frontiers | Research Topics

# Application of stem cell therapy and bioinformatics in wound repair and skin diseases

**Edited by**
Ronghua Yang, Xie Julin, Jiliang Zhou and Kun Xiong

**Published in**
Frontiers in Surgery

FRONTIERS EBOOK COPYRIGHT STATEMENT

The copyright in the text of individual articles in this ebook is the property of their respective authors or their respective institutions or funders. The copyright in graphics and images within each article may be subject to copyright of other parties. In both cases this is subject to a license granted to Frontiers.

The compilation of articles constituting this ebook is the property of Frontiers.

Each article within this ebook, and the ebook itself, are published under the most recent version of the Creative Commons CC-BY licence. The version current at the date of publication of this ebook is CC-BY 4.0. If the CC-BY licence is updated, the licence granted by Frontiers is automatically updated to the new version.

When exercising any right under the CC-BY licence, Frontiers must be attributed as the original publisher of the article or ebook, as applicable.

Authors have the responsibility of ensuring that any graphics or other materials which are the property of others may be included in the CC-BY licence, but this should be checked before relying on the CC-BY licence to reproduce those materials. Any copyright notices relating to those materials must be complied with.

Copyright and source acknowledgement notices may not be removed and must be displayed in any copy, derivative work or partial copy which includes the elements in question.

All copyright, and all rights therein, are protected by national and international copyright laws. The above represents a summary only. For further information please read Frontiers' Conditions for Website Use and Copyright Statement, and the applicable CC-BY licence.

ISSN 1664-8714
ISBN 978-2-83251-704-8
DOI 10.3389/978-2-83251-704-8

## About Frontiers

Frontiers is more than just an open access publisher of scholarly articles: it is a pioneering approach to the world of academia, radically improving the way scholarly research is managed. The grand vision of Frontiers is a world where all people have an equal opportunity to seek, share and generate knowledge. Frontiers provides immediate and permanent online open access to all its publications, but this alone is not enough to realize our grand goals.

## Frontiers journal series

The Frontiers journal series is a multi-tier and interdisciplinary set of open-access, online journals, promising a paradigm shift from the current review, selection and dissemination processes in academic publishing. All Frontiers journals are driven by researchers for researchers; therefore, they constitute a service to the scholarly community. At the same time, the *Frontiers journal series* operates on a revolutionary invention, the tiered publishing system, initially addressing specific communities of scholars, and gradually climbing up to broader public understanding, thus serving the interests of the lay society, too.

## Dedication to quality

Each Frontiers article is a landmark of the highest quality, thanks to genuinely collaborative interactions between authors and review editors, who include some of the world's best academicians. Research must be certified by peers before entering a stream of knowledge that may eventually reach the public - and shape society; therefore, Frontiers only applies the most rigorous and unbiased reviews. Frontiers revolutionizes research publishing by freely delivering the most outstanding research, evaluated with no bias from both the academic and social point of view. By applying the most advanced information technologies, Frontiers is catapulting scholarly publishing into a new generation.

## What are Frontiers Research Topics?

Frontiers Research Topics are very popular trademarks of the *Frontiers journals series*: they are collections of at least ten articles, all centered on a particular subject. With their unique mix of varied contributions from Original Research to Review Articles, Frontiers Research Topics unify the most influential researchers, the latest key findings and historical advances in a hot research area.

Find out more on how to host your own Frontiers Research Topic or contribute to one as an author by contacting the Frontiers editorial office: frontiersin.org/about/contact

# Application of stem cell therapy and bioinformatics in wound repair and skin diseases

**Topic editors**

Ronghua Yang — Guangzhou First People's Hospital, China
Xie Julin — Sun Yat-sen University, China
Jiliang Zhou — Georgia Health Sciences University, United States
Kun Xiong — Independent researcher, China

**Citation**

Yang, R., Julin, X., Zhou, J., Xiong, K., eds. (2023). *Application of stem cell therapy and bioinformatics in wound repair and skin diseases*.
Lausanne: Frontiers Media SA. doi: 10.3389/978-2-83251-704-8

# Table of contents

frontiers | Frontiers in Surgery

ORIGINAL RESEARCH
published: 05 April 2022
doi: 10.3389/fsurg.2022.878965

# Bioinformatic Analysis Reveals Hub Immune-Related Genes of Diabetic Foot Ulcers

*Yanchao Rong[1†], Hao Yang[1†], Hailin Xu[1†], Shuting Li[2], Peng Wang[1], Zhiyong Wang[1], Yi Zhang[3], Wenkai Zhu[4], Bing Tang[1*], Jiayuan Zhu[1*] and Zhicheng Hu[1*]*

[1] Department of Burn Surgery, The First Affiliated Hospital of Sun Yat-sen University, Guangzhou, China, [2] Department of Plastic Surgery, The First Affiliated Hospital of Sun Yat-sen University, Guangzhou, China, [3] Department of Burn and Plastic Surgery, Affiliated Hospital of Nantong University, Nantong, China, [4] Department of Obstetrics and Gynecology, School of Medicine, Stanford University, Stanford, CA, United States

OPEN ACCESS

**Edited by:**
Ronghua Yang,
First People's Hospital of Foshan, China

**Reviewed by:**
Shi-hui Zhu,
Second Military Medical University, China
Yinan Wang,
The First Hospital of Jilin University, China
Shenyuming Shenyuming,
Beijing Jishuitan Hospital, China

***Correspondence:**
Bing Tang
tangbing@mail.sysu.edu.cn
Jiayuan Zhu
zhujiay@mail.sysu.edu.cn
Zhicheng Hu
huzhch5@mail.sysu.edu.cn

[†] These authors have contributed equally to this work

**Specialty section:**
This article was submitted to Reconstructive and Plastic Surgery, a section of the journal Frontiers in Surgery

**Received:** 18 February 2022
**Accepted:** 17 March 2022
**Published:** 05 April 2022

**Citation:**
Rong Y, Yang H, Xu H, Li S, Wang P, Wang Z, Zhang Y, Zhu W, Tang B, Zhu J and Hu Z (2022) Bioinformatic Analysis Reveals Hub Immune-Related Genes of Diabetic Foot Ulcers. Front. Surg. 9:878965. doi: 10.3389/fsurg.2022.878965

Diabetic foot ulcer (DFU) is a complex and devastating complication of diabetes mellitus that are usually stagnant in the inflammatory phase. However, oral wound healing, which is characterized by a rapid and scarless healing process, is regarded an ideal model of wound healing. Thus, we performed a comprehensive bioinformatics analysis of the previously published data regarding oral ulcers and DFUs and found that compared to oral wound healing, the activated pathways of DFUs were enriched in cellular metabolism-related pathways but lacked the activation of inflammatory and immune-related pathways. We also found that CXCL11, DDX60, IFI44, and IFI44L were remarkable nodes since they had the most connections with other members of the module. Meanwhile, CXCL10, IRF7, and DDX58 together formed a closed-loop relationship and occupied central positions in the entire network. The real-time polymerase chain reaction and western blot was applied to validate the gene expression of the hub immune-related genes in the DFU tissues, it was found that CXCL11, IFI44, IFI44L, CXCL10 and IRF7 have a significant difference compared with normal wound tissues. Our research reveals some novel potential immune-related biomarkers and provides new insights into the molecular basis of this debilitating disease.

**Keywords: diabetic foot ulcers, bioinformatics analysis, immune, wound repair, wound healing**

## INTRODUCTION

Diabetic foot ulcer (DFU) is a complex and devastating complication of diabetes mellitus. Diabetic patients have a 15–25% chance of developing DFUs in their lifetime and a 50–70% recurrence rate in 5 years (1, 2). The refractory wound of DFUs often leads to high rates of hospitalization, amputation, and mortality. At least 25% of DFUs do not heal and 28% may result in amputation (3). In 2016, 130,000 hospital discharges for lower extremity amputation due to DFUs were reported among US adults. Meanwhile, the health care costs of DFUs pose a considerable financial burden worldwide. In England, the health care cost of DFU and the consequent amputation was estimated to be between £837 million to £962 million in 2014, which is more than the combined health care cost of breast, prostate, and lung cancers (4). In the United States, diabetes and its complications generated a total health care cost of $237 billion in 2017 (2), of which 33% was related to the treatment of DFUs (5). Unfortunately, the health care cost of DFUs is expected to increase over

the coming decades. Therefore, it is crucial to elucidate the molecular mechanisms that influence DFU progression in order to help prevent and treat these debilitating wounds.

Wound healing is a complicated process that can be divided into four integrated and overlapped phases: hemostasis, inflammation, tissue formation, and remodeling (6). Compared to the smooth and programmed healing process of acute wounds, diabetic wounds are usually stagnant in the inflammatory phase (7). After injury, neutrophils, the first inflammatory cells migrating to the wound area, clear dead cells and infectious microorganisms (8). The deregulation of neutrophil extracellular traps (NETs) activation and release (NETosis) process have been observed in the neutrophils isolated from patients with DFUs (9, 10). Afterward, monocytes appear in the wound area and are converted into macrophages (11). However, diabetes impairs the recruitment of monocytes, reduces phagocytosis, and prevents pro-inflammatory macrophages from turning into its anti-inflammatory phenotype (12). Thus, the prolonged inflammatory phase may lead to the chronic nature of DFUs wound healing. The concentration of pro-inflammatory cytokines, such as tumor necrosis factor α (TNF-α) and interleukin-1b (IL-1b), is increased and granulation and re-epithelialization are impaired in diabetic wounds (13). Therefore, maintaining a balanced inflammatory response is essential for the wound healing process.

Oral and embryonic wound healing, characterized by a rapid and scarless healing process, is regarded an ideal model of wound healing (6, 14, 15). The general principles and cellular and molecular mechanisms of skin wound healing also apply to the oral wound healing process. Hemostasis is followed by the early-stage of inflammation. Within hours of injury, the bacteria and necrotic tissues in the wound area is cleared by inflammatory cells (mostly neutrophils and monocytes) through accumulation, phagocytosis, and secretion of enzymes and toxic oxygen products (16). Within 3 days, the inflammation proceeds into its late stage. Macrophages release inflammatory cytokines and growth factors to remove apoptotic neutrophils, augment the inflammatory response, and initiate the granulation tissue formation (8, 17). Epithelialization is initiated within hours of an injury. Epithelial cells from the basal layer proliferate and migrate through the fibrin clot and eventually ensure that the wound is closed (18). Furthermore, in contrast to DFU wound, a high level of inflammatory response, followed by resolution of the inflammation (which ensures that recruited inflammatory cells are cleared from the site of injury), rapidly occurs to prevent chronic inflammation (19).

There are significant inflammatory responses in both oral and acute skin trauma, but oral mucosa has a higher inflammatory response than skin. Long-term chronic wounds have suboptimal levels of inflammation that are insufficient to promote healing. Therefore, stimulating an adequate inflammatory response can lead to better healing outcomes. In this study, we explored new immune-related gene biomarkers to improve immune status and accelerate chronic diabetic wound healing. Therefore, we performed a comprehensive bioinformatics analysis of the previously published data regarding oral ulcers and DFUs to explore the potential mechanisms of related biomarkers. Our results reveal novel potential immune-related biomarkers and provide new insights into the molecular basis of this debilitating disease.

# MATERIALS AND METHODS

## Dataset Selection

The gene expression profiles GSE37265 and GSE80178 were retrieved from the gene expression omnibus (GEO) database (https://www.ncbi.nlm.nih.gov/geo/). The GSE37265 expression profile comprises 14 oral ulcers and five normal tissues and was analyzed by the Affymetrix Human Genome U133 Plus 2.0 Array. The GSE80178 expression profile comprises six DFUs and three normal skin tissues and was analyzed by the Affymetrix Human Gene 2.0 ST Array.

## Identification of Differentially Expressed Genes

The limma (linear models for microarray data) package in R (20) was used to identify DEGs, and *P*-values were adjusted by the Benjamini and Hochberg method. Transcripts with fold expression >2.0 and adjusted $P < 0.05$ between the two groups were considered significantly different. The results are presented as volcano plots and heat maps.

## Functional Enrichment Analysis

Functional enrichment analysis of DEGs was performed by the database for annotation, visualization, and integrated discovery (DAVID) (21). The DAVID was used to perform the Kyoto encyclopedia of genes and genomes (KEGG) pathway enrichment analysis. $P < 0.05$ and false discovery rates <0.25 were considered statistically significant.

## Immune Score and Immune Cell Infiltration Analyses

The ESTIMATE algorithm was applied to calculate the scores for the level of immune cells in every sample (22). Immune cell infiltration was evaluated by the CIBERSORT algorithm (23). CIBERSORT is an analysis tool that represents the cell composition of complex tissues through analyzing gene expression data according to pre-processed gene expression profiles.

## Protein-Protein Interaction Network Analysis

The PPI network was retrieved from the STRING database and reconstructed *via* the Cytoscape software (24, 25). The degree of connectivity of each node of the network was calculated. Afterward, we used molecular complex detection (MCODE) to find clusters according to topology locating densely connected regions.

## Weighted Gene Co-expression Network Analysis

GEO expression file was examined by WGCNA using the WGCNA package in R (26). WGCNA was used to explore the relationship between the immune score and expression modules. Furthermore, the correlation between genes in corresponding

modules and gene expression profiles was defined as module membership (MM)., Each important gene's MM and gene significance (GS) were determined once the modules of interest were selected. Hub genes in each module were screened by establishing the thresholds of MM > 0.8 and GS > 0.1.

## RNA Extraction and Real-Time Polymerase Chain Reaction

DFU tissues and normal wound tissues were harvested during surgery and immediately frozen on dry ice and stored at– 80°C ($n = 3$ at each group). Total RNA extracted from rapidly frozen DRG tissues was isolated using Trizol reagent (Invitrogen). To analyze the expression level of CXCL11, DDX60, IFI44, IFI44L, CXCL10, IRF7, and DDX58, real-time polymerase chain reaction (PCR) was performed by using TaKaRa SYBR Premix Ex Taq II (Perfect Real Time). Specific primers for each gene were listed in **Figure 7A**.

## Protein Extraction and Western Blot

Total protein was extracted using a tissue protein extraction reagent (Beyotime Institute of Biotechnology, China) according to the manufacturer's instructions. Proteins were separated on the 8 or 7% SDS-polyacrylamide gel, then transferred to a PVDF membrane (Millipore, Bedford, MA). Subsequently, the membrane was blocked for 1 h in 5% skim milk at room temperature and probed with primary antibodies overnight in 0.5% skim milk at 4°C, followed by the incubation of horseradish-peroxidase-conjugated secondary antibodies for 1 h in 5% blocking buffer at room temperature. Protein bands were detected using a ECL chemiluminescence kit (Thermo Scientific, MA) with Image Quant LAS4000mini (GE Healthcare Life Sciences, UT) system. Primary and secondary antibodies are shown in **Supplementary Table 1**.

## Statistical Analyses

Statistical analyses were performed using Graph Pad Prism 7. Paired Samples test was used to compare the data between pairs of groups. $P < 0.05$ was considered statistically significant.

# RESULTS

## Evaluation of Immune Status in GSE37265

At first, we downloaded the GSE37265 dataset from the GEO database, which contains transcriptomic data of oral mucosal ulcers and normal oral mucosal tissues. The immune score of the two groups was calculated by the ESTIMATE algorithm and it was found that the immune score of the oral ulcers group was significantly higher than that of the control group ($P < 0.05$) (**Figure 1A**). Distribution of immune scores were shown in **Supplementary Table 2**. Afterward, we used the CIBERSORT algorithm to define 22 immune cell subpopulations and analyze the data from the oral ulcer and control groups. As shown in **Figure 1B**, the fraction of immune cells varied significantly among the samples and between the groups. In oral ulcers, M1 macrophages, M2 macrophages, and CD4 memory-activated T cells represented the top three highest infiltrating fractions. Inversely, T regulatory cells (Tregs), activated natural killer (NK) cells, and eosinophils were presented in lower quantities. Meanwhile, oral mucosal ulcers contained a higher fraction of CD4 naive T cells, CD4 memory-activated T cells, and M1 macrophages ($P < 0.05$) compared with normal oral mucosal tissues. However, oral mucosal ulcers contained a lower fraction of plasma cells, CD8 T cells, CD4 memory resting T cells, Tregs, activated NK cells, and resting Mast cells ($P < 0.05$) (**Figure 1C**).

## Identification and Functional Annotations of DEGs in GSE37265

Using the limma package in R, we identified the DEGs between oral mucosal ulcers (high score) and normal oral mucosal tissues (low score). As shown in the volcano plots in **Figure 2A**, a total of 1,214 DEGs (up-regulated: 885, down-regulated: 329) were identified in the GSE37265 dataset. The top 100 DEGs (up-regulated: 50, down-regulated: 50) with the highest *P*-values are shown in cluster heat maps (**Figure 2C**). To investigate the related signaling pathways, we performed the KEGG pathway analysis. Significantly enriched KEGG pathways in the DEGs from GSE37265 are shown in **Figure 2B**. Among the pathways, the TNF signaling pathway, NF-κB signaling pathway, and toll-like receptor signaling pathway are well-known pathways related to the mechanism of wound inflammation. In addition, several other pathways have been suggested to be involved in inflammatory-related mechanisms in the immune system, such as cytokine-cytokine receptor interaction, phagosome regulation, and antigen processing and presentation. KEGG pathway analysis revealed that the most significantly enriched pathway was the cytokine-cytokine receptor interaction.

## Identification of Immune-Related Modules by WGCNA

WGCNA analysis was performed on 1214 DEGs (**Figure 2**). The soft-thresholding power in WGCNA was filtered to 22 (**Figure 3A**). As shown in **Figure 3B**, the first set of modules was obtained using the Dynamic Tree Cut algorithm; afterward, correlated modules were merged. Finally, four modules were identified on the basis of the average linkage hierarchical clustering and the soft-thresholding power. However, the gray module was used for housing the genes that were not co-expressed with other genes and thus cannot be assigned to any other module, which should be ignored in our study. The pink module and the green-yellow module were highly related to the immune score (**Figure 3C**). A significant positive correlation between the pink module and the immune score was observed, while a significant negative correlation existed between the green-yellow module and the immune score. The pink module contained 406 hub genes, while the green-yellow module contained 50 hub genes. Data in these two modules were selected for further analysis.

## Identification and Functional Annotations of DEGs in GSE80178

We obtained the GSE80178 dataset from the GEO database and found that the immune score had no significant difference between the DFUs and the control groups according to the

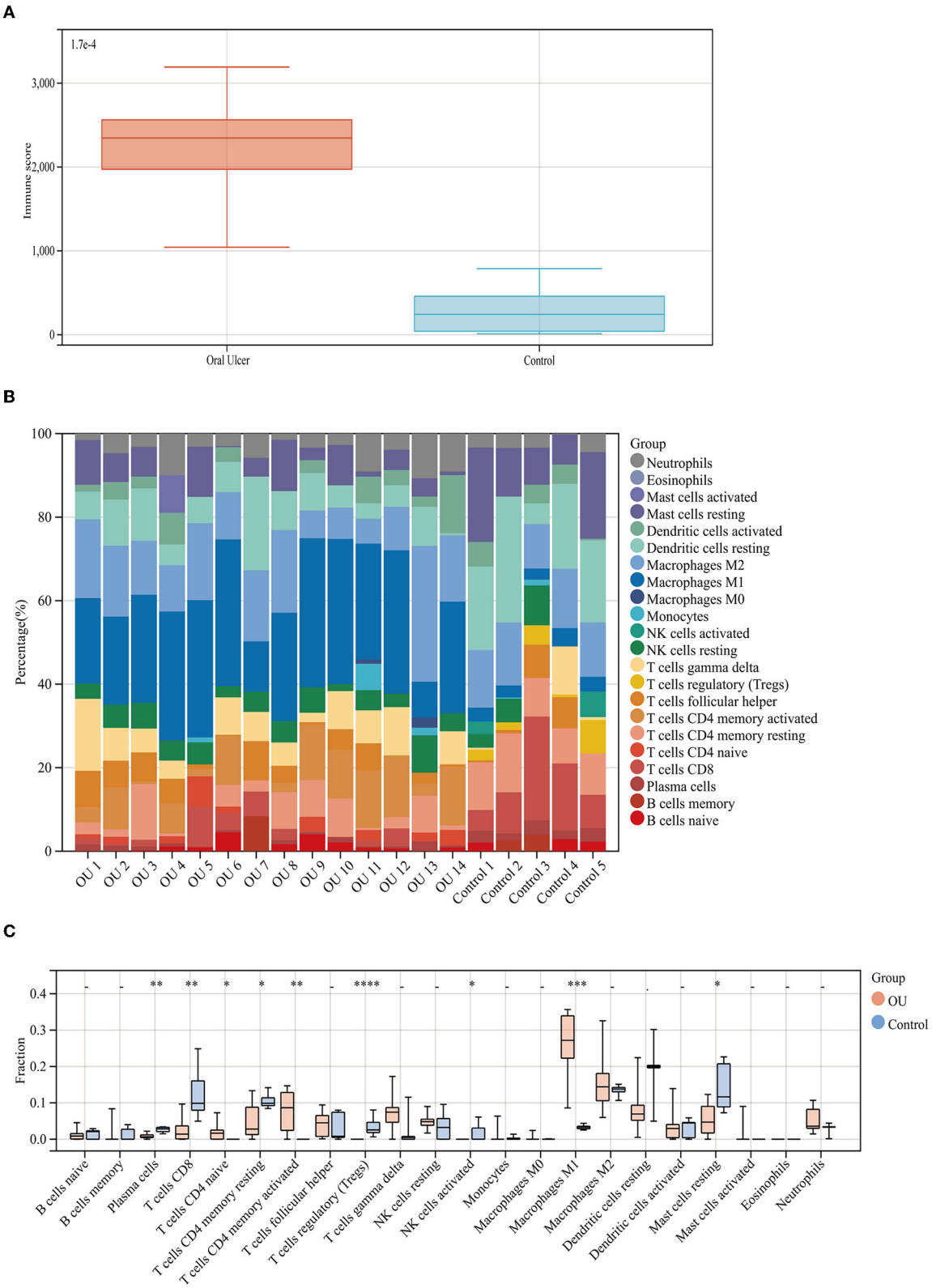


**FIGURE 1 |** Immune score and immune cell infiltration analyses. **(A)** Distribution of immune scores of oral mucosal ulcers and normal oral mucosal tissues. **(B)** The fraction of 22 subsets of immune cells from oral mucosal ulcers and normal oral mucosal tissues. **(C)** Box-plot showing the difference in immune infiltration between oral mucosal ulcers and normal oral mucosal tissues. *<0.05, **<0.01, ***<0.005, ****<0.001.

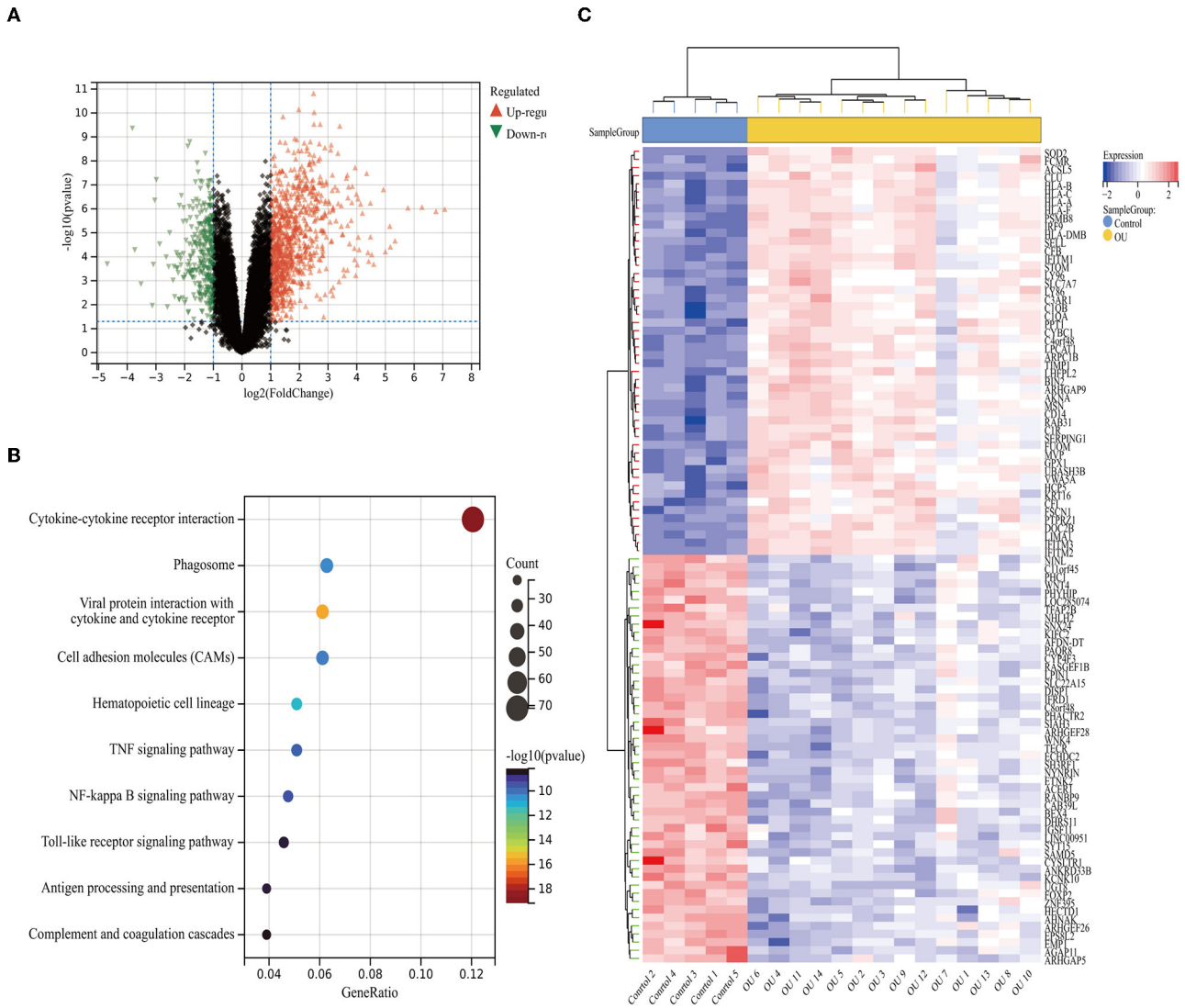


**FIGURE 2 |** The DEGs between the high and low immune score groups. **(A)** Volcano plot of the DEGs. **(B)** Heat map of the DEGs. **(C)** Mostly enriched KEGG pathways. Identification of immune-related modules by WGCNA.

ESTIMATE algorithm ($P = 0.38$) (**Figure 4A**). Distribution of immune scores were shown in **Supplementary Table 3**. Using the limma package in R, we identified the DEGs between the DFUs and the normal foot skin groups. As shown in the volcano plots, a total of 1825 DEGs (up-regulated: 409, down-regulated: 1416) were identified in the GSE80178 dataset (**Figure 4B**). The top 100 DEGs (up-regulated: 50, down-regulated: 50) with the highest *P*-values are shown in cluster heat maps (**Figure 4D**). KEGG pathway analysis is illustrated in **Figure 4C**. These DEG enrichment pathways were mainly concentrated in cellular processes and organismal systems, such as the cell cycle, interleukin-17 signaling pathway, and p53 signaling pathway. In addition, other pathways, such as glutathione metabolism, sphingolipid metabolism, and nitrogen metabolism, were primarily related to metabolic mechanism.

## Identification of Immune-Related Genes

The intersection of the analysis results of two data sets was obtained by Venn diagram (**Figure 5A**) and only 55 overlapping genes can be obtained in both groups. We defined these genes as immune-related genes and illustrated them in heat maps for each dataset. As shown in **Figure 5B**, almost all the genes were highly expressed in the oral ulcers group and lowly expressed in the DFUs group and vice versa. Overall, these immune-related genes showed opposite expression patterns in the two datasets.

## PPIs Among Immune-Related Genes

For better understanding of the interplay among the identified immune-related genes, we obtained the PPI network among the immune-related genes using the STRING tool. The network comprised 30 nodes and 116 edges (**Figure 6A**). Using MCODE,

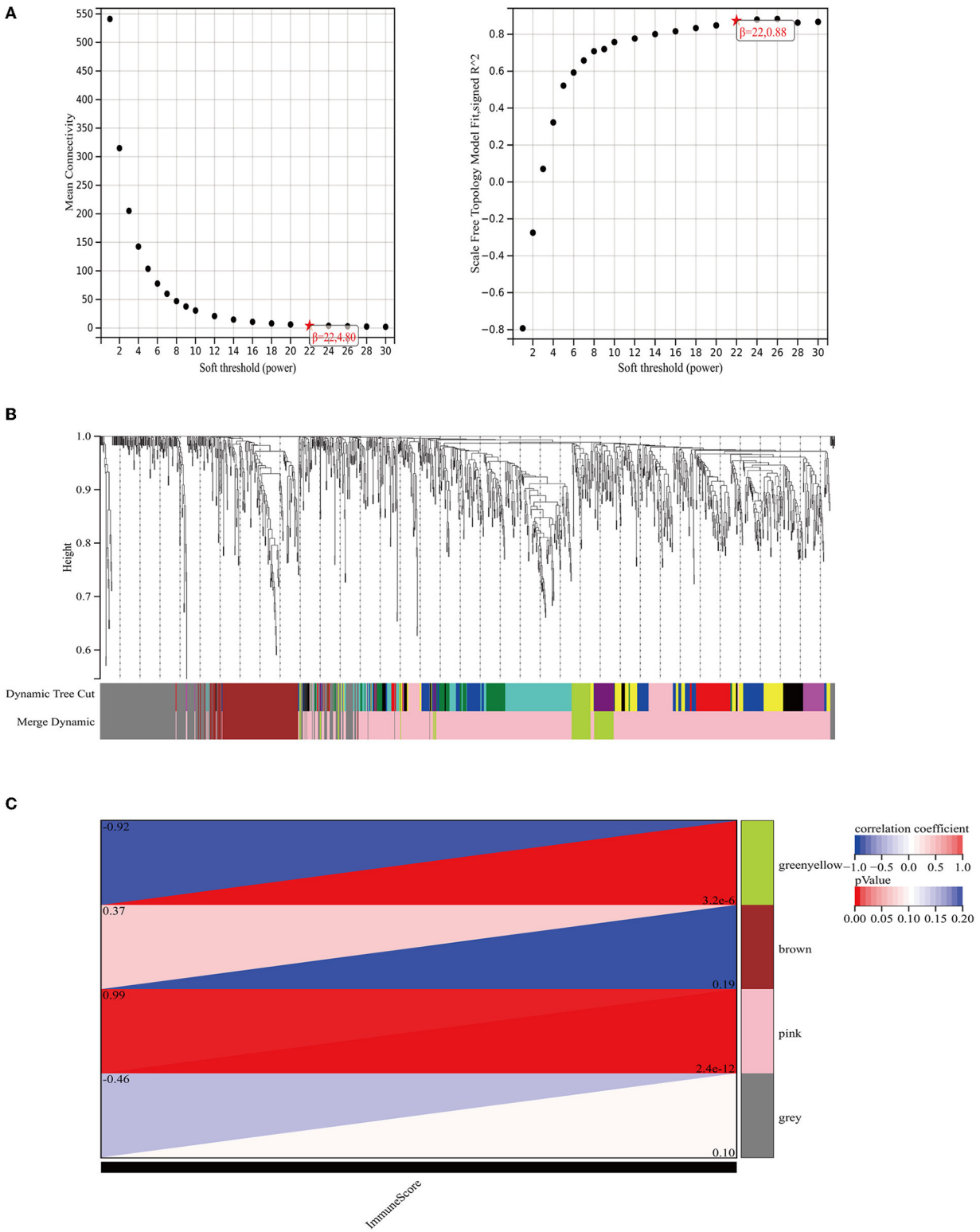


**FIGURE 3 |** The weighted immune-related gene co-expression network. **(A)** The scale-free fit index for soft-thresholding powers. The right panel shows the relationship between the soft threshold and the scale-free R2. The left panel shows the relationship between the soft threshold and the mean connectivity. **(B)** A dendrogram of the DEGs clustered based on different metrics. Each branch in the figure represents one gene and each color below represents one co-expression module. **(C)** The heat map shows the correlation between the gene module and the immune score. The correlation coefficient in each cell, decreased in size from red to blue, represents the correlation between the gene module and the immune score.

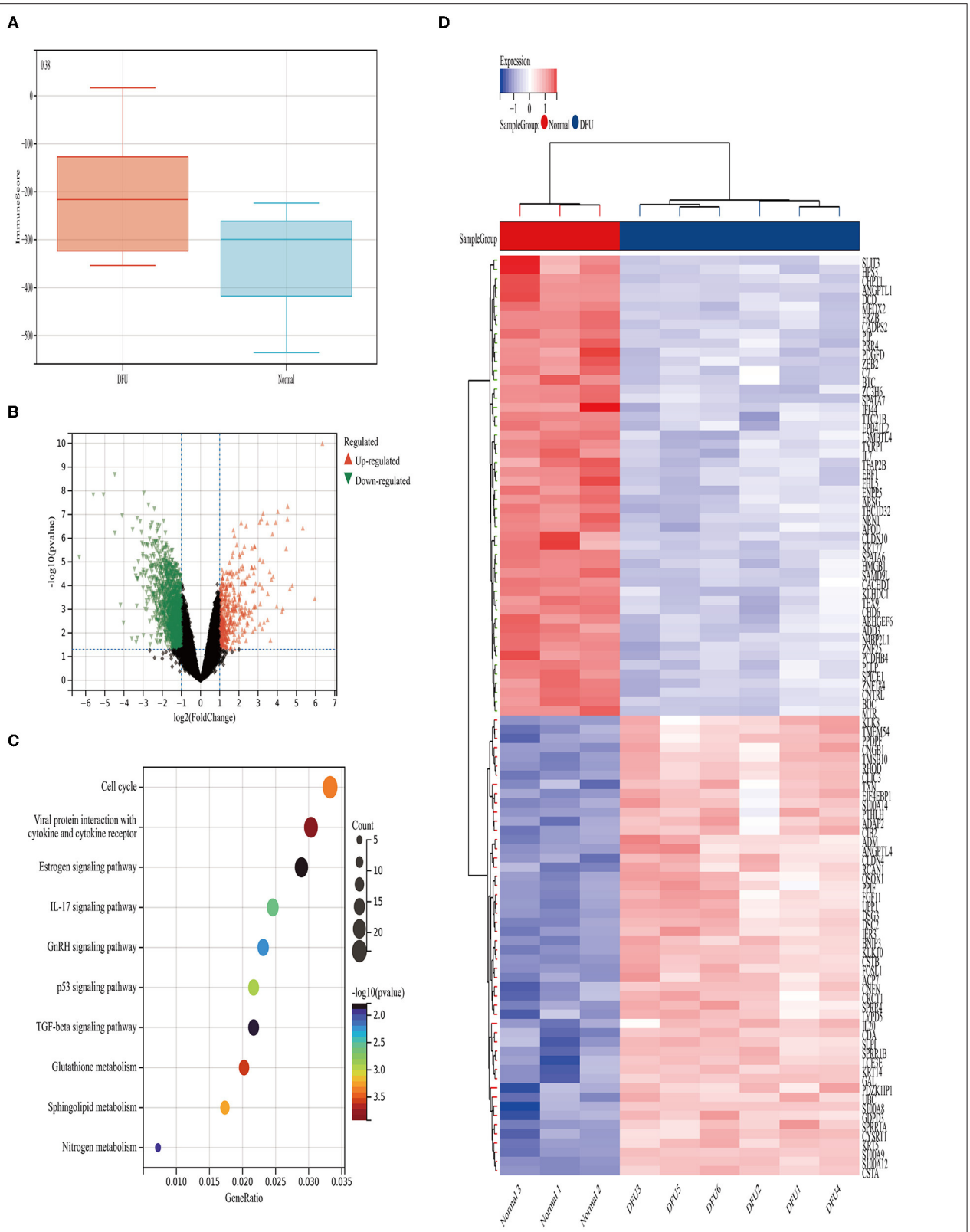


**FIGURE 4 |** Immune scores and DEGs between the DFUs group and the normal foot skin group. **(A)** Distribution of the immune scores of DFUs and normal foot skin. **(B)** Volcano plot of the DEGs. **(C)** Heat map of the DEGs. **(D)** Mostly enriched KEGG pathways.

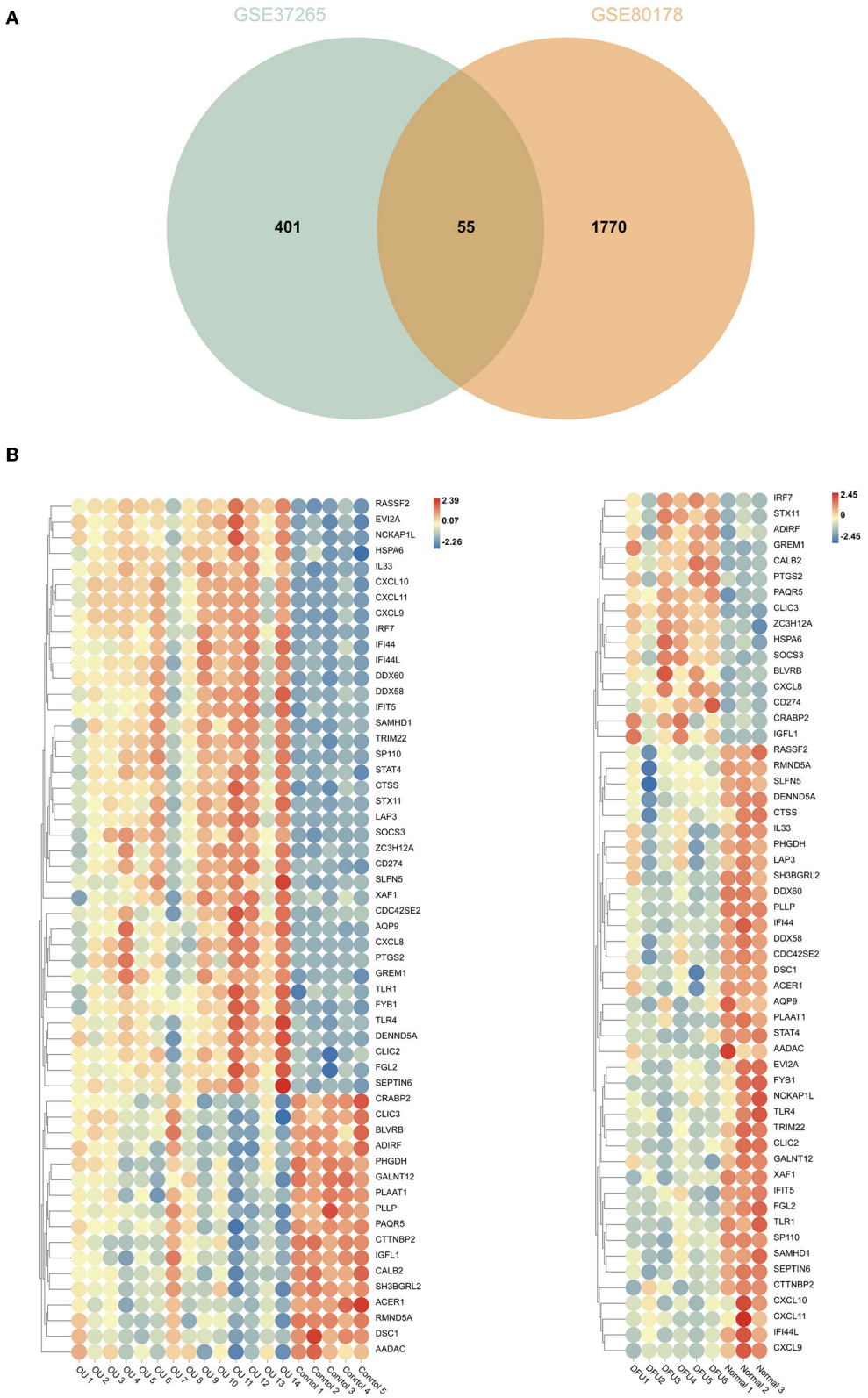


**FIGURE 5 |** Comparison of gene expression profiles with immune-related genes. **(A)** Venn diagrams showing overlapping genes in GSE37265 and GSE80178 datasets. **(B)** Heat map of immune-related genes in GSE37265 and GSE80178 datasets.

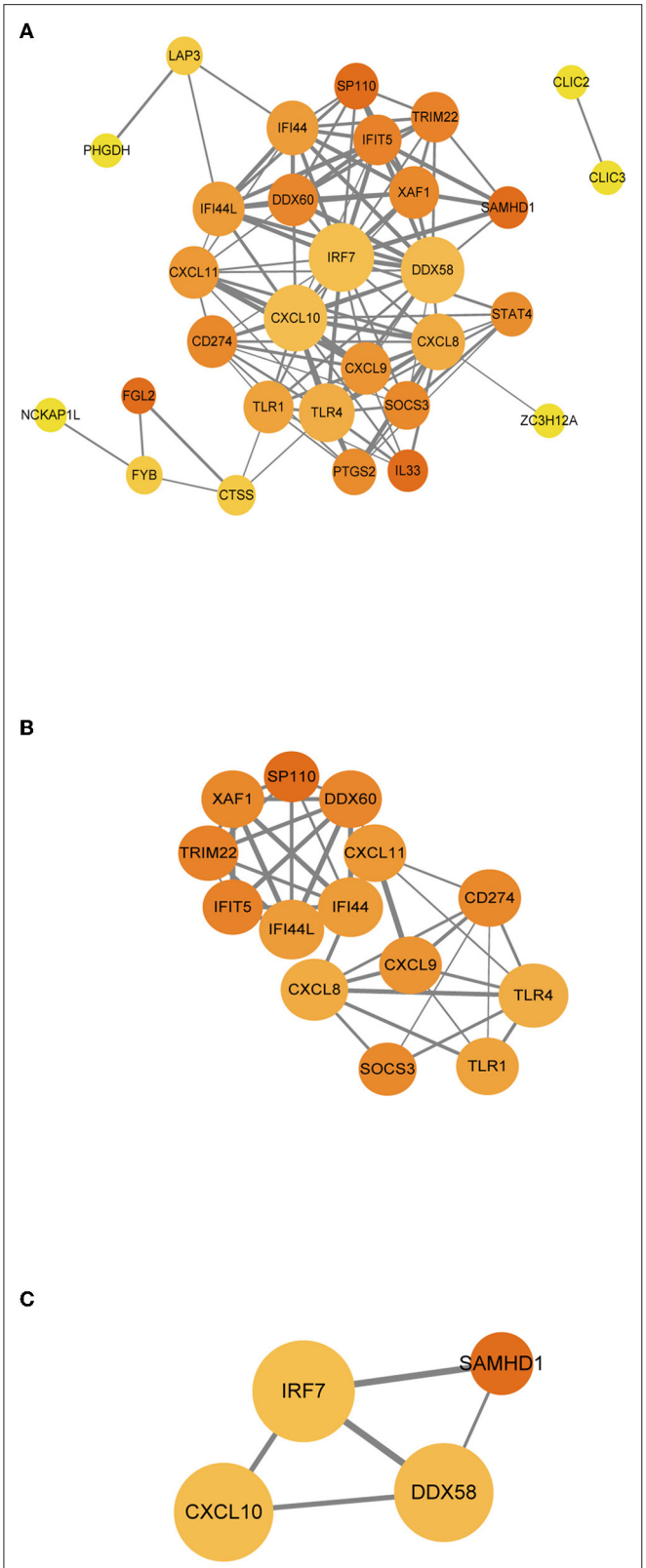


**FIGURE 6 | (A–C)** PPI networks of immune-related genes. The node color in the PPI network reflects the clustering coefficient; the node size represents the number of interacting proteins with the designated protein, while the edge size indicates the combined score.

we selected the most significant modules for further analysis. In the first module (**Figure 6B**), 40 edges involving 14 nodes were formed in the network, where CXCL11, DDX60, IFI44, and IFI44L were remarkable nodes since they had the closest connections with the other members of the module. In the second module (**Figure 6C**), CXCL10, IRF7, and DDX58 together formed a closed-loop relationship and occupied central positions in the entire network.

## Validation of Hub Immune-Related Genes

To further test these hub immune-related genes,we performed a real-time PCR validation by comparing the normal wound tissues with the DFU tissues. In line with our bioinformatic results, CXCL11, IFI44, IFI44L, CXCL10 and IRF7 had a significant difference compared with normal wound tissues ($P < 0.05$) (**Figure 7B**). However, there was no statistical difference in DDX58 and DDX60 gene expression levels observed in the DFU group compared to the Normal group ($P > 0.05$). The results of western blot also indicated that CXCL11, IFI44, IFI44L, CXCL10, and IRF7 were indeed significantly different from normal tissues (**Figure 7C**).

# DISCUSSION

DFUs and other chronic wounds are characterized by morphological and cellular changes; however, the underlying molecular biomarkers that result in these changes are poorly understood. Abnormal gene expression is closely related to a series of pathological conditions in DFUs. An altered mRNA expression is a valuable biomarker that plays an important role in the development of diabetes-related diseases (27, 28). Expanding our understanding of the mechanisms involved in diabetic wounds would improve the efficacy of wound healing and reduce the social burden. Unlike skin wounds, oral wounds heal more quickly and have fewer complications; however, our knowledge in this area is limited by the lack of detailed comparative analyses of humans. Considering that oral mucosa is recognized for quick and scarless healing, we decided to use oral ulcer as a model to explore the potential interventions related to wound immune activation during DFUs treatment.

In this study, we first analyzed the datasets of oral ulcers and DFUs using bioinformatics methods and found that the immune score of oral ulcers was significantly higher than that of the normal oral mucosa; however, there was no statistically significant difference between the immune scores of DFUs and that of normal foot skin. Afterward, KEGG function enrichment was performed on the differential genes in the two datasets, respectively, and it was found that the oral ulcers group was mainly enriched in inflammatory and immune-related pathways, while the DFU group was enriched in cellular metabolism-related pathways, lacking the activation of inflammatory and immune-related pathways. In conclusion, oral ulcers can significantly activate the immune system and initiate inflammatory responses; however, DFUs lack the corresponding activation.

Some studies have found that DFUs only have a low-intensity inflammation; in other words, the activation and function of

A

| Gene | Primers | Sequence |
|---|---|---|
| CXCL10 | Forward primer | 5'GTGGCATTCAAGGAGTACCTC |
| | Reverse primer | 5'TGATGGCCTTCGATTCTGGATT |
| CXCL11 | Forward primer | 5'GACGCTGTCTTTGCATAGGC |
| | Reverse primer | 5'GGATTTAGGCATCGTTGTCCTTT |
| DDX58 | Forward primer | 5'TGTGCTCCTACAGGTTGTGGA |
| | Reverse primer | 5'CACTGGGATCTGATTCGCAAAA |
| DDX60 | Forward primer | 5'GACAGGTCCAGGTGTCAGTTT |
| | Reverse primer | 5'TTGGTCTCGTGTGCCTTTTTG |
| IFI44 | Forward primer | 5'GGTGGGCACTAATACAACTGG |
| | Reverse primer | 5'CACACAGAATAAACGGCAGGTA |
| IFI44L | Forward primer | 5'TCTGCCATTTATGTTGTGTGACA |
| | Reverse primer | 5'CAGGTGTAATTGGTTTACGGGAA |
| IRF7 | Forward primer | 5'GCTGGACGTGACCATCATGTA |
| | Reverse primer | 5'GGGCCGTATAGGAACGTGC |

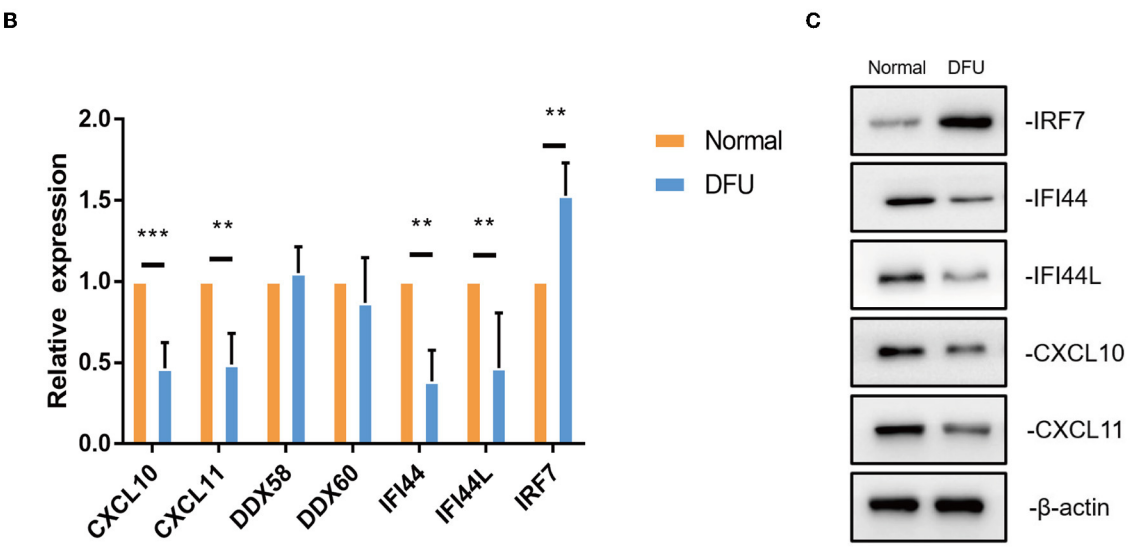


**FIGURE 7 |** The validation of hub immune-related genes. **(A,B)** Gene expression of hub immune-related genes in DFU tissues were validated by real-time PCR. **<0.05,***<0.005. **(C)**CXCL11, IFI44, IFI44L, CXCL10 and IRF7 protein levels were measured by western blot (a representative blot, from three independent experiments).

the immune cells are reduced, which provides an inadequate inflammatory response and delay in the healing process (29). In our research, we found that M1 macrophages, M2 macrophages, and CD4 memory-activated T cells were the cell types with the highest degree of infiltration on the wound surface of oral ulcers, which were significantly up-regulated compared to the control group. Macrophages play crucial roles in the inflammatory stage of wound healing (11, 30). Macrophages undergo a phenotypic transition from M1 to M2, which ensures the inflammation resolution and the wound healing progression. This process was found to be out of control in diabetic ulcers, thus resulting in dysfunctional M1 macrophage accumulation and lack of M2 macrophage (31, 32). T cells are also critical for inflammation reduction and tissue remodeling. During inflammation, macrophages secrete chemokines, such as interferon-gamma, to attract T cells to the wound, which contributes to the formation of the initial pro-inflammatory microenvironment of the wound (33). However, activated natural

killer (NK) cells and Tregs were the cell types with the lowest degree of wound infiltration, which were significantly down-regulated compared to the control group. Since NK cells inhibit wound healing, the depletion of NK cells in mice can improve the rate of wound healing (34). In contrast, wound healing was reported to be slower in Tregs-depleted mice than in wild-type mice (35). The down-regulation of Tregs in this study may be due to the transformation process of memory T cells. Tregs play an important role in maintaining skin homeostasis. Tregs secrete arginase and anti-inflammatory cytokines that promote the polarization of anti-inflammatory macrophages, inhibit inflammatory responses, and contribute to the matrix formation (36). Studies have demonstrated that NK cells are up-regulated, while Tregs are down-regulated in DFUs, and that different immune cell infiltrates would indeed cause different healing states (29).

Finally, we conducted the WGCNA analysis to find the immune-related modules and obtained 55 immune-related genes by the intersection with differential genes in the diabetes group. These genes were significantly differentiated genes in the two datasets; however, their overall expression patterns showed an opposite state. Through PPI analysis, 30 of them were closely related. By extracting the key modules, we finally identified 18 key immune-related genes. Among them, CXCL11, DDX60, IFI44, IFI44L, CXCL10, IRF7, and DDX58 were identified as the hub genes in this study. However, DDX58 and DDX60 showed no significant difference in the *in vitro* experiment, the rest genes were indeed found to be closely related to immune regulation after literature search. CXCL10 is an inflammatory chemokine secreted by monocytes, neutrophils, endothelial cells, keratinocyte, fibroblasts, mesenchymal cells, dendritic cells, and astrocytes (37). CXCL10, as one of the selective ligands of CXCR3, binds to CXCR3 and regulates immune responses by activating and recruiting leukocytes, such as T cells, eosinophils, monocytes, and NK cells (38). CXCL11 is also one of the selective ligands of CXCR3 and plays important roles in leukocyte homing and persistence of inflammation (39, 40). IFI44 was reported to negatively regulate innate immune and antiviral responses (41); it is also implicated in immune infiltration in the tumor microenvironment (42, 43). Previous studies have indicated a promising role of IFI44L in innate immunity, such as antiviral response, antitumor response, and inflammatory response (44–46). IRF7 is expressed in fibroblasts, B cells, lymphocytes, pDCs, and monocytes and plays important roles in regulating the innate and adaptive immune response (47). In this study, the above-mentioned genes showed a close relationship with immunity. Since most of the genes identified in this study have not been previously reported to be related with DFUs, there is a clear need to verify the functional importance and mechanistic roles of these genes in this pathological context. Based on the information obtained from literature, we are interested in further studies on the relationship between these genes and their functions as regulators of these debilitating chronic wounds.

## CONCLUSION

Overall, we have provided a comprehensive comparative analysis of molecular and cellular mechanisms by studying different wound healing processes in the oral cavity and skin, ultimately highlighting the fundamental mechanisms of inflammation and repair in human being, thereby providing insights for treating chronic and unhealed wounds.

## DATA AVAILABILITY STATEMENT

The original contributions presented in the study are included in the article/**Supplementary Material**, further inquiries can be directed to the corresponding authors.

## ETHICS STATEMENT

The studies involving human participants were reviewed and approved by the Institutional Review Board of The First Affiliated Hospital of Sun Yat-sen University. The patients/participants provided their written informed consent to participate in this study.

## AUTHOR CONTRIBUTIONS

ZH and JZ designed the research. YR, HY, HX, SL, PW, ZW, YZ, WZ, BT, JZ, and ZH performed the experiment. YR, HY, and ZH wrote the manuscript. YR, HY, and HX researched data. BT, JZ, and ZH reviewed/edited the manuscript. All authors contributed to the article and approved the submitted version.

## FUNDING

This work was supported by research grants 82172213 (ZH), 82072180 (JZ), 82072181 and 81871565 (BT) from National Natural Science Foundation of China, research grant 2019A1515012208 (ZH) from Guangdong Provincial Natural Science Foundation of China, and research grants 2013001 and 2018002 (JZ) from the Sun Yat-sen University Clinical Research 5010 Program, and Kelin New Star Talent Program of The First Affiliated Hospital of Sun Yat-sen University (ZH).

## ACKNOWLEDGMENTS

We appreciate the linguistic assistance provided by TopEdit (www.topeditsci.com) during the preparation of this manuscript.

## SUPPLEMENTARY MATERIAL

The Supplementary Material for this article can be found online at: https://www.frontiersin.org/articles/10.3389/fsurg.2022.878965/full#supplementary-material

## REFERENCES


1. Alavi A, Sibbald RG, Mayer D, Goodman L, Kirsner RS. Diabetic foot ulcers: Part I. Pathophysiology and prevention. *J Am Acad Dermatol.* (2014) 70: 1.e1–18. doi: 10.1016/j.jaad.2013.06.055
2. Ingelfinger JR, Armstrong DG, Boulton AJM, Bus SA. Diabetic foot ulcers and their recurrence. *New Engl J Med.* (2017) 376:2367. doi: 10.1056/NEJMra1615439
3. Prompers L, Huijberts M, Schaper N, Apelqvist J, Bakker K, Edmonds M, et al. Resource utilisation and costs associated with the treatment of diabetic foot ulcers. Prospective data from the Eurodiale Study. *Diabetologia.* (2008) 51:1826–34. doi: 10.1007/s00125-008-1089-6
4. Kerr M, Barron E, Chadwick P, Evans T, Kong WM, Rayman G, et al. The cost of diabetic foot ulcers and amputations to the National Health Service in England. *Diabet Med.* (2019) 36:995–1002. doi: 10.1111/dme.13973
5. Driver VR, Fabbi M, Lavery LA, Gibbons G. The costs of diabetic foot: the economic case for the limb salvage team. *J Vasc Surg.* (2010) 52:17–22S. doi: 10.1016/j.jvs.2010.06.003
6. Eming SA, Martin P, Tomic-Canic M. Wound repair and regeneration: mechanisms, signaling, and translation. *Sci Transl Med.* (2014) 6:265sr6. doi: 10.1126/scitranslmed.3009337
7. Ywa C, Tsa C, Jwa C, Huang X, Deng X, Cao Y, et al. An update on potential biomarkers for diagnosing diabetic foot ulcer at early stage. *Biomed Pharmacother.* (2021) 133:110991. doi: 10.1016/j.biopha.2020.110991
8. Eming SA, Wynn TA, Martin P. Inflammation and metabolism in tissue repair and regeneration. *Science.* (2017) 356:1026–30. doi: 10.1126/science.aam7928
9. Fadini GP, Menegazzo L, Rigato M, Scattolini V, Poncina N, Bruttocao A, et al. NETosis delays diabetic wound healing in mice and humans. *Diabetes.* (2016) 65:1061–71. doi: 10.2337/db15-0863
10. Wong SL, Demers M, Martinod K, Gallant M, Wang Y, Goldfine AB, et al. Diabetes primes neutrophils to undergo NETosis, which impairs wound healing. *Nat Med.* (2015) 21:815–9. doi: 10.1038/nm.3887
11. Lucas T, Waisman A, Ranjan R, Roes J, Eming SA. Differential roles of macrophages in diverse phases of skin repair. *J Immunol.* (2010) 184:3964–77. doi: 10.4049/jimmunol.0903356
12. Add A, A F, Slk B, Kag A. Targeting epigenetic mechanisms in diabetic wound healing. *Transl Res.* (2019) 204:39–50. doi: 10.1016/j.trsl.2018.10.001
13. Falanga V. Wound healing and its impairment in the diabetic foot. *Lancet.* (2005) 366:1736–43. doi: 10.1016/S0140-6736(05)67700-8
14. Szpaderska AM, Zuckerman JD, Dipietro LA. Differential injury responses in oral mucosal and cutaneous wounds. *J Dent Res.* (2003) 82:621–6. doi: 10.1177/154405910308200810
15. Turabelidze A, Guo S, Chung AY, Chen L, Dai Y, Marucha PT, et al. Intrinsic differences between oral and skin keratinocytes. *PLoS ONE.* (2014) 9:e101480. doi: 10.1371/journal.pone.0101480
16. Wikesjö UM, Selvig KA. Periodontal wound healing and regeneration. *Periodontol 2000.* (1999) 19:21–39. doi: 10.1111/j.1600-0757.1999.tb00145.x
17. Wynn T, Vannella K. Macrophages in tissue repair, regeneration, and fibrosis. *Immunity.* (2016) 44:450–62. doi: 10.1016/j.immuni.2016.02.015
18. Aukhil I. Biology of wound healing. *Surg Clin North Am.* (2010) 22:44–50. doi: 10.1034/j.1600-0757.2000.2220104.x
19. Iglesias-Bartolome R, Uchiyama A, Molinolo AA, Abusleme L, Brooks SR, Callejas-Valera JL, et al. Transcriptional signature primes human oral mucosa for rapid wound healing. *Sci Transl Med.* (2018) 10 eaap8798. doi: 10.1126/scitranslmed.aap8798
20. Robinson MD, McCarthy DJ, Smyth GK. edgeR: a Bioconductor package for differential expression analysis of digital gene expression data. *Bioinformatics.* (2010) 26:139–40. doi: 10.1093/bioinformatics/btp616
21. Huang DW, Sherman BT, Lempicki RA. Systematic and integrative analysis of large gene lists using DAVID bioinformatics resources. *Nat Protoc.* (2008) 4:44–57. doi: 10.1038/nprot.2008.211
22. Yoshihara K, Shahmoradgoli M, Martínez E, Vegesna R, Kim H, Torres-Garcia W, et al. Inferring tumour purity and stromal and immune cell admixture from expression data. *Nat Commun.* (2013) 4:2612. doi: 10.1038/ncomms3612
23. Chen B, Khodadoust MS, Liu CL, Newman AM, Alizadeh AA. Profiling tumor infiltrating immune cells with CIBERSORT. *Methods Mol Biol.* (2018) 1711:243–59. doi: 10.1007/978-1-4939-7493-1_12
24. Szklarczyk D, Franceschini A, Wyder S, Forslund K, Heller D, Huerta-Cepas J, et al. STRING v10: protein–protein interaction networks, integrated over the tree of life. *Nucleic Acids Res.* (2015) 43: D447–52. doi: 10.1093/nar/gku1003
25. Shannon P. Cytoscape: a software environment for integrated models of biomolecular interaction networks. *Genome Res.* (2003) 13:2498–504. doi: 10.1101/gr.1239303
26. Langfelder P, Horvath S. WGCNA: an R package for weighted correlation network analysis. *BMC Bioinformatics.* (2008) 9:559. doi: 10.1186/1471-2105-9-559
27. Van J, Scholey JW, Konvalinka A. Insights into diabetic kidney disease using urinary proteomics and bioinformatics. *J Am Soc Nephrol.* (2017) 28:1050−61. doi: 10.1681/ASN.2016091018
28. Ramirez HA, Liang L, Pastar I, Rosa AM, Stojadinovic O, Zwick TG, et al. Comparative genomic, microRNA, and tissue analyses reveal subtle differences between non-diabetic and diabetic foot skin. *PLoS ONE.* (2015) 10:e0137133. doi: 10.1371/journal.pone.0137133
29. Sawaya AP, Stone RC, Brooks SR, Pastar I, Jozic I, Hasneen K, et al. Deregulated immune cell recruitment orchestrated by FOXM1 impairs human diabetic wound healing. *Nat Commun.* (2020) 11:4678. doi: 10.1038/s41467-020-18276-0
30. Koh TJ, Ann DPL. Inflammation and wound healing: the role of the macrophage. *Expert Rev Mol Med.* (2011) 13:e23. doi: 10.1017/S1462399411001943
31. Mirza RE, Fang MM, Ennis WJ, Koh TJ. Blocking interleukin-1β induces a healing-associated wound macrophage phenotype and improves healing in type 2 diabetes. *Diabetes.* (2013) 62:2579–87. doi: 10.2337/db12-1450
32. Nassiri S, Zakeri I, Weingarten MS, Spiller KL. Relative expression of proinflammatory and antiinflammatory genes reveals differences between healing and nonhealing human chronic diabetic foot ulcers. *J Invest Dermatol.* (2015) 135:1700–3. doi: 10.1038/jid.2015.30
33. Palacios F, Abreu C, Prieto D, Morande P, Ruiz S, Fernández-Calero T, et al. Activation of the PI3K/AKT pathway by microRNA-22 results in CLL B-cell proliferation. *Leukemia.* (2015) 29:115–25. doi: 10.1038/leu.2014.158
34. Cuilian L, Haoran Y, Weiyun S, Ting W, Qingguo R. MicroRNA-mediated regulation of Th17/Treg balance in autoimmune disease. *Immunology.* (2018) 155:427–434. doi: 10.1111/imm.12994
35. Chen C, Zhou Y, Wang J, Yan Y, Peng L. Dysregulated MicroRNA Involvement in multiple sclerosis by induction of T Helper 17 cell differentiation. *Front Immunol.* (2018) 9:1256. doi: 10.3389/fimmu.2018.01256
36. Husakova M. MicroRNAs in the key events of systemic lupus erythematosus pathogenesis. *Biomed Pap Med Fac Univ Palacky Olomouc Czech Repub.* (2016) 160:327–42. doi: 10.5507/bp.2016.004
37. Luster AD, Ravetch JV. Biochemical characterization of a gamma interferon-inducible cytokine (IP-10). *J Exp Med.* (1987) 166:1084–97. doi: 10.1084/jem.166.4.1084
38. Jinquan T, Jing C, Jacobi HH, Reimert CM, Millner A, Quan S, et al. CXCR3 expression and activation of eosinophils: role of IFN-gamma-inducible protein-10 and monokine induced by IFN-gamma. *J Immunol.* (2000) 165:1548–56. doi: 10.4049/jimmunol.165.3.1548
39. Muehlinghaus G, Cigliano L, Huehn S, Peddinghaus A, Manz RA. Regulation of CXCR3 and CXCR4 expression during terminal differentiation of memory B cells into plasma cells. *Blood.* (2005) 105:3965–71. doi: 10.1182/blood-2004-08-2992
40. Brightling CE, Ammit AJ, Kaur D, Black JL, Wardlaw AJ, Hughes JM, et al. The CXCL10/CXCR3 axis mediates human lung mast cell migration to asthmatic airway smooth muscle. *Am J Respir Crit Care Med.* (2012) 171:1103–8. doi: 10.1164/rccm.200409-1220OC
41. Dediego ML, Nogales A, Martinez-Sobrido L, Topham DJ. Interferon-induced protein 44 interacts with cellular FK506-binding protein 5, negatively regulates host antiviral responses, and supports virus replication. *Mbio.* (2019) 10:e01839–19. doi: 10.1128/mBio.01839-19
42. Pan H, Wang X, Huang W, Dai Y, Guan J. Interferon-induced protein 44 correlated with immune infiltration serves as a potential prognostic

indicator in head and neck squamous cell carcinoma. *Front Oncol.* (2020) 10:557157. doi: 10.3389/fonc.2020.557157
43. Wisdom AJ, Hong CS, Lin AJ, Xiang Y, Kirsch DG. Neutrophils promote tumor resistance to radiation therapy. *Proc Natl Acad Sci U S A*. (2019) 116: 18584–9. doi: 10.1073/pnas.1901562116
44. Schoggins JW, Rice CM. Interferon-stimulated genes and their antiviral effector functions. *Curr Opin Virol.* (2011) 1:519–25. doi: 10.1016/j.coviro.2011.10.008
45. Huang WC, Shiao-Lin T, Chen YL, Chen PM, Chu PY. IFI44L is a novel tumor suppressor in human hepatocellular carcinoma affecting cancer stemness, metastasis, and drug resistance via regulating met/Src signaling pathway. *BMC Cancer.* (2018) 18:609. doi: 10.1186/s12885-018-4529-9
46. Dediego ML, Martinez-Sobrido L, Topham DJ. Novel functions of IFI44L as a feedback regulator of host antiviral responses. *J Virol.* (2019) 93:e01159–19. doi: 10.1128/JVI.01159-19
47. Tamura T, Yanai H, Savitsky D, Taniguchi T. The IRF family transcription factors in immunity and oncogenesis. *Annu Rev Immunol.* (2008) 26:535–84. doi: 10.1146/annurev.immunol.26.021607.090400

**Conflict of Interest:** The authors declare that the research was conducted in the absence of any commercial or financial relationships that could be construed as a potential conflict of interest.

**Publisher's Note:** All claims expressed in this article are solely those of the authors and do not necessarily represent those of their affiliated organizations, or those of the publisher, the editors and the reviewers. Any product that may be evaluated in this article, or claim that may be made by its manufacturer, is not guaranteed or endorsed by the publisher.

*Copyright © 2022 Rong, Yang, Xu, Li, Wang, Wang, Zhang, Zhu, Tang, Zhu and Hu. This is an open-access article distributed under the terms of the Creative Commons Attribution License (CC BY). The use, distribution or reproduction in other forums is permitted, provided the original author(s) and the copyright owner(s) are credited and that the original publication in this journal is cited, in accordance with accepted academic practice. No use, distribution or reproduction is permitted which does not comply with these terms.*

frontiers | Frontiers in Surgery

ORIGINAL RESEARCH
published: 19 May 2022
doi: 10.3389/fsurg.2022.917776

# High Expression of TIMELESS Predicts Poor Prognosis: A Potential Therapeutic Target for Skin Cutaneous Melanoma

*Shixin Zhao[1†], Shifeng Wen[2†], Hengdeng Liu[1†], Ziheng Zhou[1], Yiling Liu[1], Jinbao Zhong[3] and Julin Xie[1]*

[1]Department of Burn Surgery, First Affiliated Hospital of Sun Yat-Sen University, Guangzhou, China, [2]Department of Orthopedics, Guangzhou First People's Hospital, School of Medicine, South China University of Technology, Guangzhou, China, [3]Department of Dermatology, Guangzhou Institute of Dermatology, Guangzhou, China

OPEN ACCESS

**Edited by:**
Jiliang Zhou
Georgia Health Sciences University, Augusta, United States

**Reviewed by:**
Zhaocai Zhang, Second Affiliated Hospital, School of Medicine, Zhejiang University, China
Biao Cheng, General Hospital of Southern Theater Command of PLA, China

***Correspondence:**
Jinbao Zhong
zjbzpx@126.com
Julin Xie
xiejulin@mail.sysu.edu.cn

[†]These authors have contributed equally to this work and share first authorship

**Specialty section:**
This article was submitted to Reconstructive and Plastic Surgery, a section of the journal Frontiers in Surgery

**Received:** 11 April 2022
**Accepted:** 02 May 2022
**Published:** 19 May 2022

**Citation:**
Zhao S, Wen S, Liu H, Zhou Z, Liu Y, Zhong J and Xie J (2022) High Expression of TIMELESS Predicts Poor Prognosis: A Potential Therapeutic Target for Skin Cutaneous Melanoma. Front. Surg. 9:917776. doi: 10.3389/fsurg.2022.917776

**Background:** Skin cutaneous melanoma (SKCM) is the most lethal skin cancer with an increasing incidence worldwide. The poor prognosis of SKCM urgently requires us to discover prognostic biomarkers for accurate therapy. As a regulator of DNA replication, TIMELESS (TIM) has been found to be highly expressed in various malignancies but rarely reported in SKCM. The objective of this study was to evaluate the relationship between TIM and SKCM tumorigenesis and prognosis.

**Methods:** We obtained RNA sequencing data from TCGA and GTEx to analyze TIM expression and differentially expressed genes (DEGs). Subsequently, GO/KEGG, GSEA, immune cell infiltration analysis, and protein-protein interaction (PPI) network were used to perform the functional enrichment analysis of TIM-related DEGs. Moreover, the receiver operating characteristic (ROC) curves, Cox regression analysis, Kaplan–Meier (K-M) analysis, and nomograms were applied to figure out the clinical significance of TIM in SKCM. In addition, we investigated the relationship between TIM promoter methylation and SKCM prognosis through the UALCAN database. Finally, the immunohistochemical (IHC) results of normal skin and SKCM were analyzed to determine expression differences.

**Results:** TIM was significantly elevated in various malignancies, including SKCM, and high expression of TIM was associated with poor prognosis. Moreover, a total of 402 DEGs were identified between the two distinct TIM expression groups, and functional annotation showed enrichment with positive regulation of cell cycle and classic oncogenic pathways in the high TIM expression phenotype, while keratinization pathways were negatively regulated and enriched. Further analysis showed that TIM was correlated with infiltration of multiple immune cells. Finally, IHC validated the differential expression of TIM in SKCM.

**Conclusion:** TIM might play a pivotal role in tumorigenesis of SKCM and is closely related to its prognosis.

**Keywords: skin cutaneous melanoma, prognostic signature, overall survival, timeless, immune infiltration, bioinformatics**

# INTRODUCTION

Skin cutaneous melanoma (SKCM) is the most lethal skin cancer with an increasing incidence worldwide, accounting for 287,723 new cases and 60,712 deaths in 2018 (1, 2). For patients with primary SKCM, complete resection is currently considered as the first choice, providing the highest probability of cure (3). However, there are quite limited means to treat patients with metastatic SKCM. Despite the significant progress in the adjuvant therapies of SKCM, many important questions remain, such as toxicity of chemotherapy, drug resistance, and expensive cost (3). Thus, increasing incidence worldwide, poor prognosis, and limited efficacy of available therapeutic tools prompted us to undertake extensive mechanistic investigations to discover novel prognostic biomarkers and new targets for therapy that might support precision medicine.

TIM, first identified in drosophila and subsequently in mammals, is not only involved in circadian rhythms, but also in cell cycle and DNA replication . Moreover, TIM also participate in cell survival after DNA damage or replication stress by promoting TIPIN nuclear locallization and play an important role in epithelial cell morphogenesis (4). Anomalous cell cycle and molecular clockwork have been implicated in various diseases, notably tumorigenesis (5). Indeed, TIM has been demonstrated to be overexpressed in several malignancies compared to normal tissues, such as colorectal cancer, small cell lung cancer, and breast cancer (6–8). Not only that, the expression of TIM has been significantly associated with advanced tumor stages as well as poor prognosis (9). Therefore, TIM might has the potential to be used as a biomarker of cancer susceptibility, diagnosis, and prognostic outcome. Should this be the case, TIM could be a worthy therapeutic target.

In recent years, growing studies have shown that molecular factors (BRAF, MEK, PD-1) are important for biology, drug targeting, and prognosis in SKCM (10–12). To date, however, comprehensive studies of TIM in SKCM have yet to be reported. The focus of this study was to ascertain TIM expression level in SKCM and its potential prognostic significance. Moreover, the mechanisms by which TIM influences the prognosis of SKCM and its potential relationship to immune infiltration were also discussed.

# MATERIALS AND METHODS

## RNA-Sequencing Data and Ethics Statement

TPM expression values were downloaded from the UCSC XENA Project (https://xenabrowser.net/datapages/), which contains the TCGA and GTEX RNA-Seq data that was processed uniformly to provide more reliable expression analysis with tumor and normal samples (13, 14). Besides, clinicopathological information and corresponding RNA-seq data of SKCM in FPKM format were downloaded from the TCGA database (https://portal.gdc.cancer.gov/). Apart from 1 patient with incomplete clinicopathological information, a total of 471 SKCM patients were included. In this study, RNA-seq data was converted from FPKM to TPM format for further analysis. Since the UCSC XENA and TCGA database is publicly available in accordance with certain guidelines, it acknowledges that all written informed consents have been obtained before collecting data.

## Differentially Expressed Genes (DEGs) in SKCM Tumors

According to the cut-off value of 50%, 471 SKCM patients were divided into low- and high-TIM expression groups. The "DESeq2" R package was used to identify DEGs between the two groups, where the log-fold change greater than 1.5 and adjusted *P*-value less than 0.05 were set as thresholds (15). The "ggplot2" R package was used to present the results in the form of volcano plots and heatmaps.

## Functional Enrichment Analysis of TIM-Associated DEGs

The identified DEGs were then processed for functional enrichment analysis. The "clusterProfiler" and "ggplot2" R packages were used to analyze and visualize the functions of GO, including cell composition (CC), molecular function (MF), and biological process (BP), as well as KEGG pathway analysis (16).

## Gene Set Enrichment Analysis (GSEA) of TIM-Associated DEGs

The "clusterProfiler" R package was utilized for the GSEA of DEGs to clarify the functional differences between the two subgroups (16). 1,000 permutations of the gene set were performed for each analysis. We selected C2: curated gene sets from MSigDB collections as reference gene sets. Clusters with adjusted *p*-value (*p*.adj) less than 0.05 and false discovery rate (FDR) less than 0.25 were identified as statistically significant (17). The "ggplot2" R package were used for GSEA visualization.

## Relationship Between TIM and Immune Cell Infiltration in SKCM Tumors

The "GSVA" R package was utilized to analyze infiltration enrichment of 24 common immune cells, including activated dendritic cells (aDCs); B cells; CD8 T cells; Cytotoxic cells; DCs; Eosinophils; immature DCs (iDCs); Macrophages; Mast cells; Neutrophils; NK CD56bright cells; NK CD56dim cells; NK cells; Plasmacytoid DCs (pDCs); T cells; T helper cells; T central memory (Tcm); T effector memory (Tem); T follicular helper (Tfh); T gamma delta (Tgd); Th1 cells; Th17 cells; Th2

cells; Treg (18, 19). Subsequently, the spearman analysis was used to further verify the relationship between TIM expression and immune cell infiltration.

## Association of Clinicopathological Characteristics and TIM Expression in SKCM Patients

The Wilcoxon rank sum test or Pearson's chi-square test were used to compare the clinicopathological characteristics of the two distinct TIM groups. The overall survival (OS) was calculated from the date of diagnosis to the date of death or last follow-up. The disease specific survival (DSS) was calculated from the date of diagnosis to the date of death caused by SKCM. Univariate Cox proportional hazards regressions were utilized to identify the individual hazard ratio (HR) for the OS and DSS in SKCM patients. Subsequently, the significant variables in the univariate analysis ($p < 0.05$) were further subjected to multivariate analysis. The HR of individual factors was estimated by 95% confidence interval (CI).

## Clinical Significance of TIM Expression in SKCM

In order to test the predictive accuracy of TIM for SKCM diagnosis, the "pROC" and "ggplot2" R packages were used to analyze and visualize ROC curves. Prognostic data of SKCM patients, including OS and DSS, was derived from a published study (20). The "survival" R package was used for statistical analysis of survival data, and the "survminer" R package was applied for visualization of K-M curves. Finally, the R package "rms" and "survival" were applied for generating nomograms and calibration plots (20).

## Promoter Methylation and Genetic Alterations of TIM in SKCM

In order to determine if there is a relationship between TIM promoter methylation and tumor severity, we assessed the correlation between TIM promoter methylation status and cancer stages, nodal metastasis status in patients who enrolled in the UALCAN (http://ualcan.path.uab. edu/). Moreover, data and analysis of TIM mutation in SKCM were obtained from the cBioPortal database (http://www.cbioportal.org) and the images were also generated using the cBioPortal database. To further elucidate possible molecular mechanisms, we used STRING database (https://cn.string-db.org/) to construct protein-protein interaction (PPI) network and perform functional enrichment analysis.

## IHC Validation of TIM Expression

To validate the results obtained in the bioinformatic prediction analysis, we collected IHC results of normal skin and SKCM tumors from the human pathology proteinatlas (HPA) database. 4 normal skin tissues and 14 SKCM tumors were collected. The integrated optical density (IOD) of each image and the corresponding stained area were measured using ImageJ 1.8.0 software. The mean optical density (MOD) was obtained by calculating the ratio, and the mean MOD (hereafter referred to as OD value) of three random fields was used to represent the expression level of TIM protein in SKCM and normal skin tissues.

## Statistical Analysis

All statistical analysis and graphs were performed and visualized by R (3.6.3), and *P*-value less than 0.05 was considered as statistically significant.

# RESULTS

## Expression Profiles of TIM in Pan-Cancers and Related Differentially Expressed Genes in SKCM

Based on TCGA database, the expression of TIM mRNA in different cancers were determined. As shown in **Figure 1A**, among 33 cancer types, the TIM was significantly elevated in 25 cancers. More particularly, TIM expression was much higher in SKCM than in normal skin tissues ($p < 0.001$, **Figure 1B**). Interestingly, only two of the investigated cancer profiles was TIM expression decreased.

472 SKCM patients were stratified into two subgroups based on the median TIM expression. Next, we compared mRNA expression between the two groups. Finally, 402 mRNAs (146 upregulated and 256 downregulated, **Figure 1C**) were recognized as DEGs (absolute value of $\log_2FC > 1.5$, $p.adj < 0.05$) between the two subgroups. Representative DEGs were also illustrated by heatmap (**Figure 1D**).

## Functional Annotation of TIM-Associated DEGs in SKCM

In order to understand the functional implication of TIM-associated DEGs, GO and KEGG functional enrichment analysis was performed by clusterProfiler package (**Supplementary Table S1** and **Figure 2**). The association with the biological process (BP) included keratinization, keratinocyte differentiation, and skin development; cellular components (CC) included cornified envelope, intermediate filament, and immunoglobulin complex; molecular function (MF) included structural constituent of epidermis, antigen binding, and peptidase inhibitor activity. KEGG included Ras signaling pathway, salivary secretion, and vascular smooth muscle contraction (**Table 1**).

To gain further insight into the biologic pathways involved in SKCM with different TIM expression levels, GSEA was performed to identify critical signaling pathways, which showed DEGs significantly enriched in cell proliferation related clusters (**Figures 3A,B**), including cell cycle control, and DNA replication. Besides, TIM-related DEGs were also associated with formation of cornified envelope (**Figure 3C**), and keratinization (**Figure 3D**). More importantly, DEGs were also enriched in cancer pathways (**Figures 3E–I**), such as TP53 activity, FOXM1 pathway, MYC activity, PLK1 pathway, and ATM pathway. These pathways (**Supplementary Table S2**) were observed in the enrichment of MSigDB Collection (C2.all.v7.0.symbols.gmt) and the criterion for significant difference was set at FDR < 0.05, $p.adj < 0.05$.

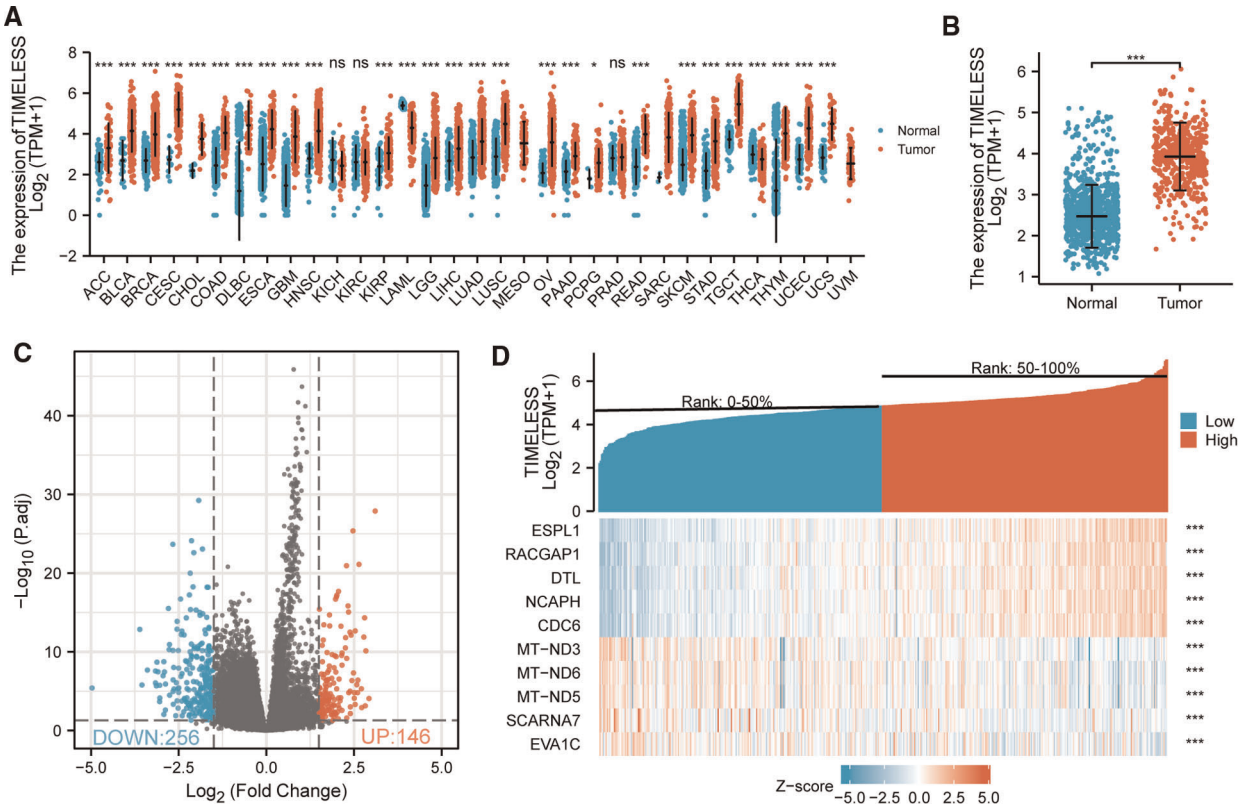


**FIGURE 1** | Differential mRNA expression profiles in skin cutaneous melanoma (SKCM) patients stratified by TIM levels. (**A**) The comparison of TIM expression between tumor and normal tissue in different malignancies based on TCGA database. ns, $p \geq 0.05$; *$p < 0.05$; **$p < 0.01$; ***$p < 0.001$. (**B**) TIM expression was higher in SKCM tumors than normal skin tissue. Based on the median TIM level, 472 SKCM patients from TCGA-SKCM project were stratified into high- and low-TIM expression groups. Shown were expression profiles of mRNA in the two subgroups; and data were presented by volcano plots (**C**) and heatmaps (**D**).

## Association of TIM and Immune Cell Infiltration in SKCM

Spearman correlation analysis showed that the expression level of TIM in the SKCM microenvironment was correlated with the immune cell infiltration level quantified by ssGSEA. As shown in **Figure 4A**, Th2 cells, and T helper cells, were both positively correlated with TIM expression. However, pDC, TReg, NK CD56bright cells, and cytotoxic cells showed a negative association with TIM. More specifically, we evaluated the infiltration levels of six most relevant immune cells—Th2 cells (**Figure 4B**, $R = 0.356$, $p < 0.001$), T helper cells (**Figure 4C**, $R = 0.180$, $p < 0.001$), pDC (**Figure 4D**, $R = -0.286$, $p < 0.001$), TReg (**Figure 4E**, $R = -0.197$, $p < 0.001$), NK CD56bright (**Figure 4F**, $R = -0.194$, $p < 0.001$), and cytotoxic cells (**Figure 4G**, $R = -0.190$, $p < 0.001$)—in distinct TIM subgroups, which showed results consistent with those in **Figure 4A**.

## Association of Clinicopathological Characteristics and TIM Expression in SKCM Patients

We examined the clinicopathological features of SKCM patients in the two distinct TIM expression subgroups. The main clinicopathological characteristics of SKCM patients were presented in **Table 2**. There was no significant difference in gender, age, body mass index (BMI), TNM stages, radiation therapy, ulceration, and Breslow depth between the two groups. However, there was a significant difference between the two subgroups in the composition of N stage, melanoma ulceration, melanoma Clark level, overall survival (OS) event, and disease specific survival (DSS) event.

## Predictive Value of TIM for SKCM Diagnosis and Prognosis

Univariate and multivariate Cox proportional hazards analysis was performed to examine the clinical advantages of TIM. As shown in **Tables 3**, **4**, the expression level of TIM is an independent risk factor for OS (HR = 1.724, $p = 0.009$) and DSS (HR = 1.593, $p = 0.034$). Subsequently, we used ROC curve to demonstrate its value on discriminating SKCM diagnosis. As the area under the curve (AUC) was 0.904, TIM showed significant high sensitivity and specificity for SKCM diagnosis (**Figure 5A**). Subsequently, K-M analyses were applied to verify the prediction of TIM on clinical outcomes. As shown in **Figures 5B, C**, OS (HR = 1.48, $p = 0.005$), and DSS (HR = 1.52, $p = 0.005$) in the high-TIM expression group

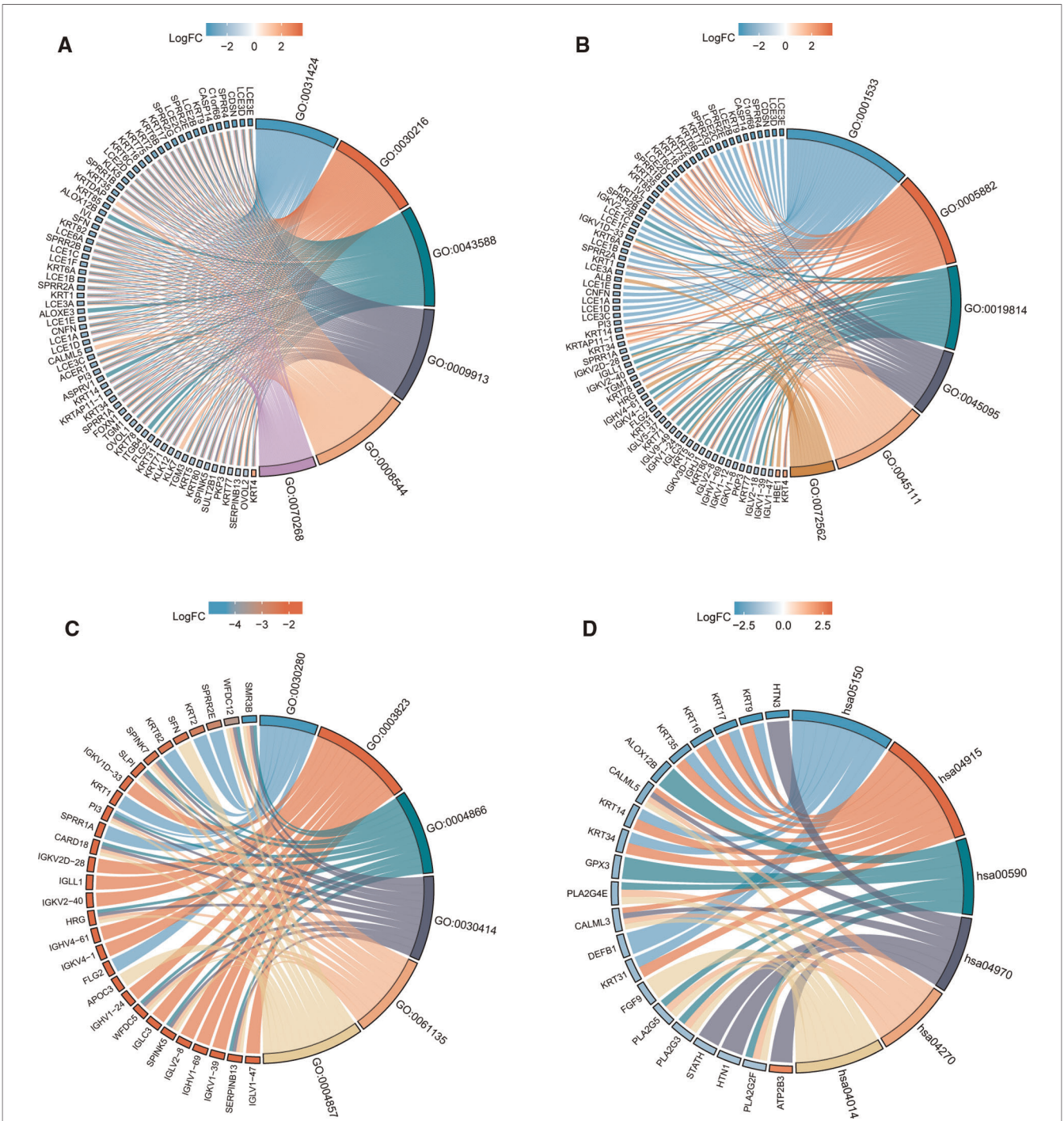


**FIGURE 2** | GO/KEGG enrichment analysis of TIM-related DEGs in TCGA-SKCM project. (**A**) Enriched GO terms in the "BP" category; (**B**) Enriched GO terms in the "MF" category. (**C**) Enriched GO terms in the "CC" category; (**D**) KEGG pathway annotations. The right semicircle represents different functional categories, while the left semicircle consists of individual DEGs. Different colors indicate different properties, and the size of the sections represents the number of DEGs.

were both statistically worse than those in the low-TIM expression group.

Moreover, to better predict the prognosis of SKCM patients, we constructed nomograms based on the results of multivariate Cox regression analysis. Four prognostic factors with statistical differences were included in the model, including clinical N stages, melanoma Clark level, Breslow depth, and TIM expression. As shown in **Figures 5D,F**, nomograms predicted OS and DSS at 1, 3, and 5 years, in which high expression of TIM predicted worse OS and DSS than low expression.

**TABLE 1** | GO/KEGG functional enrichment of TIM-related DEGs.

| Ontology | ID | Description | *p*.adj | qvalue | zscore |
|---|---|---|---|---|---|
| BP | GO:0031424 | keratinization | $8.89 \times 10^{-53}$ | $8.45 \times 10^{-53}$ | −7.15 |
| BP | GO:0030216 | keratinocyte differentiation | $4.57 \times 10^{-52}$ | $4.34 \times 10^{-52}$ | −7.49 |
| BP | GO:0043588 | skin development | $2.58 \times 10^{-51}$ | $2.45 \times 10^{-51}$ | −7.88 |
| BP | GO:0009913 | epidermal cell differentiation | $1.17 \times 10^{-50}$ | $1.11 \times 10^{-50}$ | −7.62 |
| BP | GO:0008544 | epidermis development | $1.50 \times 10^{-48}$ | $1.43 \times 10^{-48}$ | −7.88 |
| BP | GO:0070268 | cornification | $3.57 \times 10^{-42}$ | $3.39 \times 10^{-42}$ | −5.84 |
| CC | GO:0001533 | cornified envelope | $9.52 \times 10^{-38}$ | $9.13 \times 10^{-38}$ | −5.48 |
| CC | GO:0005882 | intermediate filament | $5.05 \times 10^{-13}$ | $4.84 \times 10^{-13}$ | −4.38 |
| CC | GO:0019814 | immunoglobulin complex | $1.06 \times 10^{-12}$ | $1.01 \times 10^{-12}$ | −4.47 |
| CC | GO:0045095 | keratin filament | $3.50 \times 10^{-12}$ | $3.35 \times 10^{-12}$ | −3.50 |
| CC | GO:0045111 | intermediate filament cytoskeleton | $6.31 \times 10^{-12}$ | $6.05 \times 10^{-12}$ | −4.38 |
| CC | GO:0072562 | blood microparticle | $9.07 \times 10^{-5}$ | $8.70 \times 10^{-5}$ | −2.71 |
| MF | GO:0030280 | structural constituent of epidermis | $1.54 \times 10^{-7}$ | $1.43 \times 10^{-7}$ | −2.65 |
| MF | GO:0003823 | antigen binding | $1.39 \times 10^{-4}$ | $1.29 \times 10^{-4}$ | −3.46 |
| MF | GO:0004866 | endopeptidase inhibitor activity | 0.004 | 0.004 | −3.16 |
| MF | GO:0030414 | peptidase inhibitor activity | 0.004 | 0.004 | −3.16 |
| MF | GO:0061135 | endopeptidase regulator activity | 0.004 | 0.004 | −3.16 |
| MF | GO:0004857 | enzyme inhibitor activity | 0.055 | 0.051 | −3.46 |
| KEGG | hsa05150 | Staphylococcus aureus infection | $2.80 \times 10^{-4}$ | $2.28 \times 10^{-4}$ | −2.82 |
| KEGG | hsa04915 | Estrogen signaling pathway | $2.80 \times 10^{-4}$ | $2.28 \times 10^{-4}$ | −3.00 |
| KEGG | hsa00590 | Arachidonic acid metabolism | $9.82 \times 10^{-4}$ | $7.98 \times 10^{-4}$ | −2.45 |
| KEGG | hsa04970 | Salivary secretion | 0.004 | 0.004 | −1.63 |
| KEGG | hsa04270 | Vascular smooth muscle contraction | 0.022 | 0.017 | −2.45 |
| KEGG | hsa04014 | Ras signaling pathway | 0.059 | 0.048 | −2.65 |

Additionally, we also constructed calibration plots to evaluate the prediction accuracy of two nomogram models. As shown in **Figures 5E, G**, the predicted results were highly consistent with actual survival outcomes, with the exception of the 5-year prediction for OS and DSS, which was slightly overestimated.

## Promoter Methylation and Genetic Alterations of TIM in SKCM

To explore how TIM affects the prognosis of SKCM, we first explored the methylation levels and genetic mutations of TIM. Through the UALCAN database, we found that promoter methylation of TIM was lower in SKCM patients with both primary or metastatic tumors than in the normal group (**Figure 6A**). Moreover, the tumor stage and nodal metastasis status of SKCM also supported this conclusion (**Figures 6B, C**). Meanwhile, as shown in **Figure 6D**, TIM was altered in 6% of the queried SKCM patients. According to K-M analysis, patients with TIM alterations demonstrated shorter OS (**Figure 6E**).

Next, to further investigate the mechanisms behind TIM function, PPI network and GO/KEGG enrichment analysis was performed using STRING. Both PPI network and GO/KEGG pathways showed that TIM was related to DNA replication-related genes, including TOPBP1, WDHD1, TIPIN, CLSPN, and GINS3, and the cell cycle pathway (**Figures 6F, G**). These results indicated that TIM may regulate SKCM via regulating DNA replication and cell cycle.

## IHC Validation of TIM Expression

To verify the former bioinformatic analysis results, we compared the gene expression of TIM in SKCM tissues vs normal skin controls using IHC data from the Human Protein Atlas (HPA) database. Representative images and analysis results were presented in **Figure 7**, the OD value of SKCM group was significantly higher than that of normal skin group ($p < 0.05$), consistent with the previous consequences.

# DISCUSSION

In the present study, our results disclosed for the first time that TIM was overexpressed in SKCM tissues relative to normal tissues, which was also associated with poor prognosis. In addition, TIM-specific DEGs, primarily the up-regulated ones, were enriched in cell cycle, and several oncogenic signaling-related pathways. On the contrary, down-regulated DEGs were specifically enriched in keratinization. Subsequently, we assessed the relationship between the expression of TIM and immune infiltration. Besides, promoter methylation and genetic alterations of TIM in

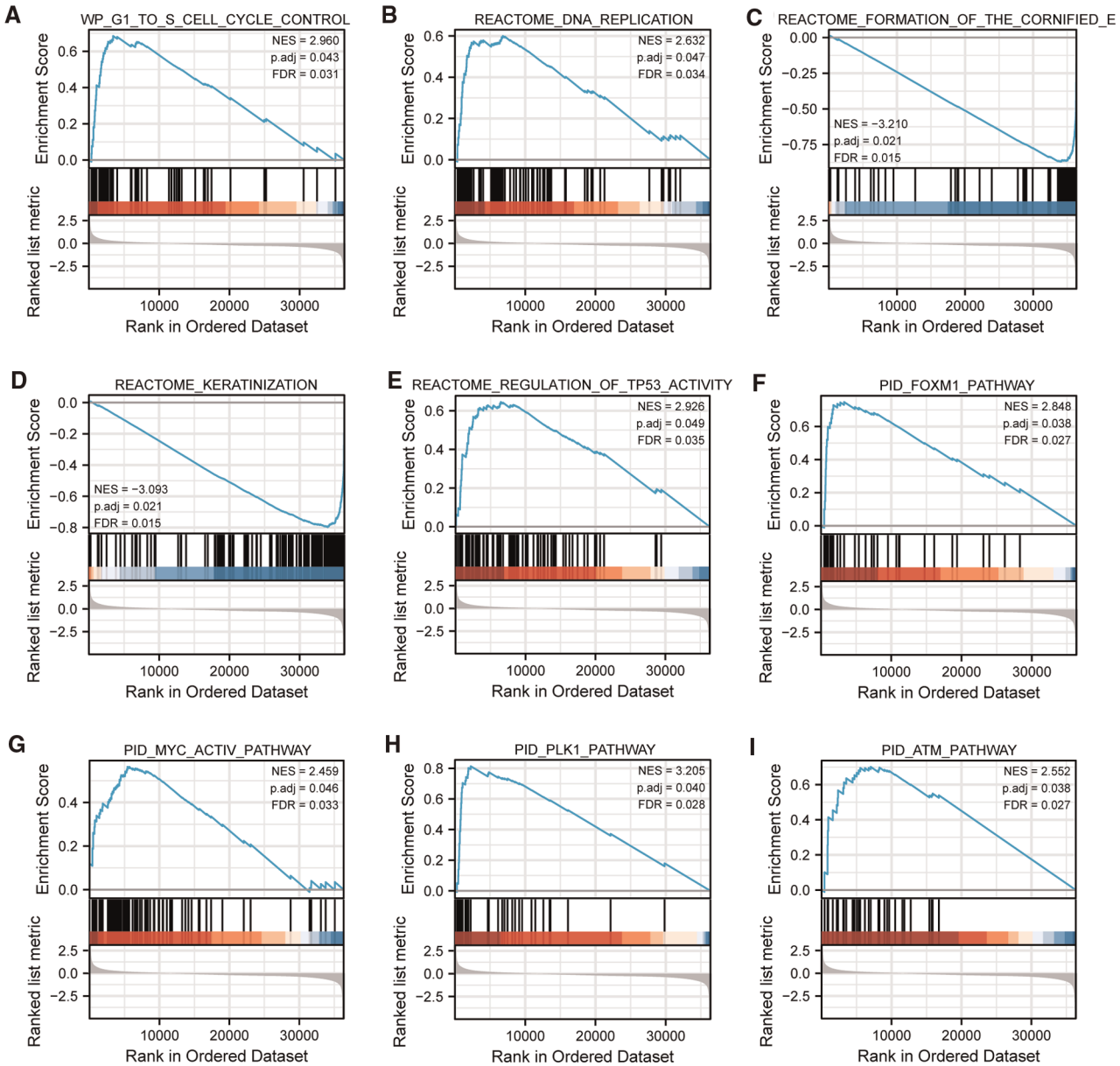


**FIGURE 3** | Representative GSEA enrichment plots of DEGs between high- and low-TIM expression groups. (**A–I**) NES, normalized enrichment score; *p*.adj, adjusted *p*-value; FDR, false discovery rate.

regulating SKCM were also further elucidated. Finally, we uncovered the value of TIM in the diagnosis of SKCM and revealed that higher expression of TIM was associated with worse clinical outcomes, such as OS and DSS.

The genes controlling accurate DNA replication were essential for normal cell proliferation, as replication errors could lead to abnormal cell proliferation. TIM was a well-characterized DNA replication regulator, and emerging evidence suggested that it played an important role in various cancers (4). In this study, we found that TIM expression was significantly elevated in a variety of solid cancers, including esophageal carcinoma, head and neck squamous cell carcinoma, and lung squamous cell carcinoma. Furthermore, TIM was also upregulated in other tumor types, such as bladder urothelial carcinoma, breast invasive carcinoma, colon adenocarcinoma, brain lower grade glioma, rectum adenocarcinoma, and uterine carcinosarcoma. Therefore, TIM may act as a key hub gene in tumor genesis and development.

We then sought to identify the biological functions and mechanisms involving TIM in SKCM. TIM, as a classic molecular clockwork in mammals, has been shown not only to be a circadian regulator, but essential for early embryonic

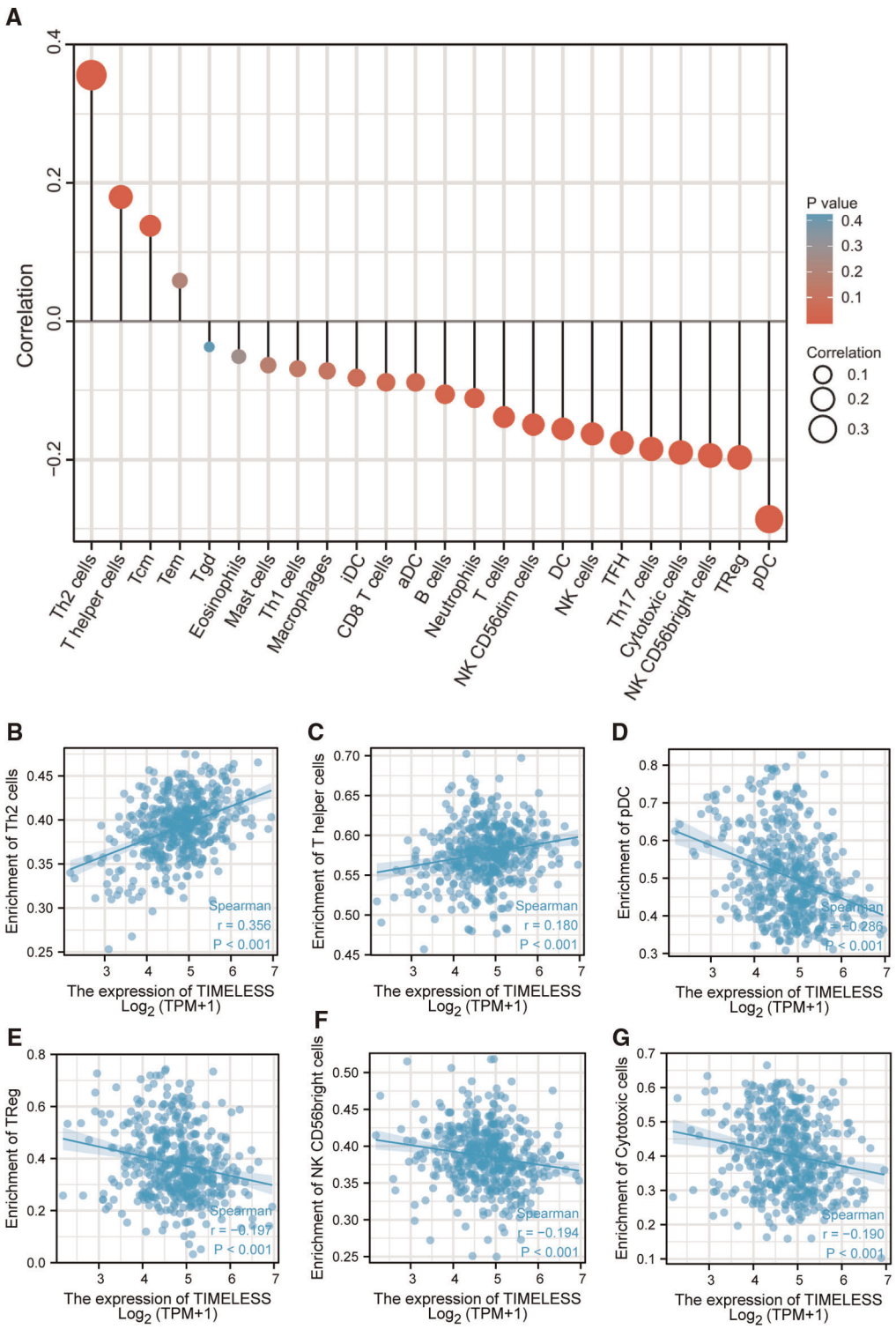


**FIGURE 4** | The expression of TIM was associated with immune infiltration in the SKCM microenvironment. (**A**) Relationships among infiltration levels of 24 immune cell types and TIM expression profiles by Spearmans analysis. The comparison of infiltration levels of most correlated immune cells, including (**B**) Th2 cells, (**C**) T helper cells, (**D**) pDC, (**E**) TReg, (**F**) NK CD56bright cells, and (**G**) cytotoxic cells was shown.

**TABLE 2 |** Association between TIM expression and clinicopathologic features in SKCM patients from the TCGA database.

| Characteristic | levels | TIM expression | | *p* | statistic |
|---|---|---|---|---|---|
| | | Low | High | | |
| T stage, n | T1/T2/T3/T4 | 16/38/44/85 | 25/41/47/68 | 0.254 | $x^2 = 4.07$ |
| N stage, n | N0/N1/N2/N3 | 100/50/25/25 | 135/24/24/31 | **0.002** | $x^2 = 14.55$ |
| M stage, n | M0/M1 | 205/11 | 213/14 | 0.776 | $x^2 = 0.08$ |
| Pathologic stage, n | Stage I/II/III/IV | 31/68/98/11 | 46/72/73/13 | 0.078 | $x^2 = 6.82$ |
| Radiation therapy, n | No/Yes | 196/34 | 187/47 | 0.167 | $x^2 = 1.91$ |
| Gender, n | Female/Male | 95/140 | 84/152 | 0.324 | $x^2 = 0.97$ |
| Age, n | ≤60/>60 | 134/97 | 118/114 | 0.147 | $x^2 = 2.10$ |
| BMI, n | ≤25/>25 | 45/82 | 39/85 | 0.593 | $x^2 = 0.29$ |
| Melanoma ulceration, n | No/Yes | 60/91 | 87/76 | **0.021** | $x^2 = 5.32$ |
| Melanoma Clark level, n | I/II/III/IV/V | 3/4/30/93/29 | 3/14/47/75/24 | **0.020** | $x^2 = 11.66$ |
| Breslow depth, n | ≤3/>3 | 87/93 | 98/82 | 0.292 | $x^2 = 1.11$ |
| OS event, n (%) | Alive/Dead | 142/91 | 105/126 | **0.001** | $x^2 = 10.57$ |
| DSS event, n (%) | Alive/Dead | 152/79 | 115/112 | **0.001** | $x^2 = 10.18$ |

*All bold values represent P values less than 0.05 to highlight statistical differences..*

**TABLE 3 |** Univariate and multivariate Cox proportional hazards analysis of TIM expression and OS for SKCM patients.

| Characteristics | Univariate analysis | | Multivariate analysis | |
|---|---|---|---|---|
| | Hazard ratio (95% CI) | *p* value | Hazard ratio (95% CI) | *p* value |
| T stage (T1&T2 vs. T3&T4) | 2.085 (1.501–2.895) | **<0.001** | 0.890 (0.506–1.567) | 0.687 |
| N stage (N0 vs. N1&N2&N3) | 1.752 (1.304–2.354) | **<0.001** | 4.844 (1.425–16.464) | **0.011** |
| M stage (M0 vs. M1) | 1.897 (1.029–3.496) | **0.040** | 2.469 (0.935–6.520) | 0.068 |
| Age (≤60 vs.>60) | 1.656 (1.251–2.192) | **<0.001** | 0.949 (0.625–1.440) | 0.806 |
| Gender (Female vs. Male) | 1.172 (0.879–1.563) | 0.281 | | |
| Pathologic stage (I&II vs. III&IV) | 1.617 (1.207–2.165) | **0.001** | 0.436 (0.127–1.503) | 0.189 |
| Melanoma ulceration (No vs. Yes) | 2.085 (1.495–2.907) | **<0.001** | 1.521 (0.998–2.316) | 0.051 |
| Melanoma Clark level (I&II&III vs. IV&V) | 2.167 (1.508–3.113) | **<0.001** | 1.793 (1.077–2.986) | **0.025** |
| BMI (≤25 vs. >25) | 0.827 (0.513–1.333) | 0.436 | | |
| Breslow depth (≤3 vs. >3) | 2.651 (1.938–3.627) | **<0.001** | 1.981 (1.169–3.357) | **0.011** |
| Radiation therapy (No vs. Yes) | 0.977 (0.694–1.377) | 0.895 | | |
| TIM (Low vs. High) | 1.480 (1.128–1.942) | **0.005** | 1.724 (1.144–2.600) | **0.009** |

*All bold values represent P values less than 0.05 to highlight statistical differences.*

development, DNA replication, and DNA damage repair (21–25). In this study, based on the functional annotation of TIM-associated DEGs, epidermal cell differentiation, keratinocyte differentiation, and skin development were closely related to TIM expression. In addition, according to the GSEA results, several cell cycle-related events and oncogenic related pathways were enriched in the high-TIM subgroup, while the downregulated DEGs were enriched in keratinization, and

**TABLE 4** | Univariate and multivariate Cox proportional hazards analysis of TIM expression and DSS for SKCM patients

| Characteristics | Univariate analysis | | Multivariate analysis | |
|---|---|---|---|---|
| | Hazard ratio (95% CI) | *p* value | Hazard ratio (95% CI) | *p* value |
| T stage (T1&T2 vs. T3&T4) | 1.887 (1.341–2.654) | **<0.001** | 0.925 (0.520–1.645) | 0.791 |
| N stage (N0 vs. N1&N2&N3) | 1.665 (1.214–2.283) | **0.002** | 6.914 (1.586–30.145) | **0.010** |
| M stage (M0 vs. M1) | 2.200 (1.190–4.069) | **0.012** | 2.758 (1.035–7.350) | **0.043** |
| Age (≤60 vs.>60) | 1.699 (1.258–2.294) | **<0.001** | 0.952 (0.613–1.480) | 0.827 |
| Gender (Female vs. Male) | 1.161 (0.855–1.575) | 0.340 | | |
| Pathologic stage (I&II vs. III&IV) | 1.536 (1.125–2.096) | **0.007** | 0.306 (0.069–1.356) | 0.119 |
| Melanoma ulceration (No vs. Yes) | 1.948 (1.372–2.767) | **<0.001** | 1.466 (0.944–2.277) | 0.088 |
| Melanoma Clark level (I&II&III vs. IV&V) | 2.128 (1.457–3.108) | **<0.001** | 1.813 (1.063–3.093) | **0.029** |
| BMI (≤25 vs. >25) | 0.937 (0.545–1.612) | 0.815 | | |
| Breslow depth (≤3 vs. >3) | 2.274 (1.628–3.177) | **<0.001** | 1.749 (1.019–3.001) | **0.042** |
| Radiation therapy (No vs. Yes) | 0.994 (0.689–1.433) | 0.973 | | |
| TIM (Low vs. High) | 1.517 (1.134–2.029) | **0.005** | 1.593 (1.035–2.452) | **0.034** |

*All bold values represent P values less than 0.05 to highlight statistical differences.*

formation of the cornified envelope. The above results indicated that TIM was not only a key regulator of DNA replication in SKCM, but also an inhibitor of keratinization. Several studies have confirmed that TIM knockdown suppressed cancer cell proliferation and clonogenic growth in colorectal cancer, lung cancer, breast and cervical cancer (8, 9, 26). Not only that, studies have verified that each melanocyte contacts with about 30 keratinocytes in the basal and suprabasal layers forming the epidermal-melanin unit (27, 28). The gap junctional intercellular communication (GJIC) formed by these two types of cells was essential for cell homeostasis. The inability to establish melanocyte-keratinocyte GJIC may contribute to the development of SKCM (29). Our functional enrichment and GSEA results confirmed that TIM inhibited keratinization while promoting cell cycle, which may be one of the reasons for the poor prognosis of SKCM. More importantly, almost all tumorigenic-related pathways enriched in the high-TIM subgroup, including TP53, FOXM1, MYC, PLK1, and ATM signaling pathways, were related to regulating cell cycle, strongly suggesting the role of TIM to accelerate DNA replication and promote tumor cell proliferation, thereby worsening the prognosis of SKCM (30–33). Therefore, TIM expression might have important significance in SKCM tumorigenesis by regulating cell cycle and inhibiting keratinization.

In immune cell infiltration analysis, TIM expression was negatively correlated with pDC, TReg, NK CD56bright cells, Cytotoxic cells, and Th17 cells. Plasmacytoid dendritic cells (pDCs) is a subset of DCs denoted by their capacity to yield extensive amount of type I interferon (IFN-α) (34). In addition to IFN-α production, pDCs can also serve as antigen-presenting cells (APCs) and regulate immune responses to various antigens. The significant role played by pDCs in regulating both the innate and adaptive components of the immune system makes them a critical player in cancer immunology. Cancers that can be detected clinically must have escaped anti-tumor immune responses to grow progressively (35). Therefore, pDCs, negatively related to TIM expression, may contribute to the immune escape of tumor cells in SKCM. In the subsequent immune response, NK cells and cytotoxic cells can cooperate to kill the tumor cells (36). Unfortunately, over-expression of TIM also caused a decrease in infiltrating cytotoxic cells and NK cells. On the other hand, we found a significant positive correlation between TIM expression and Th2 infiltrating. Although Th2 cells were best known for anti-parasites and allergic reactions, their regulation and function in the tumor microenvironment (TME) were highly controversial (37). However, emerging evidence showed that Th2 cells promoted cancer genesis, progression, and metastasis. Some studies showed that Th2 cells in the TME were related to the progression of breast cancer and cervical neoplasia (38, 39). Besides, Th2 cells had been shown to promote metastasis in breast cancer, colorectal cancer, and lung cancer (40–43). Hence, increased Th2 cell infiltration in the TME caused by TIM expression might have a role in SKCM tumorigenesis.

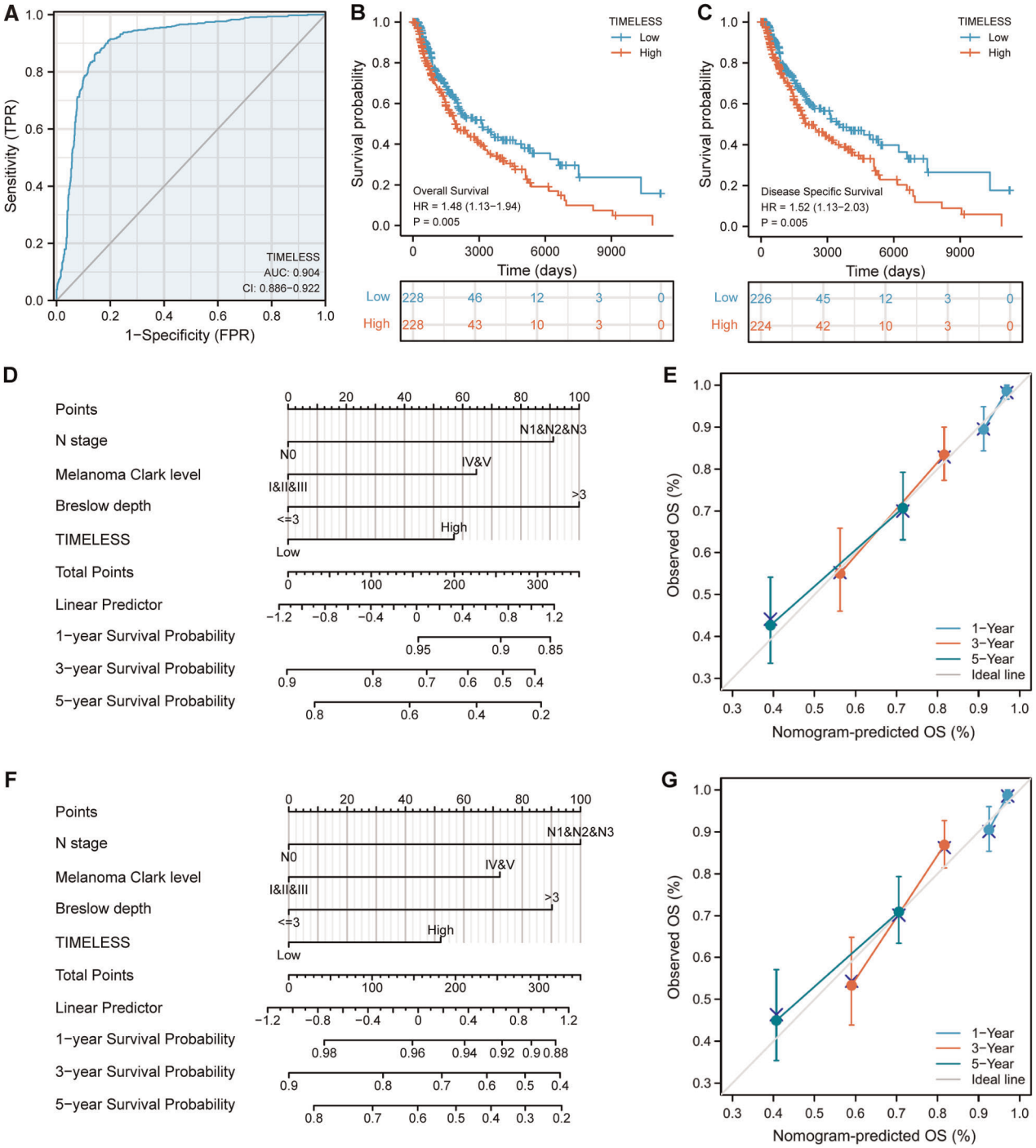


**FIGURE 5** | Predictive value of TIM for diagnosis and prognosis in SKCM patients. (**A**) ROC curve analysis evaluating the performance of TIM for SKCM diagnosis. Shown were the K-M analyses comparing OS (**B**), and DSS (**C**) between the two distinct TIM expression subgroups. (**D–G**) Construction and validation of nomograms based on TIM expression. Shown were the nomograms constructed to predict the probability of 1-, 3-, 5-year OS (**D**), and DSS (**F**) for SKCM. Calibration plots of OS, and DSS were shown in (**E,G**).

Another important issue was the clinical significance of TIM in SKCM. AUC of the ROC curve for TIM discrimination in SKCM diagnosis was 0.904, strongly suggesting that TIM was a reliable biomarker for SKCM diagnosis. Moreover, K-M survival analyses showed that patients with high TIM expression had a strikingly worse OS and DSS than patients

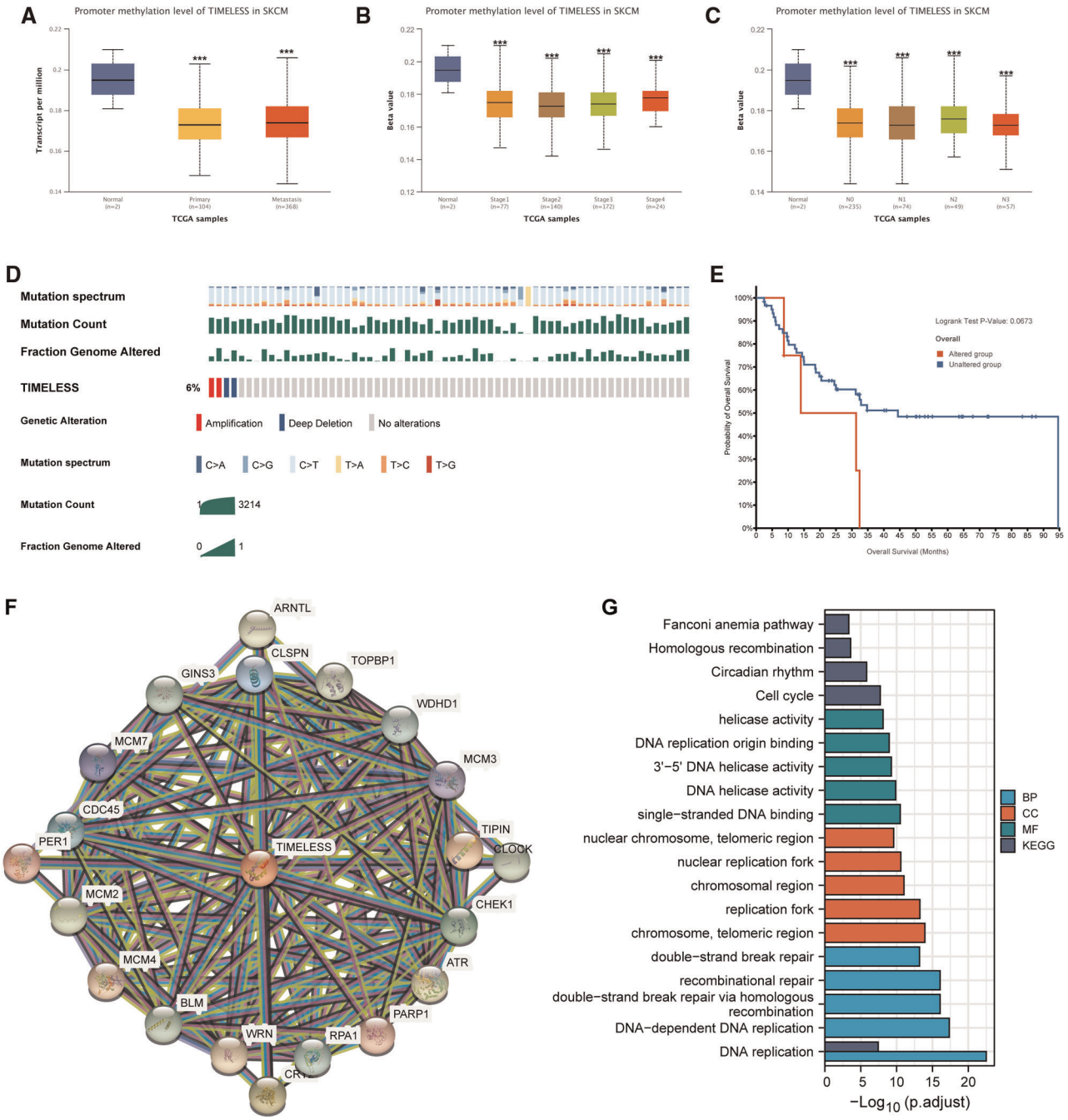


**FIGURE 6** | Promoter methylation and genetic alterations of TIM and potential regulatory mechanism of TIM in regulating SKCM. (**A–C**) Relationship between tumor type, stage, and nodal metastasis status of SKCM with the promoter methylation of TIM determined using UALCAN. (**D**) Genetic alterations of TIM in SKCM patients determined using cBioportal. (**E**) OS for TIM alterations was analyzed using cBioportal. (**F**) The neighbor gene network of 20 genes was constructed using STRING. (**G**) The bar diagrams showed the top five terms for each GO category as well as for the KEGG pathway analysis. ***$p < 0.001$.

with low TIM expression. Furthermore, the Cox analyses of this study demonstrated that TIM might be an independent predictive factor of poor prognosis for SKCM, in which N stage, melanoma Clark level, Breslow depth, and TIM expression were independent prognostic factors for OS and DSS deterioration. In addition, not only was the prognostic value of TIM confirmed in SKCM, but its expression level in a variety of tumors was negatively correlated with OS, such as papillary renal cell carcinoma (44), adrenocortical carcinoma (45), breast invasive carcinoma (46), and lung cancer (47). From the above results, it could be seen that TIM was highly expressed in these tumors and was often associated with poor

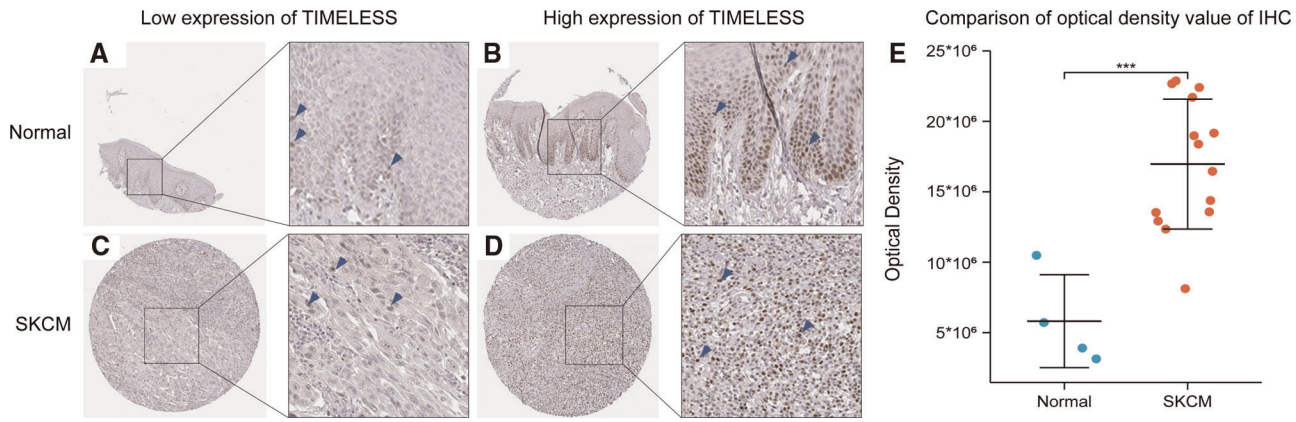


**FIGURE 7** | Representative IHC staining images of TIM in SKCM tissues and normal skin controls. (**A,B**) TIM was low (**A**) or high (**B**) in normal skin tissues. (**C,D**) TIM was low (**A**) or high (**B**) in SKCM tissues. (**E**) comparison of optical density value of IHC between SKCM tissues and normal skin controls. Blue arrows indicate positive staining.

prognosis, which further confirmed that it was a common prognostic biomarker for multiple tumor types.

As for TIM gene alternative and DNA methylation, results of Fu et al. demonstrated that hypomethylation of TIM was associated with poorer prognosis and advanced stages of breast cancer (6). These results were consistent with later observations that higher TIM was related to shorter metastatic survival, especially in ER-positive/HER2-negative women (48). According to these results, it can be hypothesized that TIM overexpression might be the result of hypomethylation in the promoter region. In our study, analysis of UALCAN revealed that TIM gene promoter methylation was lower in both primary and metastatic SKCM compared to normal controls. Few studies have scrutinized the role of TIM mutations in SKCM. Among the surveyed SKCM patients, 6% had TIM mutations, which indicated a shorter OS. These findings suggested the promoter methylation and genetic alterations of TIM played an essential role in SKCM prognosis. Therefore, further research is needed in order to fully clarify the role of promoter methylation and genetic alterations in SKCM patients.

In order to further understand the biological functions of TIM, we constructed a PPI network using STRING database and conducted functional enrichment analysis on these genes. The results showed that the functions of these genes were mainly enriched in DNA replication and cell cycle, further supporting the above predicted results. Increased expression of TIM may affect the tumogenesis and prognosis of SKCM by promoting the proliferation of melanoma cells.

The results of IHC indicated that the expression of TIM in SKCM tissues was higher than that in normal skin tissues, which was consistent with the previous prediction. Although we have disclosed the potential mechanism of TIM in SKCM tumorigenesis and its prognostic value in SKCM clinical outcomes, several factors could limit the extent to which the results can be generalized. First, as a potential novel therapeutic target, the sample size should be expanded in further research to enhance the reliability and representativeness of the results. Second, since we mainly focused on RNA-seq data from TCGA and GTEx databases, the results could be further verified by in vivo and in vitro research.

In conclusion, the highly expressed TIM in SKCM may play a pivotal role in tumorigenesis by regulating cell cycle and inhibiting melanocyte-keratinocyte GJIC. In addition, it also has prognostic value for clinical outcomes. Our results shed light on TIM as a potential therapeutic target for SKCM.

## DATA AVAILABILITY STATEMENT

The datasets presented in this study can be found in online repositories. The names of the repository/repositories and accession number(s) can be found in the article/**Supplementary Material**.

## ETHICS STATEMENT

Written informed consent was obtained from the individual(s) for the publication of any potentially identifiable images or data included in this article.

## AUTHOR CONTRIBUTIONS

SZ, SW, and HL contributed to the conception and design. JZ and JX contributed to the administrative support. ZZ and YL contributed to the provision of the study materials or patients. SZ, ZZ, and YL contributed to the collection and assembly of the data. SZ, SW, and HL contributed to the data analysis and interpretation. All the authors contributed to the writing and final approval of the manuscript.

## FUNDING

National Natural Science Foundation of China (82072178, 81871566).

## ACKNOWLEDGMENTS

We appreciate the precision medicine research platform of the First Affiliated Hospital of Sun Yat-sen University during the preparation of this manuscript.

## SUPPLEMENTARY MATERIAL

The Supplementary Material for this article can be found online at: https://www.frontiersin.org/articles/10.3389/fsurg.2022.917776/full#supplementary-material.

## REFERENCES

1. Ferlay J, Colombet M, Soerjomataram I, Mathers C, Parkin DM, Piñeros M, et al. Estimating the global cancer incidence and mortality in 2018: GLOBOCAN sources and methods. *Int J Cancer*. (2019) 144:1941–53. doi: 10.1002/ijc.31937
2. Nikolaou V, Stratigos AJ. Emerging trends in the epidemiology of melanoma. *Br J Dermatol*. (2014) 170:11–9. doi: 10.1111/bjd.12492
3. Swetter SM, Tsao H, Bichakjian CK, Curiel-Lewandrowski C, Elder DE, Gershenwald JE, et al. Guidelines of care for the management of primary cutaneous melanoma. *J Am Acad Dermatol*. (2019) 80:208–50. doi: 10.1016/j.jaad.2018.08.055
4. Mazzoccoli G, Laukkanen MO, Vinciguerra M, Colangelo T, Colantuoni V. A timeless link between circadian patterns and disease. *Trends Mol Med*. (2016) 22:68–81. doi: 10.1016/j.molmed.2015.11.007
5. Fu L, Lee CC. The circadian clock: pacemaker and tumour suppressor. *Nat Rev Cancer*. (2003) 3:350–61. doi: 10.1038/nrc1072
6. Fu A, Leaderer D, Zheng T, Hoffman AE, Stevens RG, Zhu Y. Genetic and epigenetic associations of circadian gene TIMELESS and breast cancer risk. *Mol Carcinog*. (2012) 51:923–9. doi: 10.1002/mc.20862
7. Mazzoccoli G, Vinciguerra M, Papa G, Piepoli A. Circadian clock circuitry in colorectal cancer. *World J Gastroenterol*. (2014) 20:4197–207. doi: 10.3748/wjg.v20.i15.4197
8. Yoshida K, Sato M, Hase T, Elshazley M, Yamashita R, Usami N, et al. TIMELESS is overexpressed in lung cancer and its expression correlates with poor patient survival. *Cancer Sci*. (2013) 104:171–7. doi: 10.1111/cas.12068
9. Mao Y, Fu A, Leaderer D, Zheng T, Chen K, Zhu Y. Potential cancer-related role of circadian gene TIMELESS suggested by expression profiling and in vitro analyses. *BMC Cancer*. (2013) 13:498. doi: 10.1186/1471-2407-13-498
10. Bailey MH, Tokheim C, Porta-Pardo E, Sengupta S, Bertrand D, Weerasinghe A, et al. Comprehensive characterization of cancer driver genes and mutations. *Cell*. (2018) 173:371–85.e18. doi: 10.1016/j.cell.2018.02.060
11. Danilova L, Wang H, Sunshine J, Kaunitz GJ, Cottrell TR, Xu H, et al. Association of PD-1/PD-L axis expression with cytolytic activity, mutational load, and prognosis in melanoma and other solid tumors. *Proc Natl Acad Sci U S A*. (2016) 113:E7769–77. doi: 10.1073/pnas.1607836113
12. Guan J, Gupta R, Filipp FV. Cancer systems biology of TCGA SKCM: efficient detection of genomic drivers in melanoma. *Sci Rep*. (2015) 5:7857. doi: 10.1038/srep07857
13. Begik O, Lucas MC, Liu H, Ramirez JM, Mattick JS, Novoa EM. Integrative analyses of the RNA modification machinery reveal tissue- and cancer-specific signatures. *Genome Biol*. (2020) 21:97. doi: 10.1186/s13059-020-02009-z
14. Vivian J, Rao AA, Nothaft FA, Ketchum C, Armstrong J, Novak A, et al. Toil enables reproducible, open source, big biomedical data analyses. *Nat Biotechnol*. (2017) 35:314–6. doi: 10.1038/nbt.3772
15. Love MI, Huber W, Anders S. Moderated estimation of fold change and dispersion for RNA-seq data with DESeq2. *Genome Biol*. (2014) 15:550. doi: 10.1186/s13059-014-0550-8
16. Yu G, Wang LG, Han Y, He QY. clusterProfiler: an R package for comparing biological themes among gene clusters. *Omics*. (2012) 16:284–7. doi: 10.1089/omi.2011.0118
17. Subramanian A, Tamayo P, Mootha VK, Mukherjee S, Ebert BL, Gillette MA, et al. Gene set enrichment analysis: a knowledge-based approach for interpreting genome-wide expression profiles. *Proc Natl Acad Sci U S A*. (2005) 102:15545–50. doi: 10.1073/pnas.0506580102
18. Bindea G, Mlecnik B, Tosolini M, Kirilovsky A, Waldner M, Obenauf AC, et al. Spatiotemporal dynamics of intratumoral immune cells reveal the immune landscape in human cancer. *Immunity*. (2013) 39:782–95. doi: 10.1016/j.immuni.2013.10.003
19. Hänzelmann S, Castelo R, Guinney J. GSVA: gene set variation analysis for microarray and RNA-seq data. *BMC Bioinformatics*. (2013) 14:7. doi: 10.1186/1471-2105-14-7
20. Liu J, Lichtenberg T, Hoadley KA, Poisson LM, Lazar AJ, Cherniack AD, et al. An integrated TCGA pan-cancer clinical data resource to drive high-quality survival outcome analytics. *Cell*. (2018) 173:400–16.e11. doi: 10.1016/j.cell.2018.02.052
21. Engelen E, Janssens RC, Yagita K, Smits VA, van der Horst GT, Tamanini F. Mammalian TIMELESS is involved in period determination and DNA damage-dependent phase advancing of the circadian clock. *PLoS One*. (2013) 8:e56623. doi: 10.1371/journal.pone.0056623
22. Murakami H, Keeney S. Temporospatial coordination of meiotic DNA replication and recombination via DDK recruitment to replisomes. *Cell*. (2014) 158:861–73. doi: 10.1016/j.cell.2014.06.028
23. O'Reilly LP, Zhang X, Smithgall TE. Individual Src-family tyrosine kinases direct the degradation or protection of the clock protein Timeless via differential ubiquitylation. *Cell Signal*. (2013) 25:860–6. doi: 10.1016/j.cellsig.2012.12.009
24. Gotter AL, Manganaro T, Weaver DR, Kolakowski Jr LF, Possidente B, Sriram S, et al. A time-less function for mouse timeless. *Nat Neurosci*. (2000) 3:755–6. doi: 10.1038/77653
25. Barnes JW, Tischkau SA, Barnes JA, Mitchell JW, Burgoon PW, Hickok JR, et al. Requirement of mammalian Timeless for circadian rhythmicity. *Science*. (2003) 302:439–42. doi: 10.1126/science.1086593
26. Yang X, Wood PA, Hrushesky WJ. Mammalian TIMELESS is required for ATM-dependent CHK2 activation and G2/M checkpoint control. *J Biol Chem*. (2010) 285:3030–4. doi: 10.1074/jbc.M109.050237
27. Hsu MY, Meier FE, Nesbit M, Hsu JY, Van Belle P, Elder DE, et al. E-cadherin expression in melanoma cells restores keratinocyte-mediated growth control and down-regulates expression of invasion-related adhesion receptors. *Am J Pathol*. (2000) 156:1515–25. doi: 10.1016/s0002-9440(10)65023-7
28. Haass NK, Smalley KS, Li L, Herlyn M. Adhesion, migration and communication in melanocytes and melanoma. *Pigment Cell Res*. (2005) 18:150–9. doi: 10.1111/j.1600-0749.2005.00235.x
29. Scatolini M, Patel A, Grosso E, Mello-Grand M, Ostano P, Coppo R, et al. GJB5 association with BRAF mutation and survival in cutaneous malignant melanoma. *Br J Dermatol*. (2022) 186:117–28. doi: 10.1111/bjd.20629
30. Baluapuri A, Wolf E, Eilers M. Target gene-independent functions of MYC oncoproteins. *Nat Rev Mol Cell Biol*. (2020) 21:255–67. doi: 10.1038/s41580-020-0215-2
31. Tan BC, Liu H, Lin CL, Lee SC. Functional cooperation between FACT and MCM is coordinated with cell cycle and differential complex formation. *J Biomed Sci*. (2010) 17:11. doi: 10.1186/1423-0127-17-11
32. Fischer M, Grossmann P, Padi M, DeCaprio JA. Integration of TP53, DREAM, MMB-FOXM1 and RB-E2F target gene analyses identifies cell cycle gene regulatory networks. *Nucleic Acids Res*. (2016) 44:6070–86. doi: 10.1093/nar/gkw523
33. Raab CA, Raab M, Becker S, Strebhardt K. Non-mitotic functions of polo-like kinases in cancer cells. *Biochim Biophys Acta Rev Cancer*. (2021) 1875:188467. doi: 10.1016/j.bbcan.2020.188467
34. Megjugorac NJ, Young HA, Amrute SB, Olshalsky SL, Fitzgerald-Bocarsly P. Virally stimulated plasmacytoid dendritic cells produce chemokines and induce migration of T and NK cells. *J Leukoc Biol*. (2004) 75:504–14. doi: 10.1189/jlb.0603291
35. Gajewski TF, Schreiber H, Fu YX. Innate and adaptive immune cells in the tumor microenvironment. *Nat Immunol*. (2013) 14:1014–22. doi: 10.1038/ni.2703

36. Giese MA, Hind LE, Huttenlocher A. Neutrophil plasticity in the tumor microenvironment. *Blood*. (2019) 133:2159–67. doi: 10.1182/blood-2018-11-844548
37. Schreiber S, Hammers CM, Kaasch AJ, Schraven B, Dudeck A, Kahlfuss S. Metabolic interdependency of Th2 cell-mediated type 2 immunity and the tumor microenvironment. *Front Immunol*. (2021) 12:632581. doi: 10.3389/fimmu.2021.632581
38. Feng Q, Wei H, Morihara J, Stern J, Yu M, Kiviat N, et al. Th2 type inflammation promotes the gradual progression of HPV-infected cervical cells to cervical carcinoma. *Gynecol Oncol*. (2012) 127:412–9. doi: 10.1016/j.ygyno.2012.07.098
39. Espinoza JA, Jabeen S, Batra R, Papaleo E, Haakensen V, Timmermans Wielenga V, et al. Cytokine profiling of tumor interstitial fluid of the breast and its relationship with lymphocyte infiltration and clinicopathological characteristics. *Oncoimmunology*. (2016) 5:e1248015. doi: 10.1080/2162402x.2016.1248015
40. Zhang Q, Qin J, Zhong L, Gong L, Zhang B, Zhang Y, et al. CCL5-mediated Th2 immune polarization promotes metastasis in luminal breast cancer. *Cancer Res*. (2015) 75:4312–21. doi: 10.1158/0008-5472.Can-14-3590
41. Zaynagetdinov R, Sherrill TP, Gleaves LA, McLoed AG, Saxon JA, Habermann AC, et al. Interleukin-5 facilitates lung metastasis by modulating the immune microenvironment. *Cancer Res*. (2015) 75:1624–34. doi: 10.1158/0008-5472.Can-14-2379
42. DeNardo DG, Barreto JB, Andreu P, Vasquez L, Tawfik D, Kolhatkar N, et al. CD4(+) T cells regulate pulmonary metastasis of mammary carcinomas by enhancing protumor properties of macrophages. *Cancer Cell*. (2009) 16:91–102. doi: 10.1016/j.ccr.2009.06.018
43. Chen J, Gong C, Mao H, Li Z, Fang Z, Chen Q, et al. E2F1/SP3/STAT6 axis is required for IL-4-induced epithelial-mesenchymal transition of colorectal cancer cells. *Int J Oncol*. (2018) 53:567–78. doi: 10.3892/ijo.2018.4429
44. Xia S, Lin Y, Lin J, Li X, Tan X, Huang Z. Increased expression of TICRR predicts poor clinical outcomes: a potential therapeutic target for papillary renal cell carcinoma. *Front Genet*. (2020) 11:605378. doi: 10.3389/fgene.2020.605378
45. Xie L, Wang Q, Nan F, Ge L, Dang Y, Sun X, et al. OSacc: gene expression-based survival analysis web tool for adrenocortical carcinoma. *Cancer Manag Res*. (2019) 11:9145–52. doi: 10.2147/cmar.S215586
46. Yan Z, Wang Q, Sun X, Ban B, Lu Z, Dang Y, et al. OSbrca: a web server for breast cancer prognostic biomarker investigation with massive data from tens of cohorts. *Front Oncol*. (2019) 9:1349. doi: 10.3389/fonc.2019.01349
47. Yan Z, Wang Q, Lu Z, Sun X, Song P, Dang Y, et al. OSluca: an interactive web server to evaluate prognostic biomarkers for lung cancer. *Front Genet*. (2020) 11:420. doi: 10.3389/fgene.2020.00420
48. Cadenas C, van de Sandt L, Edlund K, Lohr M, Hellwig B, Marchan R, et al. Loss of circadian clock gene expression is associated with tumor progression in breast cancer. *Cell Cycle*. (2014) 13:3282–91. doi: 10.4161/15384101.2014.954454

**Conflict of Interest:** The authors declare that the research was conducted in the absence of any commercial or financial relationships that could be construed as a potential conflict of interest.

**Publisher's Note:** All claims expressed in this article are solely those of the authors and do not necessarily represent those of their affiliated organizations, or those of the publisher, the editors and the reviewers. Any product that may be evaluated in this article, or claim that may be made by its manufacturer, is not guaranteed or endorsed by the publisher.

*Copyright © 2022 Zhao, Wen, Liu, Zhou, Liu, Zhong and Xie. This is an open-access article distributed under the terms of the Creative Commons Attribution License (CC BY). The use, distribution or reproduction in other forums is permitted, provided the original author(s) and the copyright owner(s) are credited and that the original publication in this journal is cited, in accordance with accepted academic practice. No use, distribution or reproduction is permitted which does not comply with these terms.*

frontiers | Frontiers in Surgery

MINI REVIEW
published: 14 June 2022
doi: 10.3389/fsurg.2022.935107

# Single-Cell Transcriptional Analysis Deciphers the Inflammatory Response of Skin-Resident Stromal Cells

*Baoyi Liu*[1,2], *Ang Li*[1,2], *Jingkai Xu*[1] *and Yong Cui*[1,2]*

[1]Department of Dermatology, China–Japan Friendship Hospital, Beijing, China, [2]Graduate School of Peking Union Medical College, Chinese Academy of Medical Sciences and Peking Union Medical College, Beijing, China

OPEN ACCESS

**Edited by:**
*Ronghua Yang,*
*First People's Hospital of Foshan, China*

**Reviewed by:**
*Jinhua Xu,*
*Huashan Hospital, Fudan University, China*
*Ya-gang Zuo,*
*Peking Union Medical College Hospital (CAMS), China*
*Aie Xu,*
*Third People's Hospital of Hangzhou, China*

***Correspondence:**
*Yong Cui*
*wuhucuiyong@vip.163.com*

**Specialty section:**
*This article was submitted to Reconstructive and Plastic Surgery, a section of the journal Frontiers in Surgery*

**Received:** *03 May 2022*
**Accepted:** *23 May 2022*
**Published:** *14 June 2022*

**Citation:**
*Liu B, Li A, Xu J and Cui Y (2022) Single-Cell Transcriptional Analysis Deciphers the Inflammatory Response of Skin-Resident Stromal Cells. Front. Surg. 9:935107. doi: 10.3389/fsurg.2022.935107*

The skin is the outermost barrier of the body. It has developed a sophisticated system against the ever-changing environment. The application of single-cell technologies has revolutionized dermatology research and unraveled the changes and interactions across skin resident cells in the healthy and inflamed skin. Single-cell technologies have revealed the critical roles of stromal cells in an inflammatory response and explained a series of plausible previous findings concerning skin immunity. Here, we summarized the functional diversity of skin stromal cells defined by single-cell analyses and how these cells orchestrated events leading to inflammatory diseases, including atopic dermatitis, psoriasis, vitiligo, and systemic lupus erythematosus.

**Keywords: scRNA-seq, skin resident cells, skin stromal cells, immunoregulatory axis, cellular communication**

## INTRODUCTION

The skin is the body's outermost barrier and is composed of the epidermis and dermis. It is defined by a multilayered architecture based on diverse cell populations of keratinocytes, melanocytes, fibroblasts, and endothelial cells, as well as various immune cells. Facing the ever-changing environment, it has developed a complex system that responds to stimuli such as pathogen infection, UV exposure, and toxic compounds (1). In this system, skin stromal cells have long been considered passive participants and bystanders in immunoregulation. However, recent studies have revealed that they actively participate in skin inflammatory responses.

RNA sequencing (RNA-seq) technology has long been used to dissect the molecular differences or commonalities of different inflammatory skin diseases (2). Previous bulk RNA sequencing and microarray studies on skin inflammatory diseases have revealed dysregulation of inflammatory and barrier genes, but many cell-specific transcripts often remain masked in whole-skin transcriptomic analyses. In addition, it has been difficult to systematically understand the sophisticated interplay among cells in the skin (3). Sing-cell RNA-seq (scRNA-seq) can capture tissue transcripts at the single-cell resolution and effectively solve this problem (3). The experimental procedure of scRNA-seq mainly includes four steps: sample preparation, cell enrichment, library preparation, and data analysis (4). It has been leveraged in various fields, contributing to novel discoveries and improving our understanding of embryonic medicine, developmental biology, tumor

ecosystems, immunology, and inflammatory diseases (5). scRNA-seq studies have elucidated how skin resident cells are involved in skin homeostasis regulation and inflammatory responses and revealed their immunoregulatory role (6–8). However, scRNA-seq transcriptome analysis remains challenging to define cell subpopulations due to the heterogeneity of skin cells during inflammation.

In this review, we recapitulated the main cell populations and their subpopulations of skin-resident stromal cells observed by scRNA-seq technologies in healthy and inflamed human skin and discussed their pathological alterations and "feedforward" role in recruiting immune cells in skin inflammatory diseases, including atopic dermatitis (AD), psoriasis, vitiligo, and systemic lupus erythematosus (SLE). We attempted to highlight current disagreements and consensus on skin stromal cell subsets and functions in inflammatory diseases.

## Skin Resident Cells Identified by scRNA-seq

Defining subsets of cells is an important step in scRNA-seq bioinformatics analysis. The type of obtained cells varied with different collection methods. Full-thickness skin samples contained complete skin cells, while suction blisters would lose information on fibroblasts, endothelial cells, and immune cells in the dermis (9). However, suction blisters were more accessible and often used in the study of AD (7, 10, 11). Most studies on the skin referred to the Human Cell Atlas (12) for cell identification, which could accurately distinguish skin stromal cells. However, when it comes to specific cell subtypes, especially fibroblasts with obvious heterogeneity, it was difficult for researchers to reach a consensus on grouping and naming. We would describe the disagreements and consensus on each cell subset classification in the following. The biological markers used in scRNA-seq studies are listed in **Table 1**.

**TABLE 1** | Cell defined marker of skin resident cell in scRNA-seq.

| Cell types/subtypes | Marker | Reference |
|---|---|---|
| Keratinocytes | KRT1, KRT2, KRT5 | 6–8, 13–18 |
| Basal keratinocytes | KRT5, KRT14, TP63, ITGA6, COL17A1 | 6–8, 13–17 |
| Spinous keratinocytes | KRT1, KRT10, DSG1, DSP | 6–8, 13–17 |
| Granular keratinocytes | LOR, FLG, SPINK5, KRT2, KLK11 | 6–8, 13–17 |
| Mitotic keratinocytes | CDK1, PCNA, KI67, UBE2C, TOP2A, TK1, MTK1, TOP2A | 10, 17, 18 |
| Channel keratinocytes | GJB2, GJB6, ATP1B3, ATP1A1, ATP1B1, ATP5B, FXYD3 | 10, 17, 18 |
| Follicular keratinocytes | APOC1, ACSL5, ABCC3, MGST1 APOE, CD200, SOX9, KRT19, KRT6B, KRT17, S100A2 | 10, 17, 18 |
| Melanocytes | PMEL, TYR, TYRP1, DCT, KIT, MLANA | 6, 7, 11 |
| Fibroblasts | COL1A1/A2, DCN, LUM, LUM, DCN, VIM, PDGFRA | 13, 14 |
| Papillary fibroblasts | DPP4, FAP, CD90, COL6A5, CD39, APCDD1, HSPB3, WIF1 | 16, 19–21 |
| Reticular fibroblasts | Dlk1, CD36 | 19–21 |
| Secretory-reticular fibroblasts | WISP2, SLPI, CTHRC1, MFAP5, TSPAN8 | 22 |
| Secretory-papillary fibroblasts | APCDD1, ID1, WIF1, COL18A1, PTGDS | 22 |
| Mesenchymal fibroblasts | ASPN, POSTN, GPC3, TNN, SFRP1 | 22 |
| Pro-inflammatory fibroblasts | CCL19, APOE, CXCL2, CXCL3, EFEMP1 | 22 |
| Type A | ELN, MMP2, QPCT, SFRP2 | 14 |
| Type B | APOE, C7, CYGB, IGFBP7B | 14 |
| Type C | DKK3, TNMD, TNN, SFRP1 | 14 |
| Vascular endothelial cells | PECAM1, EMCN, SELE, CD93, CLDN5, VWF, CDH5 | 6, 8, 18 |
| Lymphatic endothelial cells | LYVE1, PDPN, PROX1, CLDN5 | 6, 8, 18 |

## Keratinocytes Actively Contributed to Immunopathology in Inflamed Skin

Keratinocytes are the major cells in the epidermis, accounting for 66% of the epidermic cells from suction blisters and 37.96% of the full-thickness skin from skin biopsies in scRNA-seq (13). Keratinocytes were distinguished from other skin cells by cluster-specific expression of keratin1 (KRT1), KRT2, and KRT5 (6–8, 13–18).

Cell subtype identification of keratinocytes was consistent across various papers (6, 7, 13). Three subpopulations were separated corresponding to their stereotyped differentiation process in the normal epidermis: undifferentiated basal keratinocytes had high expression of basal epidermal proteins (KRT5 and KRT14), hemidesmosome molecules [integrin alpha-6, ITGA6; and collagen alpha-1 (XVII) chain, COL17A1] and stemness factor (tumor protein 63, TP63); upper spinous keratinocytes expressed suprabasal cell transcripts (KRT1 and KRT10); and granular keratinocytes expressed KRT2, KLK11, and late differentiation markers (Loricrin, LOR; Filaggrin, FLG; and serine protease inhibitor Kazal-type 5, SPINK5) (6–8, 13–18).

In addition, three subpopulations were unable to be distinguished by the classical differentiation model. The first undergoing proliferation was deemed as mitotic keratinocytes, as characterized by DNA synthesis and cell division transcripts, including cyclin-dependent kinase 1 (CDK1), proliferating cell nuclear antigen (PCNA), KI67, ubiquitin-conjugating enzyme E2 C (UBE2C), DNA topoisomerase 2-alpha (TOP2A), thymidine kinase (TK1), and mitogen-activated protein kinase kinase kinase 4 (MAP3K4). The second was termed "channel" keratinocytes by coordinate elevation of ion channel and cell-cell communication transcripts [gap junction beta (GJB2/6), potassium-transporting ATPase (ATP1B3/1A1/1B1/5B), and FXYD domain-containing ion transport regulator 3 (FXYD3)]. Finally, the third was separated individually as follicular keratinocytes that expressed genes associated with the

sebaceous gland [apolipoprotein (APOC1/E), long-chain-fatty-acid–CoA ligase 5 (ACSL5), ATP-binding cassette sub-family C member 3 (ABCC3), and microsomal glutathione S-transferase 1 (MGST1)], follicles (TRK19, CD200, SOX9), and (or) outer root sheath (KRT6B, KRT17, and S100A2) (10, 17, 18).

Interestingly, force-directed graph (FDG) and PAGA analyses on scRNA-seq data defined two differentiation pathways of basal keratinocytes to suprabasal cells, with or without a high level of the lamellar body (LB)-related transcripts (glucosylceramide transporter ABCA12; cytoskeleton-associated protein 4, CKAP4; and CAP-Gly domain-containing linker protein 1, CLIP1), that characterized late epidermal differentiation in healthy skin (6). When it comes to inflammation, keratinocytes showed a more complicated picture of gene expression. Gene differential expression analysis revealed that keratinocytes, especially those in spinous and granular layers, overexpressed a panel of interferon response genes [interferon alpha-inducible protein 27 (IFI27) and interferon-induced transmembrane protein 1 (IFITM1)] and damage-associated transcripts, including antimicrobial peptides, also known as alarmis (S100A7/A8/A9), wound healing states (KRT6A/16), and serpins (SERPINB4/13), consistent with previous study results (4, 6, 13). It was reported that evoked S100A8/A9 expression was a molecular event preceding any histological alteration or deregulation of cytokines and played a crucial role in enhancing keratinocyte differentiation while inhibiting proliferation (23). In addition to damage-associated molecules, keratinocytes also expressed chemokine ligands and cytokines to recruit immune cells. Reynolds et al. defined a new subpopulation of celled inflammatory differentiated keratinocytes, as suggested by coexpressing lower levels of undifferentiated and differentiated markers but additionally expressing intercellular adhesion molecule1 (ICAM1), tumor necrosis factor (TNF), and CCL20 (6). CCL20 is the only known high-affinity ligand of CCR6 and attracts IL17A-producing CCR6+ immune cells, such as dendritic cells (DCs) and T cells (24). It has been reported that the CCL20/CCR6 axis contributes to the formation of an IL17A-rich milieu in psoriasis (25). Pruritus-induced mechanical scratching also upregulated CCL20 production from keratinocytes, which could partially explain high IL17A levels in AD (24).

Several disease-specific alterations were described in keratinocytes of AD patients. Abnormally elevated genes included aquaporin-3 (AQP3, a water channel component associated with keratinocyte proliferation and transepidermal water loss) (26), tumor necrosis factor receptor superfamily member 12A (TNFRSF12A), cornifin-B (SPRR1B, promoting the cornification of keratinocytes) (10, 27), CCL2 (binding to CCR2 to polarize Th2 response) (28), CCL27, and proinflammatory cytokine IL32 (modulating keratinocyte apoptosis) (17, 29). Downregulated genes involved DEFB1, an antimicrobial against *Staphylococcus aureus* (10, 30). After dupilumab treatment, most of the activated transcripts were normalized, including S100A7/A8/A9, KRT6A, KRT16, SERPINB4, CCL2, and CCL27, whereas IFI27, TNFRSF12A, and SPRR1B remained dysregulated 1 year later (31). The relationship between these genes and recurrence is worth exploring.

Psoriatic epidermis is remarkable for the expansion of mitotic and channel subfractions with increased GJB6, which is described as a psoriasis risk gene (18). In addition, keratinocytes significantly overexpress MHC molecules (HLA-DRA, HLA-DMA, HLA-C), WNT5A, CD58, and pro-inflammatory cytokines IL36G and NFKBIZ (transcriptional regulator of IL36-driven gene expression) (13, 32). It has been described that keratinocytes are capable of directly presenting antigen to T cells and initiating an immune response (33). IL36γ could induce keratinocytes to produce CXCL1, CXCL10, and CCL20 and function as a linker between keratinocytes and DCs (34). Unexpectedly, Hughes et al. found that FOS-related antigen 1 (FOSL1) was positively correlated with diffusion pseudo-time in psoriatic KCs compared with healthy KCs by differential pseudo-time correlation analysis and further validated the distribution at the protein level by immunofluorescence staining (8). FOSL1 belongs to the FOS gene family that has been implicated as regulators of cell differentiation, proliferation, and transformation. FOSL1 was identified as the TF encoding gene of psoriasis (35), and the enhanced FOSL1 expression was significantly correlated with high psoriasis area and severity index (36). FOSL1 knockdown inhibited IL22-induced proliferation and enhanced apoptosis of keratinocytes (37). These results suggest that FOSL1 may serve as a new therapeutic target for psoriasis.

It is an intriguing finding that CCL27 expression of keratinocytes was increased in AD (17) but decreased in psoriasis (32). CCL27 is a chemotactic factor binding to CCR10 that plays an important role in the homeostatic establishment of resident lymphocytes (38). CCL27/CCR10-derived regulation would promote activated T cell product IL17A/IL22 (38). Interactions between CCL2 and CCL27 (keratinocytes) and CCR1/2 and CCR10 (T cells) might cooperatively induce the Th2 milieu in AD (17). Nevertheless, it was confusing that impaired CCL27–CCR10 interaction was present in IL17-driven psoriasis (32). This contradictory result suggested that CCL27 might serve as a molecular marker for differentiating psoriasis and AD.

Keratinocytes respond to inflammation even without visible skin damage. It was reported that keratinocytes upregulated IFN-responsive genes and fibrotic pathways in non-lesional, non-sun-exposed skin of SLE (39, 40). Keratinocytes can even recruit CXCR3+ T cells to kill surrounding melanocytes by expressing high levels of chemokines CXCL9/10/11 (16). These results emphasized that keratinocytes collaborate with immune cells and actively contribute to immunopathology.

## Melanocytes Not Bystanders of Skin Inflammation

Melanocytes account for 10% of the basal cells of the epidermis, and they can be captured at a relatively large proportion by suction blistering, defined by PMEL, tyrosinase (TYR),

tyrosinase-related protein 1/2 (TYRP1/2), KIT, and melanoma antigen (MLANA) in scRNA-seq. Melanocytes express many molecules necessary for the maintenance of the extracellular matrix and cell–cell adhesion, including fibronectins, collagens, and laminins, and adhesion to the basal keratinocyte layer by expressed cognate ligands (FN1, LAMBA4, and LAMB1) (6, 7, 11).

Pigmentation changes are very common in inflammatory skin diseases. Consistently, scRNA-seq studies indicated that melanocytes display considerable numbers of dysregulated genes, including S100 transcripts and pigmentation-associated genes (*TYR* and *MFSD12*) in inflamed skin. Despite clinical clearance of the skin, these genes are still overexpressed in spontaneously healed or dupilumab-treated AD (7, 11).

Melanocytes were previously seen as bystanders of skin inflammation, but scRNA-seq demonstrated that they are involved in a variety of inflammatory responses. They increase MHC-I signaling transcript (HLA-A, HLA-B, and HLA-E) in inflamed skin, targeting T cells (HLA-CD3D) and natural killer (NK) cells (HLA-E-KLRC1) (16). It was reported that HLA-C-presented melanocyte was attacked by CD8± T cells and further induced T cells to secrete IL17A in psoriasis lesions (41). Notably, HLA-C might also play a crucial role in transformation from acute inflammation to a chronic disease (42). Furthermore, some melanocytes significantly evoked IL4Rα, CCL18, and CXCL1 expression responses to type 2 inflammation in AD (7, 43). In vitiligo, a disease characterized by melanocyte loss, CCL18 was also overexpressed in melanocytes, which attracted CCR8+ immune cells (T and NK cells) to kill themselves (16, 44). These pieces of evidence imply that melanocytes are part of a "feedforward" inflammatory response in the epidermis, resembling keratinocytes.

Despite their pro-inflammatory role, melanocytes might be involved in inflammatory diminishing, as suggested by overexpressing matricellular protein CCN family member 3 (CCN3, limiting proinflammatory activation) (45), SERPINF1 (antiangiogenic factor) (46), and Annexin A1 (ANXA1, an anti-inflammatory factor functioning as a major mediator of glucocorticoid responses) in AD (7, 47). Consistent with this study, Rindler et al. found that melanocytes upregulated T cell reactivity inhibitor dickkopf-related protein 3 (DKK3) (48), TGF-β signaling promotor CD81 (49), and platelet-activating factor acetylhydrolase (PLA2G7), which catalyzed the degradation of the strongly pro-inflammatory phospholipid mediator platelet-activating factor (PAF) (11, 50) in spontaneously healed AD (11). Similarly, anti-inflammatory genes (CCN3 and ANXA1) remained among the top upregulated genes after 1-year dupilumab treatment, whereas inflammatory factor expression was normalized (CCL18 and CXCL1) (31).

## Heterogeneity, Dysregulated Extracellular Matrix, and Immune Regulation of Fibroblasts in Diseases

Fibroblasts make up the majority of dermal cells, marked by collagen alpha-1 (I) chain (COL1A1/A2), decorin (DCN), lumican (LUM), vimentin (VIM), and platelet-derived growth factor receptor alpha (PDGFRA). Fibroblasts play an important role in epidermal stem and progenitor cell (EpSC) maintenance (51, 52) and immune surveillance of the dermis (53). Fibroblasts account for 31.53% of the full-thickness skin cells from skin biopsies (13, 14) but are lost in suction blisters for scRNA-seq.

Fibroblasts can be spatially divided into upper papillary fibroblasts and lower reticular fibroblasts. Driskell et al. first defined dipeptidyl peptidase 4 (DPP4, also termed CD26) as a papillary fibroblast marker and delta-like non-canonical notch ligand 1 (Dlk1)+ cell as a fibroblast within the reticular layers (19). It is interesting that DPP4± fibroblasts deposit the matrix during wound healing in mice (54). In line with this study, Guerrero-Juarez. et al. identified CRABP1± papillary fibroblasts in large wounds by conducting scRNA-seq (55). These studies implied that upper papillary dermal compartments seem to be more actively involved in wound regeneration. Subsequently, fibroblast activation protein (FAP), CD90, α5 chain of collagen VI (COL6A5), CD39, APCDD1, heat shock protein beta-3 (HSPB3), and WNT inhibitory factor 1 (WIF1) were identified as papillary fibroblast markers, whereas FAP− CD90+ CD36+ fibroblasts were classified as reticular fibroblasts (20, 21). Philippeos et Al. revealed distinct properties of the upper and lower dermis using RNA-seq on the dermis separated by microdissection (21). The study demonstrated that the papillary dermis exhibited upregulation of the Wnt signaling pathway (WIF1, APCDD1, RSP01, axin-2, AXIN2) and presented an anti-inflammatory phenotype, as suggested by a significant reduction in the upregulation of PDL-1 and CD40 compared with lower fibroblasts in response to IFNγ stimulation. Reticular layers highly expressed several extracellular matrix (ECM) components (ADAM12, ADAMTS9, COL1A2, COL1A1, ELN, and FN1) and inflammatory mediators (CCL19, CCL7, CXCR4, and IL6) (21).

However, the classical markers rarely distinguish the two populations in scRNA-seq studies. Ascensión et al. conducted an integrated analysis of fibroblasts in four scRNA-seq studies and found that papillary and reticular fibroblast categories were composed of a mixture of cell subtypes (14). The classical papillary marker CD26 transcript was present in virtually all cells in the dermis without regional restriction (56). It might result from the functional heterogeneity of fibroblasts (57) or the progressive loss of clear genetic distinctions during the aging process (22). In addition, the heterogeneity of fibroblastic cells also existed across developmental time, between different anatomic skin locations (58). Therefore, fibroblast subsets identified varied among studies. How to unify the nomenclature of fibroblast subtypes is an urgent problem.

A possible strategy is to combine spatial location and function. Solé-Boldo et al. classified fibroblasts into four subpopulations: secretory-reticular fibroblasts [CCN5, antileukoproteinase, SLPI, collagen triple helix repeat-containing protein 1 (CTHRC1), microfibrillar-associated protein 5 (MFAP5), and tetraspanin-8 (TSPAN8)], secretory-papillary fibroblasts [(APCDD1, ID1, WIF1, COL18A1,

**TABLE 2** | Molecule changes of skin resident cell in inflamed skin.

| Molecular changes | Function | Disease | References |
|---|---|---|---|
| *Keratinocytes* | | | |
| IFI27, IFITM1 | Interferon response genes | AD and psoriasis | 3, 6, 13 |
| S100A7/A8/A9 | Early molecular event of inflamed skin | AD and psoriasis | 3, 6, 13 |
| KRT6A/16 | Wound healing states | AD and psoriasis | 3, 6, 13 |
| SERPINB4/13 | Protease inhibitor | AD and psoriasis | 3, 6, 13 |
| CCL20 | Attracting IL17A-producing CCR6 + immune cells | AD and psoriasis | 3, 6, 13, 24, 25 |
| AQP3 | Involved in keratinocytes proliferation and transepidermal water loss | AD | 26 |
| TNFRSF12A | Tumor necrosis factor receptor | AD | 10, 27 |
| SPRR1B | Promoting the cornification of keratinocytes | AD | 10, 27 |
| CCL2 | Binding to CCR2 to polarizing $Th_2$ response | AD | 28 |
| CCL27 | Binding to CCR10 which have important function in homeostatic establishment of resident lymphocytes | AD | 17, 38 |
| IL32 | Modulating keratinocyte apoptosis | AD | 17, 29 |
| DEFB1 | An antimicrobial against *Staphylococcus aureus* | AD | 10, 30 |
| HLA-DRA, HLA-DMA, HLA-C | Antigen presentation | Psoriasis | 13, 32 |
| WNT5A | Regulator of Wnt signaling | Psoriasis | 13, 32 |
| CD58 | Ligand of the T-lymphocyte CD2 glycoprotein | Psoriasis | 13, 32 |
| IL36G | Linker between keratinocytes and DCs | Psoriasis | 13, 32, 33 |
| NFKBIZ | Transcriptional regulator of IL36-driven gene expression | Psoriasis | 13, 32 |
| FOSL1 | Regulators of cell differentiation, proliferation, and transformation | Psoriasis | 35–37 |
| CCL27 | Binding to CCR10 which have important function in homeostatic establishment of resident lymphocytes | Psoriasis | 32, 38 |
| CXCL9/10/11 | Recruit CXCR3+ T cells to kill surrounding melanocytes | vitiligo | 16 |
| *Melanocytes* | | | |
| S100A8/A9 | Damage-associated transcripts | AD and psoriasis | 7, 11 |
| TYR, MFSD12 | Pigmentation-associated genes | AD and psoriasis | 7, 11 |
| HLA-A, HLA-B, HLA-E | Antigen presentation | AD and psoriasis | 7, 11 |
| IL4Rα, CCL18, CXCL1 | Responses to type 2 inflammation | AD | 7, 43 |
| CCN3 | Limiting proinflammatory activation | AD | 7, 45 |
| SERPINF1 | Antiangiogenic factor | AD | 7, 46 |
| ANXA1 | Mediator of glucocorticoid responses | AD | 7, 47 |
| DKK3 | T-cell reactivity inhibitor | AD | 48 |
| PLA2G7 | Catalyzing the degradation of the strongly pro-inflammatory phospholipid mediator Platelet-activating factor | AD | 11, 50 |
| CCL18 | Bind to CCR8+ immune cells (T and NK cell) | Vitiligo | 16, 44 |
| *Fibroblast* | | | |
| HLA-A, HLA-B, HLA-C, HLA-DRA | Antigen presentation | AD and psoriasis | 13 |
| CCL19 | Ligands of CCR7 which widely expressed by DCs and T cells | AD and psoriasis | 63 |
| CXCL12 | CXCR4/CXCL12 axes is involved in asthma pathology (induce a type 2 allergic response) | AD and psoriasis | 8, 13, 67 |
| SDK1, FGF7, COMP, COL5A3, COL1A1 | ECM-related proteins | Psoriasis | 13 |
| CCL26 | Classical type 2 chemokines | Psoriasis | 61 |
| IL6/LIF | Hallmark inflammatory cytokine made by fibroblasts | Psoriasis | 61 |
| IL17B | Involved in surface expression of CD80 and CD86 protein in DCs | Psoriasis | 13, 62 |
| CCL2 | Binding to CCR2 to Polarizing $Th_2$ response | AD | 28 |
| IL32 | Modulating keratinocyte apoptosis | AD | 17, 29 |
| *Vascular endothelial cells* | | | |
| ACKR1 | Interaction with CXCL8 (IL8) + macrophages | AD and psoriasis | 6 |

*AD, atopic dermatitis; NK, natural killer cells; ECM, extracellular matrix.*

prostaglandin-H2 D-isomerase (PTGDS)], mesenchymal fibroblasts [asporin (ASPN), periostin (POSTN), glypican-3 (GPC3), tenascin-N (TNN), and secreted frizzled-related protein 1 (SFRP1)], and pro-inflammatory fibroblasts [CCL19, APOE, CXCL2, CXCL3, and EGF-containing fibulin-like extracellular matrix protein 1 (EFEMP1)] that are widely spread within the dermis (22). Another study re-analyzed the four published datasets and classified fibroblasts into three major subsets: type A accounted for about 49.5% of the

fibroblasts (defined by ELN, MMP2, QPCT, and SFRP2) and was responsible for dermal cell and ECM homeostasis; type B represented 30.5% of the fibroblasts (defined by APOE, C7, CYGB, and IGFBP7B) and might play a clear role in immune surveillance and inflammation promotion; and type C represented 49.5% of the fibroblasts (defined by DKK3, TNMD, TNN, and SFRP1) and included more specialized subpopulations, such as dermal papilla cells and dermo-hypodermal junction fibroblasts (14). There were still significant differences between the two methods. To clearly describe the expression changes of fibroblasts, it is necessary to identify function-based cellular markers and arrive at a consensus for nomenclature.

Due to the different classification of fibroblast subsets among various studies, fibroblasts will be considered as a group in discussing their changes in inflammation. As expected, fibroblasts significantly increased the expression of MHC-I and MHC-II molecules (HLA-A, HLA-B, HLA-C, and HLA-DRA) in inflamed conditions (13), driving T and NK cell activation *via* targeting CD4, CD8, and CD94 (59, 60). In addition to antigen presentation, Reynolds et al. found that COL1A1+ COL1A2+ COL6A1+ fibroblasts were significantly enriched in AD and psoriatic conditions, which specialized toward ECM remodeling and maintenance, and overexpressed chemokines CXCL12 and CCL19 (6).

Consistent with the abovementioned study, Gao et al. also demonstrated that ECM-related proteins (SDK1, FGF7, COMP, COL5A3, and COL1A1) were elevated in psoriatic fibroblasts, indicating ECM remodeling in the inflamed condition (13). As major contributors to and regulators of inflammation, psoriatic fibroblasts also significantly increased cytokines CCL26, IL6, LIF, IL17B, CCL19, CXCL12, TNFRSF11B, and TNFSF13B (BAFF) (8, 13). CCL26 was a classical type 2 chemokine, while IL6 was considered a hallmark inflammatory cytokine formed by fibroblasts, and the autocrine LIF-LIFR positive feedback loop was critical for maintaining sustained I-6 transcription (61). Increased IL17B was enriched in perivascular fibroblasts (PDGFRβ+), which might be involved in the surface expression of CD80 and CD86 proteins in DCs (13, 62). CCL19 was one of the ligands of CCR7 that was widely expressed by DCs and T cells (63), suggesting that fibroblasts might communicate with these cells frequently in psoriasis. Elevated BAFF expression was strongly correlated with male psoriatic arthritis (PsA) activity and the progression of rheumatoid arthritis (64, 65), implying a consistent response of fibroblasts to inflammation throughout the body. All these results underlined dysregulated ECM and immune regulation of fibroblasts in psoriasis.

Of note, Rojahn et al. reported a new inflammatory fibroblast subpopulation only present in the upper dermis of AD lesions,

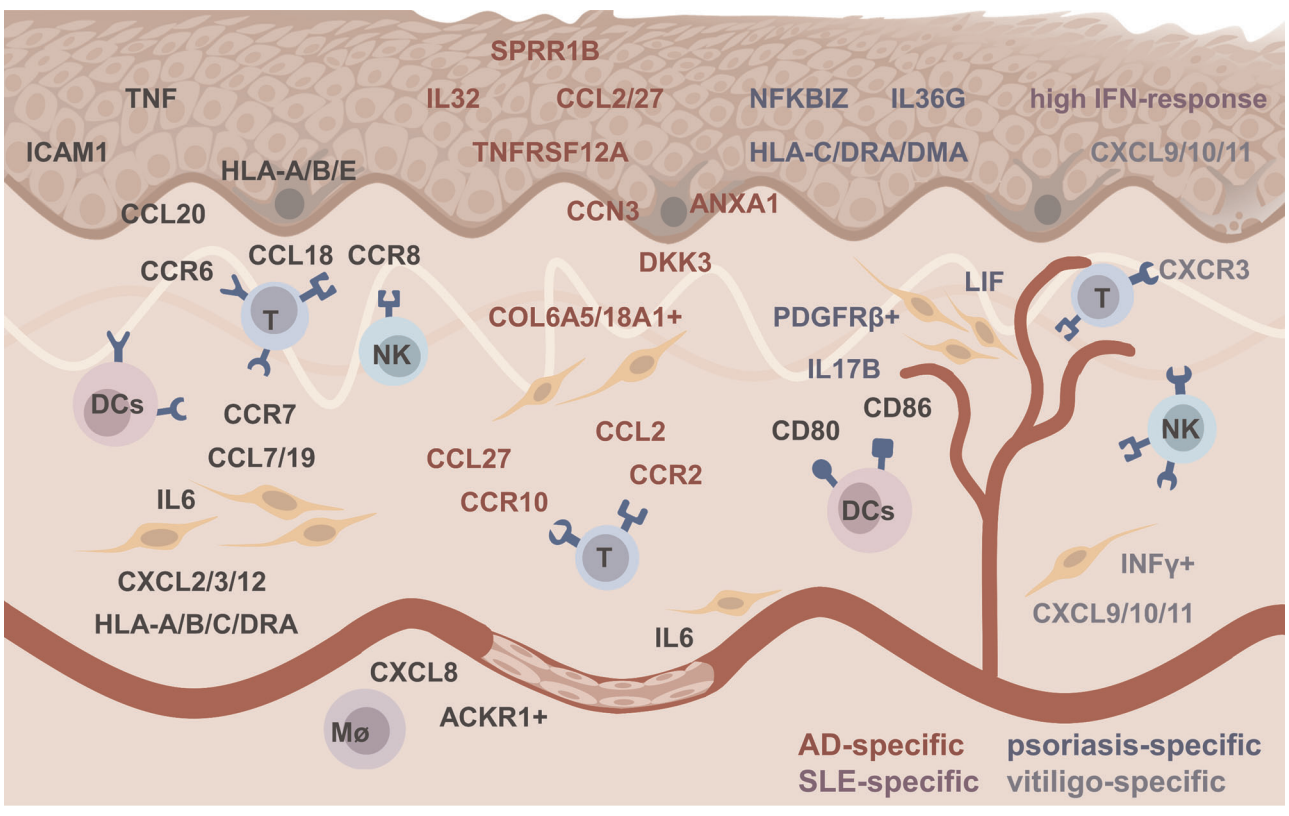


**FIGURE 1** | The feedforward role of skin stromal cell in inflamed skin. Black, red, blue, purple, and gray words represented ubiquitous, atopic dermatitis -specific, psoriasis-specific, systemic lupus erythematosus-specific, and vitiligo-specific altered genes, respectively.

marked by COL6A5 and COL18A1. These fibroblasts expressed inflammatory cytokines, including CCL2, CCL19, and IL32, similar to inflammatory keratinocytes. The study further confirmed that fibroblasts were juxtaposed to CD3+ T cells, indicating that these inflammatory fibroblasts were engaged in T cell recruitment and organization (10). The special role of this group of cells is worth studying. In addition, like upper keratinocytes and melanocytes, fibroblasts also secret CXCL9/10 in vitiligo. Xu et al. found that IFNγ-responsive fibroblasts were responsible for melanocyte loss via recruiting CD8± T cells through single-cell analysis, along with cell-type-specific genetic knockouts and engraftment experiments (66). These findings suggested that skin stromal cells induced a specific immune milieu *via* secreting the same regulatory factors in an inflammatory response.

### Endothelial Cells in Regulating Leukocyte Adhesion and Migration

There are few endothelial cells in the dermis that are not even detected in studies. Endothelial cells in the healthy adult dermis constitute the vascular endothelium (PECAM1, EMCN, SELE, CD93, CLDN5, VWF, and CDH5) and lymphatic endothelium (LYVE1, PDPN, PROX1, and CLDN5) (6, 8, 18). Reynolds et al. reported that some vascular endothelial cells, which expressed γ-synuclein (SNCG) and high level of ACKR1 (the venular capillary marker), might function as postcapillary venular cells. They found that ACKR1+ endothelial cells and CXCL8 (IL8)+ macrophages interacted with each other by cell communication analysis and further confirmed this finding with immunofluorescence staining *in situ* (6). Besides, ACKR1+ endothelial cells coexpressed inflammatory cytokines, chemokines, and leukocyte adhesion molecules including IL6, IL33, SELE, and ICAM1, implying that they might regulate leukocyte adhesion and migration (6).

## CONCLUSION

Although many technical issues remain to be resolved, scRNA-seq has demonstrated alterations in skin-intrinsic stromal cells in many inflammatory diseases (9). Thanks to scRNA-seq, we can precisely and systematically understand the heterogeneity of skin resident stromal cells, their pathological responses, and their interactions with immune cells in inflamed skin (**Table 2**). Skin stromal cells played a feedforward role by expressing chemokines, (pro)inflammatory factors, presenting antigens to immune cells, or limiting inflammation by expression regulators (**Figure 1**). These findings will greatly accelerate the development of personalized diagnostics and precision treatment.

## AUTHOR CONTRIBUTIONS

BL drafted and wrote the initial manuscript. AL, JX, and YC reviewed the manuscript. All authors contributed to the article and approved the submitted version.

## FUNDING

This work was supported by the National Natural Science Foundation of China (Grant No. 81872516, 82173418, and 82103100).

## REFERENCES

1. Wong R, Geyer S, Weninger W, Guimberteau JC, Wong JK. The dynamic anatomy and patterning of skin. *Exp Dermatol*. (2016) 25(2):92–8. doi: 10.1111/exd.12832
2. Schwingen J, Kaplan M, Kurschus FC. Review-current concepts in inflammatory skin diseases evolved by transcriptome analysis: in-depth analysis of atopic dermatitis and psoriasis. *Int J Mol Sci*. (2020) 21(3):699. doi: 10.3390/ijms21030699
3. Theocharidis G, Tekkela S, Veves A, McGrath JA, Onoufriadis A. Single-cell transcriptomics in human skin research: available technologies, technical considerations and disease applications. *Exp Dermatol*. (2022) 31(5):655–73. doi: 10.1111/exd.14547
4. Picelli S. Single-cell RNA-sequencing: the future of genome biology is now. *RNA Biol*. (2017) 14(5):637–50. doi: 10.1080/15476286.2016.1201618
5. Dubois A, Gopee N, Olabi B, Haniffa M. Defining the skin cellular community using single-cell genomics to advance precision medicine. *J Invest Dermatol*. (2021) 141(2):255–64. doi: 10.1016/j.jid.2020.05.104
6. Reynolds G, Vegh P, Fletcher J, Poyner EFM, Stephenson E, Goh I, et al. Developmental cell programs are co-opted in inflammatory skin disease. *Science*. (2021) 371(6527):eaba6500. doi: 10.1126/science.aba6500
7. Bangert C, Rindler K, Krausgruber T, Alkon N, Thaler FM, Kurz H, et al. Persistence of mature dendritic cells, T(H)2A, and Tc2 cells characterize clinically resolved atopic dermatitis under IL-4Rα blockade. *Sci Immunol*. (2021) 6(55):eabe2749. doi: 10.1126/sciimmunol.abe2749
8. Hughes TK, Wadsworth 2nd MH, Gierahn TM, Do T, Weiss D, Andrade PR, et al. Second-strand synthesis-based massively parallel scRNA-seq reveals cellular states and molecular features of human inflammatory skin pathologies. *Immunity*. (2020) 53(4):878–94.e7. doi: 10.1016/j.immuni.2020.09.015
9. Kim D, Chung KB, Kim TG. Application of single-cell RNA sequencing on human skin: technical evolution and challenges. *J Dermatol Sci*. (2020) 99(2):74–81. doi: 10.1016/j.jdermsci.2020.06.002
10. Rojahn TB, Vorstandlechner V, Krausgruber T, Bauer WM, Alkon N, Bangert C, et al. Single-cell transcriptomics combined with interstitial fluid proteomics defines cell type-specific immune regulation in atopic dermatitis. *J Allergy Clin Immunol*. (2020) 146(5):1056–69. doi: 10.1016/j.jaci.2020.03.041
11. Rindler K, Krausgruber T, Thaler FM, Alkon N, Bangert C, Kurz H, et al. Spontaneously resolved atopic dermatitis shows melanocyte and immune cell activation distinct from healthy control skin. *Front Immunol*. (2021) 12:630892. doi: 10.3389/fimmu.2021.630892
12. Rozenblatt-Rosen O, Shin JW, Rood JE, Hupalowska A, Regev A, Heyn H. Building a high-quality human cell atlas. *Nat Biotechnol*. (2021) 39(2):149–53. doi: 10.1038/s41587-020-00812-4
13. Gao Y, Yao X, Zhai Y, Li L, Li H, Sun X, et al. Single cell transcriptional zonation of human psoriasis skin identifies an alternative immunoregulatory axis conducted by skin resident cells. *Cell Death Dis*. (2021) 12(5):450. doi: 10.1038/s41419-021-03724-6
14. Ascensión AM, Fuertes-Álvarez S, Ibañez-Solé O, Izeta A, Araúzo-Bravo MJ. Human dermal fibroblast subpopulations are conserved across single-cell

RNA sequencing studies. *J Invest Dermatol*. (2021) 141(7):1735–44.e35. doi: 10.1016/j.jid.2020.11.028
15. Thompson SM, Phan QM, Winuthayanon S, Driskell IM, Driskell RR. Parallel single cell multi-omics analysis of neonatal skin reveals transitional fibroblast states that restricts differentiation into distinct fates. *J Invest Dermatol*. (2021) 17:S0022-202X(21)02608-7. doi: 10.1016/j.jid.2021.11.032
16. Gellatly KJ, Strassner JP, Essien K, Refat MA, Murphy RL, Coffin-Schmitt A, et al. scRNA-seq of human vitiligo reveals complex networks of subclinical immune activation and a role for CCR5 in T(reg) function. *Sci Transl Med*. (2021) 13(610):eabd8995. doi: 10.1126/scitranslmed.abd8995
17. He H, Suryawanshi H, Morozov P, Gay-Mimbrera J, Del Duca E, Kim HJ, et al. Single-cell transcriptome analysis of human skin identifies novel fibroblast subpopulation and enrichment of immune subsets in atopic dermatitis. *J Allergy Clin Immunol*. (2020) 145(6):1615–28. doi: 10.1016/j.jaci.2020.01.042
18. Cheng JB, Sedgewick AJ, Finnegan AI, Harirchian P, Lee J, Kwon S, et al. Transcriptional programming of normal and inflamed human epidermis at single-cell resolution. *Cell Rep*. (2018) 25(4):871–83. doi: 10.1016/j.celrep.2018.09.006
19. Driskell RR, Lichtenberger BM, Hoste E, Kretzschmar K, Simons BD, Charalambous M, et al. Distinct fibroblast lineages determine dermal architecture in skin development and repair. *Nature*. (2013) 504 (7479):277–81. doi: 10.1038/nature12783
20. Korosec A, Frech S, Gesslbauer B, Vierhapper M, Radtke C, Petzelbauer P, et al. Lineage identity and location within the dermis determine the function of papillary and reticular fibroblasts in human skin. *J Invest Dermatol*. (2019) 139(2):342–51. doi: 10.1016/j.jid.2018.07.033
21. Philippeos C, Telerman SB, Oulès B, Pisco AO, Shaw TJ, Elgueta R, et al. Spatial and single-cell transcriptional profiling identifies functionally distinct human dermal fibroblast subpopulations. *J Invest Dermatol*. (2018) 138(4):811–25. doi: 10.1016/j.jid.2018.01.016
22. Solé-Boldo L, Raddatz G, Schütz S, Mallm JP, Rippe K, Lonsdorf AS, et al. Single-cell transcriptomes of the human skin reveal age-related loss of fibroblast priming. *Commun Biol*. (2020) 3(1):188. doi: 10.1038/s42003-020-0922-4
23. Wang S, Song R, Wang Z, Jing Z, Wang S, Ma J. S100A8/A9 in inflammation. *Front Immunol*. (2018) 9:1298. doi: 10.3389/fimmu.2018.01298
24. Furue K, Ulzii D, Tanaka Y, Ito T, Tsuji G, Kido-Nakahara M, et al. Pathogenic implication of epidermal scratch injury in psoriasis and atopic dermatitis. *J Dermatol*. (2020) 47(9):979–88. doi: 10.1111/1346-8138.15507
25. Furue K, Ito T, Tsuji G, Nakahara T, Furue M. The CCL20 and CCR6 axis in psoriasis. *Scand J Immunol*. (2020) 91(3):e12846. doi: 10.1111/sji.12846
26. Bollag WB, Aitkens L, White J, Hyndman KA. Aquaporin-3 in the epidermis: more than skin deep. *Am J Physiol Cell Physiol*. (2020) 318(6):C1144–53. doi: 10.1152/ajpcell.00075.2020
27. Scholz GM, Sulaiman NS, Al Baiiaty S, Kwa MQ, Reynolds EC. A novel regulatory relationship between RIPK4 and ELF3 in keratinocytes. *Cell Signal*. (2016) 28(12):1916–22. doi: 10.1016/j.cellsig.2016.09.006
28. Kim Y, Park JY, Kim H, Chung DK. Differential role of lipoteichoic acids isolated from *Staphylococcus aureus* and *Lactobacillus plantarum* on the aggravation and alleviation of atopic dermatitis. *Microb Pathog*. (2020) 147:104360. doi: 10.1016/j.micpath.2020.104360
29. Meyer N, Zimmermann M, Bürgler S, Bassin C, Woehrl S, Moritz K, et al. IL-32 is expressed by human primary keratinocytes and modulates keratinocyte apoptosis in atopic dermatitis. *J Allergy Clin Immunol*. (2010) 125 (4):858–65.e10. doi: 10.1016/j.jaci.2010.01.016
30. Morrison G, Kilanowski F, Davidson D, Dorin J. Characterization of the mouse beta defensin 1, Defb1, mutant mouse model. *Infect Immun*. (2002) 70(6):3053–60. doi: 10.1128/iai.70.6.3053-3060.2002
31. Rojahn TB, Vorstandlechner V, Krausgruber T, Bauer WM, Alkon N, Bangert C, et al. Persistence of mature dendritic cells, TH2A, and Tc2 cells characterize clinically resolved atopic dermatitis under IL-4Rα blockade. *J Allergy Clin Immunol*. (2020) 146(5):1056–69. doi: 10.1016/j.jaci.2020.03.041
32. Kim J, Lee J, Kim HJ, Kameyama N, Nazarian R, Der E, et al. Single-cell transcriptomics applied to emigrating cells from psoriasis elucidate pathogenic versus regulatory immune cell subsets. *J Allergy Clin Immunol*. (2021) 148(5):1281–92. doi: 10.1016/j.jaci.2021.04.021
33. Black AP, Ardern-Jones MR, Kasprowicz V, Bowness P, Jones L, Bailey AS, et al. Human keratinocyte induction of rapid effector function in antigen-specific memory CD4 + and CD8+ T cells. *Eur J Immunol*. (2007) 37 (6):1485–93. doi: 10.1002/eji.200636915
34. Furue K, Yamamura K, Tsuji G, Mitoma C, Uchi H, Nakahara T, et al. Highlighting interleukin-36 signalling in plaque psoriasis and pustular psoriasis. *Acta Derm Venereol*. (2018) 98(1):5–13. doi: 10.2340/00015555-2808
35. Zeng F, Liu H, Lu D, Liu Q, Chen H, Zheng F. Integrated analysis of gene expression profiles identifies transcription factors potentially involved in psoriasis pathogenesis. *J Cell Biochem*. (2019) 120(8):12582–94. doi: 10.1002/jcb.28525
36. Sobolev VV, Zolotorenko AD, Soboleva AG, Elkin AM, Il'ina SA, Serov DN, et al. Effects of expression of transcriptional factor AP-1 FOSL1 gene on psoriatic process. *Bull Exp Biol Med*. (2011) 150(5):632–4. doi: 10.1007/s10517-011-1208-0
37. Meng J, Chen FR, Yan WJ, Lin YK. MiR-15a-5p targets FOSL1 to inhibit proliferation and promote apoptosis of keratinocytes via MAPK/ERK pathway. *J Tissue Viability*. (2021) 30(4):544–51. doi: 10.1016/j.jtv.2021.08.006
38. Li C, Xu M, Coyne J, Wang WB, Davila ML, Wang Y, et al. Psoriasis-associated impairment of CCL27/CCR10-derived regulation leads to IL-17A/IL-22-producing skin T-cell overactivation. *J Allergy Clin Immunol*. (2021) 147(2):759–63.e9. doi: 10.1016/j.jaci.2020.05.044
39. Der E, Suryawanshi H, Morozov P, Kustagi M, Goilav B, Ranabothu S, et al. Tubular cell and keratinocyte single-cell transcriptomics applied to lupus nephritis reveal type I IFN and fibrosis relevant pathways. *Nat Immunol*. (2019) 20(7):915–27. doi: 10.1038/s41590-019-0386-1
40. Der E, Ranabothu S, Suryawanshi H, Akat KM, Clancy R, Morozov P, et al. Single cell RNA sequencing to dissect the molecular heterogeneity in lupus nephritis. *JCI Insight*. (2017) 22(8):3879. doi: 10.1172/jci.insight.93009
41. Arakawa A, Siewert K, Stöhr J, Besgen P, Kim SM, Rühl G, et al. Melanocyte antigen triggers autoimmunity in human psoriasis. *J Exp Med*. (2015) 212 (13):2203–12. doi: 10.1084/jem.20151093
42. van den Bogaard EH, Tijssen HJ, Rodijk-Olthuis D, van Houwelingen KP, Coenen MJ, Marget M, et al. Cell surface expression of HLA-Cw6 by human epidermal keratinocytes: positive regulation by cytokines, lack of correlation to a variant upstream of HLA-C. *J Invest Dermatol*. (2016) 136 (9):1903–6. doi: 10.1016/j.jid.2016.05.112
43. Bitton A, Avlas S, Reichman H, Itan M, Karo-Atar D, Azouz NP, et al. A key role for IL-13 signaling via the type 2 IL-4 receptor in experimental atopic dermatitis. *Sci Immunol*. (2020) 228(2):476–84. doi: 10.1126/sciimmunol.aaw2938
44. Amniai L, Ple C, Barrier M, de Nadai P, Marquillies P, Vorng H, et al. Natural killer cells from allergic donors are defective in their response to CCL18 chemokine. *Int J Mol Sci*. (2021) 135(8):1996–2004. doi: 10.3390/ijms22083879
45. Lin Z, Natesan V, Shi H, Hamik A, Kawanami D, Hao C, et al. A novel role of CCN3 in regulating endothelial inflammation. *J Cell Commun Signal*. (2010) 4(3):141–53. doi: 10.1007/s12079-010-0095-x
46. Eslani M, Putra I, Shen X, Hamouie J, Afsharkhamseh N, Besharat S, et al. Corneal mesenchymal stromal cells are directly antiangiogenic via PEDF and sFLT-1. *Invest Ophthalmol Vis Sci*. (2017) 58(12):5507–17. doi: 10.1167/iovs.17-22680
47. Jia Y, Morand EF, Song W, Cheng Q, Stewart A, Yang YH. Regulation of lung fibroblast activation by annexin A1. *J Cell Physiol*. (2013) 228(2):476–84. doi: 10.1002/jcp.24156
48. Meister M, Tounsi A, Gaffal E, Bald T, Papatriantafyllou M, Ludwig J, et al. Self-antigen presentation by keratinocytes in the inflamed adult skin modulates T-Cell autor-reactivity. *J Invest Dermatol*. (2015) 135 (8):1996–2004. doi: 10.1038/jid.2015.130
49. Wang HX, Sharma C, Knoblich K, Granter SR, Hemler ME. EWI-2 negatively regulates TGF-β signaling leading to altered melanoma growth and metastasis. *Cell Res*. (2015) 25(3):370–85. doi: 10.1038/cr.2015.17
50. Schauberger E, Peinhaupt M, Cazares T, Lindsley AW. Lipid mediators of allergic disease: pathways, treatments, and emerging therapeutic targets. *Curr Allergy Asthma Rep*. (2016) 16(7):48. doi: 10.1007/s11882-016-0628-3
51. Schumacher M, Schuster C, Rogon ZM, Bauer T, Caushaj N, Baars S, et al. Efficient keratinocyte differentiation strictly depends on JNK-induced soluble factors in fibroblasts. *J Invest Dermatol*. (2014) 134(5):1332–41. doi: 10.1038/jid.2013.535

52. Taniguchi K, Arima K, Masuoka M, Ohta S, Shiraishi H, Ontsuka K, et al. Periostin controls keratinocyte proliferation and differentiation by interacting with the paracrine IL-1α/IL-6 loop. *J Invest Dermatol.* (2014) 134(5):1295–304. doi: 10.1038/jid.2013.500
53. Chambers ES, Vukmanovic-Stejic M. Skin barrier immunity and ageing. *Immunology*. (2020) 160(2):116–25. doi: 10.1111/imm.13152
54. Tabib T, Morse C, Wang T, Chen W, Lafyatis R. SFRP2/DPP4 and FMO1/LSP1 define major fibroblast populations in human skin. *J Invest Dermatol.* (2018) 138(4):802–10. doi: 10.1016/j.jid.2017.09.045
55. Guerrero-Juarez CF, Dedhia PH, Jin S, Ruiz-Vega R, Ma D, Liu Y, et al. Single-cell analysis reveals fibroblast heterogeneity and myeloid-derived adipocyte progenitors in murine skin wounds. *Nat Commun*. (2019) 10(1): 650. doi: 10.1038/s41467-018-08247-x
56. Vorstandlechner V, Laggner M, Kalinina P, Haslik W, Radtke C, Shaw L, et al. Deciphering the functional heterogeneity of skin fibroblasts using single-cell RNA sequencing. *Faseb j*. (2020) 34(3):3677–92. doi: 10.1096/fj.201902001RR
57. Wang T, Zhou Z, Luo E, Zhong J, Zhao D, Dong H, et al. Comprehensive RNA sequencing in primary murine keratinocytes and fibroblasts identifies novel biomarkers and provides potential therapeutic targets for skin-related diseases. *Cell Mol Biol Lett*. (2021) 26(1):42. doi: 10.1186/s11658-021-00285-6
58. Jiang D, Rinkevich Y. Distinct fibroblasts in scars and regeneration. *Curr Opin Genet Dev*. (2021) 70:7–14. doi: 10.1016/j.gde.2021.04.005
59. Fleury S, Thibodeau J, Croteau G, Labrecque N, Aronson HE, Cantin C, et al. Sékaly: HLA-DR polymorphism affects the interaction with CD4. *J Exp Med*. (1995) 182(3):733–41. doi: 10.1084/jem.182.3.733
60. Sun J, Leahy DJ, Kavathas PB. Interaction between CD8 and major histocompatibility complex (MHC) class I mediated by multiple contact surfaces that include the alpha 2 and alpha 3 domains of MHC class I. *J Exp Med*. (1995) 182(5):1275–80. doi: 10.1084/jem.182.5.1275
61. Nguyen HN, Noss EH, Mizoguchi F, Huppertz C, Wei KS, Watts GFM, et al. Autocrine loop involving IL-6 family member LIF, LIF receptor, and STAT4 drives sustained fibroblast production of inflammatory mediators. *Immunity*. (2017) 46(2):220–32. doi: 10.1016/j.immuni.2017.01.004
62. Shan B, Shao M, Zhang Q, Hepler C, Paschoal VA, Barnes SD, et al. Perivascular mesenchymal cells control adipose-tissue macrophage accrual in obesity. *Nat Metab*. (2020) 2(11):1332–49. doi: 10.1038/s42255-020-00301-7
63. Förster R, Davalos-Misslitz AC, Rot A. CCR7 and its ligands: balancing immunity and tolerance. *Nat Rev Immunol*. (2008) 8(5):362–71. doi: 10.1038/nri2297
64. Pongratz G, Straub RH, Schölmerich J, Fleck M, Härle P. Serum BAFF strongly correlates with PsA activity in male patients only – is there a role for sex hormones? *Clin Exp Rheumatol*. (2010) 28(6):813–9.
65. Reyes LI, León F, González P, Rozas MF, Labarca C, Segovia A, et al. Dexamethasone inhibits BAFF expression in fibroblast-like synoviocytes from patients with rheumatoid arthritis. *Cytokine*. (2008) 42(2):170–8. doi: 10.1016/j.cyto.2007.12.005
66. Xu Z, Chen D, Hu Y, Jiang K, Huang H, Du Y, et al. Anatomically distinct fibroblast subsets determine skin autoimmune patterns. *Nature*. (2022) 601 (7891):118–24. doi: 10.1038/s41586-021-04221-8
67. Harms M, Habib MMW, Nemska S, Nicolò A, Gilg A, Preising N, et al. An optimized derivative of an endogenous CXCR4 antagonist prevents atopic dermatitis and airway inflammation. *Acta Pharm Sin B*. (2021) 11(9): 2694–708. doi: 10.1016/j.apsb.2020.12.005


**Conflict of Interest:** The reviewer YZ declared a shared parent affiliation with the authors BL, AL, and YC to the handling editor at the time of review.

**Publisher's Note:** All claims expressed in this article are solely those of the authors and do not necessarily represent those of their affiliated organizations, or those of the publisher, the editors and the reviewers. Any product that may be evaluated in this article, or claim that may be made by its manufacturer, is not guaranteed or endorsed by the publisher.

*Copyright © 2022 Liu, Li, Xu and Cui. This is an open-access article distributed under the terms of the Creative Commons Attribution License (CC BY). The use, distribution or reproduction in other forums is permitted, provided the original author(s) and the copyright owner(s) are credited and that the original publication in this journal is cited, in accordance with accepted academic practice. No use, distribution or reproduction is permitted which does not comply with these terms.*

frontiers | Frontiers in Surgery

MINI REVIEW
published: 16 June 2022
doi: 10.3389/fsurg.2022.934828

# Research Progress of Cell Lineage Tracing and Single-Cell Sequencing Technology in Malignant Skin Tumors

*Ang Li[1,2], Baoyi Liu[1,2], Jingkai Xu[1]* and Yong Cui[1]**

[1]Department of Dermatology, China-Japan Friendship Hospital, Beijing, China, [2]Graduate School, Peking Union Medical College and Chinese Academy of Medical Sciences, Beijing, China

Cell lineage tracing and single-cell sequencing have been widely applied in development biology and oncology to reveal the molecular mechanisms in multiple basic biological processes and the differentiation of stem cells, as well as quantify the differences between single cells. They provide new methods for in-depth understanding of the origin of tumors, the heterogeneity of tumor cells, and the drug resistance mechanism of tumors, thus inspiring new strategies for tumor treatment. In this review, we summarized the progress of cell lineage tracing technology and single-cell sequencing technology in the research of malignant melanoma and cutaneous squamous cell carcinoma, attempting to spark new ideas for further research on skin tumors.

**Keywords: cell lineage tracing, single-cell sequencing, malignant melanoma, skin tumor, cutaneous squamous cell carcinoma (cSCC)**

OPEN ACCESS

***Edited by:***
*Ronghua Yang,*
*First People's Hospital of Foshan, China*

***Reviewed by:***
*Chubin ou,*
*Macquarie University, Australia*
*Xiuzu Song,*
*Third People's Hospital of Hangzhou, China*

****Correspondence:***
*Yong Cui*
*wuhucuiyong@ vip.163.com*
*Jingkai Xu*
*jkaixu1992@163.com*

***Specialty section:***
*This article was submitted to Reconstructive and Plastic Surgery, a section of the journal Frontiers in Surgery*

***Received:*** *03 May 2022*
***Accepted:*** *01 June 2022*
***Published:*** *16 June 2022*

***Citation:***
*Li A, Liu B, Xu J and Cui Y (2022) Research Progress of Cell Lineage Tracing and Single-Cell Sequencing Technology in Malignant Skin Tumors. Front. Surg. 9:934828. doi: 10.3389/fsurg.2022.934828*

## INTRODUCTION

Cutaneous malignant melanoma (MM) and cutaneous squamous cell carcinoma (cSCC) account for a high proportion of malignant skin diseases and threaten lives. Although traditional high-throughput sequencing techniques have uncovered many disease-causing or mutated genes, cellular heterogeneity is a hallmark of tumors, and sequencing results at the average level of a population of cells mask expression differences between individual cells, thereby limiting our understanding of cancer. As technology advances, cell lineage tracing and single-cell sequencing have significantly improved explanation of tumorigenesis and pathogenesis. Among the skin malignancies, MM and SCC have higher malignancy and extensive research bases. Therefore, we reviewed the application of cell lineage tracing and single-cell sequencing technology in them.

### Cell Lineage Tracing

Multicellular organisms proliferate, divide and differentiate from a single cell, and eventually form an individual with distinct organization and different morphology. This developmental process is a lineage. Cell lineage tracing refers to the use of various methods to mark a cell, and to track and observe the proliferation, differentiation and migration of all its descendants to reveal the transition of cells from one type to another, or from one state to another, through the construction of cell trajectories and gene expression changes along the timeline (1). Lineage tracing provides an important means to study organ development, tissue damage repair, and

single-cell differentiation fate. Breakthroughs in cell lineage tracing technology, especially the inducible recombinase Cre/LoxP system, have expanded the application of cell lineage tracing technology (2) (**Figure 1**).

## Single-Cell Sequencing

Single-cell sequencing refers to the amplification and sequencing of the transcriptome or genome at the single-cell level. According to the differences in sequencing molecules, single-cell sequencing mainly includes single-cell genome sequencing, transcriptome sequencing, immunology sequencing, copy number sequencing, transposase and nuclear chromatin sequencing, as well as single-cell surface protein detection. Single-cell sequencing has been applied in the fields of reproduction, immunity, stem cell differentiation, embryonic development, and tumor heterogeneity (3). Since the first single-cell transcriptome sequencing technology was available in 2009, the emergence of multiple single-cell sequencing platforms such as Fluidigm, WaferGen, 10× Genomics, inDrop, Drpo-seq, and Illumina/Bio-Rad has greatly promoted life sciences (4–7). Lineage tracing combined with single-cell sequencing technology has begun to decipher cell fate and gene expression, providing new ideas for research on skin tumor pathogenesis, drug development, and personalized medication (8, 9).

## Cutaneous Malignant Melanoma

MM is the deadliest skin cancer. The latest global cancer statistics show that in 2020, there were 324,635 new cases of cutaneous melanoma and 57,043 deaths (10). Cutaneous MM is caused by the malignant transformation of melanocytes located at the base of the epidermis, and 30% of cutaneous MM evolve from pigmented nevus. The most commonly mutated genes in cutaneous MM include *BRAF*, *PTEN*, *NRAS*,

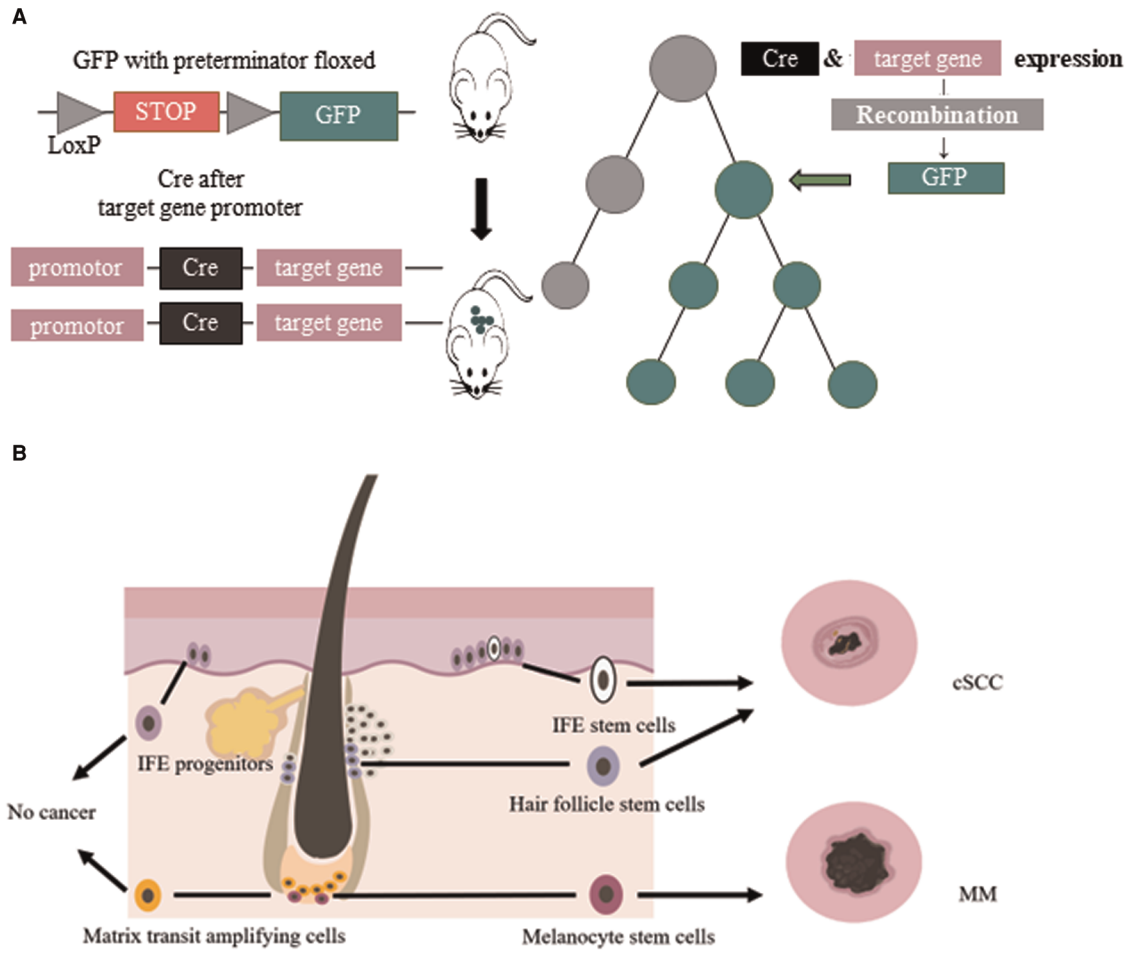


**FIGURE 1** | (**A**) Cre/LoxP system for lineage tracing: Transgenic animals with a green fluorescent protein (GFP) gene preceded by a floxed terminator, and a recombinase gene added in front of a gene specifically expressed in the target cell of interest were used. When the cell type begins to show its differentiated characteristics, the recombinase is simultaneously expressed, followed by the expression of GFP. (**B**) Cellular origins of MM and cSCC: IFE stem cells and HFSCs could develop in to cSCC. MCSCs located at the base of hair follicles could develop in to melanoma by external stimulation. Other cells, such ad IFE progenitors, do not become cancerous.

*TP53*, *CDKN2A*, *MITF*, and *BAP1* (11–13). *BRAF* mutations were discovered in about 50% of all cutaneous MM patients, about 40% of whom also carried *PTEN* mutations (12).

## Cell Lineage Tracing in MM

Lineage tracing has made valuable contributions to studying the relationship between melanocyte stem cells (MCSCs) and MM. Murine MCSCs are located in the hair follicles of the dorsal and ventral skin, both MCSCs and hair follicle stem cells undergo cyclical periods of rest (telogen) and activation (anagen) that define the hair cycle. MCSCs could proliferated to those MCSCs that do not produce melanin and mature melanocytes. Tyrosinase (Tyr) is an important molecular marker of MCSCs (14). Lineage tracing revealed that MCSCs are one of the origins of cutaneous MM, and Tyr-CreER$^{T2}$; BRaf$^{V600E}$; Pten$^{f/f}$ mice model was widely used in study MM (15–18). Kohler et al (17) identified that cutaneous MM could originate from bulge melanocytes but only after these cells have migrated out of the bulge niche and reached the lower HF region as mature melanogenic melanocytes. Moon et al. (18) identified that during melanoma development, quiescent MCSCs resists to tumorigenesis, and mature pigment-producing melanocytes might induce tumorigenesis (**Figure 1**). In the follicle cycle, the hair follicles that changing from telogen to anagen were more likely to induce tumors, while those that experiencing anagen to telogen did not present this feature. Quiescent hair follicles did not induce melanoma, but external stimuli such as UV light could activate MCSCs and lead to cutaneous MM (17). In addition, the clever combination of traditional lineage tracing and other techniques provided more precise origin tracing. Rewind, a striking new technique has been developed by Benjamin et al. (19) Combining genetic barcodes with RNA fluorescence in situ hybridization, it can directly capture rare cells in primitive subpopulations. Its application in MM directly captured drug-resistant precursor cells from V600E melanoma cells, allowing researchers to unearth some of the characteristics of such cells. In conclusion, tracing the origin of MM is of great significance for guiding and validating potential treatment options.

## Single-Cell Sequencing in Cutaneous MM

Single-cell sequencing has been widely used in studying MM, including single-cell transcriptome sequencing, single-cell exome sequencing, and single-cell immunomic sequencing (20). Tirosh et al. (21) applied single-cell transcriptome sequencing for the first time in 19 melanoma patients, analyzed the cell types of the tumor tissue, and elaborated on the expression pattern of immune cells in the tumor. The study also unveiled significant cellular heterogeneity in different regions of the tumor tissue. Analysis of tumor-associated fibroblast populations revealed that they influenced the presence of specific cellular signals and melanoma drug resistance. Since then, a multi-omics map of single-cell sequencing MM has been constructed.

Drug resistance often results in tumor recurrence, increasing financial pressure on patients, and the likelihood of death. To this end, more single-cell sequencing studies were devoted to drug resistance mechanisms in cutaneous MM (22–25). Single-cell sequencing of different MM tissues and comparison of their heterogeneity revealed the characteristics of many tumor cells and associated immune cells. An earlier study using single-cell transcriptome sequencing to analyze the cutaneous melanoma tissue of 33 human cases revealed that a tumor's T-cell signature could classify most tumors as those with a T cell exclusion program. Exclusion program was applied to samples treated with ipilimumab and anti-programmed cell death protein 1 (PD1) antibody to study its role in drug-resistant tumors (23). Single-cell transcriptome sequencing of CD8+ T cells in peripheral blood of metastatic melanoma patients who received anti-PD1 therapy revealed that the proportion of mucosa-associated invariant T cells was increased in responders (26). A Smart-seq2 study performed single-cell transcriptome sequencing of 48 tumor samples taken from biopsies of 32 patients with metastatic melanoma. In three groups of patients treated with PD1 inhibitor, anti-CTLA-4, and combination therapy, CD8+ T cells were found to be a key component of the immune checkpoint inhibitory mechanism, which is abundant in melanoma and closely related to tumor depletion. The CD8+ T cell transcription factor TCF7 can be used to assess the prognosis of immunotherapy (22). In addition, Pauken et al. (27) found melanoma-associated TM (tumor-matching CD8+ T cells, marked as NKG2D, CD39, and CX3CR1) cells in the peripheral blood of humans and mice, which also suggests that monitoring of T cells has a considerable therapeutic potential.

Combining CRISPR RNA-guided deaminase and CRISPR droplet sequencing, a study incorporated NRAS, KRAS, and MAP2K1 in the MAPK pathway of A375 melanoma cells and transferred a total of 420 sgRNAs designed for these three genes. In order to monitor the drug response to BRAF inhibitors in melanoma cells, multiple drug resistance mechanisms related to the targeted therapy of cutaneous melanoma have been discovered (25). Perturb-CITE-seq read out the single-cell transcriptome and proteome in the interaction of CRISPR-Cas9 with immune checkpoint inhibitors in melanoma cells, uncovering potential clinically relevant immune evasion mechanisms (28). Minimal residual disease (MRD) can lead to recurrence after melanoma treatment. Xenograft melanomas from BRAF-mutated patients were treated with RAF/MEK inhibition followed by the induction of an MRD model. Distinct cell subsets identified by scRNA-seq revealed that the drug-resistant state of cells within MRDs could be driven by adaptive, non-mutational events independent of mutation (29). Compared to non-acral cutaneous melanomas, acral melanoma had a lower immune infiltrate with fewer effector CD8 T cells and NK cells and a near-complete absence of γδ T cells (30) (**Figure 2**).

These single-cell sequencing studies have uncovered heterogeneous characteristics of tumors and associated immune cells, revealing mechanisms of immune evasion that are extremely beneficial in the search for novel therapies.

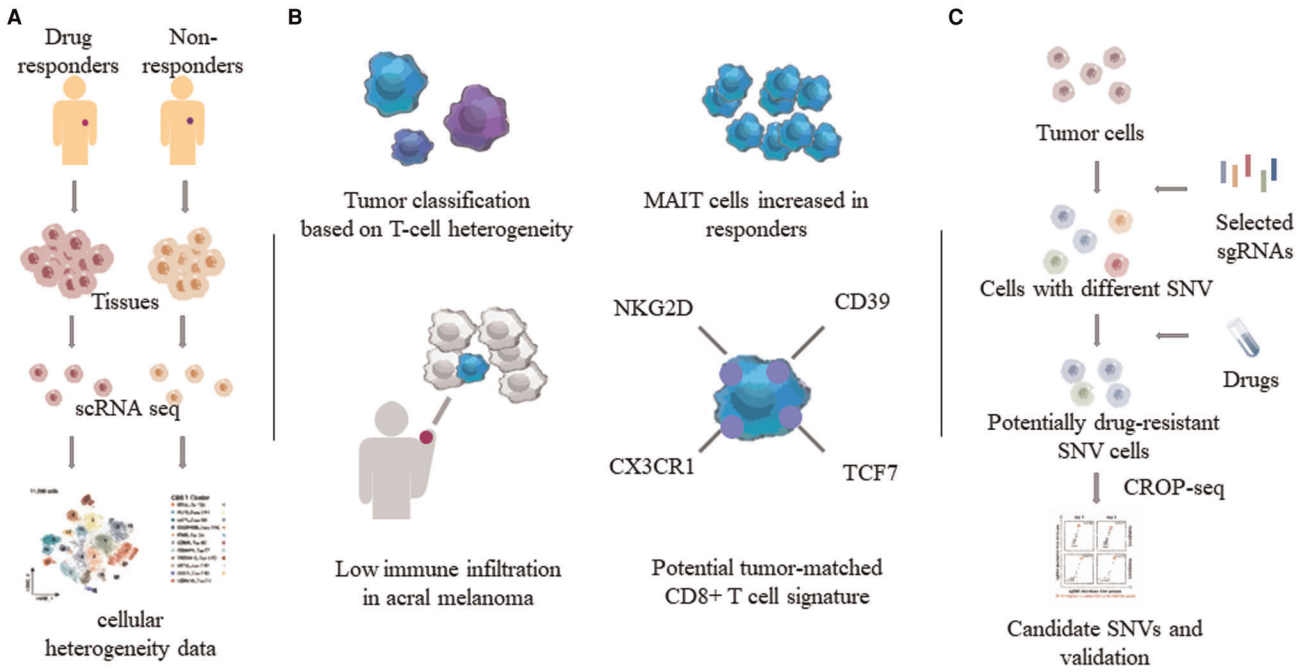


**FIGURE 2** | Heterogeneity of tumor and immune cells by single-cell sequencing. Through single-cell sequencing of different tumor tissues and related tissues such as blood, the characteristics of different tumors and tumor-related immune cells, especially T cells, were obtained. (**A**) Determination of tumor heterogeneity using single-cell sequencing. (**B**) T cell properties in MM. MAIT: mucosa-associated invariant T cells. (**C**) One combination of the CRISPR/Cas system and single-cell sequencing. SNVs: single nucleotide variants.

## Cutaneous Squamous Cell Carcinoma

Cutaneous squamous cell carcinoma (cSCC) is the second most common non-melanoma tumor among skin malignancies, following only basal cell carcinoma (31). Mutated genes associated with cSCC include *TP53*, *HRAS*, *NRAS*, *KRAS*, *CDKN2A*, *NOTCH1*, *NOTCH2*, *PIK3CA*, *TGFβ*, *PTEN*, *BRAF*, *EGFR*, etc (32). Cell lineage tracing and multiple single-cell omics studies have contributed to the tumor origin and etiology of cSCC.

### Cell Lineage Tracing in cSCC

The tumor origin theory is a major focus of current research and has important implications for the etiology of tumors. The development of single-cell lineage tracing has facilitated the traceability of cutaneous SCC. Studies have shown that cSCC could originate from interfollicular epidermis (IFE) stem cells and hair follicle stem cells (HFSCs), but not from hair follicle transient amplifying cells (TACs) or epidermal IFE precursor cells, and the malignant degree of cutaneous SCC tumors of different origins varies (33–36). $KRas^{G12D}$ mutation activation and Tp53 deletion are the most common gene mutations in cSCC. K5 and K14 are marks of IFE, HFSCs have K19, Lgr5 and Sox9 as marks, and shh can mark TACs. Cross-specific driver mice were crossed with $Kras^{G12D}$ mutant-activated mice and Tp53-null mice. In addition, cutaneous SCCs derived from HFSCs were prone to epithelial mesenchymal transition (EMT) and more invasive (36) (**Figure 1**). In K14-creER; $KRas^{G12D}$; $Tp53^{f/f}$ mice, the mesenchymal marker Vimentin of IFE stem cell-derived highly differentiated SCCs was restricted to the tumor mesenchymal region, and the expression of epidermal markers, epithelial cell adhesion molecule (Epcam) and E-cadherin, increased. However, the SCCs derived from HFSCs of Lgr5-creER; $KRas^{G12D}$; $p53^{f/f}$ mice expressed Vimentin in all intertumoral tissues, the expression of Epcam and E-cadherin decreased, and the tumors were more prone to EMT and had a higher malignancy (36, 37).

### Single-Cell Sequencing in cSCC

Sequencing studies at the whole-cell level, such as transcriptome sequencing and chromatin accessibility sequencing, have found some potential targets for tumor therapy, but there are still huge challenges in the observation of tumor heterogeneity (36, 38). By analyzing whole transcriptome profiles at single-cell resolution, the heterogeneity of tumor cells was revealed. Annotating different cell types from tumor tissues, genes belonging to the S100 gene family, SPRR gene family, and FABP5 are highly expressed in cSCC cells, and these pathways may be targets for future disease treatments (39).

The immune status of T cells is associated with the pathogenesis of SCC. In 2020, Ji et al. (40) used a combination of single-cell RNA-seq, spatial transcriptome sequencing, multiplex ion beam imaging, CRISPR screening and other methods to comprehensively analyze and study

cSCC. The study found four tumor cell subsets, three of which covered the normal epidermal state, and one formed by tumor-specific keratinocytes was localized in the fibrovascular microenvironment. Multiple potential immunosuppressive features, including co-localization of Tregs with CD8 cells in the compartmentalized tumor stroma, were confirmed. Furthermore, they identified the important role of specific tumor subpopulation-enriched gene networks in tumorigenesis through single-cell characterization of tumor cell xenografts in humans and in vivo CRISPR screening. The study clarified the spatial niche of the interaction between cSCC and stromal cell subsets and the gene network involved in cancer, which provides a basis for the study of the mechanism and treatment of cSCC. Single-cell TCR sequencing of cSCC on immunosuppressed patients receiving organ transplantation and on patients with normal immunity showed that transplant-associated SCC had a higher regulatory T cell/cytotoxic T cell ratio, which facilitated its evasion in a special immune microenvironment (41). An scRNA-seq-based study on the cSCC mouse model found that tumor-initiating stem cells selectively acquired CD80 and could directly inhibit the activity of cytotoxic T cells, suggesting an important role in activating immune checkpoint therapy (42). scRNA-seq was performed on cSCC patients before and after anti-PD-1 treatment, and it was found that pre-existing tumor-specific T cells may have limited reinvigoration capacity, and that T cell responses to checkpoint blockade were dependent on the recruitment of novel T cells (43). CD276 is highly expressed on the surface of head and neck SCCs and acts as an immune checkpoint to allow cancer stem cells to evade surveillance by the immune system. Murine models combined with single-cell sequencing showed that blocking CD276 reduced epithelial-mesenchymal transition (44).

Tumor evasion characteristics and immune cell status discovered by single-cell sequencing studies surrounding tumor tissue provide direction for targeted therapy.

## SUMMARY

With the advent of cell lineage tracing and single-cell sequencing, the origins and development of many diseases have been gradually uncovered. In tumor research, lineage tracing reveals the origin and clonal evolution of tumor cells, providing novel tumor therapeutic strategies targeting tumor stem cells. And single-cell sequencing is pivotal for understanding tumor heterogeneity, tumor microenvironment, and tumor resistance mechanisms in immunotherapy (45). Although, the application of these two techniques in skin tumors is limited by high cost, equipment, and cell capture requirements, etc., they still breed more attractive and promising research.

## AUTHOR CONTRIBUTIONS

AL: literature review and writing and editing of the paper. JX: literature review and writing of the paper. All authors contributed to the article and approved the submitted version.

## FUNDING

This work was supported by the scientific and technological innovation leading talents of "Ten Thousand Talents Program" (2018-WRJH-1), the discipline construction project of Peking Union Medical College (xhxk201903) and the fellowship of China Postdoctoral Science Foundation(2021M703654).

## REFERENCES

1. Kretzschmar K, Watt FM. Lineage tracing. *Cell*. (2012) 148(1–2):33–45. doi: 10.1016/j.cell.2012.01.002
2. Pei W, Wang X, Rossler J, Feyerabend TB, Hofer T, Rodewald HR. Using Cre-recombinase-driven Polylox barcoding for in vivo fate mapping in mice. *Nat Protoc*. (2019) 14(6):1820–40. doi: 10.1038/s41596-019-0163-5
3. Yasen A, Aini A, Wang H, Li W, Zhang C, Ran B, et al. Progress and applications of single-cell sequencing techniques. *Infect Genet Evol*. (2020) 80:104198. doi: 10.1016/j.meegid.2020.104198
4. Tang F, Barbacioru C, Wang Y, Nordman E, Lee C, Xu N, et al. mRNA-Seq whole-transcriptome analysis of a single cell. *Nat Methods*. (2009) 6 (5):377–82. doi: 10.1038/nmeth.1315
5. Zhang X, Li T, Liu F, Chen Y, Yao J, Li Z, et al. Comparative analysis of droplet-based ultra-high-throughput single-cell RNA-seq systems. *Mol Cell*. (2019) 73(1):130–42.e5. doi: 10.1016/j.molcel.2018.10.020
6. Di L, Fu Y, Sun Y, Li J, Liu L, Yao J, et al. RNA sequencing by direct tagmentation of RNA/DNA hybrids. *Proc Natl Acad Sci U S A*. (2020) 117 (6):2886–93. doi: 10.1073/pnas.1919800117
7. Gao C, Zhang M, Chen L. The comparison of two single-cell sequencing platforms: BD rhapsody and 10x genomics chromium. *Curr Genomics*. (2020) 21(8):602–9. doi: 10.2174/1389202921999200625220812
8. Pei W, Feyerabend TB, Rossler J, Wang X, Postrach D, Busch K, et al. Polylox barcoding reveals haematopoietic stem cell fates realized in vivo. *Nature*. (2017) 548(7668):456–60. doi: 10.1038/nature23653
9. Pei W, Shang F, Wang X, Fanti AK, Greco A, Busch K, et al. Resolving fates and single-cell transcriptomes of hematopoietic stem cell clones by PolyloxExpress barcoding. *Cell Stem Cell*. (2020) 27(3):383–95 e8. doi: 10.1016/j.stem.2020.07.018
10. Sung H, Ferlay J, Siegel RL, Laversanne M, Soerjomataram I, Jemal A, et al. Global cancer statistics 2020: GLOBOCAN estimates of incidence and mortality worldwide for 36 cancers in 185 countries. *CA Cancer J Clin*. (2021) 71(3):209–49. doi: 10.3322/caac.21660
11. Hayward NK, Wilmott JS, Waddell N, Johansson PA, Field MA, Nones K, et al. Whole-genome landscapes of major melanoma subtypes. *Nature*. (2017) 545(7653):175–80. doi: 10.1038/nature22071
12. Vultur A, Herlyn M. SnapShot: melanoma. *Cancer Cell*. (2013) 23(5):706-e1. doi: 10.1016/j.ccr.2013.05.001
13. Ribero S, Glass D, Bataille V. Genetic epidemiology of melanoma. *Eur J Dermatol*. (2016) 26(4):335–9. doi: 10.1684/ejd.2016.2787
14. Han R, Baden HP, Brissette JL, Weiner L. Redefining the skin's pigmentary system with a novel tyrosinase assay. *Pigment Cell Res*. (2002) 15(4):290–7. doi: 10.1034/j.1600-0749.2002.02027.x
15. Dankort D, Curley DP, Cartlidge RA, Nelson B, Karnezis AN, Damsky WE, et al. Braf(V600E) cooperates with Pten loss to induce metastatic melanoma. *Nat Genet*. (2009) 41(5):544–52. doi: 10.1038/ng.356
16. Soengas MS, Patton EE. Location, location, location: spatio-temporal cues that define the cell of origin in melanoma. *Cell Stem Cell*. (2017) 21 (5):559–61. doi: 10.1016/j.stem.2017.10.009
17. Kohler C, Nittner D, Rambow F, Radaelli E, Stanchi F, Vandamme N, et al. Mouse cutaneous melanoma induced by mutant BRaf arises from expansion

and dedifferentiation of mature pigmented melanocytes. *Cell Stem Cell*. (2017) 21(5):679–93.e6. doi: 10.1016/j.stem.2017.08.003
18. Moon H, Donahue LR, Choi E, Scumpia PO, Lowry WE, Grenier JK, et al. Melanocyte stem cell activation and translocation initiate cutaneous melanoma in response to UV exposure. *Cell Stem Cell*. (2017) 21 (5):665–78.e6. doi: 10.1016/j.stem.2017.09.001
19. Emert BL, Cote CJ, Torre EA, Dardani IP, Jiang CNL, Jain N, et al. Variability within rare cell states enables multiple paths toward drug resistance. *Nat Biotechnol*. (2021) 39(7):865–76. doi: 10.1038/s41587-021-00837-3
20. Binder H, Schmidt M, Loeffler-Wirth H, Mortensen LS, Kunz M. Melanoma single-cell biology in experimental and clinical settings. *J Clin Med*. (2021) 10(3):506. doi: 10.3390/jcm10030506
21. Tirosh I, Izar B, Prakadan SM, Wadsworth 2nd MH, Treacy D, Trombetta JJ, et al. Dissecting the multicellular ecosystem of metastatic melanoma by single-cell RNA-seq. *Science*. (2016) 352(6282):189–96. doi: 10.1126/science.aad0501
22. Sade-Feldman M, Yizhak K, Bjorgaard SL, Ray JP, de Boer CG, Jenkins RW, et al. Defining T cell states associated with response to checkpoint immunotherapy in melanoma. *Cell*. (2018) 175(4):998–1013.e20. doi: 10.1016/j.cell.2018.10.038
23. Jerby-Arnon L, Shah P, Cuoco MS, Rodman C, Su MJ, Melms JC, et al. A cancer cell program promotes T cell exclusion and resistance to checkpoint blockade. *Cell*. (2018) 175(4):984–97.e24. doi: 10.1016/j.cell.2018.09.006
24. Li H, van der Leun AM, Yofe I, Lubling Y, Gelbard-Solodkin D, van Akkooi ACJ, et al. Dysfunctional CD8 T cells form a proliferative, dynamically regulated compartment within human melanoma. *Cell*. (2019) 176 (4):775–89.e18. doi: 10.1016/j.cell.2018.11.043
25. Jun S, Lim H, Chun H, Lee JH, Bang D. Single-cell analysis of a mutant library generated using CRISPR-guided deaminase in human melanoma cells. *Commun Biol*. (2020) 3(1):154. doi: 10.1038/s42003-020-0888-2
26. De Biasi S, Gibellini L, Lo Tartaro D, Puccio S, Rabacchi C, Mazza EMC, et al. Circulating mucosal-associated invariant T cells identify patients responding to anti-PD-1 therapy. *Nat Commun*. (2021) 12(1):1669. doi: 10.1038/s41467-021-21928-4
27. Pauken KE, Shahid O, Lagattuta KA, Mahuron KM, Luber JM, Lowe MM, et al. Single-cell analyses identify circulating anti-tumor CD8 T cells and markers for their enrichment. *J Exp Med*. (2021) 218(4):e20200920. doi: 10.1084/jem.20200920
28. Bigot J, Lalanne AI, Lucibello F, Gueguen P, Houy A, Dayot S, et al. Splicing patterns in SF3B1-mutated Uveal melanoma generate shared immunogenic tumor-specific neoepitopes. *Cancer Discov*. (2021) 11(8):1938–51. doi: 10.1158/2159-8290.CD-20-0555
29. Rambow F, Rogiers A, Marin-Bejar O, Aibar S, Femel J, Dewaele M, et al. Toward minimal residual disease-directed therapy in melanoma. *Cell*. (2018) 174(4):843–55 e19. doi: 10.1016/j.cell.2018.06.025
30. Li J, Smalley I, Chen Z, Wu JY, Phadke MS, Teer JK, et al. Single cell characterization of the cellular landscape of acral melanoma identifies novel targets for immunotherapy. *Clin Cancer Res*. (2022) 28(10):2131–46. doi: 10.1158/1078-0432.CCR-21-3145
31. Que SKT, Zwald FO, Schmults CD. Cutaneous squamous cell carcinoma: Incidence, risk factors, diagnosis, and staging. *J Am Acad Dermatol*. (2018) 78(2):237–47. doi: 10.1016/j.jaad.2017.08.059
32. Pickering CR, Zhou JH, Lee JJ, Drummond JA, Peng SA, Saade RE, et al. Mutational landscape of aggressive cutaneous squamous cell carcinoma. *Clin Cancer Res*. (2014) 20(24):6582–92. doi: 10.1158/1078-0432.CCR-14-1768
33. Lapouge G, Youssef KK, Vokaer B, Achouri Y, Michaux C, Sotiropoulou PA, et al. Identifying the cellular origin of squamous skin tumors. *Proc Natl Acad Sci U S A*. (2011) 108(18):7431–6. doi: 10.1073/pnas.1012720108
34. White AC, Tran K, Khuu J, Dang C, Cui Y, Binder SW, et al. Defining the origins of Ras/p53-mediated squamous cell carcinoma. *Proc Natl Acad Sci U S A*. (2011) 108(18):7425–30. doi: 10.1073/pnas.1012670108
35. Biddle A, Liang X, Gammon L, Fazil B, Harper LJ, Emich H, et al. Cancer stem cells in squamous cell carcinoma switch between two distinct phenotypes that are preferentially migratory or proliferative. *Cancer Res*. (2011) 71(15):5317–26. doi: 10.1158/0008-5472.CAN-11-1059
36. Latil M, Nassar D, Beck B, Boumahdi S, Wang L, Brisebarre A, et al. Cell-type-specific chromatin states differentially prime squamous cell carcinoma tumor-initiating cells for epithelial to mesenchymal transition. *Cell Stem Cell*. (2017) 20(2):191–204 e5. doi: 10.1016/j.stem.2016.10.018
37. Sanchez-Danes A, Blanpain C. Deciphering the cells of origin of squamous cell carcinomas. *Nat Rev Cancer*. (2018) 18(9):549–61. doi: 10.1038/s41568-018-0024-5
38. Sastre-Perona A, Hoang-Phou S, Leitner MC, Okuniewska M, Meehan S, Schober M. De Novo PITX1 expression controls bi-stable transcriptional circuits to govern self-renewal and differentiation in squamous cell carcinoma. *Cell Stem Cell*. (2019) 24(3):390–404 e8. doi: 10.1016/j.stem.2019.01.003
39. Yan G, Li L, Zhu S, Wu Y, Liu Y, Zhu L, et al. Single-cell transcriptomic analysis reveals the critical molecular pattern of UV-induced cutaneous squamous cell carcinoma. *Cell Death Dis*. (2021) 13(1):23. doi: 10.1038/s41419-021-04477-y
40. Ji AL, Rubin AJ, Thrane K, Jiang S, Reynolds DL, Meyers RM, et al. Multimodal analysis of composition and spatial architecture in human squamous cell carcinoma. *Cell*. (2020) 182(2):497–514 e22. doi: 10.1016/j.cell.2020.05.039
41. Frazzette N, Khodadadi-Jamayran A, Doudican N, Santana A, Felsen D, Pavlick AC, et al. Decreased cytotoxic T cells and TCR clonality in organ transplant recipients with squamous cell carcinoma. *NPJ Precis Oncol*. (2020) 4:13. doi: 10.1038/s41698-020-0119-9
42. Miao Y, Yang H, Levorse J, Yuan S, Polak L, Sribour M, et al. Adaptive immune resistance emerges from tumor-initiating stem cells. *Cell*. (2019) 177(5):1172–86 e14. doi: 10.1016/j.cell.2019.03.025
43. Yost KE, Satpathy AT, Wells DK, Qi Y, Wang C, Kageyama R, et al. Clonal replacement of tumor-specific T cells following PD-1 blockade. *Nat Med*. (2019) 25(8):1251–9. doi: 10.1038/s41591-019-0522-3
44. Wang C, Li Y, Jia L, Kim JK, Li J, Deng P, et al. CD276 expression enables squamous cell carcinoma stem cells to evade immune surveillance. *Cell Stem Cell*. (2021) 28(9):1597–613.e7. doi: 10.1016/j.stem.2021.04.011
45. Bowling S, Sritharan D, Osorio FG, Nguyen M, Cheung P, Rodriguez-Fraticelli A, et al. An engineered CRISPR-Cas9 mouse line for simultaneous readout of lineage histories and gene expression profiles in single cells. *Cell*. (2020) 181(6):1410–22 e27. doi: 10.1016/j.cell.2020.04.048

**Conflict of Interest:** The authors declare that the research was conducted in the absence of any commercial or financial relationships that could be construed as a potential conflict of interest.

**Publisher's Note:** All claims expressed in this article are solely those of the authors and do not necessarily represent those of their affiliated organizations, or those of the publisher, the editors and the reviewers. Any product that may be evaluated in this article, or claim that may be made by its manufacturer, is not guaranteed or endorsed by the publisher.

*Copyright © 2022 Li, Liu, Xu and Cui. This is an open-access article distributed under the terms of the Creative Commons Attribution License (CC BY). The use, distribution or reproduction in other forums is permitted, provided the original author(s) and the copyright owner(s) are credited and that the original publication in this journal is cited, in accordance with accepted academic practice. No use, distribution or reproduction is permitted which does not comply with these terms.*

frontiers | Frontiers in Surgery

REVIEW
published: 23 June 2022
doi: 10.3389/fsurg.2022.888956

# Global Trends of Stem Cell Precision Medicine Research (2018–2022): A Bibliometric Analysis

*Muge Liu, Fan Yang and Yingbin Xu**

*Department of Burn Surgery, The First Affiliated Hospital of Sun Yat-Sen University, Guangzhou, China*

**Background:** Stem cells are a group of cells that can self-renew and have multiple differentiation capabilities. Shinya Yamanaka first discovered a method to convert somatic cells into pluripotent stem cells in 2006. Stem cell therapy can be summarized into three aspects (regenerative treatment, therapy targeted at stem cells, and establishment of disease models). Disease models are mainly established by induced pluripotent stem cells, and the research of stem cell precision medicine has been promising in recent years. Based on the construction of 3D, patient-specific disease models from pluripotent induced stem cells, proper research on disease development and treatment prognosis can be realized. Bibliometric analysis is an efficient way to quickly understand global trends and hotspots in this field.

**Methods:** A literature search of stem cell precision medicine research from 2018 to 2022 was carried out using the Web of Science Core Collection.VOSviewer, R-bibliometrix, and CiteSpace software programs were employed to perform the bibliometric analysis.

**Results:** A total of 552 publications were retrieved from 2018 to 2022. Annual publication outputs trended upward and reached a peak of 172 in 2021. The United States contributed the most publications (160, 29.0%) to the field, followed by China (63, 11.4%) and Italy (60, 10.9%). International academic collaborations were active. CANCERS was considered the most productive journal with 18 documents. NATURE was the most co-cited journal with 1860 times citations. The most cited document was entitled "Induced Pluripotent Stem Cells for Cardiovascular Disease Modeling and Precision Medicine: A Scientific Statement From the American Heart Association" with 9 times local citations. " precision medicine" ($n = 89$, 12.64%), "personalized medicine" ($n = 72$, 10.23%), "stem cells" ($n = 43$, 4.40%), and "induced pluripotent stem cells" ($n = 41$, 5.82%), "cancer stem cells" ($n = 31$, 4%), "organoids" ($n = 26$, 3.69%) were the top 6 frequent keywords.

OPEN ACCESS

***Edited by:***
*Jiliang Zhou,*
*Georgia Health Sciences University, United States*

***Reviewed by:***
*Guanghua Guo,*
*The First Affiliated Hospital of Nanchang University, China*
*Chen Xiaodong,*
*The First People's Hospital of Foshan, China*

***Correspondence:**
*Yingbin Xu*
*333xyb@163.com*

***Specialty section:***
*This article was submitted to Reconstructive and Plastic Surgery, a section of the journal Frontiers in Surgery*

***Received:*** *03 March 2022*
***Accepted:*** *30 May 2022*
***Published:*** *23 June 2022*

***Citation:***
*Liu M, Yang F and Xu Y (2022) Global Trends of Stem Cell Precision Medicine Research (2018–2022): A Bibliometric Analysis. Front. Surg. 9:888956. doi: 10.3389/fsurg.2022.888956*

**Abbreviations:** BMP, bone morphogenetic protein; CagA, cytotoxin-associated gene A; CHD1, Chromodomain-Helicase DNA-binding 1; c-Met, MET Proto-Oncogene; c-Myc, MYC Proto-Oncogene; CRISPR, clustered regularly interspaced short palindromic repeats; DNA, deoxyribonucleic acid; EGF, epidermal growth factor; FGF, fibroblast growth factor; IF, impact factor; iPSC, induced pluripotent stem cell; Klf4, Kruppel Like Factor 4; LIN28, Lin-28 Homolog; MCP, inter-country collaboration; MSC, mesenchymal stem cell; NANOG, Nanog Homeobox; Oct, octamer-binding transcription factor; RNA, ribonucleic acid; RPMI, Roswell Park Memorial Institute; SCP, intra-country collaboration; Sox2, SRY (sex determining region Y)-box 2; SPINK1: serine protease inhibitor Kazal-type 1; SPOP, speckle-type POZ protein; TEER, trans-epithelial electrical resistance; TMPRSS2-ERG, transmembrane protease serine 2:v-ets erythroblastosis virus E26 oncogene homolog; WNT, wingless-type MMTV integration site family; WoSCC, the web of science core collection

**Conclusion:** The present study performs a comprehensive investigation concerning stem cell precision medicine (2018–2022) for the first time. This research field is developing, and a deeper exploration of 3D patient-specific organoid disease models is worth more research in the future.

**Keywords: induced pluripotent stem cells (iPSCs), precision medicine, personalized medicine, organoids, bibliometric analysis**

## INTRODUCTION

Stem cells are undifferentiated or partially differentiated cells with the ability to self-renew and multiple differentiation (1). Fertilized eggs belong to totipotent stem cells. Pluripotent stem cells exist in blastocysts with 50–150 cells in mammals and differentiate into all cell types required by the body during growth and development, called embryonic stem cells (2). Adult stem cells, including hematopoietic stem cells, basal skin cells, and mesenchymal stem cells, are located in specific ecological niches in the body, like bone marrow and gonads, which can differentiate into several kinds of somatic cells (3). Stem cells can be classified as totipotent stem cells (fertilized eggs), pluripotent stem cells (embryonic stem cells), multipotent stem cells (mesenchymal stem cells), and unipotent stem cells (basal cells) by the differentiation potency.

Somatic cell nuclear transfer is the early way to create pluripotent stem cells, by which the cloned sheep, Dolly, was born (4). Shinya Yamanaka pioneered the development of induced pluripotent stem cells in 2006, using a combination of Oct3/4, Sox2, c-Myc, and Klf4 to convert mouse fibroblasts into pluripotent stem cells (5). The same chemical factors successfully transformed human fibroblasts into pluripotent stem cells (6). Junying Yu et al. optimized the combination from Oct3/4, Sox2, c-Myc, Klf4 to Oct4, Sox2, NANOG, LIN28, and successfully produced pluripotent stem cells in 2007 (7). The clinical application of stem cells can be summarized in three aspects: regenerative treatment, therapy targeted at stem cells, and disease model for research and drug development.

Using stem cells to replace the body's dysfunctional tissue has been studied since 1963 when bone-marrow cells were reported to have saved an animal from lethal radiation. Embryonic stem cells helped treat retinal diseases (8), Parkinson's disease (9), Huntington's disease (10), spinal cord injury (11), myocardial infarction (12), and type 1 diabetes (13–15) in preclinical studies. In clinical studies, embryonic stem cells have been used for cell therapy in patients with retinal diseases, and severe ischemic left ventricular dysfunction (16–20), which is safe in the medium and long term. The iPSC was transplanted into animal models for treating Parkinson's disease (21), Huntington's disease (22), Duchenne muscular dystrophy (23), Fanconi anemia (24), and hemophilia A (25) in preclinical studies. In clinical studies, induced pluripotent stem cells were also used to treat retinal diseases, but the efficacy and safety were uncertain (26). Besides self-renewal and differentiation, stem cells can regulate the activities of surrounding cells by paracrine factors. However, due to the high variability of the stem cell population, the regulatory mechanism has not been clarified. Another strategy of stem cell therapy is to activate the proliferation and differentiation potential of somatic stem cells, such as altering erythropoietin progenitor cell activity. Specific disease models can be constructed by stem cells, which are promising in disease research and new drug development. These disease models include tumors, cardiovascular disease, and nervous system disease. These disease models are mainly completed by induced pluripotent stem cells.

Precision medicine (27) is an emerging medical model which provides personalized medical diagnosis, treatment, and care for specific patients after considering their genetic information, physiological/pathological information, living environment, and many other aspects. Compared with the traditional one-size-fits-all approach, more attention is paid to the influence of individual differences on disease development. The research on stem cell precision medicine shows a significant development in recent years. Stem cell technology, especially induced pluripotent stem cell technology, gradually matures. Researchers can establish disease/patient-specific models to accurately reflect human disease mechanisms and the individual difference in drug responses based on the pluripotent and reproducible human stem cells. The realization of precision medicine is an inherent advantage that traditional disease models cannot obtain. Disease models have been established using induced pluripotent stem cells by the clustered regularly interspaced short palindromic repeats (CRISPR)/CRISPR-associated system (CRISPR-Cas9) genome engineering tool, including cardiomyopathy, valvular disease, primary microencephaly, cystic liver fibrosis, colorectal cancer, etc. Nevertheless, stem cell-based disease models are still in the early stages of development. 3D organoid models can accurately simulate organ morphology, form tissue-like architecture, and realize organ/disease development in vitro organ culture system. More complex 3D organoid multisystem models are still in development, including the addition of circulatory systems and lymphatic systems.

As an effective confirmed method of analyzing the dynamics and trends of research in a specific field, bibliometrics has rapidly developed in past decades (28). Unlike the conventional measurement of scientific documents, bibliometrics is a prevailing tool that can comprehensively investigate existing studies in a specific field. It can be easily employed with big data accessible to the public, such as Web of Science, PubMed, and MEDLINE. Statistical tools, including R-bibliometrix, VOSviewer, CiteSpace, BICOMB, and BibExcel, are integrated as an automatic workflow to carry out multistep bibliometric

analyses. In prior studies, bibliometric analysis has been successfully performed in various disciplines, especially in environmental science and medicine (29).

In this study, we aim to explore the following objects in the field of stem cell precision medicine: 1. productivity of publications; 2. productive countries/regions; 3. leading affiliations; 4. influential journals; 5. key documents/references; and 6. key words. With the technology of bibliometric analysis, we can conduct a quick review of the research process of stem cell precision medicine in the last five years to provide reference value to clinicians and scholars in future studies.

# METHOD

## Data Collection

We carried out the Web of Science database to conduct a comprehensive literature retrieval for 2018 to 2022. The process was limited within the Web of Science Core Collection, and no restriction on the edition. The retrieval strategy was as follows: Topic =(" stem cell*" or "pluripotent stem cell*" or "PSC*" or "MSC*" or "iPSC*"). Related Documents, including" articles" and "reviews", were selected. All search was performed on a single day, January 22, 2022. Documents were downloaded as original data from WoS for further bibliometric analysis.

## Statistical Analysis

Indicators, including the annual publications, countries, affiliations, and languages, were extracted from the WoS and managed using Microsoft Excel for Mac 2018 edition 16.18 (181014). The R-bibliometrix was performed to sort the countries and regions, institutions, individuals, and citations in the order of publications productivity. Impact Factor was obtained from WoS and consistent with the latest vision of Journal Citation Reports 2020 as a measurement of journal analysis. To better understand the academic relationships among different countries, we used VOSviewer (1.6.16) to visualize the intensity of collaborations with the lines connecting countries. The "treemap" function of the R-bibliometrics was employed to sort the author's keywords in the order of frequency. CiteSpace (5.7.R5) was used to conduct the burst of reference citations from 2018 to 2022, and the minimum duration of burst was set for one year.

# RESULTS

## Annual Output

The total number of publications on stem cell precision medicine research was 552 from 2018 to 2022, of which articles and reviews accounted for 280 (50.72%) and 272 (49.28%), respectively. The languages of publications were mainly English 544 (98.55%) and other languages including French, German, etc. The annual outputs of stem cell precision medicine publications are shown in **Figure 1**. This period's continuously increasing trends were shown with the peak point at 2021 of 172.

## Country/Region Analysis

We identified 50 countries that contributed to stem cell precision medicine research. The top 10 productive countries were selected and presented in **Table 1**. The United States was

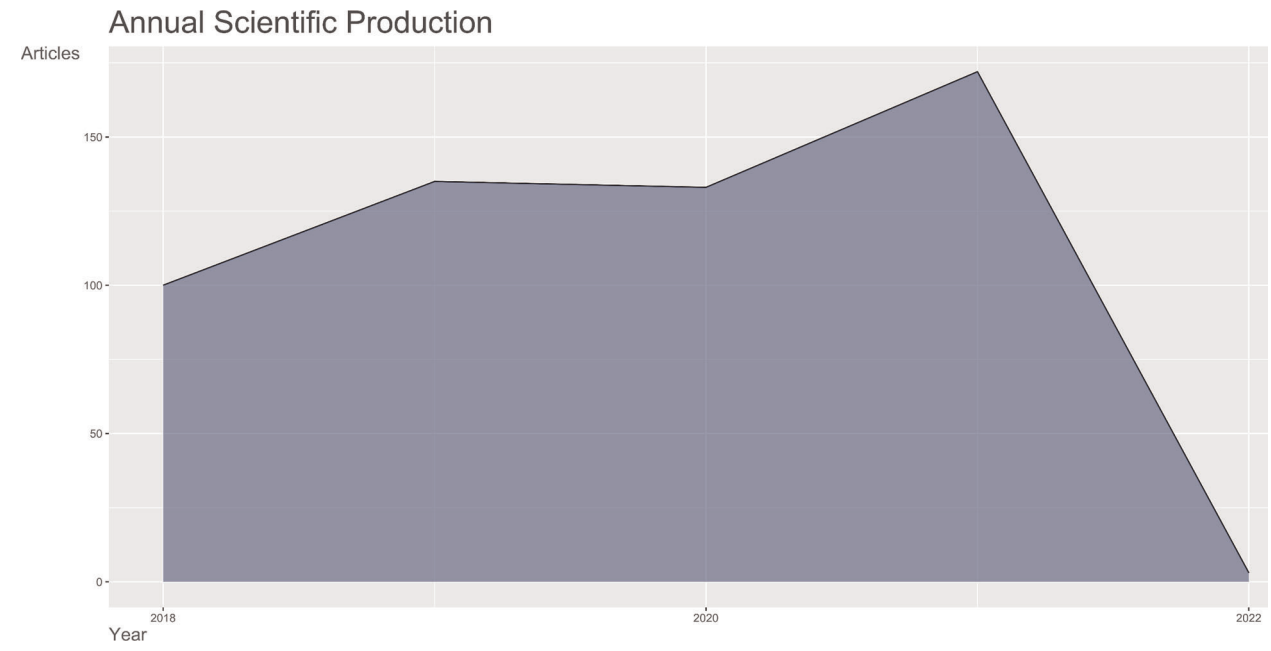


**FIGURE 1** | Annul number of publications in the field of stem cell precision medicine (2018–2022).

**TABLE 1** | The top 10 most productive countries of stem cell precision medicine research.

| Country | Articles | SCP | MCP | MCP_Ratio |
|---|---|---|---|---|
| USA | 160 (28.99%) | 124 | 36 | 0.225 |
| CHINA | 63 (11.41%) | 50 | 13 | 0.2063 |
| ITALY | 60 (10.87%) | 43 | 17 | 0.2833 |
| GERMANY | 38 (6.88%) | 20 | 18 | 0.4737 |
| UNITED KINGDOM | 22 (3.99%) | 11 | 11 | 0.5 |
| JAPAN | 21 (3.80%) | 19 | 2 | 0.0952 |
| FRANCE | 16 (2.90%) | 12 | 4 | 0.25 |
| INDIA | 15 (2.72%) | 13 | 2 | 0.1333 |
| CANADA | 12 (2.17%) | 9 | 3 | 0.25 |
| KOREA | 12 (2.17%) | 10 | 2 | 0.1667 |

*SCP, intra-country collaboration; MCP, inter-country collaboration.*

the most productive country ($n = 160$), followed by China ($n = 63$), Italy ($n = 60$), Germany ($n = 38$), and the UK ($n = 22$). In **Figure 2**, the larger circle represented more publications, and the thicker line represented more collaborations. Active collaborations were observed, as the United States had active academic exchanges with many countries, including Italy, China, Germany, England, Japan, India, and so on.

The top 10 productive affiliations worldwide are listed in **Table 2**. Among these affiliations, seven were located in America, while the rest three were located in Austria, Canada, and Italy. The top 3 productive affiliations were Stanford University, Medical University of Vienna, and Harvard Medical School, which respectively contributed 42, 30, and 29 pieces of research on stem cell precision medicine.

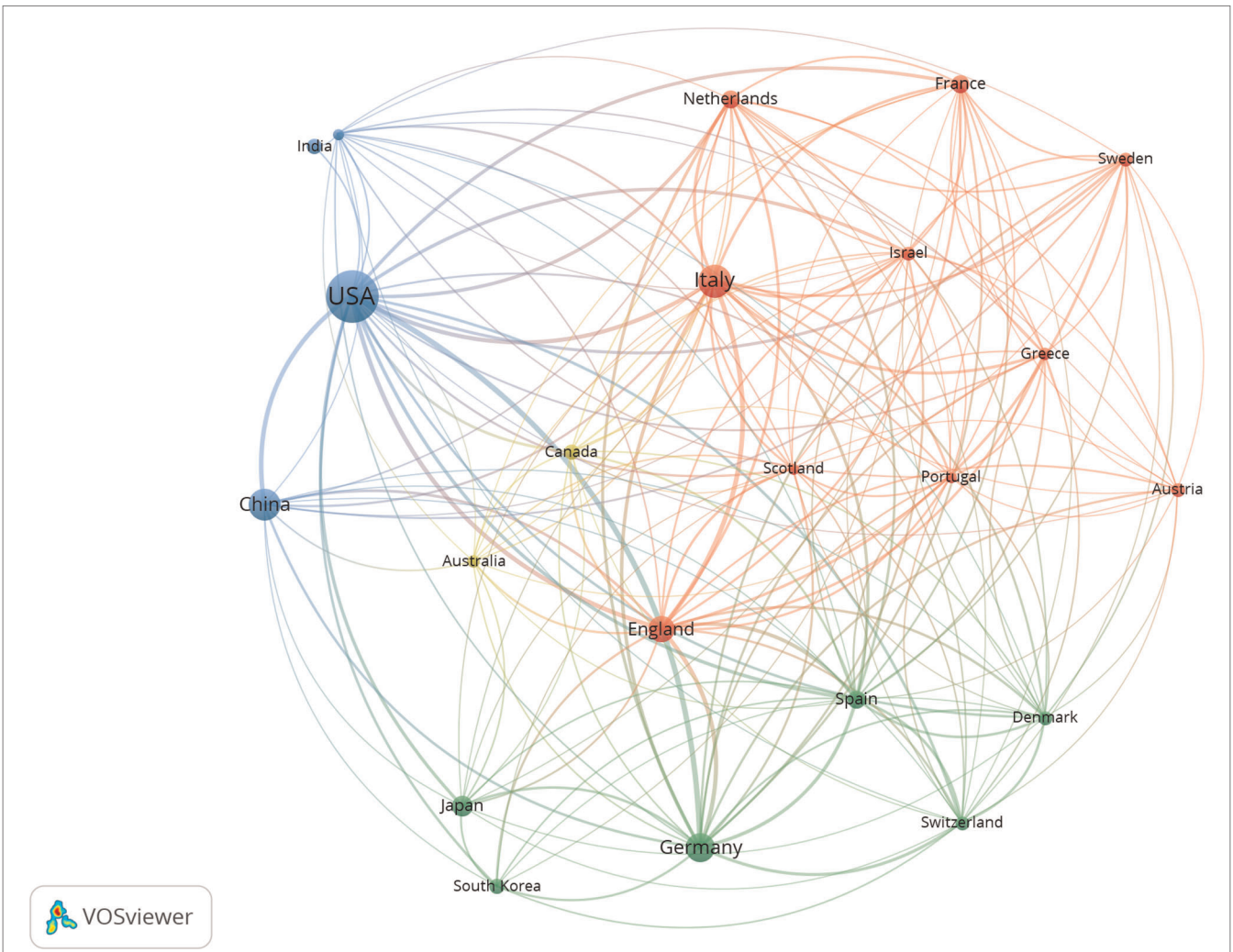


**FIGURE 2** | Geographical distribution and collaborations among countries in stem cell precision medicine. The circles represent countries, with the larger circle corresponding to more publications. The connecting lines represent the academic cooperation between countries, with the thicker line corresponding to closer cooperation. Different colors represent different clusters automatically calculated by VOSviewer.

## Journal Analysis

We identified 344 journals associated with publications of stem cell precision medicine from 2018 to 2022. The journals with more than 10 publications in this field are shown in **Table 3**. As of January 2022, the top 3 productive journals were CANCERS, CELLS, and INTERNATIONAL JOURNAL OF MOLECULAR SCIENCES, with 18, 15, and 14 publications. The journals with the three highest impact factors were BIOMATERIALS, EBIOMEDICINE, FRONTIERS IN CELL AND DEVELOPMENTAL BIOLOGY, which published 5, 5, and 6 articles.

The term co-citation refers to a situation where two documents both appear in the reference of the third document. A total of 10 journals had been co-cited no less than 570 times (T = 570), as shown in **Table 4**. NATURE had the highest co-citation frequency of 1,860, followed by CELL and J Cell Stem Cell, which had been co-cited up to 1,241 and 1,218 times, respectively. Scientific Reports was both in the top 10 productive and co-cited journals.

In VOSviewer, we created a map to reflect the co-citation relationships among journals whose publications had been at least co-cited 570 times (**Figure 3**). NATURE was represented by the giant circle in the center and had active co-citation relationships with other journals, especially with CELL, Cell Stem Cell, PROCEEDINGS OF THE NATIONAL ACADEMY OF SCIENCES OF THE UNITED STATES OF AMERICA, and so on.

## Document Analysis

The top 10 documents in terms of local citation times are listed in **Table 5**. The most cited document was entitled "Induced Pluripotent Stem Cells for Cardiovascular Disease Modeling and Precision Medicine: A Scientific Statement From the American Heart Association" on CIRCULATION-GENOMIC AND PRECISION MEDICINE, which was published by Musunuru K in 2018 with 9 local citations. The second was "Disease Modeling Using 3D Organoids Derived from Human

**TABLE 2 |** The top 10 most productive affiliations of stem cell precision medicine research.

| Affiliations | Articles | Nation |
|---|---|---|
| Stanford University | 42 | USA |
| Medical University of Vienna | 30 | Austria |
| Harvard Medical School | 29 | USA |
| Icahn School of Medicine at Mount Sinai | 24 | USA |
| University of Pennsylvania | 22 | USA |
| University of Toronto | 19 | Canada |
| University of Illinois Chicago | 17 | USA |
| University of Pittsburgh | 17 | USA |
| University of Washington | 17 | USA |
| University of Milan | 16 | Italy |

**TABLE 3 |** The top 10 most productive journals of stem cell precision medicine research.

| Sources | Articles | IF2020 | JCR2020 |
|---|---|---|---|
| CANCERS | 18 | 6.639 | Q1 (ONCOLOGY) |
| CELLS | 15 | 6.600 | Q2 (CELL BIOLOGY) |
| INTERNATIONAL JOURNAL OF MOLECULAR SCIENCES | 14 | 5.924 | Q1 (BIOCHEMISTRY & MOLECULAR BIOLOGY) Q2 (CHEMISTRY, MULTIDISCIPLINARY) |
| JOURNAL OF PERSONALIZED MEDICINE | 9 | 4.945 | Q1 (HEALTH CARE SCIENCES & SERVICES) Q1 (MEDICINE, GENERAL & INTERNAL) |
| SCIENTIFIC REPORTS | 7 | 4.380 | Q1 (MULTIDISCIPLINARY SCIENCES) |
| FRONTIERS IN CELL AND DEVELOPMENTAL BIOLOGY | 6 | 6.684 | Q1 (DEVELOPMENTAL BIOLOGY) Q2 (CELL BIOLOGY) |
| JOURNAL OF CLINICAL MEDICINE | 6 | 4.242 | Q1 (MEDICINE, GENERAL & INTERNAL) |
| BIOMATERIALS | 5 | 12.479 | Q1 (ENGINEERING, BIOMEDICAL) Q1 (MATERIALS SCIENCE, BIOMATERIALS) |
| EBIOMEDICINE | 5 | 8.143 | Q1 (MEDICINE, RESEARCH & EXPERIMENTAL) |
| FRONTIERS IN BIOENGINEERING AND BIOTECHNOLOGY | 5 | 5.890 | Q1 (MULTIDISCIPLINARY SCIENCES) |

**TABLE 4 |** The 10 most co-cited journals of stem cell precision medicine research from 2018 to 2022.

| Sources | Citation | IF2020 | JCR2020 |
|---|---|---|---|
| NATURE | 1,860 | 49.962 | Q1 (MULTIDISCIPLINARY SCIENCES) |
| CELL | 1,241 | 41.584 | Q1 (BIOCHEMISTRY & MOLECULAR BIOLOGY) Q1 (CELL BIOLOGY) |
| Cell Stem Cell | 1,218 | 24.633 | Q1 (CELL & TISSUE ENGINEERING) Q1 (CELL BIOLOGY) |
| PROCEEDINGS OF THE NATIONAL ACADEMY OF SCIENCES OF THE UNITED STATES OF AMERICA | 1,120 | 11.205 | Q1 (MULTIDISCIPLINARY SCIENCES) |
| BLOOD | 1,080 | 23.629 | Q1 (HEMATOLOGY) |
| SCIENCE | 986 | 47.728 | Q1 (MULTIDISCIPLINARY SCIENCES) |
| PLoS One | 903 | 3.24 | Q2 (MULTIDISCIPLINARY SCIENCES) |
| Scientific Reports | 884 | 4.38 | Q1 (MULTIDISCIPLINARY SCIENCES) |
| NEW ENGLAND JOURNAL OF MEDICINE | 686 | 91.253 | Q1 (MEDICINE, GENERAL & INTERNAL) |
| Nature Communications | 593 | 14.919 | Q1 (MULTIDISCIPLINARY SCIENCES) |

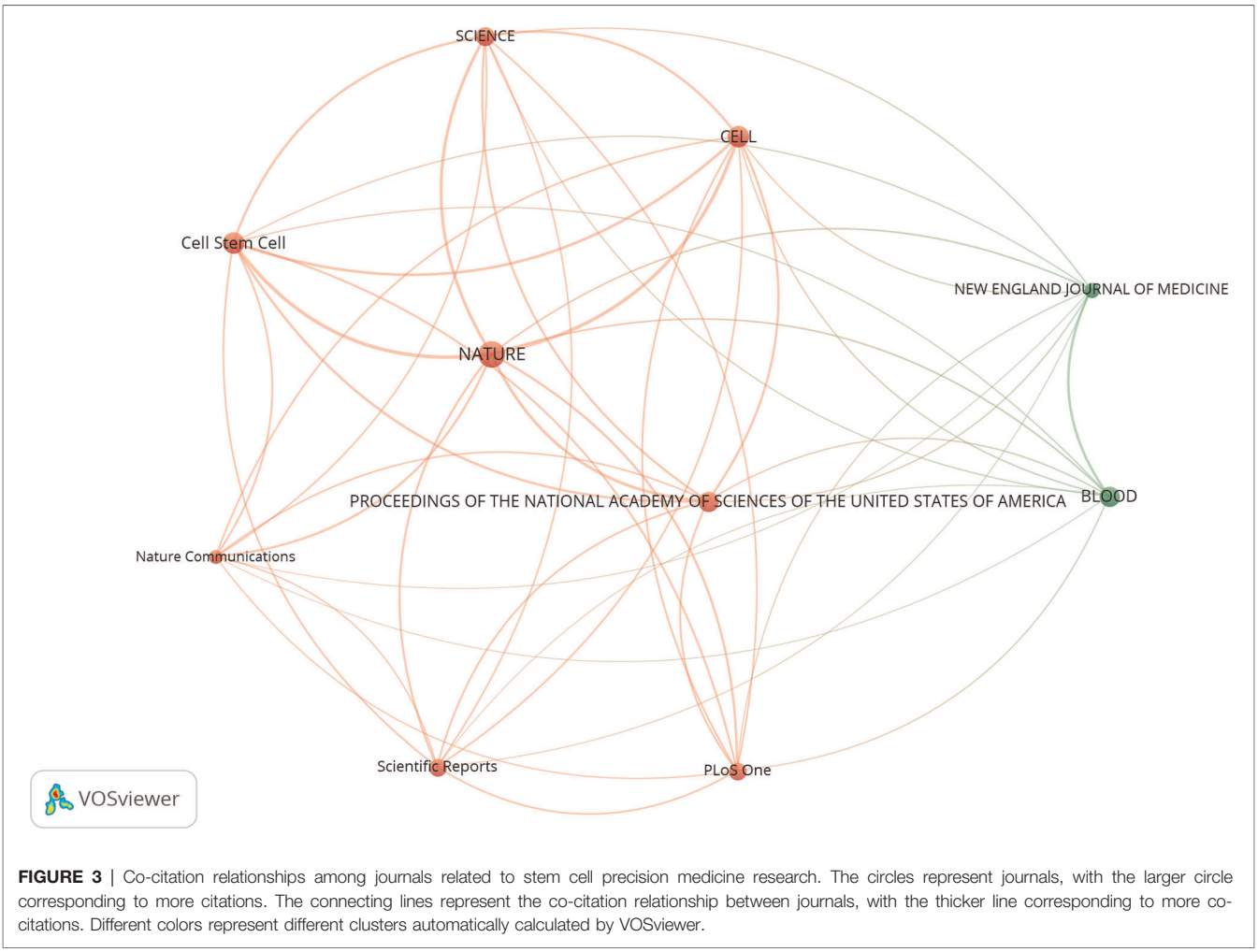


**FIGURE 3** | Co-citation relationships among journals related to stem cell precision medicine research. The circles represent journals, with the larger circle corresponding to more citations. The connecting lines represent the co-citation relationship between journals, with the thicker line corresponding to more co-citations. Different colors represent different clusters automatically calculated by VOSviewer.

Induced Pluripotent Stem Cells" on INTERNATIONAL JOURNAL OF MOLECULAR SCIENCES, published by Ho BX in 2018 with 7 local citations. The third was "Organs-on-a-Chip: A Fast Track for Engineered Human Tissues in Drug Development" on CELL STEM CELL, published by Ronaldson-Bouchard K in 2018 with 6 local citations.

The top 10 references with the highest co-citations are listed in **Table 6**. "Induction of pluripotent stem cells from adult human fibroblasts by defined factors" had the most co-citations ($n = 91$), followed by "Induction of pluripotent stem cells from mouse embryonic and adult fibroblast cultures by defined factors" ($n = 84$) and "Cerebral organoids model human brain development and microcephaly" ($n = 46$). The top 10 references had at least over 28 co-citations (T = 28) and a map constructed in the VOSveiwer, to present the co-citation relationships between the references (**Figure 4**). The top co-cited references tended to have co-citation relationships according to the thickness of lines between them.

## Key Words Analysis

Keywords were set as "author keywords" in the VOSviewer, and the top 50 keywords were automatically listed in terms of frequencies (sizes of cubes) in **Figure 5A**. We found that the top 50 keywords with frequency rates higher than 3% account for 12% and they were "precision medicine" ($n = 89$, 12.64%), "personalized medicine" ($n = 72$, 10.23%), "stem cells" ($n = 43$, 4.40%), "induced pluripotent stem cells" ($n = 41$, 5.82%), " cancer stem cells" ($n = 31$, 4%), and "organoids" ($n = 26$, 3.69%). A map (**Figure 5B**) was built to reflect the co-occurrence relationships between high-frequency keywords. "stem cells" "induced pluripotent stem cells" "cancer stem cells" "organoids" and "regenerative medicine" had strong co-occurrence relationships with "precision medicine" and "personalized medicine", which reflected the classic research direction and basic theory of stem cell precision medicine research.

## Burst Analysis

With CiteSpace, we performed a burst analysis of reference citations, and five references were selected during the period. As shown in **Figure 6**, the reference entitled "Organogenesis in a dish: modeling development and disease using organoid technologies" had the highest burst strength (4.09), followed by "Microfluidic organs-on-chips" (2.8) and "Organoid cultures derived from patients with advanced prostate cancer" (2.03).

**TABLE 5 |** The 10 most cited documents of stem cell precision medicine in the past 5 years.

| Document | First author | Journal | Year | Local Citations |
|---|---|---|---|---|
| Induced Pluripotent Stem Cells for Cardiovascular Disease Modeling and Precision Medicine: A Scientific Statement From the American Heart Association | Musunuru K | CIRCULATION-GENOMIC AND PRECISION MEDICINE | 2018 | 9 |
| Disease Modeling Using 3D Organoids Derived from Human Induced Pluripotent Stem Cells | Ho BX | INTERNATIONAL JOURNAL OF MOLECULAR SCIENCES | 2018 | 7 |
| Organs-on-a-Chip: A Fast Track for Engineered Human Tissues in Drug Development | Ronaldson-Bouchard K | CELL STEM CELL | 2018 | 6 |
| Human iPSC banking: barriers and opportunities | Huang CY | JOURNAL OF BIOMEDICAL SCIENCE | 2019 | 6 |
| Patient and Disease-Specific Induced Pluripotent Stem Cells for Discovery of Personalized Cardiovascular Drugs and Therapeutics | Paik DT | PHARMACOLOGICAL REVIEWS | 2020 | 6 |
| Enhanced Utilization of Induced Pluripotent Stem Cell-Derived Human Intestinal Organoids Using Microengineered Chips | Workman MJ | CELLULAR AND MOLECULAR GASTROENTEROLOGY AND HEPATOLOGY | 2018 | 5 |
| Human iPSC-Derived Blood-Brain Barrier Chips Enable Disease Modeling and Personalized Medicine Applications | Vatine GD | CELL STEM CELL | 2019 | 5 |
| Personalised organs-on-chips: functional testing for precision medicine | van den Berg A | LAB ON A CHIP | 2019 | 5 |
| Personalized medicine in cardio-oncology: the role of induced pluripotent stem cell | Sayed N | CARDIOVASCULAR RESEARCH | 2019 | 5 |
| Towards Precision Medicine With Human iPSCs for Cardiac Channelopathies | Wu JC | CIRCULATION RESEARCH | 2019 | 5 |

**TABLE 6 |** The 10 most co-cited references of stem cell precision medicine in the past 5 years.

| Document | First author | Journal | Year | Co-Citations |
|---|---|---|---|---|
| Induction of pluripotent stem cells from adult human fibroblasts by defined factors | Takahashi K | CELL | 2007 | 91 |
| Induction of pluripotent stem cells from mouse embryonic and adult fibroblast cultures by defined factors | Takahashi K | CELL | 2006 | 84 |
| Cerebral organoids model human brain development and microcephaly | Lancaster MA | NATURE | 2013 | 46 |
| Single Lgr5 stem cells build crypt-villus structures in vitro without a mesenchymal niche | Sato T | NATURE | 2009 | 43 |
| Induced pluripotent stem cell lines derived from human somatic cells | Yu J | SCIENCE | 2007 | 40 |
| Organogenesis in a dish: modeling development and disease using organoid technologies | Lancaster MA | SCIENCE | 2014 | 38 |
| Embryonic stem cell lines derived from human blastocysts | Thomson JA | SCIENCE | 1998 | 36 |
| Modeling Development and Disease with Organoids | Clevers H | CELL | 2016 | 33 |
| Long-term expansion of epithelial organoids from human colon, adenoma, adenocarcinoma, and Barrett's epithelium | Sato T | GASTROENTEROLOGY | 2011 | 30 |
| Prospective derivation of a living organoid biobank of colorectal cancer patients | van de Wetering M | CELL | 2015 | 28 |

# DISCUSSION

## Research Status and Trends

We performed a worldwide investigation of the literature on stem cell precision medicine from WoSCC from 2018 to 2022 by bibliometric analysis. Each year's total output of publications can reflect academics' overall development and attention in a specific research field. The general trend of research output regarding stem cell precision medicine was rising. A peak was reached in 2021, suggesting that this field had been a subject of ongoing concern and has been well developed. There were 100 papers published in 2018 and 172 papers (articles and reviews) published in 2021.

North America, Asia, and Europe were the central regions of research production. The United States undoubtedly dominated the research field of stem cell precision medicine, contributing approximately 30% of the existing publications. The leading academics with advanced research conditions and technologies might attribute such a apparent superiority. Seven of the top 10 contributing institutions were all from the United States, including Stanford University, Harvard Medical School, Icahn School of Medicine at Mount Sinai, University of Pennsylvania, University of Illinois Chicago, University of Pittsburgh, and University of Washington. Notably, the United States had active intercountry collaborations but a relatively lower MCP ratio, suggesting that research on stem

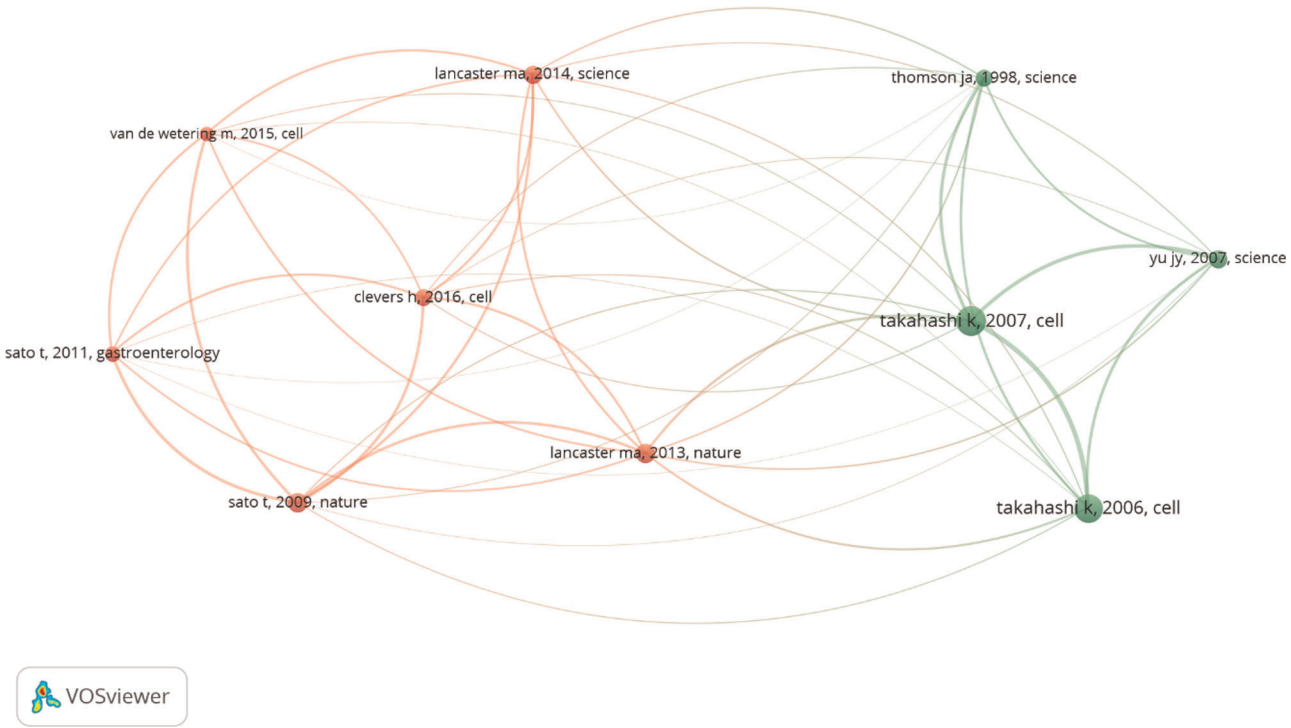


**FIGURE 4** | The co-citation relationships among references (T > 28) of stem cell precision medicine (2018–2022). The circles represent references, with the larger circle corresponding to more citations. The connecting lines represent the co-citation relationship between references, with the thicker line corresponding to more co-citations. Different colors represent different clusters automatically calculated by VOSviewer.

cell precision medicine in America was more independent and advanced than in other countries.

Moreover, the United States retained enormous influence and had comprehensive and active scientific research cooperation with other countries, including China, Italy, Germany, England, and Japan. Remarkably, China surpassed European countries and ranked in the top 3 in terms of publications on stem cell precision medicine. Most of the high-yielding institutions were from the US, and there were only three institutions from Australia, Canada, and Italy. This information indicated that China was an Asian country with high research yields but relatively decentralized research units. These differences might be attributed to the importance the governments attached to scientific research in recent years, the availability of sufficient funding, and the rapid development of research capacity.

Journal of associated publications can reflect the overall quality of the research. The top 3 productive journals with publications relating to stem cell precision medicine were CANCERS, CELLS, and INTERNATIONAL JOURNAL OF MOLECULAR SCIENCES. The top 3 co-cited journals in this field were NATURE, CELL, and Cell Stem Cell. The top 3 journals all ranked in Q1 in Journal Citation Reports for co-citing journals, while the highest impact factor of the top 10 reached 91.253 (2020). Scientific Reports both Ranked in the top 10 as for production and co-citation. In the past five years, papers on stem cell precision medicine had not been published in top journals, but the overall journals were still distributed in the Q1 area. Generally, the quality of studies on stem cell precision medicine was considerable.

## Background Knowledge

Highly cited papers can reflect the influential background knowledge of a field. There was no overlap between highly cited articles and highly co-cited references recently. Highly co-cited references are often the classic theories in the research field after time test. Most of the highly co-cited references in our research came from NATURE, CELL, and SCIENCE, suggesting that crucial research background knowledge in the future was likely to be found in these journals. The most cited document was "Induced Pluripotent Stem Cells for Cardiovascular Disease Modeling and Precision Medicine: A Scientific Statement From the American Heart Association" by Musunuru K in 2018. In this study, the authors stated that there were currently two ways to model cardiovascular disease using induced pluripotent stem cells: iPSC from patient-specific cells (such as skin fibroblasts) or gene editing. Cardiovascular disease models based on iPSC had covered cardiomyopathy, rhythm abnormalities, valvular and vascular diseases, ischemic heart disease, familial pulmonary hypertension, etc. However, there were still relatively intuitive differences between cardiomyocytes


**FIGURE 5** | (Continued)

differentiated from iPSC and adult cardiomyocytes, reflected in cell shape, electrophysiology, calcium handling, mitochondrial physiology, and response to epinephrine signals. In terms of precision medicine, cardiovascular organoids constructed from induced stem cells played a role in screening DNA mutations of patient-specific diseases, disease development mechanisms, and treatment methods. In the future, we look forward to more large-scale production of induced pluripotent stem cells and the construction of stem cell banks for drug toxicity testing and other important directions (30).

The second document, "Disease Modeling Using 3D Organoids Derived from Human Induced Pluripotent Stem Cells" by Ho BX published in 2018 emphasized that 3D organoids from induced pluripotent stem cells could highly simulate the natural physiological environment compared with 2D models. It had advantages in constructing vascularization models and studying complex inflammation models. The author summarized the organoid disease models built by human-induced pluripotent stem cells, including the brain, liver, pancreas, small intestine, stomach, kidney, bladder, lung, retina, etc. However, there were still shortcomings in 3D organoids. The modeling technology of induced pluripotent stem cell 3D organoids was complex and required high technical requirements. Further, cells (endothelial cells, monocytes, macrophages, etc.) and cell physiology changes (leukocyte migration, monocyte differentiation, etc.) were constructed based on vascularization. The vascularization in the model was not yet complete, and wide vascular networks could not be built at this stage. Despite these, human-induced pluripotent stem cells still played an essential role in building disease models and drug screening (31).

The third one, "Organs-on-a-Chip: A Fast Track for Engineered Human Tissues in Drug Development" by Ronaldson-Bouchard K described the critical role of organ-on-a-chip in drug development. Human-induced pluripotent stem cells were involved in developing part of the organ-on-a-chip construction. The construction method of the single organoid chip included primary cells, cell lines, iPSCs, MSCs, and other cells. Multiple organ chips could be connected by static, singe-loop perfusion, recirculation, and recirculation-tissue-specific media (32). The fourth highly cited document was "Human iPSC banking: barriers and opportunities" by Huang CY in 2019, which focused on summarizing the current development of iPSC banks and introduced the cell sources, reprogramming methods, characterization methods, and operational situation of worldwide iPSC banks (33). Paik DT emphasized the vital

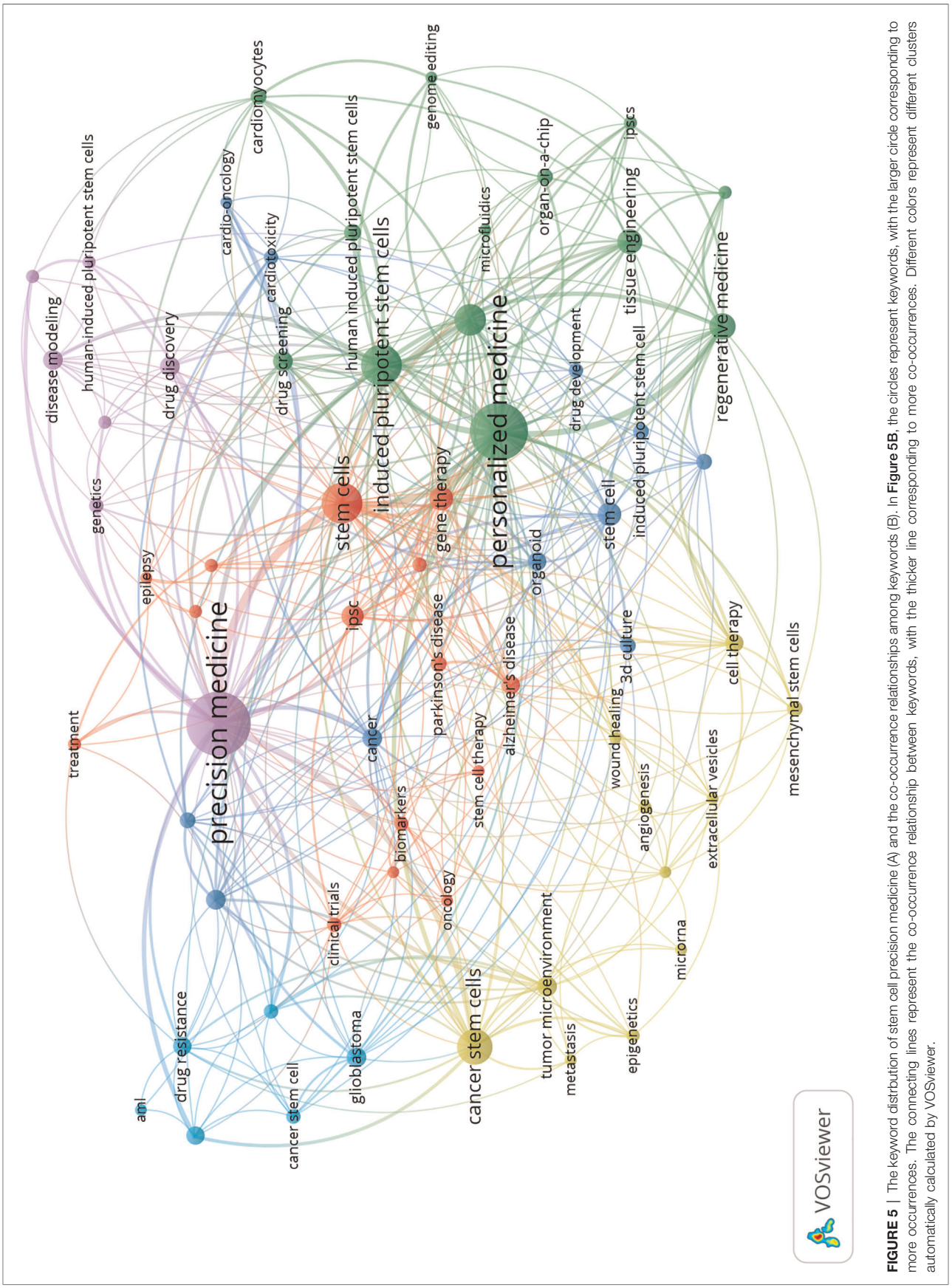


**FIGURE 5** | The keyword distribution of stem cell precision medicine (A) and the co-occurrence relationships among keywords (B). In **Figure 5B**, the circles represent keywords, with the larger circle corresponding to more occurrences. The connecting lines represent the co-occurrence relationship between keywords, with the thicker line corresponding to more co-occurrences. Different colors represent different clusters automatically calculated by VOSviewer.

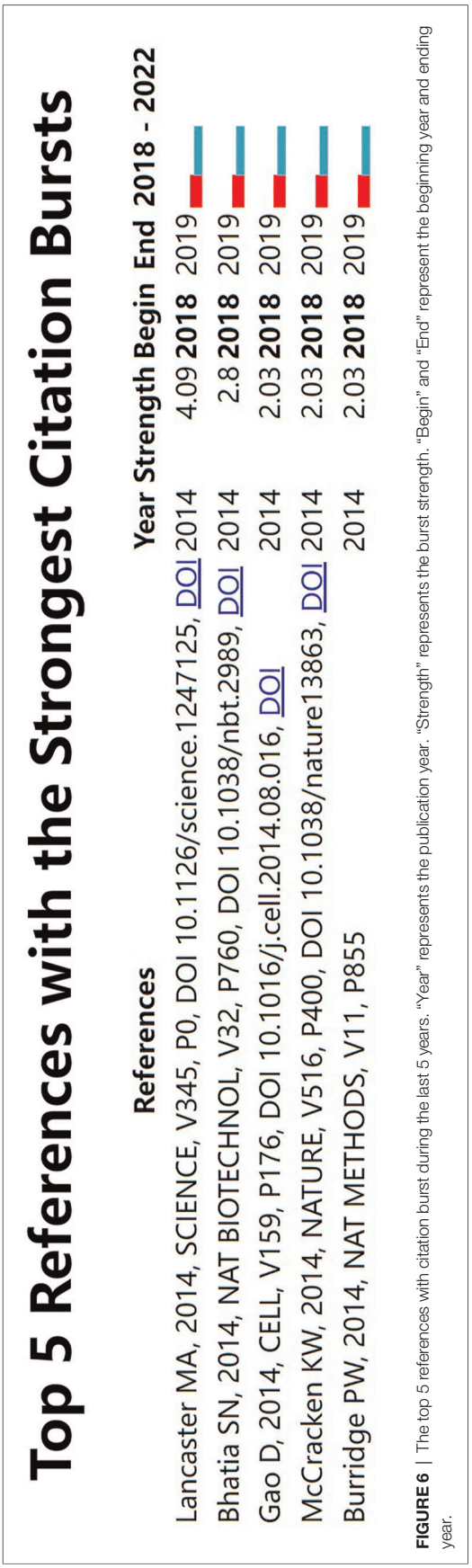


**FIGURE 6** | The top 5 references with citation burst during the last 5 years. "Year" represents the publication year. "Strength" represents the burst strength. "Begin" and "End" represent the beginning year and ending year.

role of patient-specific induced pluripotent stem cells in screening personalized cardiovascular drugs in "Patient and Disease-Specific Induced Pluripotent Stem Cells for Discovery of Personalized Cardiovascular Drugs and Therapeutics" in 2020 (34). This paper supplemented and enriched the one by Musunuru K in 2018. The top 5 highly cited documents highlight two key points. The construction of disease models by iPSC is essential for achieving precise treatment. Moreover, the research on cardiovascular disease models has recently received sufficient attention and development.

Co-cited references can reflect the general and influential views of background knowledge. Highly-cited references concentrated on the early stages of induced pluripotent stem cells. Studies include:

- The original investigator Takahashi K's research on the iPSC construction of mice and huma;
- Yu J's improvements to the induction protocol of human iPSC;
- The construction of brain-like and intestinal-like models;

In 2006, Takahashi K successfully reprogrammed mouse embryonic and adult fibroblasts into pluripotent stem cells for the first time through Oct3/4, Sox2, c-Myc, and Klf4 (5). The above four factors were used to successfully reprogram human skin fibroblasts into pluripotent stem cells in the following year (6). At the same time, Yu J also successfully reprogrammed human mature somatic cells into pluripotent stem cells using different combinations of factors (OCT4, SOX2, NANOG, and LIN28) (7). In 2009, Sato T constructed intestinal crypt-villus units using Lgr5 stem cells in crypts of the small intestine, which served as an important basis for subsequent organoid model construction (35). Lancaster MA constructed 3D brain organoids from human induced pluripotent stem cells in 2013, which contained developmental characteristics of the human cerebral cortex. Lancaster MA used RNA interference technology in the model for studying microcephaly (36). We believe that this information from the above studies is vital for further studies.

## Hotspots

The information imparted by keywords is worth further exploration. In addition to search keywords, the other top 10 keywords included "cancer stem cells," "organoids," "regenerative medicine," "tissue engineering," and "gene therapy." The number of occurrences of keywords reflects the hotspots of the research. As shown in the highly-cited documents and references, the current research hotspots focused on establishing individualized disease models, including tumor and non-tumor diseases. Gene therapy was part of the mechanistic studies in organoid models. The research on the regenerative potential of stem cells corresponded to the current stem cell replacement therapy and future tissue engineering. The construction of patient-specific complete organs based on induced pluripotent stem cells was the ultimate goal of regenerative medicine and needed more research in the future.

### Citation Burst

The references with intense citation burst reflect the surge of citations at a specific time. We summarized the strong citation burst references to analyze the dynamics of attention on stem cell precision medicine. The document with the strongest citation burst was titled "Organogenesis in a dish: Modeling development and disease using organoid technologies" by Lancaster MA on SCIENCE, which summarized the current uses and prospects of induced pluripotent stem cells. Human-derived cells were transformed into pluripotent stem cells, and pluripotent stem cells of a specific genotype could be constructed with gene-editing tools or the patient's genes. Furthermore, organoids were built and used for disease simulation, drug testing, and even organ replacement (37). The second strongest paper was a perspective titled "Microfluidic organs-on-chips" by Bhatia SN on Nature Biotechnology. The author conducted a comprehensive review on organs-on-chips and illuminates the basic definition (Microfluidic culture devices and Control of system parameters). Compared with the 3D static modeling method, the microfluidic organ-on-a-chip model consisted of independent but closely related subsystems. Each system could achieve fine adjustment (like cell type and location, molecular and oxygen gradients, flow levels and pattern, mechanical forcing regimens, etc.) and affect other systems through microfluidic media. Organ-on-a-Chip could control fluid flow and enhance many cells' differentiation, function, and long-term survival. Besides, the fluid environment allowed the organ to interact with circulating cells, like blood cells and tumor cells. Cells in the model could be precisely located and integrated with fluorescence confocal microscopy, microfluorescence, TEER measurement, multi-electrode arrays for organ physiology, disease research or drug screening, and even the adsorption, distribution, metabolism, elimination, and toxicity of drugs (38).

The third was "Organoid Cultures Derived from Patients with Advanced Prostate Cancer" by Gao D on CELL. Dong Gao et al. constructed a 3D organoid model system from patient prostate cancer biopsy samples and circulating tumor cells. They used this model to simulate numerous prostate cancer molecular changes, including but not limited to TMPRSS2-ERG fusion, SPOP mutation, SPINK1 overexpression, and CHD1 loss. The author was optimistic that the model would help further prostate cancer pathogenesis research and drug screening (39). In the same year, McCracken KW et al. reported in NATURE that they de novo generated a 3D model of gastric tissue by controlling the activation of FGF, WNT, BMP, retinoic acid, and EGF signaling pathways in human pluripotent stem cells. The author discovered that H. pylori infection resulted in the virulence factor CagA action with the c-Met receptor, thus leading to epithelial proliferation (40). Burridge PW published his research in Nature Methods to optimize the cardiac differentiation culture conditions of human-induced pluripotent stem cells, using a medium consisting of the basal medium RPMI 1,640, L-ascorbic acid 2-phosphate, and rice-derived recombinant human albumin. This culture condition yielded 95% tnnt2 + cardiomyocytes in the small molecule-based differentiation induction and achieved a 1:100 productivity in 11 human induced pluripotent stem cell lines (41).

From the citation burst references, we can also see that stem cell precision medicine has focused on creating and applying 3D, patient-specific disease models involving prostate cancer, stomach, and heart in the last five years. In the future, the establishment of multi-organ and multi-disease 3D organoid models will remain an important development direction for the application of induced pluripotent stem cells.

## LIMITATIONS

Our study was based on the tools of bibliometrics, in which the error of document statistics was hard to avoid. Our literature search was limited to WoSCC, and the analysis based on one data source might lead to biased results. The bibliometric method is closely related to time. The results of the analysis vary significantly with the choice of time span. Our study was limited to the last five years, which meant that our results were time-bound, and we could not fully understand the disease. Meanwhile, the analysis results are not suitable for continued use in the future. Especially, the burst analysis is a relatively niche approach to literature analysis in CiteSpace that calculates the surge of citations in a period. This analysis results reflect the "speed" of citations rather than the "number" of citations. It represents those papers which have attracted attention at some point, and the relevant papers may be previously published studies which have recently attracted attention. Furthermore, the bibliometric analysis is based on a certain form of publication. The result is that other forms of study or unpublished studies are not considered in our research, which may influence the authority of our conclusions. In addition, our study can also be affected by changes in journal titles. Nevertheless, our study was built on the most extensive database and had well-developed and optimized tools, which to a large extent, could be a future reference for clinicians and researchers studying stem cell precision medicine.

## CONCLUSION

In the present study, we conducted a comprehensive analysis of the existing research in stem cell precision medicine from 2018 to 2022, applying bibliometrics tools. Globally the study of stem cell precision medicine was undergoing a stable development over the last five years, and the year 2021 peaked its literature quantity. The United States was the most influential country regarding the number of research production and had active academic cooperation with countries, including Italy, China, Germany, and other countries. Notably, Asian countries led by China had recently taken a significant role in this field. CANCERS (IF 6.639) was the journal with the highest production of publications in stem cell precision medicine. BIOMATERIALS had the highest IF (12.479) among the top 10 productive journals. The most cited document on stem cell

precision medicine was "Induced Pluripotent Stem Cells for Cardiovascular Disease Modeling and Precision Medicine: A Scientific Statement From the American Heart Association," published by Musunuru K in 2018 with a local citation of 9 times. Takahashi K et al. published the study "Induction of pluripotent stem cells from adult human fibroblasts by defined factors," in CELL, which had been co-cited with other references for 91 times recently. "precision medicine" ($n = 89$, 12.64%), "personalized medicine" ($n = 72$, 10.23%), "stem cells" ($n = 43$, 4.40%), "induced pluripotent stem cells" ($n = 41$, 5.82%), "cancer stem cells" ($n = 31$, 4%) and "organoids" ($n = 26$, 3.69%) co-occurred closely and were high-frequency keywords. They represented the disciplinary basis of stem cell precision medicine. The content of the top three citation burst documents focused on the current and future uses of induced pluripotent stem cells, giving optimism for their use in disease modeling, drug trials, and even organ replacement. These areas were relatively popular directions for stem cell precision medicine and worth further research in the future.

## DATA AVAILABILITY STATEMENT

The datasets used and analysed during the current study are available from the corresponding author on reasonable request.

## AUTHOR CONTRIBUTIONS

ML and FY designed this study. ML collected data and performed the analysis. FY was the main contributor who wrote the manuscript. YX revised the manuscript. All authors contributed to the article and approved the submitted version.

## REFERENCES


1. Saba JA, Liakath-Ali K, Green R, Watt FM. Translational control of stem cell function. *Nat Rev Mol Cell Biol*. (2021) 22(10):671–90. doi: 10.1038/s41580-021-00386-2
2. Solter D. From teratocarcinomas to embryonic stem cells and beyond: a history of embryonic stem cell research. *Nat Rev Genet*. (2006) 7(4): 319–27. doi: 10.1038/nrg1827
3. Goodell MA, Nguyen H, Shroyer N. Somatic stem cell heterogeneity: diversity in the blood, skin and intestinal sStem cell compartments. *Nat Rev Mol Cell Biol*. (2015) 16(5):299–309. doi: 10.1038/nrm3980
4. Matoba S, Zhang Y. Somatic cell nuclear transfer reprogramming: mechanisms and applications. *Cell Stem Cell*. (2018) 23(4):471–85. doi: 10.1016/j.stem.2018.06.018
5. Takahashi K, Yamanaka S. Induction of pluripotent stem cells from mouse embryonic and adult fibroblast cultures by defined factors. *Cell*. (2006) 126(4):663–76. doi: 10.1016/j.cell.2006.07.024
6. Takahashi K, Tanabe K, Ohnuki M, Narita M, Ichisaka T, Tomoda K, et al. Induction of pluripotent stem cells from adult human fibroblasts by defined factors. *Cell*. (2007) 131(5):861–72. doi: 10.1016/j.cell.2007.11.019
7. Yu J, Vodyanik MA, Smuga-Otto K, Antosiewicz-Bourget J, Frane JL, Tian S, et al. Induced pluripotent stem cell lines derived from human somatic cells. *Science*. (2007) 318(5858):1917–20. doi: 10.1126/science.1151526
8. Lamba DA, Gust J, Reh TA. Transplantation of human embryonic stem cell-derived photoreceptors restores some visual function in crx-deficient mice. *Cell Stem Cell*. (2009) 4(1):73–9. doi: 10.1016/j.stem.2008.10.015
9. Yang D, Zhang Z-J, Oldenburg M, Ayala M, Zhang S-C. Human embryonic stem cell-derived dopaminergic neurons reverse functional deficit in parkinsonian rats. *Stem Cells*. (2008) 26(1):55–63. doi: 10.1634/stemcells.2007-0494
10. Ma L, Hu B, Liu Y, Vermilyea SC, Liu H, Gao L, et al. Human embryonic stem cell-derived GABA neurons correct locomotion deficits in quinolinic acid-lesioned mice. *Cell Stem Cell*. (2012) 10(4):455–64. doi: 10.1016/j.stem.2012.01.021
11. Keirstead HS, Nistor G, Bernal G, Totoiu M, Cloutier F, Sharp K, et al. Human embryonic stem cell-derived oligodendrocyte progenitor cell transplants remyelinate and restore locomotion after spinal cord injury. *J Neurosci*. (2005) 25(19):4694–705. doi: 10.1523/JNEUROSCI.0311-05.2005
12. Fernandes S, Chong JJH, Paige SL, Iwata M, Torok-Storb B, Keller G, et al. Comparison of human embryonic stem cell-derived cardiomyocytes, cardiovascular progenitors, and bone marrow mononuclear cells for cardiac repair. *Stem Cell Rep*. (2015) 5(5):753–62. doi: 10.1016/j.stemcr.2015.09.011
13. Vegas AJ, Veiseh O, Gürtler M, Millman JR, Pagliuca FW, Bader AR, et al. Long-term glycemic control using polymer-encapsulated human stem cell-derived beta cells in immune-competent mice. *Nat Med*. (2016) 22 (3):306–11. doi: 10.1038/nm.4030
14. Pagliuca FW, Millman JR, Gürtler M, Segel M, Van Dervort A, Ryu JH, et al. Generation of functional human pancreatic β cells in vitro. *Cell*. (2014) 159 (2):428–39. doi: 10.1016/j.cell.2014.09.040
15. Rezania A, Bruin JE, Arora P, Rubin A, Batushansky I, Asadi A, et al. Reversal of diabetes with insulin-producing cells derived in vitro from human pluripotent stem cells. *Nat Biotechnol*. (2014) 32(11):1121–33. doi: 10.1038/nbt.3033
16. Stern JH, Tian Y, Funderburgh J, Pellegrini G, Zhang K, Goldberg JL, et al. Regenerating eye tissues to preserve and restore vision. *Cell Stem Cell*. (2018) 22(6):834–49. doi: 10.1016/j.stem.2018.05.013
17. Da Cruz L, Fynes K, Georgiadis O, Kerby J, Luo YH, Ahmado A, et al. Phase 1 clinical study of an embryonic stem cell-derived retinal pigment epithelium patch in age-related macular degeneration. *Nat Biotechnol*. (2018) 36 (4):328–37. doi: 10.1038/nbt.4114
18. Mehat MS, Sundaram V, Ripamonti C, Robson AG, Smith AJ, Borooah S, et al. Transplantation of human embryonic stem cell-derived retinal pigment epithelial cells in macular degeneration. *Ophthalmol*. (2018) 125 (11):1765–75. doi: 10.1016/j.ophtha.2018.04.037
19. Schwartz SD, Regillo CD, Lam BL, Eliott D, Rosenfeld PJ, Gregori NZ, et al. Human embryonic stem cell-derived retinal pigment epithelium in patients with age-related macular degeneration and stargardt's macular dystrophy: follow-up of two open-label phase 1/2 studies. *Lancet*. (2015) 385 (9967):509–16. doi: 10.1016/S0140-6736(14)61376-3
20. Menasché P, Vanneaux V, Hagège A, Bel A, Cholley B, Parouchev A, et al. Transplantation of human embryonic stem cell–derived cardiovascular progenitors for severe ischemic left ventricular dysfunction. *J Am Coll Cardiol*. (2018) 71(4):429–38. doi: 10.1016/j.jacc.2017.11.047
21. Kikuchi T, Morizane A, Doi D, Magotani H, Onoe H, Hayashi T, et al. Human IPS cell-derived dopaminergic neurons function in a primate parkinson's disease model. *Nature*. (2017) 548(7669):592–6. doi: 10.1038/nature23664
22. An MC, Zhang N, Scott G, Montoro D, Wittkop T, Mooney S, et al. Genetic correction of huntington's disease phenotypes in induced pluripotent stem cells. *Cell Stem Cell*. (2012) 11(2): 253–63. doi: 10.1016/j.stem.2012.04.026
23. Hicks MR, Hiserodt J, Paras K, Fujiwara W, Eskin A, Jan M, et al. ERBB3 and NGFR mark a distinct skeletal muscle progenitor cell in human development and HPSCs. *Nat Cell Biol*. (2018) 20(1):46–57. doi: 10.1038/s41556-017-0010-2
24. Raya Á, Rodríguez-Piz I, Guenechea G, Vassena R, Navarro S, Barrero MJ, et al. Disease-corrected haematopoietic progenitors from fanconi anaemia induced pluripotent stem cells. *Nature*. (2009) 460(7251):53–9. doi: 10.1038/nature08129
25. Xu D, Alipio Z, Fink LM, Adcock DM, Yang J, Ward DC, et al. Phenotypic correction of murine hemophilia a using an IPS cell-based therapy. *Proc Natl Acad Sci USA*. (2009) 106(3): 808–13. doi: 10.1073/pnas.0812090106

26. Mandai M, Watanabe A, Kurimoto Y, Hirami Y, Morinaga C, Daimon T, et al. Autologous induced stem-cell–derived retinal cells for macular degeneration. *N Engl J Med*. (2017) 376(11):1038–46. doi: 10.1056/nejmoa1608368
27. Gomez-Lopez G, Dopazo J, Cigudosa JC, Valencia A, Al-Shahrour F. Precision medicine needs pioneering clinical bioinformaticians. *Brief Bioinform*. (2017) 20(3):752–66. doi: 10.1093/bib/bbx144
28. Devos P, Ménard J. Trends in worldwide research in hypertension over the period 1999-2018: a bibliometric study. *Hypertens*. (2020) 18(4):1649–55. doi: 10.1161/HYPERTENSIONAHA.120.15711
29. Xiao Y, Wu H, Wang G, Mei H. Mapping the worldwide trends on energy poverty research: a bibliometric analysis (1999–2019). *Int J Environ Res Public Health*. (2021) 18(4):1–22. doi: 10.3390/ijerph18041764
30. Musunuru K, Sheikh F, Gupta RM, Houser SR, Maher KO, Milan DJ, et al. Induced pluripotent stem cells for cardiovascular disease modeling and precision medicine: a scientific statement from the American heart association. *Circ Genom Precis Med*. (2018) 11:e000043. doi: 10.1161/HCG.0000000000000043
31. Ho BX, Pek NMQ, Soh BS. Disease modeling using 3D organoids derived from human induced pluripotent stem cells. *Int J Mol Sci*. (2018) 19 (4):936. doi: 10.3390/ijms19040936
32. Ronaldson-Bouchard K, Vunjak-Novakovic G. Organs-on-a-chip: a fast track for engineered human tissues in drug development. *Cell Stem Cell*. (2018) 22(3):310–24. doi: 10.1016/j.stem.2018.02.011
33. Huang CY, Liu CL, Ting CY, Chiu YT, Cheng YC, Nicholson MW, et al. Human IPSC banking: barriers and opportunities. *J Biomed Sci*. (2019) 26 (1):1–14. doi: 10.1186/s12929-019-0578-x
34. Paik DT, Chandy M, Wu JC. Patient and disease–specific induced pluripotent stem cells for discovery of personalized cardiovascular drugs and therapeutics. *Pharmacol Rev*. (2020) 72(1):320–42. doi: 10.1124/pr.116.013003
35. Sato T, Vries RG, Snippert HJ, Van De Wetering M, Barker N, Stange DE, et al. Single Lgr5 stem cells build crypt-villus structures in vitro without a mesenchymal niche. *Nature*. (2009) 459(7244):262–5. doi: 10.1038/nature07935
36. Lancaster MA, Renner M, Martin CA, Wenzel D, Bicknell LS, Hurles ME, et al. Cerebral organoids model human brain development and microcephaly. *Nature*. (2013) 501(7467):373–9. doi: 10.1038/nature12517
37. Lancaster MA, Knoblich JA. Organogenesisin a dish: modeling development and disease using organoid technologies. *Science*. (2014) 345(6194):1247125. doi: 10.1126/science.1247125
38. Bhatia SN, Ingber DE. Microfluidic organs-on-chips. *Nat Biotechnol*. (2014) 32(8):760–72. doi: 10.1038/nbt.2989
39. Gao D, Vela I, Sboner A, Iaquinta PJ, Karthaus WR, Gopalan A, et al. Organoid cultures derived from patients with advanced prostate cancer. *Cell*. (2014) 159(1):176–87. doi: 10.1016/j.cell.2014.08.016
40. McCracken KW, Catá EM, Crawford CM, Sinagoga KL, Schumacher M, Rockich BE, et al. Modelling human development and disease in pluripotent stem-cell-derived gastric organoids. *Nature*. (2014) 516 (7531):400–4. doi: 10.1038/nature13863
41. Burridge PW, Matsa E, Shukla P, Lin ZC, Churko JM, Ebert AD, et al. Chemically defned generation of human cardiomyocytes. *Nat Methods*. (2014) 11(8):855–60. doi: 10.1038/nMeth.2999


**Conflict of Interest:** The authors declare that the research was conducted in the absence of any commercial or financial relationships that could be construed as a potential conflict of interest.

**Publisher's Note:** All claims expressed in this article are solely those of the authors and do not necessarily represent those of their affiliated organizations, or those of the publisher, the editors and the reviewers. Any product that may be evaluated in this article, or claim that may be made by its manufacturer, is not guaranteed or endorsed by the publisher.

*Copyright © 2022 Liu, Yang and Xu. This is an open-access article distributed under the terms of the Creative Commons Attribution License (CC BY). The use, distribution or reproduction in other forums is permitted, provided the original author(s) and the copyright owner(s) are credited and that the original publication in this journal is cited, in accordance with accepted academic practice. No use, distribution or reproduction is permitted which does not comply with these terms.*

frontiers | Frontiers in Surgery

ORIGINAL RESEARCH
published: 08 July 2022
doi: 10.3389/fsurg.2022.950967

# Anti-Aging Effect of the Stromal Vascular Fraction/Adipose-Derived Stem Cells in a Mouse Model of Skin Aging Induced by UVB Irradiation

*Jingru Wang*[1,2], *Yuanwen Chen*[3], *Jia He*[2], *Guiqiang Li*[2], *Xiaodong Chen*[2]* *and Hongwei Liu*[1]*

[1]Department of Plastic Surgery, The First Affiliated Hospital of Jinan University, Guangzhou, China, [2]Department of Burn Surgery, First People's Hospital of Foshan, Foshan, China, [3]Department of Burn and Plastic Surgery, The People's Hospital of Baoan shenzhen, Shenzhen, China

OPEN ACCESS

**Edited by:**
*Jiliang Zhou,*
*Georgia Health Sciences University, United States*

**Reviewed by:**
*Xiaoling Guo,*
*Wenzhou Medical University, China*
*Jingjing Fan,*
*Xinjiang Medical University, China*

***Correspondence:**
*Xiaodong Chen*
*Cxd234@163.com*
*Hongwei Liu*
*liuhongwei0521@hotmail.com*

**Specialty section:**
*This article was submitted to Reconstructive and Plastic Surgery, a section of the journal Frontiers in Surgery*

**Received:** *23 May 2022*
**Accepted:** *23 June 2022*
**Published:** *08 July 2022*

**Citation:**
*Wang J, Chen Y, He J, Li G, Chen X and Liu H (2022) Anti-Aging Effect of the Stromal Vascular Fraction/ Adipose-Derived Stem Cells in a Mouse Model of Skin Aging Induced by UVB Irradiation. Front. Surg. 9:950967. doi: 10.3389/fsurg.2022.950967*

Adipose-derived stem cells(ADSCs) have been used for anti-photo-aging. But the purification of ADSCs requires *in vitro* amplification and culture, there is considerable risk of direct treatment for patients. Stromal vascular fraction(SVF) is a biologically and clinically interesting heterogeneous cell population contains ADSCs. There are few reports on anti-aging effects of SVF in photo-aging skin. The present study investigated the anti-aging effect of stromal vascular fraction (SVF) and adipose-derived stem cells (ADSCs) injection in photo-aging skin. The relationship between the dosage of injection and effect was also discussed. Thirty healthy, 6-week-old, nude rats were randomly divided into the control and experimental groups. The experimental group needing ultraviolet B (UVB) irradiation five days per week, and a duration of 8 weeks. According to different dose regimens of SVF and ADSCs, experiment rats were randomly grouped as the model control group, low-dose (LD) treatment group, middle-dose (MD) treatment group and high-dose (HD) treatment group. At 7 and 28 days post-treatment, specimens were harvested for histological and immunohistochemical analysis. We found that certain concentrations of cells (MD and HD groups) could improve the texture of photoaged skin. Changes in the epidermal cell layer were clearly observed after 7 days of treatment. The epidermal layer becomes thinner and more tender. After 28 days of treatment, the dermal tissue was thickened and the collagen content and proportion were improved. All these indicators showed no significant difference between the same dosages in the two treatment groups. Our results demonstrate that SVF may have anti-aging potential in photo-aging skin and the ADSCs play an important role in SVF. SVF maybe a potential agent for photo-anging skin and the most effective dose of SVF was $10^6$ cells /100 μl/ injection point. The proper injection interval may be 1.5 cm.

**Keywords: adipose-derived stem cells, stromal vascular fraction, anti photo-aging, dose-effect relationship, cell-mediated therapy**

## INTRODUCTION

Since skin is the largest human organ, it's aging is the most intuitive form of aging. Skin aging is a complex biological process, which is influenced by endogenous (genetic, psychological, etc.) and exogenous factors (1). Under the combined action of these factors, the structure, function, and appearance of the skin changes.

Ultraviolet (UV) exposure is one of the major causative factors for skin aging. Ultraviolet B (UVB) radiation causes connective tissue damage more efficiently than longer wavelength radiation, so it is thought to play a major role in the production of skin wrinkles (2). Long-term UV exposure causes skin wrinkles, roughness, and loss of elasticity (3). Collagen bundles, as the main structural protein of human skin, maintain the skin tensity. Collagen type I (85%–95%) and collagen type III (10%–15%) are the main protein components of the dermis in adults (2, 4). Long-term sun exposure hinders the synthesis of collagen I, ultimately leading to a reduction in the mature collagen bundles and increase in the immature collagen type III, which causes skin wrinkles and sagging (3, 5). UV irradiation can also stimulate dermal inflammatory reaction and activate the inflammatory mediators and cytokines to release resolvase, which gradually dissolves the contents of the dermis (6). Continuous or repetitive protease hydrolysis of extracellular matrix (ECM) is one of the basic characteristics of skin aging process. The imbalance between synthesis and degradation of dermal ECM also leads to wrinkles. The synergistic effect of matrix metalloproteinases (MMPs) family majorly contributes to the degradation of ECM (3, 6, 7) especially MMP-1 and MMP-3. In addition to the changes in the dermis, the histological changes, and the changes in the epidermis due to photo-aging include hyperkeratosis, irregular thickening or atrophy and abnormal proliferation of basal layer cells (6).

Cell therapy has become a primary treatment in all fields of modern medicine. Stem cells have been used for wound healing and tumor treatment. Adipose-derived stem cells (ADSCs) are pluripotent mesenchymal stem cells, which are isolated from adipose tissue by liposuction (8). Numerous studies have shown that ADSCs stimulate the proliferation, secretion, and migration of fibroblast cells, and promote blood vessel regeneration by their paracrine and autocrine effects during the repair and reconstruction of skin tissue injury (8–12). Moreover, previous studies have suggested that ADSCs improve the quality of aging skin by promoting collagen synthesis and anti-oxidation (13, 14). However, the purification of ADSCs requires *in vitro* amplification and culture. There is considerable risk of direct treatment for patients. Stromal vascular fraction (SVF) is a biologically and clinically interesting heterogeneous cell population, which can be employed directly or cultured for selection and expansion of an adherent population, called the ADSCs, whose content is 20%–30% (15). There are very few reports on anti-aging effects of SVF in photo-damaged aged skin. Thus, in the present study, we employed a UVB-induced nude rat model and subcutaneously injected SVF to explore its influence on photo-aging skin. We also explored the action of ADSCs using the corresponding dose relationship to SVF.

## MATERIALS AND METHODS

### Isolation of SVF

Subcutaneous adipose tissue was obtained by tumescent liposuction from healthy women donors ($n = 6$, aged 28–34 years) after informed consent, as approved by the institutional review boards. The adipose tissue samples were washed three times with phosphate buffered saline (PBS), and then the washed aspirates were digested with 0.1% collagenase type I (Sigma, America) for 30 min at 37°C with gentle constant shaking, and centrifuged at 300 g for 10 min. Pellets were resuspended in PBS and filtered with 200 μm nylon mesh followed by centrifugation at 300 g for 10 min. Then, the pellets were resuspended in lysis buffer (0.3% NaCl solution) for 10 min at 37°C, and centrifuged for 5 min at 300 × g to obtain the SVF (16). The percentage of ADSCs in SVF was examined by surface marker expression using flow cytometric analysis with an LSR2 (Becton Dickinson, San Jose, CA). The following monoclonal antibodies were used: CD44 (Miltenyi Biotec, Germany), CD45 (Miltenyi Biotec, Germany), CD34 (BD Biosciences, San Diego, CA), CD29 (BD Biosciences, San Diego, CA), HLA-DR (BD Biosciences, San Diego, CA).

### Isolation and Culture of ADSCs

SVF was isolated as mentioned above and then the cell number of SVF was counted with a cell counter. For culture of ADSCs, the pellet was resuspended in DMEM/low glucose with 10% fetal calf serum, supplemented with 100 U/ml of penicillin and 100 μg of streptomycin, and transferred to T25 flasks at a density of $10^4$ nucleated cells. Primary cells were cultured for three days, non-adherent cells were removed by replacing the medium and the adherent cells were cultured for another day, defined as "Passage 0" (P0). The medium was changed every three days until reaching 70%–80% confluence, the adherent cells were detached by trypsin containing EDTA (Gibco USA) and plated in the same medium at a density of 2,000 cells/$cm^2$. *In vitro* cultured ADSCs were subjected to adipogenic differentiation, osteogenic differentiation and chondrogenic differentiation, and detected using Oil-red O, Alizarin red, and Alcian blue staining (**Figure 1**). Cells of P3 were used in the subsequent experiments.

### UVB-induced Aging Model

Thirty female nude rats were purchased from Charles River Laboratories [SCXK (Jing) 202012-0001]. All rats were housed in climate-controlled quarters (22 ± 1°C, 40%–60% humidity) at the institute of laboratory animal science, Jinan university, with a 12/12 h light/dark cycle. They were acclimatized for one week prior to study initiation, and allowed free access to food and water. The rats were randomly divided into the control group ($n = 6$) and the experimental group ($n = 24$). The experimental model group was further randomly divided into four groups ($n = 6$ each).

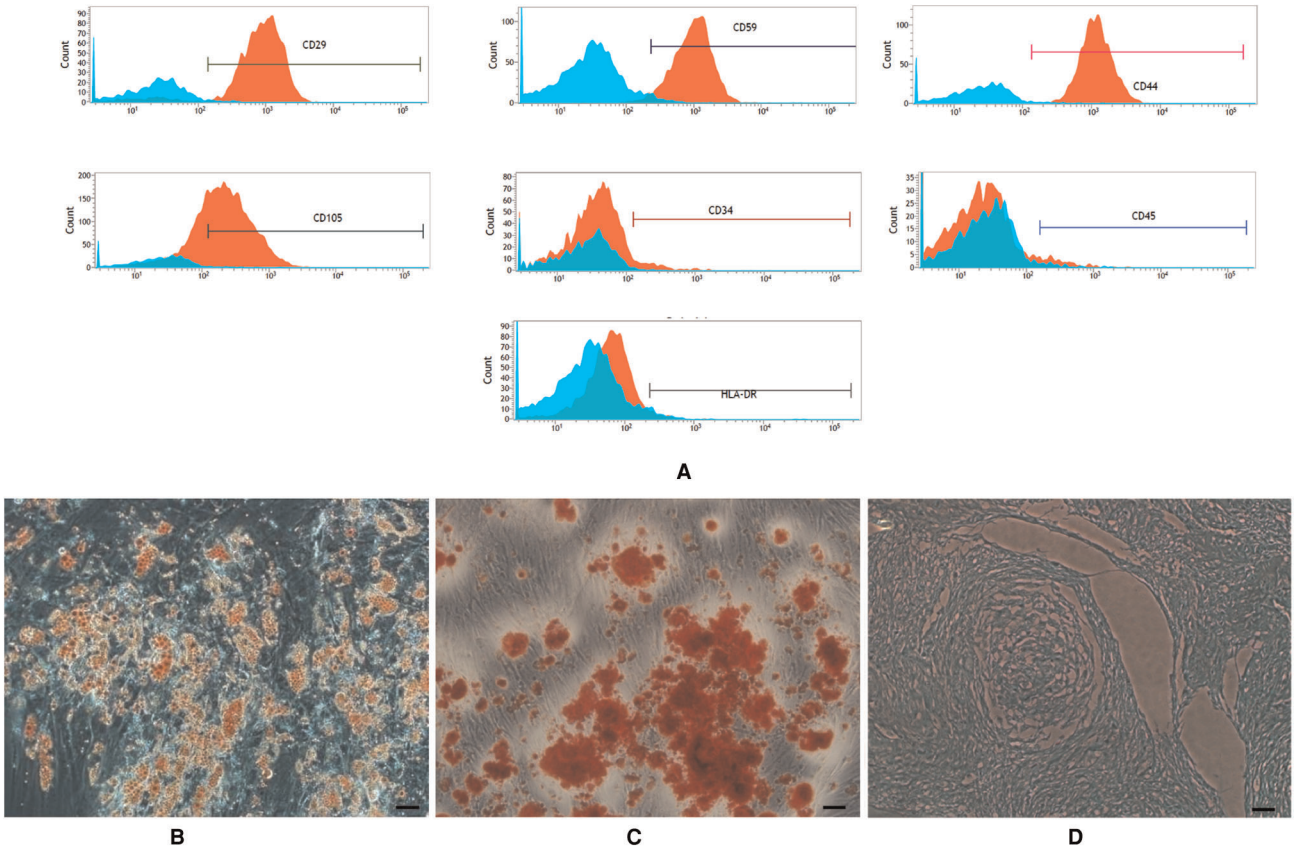


**FIGURE 1** | (**A**) expression of surface marker of the third generation of ADSCs. Flow cytometry labeling of surface markers showed (**B–D**): Multi-lineage differentiation potential of adipose-derived stem cells (ADSCs). (**B**) Oil Red O staining. (**C**) Alizarin red staining. (**D**) Alcian blue staining (scale bars = 50 μm).

The skin wrinkles were induced by UVB irradiation as previously described by Kim Bissett et al (17). The rats were irradiated dorsally using the UVB lamps (Toshiba, 15, W 2 tube, irradiance 290–320 nm) for eight weeks, five times a week. The distance between the lamps and the animals' backs was 50 cm. During exposure, the animals could freely move around in the cages. Irradiation intensity at the skin surface was measured using a UV meter. The irradiation dose was one minimal erythemal dose (MED; 60 mJ/cm$^2$) in the first week, two MED in the second week, three MED in the third week, and four MED in the fourth week, through eight weeks. The total UVB dose was approximately 130 MED (7.8 J/cm$^2$).

## Measurement of the Injection Area

100 μl methylene blue solution was subcutaneously injected into the rats. The diffusion range was measured by a ruler.

## Animal Experiments

After wrinkle induction, the nude rats of the UVB model group were randomly divided into four groups ($n = 6$). Three groups of animals received cell therapy. SVF ($1 \times 10^4$, $1 \times 10^5$, $1 \times 10^6$ cells/100 μl/site) were subcutaneously injected into the restricted area of one side of dorsal skin, and ADSCs ($2 \times 10^3$, $2 \times 10^4$, $2 \times 10^5$ cells/100 μl/site) were subcutaneously injected into the other side (Our experiments confirm that the average percentage of ADSCs in SVF isolated from adipose tissue of healthy women was 25.79 ± 5.7%. To facilitate counting and confirm the minimum effective quantities we chose 20% as the experimental parameters.) The same volume of physiological saline was injected into the UVB model control group and the control group. We marked the injection point daily with a marking pen. One week after injection, biopsy specimens were taken with a 5-mm punch. Skin samples were fixed with 4% paraformaldehyde for histopathology. Four weeks after injection, all animals were sacrificed and skin samples were collected. The skin tissue was divided into two parts. One part was fixed with 4% paraformaldehyde as aforementioned and the other part was stored in liquid nitrogen for subsequent analysis.

## Histological Examination

Skin tissues were dehydrated and paraffin-embedded after 24 h fixation, and serially sectioned (4 μm) for hematoxylin and eosin (H&E) staining. The pictures of each section were taken under ×40 or ×400 magnification. Dermal thickness (the distance between subcutaneous fat and the dermoepidermal junction)

and epidermal thickness (the distance from the granular layer to basal layer) were measured randomly at five sites on each picture.

## Quantitative Polymerase Chain Reaction (qPCR) Analysis

Total RNA was extracted from skin samples stored in liquid nitrogen using TRIzol (Invitrogen, Carlsbad, CA, USA), and then resuspended in RNase-free water. The RNA was electrophoresed in 1% agarose gels to confirm its quality and quantity. Equal amounts of RNA (1 μg) were reverse-transcribed using a cDNA synthesis kit (Toyobo CO. LTD., Japan).

qPCR was performed on a CFX 96™ Real-Time PCR detection system (Bio-Rad mini option, USA) using SYBR Green I PCR Master Mix (Takara BIOINC., Japan). The following oligonucleotides were used as primers: the internal control *β*-actin (F:5′-GAGTACAACCTTCTTGCAGCTC-3′ and R: 5′-CATACCCACCATCACACCCTG-3′), rat collagen I-$\alpha_1$ (F: 5′-GATGGACTCAACGGTCTCCC-3′ and R: 5′-CGGCCACCATCTTGAGACTT-3′), rat collagen III (F: 5′-CT GAAGGGCAGGGAACAACT-3′, R: 5′-ATCCCGAGTCGCA GACACATA-3′), and rat MMP-3 (F: 5′-GATGGACTCAACG GTCTCCC-3′, R: 5′-CGGCCACCATCTTGAGACTT-3′). The two-step qPCR amplification standard procedure was as follows: Step 1, 95°C, 30 s; Step 2, 40 cycles with 95°C, 5 s and 60°C, 30 s. The quantity of PCR products was calculated from the cycle threshold value. The levels of gene expression were normalized with those of *β-actin* gene. The data was calculated with the formula of relative expression quantity = $2^{-\triangle\triangle Ct}$.

## Immunohistochemistry Staining of Ki67

Immunohistochemistry was used to detect the cell proliferation of basal cell layer. Two types of markers were used, respectively: Anti-Ki67 antibody (Abcam, Cambridge, UK). Paraffin sections (4 μm) of each group of 7-day skin samples were dehydrated and rehydrated before immunohistochemical staining. After rehydration, the sections were incubated for 5 min in PBS, followed by microwave antigen retrieval for 10 min in sodium citrate buffer (pH = 6.0). The slide was removed from the microwave oven and allowed to cool at room temperature. Slides were washed with PBS for 5 min, three times and incubated in 3% $H_2O_2$ for 20 min, washed again in PBS, and blocked using a protein block solution for 30 min at room temperature. Then, sections were incubated with the primary antibody at 4°C overnight (over 10 h). The next day, the sections were removed from the fridge and rewarmed to room temperature for 1 h. The sections were washed with PBS for three times and then incubated with a biotinylated secondary antibody for 1 h. Slides were counterstained with diaminobenzidine and visualized on an Olympus microscope. The numbers of Ki67-positive nuclei were quantified using the Image J software on five non-consecutive tissue sections for each image, respectively.

## Statistical Analysis

All values are expressed as mean ± standard deviation. The data were evaluated by analysis of variance followed by a Newman-Keuls' test for multiple comparisons. The difference was considered to be significant if $P < 0.05$.

# RESULTS

## Percentage of ADSCs in SVF

Flow cytometric analyses showed that the average percentage of ADSCs in SVF isolated from adipose tissue of healthy women was 25.79 ± 5.7%.

## Characterization of ADSCs

ADSCs expanded easily *in vitro* and exhibited a fibroblast-like morphology. Characteristic expressions of stem cell-related surface markers were confirmed by flow cytometry. ADSCs expressed CD29, CD59, CD44 and CD105, but not CD34, CD45 and HLA-DR (**Figure 1A**). ADSCs were incubated in media known to induce an adipogenic, osteogenic, or chondrogenic lineage. Adipogenic, osteogenic, and chondrogenic differentiation was confirmed by Oil Red O staining (**Figure 1B**), Alizarin red S staining (**Figure 1C**), and Alcian blue staining (**Figure 1D**).

## Diffusion Range of Subcutaneously Injected Methylene Blue Solution in the Back Skin of Rats

The methylene blue solution diffused as a circle with a diameter of 1.5 cm after subcutaneous injection (**Figure 2**).

## Effect of SVF and ADSCs Injection on Epidermal Thickness and the Proportion of Stratum Corneum in the Epidermis

H&E staining showed significant changes in skin samples from treated rats compared to control rats after seven days (**Figure 3A**). Measurement of the epidermal thickness showed decrease in the MD and HD groups of SVF and ADSCs ($P < 0.05$) (**Figure 3B**). No difference was observed in the matched groups between SVF and ADSCs (**Figure 3B**). The proportion of stratum corneum in the epidermis was also decreased in the MD and HD groups of SVF and ADSCs ($P < 0.05$) (**Figure 3C**). No difference was observed in the matched groups between SVF and ADSCs (**Figure 3C**).

## Analysis of the Proliferation of the Basal Layer of Epidermis

UVB exposure stimulated abnormal proliferation of the basal layer cells. SVF and ADSCs treatment decreased the abnormal proliferation (**Figure 4A**). We measured Ki67-positive nuclei to further confirm the efficacy. As shown in **Figure 4B** all of the treated groups had lower proliferation rates ($P < 0.05$). The efficacy was significantly higher in the HD treatment group. No difference was observed in the matched groups between SVF and ADSCs (**Figure 4B**).

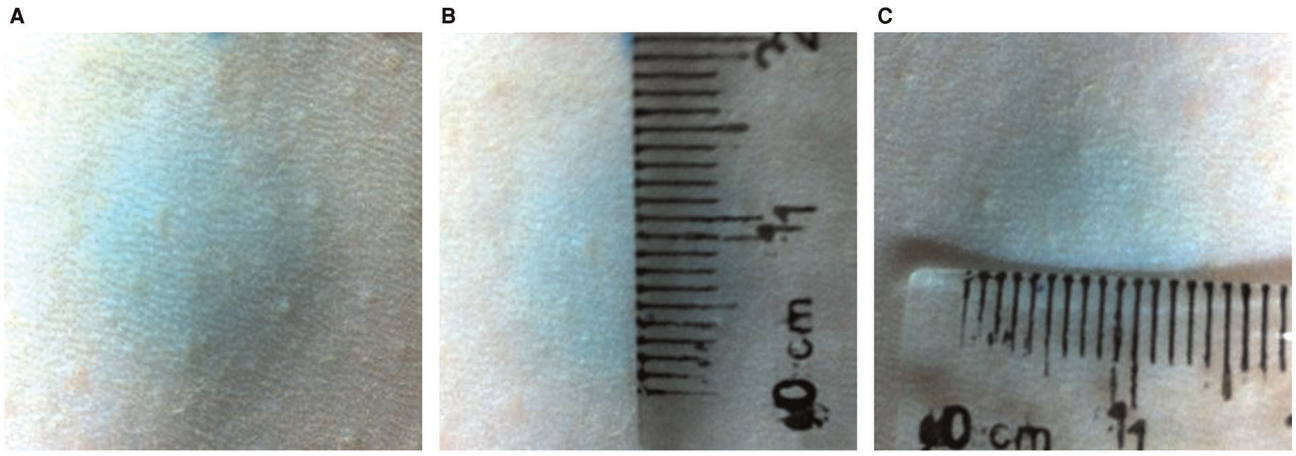


**FIGURE 2** | The diffusion range of 100 μl methylene blue solution subcutaneous injection the back skin of rats. The methylene blue solution diffused as a circle with a diameter of 1.5 cm after subcutaneous injection.

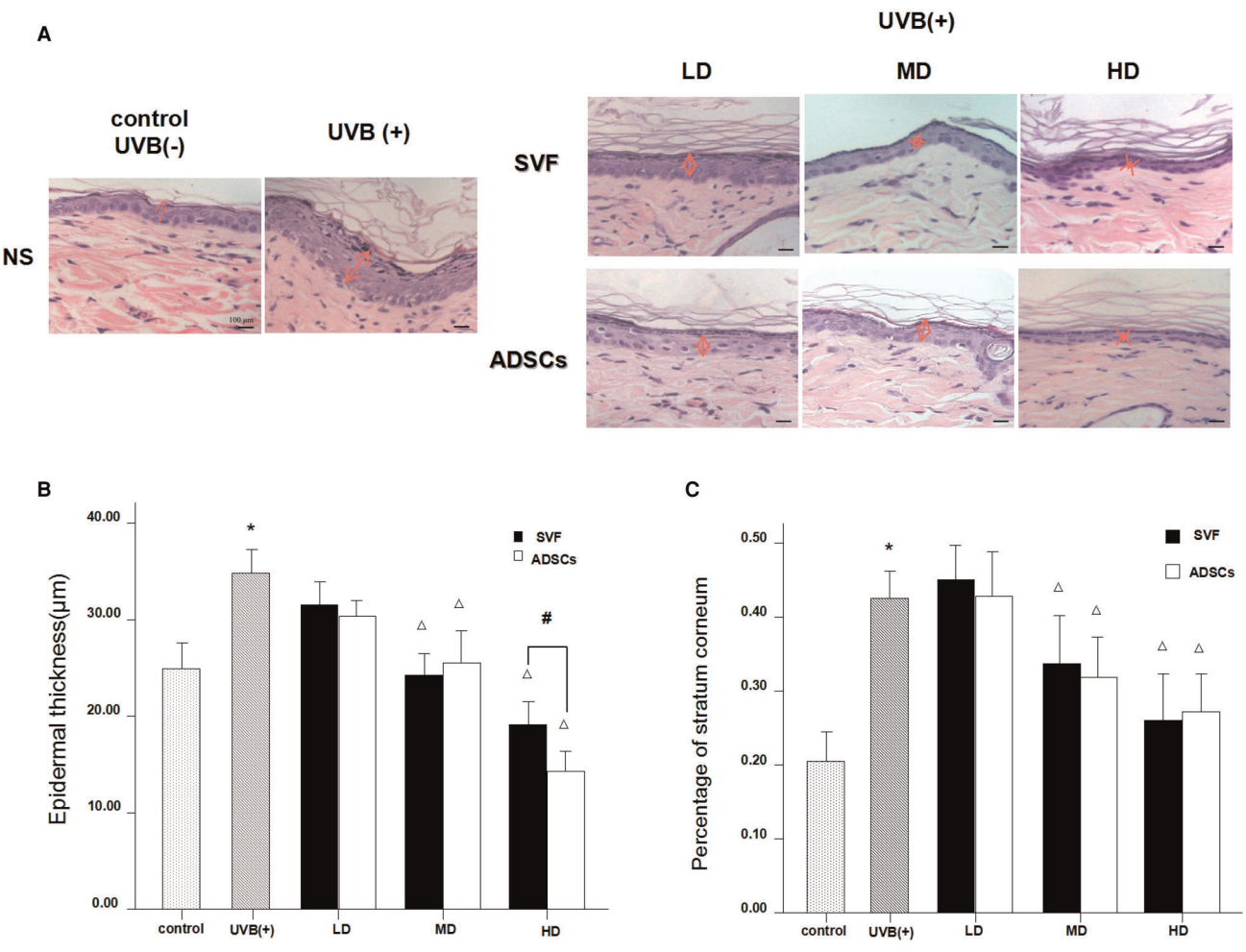


**FIGURE 3** | Haematoxylin staining showed the changes of epidermal thickness of nude rats exposed to UVB 7 days after SVF treatment and ADSCs treatment (×400). (**A**) UVB exposure decreased the epidermal thickness of nude rats and SVF and ADSCs treatment increased the epidermal thickness of aging skin. (**B**) The epidermal thickness of UVB exposed group and SVF and ADSCs treatment groups. (**C**) Percentage of stratum corneum of UVB exposed group and SVF and ADSCs treatment groups. Mean ± SD. $n = 6$. $^{*}P < 0.05$ vs control group. $^{\triangle}P < 0.05$ vs UVB(+) group. $^{\#}P < 0.05$ between the groups with line marker.

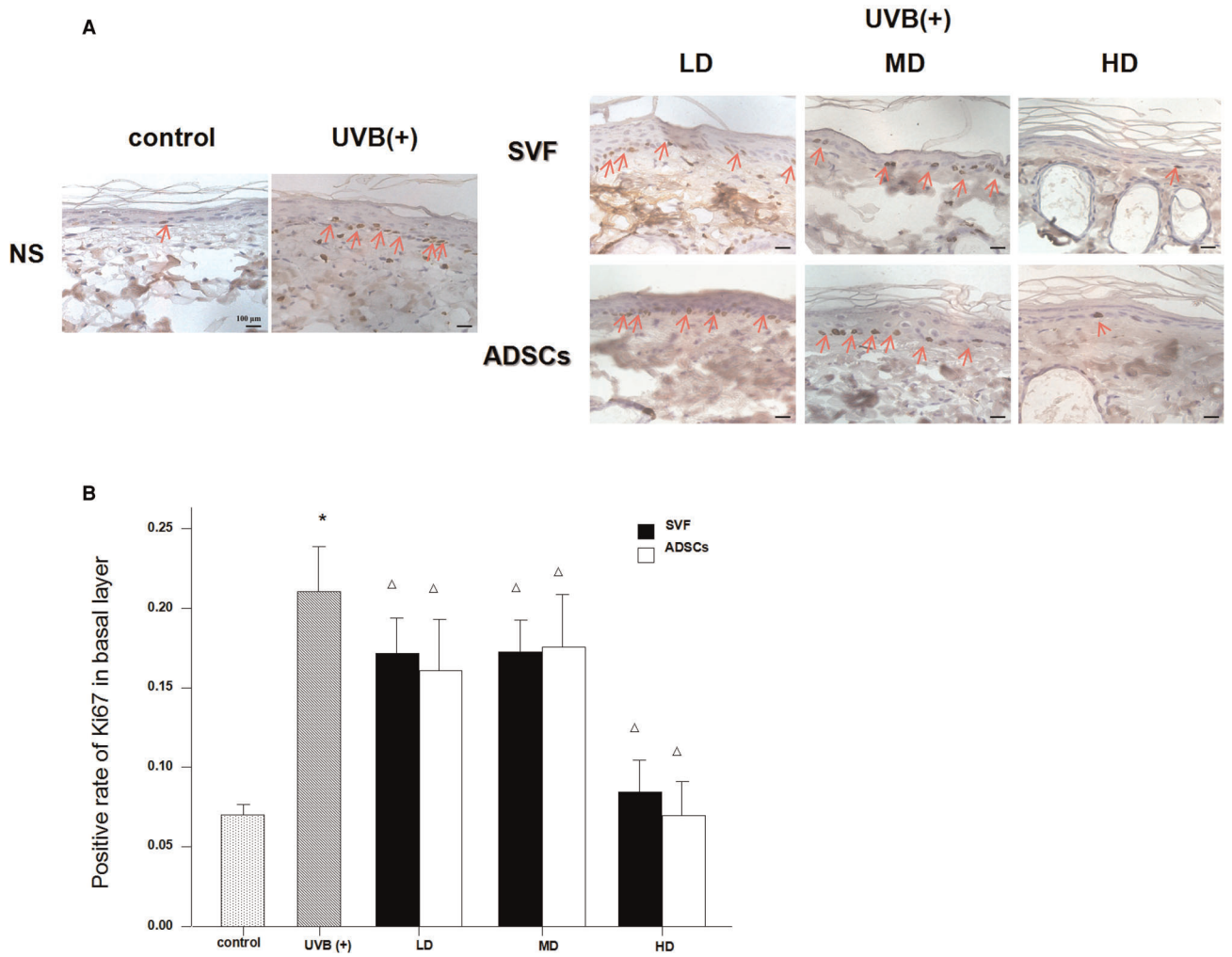


**FIGURE 4** | Ki67 immunostain showed the proliferation of basal cell nuclei that treated with ADSCs and SVF after 7 days (×400). (**A**) UVB exposure stimulated abnormal proliferation of the basal layer cells. SVF and ADSCs treatment decreased the abnormal proliferation. (**B**) All of the treated groups had lower proliferation rates ($p < 0.05$). The efficacy was significantly higher in the HD treatment group. No difference was observed in the matched groups between SVF and ADSCs. Mean ± SD. $n = 6$. *$P < 0.05$ vs control group. △$P < 0.05$ vs UVB (+) group.

## Effect of SVF and ADSCs Injection on Dermal Thickness

**Figure 5A** shows the histological measurements of the dermal thickness of the nude rats by H&E staining after 28 d. The dermal thickness increased in the HD groups with SVF and ADSCs treatment ($P < 0.05$) (**Figure 5B**). No difference was observed in the matched groups between SVF and ADSCs (**Figure 5B**).

## Relative mRNA Expression of Collagen Type I, Collagen Type III and Matrix Metalloproteinase 3 (MMP-3) in Dermis

The mRNA expression levels of collagen type I, collagen type III and MMP-3 were compared between the experimental groups. As shown in **Figure 6**, the relative mRNA expression of collagen type I was increased in the MD and HD groups of SVF and ADSCs ($P < 0.05$). As shown in **Figure 7**, collagen type III expression was decreased in the MD and HD groups of SVF and ADSCs ($P < 0.05$). The relative mRNA expression of MMP-3 was decreased in all groups (**Figure 8**), and the MD and HD groups showed statistically significant decrease ($P < 0.05$). No difference was observed in the matched groups between SVF and ADSCs in the above targets (**Figures 6–8**).

# DISCUSSION

Cell therapy has become an important component in the development of modern medicine. For example, stem cells, which have reproductive capacity, are used to treat therioma or restore organ functions after damage by disease or trauma.

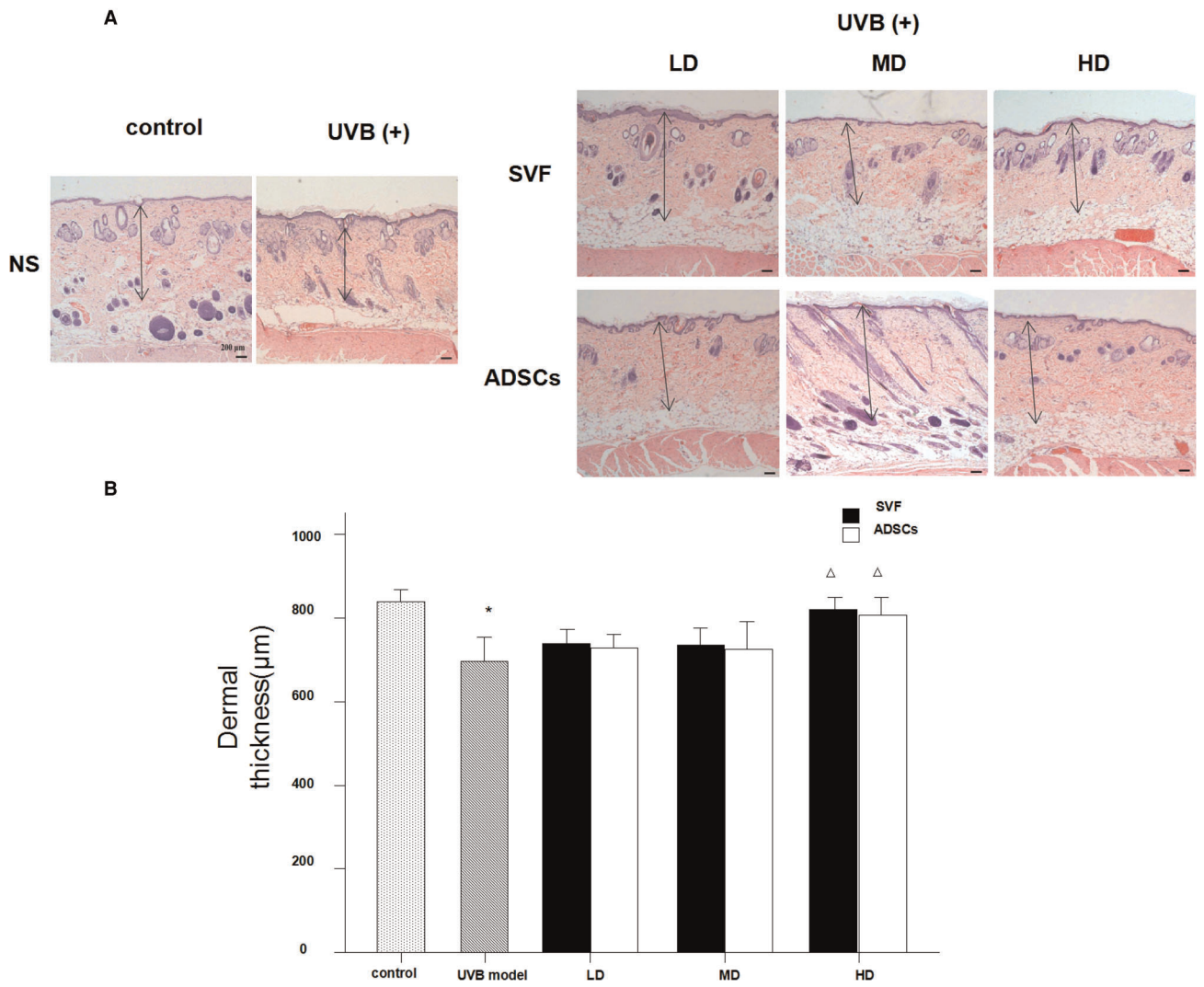


**FIGURE 5** | Haematoxylin staining showed the changes of dermal thickness of nude rats exposed to UVB 28 days after SVF treatment (×40). (**A**) UVB exposure decreased dermal thickness and SVF and ADSCs treatment increased dermal thickness of aging skin. (**B**) The dermal thickness of UVB exposed group and SVF and ADSCs treatment groups. Mean ± SD. $n = 6$. $^{*}P < 0.05$ vs control group. $^{\triangle}P < 0.05$ vs UVB model group.

Embryonic stem cells obtained from fetuses were considered to be the best source, and have been thoroughly investigated. However, there are serious ethical issues and carcinogenic potential that hinder their clinical application (18). Therefore, adult stem cells have been used as they do not have the ethical problems related to embryonic stem cells. In recent years, literature related to SVF cells and ADSCs has been considerably augmented. These studies have demonstrated the safety and efficacy of autologous SVF use in regenerative cell therapy for wound healing, skeletal regeneration, cardiovascular and peripheral vascular diseases, and tissue engineering (19, 20). However, there are few reports on its anti photo-aging potential. SVFs are widely present in fat tissue, which contains 20%–30% ADSCs, and can be easily harvested during aesthetic lipoaspiration procedures. Hence, sufficient quantity of cells can be easily obtained from patients with less pain. The cells can be immediately used during the surgery. Moreover, it can avoid the biological safety issues and reduce the risk of infection due to absence of exogenous substance during the operation. The present study demonstrated that SVF, which contains ADSCs, has effective anti-wrinkle properties, as observed by the effects on epidermal thickness, epidermal stratum corneum thickness, abnormal proliferation of basal layer, dermal thickness and relative mRNA expressions of dermal collagen I, collagen III and MMP-3.

The epidermal turnover time of healthy human skin is 28 days. However, in the case of foreign invasion and destruction

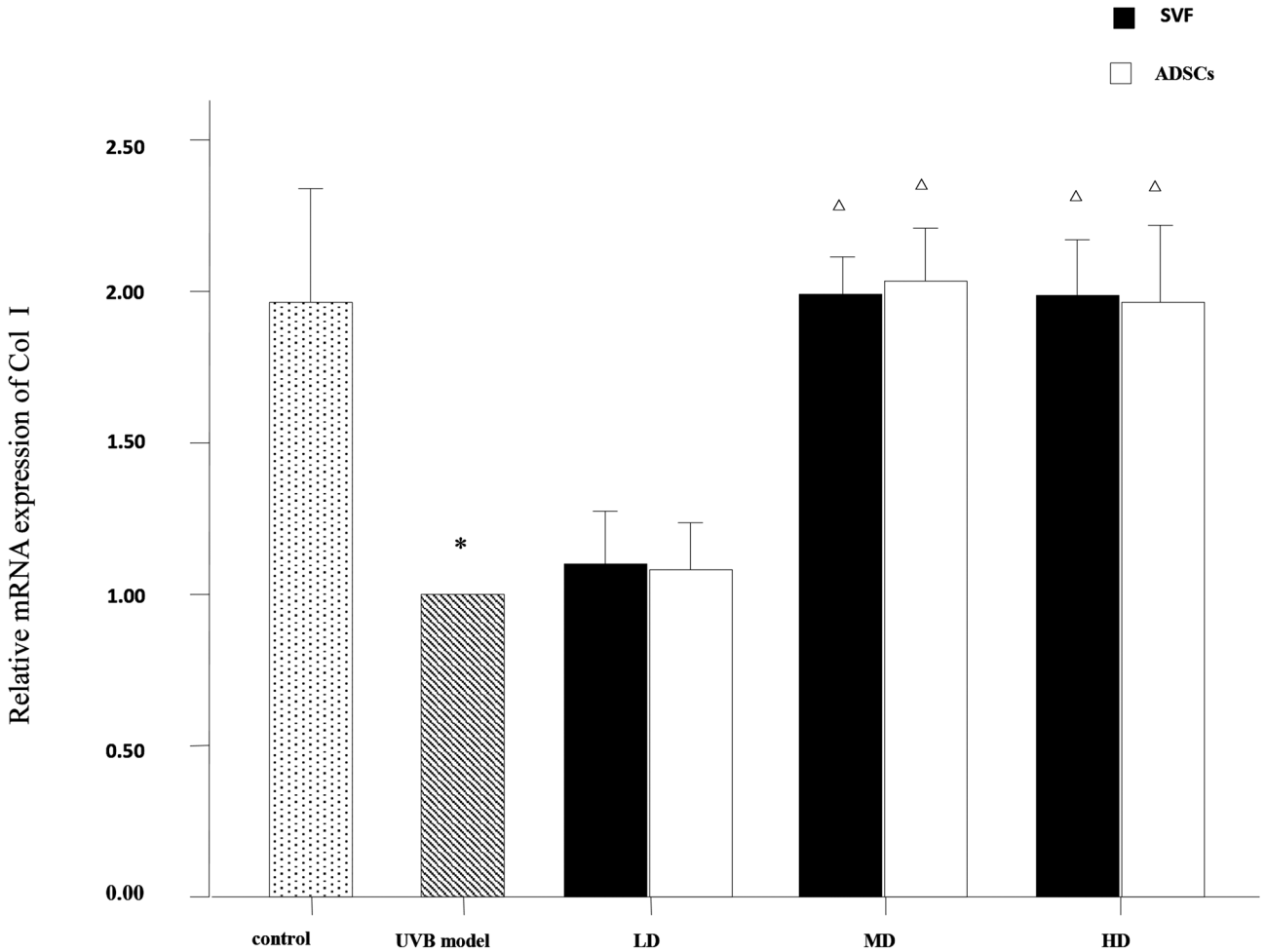


**FIGURE 6** | Quantitative polymerase chain reaction (qPCR) showed the relative mRNA expression of collagen I of nude rats exposed to UVB 28 days after SVF and ADSCs treatment. Mean ± SD. $n = 6$. $^{*}P < 0.05$ vs control group. $^{\triangle}P < 0.05$ vs UVB model group.

of the stratum corneum, the basal cell division is activated to remove foreign bodies for repair. The chemical (organic solvents, etc.) or physical (UVB, etc.) irritation may trigger epidermal hyperplasia and abnormal dyskeratosis (21). In our study, we observed that long-term UVB irradiation increased the epidermal thickness, especially in the stratum corneum, and the proportion of stratum corneum was obviously increased in the epidermis. Moreover, long-term exposure to UV irradiation led to disarrangement of the basal cells and changes in the morphology of nuclei. UV irradiation activated the proliferation of epidermal keratinocytes, which is an adaptive process of cell apoptosis, and DNA damage can cause abnormal proliferation of cells in the absence of repair (22, 23). After the SVF and ADSCs treatment, the abnormal proliferation of basal layer cells was significantly decreased. The proliferating phase cells were similar to normal skin when the cell concentration reached $10^6$/100 μl in the SVF treatment group. The same result was observed at the cell concentration of $2 \times 10^5$/100 μl in the ADSCs treatment group. Hence, SVF was involved in the regulation of anti-UV damage in photo-aging skin, and ADSCs played a major role in this process. The underlying mechanism needs further study. SVF possibly repairs the epidermal damage of UV irradiation by the following processes: (1) SVF can inhibit the abnormal proliferation of basal cells; (2) SVF can accelerate the epidermal turnover rate; (3) SVF facilitates the division, maturity and loss of skin cells in a renewed state of equilibrium.

Photo-aging is a complex reparative process, with similarities to pathological skin wounds. It has been reported that adult stem cells can promote the proliferation of fibroblasts and the formation of new blood vessels by secreting cytokines, and promote the growth and epithelialization of granulation tissue, in order to promote wound healing (9, 10); while collagen repair is facilitated by promoting the secretion of fibroblasts in dermal tissue (11, 13, 15). Collagen accounts for about 90% of the human dermal protein and the major collagenous constituents of healthy dermis are the collagen type I (85%–95%) and type III (10%–15%) (2, 4). Aging decreases the

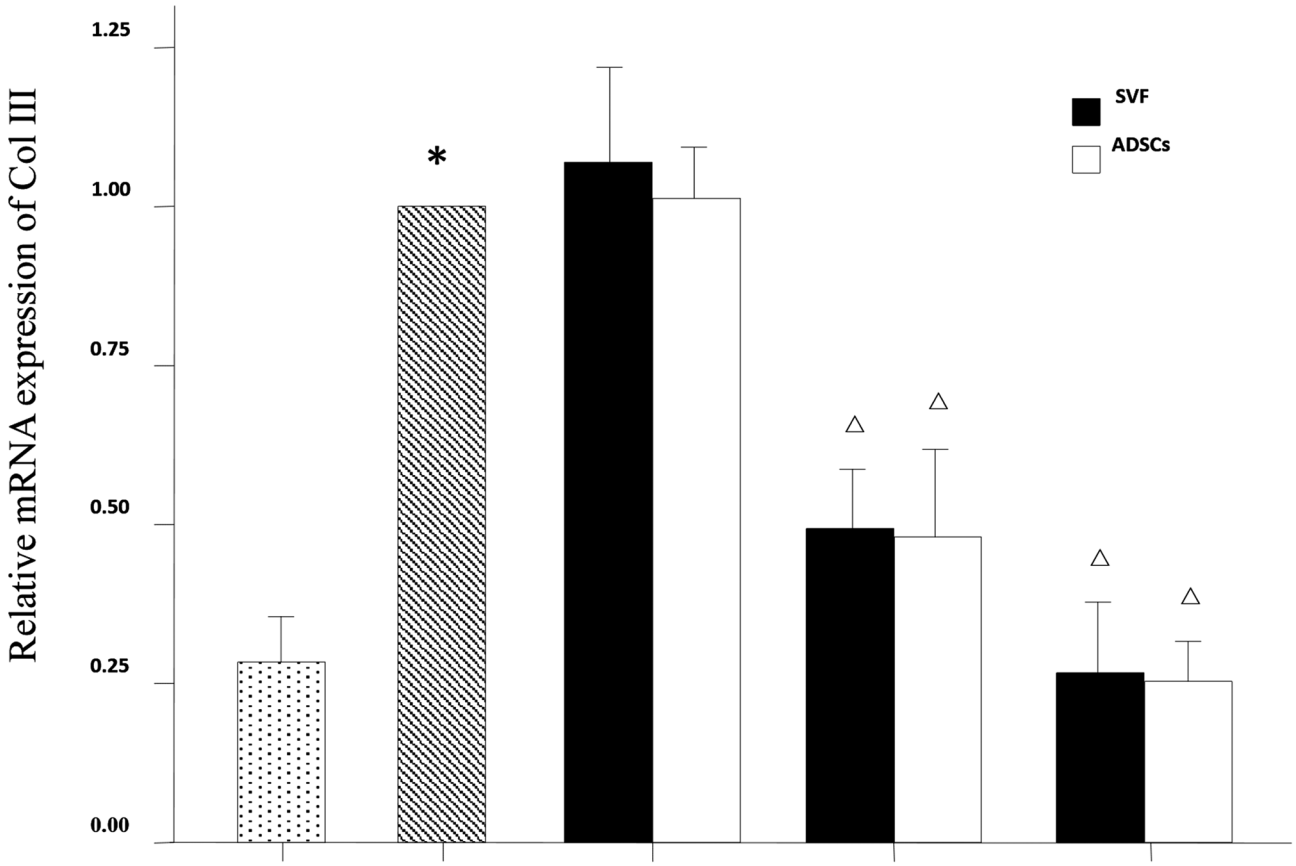


**FIGURE 7** | qPCR showed the relative mRNA expression of collagen III of nude rats exposed to UVB 28 days after SVF and ADSCs treatment. Mean ± SD. $n = 6$. $^{*}P < 0.05$ vs control group. $^{\triangle}P < 0.05$ vs UVB model group.

content of collagen I and increases collagen III ratio in the same part of the skin, which is more pronounced in the UVB-exposed area (24). The decrease in collagen content and the change in collagen ratio leads to skin relaxation and eventual collapse to form the wrinkles (1, 23). These changes have been shown to correlate well with clinical severity of photo-aging (4). The present study showed that subcutaneous injection of SVF can increase the thickness of dermis, promote the relative mRNA expression of collagen type I, and inhibit the relative mRNA expression of collagen type III. Both middle-dose and high-dose of SVF treatment could improve the proportion of collagen type I and type III in dermis, which resembled young and healthy skin tissue.

Collagen reduction results from a combination of increased enzymatic breakdown *via* the actions of MMPs (5). MMPs are a family of proteins containing zinc that can cause tissue damage by degradation of the ECM leading to wrinkle formation (4). Excessive UV irradiation enhances the secretion of MMPs by keratinocytes, fibroblasts, and inflammatory cells. MMP-1, MMP-3 and MMP-9 are stimulated by UV irradiation, and alter collagen type I, which is related to the quality of the skin. MMP-1 initiates collagen fiber fracture process and MMP-3 leads to its degradation (5). MMP-3 can also activate pro-MMP-1. The amount of MMP-3 in the dermal tissue has a direct impact on the degradation efficiency of collagen (4, 11). Therefore, MMP-3 expression is an important determinant of wrinkle formation. MMP-3 mRNA expression can be used as an indicator of altered collagen content in the skin (11). The results of the present study showed that the relative expression of MMP-3 mRNA was decreased in all the SVF treatment groups. We hypothesized that SVF may hinder the degradation rate of collagen protein by down-regulating the expression of MMP-3 mRNA, which leads to a new homeostasis between synthesis and degradation of collagen protein and increases the collagen content in order to improve the quality of photo-aging skin.

The SVF contains multiple components, it is not clear whether the efficacy of anti-aging is attributable to the ADSCs or other components of fat tissue. The results of this study showed no significant difference in the corresponding dose group between SVF and ADSCs in all observed targets. Therefor, we infer that ADSCs is the main cellular component of SVF, which has a major effect in increasing the dermal thickness and collagen content (1, 18).

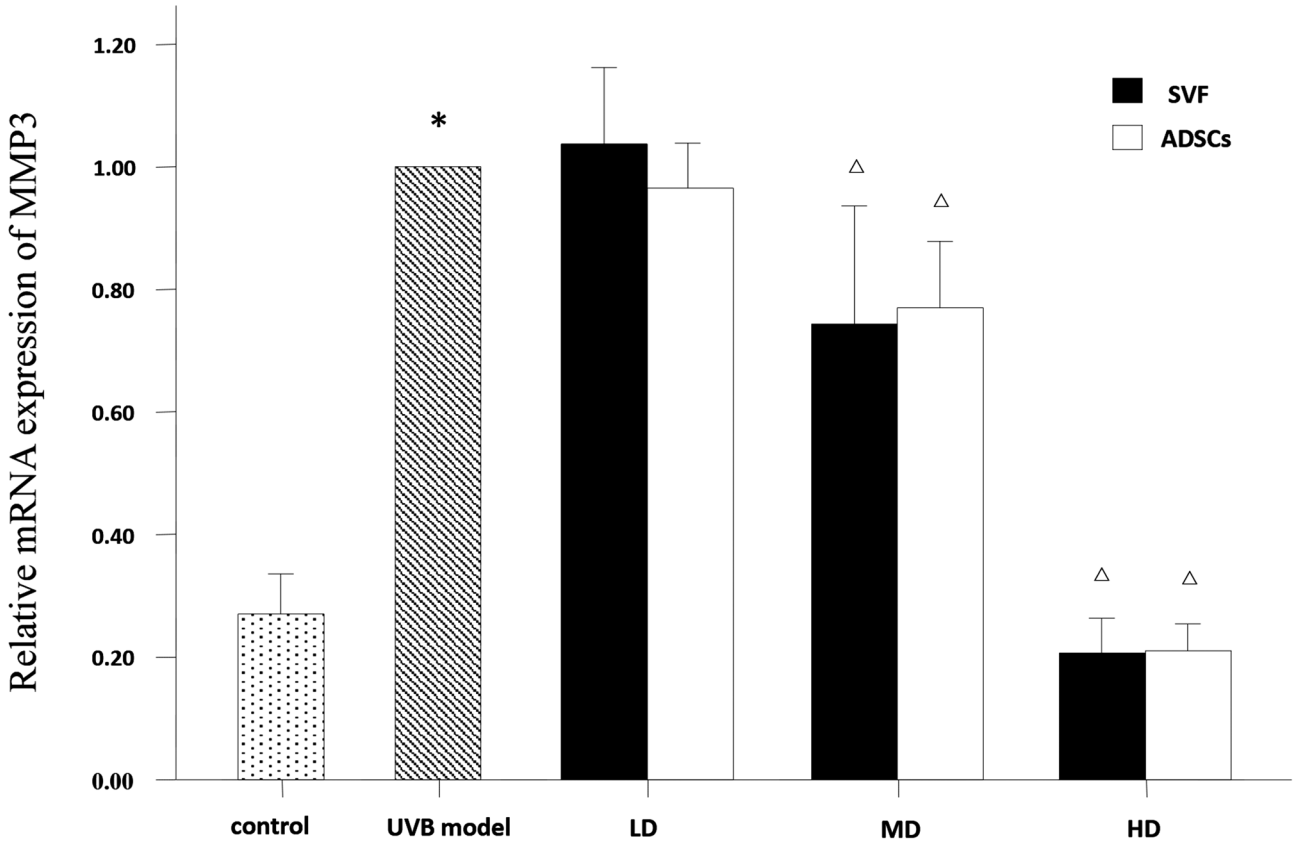


**FIGURE 8** | qPCRed the relative mRNA expression of MMP3 of nude rats exposed to UVB 28 days after SVF and ADSCs treatment. Mean ± SD. $n = 6$. *$P < 0.05$ vs control group. $^{\triangle}P < 0.05$ vs UVB model group.

The therapeutic role of SVF in photo-aging has been demonstrated, but how to put it into clinical application is still a question worth exploring. The use dose and injection method of SVF were also discussed in our study. Based on the operability and clinical application, we selected low, medium and high doses ($1 \times 10^4$, $1 \times 10^5$, $1 \times 10^6$cells/100 μl/site) of SVF. We found that it acted on the epidermis and germinal layer cells when the cell numbers reached $10^5$cells/100 μl/site. But this treatment concentration did not improve the dermal thickness. Quantitative polymerase chain reaction (qPCR) analysis show that the relative mRNA expression of collagen type I was increased and collagen type III expression was decreased in MD group. Due to the deficiency of our experiments, the protein content in the dermis was not further determined, so we cannot deny that this is an effective concentration. Therefore, we considered that $10^5$cells/100 μl/site as the effective concentration, but $10^6$cells/100 μl/site as the optimal concentration. To determine the mode of injection, 100 μl methylene blue solution was subcutaneously injected into the rats. The methylene blue solution diffused as a circle with a diameter of 1.5 cm after subcutaneous injection. This suggests that we should be 1.5 cm apart between the two injection points.

## CONCLUSIONS

In summary, our study demonstrated that SVF had anti photo-aging effect in the UVB-irradiated mouse model. By comparing the effect of SVF and corresponding dose of ADSCs, ADSCs were found to play a major role in SVF. Although the multiplication capacity of basal cells and the relative expression of MMP-3 mRNA were significantly improved at all doses of SVF, analyses of epidermal and dermal thicknesses and the relative mRNA expression of collagen type I and type III suggested that the clinical dose of SVF in humans should be the high-dose in mice, which is $10^6$cells/100 μl/site. The methylene blue solution injection in rat skin indicated that the best injection interval is 1.5 cm. Although some progress has been made on the use of SVF, the underlying mechanism and the role of other endogenous cells need to be addressed.

## DATA AVAILABILITY STATEMENT

The original contributions presented in the study are included in the article/Supplementary Material, further inquiries can be directed to the corresponding author/s.

## ETHICS STATEMENT

The studies involving human participants were reviewed and approved by The Medical Ethics Committee of the First Affiliated Hospital of Jinan University. The patients/participants provided their written informed consent to participate in this study.

The animal study was reviewed and approved by The Experimental Animal Ethics Committee of Jinan University.

## AUTHOR CONTRIBUTIONS

JW: Conception and design, provision of study material, collection of data, manuscript writing and final approval of the manuscript. YC & JH: Provision of study material, collection of data and final approval of the manuscript. GL: Collection of data and final approval of the manuscript. XC & HL: Conception and design, data analysis, manuscript writing and final approval of the manuscript. All authors have read and agreed to the published version of the manuscript.

## REFERENCES


1. Ganceviciene R, Liakou AI, Theodoridis A, Makrantonaki E, Zouboulis CC. Skin anti-aging strategies. *Dermato-endocrinology*. (2012) 4(3):308–19. doi: 10.4161/derm.22804
2. Park HM, Kim HJ, Jang YP, Kim SY. Direct analysis in real time mass spectrometry (DART-MS) analysis of skin metabolome changes in the ultraviolet B-induced mice. *Biomol Ther (Seoul)*. (2013) 21(6):470–5. doi: 10.4062/biomolther.2013.071
3. Fisher GJ, Wang ZQ, Datta SC, Varani J, Kang S, Voorhees JJ. Pathophysiology of premature skin aging induced by ultraviolet light. *N Engl J Med*. (1997) 337(20):1419–28. doi: 10.1056/nejm199711133372003
4. Kim HH, Lee MJ, Lee SR, Kim KH, Cho KH, Eun HC, et al. Augmentation of UV-induced skin wrinkling by infrared irradiation in hairless mice. *Mech Ageing Dev*. (2005) 126(11):1170–7. doi: 10.1016/j.mad.2005.06.003
5. Quan TH, Qin ZP, Xia W, Shao Y, Voorhees JJ, Fisher GJ. Matrix-degrading metalloproteinases in photoaging. *J Investig Dermatol Symp Proc* (2009) 14 (1):20–4.
6. Chung JH, Hanft VN, Kang S. Aging and photoaging. *J Am Acad Dermatol*. (2003) 49(4):690–7. doi: 10.1067/s0190-9622(03)02127-3
7. Bosch R, Philips N, Suárez-Pérez JA, Juarranz A, Devmurari A, Chalensouk-Khaosaat J, et al. Mechanisms of photoaging and cutaneous photocarcinogenesis, and photoprotective strategies with phytochemicals. *Antioxidants (Basel, Switzerland)*. (2015) 4(2):248–68. doi: 10.3390/antiox4020248
8. Zuk PA, Zhu M, Mizuno H, Huang J, Futrell JW, Katz AJ, et al. Multilineage cells from human adipose tissue: implications for cell-based therapies. *Tissue Eng*. (2001) 7(2):211–28. doi: 10.1089/107632701300062859
9. Rehman J, Traktuev D, Li J, Merfeld-Clauss S, Temm-Grove C, Bovenkerk J, et al. Secretion of angiogenic and antiapoptotic factors by human adipose stromal cells. *Circulation*. (2004) 109(10):1292–8. doi: 10.1161/01.cir.0000121425.42966.f1
10. Kim WS, Park BS, Sung JH. The wound-healing and antioxidant effects of adipose-derived stem cells. *Expert Opin Biol Ther*. (2009) 9(7):879–87. doi: 10.1517/14712590903039684
11. Kim BH, Son WC, Yim CO, Kang SK, Ra JC, Kim YC. Anti-wrinkle effects of adipose tissue-derived mesenchymal stem cells in a UV-irradiated hairless mouse model. *Tissue Eng Regen Med*. (2010) 7(5):583–91.
12. Kim WS, Park BS, Park SH, Kim HK, Sung JH. Antiwrinkle effect of adipose-derived stem cell: activation of dermal fibroblast by secretory factors. *J Dermatol Sci*. (2009) 53(2):96–102. doi: 10.1016/j.jdermsci.2008.08.007
13. Kim WS, Park BS, Sung JH. Protective role of adipose-derived stem cells and their soluble factors in photoaging. *Arch Dermatol Res*. (2009) 301(5):329–36. doi: 10.1007/s00403-009-0951-9
14. Kim WS, Park SH, Ahn SJ, Kim HK, Park JS, Lee GY, et al. Whitening effect of adipose-derived stem cells: a critical role of TGF-beta 1. *Biol Pharm Bull*. (2008) 31(4):606–10. doi: 10.1248/bpb.31.606
15. Park BS, Jang KA, Sung JH, Park JS, Kwon YH, Kim KJ, et al. Adipose-derived stem cells and their secretory factors as a promising therapy for skin aging. *Dermatol Surg*. (2008) 34(10):1323–6. doi: 10.1111/j.1524-4725.2008.34283.x
16. Alharbi Z, Opländer C, Almakadi S, Fritz A, Vogt M, Pallua N. Conventional vs. Micro-fat harvesting: how fat harvesting technique affects tissue-engineering approaches using adipose tissue-derived stem/stromal cells. *J Plast Reconstr Aesthet Surg*. (2013) 66(9):1271–8. doi: 10.1016/j.bjps.2013.04.015
17. Bissett DL, Hannon DP, Orr TV. An animal model of solar-aged skin: histological, physical, and visible changes in UV-irradiated hairless mouse skin. *Photochem Photobiol*. (1987) 46(3):367–78. doi: 10.1111/j.1751-1097.1987.tb04783.x
18. Kim JH, Jung M, Kim HS, Kim YM, Choi EH. Adipose-derived stem cells as a new therapeutic modality for ageing skin. *Exp Dermatol*. (2011) 20(5):383–7. doi: 10.1111/j.1600-0625.2010.01221.x
19. Klumpers DD, Mooney DJ, Smit TH. From skeletal development to tissue engineering: lessons from the micromass assay. *Tissue Eng Part B Rev*. (2015) 21(5):427–37. doi: 10.1089/ten.TEB.2014.0704
20. Zhou L, Xia J, Qiu X, Wang P, Jia R, Chen Y, et al. In vitro evaluation of endothelial progenitor cells from adipose tissue as potential angiogenic cell sources for bladder angiogenesis. *PLoS One*. (2015) 10(2):e0117644. doi: 10.1371/journal.pone.0117644
21. Harding CR. The stratum corneum: structure and function in health and disease. *Dermatol Ther*. (2004) 17(Suppl 1):6–15. doi: 10.1111/j.1396-0296.2004.04s1001.x
22. Kramer E, Herman O, Frand J, Leibou L, Schreiber L, Vaknine H. Ki67 as a biologic marker of basal cell carcinoma: a retrospective study. *Israel Med Assoc J*. (2014) 16(4):229–32.
23. Ichihashi M, Ueda M, Budiyanto A, Bito T, Oka M, Fukunaga M, et al. UV-induced skin damage. *Toxicology*. (2003) 189(1-2):21–39. doi: 10.1016/s0300-483x(03)00150-1
24. Schwartz E, Cruickshank FA, Christensen CC, Perlish JS, Lebwohl M. Collagen alterations in chronically sun-damaged human skin. *Photochem Photobiol*. (1993) 58(6):841–4. doi: 10.1111/j.1751-1097.1993.tb04981.x


**Conflict of Interest:** The authors declare that the research was conducted in the absence of any commercial or financial relationships that could be construed as a potential conflict of interest.

**Publisher's Note:** All claims expressed in this article are solely those of the authors and do not necessarily represent those of their affiliated organizations, or those of the publisher, the editors and the reviewers. Any product that may be evaluated in this article, or claim that may be made by its manufacturer, is not guaranteed or endorsed by the publisher.

*Copyright © 2022 Wang, Chen, He, Li, Chen and Liu. This is an open-access article distributed under the terms of the Creative Commons Attribution License (CC BY). The use, distribution or reproduction in other forums is permitted, provided the original author(s) and the copyright owner(s) are credited and that the original publication in this journal is cited, in accordance with accepted academic practice. No use, distribution or reproduction is permitted which does not comply with these terms.*

frontiers | Frontiers in Surgery

TYPE Original Research
PUBLISHED 21 July 2022
DOI 10.3389/fsurg.2022.860806

Check for updates

OPEN ACCESS

EDITED BY
Kun Xiong,
Central South University, China

REVIEWED BY
Mattia Riefolo,
University of Bologna, Italy
Jinchun Wu,
Zhongshan Hospital Affiliated to Fudan University (QingPu Branch), China

*CORRESPONDENCE
Yan Han
13720086335@163.com
Yi Yang
sydyy@163.com

†These authors have contributed equally to this work.

SPECIALTY SECTION
This article was submitted to Reconstructive and Plastic Surgery, a section of the journal Frontiers in Surgery

RECEIVED 23 January 2022
ACCEPTED 07 July 2022
PUBLISHED 21 July 2022

CITATION
Xu Y, Chen Y, Niu Z, Yang Z, Xing J, Yin X, Guo L, Zhang Q, Yang Y and Han Y (2022) Ferroptosis-related lncRNA signature predicts prognosis and immunotherapy efficacy in cutaneous melanoma.
Front. Surg. 9:860806.
doi: 10.3389/fsurg.2022.860806

COPYRIGHT
© 2022 Xu, Chen, Niu, Yang, Xing, Yin, Guo, Zhang, Yang and Han. This is an open-access article distributed under the terms of the Creative Commons Attribution License (CC BY). The use, distribution or reproduction in other forums is permitted, provided the original author(s) and the copyright owner(s) are credited and that the original publication in this journal is cited, in accordance with accepted academic practice. No use, distribution or reproduction is permitted which does not comply with these terms.

# Ferroptosis-related lncRNA signature predicts prognosis and immunotherapy efficacy in cutaneous melanoma

Yujian Xu[1†], Youbai Chen[1†], Zehao Niu[1†], Zheng Yang[1], Jiahua Xing[1], Xiangye Yin[1], Lingli Guo[1], Qixu Zhang[2], Yi Yang[3*] and Yan Han[1*]

[1]Department of Plastic and Reconstructive Surgery, Chinese PLA General Hospital, Beijing, China, [2]Department of Plastic Surgery, The University of Texas MD Anderson Cancer Center, Houston, TX, United States, [3]Department of Dermatology, Chinese PLA General Hospital, Beijing, China

**Purpose:** Ferroptosis-related lncRNAs are promising biomarkers for predicting the prognosis of many cancers. However, a ferroptosis-related signature to predict the prognosis of cutaneous melanoma (CM) has not been identified. The purpose of this study was to construct a ferroptosis-related lncRNA signature to predict prognosis and immunotherapy efficacy in CM.

**Methods:** Ferroptosis-related differentially expressed genes (FDEGs) and lncRNAs (FDELs) were identified using TCGA, GTEx, and FerrDb datasets. We performed Cox and LASSO regressions to identify key FDELs, and constructed a risk score to stratify patients into high- and low-risk groups. The lncRNA signature was evaluated using the areas under the receiver operating characteristic curves (AUCs) and Kaplan-Meier analyses in the training, testing, and entire cohorts. Multivariate Cox regression analyses including the lncRNA signature and common clinicopathological characteristics were performed to identify independent predictors of overall survival (OS). A nomogram was developed for clinical use. We performed gene set enrichment analyses (GSEA) to identify significantly enriched pathways. Differences in the tumor microenvironment (TME) between the 2 groups were assessed using 7 algorithms. To predict the efficacy of immune checkpoint inhibitors (ICI), we analyzed the association between *PD1* and *CTLA4* expression and the risk score. Finally, differences in Tumor Mutational Burden (TMB) and molecular drugs Sensitivity between the 2 groups were performed.

**Results:** We identified 5 lncRNAs (AATBC, AC145423.2, LINC01871, AC125807.2, and AC245041.1) to construct the risk score. The AUC of the lncRNA signature was 0.743 in the training cohort and was validated in the testing and entire cohorts. Kaplan-Meier analyses revealed that the high-risk group had poorer prognosis. Multivariate Cox regression showed that the lncRNA signature was an independent predictor of OS with higher accuracy than traditional clinicopathological features. The 1-, 3-, and 5-year survival probabilities for CM patients were 92.7%, 57.2%, and 40.2% with an AUC of 0.804, indicating a good accuracy and reliability of the nomogram. GSEA showed that the high-risk group had lower ferroptosis and immune response. TME analyses confirmed that the high-risk group had lower immune cell infiltration (e.g., CD8+ T cells, CD4+ memory-activated T cells,

and M1 macrophages) and lower immune functions (e.g., immune checkpoint activation). Low-risk patients whose disease expressed *PD1* or *CTLA4* were likely to respond better to ICIs. The analysis demonstrated that the TMB had significantly difference between low- and high- risk groups. Chemotherapy drugs, such as sorafenib, Imatinib, ABT.888 (Veliparib), Docetaxel, and Paclitaxel showed Significant differences in the estimated IC50 between the two risk groups.

**Conclusion:** Our novel ferroptosis-related lncRNA signature was able to accurately predict the prognosis and ICI outcomes of CM patients. These ferroptosis-related lncRNAs might be potential biomarkers and therapeutic targets for CM.

KEYWORDS

cutaneous melanoma, ferroptosis, immune infiltration, immune checkpoint, long non-coding RNA

# Introduction

Cutaneous melanoma (CM), which is characterized by the malignant transformation and over-proliferation of melanocytes, has an increasing incidence and accounts for more than 75% of skin cancer-related deaths (1, 2). Although most cases of primary localized CM can be cured with surgical resection, advanced metastatic CM has a poor prognosis. The 5-year survival rates of patients with localized, regionally metastatic, and distantly metastatic CM are 98%, 63%, and 16%, respectively (3). Current prognosis prediction in CM patients depends primarily on clinicopathological factors (e.g., patient demographics, Breslow thickness, ulceration, TNM stage). Although these factors are useful for treatment decisions, they are not appropriate for the early identification of high-risk patients owing to molecular and tumor microenvironment (TME) heterogeneity (4, 5). Recent studies have shown that targeted therapy (e.g., BRAF inhibitors, MEK inhibitors) and immunotherapy with immune checkpoint inhibitors (ICIs) targeting cytotoxic T-lymphocyte antigen-4 (CTLA4) and programmed cell death protein 1 (PD1) can significantly improve the survival of CM patients (6). However, many CM patients have primary or acquired resistance to ICIs. Therefore, it is critical to identify novel molecular biomarkers to better predict the prognosis of CM patients and improve the efficacy of immunotherapy in this population.

Ferroptosis, a type of programmed cell death characterized by the accumulation of reactive oxygen species caused by iron accumulation and lipid peroxidation (7), have been proved to be different from apoptosis, necroptosis and pyroptosis (8). Ferroptosis affects cell proliferation, metastasis, and immune response in cancers. Because ferroptosis-related genes have important regulatory roles in cancer progression, they have been used to construct risk scores to predict the prognosis of many cancers, including melanoma based on mRNA expressions (9, 10). However, existing ferroptosis-related gene signatures have a poor predictive ability for the prognosis of CM patients in the most recent studies. Therefore, signatures based on ferroptosis-related non-coding RNAs may be better prognostic biomarkers owing to their higher cell/tissue specificity than protein-coding genes.

Long non-coding RNAs (lncRNAs) are a group of endogenous non-protein-coding RNAs that regulate many cellular processes, including proliferation, differentiation, migration, and invasion. They are also involved in innate and adaptive immunity by mediating the TME, and regulate ferroptosis in cancers. In addition, ferroptosis-related lncRNA signatures are useful predictors of the prognosis of many cancers, including lung adenocarcinoma (11–13), breast cancer (14, 15), gastric cancer (16, 17), bladder cancer (18), colon cancer (19), hepatocellular carcinoma (19), head and neck squamous cell carcinoma (20), and glioma (21). Ferroptosis-related lncRNAs may also have value in predicting CM prognosis. However, a ferroptosis-related lncRNA signature to predict the prognosis of CM has not yet been identified.

In the present study, we aimed to (1) identify a ferroptosis-related lncRNA signature to differentiate high- and low-risk CM patients; (2) construct a nomogram including the lncRNA signature to predict the survival of CM patients; and (3) identify differences in the TME between high- and low-risk patients and predict their responses to ICIs.

# Materials and methods

## Data acquisition

The flow chart of the present study is shown in **Scheme 1**. The fragments per kilobase of per million (FPKM) of CM transcriptome, lncRNA counts data and corresponding clinical data of CM were downloaded from TCGA database (https://tcga-data.ncinih.gov/tcga/). The transcriptome samples included 471 tumor samples and 1 normal sample. Among them, 461 clinical samples were included for prognosis

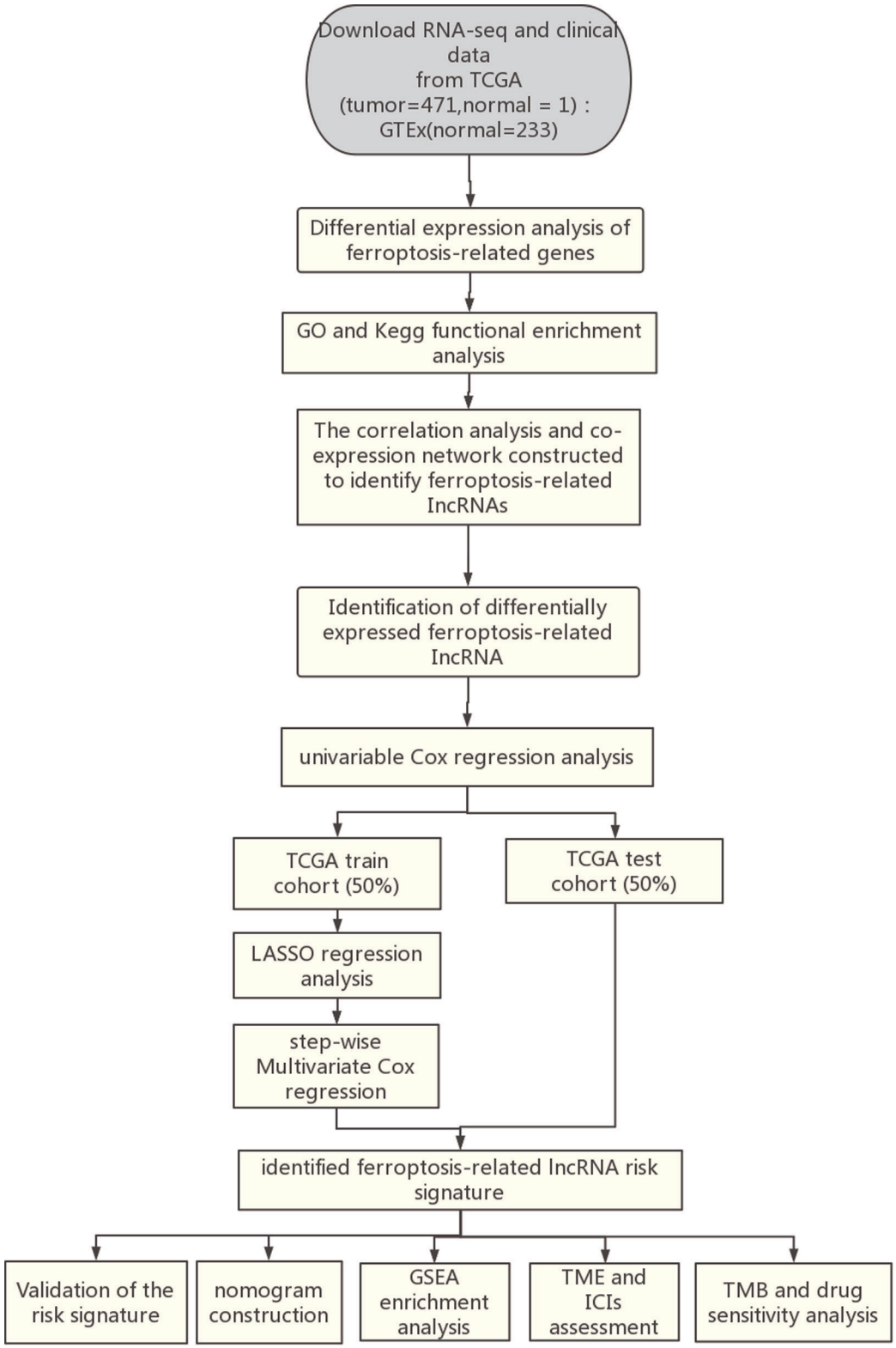


SCHEME 1
Flowchart of the analysis process.

analysis because 10 patients had missing survival time. The clinical characteristics of the 461 patients are displayed in **Supplementary Table S1**. In addition, 233 normal skin samples with transcriptome data were downloaded from GTEx database (https://gtexportal.org/home/), then normalized and processed with TCGA biolinks package (22). The batch effects between TCGA and GTEx data were eliminated by R software package "limma". The final datasets contained RNA expression profile of 471 CM samples and 234 normal samples. Sixty ferroptosis-related genes (**Supplementary Table S2**) that have been validated in previous studies (23–25) were obtained from the FerrDb database (26).

## Identification of ferroptosis-related differentially expressed genes and lncRNAs

To identify the ferroptosis-related differentially expressed genes (FDEGs) between tumor and normal samples, we analyzed the datasets using the classical Bayesian algorithm in the "limma" package in R (27). The ggplot2 package was used to create heatmap plots (28). We performed Gene Ontology (GO) and Kyoto Encyclopedia of Genes and Genomes (KEGG) enrichment analyses to evaluate the biological processes and pathways associated with these FDEGs. Analyses of Pearson correlation between lncRNAs and FDEGs were performed to identify ferroptosis-related lncRNAs. The association was considered significant if the square of the correlation coefficient $|R^2| > 0.4$ and $P < 0.001$. Cytoscape software 3.8.0 was used to visualize the network of gene-lncRNA co-expression (29). All ferroptosis-related lncRNAs in the co-expression network were included in the differential expression analysis. Ferroptosis-related differentially expressed lncRNAs (FDELs) (false discovery rate [FDR] < 0.05 and log2FC ≥ 1) were identified using the "limma" package and illustrated in heatmap and volcano plots

## Construction of the ferroptosis-related lncRNA signature

We first performed univariate Cox regression to identify candidate FDELs that were significantly associated with overall survival (OS). We then performed least absolute shrinkage and selection operator (LASSO) regression to identify the key FDELs based on the optimal lambda value. We performed stepwise multivariate Cox regression including these key FDELs to construct a risk score. The risk score was calculated as follows: risk score $= \sum_{i=1}^{n} \beta_i *$ (expression of $\text{lncRNA}_i$), where n is the number of key lncRNAs and $\beta$ is the regression coefficient. Using the median risk score as a cutoff value, we classified all patients as high-risk (≥median risk score) or low-risk (<median risk score).

## Validation of the ferroptosis-related lncRNA signature

All 461 CM samples were randomly divided into a training cohort ($n = 231$) and a test cohort ($n = 230$) using the caret package in R. The detailed baseline characteristics of the training and testing cohort showed no statistical significance (**Supplementary Table S3**). The receiver operating characteristic (ROC) curves were applied and area under the curves (AUCs) were calculated to evaluate the accuracy of the prognostic lncRNA signature in the training, test, and entire cohorts. The risk level distribution and survival status distribution were illustrated. Kaplan-Meier analyses and log-rank tests were performed to compare survival differences between the high- and low-risk groups. In addition, principal component analysis (PCA) (30) and t-distributed stochastic neighbor embedding (t-SNE) (31) were used for dimensionality reduction and clustering visualization based on the risk score.

## Independence predictor identification and nomogram construction

To determine whether the risk score was an independent predictor of survival, we performed univariate and multivariate Cox regression analyses, which included the risk score, patient age, patient sex, melanoma stage, and TNM stage (T: tumor size; N: lymph node involvement; M: metastasis), in the entire cohort. Hazard ratios (HRs) and 95% confidence intervals (CIs) for each predictor were calculated. AUCs for 3-year OS predicted with the independent risk factors as shown by multivariate Cox regression were calculated to evaluate the predictive value of the lncRNA signature. We also developed a nomogram that included the abovementioned risk factors for the practical prediction of 1-, 3-, and 5-year OS. The performance of the nomogram was evaluated using a calibration curve analysis and C-index.

## Gene set enrichment analysis

We performed gene set enrichment analysis (GSEA) (32) to identify significantly differentially enriched pathways between the high- and low-risk groups. Gene expression was used as a phenotype label (33). The number of random sample permutations was set at 1,000. Statistical significance was set

at a |normalized enrichment score| >1, nominal *P*-value <0.05, and FDR q-value <0.25 (34).

## TME assessment

The tumor purity, ESTIMATE score, immune score, and stromal score for each melanoma sample were calculated using the ESTIMATE algorithm (17). In addition, the single-sample GSEA (ssGSEA) (35), TIMER, CIBERSORT (36), MCPcounter, QUANTISEQ, XCELL, and EPIC algorithms were used to compare cellular components and immune responses between high- and low-risk groups. The differences in immune cell infiltration were shown in heatmap, violin, and radar plots. Furthermore, the ssGSEA scores of the 16 most commonly involved immune cells and 13 most commonly involved immune functions in TME were compared between the 2 groups.

## ICI efficacy

To predict the efficacy of ICIs, we systematically searched the ICI-related gene expression profiles and identified 44 ICI-related genes that might be correlated with ICI response. Among these genes, *PD1* and *CTLA4* were previously reported to be crucial targets of ICIs in CM (6, 37). The association between the expression of the *PD1* and *CTLA4* genes and the risk score was analyzed using data from The Cancer Immunome Atlas data (https://tcia.at/) to investigate the role of ferroptosis in the efficacy of ICIs.

## Tumor Mutational Burden (TMB) and drugs sensitivity analysis

The somatic mutational profile of CM was downloaded from the TCGA. The quantity and quality of the gene mutations were analyzed in the 2 groups with the "Maftools" package in R (38). In addition, we used the "pRRophetic" package in R to evaluate the half maximal inhibitory concentration (IC50) of common chemotherapy and molecular drugs.

## Statistical analysis

All statistical analyses were performed using R version 3.6.1 (Institute for Statistics and Mathematics, Vienna, Austria; https://www.r-project.org) and its (packages: limma, impute, bioconductor, ggplot2, rms, glmnet, preprocess Core, forest plot, survminer, survival ROC, beeswarm, etc.) as described previously (39). Normally and non-normally distributed variables were analyzed using the unpaired Student' t-test and the Wilcoxon test, respectively. The Benjamin-i-Hochberg method was used to identify FDELs based on FDR. All statistical tests were 2-sided with $P \leq 0.05$ being statistically significant.

# Results

## Identification of FDEGs and FDELs

We identified 53 FDEGs (25 upregulated and 28 downregulated) between the normal and tumor samples (**Figure 1A**). The results of GO (**Figure 1B**) and KEGG (**Figure 1C**) analyses indicated that FDEGs were mainly enriched in ferroptosis-related biological processes (e.g., response to oxidative stress) and signaling pathways (e.g., ferroptosis). Pearson correlation analysis identified 387 ferroptosis-related lncRNAs (326 upregulated and 61 downregulated) (**Supplementary Table S4**). The ferroptosis-related lncRNAs were visualized in a gene-lncRNA co-expression network (**Figure 1D**). As shown in the heatmap (**Figure 1E**) and volcano plot (**Figure 1F**), there were 161 FDELs (130 upregulated and 31 downregulated).

## Construction of the lncRNA signature

The univariate Cox regression analysis revealed that 50 of the 161 FDELs were significantly associated with OS (**Figure 2A**). LASSO regression revealed 8 of these 50 lncRNAs to be key to prognosis (**Figures 2B,C**). Stepwise multivariate Cox regression finally identified 5 lncRNAs (AATBC, AC145423.2, LINC01871, AC125807.2, and AC245041.1) for construction of the prognostic lncRNA signature (**Figure 2D**). Among these 5 lncRNAs, only LINC01871 was a protective factor, whereas the other 4 were risk factors (**Figure 2E**). The results of the univariate and multivariate Cox regression analyses of the 5 lncRNAs in the training cohort are shown in **Supplementary Table S3**. The risk score was calculated as follows: Risk score = 0.147 × expression of AATBC + 0.175 × expression of AC145423.2 - 0.091 × expression of LINC01871 + 0.165 × expression of AC125807.2 + 0.376 × expression of AC245041.1. All patients were divided into high- or low-risk group based on the median risk score of 0.995.

## Validation of the lncRNA signature

The AUC of the lncRNA signature for predicting 5-year OS in the TCGA training cohort was 0.743 (**Figure 3A**), indicating

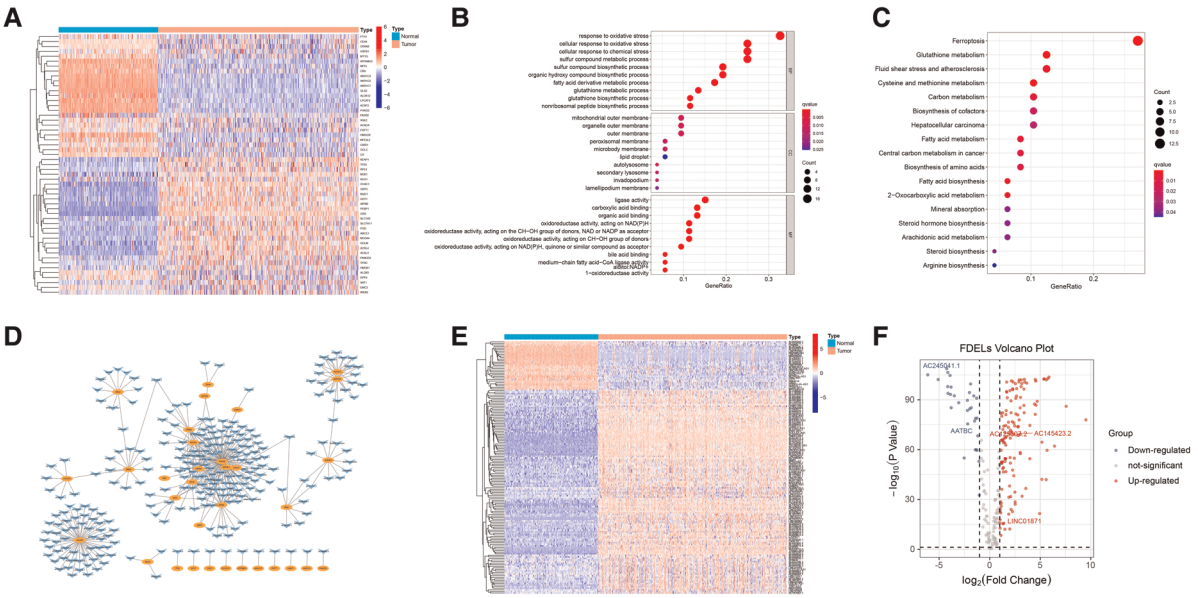


FIGURE 1
FDEG and FDEL identification and functional enrichment analyses. (**A**) The heatmap illustrates 53 FDEGs. (**B**) GO analysis of the FDEGs. (**C**) KEGG analysis of the FDEGs. (**D**) Co-expression network of FDEGs and FDELs. Yellow nodes indicate FDEGs; blue arrows FDELs. (**E**,**F**) A heatmap and volcano plot show 161 FDELs and 5 studied LncRNAs.

that the lncRNA signature offered accurate prediction. The mortality rate increased and survival time decreased as the risk score increased (**Figures 3B,C**). The OS rate of the high-risk group was significantly poorer than that of the low-risk group (**Figure 3D**). The ability of the 5-lncRNA signature to discriminate between high- and low-risk patients was validated in the testing cohort (**Figures 3E–H**) and entire TCGA cohort (**Figures 3I–L**). PCA and t-SNE analyses confirmed that the risk score had reliable clustering ability in the training cohort (**Figures 3M,N**), testing cohort (**Figures 3O,P**), and entire cohort (**Figures 3Q,R**).

## Independence predictors and comprehensive nomogram

The clinicopathological features of all 471 CM patients are shown in **Supplementary Table S5**. The HRs of the risk score in the univariate and multivariate Cox regression analyses were 1.499 (95% CI: 1.302–1.725, $P < .001$) and 1.338 (95% CI:1.154–1.552, $P < .001$), respectively (**Figures 4A,B**), indicating that the lncRNA signature was an independent predictor of OS.

We developed a nomogram that included the risk score and traditional clinicopathological factors for clinical use. The 1-, 3-, and 5-year survival probabilities for CM patients predicted with the nomogram were 92.7%, 57.2%, and 40.2%, respectively (**Figure 4C**). The AUC of the risk score for predicting 3-year OS (0.713) was greater than the AUCs of other clinicopathological features for predicting 3-year OS (684–0.693), indicating that the risk score had a better predictive ability (**Figure 4D**). In addition, the AUC of a prediction model that included the statistically significant variables in the multivariate analysis (i.e., risk score, age, T stage, and N stage) was 0.804, indicating that the novel risk score significantly increased the predictive accuracy of nomogram construction. The calibration curve analysis demonstrated excellent agreement between nomogram predictions and actual observations, indicating that the nomogram was stable and accurate in predicting the prognosis of CM (**Figure 4E**). Finally, the comparison of signature with other models showed that our AUC was superior to the existing signatures (**Figure 4F**). The calculation of C-index of Nomogram and signature were performed to reflect the validity of the nomogram and model, and two results are respectively 0.696 and 0.739 (**Figure 4G**).

## GSEA

The results of GSEA showed that ferroptosis, apoptosis, immune system process, immune response, antigen processing and presentation, T-cell receptor, B-cell receptor, and natural killer cell-mediated cytotoxicity pathways were inhibited in

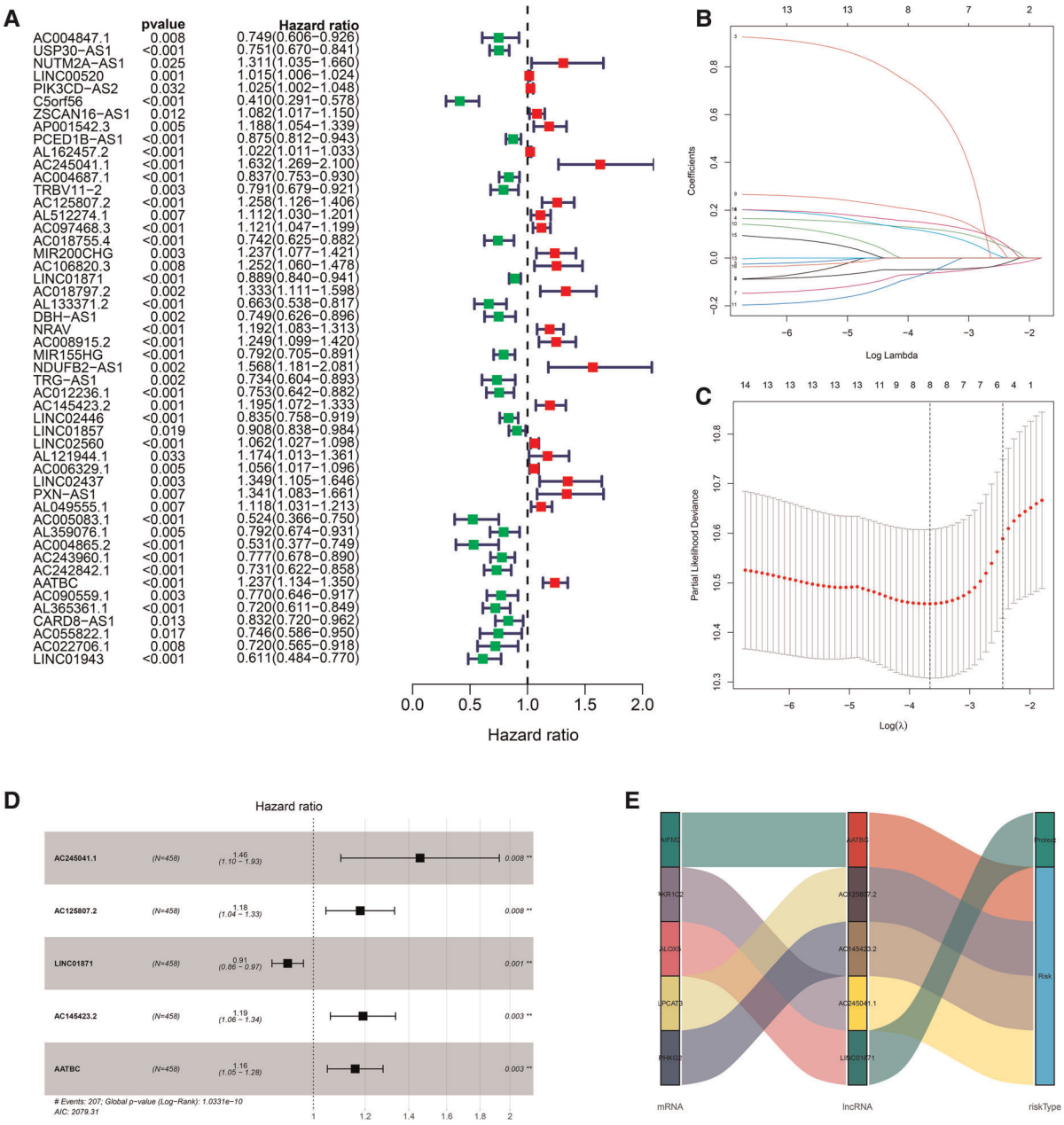


FIGURE 2
Construction of the prognostic ferroptosis-related lncRNA signature. (**A**) Univariate Cox regression revealed that 50 of the 161 FDELs were associated with OS. (**B**) LASSO regression identified 8 FDELs from the 50 lncRNAs, Dynamic LASSO coefficient profiling. (**C**) Selection of the tuning parameter (lambda); and the dashed lines on the left and right indicate the "lambda. min" and "lambda.1se" criteria, respectively. (**D**) Stepwise Cox regression finally identified 5 FDELs (AATBC, AC145423.2, LINC01871, AC125807.2, and AC245041.1) to construct the risk score ($P < 0.001$). (**E**) Sankey diagram shows the associations among FDELs, FDEGs, and risk types.

the high-risk group (Figures 5A–H). The lower level of ferroptosis and immune response in the high-risk group suggested that the association between ferroptosis and the immune TME play an important role in CM prognosis; therefore, we further compared immune cell infiltration and functions between the high- and low-risk groups.

## TME assessment

Significant differences in immune cell infiltration between the high- and low-risk groups are illustrated in Figure 6A. Compared with the low-risk group, the high-risk group had significantly higher tumor purity (Figure 6B), but lower

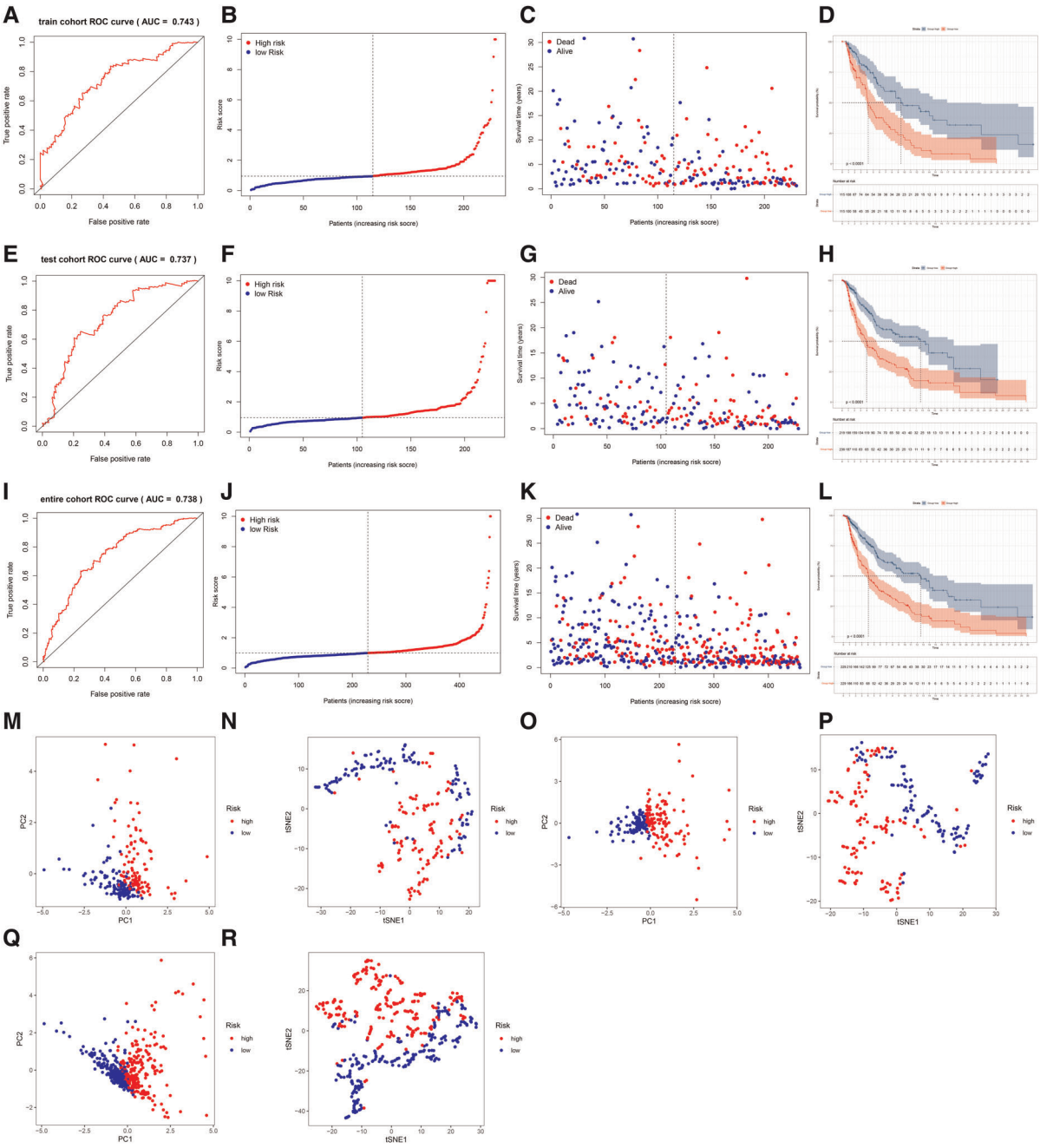


FIGURE 3
Evaluation and validation of the lncRNA signature in the training, testing, and entire cohorts. (**A**) AUC of the lncRNA signature for predicting 5-year survival in the training cohort. (**B**) The rank of the calculated risk score in the training cohort. (**C**) The survival status and survival time in the training cohort. (**D**) Kaplan-Meier survival curves of the high-risk patients and low-risk patients in the training cohort. (**E–H**) The lncRNA signature was validated in the testing cohort. (**I–L**) The lncRNA signature was validated in the entire cohort. (**M**,**N**) PCA and t-SNE analysis of the training cohort. (**O**,**P**) PCA and t-SNE analysis of the test cohort. (**Q**,**R**) PCA and t-SNE analysis of the entire cohort.

ESTIMATE scores (Figure 6C), stromal scores (Figure 6D), and immune score (Figure 6E), indicating that the high-risk group had a lower immune response. The high-risk group also had significantly fewer CD8+ T cells, CD4+ memory-activated T cells and M1 macrophages, but more M0 and M2 macrophages (Figure 6F). In addition, a comparison of ssGSEA scores for immune cells confirmed that the high-risk group had significantly fewer B cells, T cells, dendritic cells, macrophages, and nature killer cells than the low-risk group did (Figure 7A). ssGSEA score for immune functions

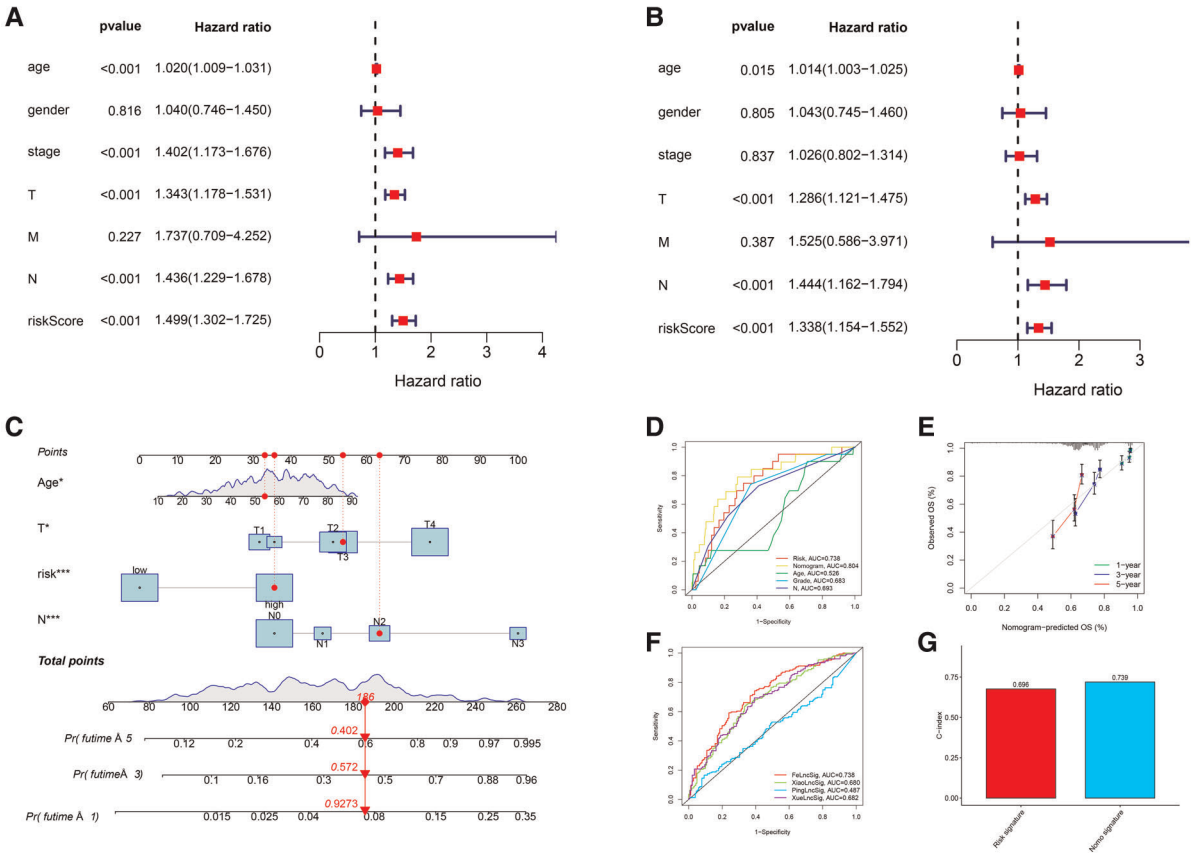


FIGURE 4
Independent prognostic value of the lncRNA signature and the comprehensive nomogram. (**A**) Univariate Cox regression identified individual factors related to OS. (**B**) Multivariate Cox regression identified independent predictors of OS. Our lncRNA signature was an independent predictor of OS with a hazard ratio of 1.338 (95% CI, 1.154-1.552, $P < .001$). (**C**) The nomogram including the lncRNA signature, age, T stage, and N stage for the practical prediction of the prognosis of CM patients. (**D**) AUCs of nomogram, signature and other clinicopathological characteristics for predicting 3-year OS. (**E**) A calibration curve analysis showed that the nomogram predictions were consistent with actual observations. (**F**) The ROC comparison of the studied signature with existing signatures. (**G**) The C-index of Nomogram.

demonstrated that pathways related to immune checkpoints, antigen-presenting cell, cell chemokine receptors, inflammation regulation, human leukocyte antigen, major histocompatibility complex, T cell functions, and type I/II interferon response were significantly downregulated in the high-risk group (Figure 7B).

## ICI efficacy

The differences in the expression of 44 ICI-related genes between the high- and low-risk groups are shown in Figure 8A. The high-risk group had significantly lower expression levels of *PD-1* and *CTLA-4*. Among patients whose disease expressed either of these ICI-related genes, low-risk patients were likely to have a better response to ICIs than high-risk patients were, through the Cancer Immune Atlas (TCIA) database (Figures 8B–E). These results suggest that a higher level of ferroptosis facilitated a higher immune response in the TME, leading to increase the efficacy of ICIs in CM patients. Then, we also used TIDE (Tumor Immune Dysfunction and Exclusion) score to evaluate the response to immunotherapy, and the results showed TIDE and Dysfunction scores were higher in low-risk group than high-risk group (Figures 8F,G). The prognostic performance in immunotherapy cohorts were displayed through survival cures, indicating that cohorts with low risk combined with high ICI score have the better prognosis than other cohorts, especially with *PD-1* expression positive (Figure 8H).

## Tumor Mutational Burden (TMB) and drugs sensitivity analysis

The analysis demonstrated that the TMB had significantly difference between low- and high- risk groups (Figure 9A),

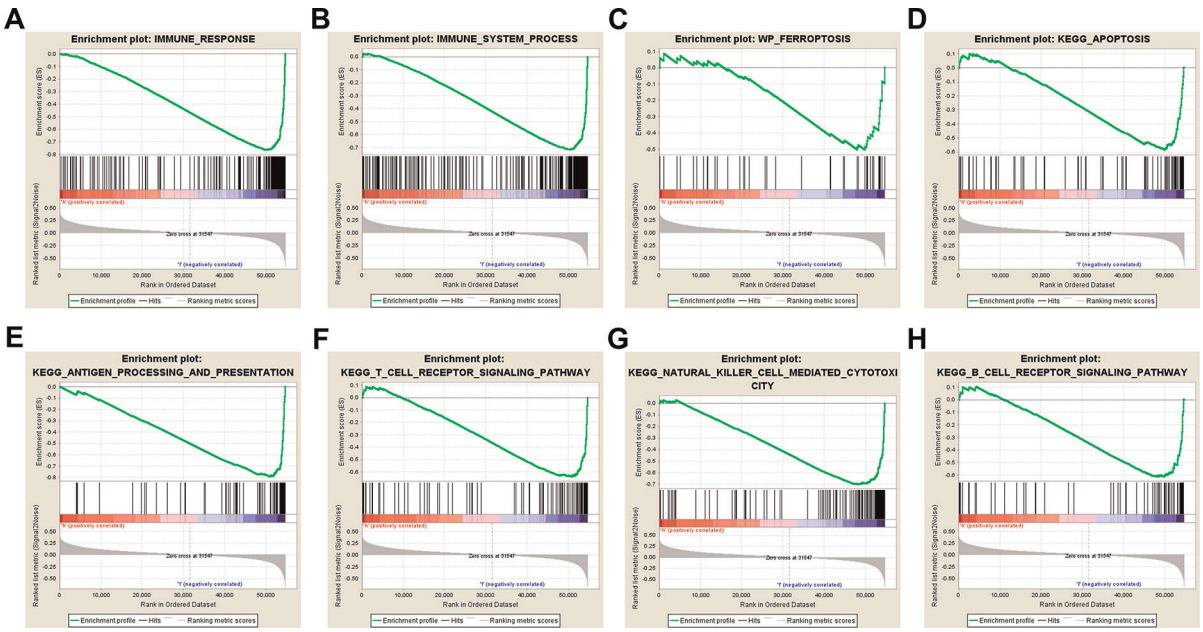


FIGURE 5
Gene set enrichment analysis. Immune-related and ferroptosis-related pathways were significantly enriched in the low-risk group. (A) Immune system process. (B) Immune response. (C) Ferroptosis. (D) Apoptosis. (E) Antigen processing and presentation. (F) T-cell receptor signaling pathway. (G) Natural killer cell-mediated cytotoxicity. (H) B-cell receptor signaling pathway.

and TMB has a significant impact on patient prognosis between low- and high- risk groups (**Figures 9B,C**). Then, we then identified the top 20 genes with the highest mutation rates in the two risk subgroups. The mutation rates of TTN, MUC16, BRAF, and DNAH5 were higher than 30% in both groups (**Figures 9D,E**). Mutation of the TTN gene was more common in the high-risk subgroup. Genetic mutations can affect the tumor response to chemotherapy and targeted therapy (**Figure 9F**); therefore, we investigated the association between the risk model and the efficacy of chemotherapy and targeted therapy drugs in patients with CM. We listed 10 common target drugs (**Figure 9G**) and 10 Chemotherapy drugs (**Figure 9H**) used for CM, such as sorafenib, Imatinib, ABT.888 (Veliparib), Docetaxel, and Paclitaxel (**Figure 9H**). Significant differences in the estimated IC50 between the two risk groups were observed, which suggest that the risk model might be used to identify potential biomarkers for chemotherapy and targeted therapy sensitivity.

## Discussion

We performed comprehensive analyses utilizing the TCGA, GTEx, and FerrDb databases and identified 5 key lncRNAs to construct a risk score that stratified CM patients into high- and low-risk groups. The lncRNA signature was an independent prognostic predictor of OS with fair accuracy. The nomogram that included the lncRNA signature and other clinicopathological factors had good accuracy and reliability in predicting the OS of CM patients. The high-risk group was associated with lower ferroptosis, immune response, immune cell infiltration and immune function. High-risk patients had also lower expression of ICI-related genes such as *PD-1* and *CTLA-4*, and thus had poorer responses to ICIs. These results collectively demonstrate that this novel ferroptosis-related lncRNA signature can predict the prognosis of CM and the efficacy of ICIs in CM patients.

Ferroptosis-related lncRNA signatures have considerable predictive value for the prognosis of CM. Recent studies have developed several lncRNA signatures related to autophagy (40) and immunity (41–44) to predict the prognosis of CM. In these studies, the numbers of lncRNAs used for signature construction ranged from 3 to 24 (**Supplementary Table S6**). Similarly, we constructed a risk score based on 5 lncRNAs we identified (AATBC, AC145423.2, AC125807.2, AC245041.1, and LINC01871). The regulatory roles and molecular mechanisms of these 5 lncRNAs have been shown in previous studies.

AATBC (apoptosis-associated transcript in bladder cancer) was originally discovered in bladder cancer by Zhao et al. (45), who found that AATBC overexpression of AATBC is positively correlated with tumor grade and stage. A transcriptomic analysis of high-throughput sequencing data (46) confirmed that AATBC can harbor bladder cancer-related miRNA recognition elements. Wang et al. (47) identified a multi-

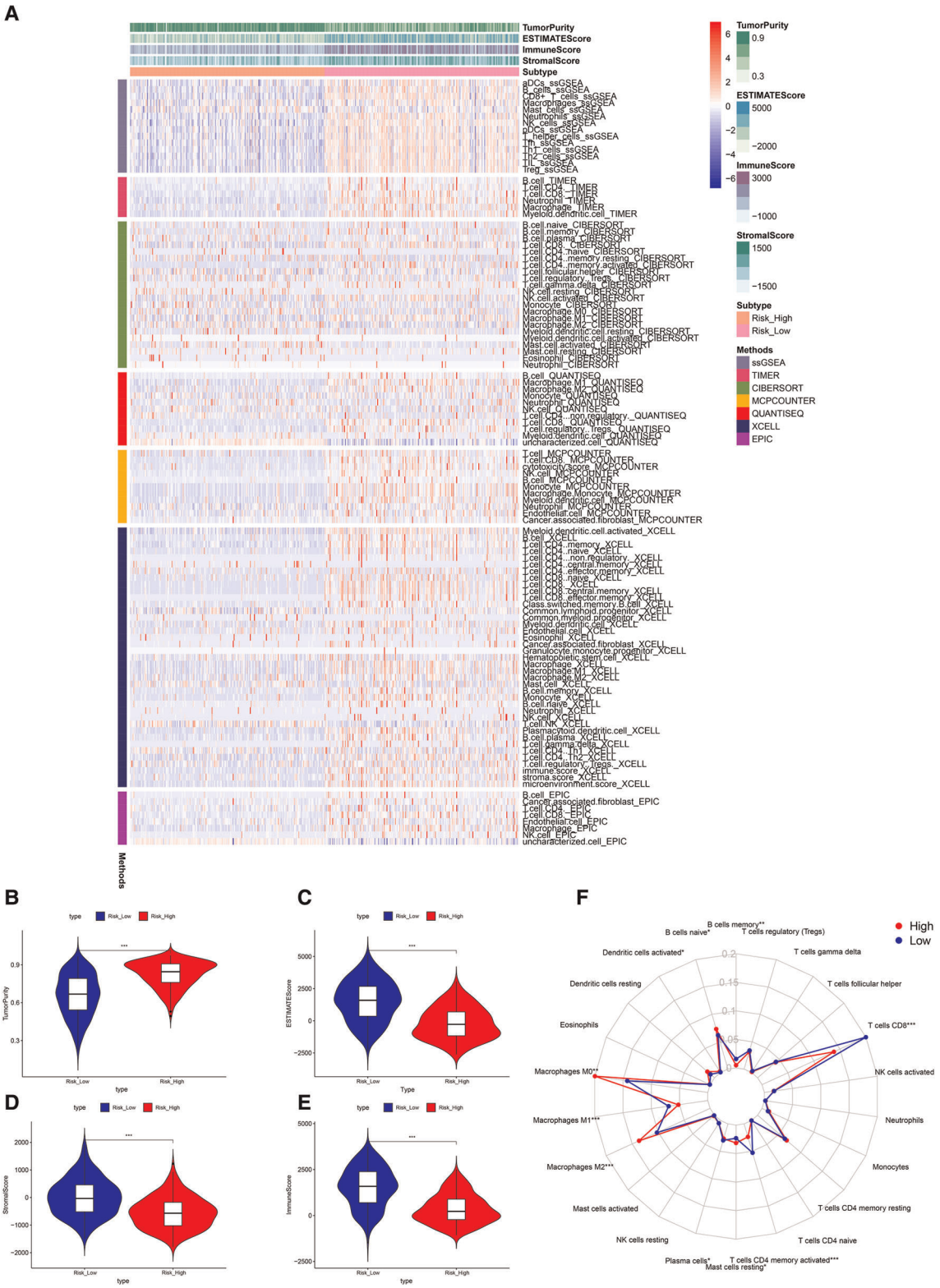


FIGURE 6
Tumor microenvironment analyses. (**A**) Immunity heatmap including the Tumor purity score, ESTIMATE score, immune score, stromal score and 7 other algorithms (ssGSEA, TIMER, CIBERSORT, MCPcounter, QUANTISEQ, XCELL, and EPIC). (**B**) The high-risk group had significantly higher tumor purity. (**C**–**E**) The high-risk group had significantly lower ESTIMATE, stromal, and immune scores. (**F**) A radar plot shows that the high-risk group had significantly fewer CD8+ T cells, CD4+ memory activated T cells and M1 macrophages, but more M0 and M2 macrophages. *$P < 0.05$; **$P < 0.01$; ***$P < 0.001$.

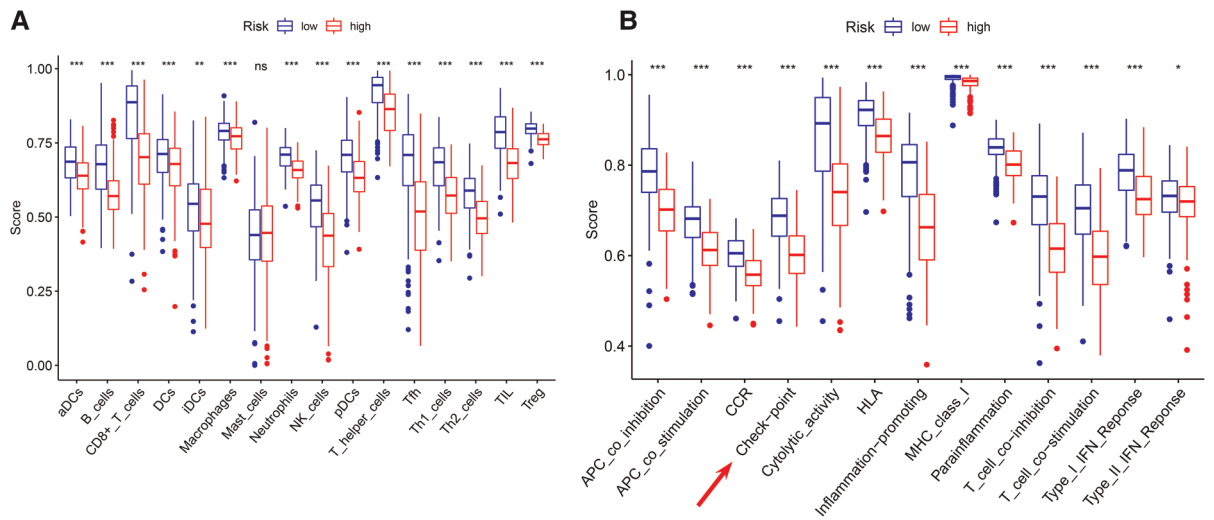


FIGURE 7
ssGSEA analyses (**A**) comparison of ssGSEA scores for 16 immune cells between the high- and low-risk groups. (**B**) A comparison of the 2 groups' ssGSEA scores for 13 immune functions indicates that the high-risk group had a significantly lower the checkpoint score. *$P < 0.05$; **$P < 0.01$; ***$P < 0.001$.

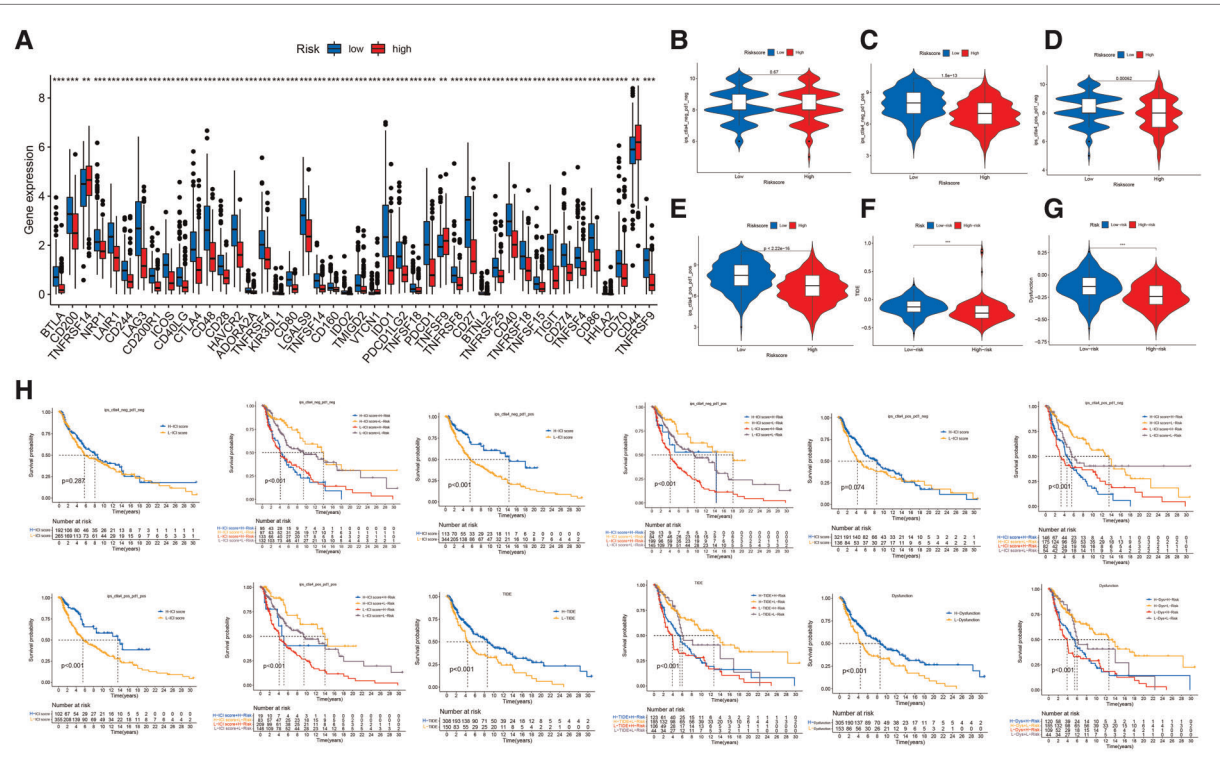


FIGURE 8
Immune checkpoint differences. (**A**) The expression of 44 immune checkpoint genes differed significantly between the high- and low-risk groups. The low-risk group had significantly higher expression of CD274 (*PDL-1*) and *CLAT-4* ($P < .001$). (**B**) The difference in ICI efficacy was not significant between the 2 groups if PD-1 and CLAT4 were both negatively expressed. (**C–E**) Low-risk patients with PD-1 or CTLA4 expression were likely to respond better to ICIs than high-risk patients were. (**F,G**) The TIDE and Dysfunction scores were higher in low-risk group than high-risk group. (**H**) The prognostic performance in immunotherapy cohorts.

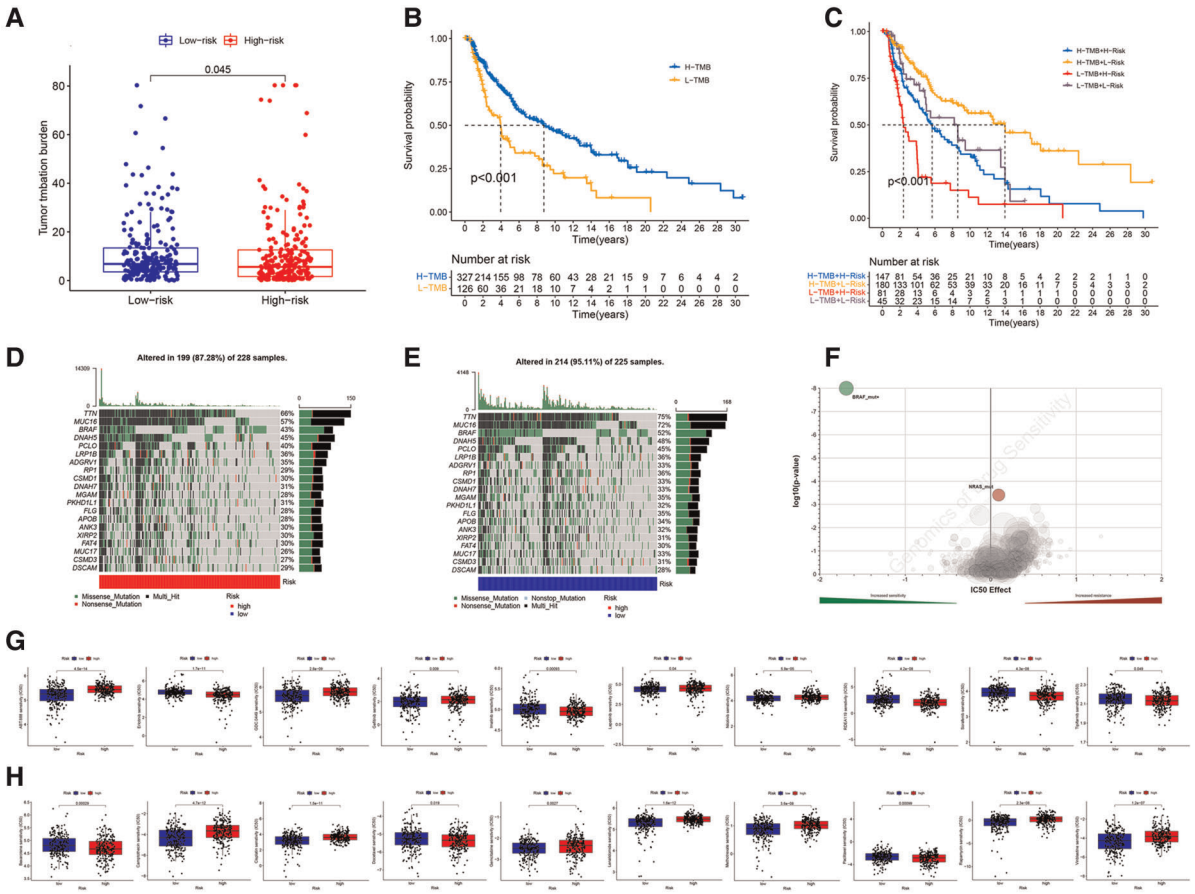


FIGURE 9
TMB and drugs sensitivity analysis. (**A**) The TMB in different risk groups. ($P < .001$). (**B**,**C**) The prognostic performance of TMB scores in survival cures. (**D**–**E**) The mutation rates of the top 20 genes in different risk groups. (**F**) The IC50 score with mutation. (**G**) The target drugs sensitivity in different risk groups. (**H**) The Chemotherapy drugs sensitivity in different risk groups.

RNA-type-based signature that included AATBC for predicting recurrence-free survival in patients with uterine corpus endometrial carcinoma. Tang et al. (48) found that AATBC overexpression promotes the migration and invasion of nasopharyngeal carcinoma cells *in vitro*, as well as their metastasis *in vivo*, through the miR-1237-3p-PNN-ZEB1 axis, leading to poor survival. Tang et al. (48) showed that AATBC is highly expressed in breast cancer and promotes cancer migration and invasion by activating the YAP1/Hippo signaling pathway through the AATBC-YBX1-MST1 axis. Zhang et al. (49) demonstrated that AATBC overexpression promotes the proliferation and migration of prostate cancer cells *via* the miR-1245b-5p-CASK axis. The role of AATBC in CM was reported by Yan et al. (50), who constructed a prognostic model with 7 gene instability–related lncRNAs, including AATBC. Their cell experiments verified that AATBC knockdown can inhibit the proliferation and invasion of CM. In accordance with these studies, we found that AATBC is a risk factor for poor prognosis in CM patients.

Unlike that of AATBC, the regulatory roles of the other 3 risk factors (AC145423.2, AC125807.2 and AC245041.1), have been rarely reported. Xuan et al. (51) identified 7 autophagy-related lncRNAs including AC145423.2 to build a risk score, for dividing clear cell renal cell carcinoma patients into low- and high-risk groups. Hou et al. (52) constructed a competing endogenous RNA network that included AC125807.2 and 11 other lncRNAs, and found AC125807.2 to be an independent prognostic predictor of OS in patients with lung adenocarcinoma. Huang et al. (53), who established a ferroptosis-related lncRNA signature, which included AC245041.1, for gastric cancer, found that higher AC245041.1 expression is correlated with poorer OS. In agreement with these studies, our results showed that AC145423.2, AC125807.2 and AC245041.1 are associated with poor prognosis in CM patients. However, the mechanism underlying how lncRNA regulates ferroptosis remains elusive and requires further investigation.

Previous studies have shown that LINC01871 is related to stemness, autophagy, and immunity in breast, gastric, cervical,

and endometrial cancers. For example, Li et al. (54) identified 12 stemness-related lncRNA including LINC01871, to predict the prognosis of breast cancer. In a second, they identified 11 autophagy-related lncRNAs including LINC01871, in breast cancer (55). Ma et al. (56) established a signature comprising 8 immune-related lncRNA including LINC01871, to predict the survival of breast cancer patients. Moreover, LINC01871 has a strong positive correlation with ICI-related genes such as *CTLA4* and *PD1*, which suggested that the lncRNAs has critical roles in the immune response and immunotherapy outcomes. Wu et al. (57) identified 5 autophagy-related lncRNAs including LINC01871, to construct a risk score and a nomogram to predict the prognosis of breast cancer patients. Mathias et al. (58) investigated the role of LINC01871 in 5 molecular subtypes of breast cancer and found that LINC01871 is associated with immune response activation and favorable OS in patients with basal-like breast cancers. He et al. (59), in a multi-omics data analysis, identified molecular features (e.g., genes, miRNAs, lncRNAs, proteins, pathways) that correlated with tumor immunity in gastric cancer. They found that LINC01871 was positively associated with cancer immunity (expression levels of CD8+ T cell, cytolytic immune activity, and PD-L1), which suggests that LINC01871 is a useful biomarker for assessing immunotherapy response. In addition, Chen et al. (60) constructed a signature of 6 immune-related lncRNAs, including LINC01871, to predict the prognosis of cervical cancer. Similarly, Wang et al. (61) identified a signature of 5 autophagy-related lncRNAs, including LINC01871, to predict the prognosis of endometrial cancer patients. Together, these studies demonstrate that LINC01871 is positively associated with the immune response, and thus a protective factor for cancer prognosis. This is consistent with our finding that LINC01871 is the only ferraptosis-related protective factor for OS in CM.

The AUCs of lncRNA signature for OS prediction significantly varied in previous studies, and (**Supplementary Table S5**). Our ferroptosis-related lncRNA signature had AUCs for predicting 5-year OS of 0.743, 0.737, and 0.738 in the training, testing, and entire cohorts, respectively. These results are in line with those of the studies by Yoshihara et al. (17), Xiao et al. (62), and Wang et al. (42), whose signatures for predicting survival also had an AUCs of 0.7–0.8. And the HRs of lncRNA signatures ranged from 1.024 to 2.043 ($P < 0.05$ for all), also listing in **Supplementary Table S5**. In accordance with these studies' findings, our multivariate Cox regression analysis showed that our lncRNA signature had an HR of 1.338, indicating that the mortality risk of a CM patient would increase by 33.8% as the risk score increased by 1 point.

Our nomogram integrated the independent risk factors identified in the multivariate Cox regression analysis. This combination significantly increased the predictive accuracy of Ferroptosis-related signature in clinical application, as it had an AUC of 0.804 for predicting 3-year OS in the entire cohort. The calibration curve analysis demonstrated excellent agreement between nomogram predictions and actual observations, indicating that our nomogram was stable and accurate in predicting the prognosis of CM. Few others have developed nomograms for the prediction of CM prognosis. Although Xiao et al. (62) constructed a nomogram that included the same predictors as ours, they did not report the AUC of the nomogram or evaluate its performance. Tian et al. (63) noted that the AUCs of their nomogram for predicting 3-year OS were 0.816 and 0.740 in the training and testing cohorts, respectively, but their nomogram had more variables than ours and was not verified by calibration curve analysis.

The imbalance of immunity in the TME plays an important role in the development and progression of CM. Ferroptosis is associated with the immune TME and the response of CM to immunotherapies (64). Specific ferroptosis-related lncRNAs can regulate the TME by affecting antigen release/ presentation, immune activation, immune cells migration/ infiltration, and even enhancing the efficacy of ICIs (65–68). Previous studies showed that patients with lower immune cell (e.g., CD8 + T cells, M1 macrophages) infiltration and function have poorer survival (69). For example, Wang et al. (42) found that high-risk CM patients have lower immune functions than low-risk patients do. Xiao et al. (62) showed that high-risk CM patients have lower levels of CD8+ T cells, CD4+ memory-activated T cells, and M1 macrophages, but higher levels of M0 macrophages. Their results were consistent with those of Ping et al. (41), who found that high-risk CM patients have lower levels of B cells, CD4+ T cells, monocytes, and CD8+ T cells, but higher levels of M0 macrophages. Thus, it may have lower responses to chemotherapeutics (i.e., cisplatin, vinblastine, paclitaxel) and ICIs. In accordance with those studies, the present study demonstrated that high-risk patients have significantly lower immune cell (e.g., CD8+ T cells) infiltration and immune function (e.g., immune checkpoint activation), possibly because immunotherapy-activated CD8+ T cells enhance lipid peroxidation and ferroptosis as a cytotoxic mechanism in CM cells and ultimately promote the efficacy of anti-CTLA-4 and anti-PD-1 therapies (70).

The present study had several limitations. First, the 5 lncRNAs were identified and validated using a single data source (TCGA). It would have been better if we tested the prognostic value of these lncRNAs in another independent patient cohort. its prognostic values were tested in another independent patient cohort. Second, the molecular mechanism of these lncRNAs remains unclear and requires further validation using cellular/ molecular biological experiments. Despite these limitations, this is the first study to identify a ferroptosis-related lncRNA signature for the prediction of

prognosis and immunotherapy efficacy in CM patients. Owing to its relevance to the immune TME and ICI-related gene expression, these ferroptosis-related lncRNAs may be potential biomarkers and therapeutic targets for CM. The lncRNA signature may help improve the efficacy of personalized immunotherapy.

Our novel ferroptosis-related lncRNA signature was able to accurately predict the prognosis of CM patients and their outcomes. The novel ferroptosis-related lncRNA signature was able to accurately predict the prognosis and outcome of ICI therapies. These ferroptosis-related lncRNAs might be potential biomarkers and therapeutic targets for CM.

## Data availability statement

The original contributions presented in the study are included in the article/**Suplementary Material**, further inquiries can be directed to the corresponding author/s.

## Author contributions

YX and YC are responsible for data processing and article writing. ZN is responsible for sorting out the results. LG and QZ are responsible for determining the research ideas. ZY, JX and XY reviewed the research and articles. General idea of YH and YY evaluation study. All authors contributed to the article and approved the submitted version.

## Acknowledgments

We are grateful to those who provide and maintain the public databases, and datasets we used in this study.

## Supplementary material

The Supplementary Material for this article can be found online at: https://www.frontiersin.org/articles/10.3389/fsurg.2022.860806/full#supplementary-material.

## Conflict of interest

The authors declare that the research was conducted in the absence of any commercial or financial relationships that could be construed as a potential conflict of interest.

## Publisher's note

All claims expressed in this article are solely those of the authors and do not necessarily represent those of their affiliated organizations, or those of the publisher, the editors and the reviewers. Any product that may be evaluated in this article, or claim that may be made by its manufacturer, is not guaranteed or endorsed by the publisher.

## References

1. Siegel RL, Miller KD, Fuchs HE, Jemal A. Cancer statistics, 2021. *CA Cancer J Clin*. (2021) 71:7–33. doi: 10.3322/caac.21654

2. Trager MH, Queen D, Samie FH, Carvajal RD, Bickers DR, Geskin LJ. Advances in prevention and surveillance of cutaneous malignancies. *Am J Med*. (2020) 133:417–23. doi: 10.1016/j.amjmed.2019.10.008

3. Davis LE, Shalin SC, Tackett AJ. Current state of melanoma diagnosis and treatment. *Cancer Biol Ther*. (2019) 20:1366–79. doi: 10.1080/15384047.2019.1640032

4. Leonardi GC, Falzone L, Salemi R, Zanghì A, Spandidos DA, Mccubrey JA, et al. Cutaneous melanoma: from pathogenesis to therapy (Review). *Int J Oncol*. (2018) 52:1071–80. doi: 10.3892/ijo.2018.4287

5. Simiczyjew A, Dratkiewicz E, Mazurkiewicz J, Ziętek M, Matkowski R, Nowak D. The influence of tumor microenvironment on immune escape of melanoma. *Int J Mol Sci*. (2020) 21(21). doi: 10.3390/ijms21218359

6. Van Allen EM, Miao D, Schilling B, Shukla SA, Blank C, Zimmer L, et al. Genomic correlates of response to CTLA-4 blockade in metastatic melanoma. *Science*. (2015) 350:207–11. doi: 10.1126/science.aad0095

7. Wang Z, Jin D, Ma D, Ji C, Wu W, Xu L, et al. Ferroptosis suppressed the growth of melanoma that may be related to DNA damage. *Dermatol Ther*. (2019) 32:e12921. doi: 10.1111/dth.12921

8. Van der Meeren L, Verduijn J, Krysko DV, Skirtach AG. AFM Analysis enables differentiation between apoptosis, necroptosis, and ferroptosis in murine cancer cells. *iScience*. (2020) 23:101816. doi: 10.1016/j.isci.2020.101816

9. Zeng N, Ma L, Cheng Y, Xia Q, Li Y, Chen Y, et al. Construction of a ferroptosis-related gene signature for predicting survival and immune microenvironment in melanoma patients. *Int J Gen Med*. (2021) 14:6423–38. doi: 10.2147/IJGM.S327348

10. Xu C, Chen H. A ferroptosis-related gene model predicts prognosis and immune microenvironment for cutaneous melanoma. *Front Genet*. (2021) 12:697043. doi: 10.3389/fgene.2021.697043

11. Guo Y, Qu Z, Li D, Bai F, Xing J, Ding Q, et al. Identification of a prognostic ferroptosis-related lncRNA signature in the tumor microenvironment of lung adenocarcinoma. *Cell Death Discov*. (2021) 7:190. doi: 10.1038/s41420-021-00576-z

12. Lu L, Liu LP, Zhao QQ, Gui R, Zhao QY. Identification of a ferroptosis-related LncRNA signature as a novel prognosis model for lung adenocarcinoma. *Front Oncol*. (2021) 11:675545. doi: 10.3389/fonc.2021.675545

13. Zheng Z, Zhang Q, Wu W, Xue Y, Liu S, Chen Q, et al. Identification and validation of a ferroptosis-related long non-coding RNA signature for predicting the outcome of lung adenocarcinoma. *Front Genet*. (2021) 12:690509. doi: 10.3389/fgene.2021.690509

14. Wu ZH, Tang Y, Yu H, Li HD. The role of ferroptosis in breast cancer patients: a comprehensive analysis. *Cell Death Discov*. (2021) 7:93. doi: 10.1038/s41420-021-00473-5

15. Zhang K, Ping L, Du T, Liang G, Huang Y, Li Z, et al. A ferroptosis-related lncRNAs signature predicts prognosis and immune microenvironment for breast cancer. *Front Mol Biosci*. (2021) 8:678877. doi: 10.3389/fmolb.2021.678877

16. Chen W, Feng Z, Huang J, Fu P, Xiong J, Cao Y, et al. Identification of ferroptosis-related long noncoding RNA and construction of a novel prognostic signature for gastric cancer. *Dis Markers*. (2021) 2021:7724997. doi: 10.1155/2021/7724997

17. Yoshihara K, Shahmoradgoli M, Martínez E, Vegesna R, Kim H, Torres-Garcia W, et al. Inferring tumour purity and stromal and immune cell

admixture from expression data. *Nat Commun*. (2013) 4:2612. doi: 10.1038/ncomms3612

18. Zhou R, Liang J, Tian H, Chen Q, Yang C, Liu C. Development of a ferroptosis-related lncRNA signature to predict the prognosis and immune landscape of bladder cancer. *Dis Markers*. (2021) 2021:1031906. doi: 10.1155/2021/1031906

19. Cai HJ, Zhuang ZC, Wu Y, Zhang YY, Liu X, Zhuang JF, et al. Development and validation of a ferroptosis-related lncRNAs prognosis signature in colon cancer. *Bosn J Basic Med Sci*. (2021) 21(5):569–76. doi: 10.17305/bjbms.2020.5617

20. Tang Y, Li C, Zhang YJ, Wu ZH. Ferroptosis-Related Long Non-Coding RNA signature predicts the prognosis of Head and neck squamous cell carcinoma. *Int J Biol Sci*. (2021) 17:702–11. doi: 10.7150/ijbs.55552

21. Zheng J, Zhou Z, Qiu Y, Wang M, Yu H, Wu Z, et al. A prognostic ferroptosis-related lncRNAs signature associated with immune landscape and radiotherapy response in glioma. *Front Cell Dev Biol*. (2021) 9:675555. doi: 10.3389/fcell.2021.675555

22. Mounir M, Lucchetta M, Silva TC, Olsen C, Bontempi G, Chen X, et al. New functionalities in the TCGAbiolinks package for the study and integration of cancer data from GDC and GTEx. *PLoS Comput Biol*. (2019) 15:e1006701. doi: 10.1371/journal.pcbi.1006701

23. Hassannia B, Vandenabeele P, Vanden Berghe T. Targeting ferroptosis to iron out cancer. *Cancer Cell*. (2019) 35:830–49. doi: 10.1016/j.ccell.2019.04.002

24. Stockwell BR, Friedmann Angeli JP, Bayir H, Bush AI, Conrad M, Dixon SJ, et al. Ferroptosis: a regulated cell death nexus linking metabolism, redox biology, and disease. *Cell*. (2017) 171:273–85. doi: 10.1016/j.cell.2017.09.021

25. Zheng J, Conrad M. The metabolic underpinnings of ferroptosis. *Cell Metab*. (2020) 32:920–37. doi: 10.1016/j.cmet.2020.10.011

26. Zhou N, Bao J. Ferrdb: a manually curated resource for regulators and markers of ferroptosis and ferroptosis-disease associations. *Database (Oxford)*. (2020) 2020:baaa021. doi: 10.1093/database/baaa021

27. Ritchie ME, Phipson B, Wu D, Hu Y, Law CW, Shi W, et al. Limma powers differential expression analyses for RNA-sequencing and microarray studies. *Nucleic Acids Res*. (2015) 43:e47. doi: 10.1093/nar/gkv007

28. Ito K, Murphy D. Application of ggplot2 to pharmacometric graphics. *CPT Pharmacometrics Syst Pharmacol*. (2013) 2:e79. doi: 10.1038/psp.2013.56

29. Shannon P, Markiel A, Ozier O, Baliga NS, Wang JT, Ramage D, et al. Cytoscape: a software environment for integrated models of biomolecular interaction networks. *Genome Res*. (2003) 13:2498–504. doi: 10.1101/gr.1239303

30. Ringnér M. What is principal component analysis. *Nat Biotechnol*. (2008) 26:303–4. doi: 10.1038/nbt0308-303

31. Kanaan-Izquierdo S, Ziyatdinov A, Burgueño MA, Perera-Lluna A. Multiview: a software package for multiview pattern recognition methods. *Bioinformatics (Oxford, England)*. (2019) 35:2877–9. doi: 10.1093/bioinformatics/bty1039

32. Subramanian A, Kuehn H, Gould J, Tamayo P, Mesirov JP. GSEA-P: a desktop application for gene set enrichment analysis. *Bioinformatics (Oxford, England)*. (2007) 23:3251–3. doi: 10.1093/bioinformatics/btm369

33. Subramanian A, Tamayo P, Mootha VK, Mukherjee S, Ebert BL, Gillette MA, et al. Gene set enrichment analysis: a knowledge-based approach for interpreting genome-wide expression profiles. *Proc Natl Acad Sci USA*. (2005) 102:15545–50. doi: 10.1073/pnas.0506580102

34. Yoon S, Kim SY, Nam D. Improving gene-set enrichment analysis of RNA-seq data with small replicates. *PLoS ONE*. (2016) 11:e0165919. doi: 10.1371/journal.pone.0165919

35. Foroutan M, Bhuva DD, Lyu R, Horan K, Cursons J, Davis MJ. Single sample scoring of molecular phenotypes. *BMC Bioinformatics*. (2018) 19:404. doi: 10.1186/s12859-018-2435-4

36. Chen B, Khodadoust MS, Liu CL, Newman AM, Alizadeh AA. Profiling tumor infiltrating immune cells with CIBERSORT. *Methods Mol Biol*. (2018) 1711:243–59. doi: 10.1007/978-1-4939-7493-1_12

37. Daassi D, Mahoney KM, Freeman GJ. The importance of exosomal PDL1 in tumour immune evasion. *Nat Rev Immunol*. (2020) 20:209–15. doi: 10.1038/s41577-019-0264-y

38. Mayakonda A, Lin DC, Assenov Y, Plass C, Koeffler HP. Maftools: efficient and comprehensive analysis of somatic variants in cancer. *Genome Res*. (2018) 28:1747–56. doi: 10.1101/gr.239244.118

39. Löffler-Wirth H, Kalcher M, Binder H. oposSOM: r-package for high-dimensional portraying of genome-wide expression landscapes on bioconductor. *Bioinformatics (Oxford, England)*. (2015) 31:3225–7. doi: 10.1093/bioinformatics/btv342

40. Ding Y, Li T, Li M, Tayier T, Zhang M, Chen L, et al. A novel autophagy-related lncRNA gene signature to improve the prognosis of patients with melanoma. *Biomed Res Int*. (2021) 2021:8848227. doi: 10.1155/2021/8848227

41. Ping S, Wang S, He J, Chen J. Identification and validation of immune-related lncRNA signature as a prognostic model for skin cutaneous melanoma. *Pharmgenomics Pers Med*. (2021) 14:667–81. doi: 10.2147/PGPM.S310299

42. Wang Y, Ba HJ, Wen XZ, Zhou M, Küçük C, Tamagnone L, et al. A prognostic model for melanoma patients on the basis of immune-related lncRNAs. *Aging (Albany NY)*. (2021) 13:6554–64. doi: 10.18632/aging.202730

43. Xiao B, Liu L, Li A, Wang P, Xiang C, Li H, et al. Identification and validation of immune-related lncRNA prognostic signatures for melanoma. *Immun Inflamm Dis*. (2021) 9:1044–54. doi: 10.1002/iid3.468

44. Zhou JG, Donaubauer AJ, Frey B, Becker I, Rutzner S, Eckstein M, et al. Prospective development and validation of a liquid immune profile-based signature (LIPS) to predict response of patients with recurrent/metastatic cancer to immune checkpoint inhibitors. *J Immunother Cancer*. (2021) 9(2):e001845. doi: 10.1136/jitc-2020-001845

45. Zhao F, Lin T, He W, Han J, Zhu D, Hu K, et al. Knockdown of a novel lincRNA AATBC suppresses proliferation and induces apoptosis in bladder cancer. *Oncotarget*. (2015) 6:1064–78. doi: 10.18632/oncotarget.2833

46. Li M, Liu Y, Zhang X, Liu J, Wang P. Transcriptomic analysis of high-throughput sequencing about circRNA, lncRNA and mRNA in bladder cancer. *Gene*. (2018) 677:189–97. doi: 10.1016/j.gene.2018.07.041

47. Wang P, Zeng Z, Shen X, Tian X, Ye Q. Identification of a multi-RNA-type-based signature for recurrence-free survival prediction in patients with uterine corpus endometrial carcinoma. *DNA Cell Biol*. (2020) 39:615–30. doi: 10.1089/dna.2019.5148

48. Tang T, Yang L, Cao Y, Wang M, Zhang S, Gong Z, et al. LncRNA AATBC regulates Pinin to promote metastasis in nasopharyngeal carcinoma. *Mol Oncol*. (2020) 14:2251–70. doi: 10.1002/1878-0261.12703

49. Zhang W, Liu Q, Zhao J, Wang T, Wang J. Long noncoding RNA AATBC promotes the proliferation and migration of prostate cancer cell through miR-1245b-5p/CASK axis. *Cancer Manag Res*. (2021) 13:5091–100. doi: 10.2147/CMAR.S310529

50. Yan K, Wang Y, Shao Y, Xiao T. Gene instability-related lncRNA prognostic model of melanoma patients via machine learning strategy. *J Oncol*. (2021) 2021:5582920. doi: 10.1155/2021/5582920

51. Xuan Y, Chen W, Liu K, Gao Y, Zuo S, Wang B, et al. A risk signature with autophagy-related long noncoding RNAs for predicting the prognosis of clear cell renal cell carcinoma: based on the TCGA database and bioinformatics. *Dis Markers*. (2021) 2021:8849977. doi: 10.1155/2021/8849977

52. Hou J, Yao C. Potential prognostic biomarkers of lung adenocarcinoma based on bioinformatic analysis. *Biomed Res Int*. (2021) 2021:8859996. doi: 10.1155/2021/8859996

53. Huang S, Li D, Zhuang L, Sun L, Wu J. Identification of Arp2/3 complex subunits as prognostic biomarkers for hepatocellular carcinoma. *Front Mol Biosci*. (2021) 8:690151. doi: 10.3389/fmolb.2021.690151

54. Li X, Li Y, Yu X, Jin F. Identification and validation of stemness-related lncRNA prognostic signature for breast cancer. *J Transl Med*. (2020) 18:331. doi: 10.1186/s12967-020-02497-4

55. Li X, Jin F, Li Y. A novel autophagy-related lncRNA prognostic risk model for breast cancer. *J Cell Mol Med*. (2021) 25:4–14. doi: 10.1111/jcmm.15980

56. Ma W, Zhao F, Yu X, Guan S, Suo H, Tao Z, et al. Immune-related lncRNAs as predictors of survival in breast cancer: a prognostic signature. *J Transl Med*. (2020) 18:442. doi: 10.1186/s12967-020-02522-6

57. Wu Q, Li Q, Zhu W, Zhang X, Li H. Identification of autophagy-related long non-coding RNA prognostic signature for breast cancer. *J Cell Mol Med*. (2021) 25:4088–98. doi: 10.1111/jcmm.16378

58. Mathias C, Muzzi J, Antunes BB, Gradia DF, Castro M, Carvalho de Oliveira J. Unraveling immune-related lncRNAs in breast cancer molecular subtypes. *Front Oncol*. (2021) 11:692170. doi: 10.3389/fonc.2021.692170

59. He Y, Wang X. Identification of molecular features correlating with tumor immunity in gastric cancer by multi-omics data analysis. *Ann Transl Med*. (2020) 8:1050. doi: 10.21037/atm-20-922

60. Chen Q, Hu L, Huang D, Chen K, Qiu X, Qiu B. Six-lncRNA immune prognostic signature for cervical cancer. *Front Genet*. (2020) 11:533628. doi: 10.3389/fgene.2020.533628

61. Wang Z, Zhang J, Liu Y, Zhao R, Zhou X, Wang H. An integrated autophagy-related long noncoding RNA signature as a prognostic biomarker for human endometrial cancer: a bioinformatics-based approach. *Biomed Res Int*. (2020) 2020:5717498. doi: 10.1155/2020/5717498

62. Xiao B, Liu L, Chen Z, Li A, Wang P, Xiang C, et al. Identification of epithelial-mesenchymal transition-related prognostic lncRNAs biomarkers associated with melanoma microenvironment. *Front Cell Dev Biol*. (2021) 9:679133. doi: 10.3389/fcell.2021.679133

63. Tian J, Yang Y, Li MY, Zhang Y. A novel RNA sequencing-based prognostic nomogram to predict survival for patients with cutaneous melanoma: clinical trial/experimental study. *Medicine (Baltimore)*. (2020) 99:e18868. doi: 10.1097/MD.0000000000018868

64. Drijvers JM, Gillis JE, Muijlwijk T, Nguyen TH, Gaudiano EF, Harris IS, et al. Pharmacologic screening identifies metabolic vulnerabilities of CD8(+) T cells. *Cancer Immunol Res*. (2021) 9:184–99. doi: 10.1158/2326-6066.CIR-20-0384

65. Carpenter S, Aiello D, Atianand MK, Ricci EP, Gandhi P, Hall LL, et al. A long noncoding RNA mediates both activation and repression of immune response genes. *Science*. (2013) 341:789–92. doi: 10.1126/science.1240925

66. Gomez JA, Wapinski OL, Yang YW, Bureau JF, Gopinath S, Monack DM, et al. The NeST long ncRNA controls microbial susceptibility and epigenetic activation of the interferon-$\gamma$ locus. *Cell*. (2013) 152:743–54. doi: 10.1016/j.cell.2013.01.015

67. Hu R, Sun X. lncRNATargets: a platform for lncRNA target prediction based on nucleic acid thermodynamics. *J Bioinform Comput Biol*. (2016) 14:1650016. doi: 10.1142/S0219720016500165

68. Zhang H, Chen Z, Wang X, Huang Z, He Z, Chen Y. Long non-coding RNA: a new player in cancer. *J Hematol Oncol*. (2013) 6:37. doi: 10.1186/1756-8722-6-37

69. Wang P, Zhang X, Sun N, Zhao Z, He J. Comprehensive analysis of the tumor microenvironment in cutaneous melanoma associated with immune infiltration. *J Cancer*. (2020) 11:3858–70. doi: 10.7150/jca.44413

70. Long W, Ouyang H, Wan W, Yan W, Zhou C, Huang H, et al. "Two in one": simultaneous functionalization and DOX loading for fabrication of nanodiamond-based pH responsive drug delivery system. *Mater Sci Eng C Mater Biol Appl*. (2020) 108:110413. doi: 10.1016/j.msec.2019.110413

frontiers | Frontiers in Surgery

TYPE Review
PUBLISHED 12 August 2022
DOI 10.3389/fsurg.2022.933781

Check for updates

OPEN ACCESS

EDITED BY
Xie Julin,
Sun Yat-sen University, China

REVIEWED BY
Rongbiao Pi,
Sun Yat-sen University, China
Qiwei Yang,
Second Military Medical University, China
Wenzhen Liao,
Southern Medical University, China

*CORRESPONDENCE
Xiang Zeng
zengxiang@stemcell-x.org
Wei Zhu
zhuwei0921@gzucm.edu.cn

SPECIALTY SECTION
This article was submitted to Reconstructive and Plastic Surgery, a section of the journal Frontiers in Surgery

RECEIVED 01 May 2022
ACCEPTED 01 August 2022
PUBLISHED 12 August 2022

CITATION
Chen G, Chen H, Zeng X and Zhu W (2022) Stem cell-derived exosomal transcriptomes for wound healing.
Front. Surg. 9:933781.
doi: 10.3389/fsurg.2022.933781

COPYRIGHT
© 2022 Chen, Chen, Zeng and Zhu. This is an open-access article distributed under the terms of the Creative Commons Attribution License (CC BY). The use, distribution or reproduction in other forums is permitted, provided the original author(s) and the copyright owner(s) are credited and that the original publication in this journal is cited, in accordance with accepted academic practice. No use, distribution or reproduction is permitted which does not comply with these terms.

# Stem cell-derived exosomal transcriptomes for wound healing

Guiling Chen[1,2,3,4], Hankun Chen[5], Xiang Zeng[1,2,3,4]* and Wei Zhu[1,2,4]*

[1]The Second Clinical College of Guangzhou University of Chinese Medicine, Guangzhou, China, [2]The Second Affiliated Hospital of Guangzhou University of Chinese Medicine, Guangzhou, China, [3]National Institute of Stem Cell Clinical Research, Guangdong Provincial Hospital of Chinese Medicine, Guangzhou, China, [4]Guangdong Provincial Academy of Chinese Medical Sciences, Guangzhou, China, [5]Research and Development Department, Guangzhou Qinglan Biotechnology Company Limited, Guangzhou, China

Wound healing is a complex and integrated process of the interaction of various components within the injured tissue. Accumulating evidence suggested that stem cell-derived exosomal transcriptomes could serve as key regulatory molecules in wound healing in stem cell therapy. Stem cell-derived exosomal transcriptomes mainly consist of long noncoding RNAs (lncRNAs), microRNAs (miRNAs), circular RNAs (circRNAs) and messenger RNAs (mRNAs). In this article we presented a brief introduction on the wound repair process and exosomal transcriptomes. Meanwhile, we summarized our current knowledge of the involvement of exosomal transcriptomes in physiological and pathological wound repair process including inflammation, angiogenesis, and scar formation.

KEYWORDS

wound healing, stem cell, exosome, microRNA, long noncoding RNA, circular RNA, messenger RNA

## Introduction

Skin wounds are classified primarily into acute and chronic wounds. Acute wounds included cuts, scrapes, burns, trauma, needle punctures, and surgical incisions. While chronic wounds refer to wounds like diabetic foot ulcers, pressure ulcers and infected wounds (1). The healing of wound is the process of tissue regeneration involving the synergistic and integrated actions of cells and intercellular factors, cells and cells, cells and the microenvironment. The normal wound healing involves four successive but overlapping phases, including the hemostasis phase, the inflammatory phase, the proliferative phase, and the remodeling phase (2). Many factors affect and interfere with normal wound healing, such as infection, medication, complex comorbidities, age, obesity, smoking and nutrition (3, 4). Any disturbance in these four phases affects wound healing or even proper functioning of the skin, results in the formation of chronic non-healing wounds or repaired with hypertrophic scar tissue or keloids (5).

Currently, therapeutic research on wound healing is focused on the use of small molecules, including growth factors, insulin, stromal cell-derived factor-1, antimicrobial peptides, platelet rich plasma, and so on (6). In addition, silk biomaterials, artificial skin grafts, honey are also potential therapeutic means for

wound healing (7–9). In recent decades, stem cell therapy has become a promising approach in wound healing due to its distinguished functions on tissue regeneration, immunoregulation and angiogenesis (10). Stem cells participate in the regulation of inflammatory, proliferative and remodeling phases *via* paracrine of cytokines, chemokines and growth factors. Stem cells ranging from immature pluripotent stem cells to more restricted multipotent progenitor cells have been investigated for their abilities in facilitating wound healing in several animal models and clinical trials (11). However, because stem cells do not readily survive in the wound microenvironment in a large portion of cases, their effects in wound healing may be difficult to be accomplished (12). One fundamental hurdle is that reactive oxygen species can weaken stem cell function and therefore impair wound healing (13). In addition, small molecules are easily degraded in wound fluids and carry risks of drug resistance, new therapies are still being explored.

Stem cell-derived exosomes have demonstrated great potentials to provide therapeutical benefits in nearly all stages of wound healing process, including alleviating inflammation (14), promoting vascularization (15), promoting proliferation and migration of epithelial cells and fibroblasts (16), while reducing scar formation (17). However, the exact mechanism of action remains to be explored. Growing evidences have shown that exosome-derived transcriptomes (RNAs) participate in comprehensive biological and functional aspects of physiological conditions (18–20). Therefore, stem cell derived exosomal transcriptomes attracted great research interests (21–24). In this review, we summarized the process of wound healing and several key RNAs of exosome transcriptomes involved, such as messenger RNAs (mRNAs), microRNAs (miRNAs), long non-coding RNAs (lncRNAs) and circular RNAs (circRNAs), with the focus on the effects of several transcriptional molecules of stem cell derived exosomes on wound healing.

## Wound healing process

Wound healing is a complex and dynamic process to skin injury. Wound healing is classically divided into four overlapping phases: hemostasis, inflammation, proliferation and remodeling. During the hemostatic phase, platelets and circulating coagulant factors accumulate and interact at the site of tissue injury, followed by activation of endothelial cells. Inflammation state involves complex mechanisms among resident immune cells, circulating leucocytes and their pro-inflammatory cytokines and chemokines. Uncontrolled and excessive inflammation promotes tissue injury and delays healing, thereby causing chronic wounds or scars. The proliferative phase of healing is characterized by extensive activation of keratinocytes, epidermal stem cells, fibroblasts, macrophages and endothelial cells to orchestrate wound closure and angiogenesis. Extracellular matrix (ECM) remodeling spans the entire wound healing process. Fibroblasts, myofibroblasts, collagen, transforming growth factor (TGF)-β, proteoglycans and matrix metalloproteinases are major players involved in ECM remodeling, balancing collagen synthesis and degradation (25, 26).

Disturbance of any of the above stages of the normal wound healing process can lead to pathological wound healing, which mainly includes two types: excessive scarring and chronic wound healing. Persistent activation of TGF-β pathway provided a deviant signal to myofibroblasts, leading to continuous production of ECM triggering pathological scarring (27). Hyper-proliferation of fibroblasts and excessive collagen deposition may lead to hypertrophic scar formation as well (28). Chronic wounds are typically caused by a temporal arrest in the inflammation phase with no further progress to the stages of healing. Chronic wounds are characterized by massive immune cell infiltration, excessive levels of proinflammatory cytokines, persistent infection, the formation of biofilms of drug-resistant microorganisms, and appearance of senescent cells which are unresponsive to restorative stimuli (29, 30).

## Exosomes and exosomal transcriptomes

Exosomes are bioactive membranous vesicles with a diameter of 40–100 nm secreted by many type of cells. They were discovered for the first time in sheep reticulocytes in 1983 (31). Exosome formation begins with endocytosis on the surface of the cell membrane with the formation of early endosomes *via* inward budding (32). Recently, various nucleic acids have been identified within exosomes, including mRNAs and non-coding RNAs such as miRNAs, lncRNAs, circRNAs, ribosomal RNAs (rRNAs), transfer RNAs (tRNAs), small nucleolar RNAs (snoRNAs), small nuclear RNAs (snRNAs) and piwi-interacting RNAs (piRNAs). These RNAs are transferred from parent cells to recipient cells through exosomes to exert specific functions (33, 34). Secreted exosomes can be transferred to recipient cells *via* endocytosis, direct membrane fusion, and receptor ligand interactions. Exosomes are associated with a wide spectrum of physiological and pathological processes including but not limited to immune responses, viral pathogenicity, pregnancy, cardiovascular diseases, central nervous system-related diseases, cancer progression and so on. In addition, exosomes have potential as diagnostic and therapeutic tools for a variety of diseases, including neurodegenerative diseases, cardiovascular dysfunction, and cancer (35).

Exosomal transcriptomes mainly contain mRNAs, lncRNAs, miRNAs and circRNAs, which have been

intensively studied in a number of studies. mRNAs, macromolecules carry codes from the DNA in the nucleus to the cytoplasm (the ribosomes), where protein synthesis occurs, were first found highly enriched in exosomes released by mast cells (36, 37). mRNAs in exosomes differ significantly from those in the cytoplasm of the donor cells (37). Exosomal mRNAs could be transferred to other cells and be translated into proteins in the target cells (37, 38). Exosomes derived from cells growing under oxidative stress may induce tolerance of the recipient cells to external stress by mRNAs transported by exosomes (39). In addition, exosomal mRNAs may potentially play a role in epigenetic inheritance in mammals (40).

Although 70% of the human genome is transcribed into RNAs, only 2% of these transcripts are translated into proteins. The remaining transcripts are defined as noncoding RNAs, including lncRNAs, miRNAs and circRNAs, which participate in the regulation of mRNA and protein function, in the binding with DNA to modulate gene transcription, or in acting as the competing endogenous RNA (ceRNA) or miRNA sponges to regulate gene expression (**Figure 1**). LncRNAs are a category of cellular RNAs which are longer than 200 nucleotides in length but in lack of the open reading frames. This class comprises, among others, long intergenic noncoding RNAs (lincRNAs), antisense RNAs, and sense overlapping lncRNAs. LncRNAs may serve as biomarkers of cancer, such as nuclear enriched abundant transcript 1 (NEAT1), HOX Transcript Antisense RNA (HOTAIR), metastasis-associated lung adenocarcinoma transcript 1 (MALAT-1), H19. Moreover, lncRNAs participated in cancer development, progression, metastasis and prognosis (41), and other diseases like cerebrovascular diseases, cardiac diseases, inflammatory bowel diseases, metabolic syndrome related disorders as well (42–45).The abundance of exosomal lncRNAs correlates with their expression levels in the cell of origin (46).

Among the RNAs in exosomes, miRNAs have attracted the most attention due to their roles in gene expression regulation. MiRNAs are a class of 17–24 nt, small, noncoding and evolutionarily conserved RNAs, They can mediate post-transcriptional gene silencing by targeting the 3′-UTR of target mRNAs under the control of the RNA-induced silencing complex (47–49). MiRNAs can regulate cell proliferation and differentiation (50), and thus participate in development (51, 52). They can also serve as therapeutic targets and prognostic markers for diseases and cancers (53, 54).

CircRNAs are a new category of single-stranded RNAs characterized by their covalently closed loop structures lacking of 5′ caps or a 3′ poly(A) tails in all eukaryotic cells. They are generated through a particular mechanism of alternative splicing called “back-splicing”. In 2015, Li et al. reported for the first time that exosomes contained abundant circRNAs. Genome-wide RNA-seq analysis found that circRNAs were enriched in the exosomes relative to the parental cells. It has been reported that the sorting of circRNAs to exosomes can be controlled by modulating the levels of relevant miRNAs in parental cells and can transfer bioactive substance to target cells (55). It has been confirmed that circRNAs could exert biological functions in multiple aspects, including participating in neuronal development (56) and the pathogenesis of cancer, cardiovascular, neurological, and autoimmune diseases (57–60). In addition, circRNAs serve as potential biomarkers for many diseases (61), especially cancer (62).

## Advantages of exosomes and exosomal transcriptomes in wound healing

Harsh wound microenvironments, such as deficiency of nutritional factors, enhanced inflammatory response, increased reactive oxygen species, and impaired vasculature, all resulted in poor survival of the transplanted stem cells (63).

Stem cell derived exosomes carrying bioactive contents of parental stem cells, transmit signals and participate in the remodeling of extracellular matrix through paracrine mechanism. Exosomes are less immunogenic, more stable and easier to store relative to their donor stem cells, and therefore can be used as an alternative therapy for stem cells in wound healing regulation. There have been clinical trials on stem cell derived exosomes for the treatment of diabetic wounds registered on the Clinicaltrial.gov website [NCT05243368]. Besides, patents on stem cell derived exosomes as wound dressings have been published [CN114376989A& CN114377194A]. However, the low yields of stem cell derived exosomes require a large number of stem cells to be consumed. Exosome components are complex and can hardly be purified due to the limitation of extraction techniques. The transcriptomes of exsomes, however, as intercellular transport cargos of exosomes, is relatively well-defined in composition and more suitable for research. Moreover, their functions in wound healing can be defined by loss- or gain-of-function experiments after overexpression or knockdown their expressions in the parent cells. Unlike the great risks such as mutagenesis, toxicity, and limited capacity for genetic cargo posed by viral vectors, exosomal RNAs transferring presented good safety and biocompatibility (64).

At present, research on stem cell derived exosomes mainly focuses on those derived from mesenchymal stem cells (65–67). However, there are still some studies on exosomes from other sources of stem cells, such as pluripotent stem cells (68, 69) or embryonic stem cells (70). Consistent with the major functions of the parental cells, exosomes derived from MSCs embrace immunomodulatory as well as regenerative effects on the recipient cells (21, 71).

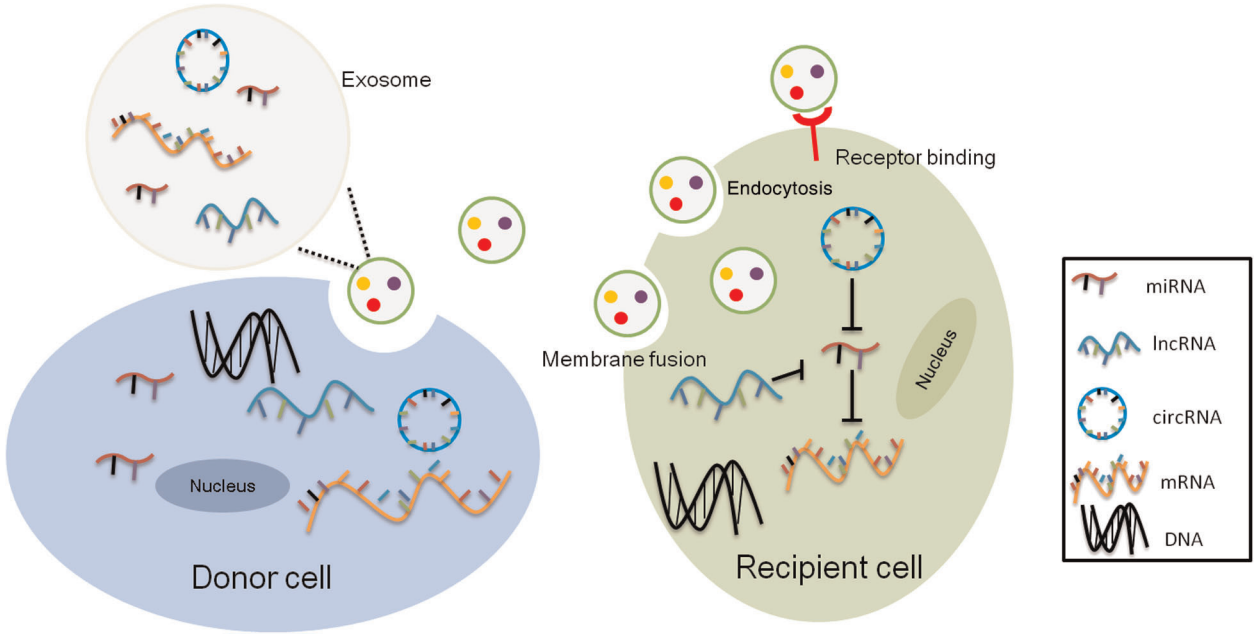


FIGURE 1
Intercellular transcriptomes delivery by exosomes. Exosomal noncoding RNAs, mainly microRNAs (miRNAs), long noncoding RNAs (lncRNAs), and circular RNAs (circRNAs) from donor cells act as competitive endogenous RNAs (ceRNAs) for binding to common miRNA response elements (MREs) from recipient cells altering their activity.

## Transcriptomes of stem cell exosomes and wound healing

The stem cell derived exosomal transcriptomes have been shown to promote wound healing in terms of anti-inflammation, cell proliferation and migration, blood vessel formation, and inhibition of scar formation, and the effects on wound healing of four transcriptomes, including miRNAs, lncRNAs, circRNAs, as well as mRNAs, will be illustrated below (see **Figure 2**).

### Stem cell derived exosomal miRNAs and wound healing

A number of studies have demonstrated that miRNAs were the active molecules of stem cell derived exosomes to regulate the functions of the recipient cells (72, 73). In wound healing for examples, miRNAs in the stem cell derived-exosomes have shown potent effects on regeneration, anti-inflammatory and anti-scarring to the wounds (see **Table 1**).

#### Exosomal miRNAs on skin regeneration

During wound healing process, regeneration is mainly manifested by promoting fibroblasts proliferation, boosting vascularization, formation of granulation tissue, and enhancing re-epithelialization, among other phathophyioloigcal events. Four miRNAs (miR-126-3p, miR-21-3p, miR-146a-3p and miR-21-5p) were reported to have the potentials to enhance the proliferation and migration of the fibroblasts and endothelial cells, and to promote angiogenesis of human endothelial cells through phosphatase and tension homologs (PTEN), PI3K/AKT and ERK signaling pathways, respectively (74–77). Local application of miRNA-21-3p-enriched umbilical cord blood-exosomes into mouse skin wounds accelerated re-epithelialization, reduced scar width, and enhanced angiogenesis. Inhibition of PTEN and sprouty RTK signaling antagonist 1 may be the key function of miR-21-3p (75). MiR-146a-3p, derived from ADSC-exosomes could promote the proliferation and migration of fibroblasts by inducing the expressions of serpin family H member 1 and p-ERK2 to rapidly reduce the wound area and foster the formation of new blood vessels in rats with wounds (74). An *in vitro* study by Tao et al. found that exosomes over-expressing miR-126-3p derived from synovium mesenchymal stem cells stimulated the proliferation of human dermal fibroblasts and human dermal microvascular endothelial cells (HMEC-1) in a dose-dependent manner, and enhanced HMEC-1 migration and tube formation as well. In addition, exosomes overloaded with miR-126-3p accelerated re-epithelialization, activated angiogenesis, and promoted collagen maturation in diabetic wound healing (76). Gao et al. suggested that exosomes enriced in miR-135a from human amniotic mesenchymal stem cells have

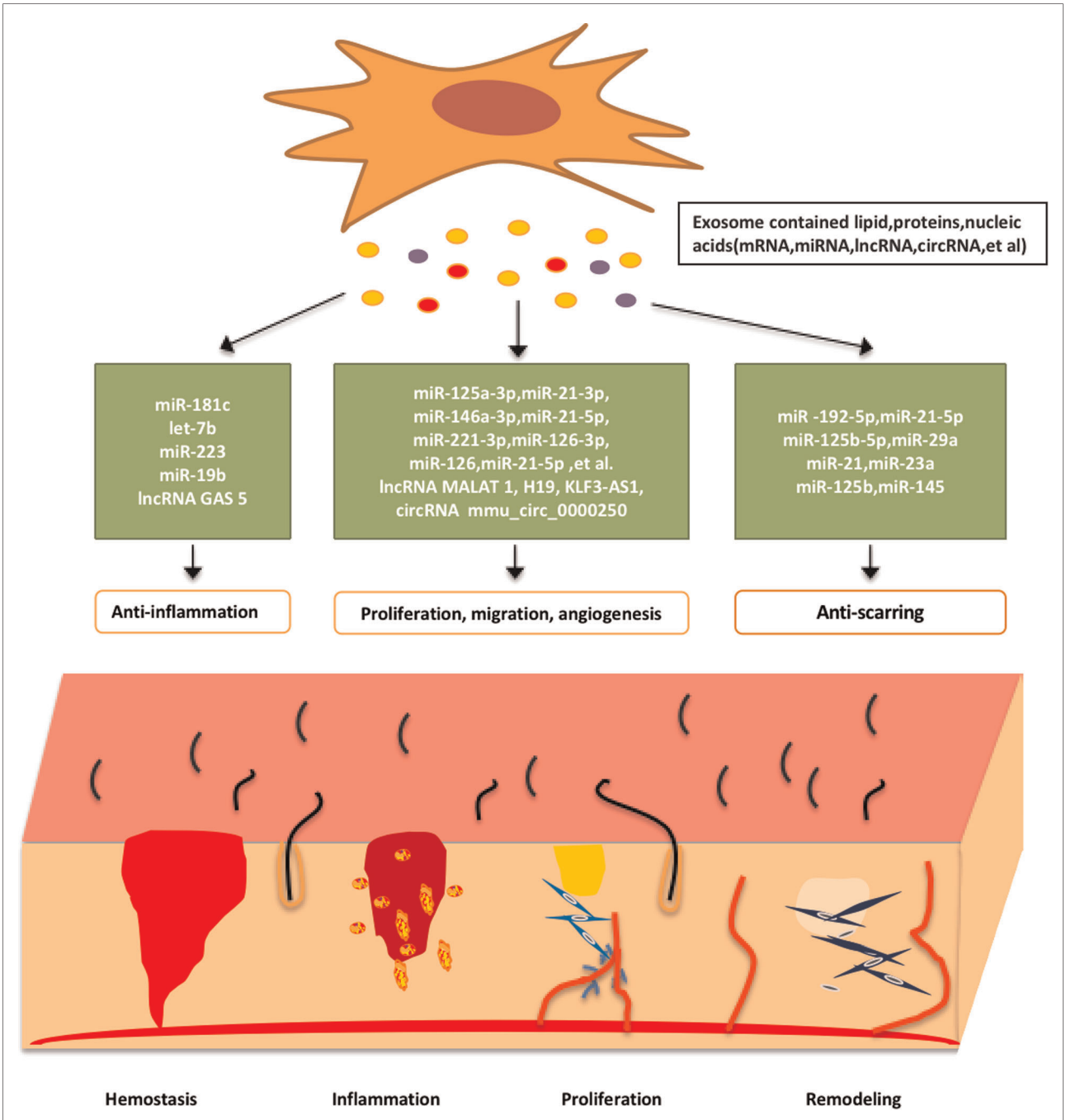


FIGURE 2
Schematic demonstration of the exosomal RNAs derived from stem cells promote wound healing by enhancing angiogenesis, cell proliferation and migration, reducing inflammation, and anti-scarring.

shown efficacy in enhacing epidermal cell migration to promote wound healing in SD rats. Furthermore, knockdown of miR-135a in ADSC-exosomes validly attenuated the effect of exosomes on BJ fibroblasts migration. The study suggested that the abovementioned function of miR-135a may be realized through inhibiting the expression of large tumor suppressor kinase 2 (78).

MiRNAs from other stem cell derived exosomes have been reported to enhance cell proliferation and migration to improve wound healing. MiR-200a-enriched embryonic stem cell derived exosomes were capble of rejuvenating vascular endothelial cell senescence and restore impaired proliferation, migration, and tube formation by downregulating Keap1 to activated nuclear factor erythroid2-related factor 2 (79).

TABLE 1 Stem cell-exosome derived miRNA-mediated regulation of wound healing.

| Exosome derived miRNAs | Donor cells | Recipient cells | Potential target factor | Functions | References |
|---|---|---|---|---|---|
| miR-125a-3p | ADSCs | HUVECs | PTEN↓ | Promote cell viability, migration and angiogenesis | (106) |
| miR-21-3p | Umbilical cord blood | Fibroblasts and endothelial cells | PTEN↓<br>SPRY1↓ | Promote fibroblast proliferation and migration, enhance endothelial cell angiogenic activity | (75) |
| miR -146a | ADSCs | Fibroblasts | Serpin family H member 1 and p-ERK2↑ | Promote the migration and proliferation of fibroblasts, and neovascularization | (74) |
| miR-21-5p | BMSCs | Fibroblasts and HUVECs | SPRY2↓; PI3K/AKT and ERK1/2↑ | Promote the proliferation, migration and angiogenesis of fibroblasts and HUVECs | (77) |
| miR-221-3p | BMSCs | Endothelial cells | AKT/eNOS↑ | Promote endothelial cells proliferation, migration, tube formation and VEGF levels | (107) |
| miR-126-3p | Synovium mesenchymal stem cells | Fibroblasts and HMEC-1 | — | Promote proliferation of human dermal fibroblasts and human dermal microvascular endothelial cells (HMEC-1);<br>Promote g HMEC-1 migration and tube formation<br>Promote collagen maturation | (76) |
| miR-126 | BMSCs | HUVECs | PI3K/AKT ↑ | Promote the HUVECs proliferation, migration and angiogenesis | (108) |
| miR-21-5p and let-7c-5p | BMSCs | HUVECs | – | Enhance cell proliferation rate, migration and tube formation | (109) |
| miR-200a | Embryonic stem cells | Endothelial cells | Kelch-like ECH- associated protein 1↓ nuclear factor erythroid2-related factor 2↑ | Rejuvenate the senescence of endothelial cells and recover compromised proliferation, migratory capacity, and tube formation | (79) |
| miR-125a | ADSCs | Endothelial cells | DLL4↓ | Promote endothelial cell angiogenesis | (110) |
| miR-21 | ADSCs | HaCaT cells | PI3K/AKT ↑ | Enhance the migration and proliferation | (111) |
| miR-135a | Human amnion mesenchymal stem cells | BJ cells | Large tumor suppressor kinase 2↓ | Promote cell migration and transformation | (78) |
| miR-378 | ADSCs | HaCaT cells | Caspase-3↑ | Promote proliferation and migration and reducing apoptosis | (112) |
| miR -93-3p | BMSCs | HaCaT cells | Apoptotic peptidase activating factor 1 ↓ | Promote proliferation and migration and reducing apoptosis | (113) |
| miR-100-5p and miR-1246 | Stem cells of human deciduous exfoliated teeth | HUVECs | VEGFA↓ | Inhibite cell proliferation and migration and inducing apoptosis | (80) |
| miR-181c | UCMSCs | Macrophages | TLR4↓ | Alleviate inflammation | (81) |
| let-7b | UCMSCs | Macrophages | TLR4/NF-κB/STAT3/AKT↓ | Regulate macrophage plasticity and alleviating inflammation | (82) |
| miR-223 | BMSCs | Macrophages | Pknox1↓ | Promote macrophage toward M2 polarization | (83) |
| miR-19b | ADSCs | Fibroblasts | CCL1↓TGF-β↑ | Regulate inflammation | (84) |
| miR -192-5p | ADSCs | Fibroblasts | IL-17RA↓Smad↓ | Anti- fibrosis | (87) |
| miR-21-5p and miR-125b-5p | UCMSCs | Fibroblasts | TGF-β receptor type II and TGF-β receptor type I ↓ | Anti-myofibroblast differentiation | (17) |
| miR-29a | ADSCs | Fibroblasts | TGF-β2/Smad3↓ | Inhibit fibrosis and scar hyperplasia of fibroblasts | (86) |
| miR-21, mir-23a, miR-125b, and miR-145 | UCMSCs | Myofibroblasts | TGF-β/SMAD2↓ | Suppress α-smooth muscle actin formation and collagen deposition | (88) |

ADSC, adipose-derived mesenchymal stem cell; BMSC, bone marrow-derived mesenchymal stem cell; UCMSC, human umbilical cord-derived mesenchymal stem cells. HUVECs, human umbilical vein endothelial cells; HMEC-1, human dermal microvascular endothelial cells; PTEN, phosphatase and tensin homolog; SPRY, sprouty RTK signaling antagonist; TGF-β, transforming growth factor-β; ↑, upregulated; ↓, downregulated.

Although most stem cell-exosomes derived miRNAs can promote cell proliferation, migration, and angiogenesis, a small proportion of miRNAs play a part in inhibiting wound healing. Exosomes enriched with miR-100-5p and miR-1246 from human deciduous tooth exfoliated dental stem cells were found to decrease cell proliferation and migration of HUVECs, induce cell apoptosis, and suppress tube like structure formation of HUVECs by downregulating several angiogenesis related factors, including VEGFA, MMP-9 and angiopoietin 1 (80), suggesting that miR-100-5p and miR-1246 play an anti-angiogenic role in wound healing.

### Exosomal miRNAs on anti-inflammation

The inflammatory response performs multiple tasks at the wound site by improving wound debridement and producing chemokines, metabolites, and growth factors. If this orchestrated response becomes dysregulated, wounds can become chronic or progressive fibrosis, both of which can impair tissue function and ultimately lead to organ failure and even death. Investigations have shown that miR-181c in UCMSC exosomes played a critical role in regulating burn induced inflammation. Exosomes overexpressing miR-181c potently inhibited toll-like receptor 4 (TLR4) signaling and attenuated inflammation in skin-burned rats, and significantly reduced lipopolysaccharide (LPS) induced TLR4 expression and inflammatory responses in macrophages (81). Besides, macrophages have been shown to play a central role in the inflammatory phase of tissue repair, such as the removal of dead cells, debris and pathogens. The dynamic plasticity allows them to mediate tissue damage and repair functions. For instance, LPS-pretreated UCMSC-derived exosomes can uniquely express miR let-7b, and upregulate of the expression of anti-inflammatory cytokines and promote M2 macrophage activation. Let-7b regulated macrophage polarization by downregulating TLR4/NF-κB/STAT3/AKT signaling pathway (82). In another study, miR-223 derived from BMSC-exosomes regulated macrophage polarization by targeting pknox1, suggesting that macrophage M2 polarization may accelerate wound healing *via* miR-223 (83). MiR-19b, derived from ADSC exosomes, were significantly increased in recipient cells and were able to decrease inflammatory CCL1 levels acting through TGF-β pathway in $H_2O_2$ pretreated HaCaT cells (84).

### Exosomal miRNAs on anti-scarring

Skin fibrosis results from poor wound healing following severe tissue damage such as severe burns, trauma, and major surgery. Pathological skin fibrosis tends to cause scarring. Dysregulation of each stage of wound healing, including the inflammatory, proliferative and remodeling stages, can lead to skin fibrosis (85). In vivo, ADSC derived exosomes over-expressing miR-29a inhibited the proliferation, migration, fibrosis and scar hyperplasia of human hypertrophic scar fibroblasts after scald wound in mice by targeting TGF-β2/Smad3 signaling pathway (86). Besides, ADSC exosomal miR-192-5p reduced pro-fibrotic protein levels and ameliorated hypertrophic scar fibrosis in mice through the IL-17RA /Smad axis (87).

Myofibroblasts aggregation also results in excessive scarring. A study examined UCMSC exosomal miRNAs by high-throughput sequencing and found that a group of specific miRNAs (miR-21, miR-23a, miR-125b and miR-145) played a key role during myofibroblast formation. In vivo and *in vitro* studies have validated that these miRNAs inhibited α-smooth muscle actin formation and collagen deposition through suppressing TGFβ/Smad2 axis (88).UCB exosomes were identified to contain abundant miRNAs. MiR-21-5p and miR-125b-5p from UCB exosomes were found essential for TGF-β1-induced anti-myofibroblast differentiation in human dermal fibroblasts by repressing receptor type II (TGFBR2) and TGF-β receptor type I (TGFBR1) respectively (17).

## Stem cell derived exosomal lncRNAs and wound healing

Stem cell-derived exosomal lncRNAs promotes wound healing in cell proliferation, migration, angiogenesis, anti-inflammatory and anti-fibrosis (see **Table 2**).

The lncRNA MALAT 1, a lncRNA abundant in exosomes from ADSCs, was validated to have the function in promoting human dermal fibroblasts migration and ischemic wound healing (89). Another study demonstrated that MALAT1-enriched exosomes derived from ADSCs promoted cell proliferation, migration and apoptosis in $H_2O_2$ induced HaCaT and human dermal fibroblasts by targeting miR-124 and activating the Wnt/β-catenin pathway (90).

LncRNA H19 (H19) was one of the first discovered lncRNAs and was found enriched in MSC-exosomes. ADSC exosomes inhibited the expression of miR-19b *via* lncRNA H19, thereby upregulating SOX9 to activate the Wnt/β-catenin pathway, resulting in accelerating the proliferation, migration and invasion of human skin fibroblasts. In vivo experiments also confirmed that exosomes from ADSCs promoted mouse skin wound healing through H19 (91). In a streptozotocin-induced diabetic foot mouse model, BMSCs-derived lncRNA H19 transferred to fibroblasts *via* exosomes, prevented fibroblasts apoptosis and inflammation by attenuating miR-152-3p-mediated PTEN repression to improve diabetic wound healing (92).

Another lncRNA KLF3-AS1 from BMSC exosomes induced angiogenesis to promote wound healing in diabetic skin. KLF3-AS1 accelerated the proliferation, migration and tube formation of HUVECs, while inhibited the apoptosis of HUVECs challenged by high glucose. In vivo, exosomes from BMSCs over-expressing KLF3-AS1 also promoted skin wound healing

TABLE 2 Stem cell-exosome derived lncRNA/cirRNA-mediated regulation of wound healing.

| Exosome derived lncRNAs/circRNA | Donor cells | Recipient cells | Potential target factor | Functions | References |
|---|---|---|---|---|---|
| lncRNA MALAT 1 | ADSCs | Fibroblasts | – | Enhance cell migration | (89) |
| lncRNA MALAT 1 | ADSCs | HaCaT and fibroblasts | miR-124<br>Wnt/β-catenin↑ | Promote cell proliferation, migration | (90) |
| lncRNA H19 | ADSCs | Fibroblasts | miR-19b↓<br>SOX9↑<br>Wnt/β-catenin↑ | Accelerate fibroblasts proliferation, migration and invasion | (91) |
| lncRNA H19 | BMSCs | Fibroblasts | miR-152-3p↓<br>PTEN↑<br>PI3K/AKT↓ | Prevent the apoptosis and inflammation of fibroblasts | (92) |
| lncRNA KLF3-AS1 | BMSCs | HUVECs | miR-383↓<br>VEGFA↑ | Accelerate the proliferation, migration and tube formation of HUVECs<br>Inhibit the apoptosis of HUVECs challenged by high glucose | (93) |
| lncRNA GAS 5 | ADSCs | Fibroblasts | TLR-7↓ | Modulate inflammation and accelerate the healing of chronic recalcitrant wounds | (94) |
| circRNA 0000250 | ADSCs | EPCs | miR-128-3p↓<br>SIRT1↑ | Enhance autophagy, reduce apoptosis of EPCs, facilitate skin angiogenesis | (96) |

ADSC, adipose-derived mesenchymal stem cell; BMSC, bone marrow-derived mesenchymal stem cell; EPCs, endothelial progenitor cells; PTEN, phosphatasetensin homolog; ↑, upregulated; ↓, downregulated.

in diabetic mice through increasing angiogenesis, and decreasing inflammation and miR-383 expression (93). Besides, LncRNA GAS 5, which is highly enriched in exosomes from ADSCs, was found to attenuate LPS induced inflammation in human skin fibroblasts, indicating it may have a role in promoting healing of chronic recalcitrant wounds (94). HOTAIR, a long noncoding RNA from extracellular vesicles of BMSCs, was confirmed to participate in promoting angiogenesis and wound healing in diabetic db/db mouse (95).

## Stem cell derived exosomal circRNAs and wound healing

The roles of circRNAs in wound healing have also received increasing attention because studies have shown that circRNAs involved in the physiological process of wound healing (see **Table 2**). CircRNAs are crucial in regulating different disease microenvironments. ADSC-exosomes containing high concentrations of mmu_circ_0000250 facilitated the recovery of endothelial progenitor cells (EPCs) function by enhancing autophagy, and reducing apoptosis of EPCs under high glucose conditions. In diabetic mouse wounds, mmu_circ_0000250-enriched exosomes facilitated skin angiogenesis and inhibited apoptosis through autophagy activation *via* inhibiting miR-128-3p and upregulating SIRT1 (96). Circ-Gcap14 from hypoxic preconditioned ADSCs increased the expression of angiogenic growth factors and accelerated diabetic wound closure by inhibiting downstream miR-18a-5p and promoting the expression of HIF-1α in a mouse wound model (97).

## Stem cell derived exosomal mRNAs and wound healing

Current studies have confirmed that mRNAs are enriched in exosomes, can be transferred to recipient cells and perform coding functions. Few studies have focused on the contribution of exosomal mRNAs in wound healing. A study revealed that microvesicles derived from UCMSCs improved the dedifferentiation and proliferation of damaged tubular cells by transferring hepatocyte growth factor (HGF) mRNAs and enhancing HGF synthesis, thereby accelerating renal regeneration and delaying fibrosis (98). Deregibus et al. first reported that endothelial progenitor cell-derived microvesicles improved angiogenesis through transfered mRNAs associated with PI3K/AKT and endothelial NOS signaling pathways (99). Future research may focus on how to transport functional mRNAs to encode active molecules for wound healing.

# Conclusion and perspective

In recent years, there have been a large number of studies confirming that exosomes derived from different stem cell types are effective for wound healing (15, 79, 81, 100, 101). Since the targets of exosomes on recipient cells are not well-defined, the investigation of their molecular mechanisms is necessary. The skin wound healing process is a precisely regulated, therefore, the functions of the transcriptomes of exosomes on skin wound healing are complex. At present, the majority of the research work concentrated on how miRNAs from the stem cell derived exosomal transcriptomes act on

fibroblast proliferation and migration in wound healing, and yet a few studies aimed at lncRNAs, circRNAs and mRNAs. This article reviews the major effects of mRNAs, miRNAs, lnc RNAs, circRNAs, and other stem cell derived exosomal transcriptomes on wound healing. Most of these exosomal RNAs were derived from mesenchymal stem cells, especially ADSCs and BMSCs. Although these RNAs are from different sources, their functions are nearly identical.

Exosomes are abundant in RNAs, including coding or non coding RNAs (ncRNAs). It is worth exploring whether RNAs interact with each other. The prevailing hypothesis is competitive endogenous RNA (ceRNA) hypothesis regarding the interplay between RNAs currently. The current research on stem cell derived exosomes and ceRNAs is still lacking. Han et al. investigated the interaction between differentially expressed lncRNAs, miRNAs and mRNAs during wound healing in normal individuals. After analyzing the ceRNA network, four up-regulated lncRNAs (MEG8, MEG3, MIR181A1HG, MIR4435-2HG) were found express during wound healing. MEG8/MEG3 may regulate fibroblast proliferation, differentiation and apoptosis *via* hsa-miR-296-3p/miR-6763-5p (102).With this lead, more studies regarding the interaction between ceRNA and other RNAs in wound healing are warranted.

To date, there have been a number of studies on the clinical application of ncRNAs which served as biomarkers for judging disease progression and prognosis of patients (103–105). However, the application of stem cell-derived exosomal transcriptomes remains at the basic research stage, and some urgent concerns need to be solved before clinical translation. For example, which source of exosomal transcriptomes is with the most potent efficacy? Which ncRNA plays the major regulatory role? Do lncRNAs alone or co-working with other exosomal components such as lipids and proteins participate in wound healing? How to improve the yields of specific RNAs from exosomes? Although the above challenges exist, with the rise of gene editing technology and the continuous development of RNA delivery techniques, it is foreseeable that stem cell derived exosomal transcriptomes can be widely used in the field of regenerative medicine in the near future.

## Author contributions

WZ designed the overall review. GC wrote the manuscript and drew the figures. HC polished the manuscript. WZ and XZ gave final approval of the manuscript. All authors contributed to the article and approved the submitted version.

## Funding

This work was supported by the special foundation of Guangzhou Key Laboratory (No. 542 202002010004), Guangzhou Science and Technology Plan Project (No. 202201020296), Guangdong Provincial Hospital of Chinese Medicine Science and Technology Research Program (No.YN2019MJ11), the Startup Grant of Guangdong Provincial Hospital of Chinese Medicine to Xiang Zeng (2022KT1032), and the scientific research project of Guangdong Administration of Traditional Chinese Medicine (No. 20211315&20222082).

## Conflict of interest

Author HC was employed by Guangzhou Qinglan Biotechnology Company Limited. The remaining authors declare that the research was conducted in the absence of any commercial or financial relationships that could be construed as a potential conflict of interest

## Publisher's note

All claims expressed in this article are solely those of the authors and do not necessarily represent those of their affiliated organizations, or those of the publisher, the editors and the reviewers. Any product that may be evaluated in this article, or claim that may be made by its manufacturer, is not guaranteed or endorsed by the publisher.

## References

1. Clark M, Adcock L. Cadth Rapid Response Reports. Honey for Wound Management: A Review of Clinical Effectiveness and Guidelines. Ottawa (ON): Canadian Agency for Drugs and Technologies in Health. Copyright © 2018 Canadian Agency for Drugs and Technologies in Health. (2018).

2. Wang PH, Huang BS, Horng HC, Yeh CC, Chen YJ. Wound healing. *J Chin Med Assoc*. (2018) 81(2):94–101. doi: 10.1016/j.jcma.2017.11.002

3. Bonifant H, Holloway S. A review of the effects of ageing on skin integrity and wound healing. *Br J Community Nurs*. (2019) 24(Sup3):S28–S33. doi: 10.12968/bjcn.2019.24.Sup3.S28

4. Gould LJ, Fulton AT. Wound healing in older adults. *R I Med J*. (2016) 99 (2):34–6.

5. Thapa RK, Diep DB, Tønnesen HH. Topical antimicrobial peptide formulations for wound healing: current developments and future prospects. *Acta Biomater*. (2020) 103:52–67. doi: 10.1016/j.actbio.2019.12.025

6. Veith AP, Henderson K, Spencer A, Sligar AD, Baker AB. Therapeutic strategies for enhancing angiogenesis in wound healing. *Adv Drug Delivery Rev*. (2019) 146:97–125. doi: 10.1016/j.addr.2018.09.010

7. Chouhan D, Mandal BB. Silk biomaterials in wound healing and skin regeneration therapeutics: from bench to bedside. *Acta Biomater*. (2020) 103:24–51. doi: 10.1016/j.actbio.2019.11.050

8. Kim HS, Sun X, Lee JH, Kim HW, Fu X, Leong KW. Advanced drug delivery systems and artificial skin grafts for skin wound healing. *Adv Drug Delivery Rev*. (2019) 146:209–39. doi: 10.1016/j.addr.2018.12.014

9. Saikaly SK, Khachemoune A. Honey and wound healing: an update. *Am J Clin Dermatol*. (2017) 18(2):237–51. doi: 10.1007/s40257-016-0247-8

10. Mazini L, Rochette L, Admou B. Hopes and limits of adipose-derived stem cells (adscs) and mesenchymal stem cells (mscs) in wound healing. *Int J Mol Sci*. (2020) 21(4):1–19. doi: 10.3390/ijms21041306

11. Duscher D, Barrera J, Wong VW, Maan ZN, Whittam AJ, Januszyk M, et al. Stem cells in wound healing: the future of regenerative medicine? A mini-review. *Gerontology*. (2016) 62(2):216–25. doi: 10.1159/000381877

12. King A, Balaji S, Keswani SG, Crombleholme TM. The role of stem cells in wound angiogenesis. *Adv Wound Care*. (2014) 3(10):614–25. doi: 10.1089/wound.2013.0497

13. Gonçalves RV, Costa AMA. Oxidative stress and tissue repair: mechanism, biomarkers, and therapeutics. *Oxid Med Cell Longevity*. (2021) 2021:6204096. doi: 10.1155/2021/6204096

14. Liu W, Yu M, Xie D, Wang L, Ye C, Zhu Q, et al. Melatonin-Stimulated Msc-derived exosomes improve diabetic wound healing through regulating macrophage M1 and M2 polarization by targeting the Pten/Akt pathway. *Stem Cell Res Ther*. (2020) 11(1):259. doi: 10.1186/s13287-020-01756-x

15. Zhang J, Guan J, Niu X, Hu G, Guo S, Li Q, et al. Exosomes released from human induced pluripotent stem cells-derived Mscs facilitate cutaneous wound healing by promoting collagen synthesis and angiogenesis. *J Transl Med*. (2015) 13:49. doi: 10.1186/s12967-015-0417-0

16. Ma T, Fu B, Yang X, Xiao Y, Pan M. Adipose mesenchymal stem cell-derived exosomes promote cell proliferation, migration, and inhibit cell apoptosis via Wnt/*B*-catenin signaling in cutaneous wound healing. *J Cell Biochem*. (2019) 120(6):10847–54. doi: 10.1002/jcb.28376

17. Zhang Y, Pan Y, Liu Y, Li X, Tang L, Duan M, et al. Exosomes derived from human umbilical cord blood mesenchymal stem cells stimulate regenerative wound healing via transforming growth factor-*B* receptor inhibition. *Stem Cell Res Ther*. (2021) 12(1):434. doi: 10.1186/s13287-021-02517-0

18. Yue B, Yang H, Wang J, Ru W. Exosome biogenesis, secretion and function of exosomal mirnas in skeletal muscle myogenesis. *Cell Prolif*. (2020) 53(7):e12857. doi: 10.1111/cpr.12857

19. Melnik BC, Stremmel W, Weiskirchen R. Exosome-Derived micrornas of human milk and their effects on infant health and development. *Biomolecules*. (2021) 11(6):1–47. doi: 10.3390/biom11060851

20. Chang W, Wang J. Exosomes and their noncoding Rna cargo are emerging as new modulators for diabetes Mellitus. *Cells*. (2019) 8(8):1–15. doi: 10.3390/cells8080853

21. Harrell CR, Jovicic N. Mesenchymal stem cell-derived exosomes and other extracellular vesicles as new remedies in the therapy of inflammatory diseases. *Cells*. (2019) 8(12):1–22. doi: 10.3390/cells8121605

22. Mao Q, Liang XL, Zhang CL, Pang YH, Lu YX. Lncrna Klf3-As1 in human mesenchymal stem cell-derived exosomes ameliorates pyroptosis of cardiomyocytes and myocardial infarction through Mir-138-5p/Sirt1 axis. *Stem Cell Res Ther*. (2019) 10(1):393. doi: 10.1186/s13287-019-1522-4

23. Zhang X, Sai B, Wang F, Wang L, Wang Y, Zheng L, et al. Hypoxic bmsc-derived exosomal mirnas promote metastasis of lung cancer cells via Stat3-induced Emt. *Mol Cancer*. (2019) 18(1):40. doi: 10.1186/s12943-019-0959-5

24. Xing X, Li Z, Yang X, Li M, Liu C, Pang Y, et al. Adipose-Derived mesenchymal stem cells-derived exosome-mediated microrna-342-5p protects endothelial cells against atherosclerosis. *Aging*. (2020) 12(4):3880–98. doi: 10.18632/aging.102857

25. Darby IA, Laverdet B, Bonté F, Desmoulière A. Fibroblasts and myofibroblasts in wound healing. *Clin Cosmet Investig Dermatol*. (2014) 7:301–11. doi: 10.2147/ccid.s50046

26. Xue M, Jackson CJ. Extracellular matrix reorganization during wound healing and its impact on abnormal scarring. *Adv Wound Care*. (2015) 4(3):119–36. doi: 10.1089/wound.2013.0485

27. Sarrazy V, Billet F, Micallef L, Coulomb B, Desmoulière A. Mechanisms of pathological scarring: role of myofibroblasts and current developments. *Wound Repair Regen*. (2011) 19(Suppl 1):S10–5. doi: 10.1111/j.1524-475X.2011.00708.x

28. Zeng G, Zhong F, Li J, Luo S, Zhang P. Resveratrol-mediated reduction of collagen by inhibiting proliferation and producing apoptosis in human hypertrophic scar fibroblasts. *Biosci Biotechnol Biochem*. (2013) 77(12):2389–96. doi: 10.1271/bbb.130502

29. Bowers S, Franco E. Chronic wounds: evaluation and management. *Am Fam Physician*. (2020) 101(3):159–66.

30. Wilkinson HN, Hardman MJ. Wound healing: cellular mechanisms and pathological outcomes. *Open Biol*. (2020) 10(9):200223. doi: 10.1098/rsob.200223

31. Pan BT, Johnstone RM. Fate of the transferrin receptor during maturation of sheep reticulocytes in vitro: selective externalization of the receptor. *Cell*. (1983) 33(3):967–78. doi: 10.1016/0092-8674(83)90040-5

32. Liu J, Ren L, Li S, Li W, Zheng X, Yang Y, et al. The biology, function, and applications of exosomes in cancer. *Acta Pharm Sin B*. (2021) 11(9):2783–97. doi: 10.1016/j.apsb.2021.01.001

33. Van den Boorn JG, Dassler J, Coch C, Schlee M, Hartmann G. Exosomes as nucleic acid nanocarriers. *Adv Drug Delivery Rev*. (2013) 65(3):331–5. doi: 10.1016/j.addr.2012.06.011

34. Xie Y, Dang W, Zhang S, Yue W, Yang L, Zhai X, et al. The role of exosomal noncoding Rnas in cancer. *Mol Cancer*. (2019) 18(1):37. doi: 10.1186/s12943-019-0984-4

35. Kalluri R, LeBleu VS. The biology, function, and biomedical applications of exosomes. *Science*. (2020) 367(6478):1–40. doi: 10.1126/science.aau6977

36. Chen M, Xu R, Ji H, Greening DW, Rai A, Izumikawa K, et al. Transcriptome and long noncoding RNA sequencing of three extracellular vesicle subtypes released from the human colon cancer Lim1863 cell line. *Sci Rep*. (2016) 6:38397. doi: 10.1038/srep38397

37. Valadi H, Ekström K, Bossios A, Sjöstrand M, Lee JJ, Lötvall JO. Exosome-Mediated transfer of MRNAs and MicroRNAs is a novel mechanism of genetic exchange between cells. *Nat Cell Biol*. (2007) 9(6):654–9. doi: 10.1038/ncb1596

38. Jiang H, Li Z, Li X, Xia J. Intercellular transfer of messenger RNAs in multiorgan tumorigenesis by tumor cell-derived exosomes. *Mol Med Rep*. (2015) 11(6):4657–63. doi: 10.3892/mmr.2015.3312

39. Eldh M, Ekström K, Valadi H, Sjöstrand M, Olsson B, Jernås M, et al. Exosomes communicate protective messages during oxidative stress; possible role of exosomal shuttle RNA. *PLoS One*. (2010) 5(12):e15353. doi: 10.1371/journal.pone.0015353

40. Sharma A. Bioinformatic analysis revealing association of exosomal mrnas and proteins in epigenetic inheritance. *J Theor Biol*. (2014) 357:143–9. doi: 10.1016/j.jtbi.2014.05.019

41. Lorenzi L, Avila Cobos F. Long noncoding RNA expression profiling in cancer: challenges and opportunities. *Genes Chromosom Cancer*. (2019) 58(4):191–9. doi: 10.1002/gcc.22709

42. Zhang H, Liu B, Shi X, Sun X. Long noncoding rnas: potential therapeutic targets in cardiocerebrovascular diseases. *Pharmacol Ther*. (2021) 221:107744. doi: 10.1016/j.pharmthera.2020.107744

43. Greco S, Salgado Somoza A, Devaux Y, Martelli F. Long noncoding RNAs and cardiac disease. *Antioxid Redox Signal*. (2018) 29(9):880–901. doi: 10.1089/ars.2017.7126

44. Lin L, Zhou G, Chen P, Wang Y, Han J, Chen M, et al. Which long noncoding RNAs and circular RNAs contribute to inflammatory bowel disease? *Cell Death Dis*. (2020) 11(6):456. doi: 10.1038/s41419-020-2657-z

45. Losko M, Kotlinowski J. Long noncoding rnas in metabolic syndrome related disorders. *Mediat Inflamm*. (2016) 2016:5365209. doi: 10.1155/2016/5365209

46. Naderi-Meshkin H, Lai X, Amirkhah R, Vera J, Rasko JEJ, Schmitz U. Exosomal LncRNAs and cancer: connecting the missing links. *Bioinformatics*. (2019) 35(2):352–60. doi: 10.1093/bioinformatics/bty527

47. Bartel DP. MicroRNAs: genomics, biogenesis, mechanism, and function. *Cell*. (2004) 116(2):281–97. doi: 10.1016/s0092-8674(04)00045-5

48. Sonenberg N, Hinnebusch AG. Regulation of translation initiation in eukaryotes: mechanisms and biological targets. *Cell*. (2009) 136(4):731–45. doi: 10.1016/j.cell.2009.01.042

49. Tafrihi M, Hasheminasab E. Mirnas: biology, biogenesis, their web-based tools, and databases. *MicroRNA*. (2019) 8(1):4–27. doi: 10.2174/2211536607666180827111633

50. Kabekkodu SP, Shukla V, Varghese VK, D'Souza J, Chakrabarty S, Satyamoorthy K. Clustered mirnas and their role in biological functions and diseases. *Biol Rev Camb Philos Soc*. (2018) 93(4):1955–86. doi: 10.1111/brv.12428

51. Kosik KS, Nowakowski T. Evolution of new mirnas and cerebro-cortical development. *Annu Rev Neurosci*. (2018) 41:119–37. doi: 10.1146/annurev-neuro-080317-061822

52. Shvedova M, Kobayashi T. Micrornas in cartilage development and dysplasia. *Bone*. (2020) 140:115564. doi: 10.1016/j.bone.2020.115564

53. Lu Q, Wu R, Zhao M, Garcia-Gomez A, Ballestar E. Mirnas as therapeutic targets in inflammatory disease. *Trends Pharmacol Sci*. (2019) 40(11):853–65. doi: 10.1016/j.tips.2019.09.007

54. Shah V, Shah J. Recent trends in targeting mirnas for cancer therapy. *J Pharm Pharmacol*. (2020) 72(12):1732–49. doi: 10.1111/jphp.13351

55. Li Y, Zheng Q, Bao C, Li S, Guo W, Zhao J, et al. Circular Rna is enriched and stable in exosomes: a promising biomarker for cancer diagnosis. *Cell Res*. (2015) 25(8):981–4. doi: 10.1038/cr.2015.82

56. Mehta SL, Dempsey RJ, Vemuganti R. Role of circular rnas in brain development and Cns diseases. *Prog Neurobiol*. (2020) 186:101746. doi: 10.1016/j.pneurobio.2020.101746

57. Cao YZ, Sun JY, Chen YX, Wen CC, Wei L. The roles of circrnas in cancers: perspectives from molecular functions. *Gene*. (2021) 767:145182. doi: 10.1016/j.gene.2020.145182

58. Li J, Sun C, Cui H, Sun J, Zhou P. Role of circrnas in neurodevelopment and neurodegenerative diseases. *J Mol Neurosci*. (2021) 71(9):1743–51. doi: 10.1007/s12031-021-01882-y

59. Xia X, Tang X, Wang S. Roles of circrnas in autoimmune diseases. *Front Immunol*. (2019) 10:639. doi: 10.3389/fimmu.2019.00639

60. Yu Z, Huang Q, Zhang Q, Wu H, Zhong Z. Circrnas open a new era in the study of cardiovascular disease (review). *Int J Mol Med*. (2021) 47(1):49–64. doi: 10.3892/ijmm.2020.4792

61. Ma Y, Liu Y, Jiang Z. Circrnas: a new perspective of biomarkers in the nervous system. *Biomed Pharmacother*. (2020) 128:110251. doi: 10.1016/j.biopha.2020.110251

62. Solé C, Mentxaka G, Lawrie CH. The use of circrnas as biomarkers of cancer. *Methods Mol Biol*. (2021) 2348:307–41. doi: 10.1007/978-1-0716-1581-2_21

63. Sylakowski K, Bradshaw A, Wells A. Mesenchymal stem cell/multipotent stromal cell augmentation of wound healing: lessons from the physiology of matrix and hypoxia support. *Am J Pathol*. (2020) 190(7):1370–81. doi: 10.1016/j.ajpath.2020.03.017

64. Meng Z, Zhou D, Gao Y, Zeng M, Wang W. Mirna delivery for skin wound healing. *Adv Drug Delivery Rev*. (2018) 129:308–18. doi: 10.1016/j.addr.2017.12.011

65. Huang Y, He B, Wang L, Yuan B, Shu H, Zhang F, et al. Bone marrow mesenchymal stem cell-derived exosomes promote rotator cuff tendon-bone healing by promoting angiogenesis and regulating M1 macrophages in rats. *Stem Cell Res Ther*. (2020) 11(1):496. doi: 10.1186/s13287-020-02005-x

66. Liu W, Rong Y, Wang J, Zhou Z, Ge X, Ji C, et al. Exosome-Shuttled mir-216a-5p from hypoxic preconditioned mesenchymal stem cells repair traumatic spinal cord injury by shifting microglial M1/M2 polarization. *J Neuroinflammation*. (2020) 17(1):47. doi: 10.1186/s12974-020-1726-7

67. Wen Z, Mai Z, Zhu X, Wu T, Chen Y, Geng D. Mesenchymal stem cell-derived exosomes ameliorate cardiomyocyte apoptosis in hypoxic conditions through Microrna144 by targeting the Pten/Akt pathway. *Stem Cell Res Ther*. (2020) 11(1):36. doi: 10.1186/s13287-020-1563-8

68. Sahoo S, Klychko E, Thorne T, Misener S, Schultz KM, Millay M, et al. Exosomes from human Cd34(+) stem cells mediate their proangiogenic paracrine activity. *Circ Res*. (2011) 109(7):724–8. doi: 10.1161/circresaha.111.253286

69. Wang Y, Zhang L, Li Y, Chen L, Wang X, Guo W, et al. Exosomes/microvesicles from induced pluripotent stem cells deliver cardioprotective mirnas and prevent cardiomyocyte apoptosis in the ischemic myocardium. *Int J Cardiol*. (2015) 192:61–9. doi: 10.1016/j.ijcard.2015.05.020

70. Khan M, Nickoloff E, Abramova T, Johnson J, Verma SK, Krishnamurthy P, et al. Embryonic stem cell-derived exosomes promote endogenous repair mechanisms and enhance cardiac function following myocardial infarction. *Circ Res*. (2015) 117(1):52–64. doi: 10.1161/circresaha.117.305990

71. Ha DH, Kim HK, Lee J, Kwon HH, Park GH, Yang SH, et al. Mesenchymal stem/stromal cell-derived exosomes for immunomodulatory therapeutics and skin regeneration. *Cells*. (2020) 9(5):1–45. doi: 10.3390/cells9051157

72. Nakano M, Fujimiya M. Potential effects of mesenchymal stem cell derived extracellular vesicles and exosomal mirnas in neurological disorders. *Neural Regen Res*. (2021) 16(12):2359–66. doi: 10.4103/1673-5374.313026

73. Zhang Y, Kim MS, Jia B, Yan J, Zuniga-Hertz JP, Han C, et al. Hypothalamic stem cells control ageing speed partly through exosomal mirnas. *Nature*. (2017) 548(7665):52–7. doi: 10.1038/nature23282

74. Md G C, Md Y W, Md L Z, Md Y Z. Effect of microrna-146a modified adipose-derived stem cell exosomes on rat back wound healing. *Int J Low Extrem Wounds*. (2021):15347346211038092. doi: 10.1177/15347346211038092 [Epub ahead of print].

75. Hu Y, Rao SS, Wang ZX, Cao J, Tan YJ, Luo J, et al. Exosomes from human umbilical cord blood accelerate cutaneous wound healing through Mir-21-3p-mediated promotion of angiogenesis and fibroblast function. *Theranostics*. (2018) 8(1):169–84. doi: 10.7150/thno.21234

76. Tao SC, Guo SC, Li M, Ke QF, Guo YP, Zhang CQ. Chitosan wound dressings incorporating exosomes derived from microrna-126-overexpressing synovium mesenchymal stem cells provide sustained release of exosomes and heal full-thickness skin defects in a diabetic rat model. *Stem Cells Transl Med*. (2017) 6(3):736–47. doi: 10.5966/sctm.2016-0275

77. Wu D, Kang L, Tian J, Wu Y, Liu J, Li Z, et al. Exosomes derived from bone mesenchymal stem cells with the stimulation of Fe(3)O(4) nanoparticles and static magnetic field enhance wound healing through upregulated Mir-21-5p. *Int J Nanomed*. (2020) 15:7979–93. doi: 10.2147/ijn.s275650

78. Gao S, Chen T, Hao Y, Zhang F, Tang X, Wang D, et al. Exosomal Mir-135a derived from human amnion mesenchymal stem cells promotes cutaneous wound healing in rats and fibroblast migration by directly inhibiting Lats2 expression. *Stem Cell Res Ther*. (2020) 11(1):56. doi: 10.1186/s13287-020-1570-9

79. Chen B, Sun Y, Zhang J, Zhu Q, Yang Y, Niu X, et al. Human embryonic stem cell-derived exosomes promote pressure ulcer healing in aged mice by rejuvenating senescent endothelial cells. *Stem Cell Res Ther*. (2019) 10(1):142. doi: 10.1186/s13287-019-1253-6

80. Liu P, Zhang Q, Mi J, Wang S, Xu Q, Zhuang D, et al. Exosomes derived from stem cells of human deciduous exfoliated teeth inhibit angiogenesis in vivo and in vitro via the transfer of Mir-100-5p and Mir-1246. *Stem Cell Res Ther*. (2022) 13(1):89. doi: 10.1186/s13287-022-02764-9

81. Li X, Liu L, Yang J, Yu Y, Chai J, Wang L, et al. Exosome derived from human umbilical cord mesenchymal stem cell mediates Mir-181c attenuating burn-induced excessive inflammation. *EBioMedicine*. (2016) 8:72–82. doi: 10.1016/j.ebiom.2016.04.030

82. Ti D, Hao H, Tong C, Liu J, Dong L, Zheng J, et al. Lps-Preconditioned mesenchymal stromal cells modify macrophage polarization for resolution of chronic inflammation via exosome-shuttled Let-7b. *J Transl Med*. (2015) 13:308. doi: 10.1186/s12967-015-0642-6

83. He X, Dong Z, Cao Y, Wang H, Liu S, Liao L, et al. Msc-derived exosome promotes M2 polarization and enhances cutaneous wound healing. *Stem Cells Int*. (2019) 2019:7132708. doi: 10.1155/2019/7132708

84. Cao G, Chen B, Zhang X, Chen H. Human adipose-derived mesenchymal stem cells-derived exosomal microrna-19b promotes the healing of skin wounds through modulation of the Ccl1/Tgf-*B* signaling axis. *Clin Cosmet Investig Dermatol*. (2020) 13:957–71. doi: 10.2147/ccid.s274370

85. Ayadi A E, Jay JW, Prasai A. Current approaches targeting the wound healing phases to attenuate fibrosis and scarring. *Int J Mol Sci*. (2020) 21(3):1–28. doi: 10.3390/ijms21031105

86. Yuan R, Dai X, Li Y, Li C, Liu L. Exosomes from Mir-29a-modified adipose-derived mesenchymal stem cells reduce excessive scar formation by inhibiting Tgf-*B*2/Smad3 signaling. *Mol Med Rep*. (2021) 24(5):1–12. doi: 10.3892/mmr.2021.12398

87. Li Y, Zhang J, Shi J, Liu K, Wang X, Jia Y, et al. Correction to: exosomes derived from human adipose mesenchymal stem cells attenuate hypertrophic scar fibrosis by Mir-192-5p/Il-17ra/Smad axis. *Stem Cell Res Ther*. (2021) 12(1):490. doi: 10.1186/s13287-021-02568-3

88. Fang S, Xu C, Zhang Y, Xue C, Yang C, Bi H, et al. Umbilical cord-derived mesenchymal stem cell-derived exosomal micrornas suppress myofibroblast differentiation by inhibiting the transforming growth factor-*B*/Smad2 pathway during wound healing. *Stem Cells Transl Med*. (2016) 5(10):1425–39. doi: 10.5966/sctm.2015-0367

89. Cooper DR, Wang C, Patel R, Trujillo A, Patel NA, Prather J, et al. Human adipose-derived stem cell conditioned media and exosomes containing Malat1 promote human dermal fibroblast migration and ischemic wound healing. *Adv Wound Care*. (2018) 7(9):299–308. doi: 10.1089/wound.2017.0775

90. He L, Zhu C, Jia J, Hao XY, Yu XY, Liu XY, et al. Adsc-Exos containing Malat1 promotes wound healing by targeting Mir-124 through activating Wnt/*B*-catenin pathway. *Biosci Rep*. (2020) 40(5):1–13. doi: 10.1042/bsr20192549

91. Qian L, Pi L, Fang BR, Meng XX. Adipose mesenchymal stem cell-derived exosomes accelerate skin wound healing via the Lncrna H19/Mir-19b/Sox9 axis. *Lab Invest*. (2021) 101(9):1254–66. doi: 10.1038/s41374-021-00611-8

92. Li B, Luan S, Chen J, Zhou Y, Wang T, Li Z, et al. The Msc-derived exosomal Lncrna H19 promotes wound healing in diabetic foot ulcers by upregulating pten via microrna-152-3p. *Mol Ther Nucleic*. (2020) 19:814–26. doi: 10.1016/j.omtn.2019.11.034

93. Han ZF, Cao JH, Liu ZY, Yang Z, Qi RX, Xu HL. Exosomal Lncrna Klf3-As1 derived from bone marrow mesenchymal stem cells stimulates angiogenesis to promote diabetic cutaneous wound healing. *Diabetes Res Clin Pract*. (2022) 183:109126. doi: 10.1016/j.diabres.2021.109126

94. Patel RS, Impreso S, Lui A. Long noncoding Rna Gas5 contained in exosomes derived from human adipose stem cells promotes repair and modulates inflammation

in a chronic dermal wound healing model. *Biology*. (2022) 11(3):1–19. doi: 10.3390/biology11030426

95. Born LJ, Chang KH, Shoureshi P, Lay F, Bengali S, Hsu ATW, et al. Hotair-loaded mesenchymal stem/stromal cell extracellular vesicles enhance angiogenesis and wound healing. *Adv Healthcare Mater*. (2022) 11(5):e2002070. doi: 10.1002/adhm.202002070

96. Shi R, Jin Y, Hu W, Lian W, Cao C, Han S, et al. Exosomes derived from Mmu_Circ_0000250-modified adipose-derived mesenchymal stem cells promote wound healing in diabetic mice by inducing Mir-128-3p/Sirt1-mediated autophagy. *Am J Physiol Cell Physiol*. (2020) 318(5):C848–C56. doi: 10.1152/ajpcell.00041.2020

97. Wang Z, Feng C, Liu H, Meng T, Huang W, Long X, et al. Hypoxic pretreatment of adipose-derived stem cells accelerates diabetic wound healing via Circ-Gcap14 and Hif-1$\alpha$/Vegf mediated angiopoiesis. *Int J Stem Cells*. (2021) 14(4):447–54. doi: 10.15283/ijsc21050

98. Ju GQ, Cheng J, Zhong L, Wu S, Zou XY, Zhang GY, et al. Microvesicles derived from human umbilical cord mesenchymal stem cells facilitate tubular epithelial cell dedifferentiation and growth via hepatocyte growth factor induction. *PLoS One*. (2015) 10(3):e0121534. doi: 10.1371/journal.pone.0121534

99. Deregibus MC, Cantaluppi V, Calogero R, Lo Iacono M, Tetta C, Biancone L, et al. Endothelial progenitor cell derived microvesicles activate an angiogenic program in endothelial cells by a horizontal transfer of mrna. *Blood*. (2007) 110 (7):2440–8. doi: 10.1182/blood-2007-03-078709

100. Liu J, Yan Z, Yang F, Huang Y, Yu Y, Zhou L, et al. Exosomes derived from human umbilical cord mesenchymal stem cells accelerate cutaneous wound healing by enhancing angiogenesis through delivering angiopoietin-2. *Stem Cell Rev Rep*. (2021) 17(2):305–17. doi: 10.1007/s12015-020-09992-7

101. Shabbir A, Cox A, Rodriguez-Menocal L, Salgado M, Van Badiavas E. Mesenchymal stem cell exosomes induce proliferation and migration of normal and chronic wound fibroblasts, and enhance angiogenesis in vitro. *Stem Cells Dev*. (2015) 24(14):1635–47. doi: 10.1089/scd.2014.0316

102. Han B, Xu S, Liu X, Shi J, Liu Z, Zhang Y, et al. Competing endogenous Rna network in non-keloid-prone individuals during wound healing. *J Craniofac Surg*. (2022) 33(1):29–34. doi: 10.1097/scs.0000000000007824

103. Huang M, He YR, Liang LC, Huang Q, Zhu ZQ. Circular Rna Hsa_Circ_0000745 may serve as a diagnostic marker for gastric cancer. *World J Gastroenterol*. (2017) 23(34):6330–8. doi: 10.3748/wjg.v23.i34.6330

104. Pichu S, Vimalraj S, Viswanathan V. Impact of microrna-210 on wound healing among the patients with diabetic foot ulcer. *PLoS One*. (2021) 16(7): e0254921. doi: 10.1371/journal.pone.0254921

105. Yu Y, Zhang W, Li A, Chen Y, Ou Q, He Z, et al. Association of long noncoding Rna biomarkers with clinical immune subtype and prediction of immunotherapy response in patients with cancer. *JAMA Netw. Open*. (2020) 3 (4):e202149. doi: 10.1001/jamanetworkopen.2020.2149

106. Pi L, Yang L, Fang BR, Meng XX, Qian L. Exosomal microrna-125a-3p from human adipose-derived mesenchymal stem cells promotes angiogenesis of wound healing through inhibiting pten. *Mol Cell Biochem*. (2022) 477 (1):115–27. doi: 10.1007/s11010-021-04251-w

107. Yu M, Liu W, Li J, Lu J, Lu H, Jia W, et al. Exosomes derived from atorvastatin-pretreated Msc accelerate diabetic wound repair by enhancing angiogenesis via Akt/Enos pathway. *Stem Cell Res Ther*. (2020) 11(1):350. doi: 10.1186/s13287-020-01824-2

108. Zhang L, Ouyang P, He G, Wang X, Song D, Yang Y, et al. Exosomes from microrna-126 overexpressing mesenchymal stem cells promote angiogenesis by targeting the Pik3r2-mediated Pi3k/Akt signalling pathway. *J Cell Mol Med*. (2021) 25(4):2148–62. doi: 10.1111/jcmm.16192

109. Wang W, Zhao Y, Li H, Zhang Y, Jia X, Wang C, et al. Exosomes secreted from mesenchymal stem cells mediate the regeneration of endothelial cells treated with rapamycin by delivering pro-angiogenic micrornas. *Exp Cell Res*. (2021) 399 (1):112449. doi: 10.1016/j.yexcr.2020.112449

110. Liang X, Zhang L, Wang S, Han Q, Zhao RC. Exosomes secreted by mesenchymal stem cells promote endothelial cell angiogenesis by transferring Mir-125a. *J Cell Sci*. (2016) 129(11):2182–9. doi: 10.1242/jcs.170373

111. Yang C, Luo L, Bai X, Shen K, Liu K, Wang J, et al. Highly-expressed micorna-21 in adipose derived stem cell exosomes can enhance the migration and proliferation of the Hacat cells by increasing the Mmp-9 expression through the Pi3k/Akt pathway. *Arch Biochem Biophys*. (2020) 681:108259. doi: 10.1016/j.abb.2020.108259

112. Zheng T, Shao W, Tian J. Exosomes derived from adscs containing Mir-378 promotes wound healing by targeting caspase-3. *J Biochem Mol Toxicol*. (2021) 35 (10):e22881. doi: 10.1002/jbt.22881

113. Shen C, Tao C, Zhang A, Li X, Guo Y, Wei H, et al. Exosomal microrna-93-3p secreted by bone marrow mesenchymal stem cells downregulates apoptotic peptidase activating factor 1 to promote wound healing. *Bioengineered*. (2022) 13(1):27–37. doi: 10.1080/21655979.2021.1997077

frontiers | Frontiers in Surgery

TYPE Original Research
PUBLISHED 17 August 2022
DOI 10.3389/fsurg.2022.990749

Check for updates

OPEN ACCESS

EDITED BY
Jiliang Zhou,
Georgia Health Sciences University, United States

REVIEWED BY
Huimei Wang,
Fudan University, China
Shilin Xia,
Dalian Medical University, China

*CORRESPONDENCE
Jiehua Li
jiehuali_fs@163.com
Xiaobing Pi
pxbingice@163.com
Ronghua Yang
a_hwa991316@163.com

[†]These authors have contributed equally to this work and share first authorship

SPECIALTY SECTION
This article was submitted to Reconstructive and Plastic Surgery, a section of the journal Frontiers in Surgery

RECEIVED 10 July 2022
ACCEPTED 01 August 2022
PUBLISHED 17 August 2022

CITATION
Zhou S, Han Y, Yang R, Pi X and Li J (2022) TIMM13 as a prognostic biomarker and associated with immune infiltration in skin cutaneous melanoma (SKCM).
Front. Surg. 9:990749.
doi: 10.3389/fsurg.2022.990749

COPYRIGHT
© 2022 Zhou, Han, Yang, Pi and Li. This is an open-access article distributed under the terms of the Creative Commons Attribution License (CC BY). The use, distribution or reproduction in other forums is permitted, provided the original author(s) and the copyright owner(s) are credited and that the original publication in this journal is cited, in accordance with accepted academic practice. No use, distribution or reproduction is permitted which does not comply with these terms.

# TIMM13 as a prognostic biomarker and associated with immune infiltration in skin cutaneous melanoma (SKCM)

Sitong Zhou[1†], Yuanyuan Han[2†], Ronghua Yang[3*], Xiaobing Pi[1*] and Jiehua Li[1*]

[1]Department of Dermatology, The First People's Hospital of Foshan, Foshan, China, [2]Institute of Medical Biology, Chinese Academy of Medical Sciences and Peking Union Medical College, Yunnan Key Laboratory of Vaccine Research and Development on Severe Infectious Diseases, Kunming, China, [3]Department of Burn and Plastic Surgery, Guangzhou First People's Hospital, South China University of Technology, Guangzhou, China

**Objective:** Providing protection against aggregation and guiding hydrophobic precursors through the mitochondria's intermembrane space, this protein functions as a chaperone-like protein. SLC25A12 is imported by TIMM8 as a result of its interaction with TIMM13. In spite of this, it is still unknown how TIMM13 interacts with skin cutaneous melanoma (SKCM) and tumor-infiltrating lymphocytes (TILs).

**Methods:** Aberrant expression of TIMM13 in SKCM and its clinical outcome was evaluated with the help of multiple databases, including the Xiantao tool (https://www.xiantao.love/), HPA, and UALCAN. TISIDB and Tumor Immune Estimation Resources (TIMER) databases were applied to explore the association between TIMM13 and tumor infiltration immune cells. OS nomogram was constructed, and model performance was examined. Finally, TIMM13 protein expression was validated by immunohistochemistry (IHC).

**Results:** TIMM13 expression was higher in SKCM samples than in peritumor samples. TIMM13 was strongly associated with sample type, subgroup, cancer stage, lymph node stage, and worse survival. Further, upregulation of TIMM13 was significantly associated with immunoregulators, and chemokines, as well as T cells, B cells, monocytes, neutrophils, macrophages, and T-cell regulators. An analysis of bioinformatic data uncovered that TIMM13 expression was strongly associated with PD1 (T-cell exhaustion marker). The nomogram showed good predictive performance based on calibration plot. TIMM13 was highly expressed in melanoma tissue samples than in normal samples.

**Conclusion:** In brief, TIMM13 may be a prognostic biomarker for SKCM. It might modulate the tumor immune microenvironment and lead to a poorer prognosis. In addition, it is necessary to study the targeted therapy of TIMM13.

KEYWORDS

cutaneous melanoma, translocase of inner mitochondrial membrane 13 (TIMM13), prognosis, biomarker, tumor immune microenvironment

# Introduction

There are two main types of melanoma: cutaneous and uveal (1). Melanin-producing melanocytes in the skin are transformed into melanoma cells through malignant transformation (2). More than 75% of skin cancer deaths are caused by melanoma, even though it represents only 5% of all skin cancer cases (3). Cutaneous melanoma is considered the most aggressive type of skin cancer (4). There are approximately 232,100 (1.7%) new cases of cutaneous melanoma diagnosed worldwide (excluding nonmelanoma skin cancers), and the incidence of cutaneous melanoma is around 55,500 deaths per year (0.7% of all cancer deaths) (5). Before the FDA's approved targeted and immunotherapy strategies in 2011 and 2014, metastatic melanoma was thought to be incurable and not treatable (6). These strategies are effective in treating some cases of melanoma, but not all, due to toxicity, intrinsic resistance to drugs, and other unidentified causes (7). It is necessary to perform surgery, radiotherapy, chemotherapy, and conduct clinical trials to cure resistant melanoma cells (8). With SKCM, the discovery of new immunotherapy targets and the detection of immune-related biomarkers are urgent tasks.

The TIMM13 gene encodes a chaperone protein that is part of the evolutionarily conserved TIMM (translocase of inner mitochondrial membrane) family that assists in the transport of proteins into mitochondria from the cytosol (9). The TIMM13 gene prevents hydrophobic precursors from aggregating and guides the proteins passing the mitochondrial intermembrane. SLC25A12/ARALAR1 and SLC25A13/ARALAR2 are imported by the TIMM8-TIMM13 complex (10). Timm13 is associated with Mohr-Tranebjaerg Syndrome and Visual Cortex Disease (11). It is related to the Peroxisomal lipid metabolism pathway (12). Studies have shown that TIMM13 was differently expressed in metastatic susceptibility (13), hepatocellular carcinoma (14), breast cancer (15) et al. These research proposed that TIMM13 may impact cancer profoundly, and it may be considered a new target for dealing with various malignant tumors. However, the possible mechanisms of TIMM13 in tumorigenesis and immune involvement in SKCM is still unclear.

In the study, the expression of TIMM13 and its connection with the clinical outcomes of SKCM were explored by various databases, including the Xiantao tool, HPA, and UALCAN databases. In addition, the Xiantao tool and TIMER database was conducted to explore the connection of TIMM13 with the infiltration of immune cells. The TISIDB database was used to study the relationship between TIMM13 and immunomodulators, immunostimulators, and chemokines. This research revealed the important function of TIMM13 in SKCM, and then the possible relationship and possibility of TIMM13 regulating tumor invasion of immune cells.

# Materials and methods

## Interaction analysis of gene expression profiling

The Xiantao tool online database (https://www.xiantao.love/) (16) is an integrated platform using R software (3.6.3) for obtaining analytical data from TCGA (https://portal.gdc.cancer.gov/) (17) and The Genotype–Tissue Expression (GTEx) (https://gtexportal.org/home/) (18). R packages used in the Xiantao tool were set as default. In the study, we evaluated TIMM13 expression in SKCM and normal tissues using the Xiantao data source.

## UALCAN database analysis

The UALCAN website (http://ualcan.path.uab.edu/) contains massive bioinformatics and clinical data on 31 TCGA malignant tumors (19). It can be used to make a gene expression comparison between SKCM and normal samples, at different tumor stages, different subtypes, and other clinicopathological characteristics. In the research, the expression level of TIMM13 will be determined by the main clinicopathological characteristics, such as tissue category (healthy or tumor), SKCM stage (stages 1, 2, 3, 4), lymph node stage (N01 stage, 2, 3), cancer subgroup, etc. The clinicopathological features (tumor degree, stage) and TIMM13 expression distribution of patients were collected by the UALCAN database and Xiantao tool for correlation analysis.

## Survival analysis for SKCM

Based on the median of the expression of TIMM13, patients were divided into a high TIMM13 expression group and a low TIMM13 expression group. The prognostic significance of TIMM13 in SKCM, including overall survival (OS), and progression-free interval (PFI), were explored using the Xiantao tool between the high TIMM13 expression group and low TIMM13 expression group. The hazard ratio (HR) with 95% confidence intervals and log-rank p-value was estimated. $P < 0.05$ was regarded as statistical significance.

## Tumor immune infiltration analysis

ssSGSEA method was applied to explore the potential connection between TIMM13 mRNA expression and immune infiltration level in SKCM by TIMER 2.0 (http://timer.cistrome.org/) (20). In addition, TILs gene markers and TILs gene expression were analyzed by the Xiantao

tool. Then we drew the expression dispersion maps between a pair of custom genes for SKCM and the statistical significance of the correlation was estimated by Spearman's method. log2 RSEM was applied to exhibit the levels of gene expression.

## TISIDB database analysis

TISIDB (http://cis.hku.hk/TISIDB/) (21) is an online platform for studying tumor-immune system interaction, which combines various heterogeneous data sources. This database can assist us to know the interaction between tumors and immune cells, predict the responses of the body to immunotherapy, and find out novel immunotherapy targets. It will be a precious basis for tumor immunology studies and treatment. In this study, we used TISIDB to study the relationship between TIMM13 and 28 TILs, 45 immunopotentiators, 24 immunosuppressants, 41 chemokines, and 18 receptors in SKCM.

## Building and validation of a nomogram

A nomogram is a statistical model of prognosis presented as a simple graph. In the nomogram, each sample is assigned a point for each of its variables and the resulting total score predicts 1-, 3-, and 5-year survival rates. We used independent prognostic factors to build a nomogram using the "rms" package. A calibration plot (by a bootstrap method with 500 resamples) was used to validate the nomogram and concordance index (C-index).

## Immunohistochemistry (IHC) staining

Paraffin-embedded tissues were sectioned at 4 μm for IHC analysis. Antigens were retrieved by incubating the samples in citrate buffer (pH 6.0) for 15 min at 100 °C in a microwave oven and naturally cooled to room temperature. After blocking with a mixture of methanol and 0.75% hydrogen peroxide, sections were incubated overnight with appropriate dilatation of primary antibodies (TIMM13, Invitrogen, 1:150) followed by incubation with a secondary antibody conjugated with HRP (goat anti-rabbit, 1:500, Cell Signalling Technology). The sections were washed three times with PBS and incubated with AEC (ZSGB-BIO).

## Statistical analysis

Statistical analyses were performed with the Student t test, the Mann-Whitney U test, or analysis of variance, as appropriate. For nonparametric (non-normally distributed) data, Mann–Whitney U test was used for statistical analysis. The survival curve was drawn by KM plot by log-rank test. We calculated Spearman's correlation coefficient to explore the relationship between TIMM13 expression and immune infiltration levels, immunomodulators, and chemokines. Statistically significant was regarded as $p < 0.05$.

# Results

## High expression of TIMM13 in SKCM tissue

The differential expression of TIMM13 in tumor and normal tissues were studied by RNA-seq data of different types of cancer from TCGA. The conclusion was shown in **Figure 1A**. According to Xiantao tool, we found that the expression of TIMM13 upregulated in almost all cancer tissues such as ACC, BLCA and SKCM, but downregulated in KIRC, LAML and PCPG.

To validate these results in SKCM, cancer samples from the TCGA database and normal samples from GTEx database were tested by xiantao tool. As shown in **Figure 1B**, it was found that TIMM13 mRNA expression was significantly higher in SKCM samples (469 cases) than that in normal samples (813 cases) ($p < 0.05$) from GETx. Based on the HPA website, immunohistochemistry confirmed the TIMM13 protein expression pattern (**Figure 1C**). It is worth noting that the increased expression of TIMM13 mRNA was negatively correlated with PD1 (**Figure 1D**), where the AUC of TIMM13 in SKCM is 0.757 (95% CI is 0.727 to 0.786) (**Figure 1E**). It is suggested that TIMM13 was significantly elevated in SKCM tissues, which may be a potential biomarker for the diagnosis of SKCM.

## Relationship between TIMM13 expression and patient clinical pathology in SKCM

Using the UALCAN and the Xiantao tool, we investigated the relationship between TIMM13 expression and several clinicopathological features, such as tumor type, stage, lymph node stage, and TP53 mutation shown in **Figure 2A**, the expression of TIMM13 in SKCM metastatic cancer tissues was significantly higher than that in primary cancer tissues and normal cancer tissues ($p = 0.0018$). There was no significant difference between different cancer stages (**Figure 2B**), different lymph nodes (**Figure 2C**) and TP53 mutation (**Figure 2D**). Secondly, in order to further understand the function and possible mechanism of

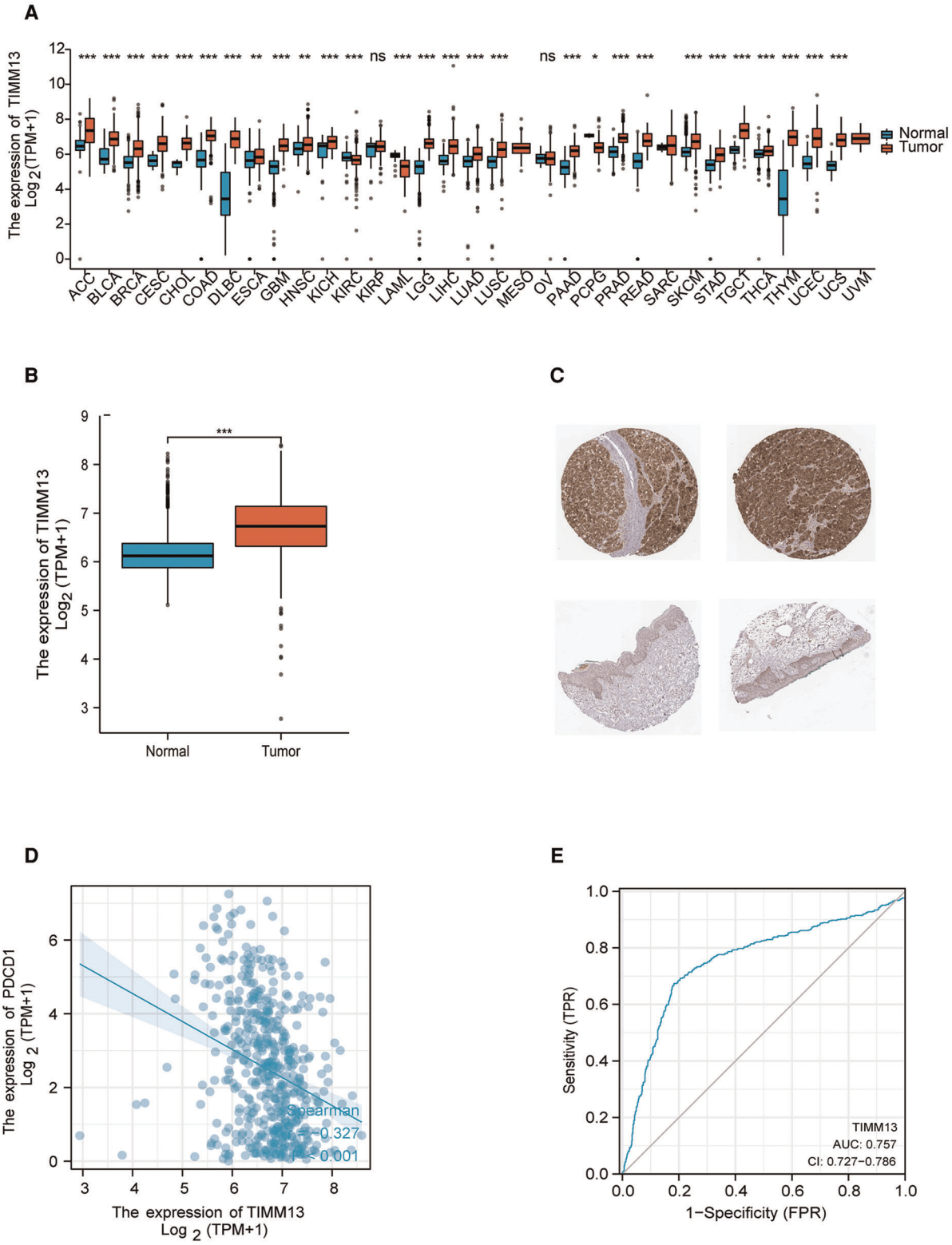


FIGURE 1
TIMM13 expression levels. (A) Increased or decreased TIMM13 in different tumor types from The Cancer Genome Atlas (TCGA) database were determined by Xiantao tool (*$p < 0.05$, **$p < 0.01$, ***$p < 0.001$). (B) Increased TIMM13 in SKCM tissues compared with normal tissues. (C) TIMM13 immunohistochemical staining levels in SKCM tissues (up) and normal tissues (down) by using HPA database. (D) The correlation analysis between TIMM13 and PD1 mRNA level. (E) The receiver-operating characteristic (ROC) curve analysis of TIMM13 in SKCM patients.

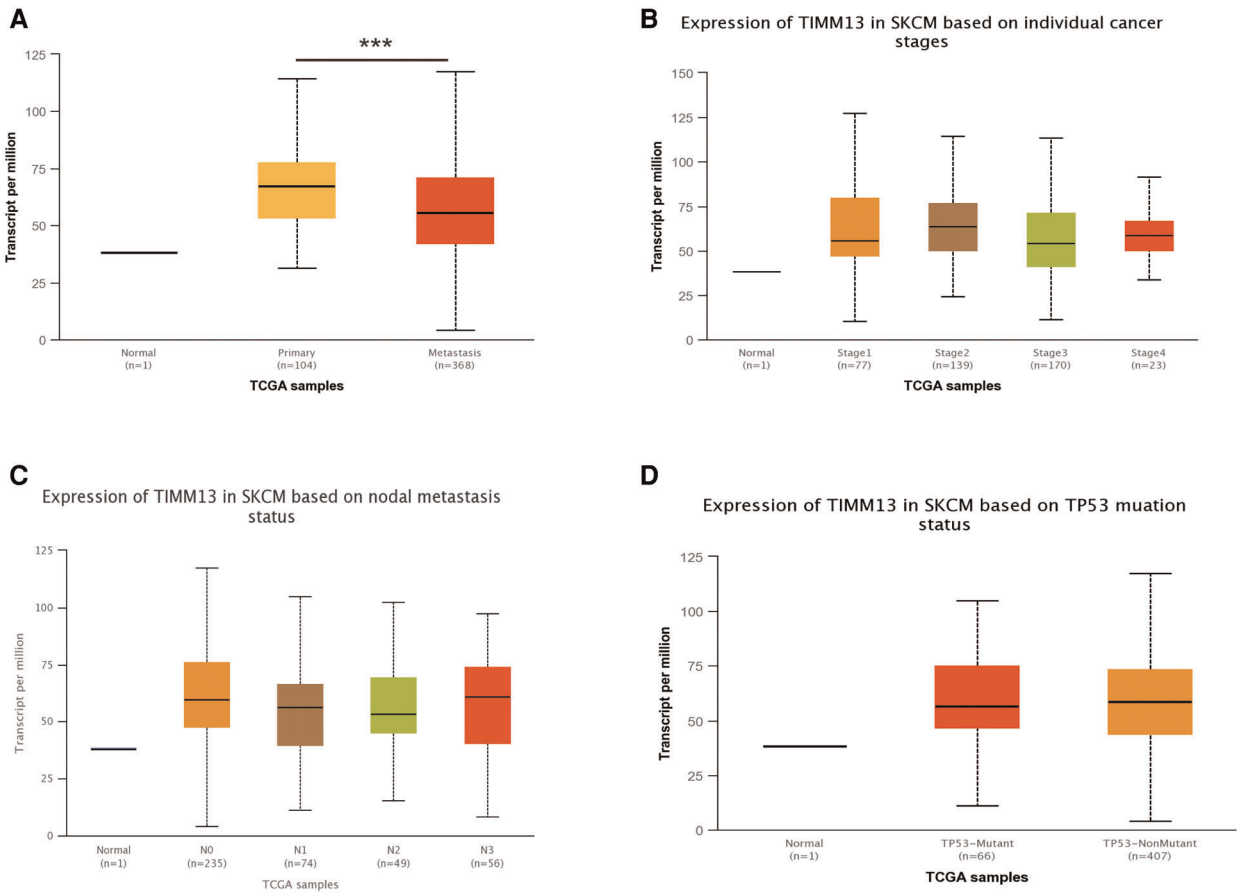


FIGURE 2
Correlation between TIMM13 mRNA expression level and clinicopathological parameters of SKCM through the UALCAN database. (A) Sample type (normal/primary tumor). (B) Cancer stage (stage 1, 2, 3, and 4). (C) Lymph node stage (N0 1, 2, and 3). (D) TP53 mutation subgroup. N, normal; P, primary tumor; S1, stage 1; S2, stage 2; S3, stage 3; S4, stage 4.

TIMM13 in tumorigenesis, we used univariate and multivariate Cox regression analysis to observe the correlation between TIMM13 expression and clinicopathological features of SKCM. The up-regulation of TIMM13 expression was related to a poorer OS (HR = 2. 199, $p < 0.001$) (Table 1), DSS (Table 2) (HR = 2. 442, $p < 0.001$) and PFI (Table 3) (HR = 1. 439, $p = 0.027$) in SKCM patients. The increase of TIMM13 mRNA expression was related to a poorer OS in T4 stage (HR = 4. 500, $p = 0.010$), N2 stage (HR = 3. 617, $p = 0.048$), N3 stage (HR = 11. 432, $p < 0.001$), melanoma ulceration (HR = 1. 650, $p = 0.030$), and Melanoma Clark V level (HR = 4. 519, $p = 0.043$) SKCM patients. Furthermore, we found that DSS and PFI in T4 stage (DSS HR = 3.415, $p = 0.039$), N1 stage (DSS HR = 4.736, $p = 0.044$), N2 stage (DSS HR = 5.521, $p = 0.027$), N3 stage (DSS HR = 17.411, $p < 0.001$; PFI HR = 5.829, $p < 0.001$), Melanoma Clark V level (DSS HR = 5.338, $p = 0.028$; PFI HR = 3.211, $p = 0.021$) were associated with TIMM13 expression. It was a hint that the prognostic effect of TIMM13 in SKCM might be influenced by their clinical characteristics.

## Increased TIMM13 mRNA expression associated with poor overall survival in SKCM patients

It was suggested that the expression level of TIMM13 mRNA in SKCM patients is higher than that in the normal control group. Therefore, whether the expression of TIMM13 was related to tumor prognosis needs further study. In this study, the expression of TIMM13 and its relationship with prognosis were detected by the Kaplan–Meier survival curve to determine whether TIMM13 can be used as a biomarker for prognosis of SKCM. It was worth noting that the high expression of TIMM13 was associated with a poorer outcome of SKCM. High expression of TIMM13 was associated with poorer OS, and PFI (Figures 3A,B).

TABLE 1 Univariate and multivariate Cox regression analysis of OS.

| Characteristics | Total (*N*) | Univariate analysis | | Multivariate analysis | |
|---|---|---|---|---|---|
| | | Hazard ratio (95% CI) | *p*-value | Hazard ratio (95% CI) | *p*-value |
| Gender | 456 | | | | |
| Female | 172 | Reference | | | |
| Male | 284 | 1.172 (0.879-1.563) | 0.281 | | |
| Pathologic stage | 410 | | | | |
| Stage I | 77 | Reference | | | |
| Stage II | 140 | 1.586 (1.054-2.385) | **0.027** | 0.279 (0.111-0.703) | **0.007** |
| Stage III | 170 | 1.983 (1.344-2.927) | **<0.001** | 0.166 (0.040-0.695) | **0.014** |
| Stage IV | 23 | 3.517 (1.781-6.944) | **<0.001** | 0.221 (0.047-1.045) | 0.057 |
| T stage | 361 | | | | |
| T1 | 41 | Reference | | | |
| T2 | 77 | 1.495 (0.811-2.756) | 0.197 | 1.529 (0.620-3.768) | 0.356 |
| T3 | 90 | 2.097 (1.158-3.798) | **0.015** | 2.924 (0.964-8.871) | 0.058 |
| T4 | 153 | 3.711 (2.070-6.653) | **<0.001** | 4.500 (1.435-14.111) | **0.010** |
| N stage | 402 | | | | |
| N0 | 224 | Reference | | | |
| N1 | 73 | 1.497 (1.014-2.210) | **0.043** | 3.489 (0.988-12.327) | 0.052 |
| N2 | 49 | 1.534 (0.972-2.419) | 0.066 | 3.617 (1.012-12.930) | **0.048** |
| N3 | 56 | 2.731 (1.769-4.215) | **<0.001** | 11.432 (3.201-40.822) | **<0.001** |
| M stage | 430 | | | | |
| M0 | 406 | Reference | | | |
| M1 | 24 | 1.897 (1.029-3.496) | **0.040** | | |
| Tumor tissue site | 392 | | | | |
| Extremities | 190 | Reference | | | |
| Trunk | 166 | 0.940 (0.693-1.275) | 0.691 | | |
| Head and Neck | 36 | 1.269 (0.755-2.131) | 0.368 | | |
| Melanoma ulceration | 313 | | | | |
| No | 146 | Reference | | | |
| Yes | 167 | 2.085 (1.495-2.907) | **<0.001** | 1.650 (1.050-2.592) | **0.030** |
| Melanoma clark level | 315 | | | | |
| I and II | 19 | Reference | | | |
| III | 76 | 1.679 (0.704-4.002) | 0.243 | 2.340 (0.606-9.039) | 0.218 |
| IV | 167 | 2.945 (1.286-6.747) | **0.011** | 2.704 (0.701-10.435) | 0.149 |
| V | 53 | 5.449 (2.253-13.177) | **<0.001** | 4.519 (1.046-19.532) | **0.043** |
| Age | 456 | | | | |
| ≤60 | 246 | Reference | | | |
| >60 | 210 | 1.656 (1.251-2.192) | **<0.001** | 1.258 (0.847-1.870) | 0.256 |
| TIMM13 | 456 | | | | |
| Low | 230 | Reference | | | |
| High | 226 | 1.711 (1.307-2.241) | **<0.001** | 2.199 (1.498-3.228) | **<0.001** |

Bold values represent significantly different.

## Correlation between immune infiltration and TIMM13 expression in SKCM

Immune infiltration plays an important role in tumor progression. We observed whether the expression of TIMM13 affected the number of tumors infiltrating lymphocytes (TILs) in SKCM by using the Xiantao tool. As a result, the expression of TIMM13 was negatively correlated with StromalScore, ImmuneScore, and ESTIMATEScore of SKCM (rho = −0.307, $p < 0.001$; rho = −0.398, $p < 0.001$; rho = −0.393, $p < 0.001$,

TABLE 2 Univariate and multivariate Cox regression analysis of DSS.

| Characteristics | Total (*N*) | Univariate analysis | | Multivariate analysis | |
|---|---|---|---|---|---|
| | | Hazard ratio (95% CI) | *p*-value | Hazard ratio (95% CI) | *p*-value |
| Gender | 450 | | | | |
| Female | 172 | Reference | | | |
| Male | 278 | 1.161 (0.855-1.575) | 0.340 | | |
| Pathologic stage | 405 | | | | |
| Stage I | 76 | Reference | | | |
| Stage II | 139 | 1.496 (0.977-2.291) | 0.064 | 0.299 (0.115-0.773) | **0.013** |
| Stage III | 167 | 1.777 (1.181-2.672) | **0.006** | 0.125 (0.024-0.660) | **0.014** |
| Stage IV | 23 | 3.800 (1.914-7.547) | **<0.001** | 0.178 (0.031-1.019) | 0.052 |
| T stage | 356 | | | | |
| T1 | 41 | Reference | | | |
| T2 | 76 | 1.435 (0.775-2.657) | 0.250 | 1.390 (0.557-3.470) | 0.481 |
| T3 | 88 | 1.934 (1.060-3.529) | **0.032** | 2.562 (0.835-7.863) | 0.100 |
| T4 | 151 | 3.110 (1.715-5.637) | **<0.001** | 3.415 (1.066-10.944) | **0.039** |
| N stage | 396 | | | | |
| N0 | 221 | Reference | | | |
| N1 | 71 | 1.279 (0.827-1.976) | 0.269 | 4.736 (1.041-21.537) | **0.044** |
| N2 | 49 | 1.473 (0.905-2.398) | 0.120 | 5.521 (1.212-25.162) | **0.027** |
| N3 | 55 | 2.920 (1.867-4.565) | **<0.001** | 17.411 (3.852-78.698) | **<0.001** |
| M stage | 424 | | | | |
| M0 | 400 | Reference | | | |
| M1 | 24 | 2.200 (1.190-4.069) | **0.012** | | |
| Tumor tissue site | 386 | | | | |
| Extremities | 188 | Reference | | | |
| Trunk | 164 | 0.920 (0.664-1.274) | 0.615 | | |
| Head and neck | 34 | 1.271 (0.720-2.244) | 0.407 | | |
| Melanoma ulceration | 309 | | | | |
| No | 145 | Reference | | | |
| Yes | 164 | 1.948 (1.372-2.767) | **<0.001** | 1.593 (0.993-2.555) | 0.053 |
| Melanoma clark level | 310 | | | | |
| I and II | 19 | Reference | | | |
| III | 76 | 1.898 (0.739-4.877) | 0.183 | 2.270 (0.580-8.891) | 0.239 |
| IV | 163 | 3.235 (1.307-8.005) | **0.011** | 2.814 (0.723-10.951) | 0.136 |
| V | 52 | 5.779 (2.206-15.141) | **<0.001** | 5.338 (1.204-23.670) | **0.028** |
| Age | 450 | | | | |
| ≤60 | 244 | Reference | | | |
| >60 | 206 | 1.699 (1.258-2.294) | **<0.001** | 1.246 (0.819-1.895) | 0.304 |
| TIMM13 | 450 | | | | |
| Low | 227 | Reference | | | |
| High | 223 | 1.798 (1.348-2.399) | **<0.001** | 2.442 (1.621-3.677) | **<0.001** |

Bold values represent significantly different.

respectively) (Figure 4A). Our results also revealed a significant correlation between TIMM13 and TILs abundance (Figure 4B). The high expression of TIMM13 was negatively correlated with the infiltration of Th1 cells (rho = −0.416) (Figure 4C) and T lymphocytes (Rho = −0.415) (Figure 4D), aDC cells (rho = −0.338) (Figure 4E), TFH cells (rho = −0.366) (Figure 4F), B lymphocytes (Rho = −0.359) (Figure 4G) and T helper T cells (rho = −0.354) (Figure 4H). All the *p*-values above were <0.001.

TABLE 3 Univariate and multivariate Cox regression analysis of PFI.

| Characteristics | Total (*N*) | Univariate analysis | | Multivariate analysis | |
|---|---|---|---|---|---|
| | | Hazard ratio (95% CI) | *p*-value | Hazard ratio (95% CI) | *p*-value |
| Gender | 457 | | | | |
| Female | 172 | Reference | | | |
| Male | 285 | 1.037 (0.821-1.309) | 0.763 | | |
| Pathologic stage | 411 | | | | |
| Stage I | 77 | Reference | | | |
| Stage II | 140 | 1.381 (0.980-1.944) | 0.065 | 0.411 (0.193-0.877) | **0.021** |
| Stage III | 171 | 1.968 (1.426-2.715) | **<0.001** | 0.363 (0.112-1.179) | 0.092 |
| Stage IV | 23 | 3.438 (1.989-5.942) | **<0.001** | 0.379 (0.115-1.254) | 0.112 |
| T stage | 362 | | | | |
| T1 | 41 | Reference | | | |
| T2 | 77 | 0.995 (0.639-1.548) | 0.982 | 1.196 (0.598-2.390) | 0.613 |
| T3 | 91 | 1.325 (0.859-2.044) | 0.203 | 1.817 (0.770-4.287) | 0.173 |
| T4 | 153 | 2.129 (1.387-3.268) | **<0.001** | 1.975 (0.812-4.802) | 0.133 |
| N stage | 403 | | | | |
| N0 | 224 | Reference | | | |
| N1 | 74 | 1.634 (1.183-2.258) | **0.003** | 2.496 (0.888-7.014) | 0.083 |
| N2 | 49 | 1.502 (1.023-2.205) | **0.038** | 2.579 (0.904-7.353) | 0.076 |
| N3 | 56 | 2.965 (2.096-4.195) | **<0.001** | 5.829 (2.132-15.933) | **<0.001** |
| M stage | 431 | | | | |
| M0 | 407 | Reference | | | |
| M1 | 24 | 2.026 (1.255-3.269) | **0.004** | | |
| Tumor tissue site | 393 | | | | |
| Extremities | 190 | Reference | | | |
| Trunk | 167 | 1.075 (0.834-1.386) | 0.577 | | |
| Head and neck | 36 | 1.364 (0.866-2.150) | 0.180 | | |
| Melanoma ulceration | 313 | | | | |
| No | 146 | Reference | | | |
| Yes | 167 | 1.626 (1.228-2.152) | **<0.001** | 1.443 (0.982-2.121) | 0.062 |
| Melanoma clark level | 315 | | | | |
| I and II | 19 | Reference | | | |
| III | 76 | 1.333 (0.709-2.505) | 0.372 | 1.170 (0.496-2.758) | 0.720 |
| IV | 167 | 1.908 (1.048-3.473) | **0.034** | 1.223 (0.513-2.915) | 0.650 |
| V | 53 | 4.821 (2.486-9.349) | **<0.001** | 3.211 (1.193-8.645) | **0.021** |
| Age | 457 | | | | |
| ≤60 | 247 | Reference | | | |
| >60 | 210 | 1.576 (1.240-2.002) | **<0.001** | 1.395 (0.988-1.970) | 0.059 |
| TIMM13 | 457 | | | | |
| Low | 230 | Reference | | | |
| High | 227 | 1.303 (1.041-1.631) | **0.021** | 1.439 (1.041-1.990) | **0.027** |

Bold values represent significantly different.

Similar results were obtained by detecting CD8 + T lymphocyte infiltration using the TIMER database, suggesting that TIMM13 could play a key role in inhibiting SKCM immune infiltration and was related to tumor microenvironment.

The correlation between TIMM13 and different TILs' biomarkers in SKCM was studied by using the Xiantao tool. We found that TIMM13 was associated with most TILs' markers in SKCM. Several functional T lymphocytes,

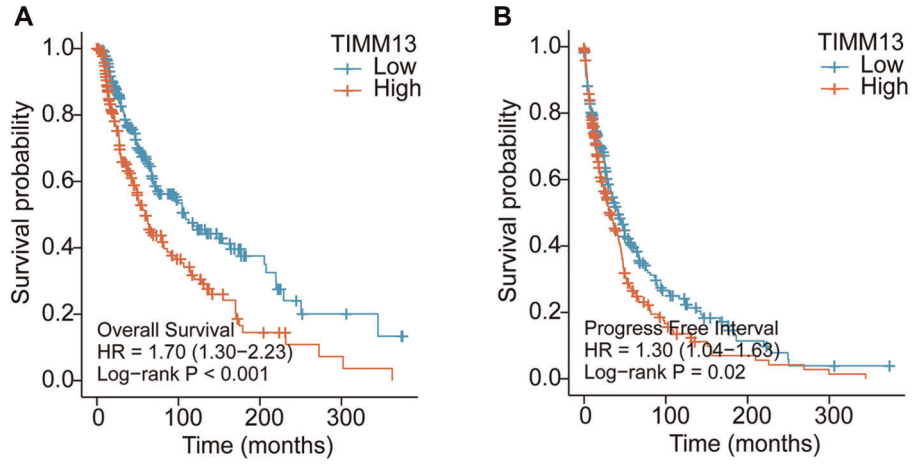


FIGURE 3
Kaplan–Meier survival curves comparing the high and low expression of TIMM13 in SKCM by using Xiantao tool. Survival curves of OS (A), FPI (B) in the SKCM patients. OS, overall survival; PFI, progression free interval.

including Th1, Tregs and exhausted T lymphocytes, were also investigated. In particular, TIMM13 is significantly associated with most sets of TILs immunomarkers in SKCM (Table 4).

Furthermore, TIMM13 was significantly associated with most of monocytes, TAM, M2 macrophages and T cell exhaustion markers in SKCM (Table 4). As shown in the table, PD-1, PDL1, CTLA4, LAG3, TIM-3, GZMB of T-cell exhaustion, and CCL-2, CD68, IL10 of TAMs, IRF5 of M1 phenotype and CD163, VSIG4 and MS4A4A of M2 phenotype were almost negatively correlated with TIMM13 in SKCM ($p < 0.0001$). It was suggested that TIMM13 could regulate exhaustion, and macrophage polarization in SKCM.

## The expression of TIMM13 is related to immunoinhibitors and immunostimulators in SKCM

Immunoinhibitors and immunostimulators are substances that influence the function of the immune system. This study showed that TIMM13 was significantly associated with immunoinhibitors ($p < 0.001$), such as BTLA (rho = −0.389), CD274 (rho = −0.476), CD96 (rho = −0.404), IL10 (rho = −0.328), PDCD1LG2 (rho = −0.458), and TIGIT (rho = −0.342) (Figure 5A). The expression of TIMM13 was also significantly associated with immunostimulators ($p < 0.001$), including CD28 (rho = −0.389), CD80 (rho = −0.44), IL2RA (rho = −0.434), TNFRSF9 (rho = −0.417), TNFSF13B (rho = −0.402), TNFSF4 (rho = −0.396) (Figure 5B). These results proposed that TIMM13 was intimately engaged in the regulation of the immune interaction and might modulate tumor immune escape.

## Correlation between the TIMM13 expression and chemokines/receptors in SKCM

Chemokines played a great function in controlling the infiltration degree of immune cell. This research implicated a significant association between TIMM13 expression and chemokines. For instance, the expression of TIMM13 was significantly associated with CCL8 (rho = −0.293), CXCL9 (rho = −0.359), CXCL10 (rho = −0.347), CXCL10 (rho = −0.347), CXCL11 (rho = −0.375), CXCL12 (rho = −0.33), and CXCL13 (rho = −0.372) (Figure 6A). All the values of $p$ were < 0.001. At the same time, we found that the expression of TIMM13 was also significantly related with chemokine receptors ($p < 0.001$), including CCR1 (rho = −0.375), CCR2 (rho = −0.429), CCR4 (rho = −0.441), CCR5 (rho = −0.362), CCR8 (rho = −0.432), XCR1 (rho = −0.385) (Figure 6B). These results further suggested that TIMM13 may be an immunoregulatory factor in SKCM.

## Construction and validation of a nomogram

A nomogram was built for the training set based on the gender, pathologic stage, TNM stage, age, and TIMM13 expression (Figure 7A). The C-index of the nomogram was 0.715(0.693–0.736). The calibration plots for the 1-, 3-, and 5-year survivals indicated good agreement between the actual observations and the predictions (Figure 7B). These results indicated that the prediction performance of the nomogram was good.

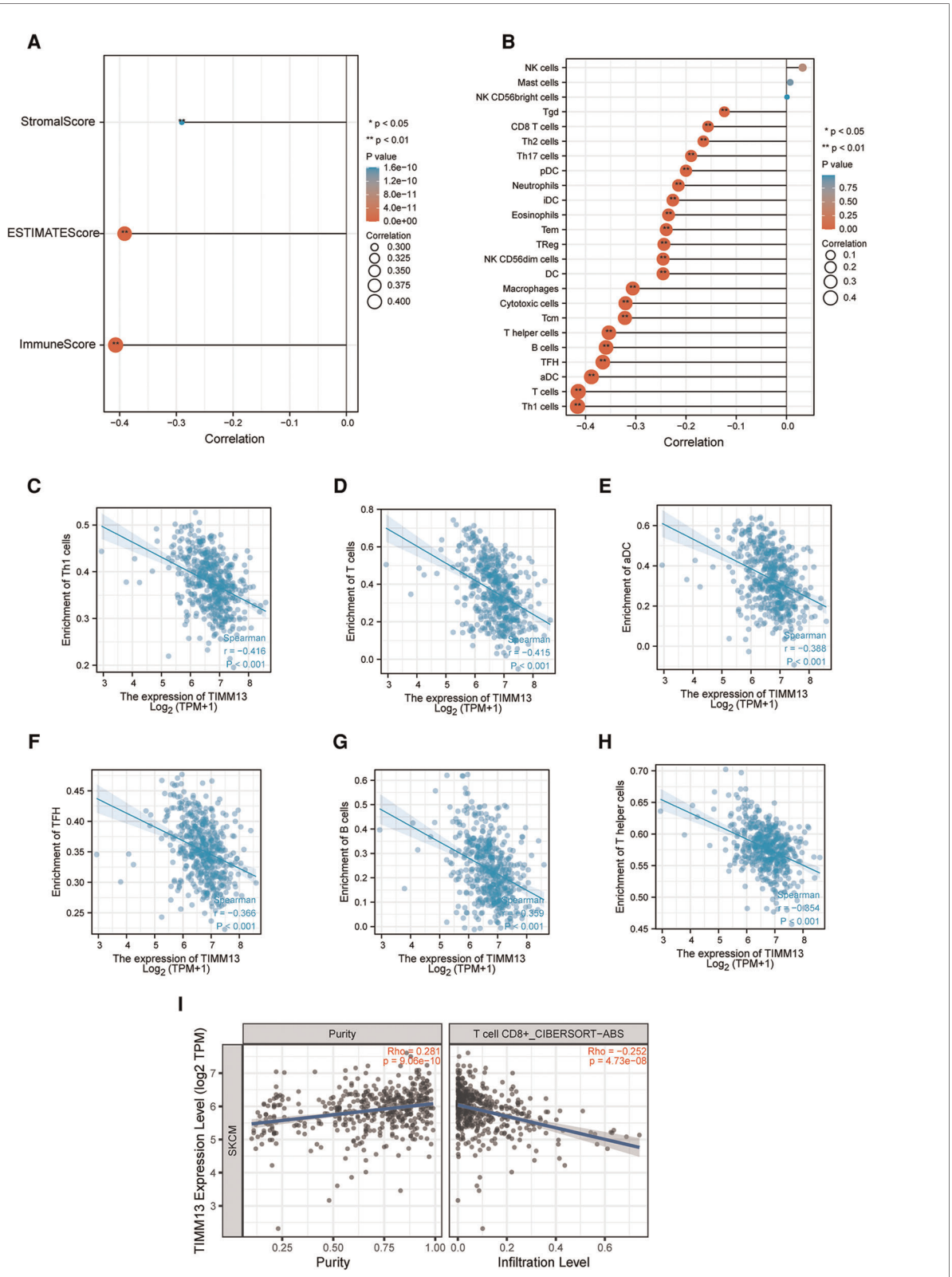


FIGURE 4
Correlation of TIMM13 expression with immune infiltration in SKCM. (A) Correlation of TIMM13 expression with infiltration levels of StomalScore, ESTIMATEScore, and ImmuneScore in SKCM available at Xiantao tool. (B) Correlation of TIMM13 expression with infiltration levels of immune cells in SKCM available at Xiantao tool. Correlation of ITGAL expression with infiltration levels of Th1 cells (C), T cells (D), aDC (E), TFH (F), B cells (G), and T helper in SKCM (H). (I) Correlation between the expression of TIMM13 and the abundance of TILs in SKCM validation at TIMER database.

TABLE 4 Correlation analysis between ITGAL and related genes and markers of immune cells in Xiantao tool.

| Description | Gene markers | Cor | *p* |
|---|---|---|---|
| $CD8^+$ T cell | CD8A | −0.373 | <0.001 |
| | CD8B | −0.353 | <0.001 |
| T cell (general) | CD3D | −0.358 | <0.001 |
| | CD3E | −0.353 | <0.001 |
| | CD2 | −0.370 | <0.001 |
| B cell | CD19 | −0.315 | <0.001 |
| | CD79A | −0.323 | <0.001 |
| Monocyte | CD86 | −0.368 | <0.001 |
| | CD115 (CSF1R) | −0.287 | <0.001 |
| TAM | CCL2 | −0.200 | <0.001 |
| | CD68 | −0.165 | <0.001 |
| | IL10 | −0.240 | <0.001 |
| M1 Macrophage | IRF5 | −0.304 | <0.001 |
| M2 Macrophage | CD163 | −0.285 | <0.001 |
| | VSIG4 | −0.248 | <0.001 |
| | MS4A4A | −0.322 | <0.001 |
| Neutrophils | CD11b (ITGAM) | −0.286 | <0.001 |
| | CCR7 | −0.303 | <0.001 |
| Natural killer cell | KIR2DL1 | −0.131 | 0.004 |
| | KIR3DL1 | −0.154 | <0.001 |
| | KIR3DL2 | −0.271 | <0.001 |
| | KIR2DS4 | −0.133 | 0.004 |
| Dendritic cell | HLA-DPB1 | −0.301 | <0.001 |
| | HLA-DQB1 | −0.287 | <0.001 |
| | HLA-DRA | −0.345 | <0.001 |
| | HLA-DPA1 | −0.330 | <0.001 |
| | BDCA-1(CD1C) | −0.255 | <0.001 |
| | BDCA-4(NRP1) | −0.156 | <0.001 |
| | CD11c (ITGAX) | −0.2271 | <0.001 |
| Th1 | T -bet (TBX21) | −0.337 | <0.001 |
| | STAT4 | −0.372 | <0.001 |
| | STAT1 | −0.308 | <0.001 |
| | IFN-$\gamma$ (IFNG) | −0.365 | <0.001 |
| | TNF-$\alpha$ (TNF) | −0.262 | <0.001 |
| Th2 | GATA3 | −0.280 | <0.001 |
| | STAT5A | −0.091 | 0.050 |
| Tfh | BCL6 | −0.267 | <0.001 |
| | IL21 | −0.384 | <0.001 |
| Th17 | STAT3 | −0.201 | <0.001 |
| Treg | FOXP3 | −0.249 | <0.001 |
| | CCR8 | −0.371 | <0.001 |
| | STAT5B | −0.217 | <0.001 |
| T cell exhaustion | PD-1 (PDCD1) | −0.288 | <0.001 |
| | PDL1(PDCD1LG2) | −0.371 | <0.001 |
| | CTLA4 | −0.306 | <0.001 |
| | LAG3 | −0.260 | <0.001 |
| | TIM-3 (HAVCR2) | −0.345 | <0.001 |
| | GZMB | −0.270 | <0.001 |

## Histologic analysis

We next explored the protein expression levels of TIMM13 between melanoma and normal skin tissues. The IHC staining results showed that TIMM13 showed higher expression levels in melanoma tissues ($n = 25$) than in normal skin tissues ($n = 15$) (**Figures 8A,B**). The patients' characteristics were shown in **Table 5**.

# Discussion

In this study, the expression level of TIMM13 in SKCM and its clinical significance were comprehensively studied by bioinformatics. Our results showed that poor prognosis was in accordance with high expression of TIMM13 in SKCM. The expression of TIMM13 is closely related to the infiltration of various immune cells, immunomodulators, chemokines and receptors in SKCM. Therefore, our study provided new insights into the key functions of TIMM13, which might be a prognostic biomarker related to immune infiltration of SKCM.

TIMM13 partners with TIMM8a in the mitochondrial intermembrane space to form a 70 kDa complex and facilitates the import of the inner membrane substrate TIMM23 (9). Kim SH et al. reported that TIMM13 functions as a target gene of miRNA-1273g-3p to contribute to Alzheimer's Disease pathogenesis by regulating expression of mitochondrial genes (22). Roesch K et al. reported that human deafness dystonia syndrome was caused by a defect in assembly of the DDP1/TIMM8a-TIMM13 complex. Timm13 is related to Mohr-Tranebjaerg Syndrome and Visual Cortex Disease. Among its related pathways are Peroxisomal lipid metabolism. Several studies have shown that TIMM13 was differently expressed in metastatic susceptibility (13), hepatocellular carcinoma (14), breast cancer (15) et al. These researchers suggested that TIMM13 might have a significant influence on cancer, and may be a novel target in treating a variety of malignancies. However, the possible function of TIMM13 in regulating tumor immunity and its clinical significance in SKCM are still unknown.

Therefore, we computed the TIMM13 expression for SKCM using the Xiantao tool and the UALCAN database. We found that TIMM13 was abnormally expressed in the tissues of various malignant tumors. TIMM13 in SKCM was significantly higher than that in adjacent tissues. Using the HPA database, we also found that TIMM13mRNA and protein levels in most SKCM samples were higher than those in matched paracancer samples. It was suggested that the expression level of TIMM13 could be used as a diagnostic indicator of SKCM with the AUC is 0.757. In addition, in order to determine whether TIMM13 could be used as a biomarker for prognosis, we analyzed the correlation between TIMM13 expression and OS, and FPI in SKCM patients with the Xiantao tool. Furthermore, to confirm whether TIMM13 can be used as a prognostic biomarker, we used the xiantao tool to analyze the correlation between the TIMM13 expression and OS, DSS, and FPI in SKCM patients. Notably, analysis of this database indicated that the higher TIMM13 expression correlated with HR for worse OS DSS, and poorer

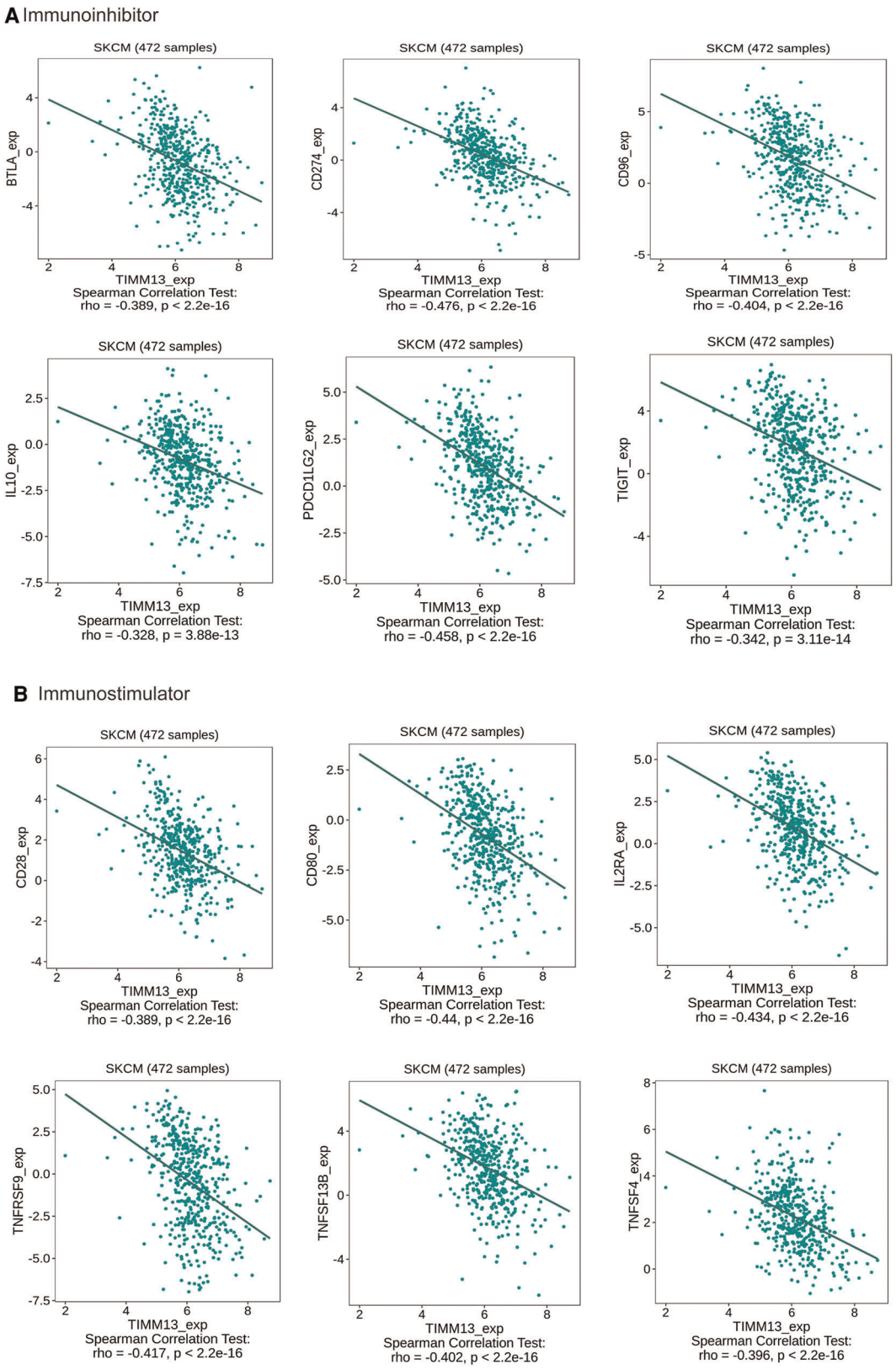


FIGURE 5
The expression of TIMM13 is associated with immunomodulators in SKCM. (A) Correlation between TIMM13 expression and immunoinhibitors in SKCM available at TISIDB database. (B) Correlation between TIMM13 expression and immunostimulators in SKCM available at TISIDB database. Color images are available online.

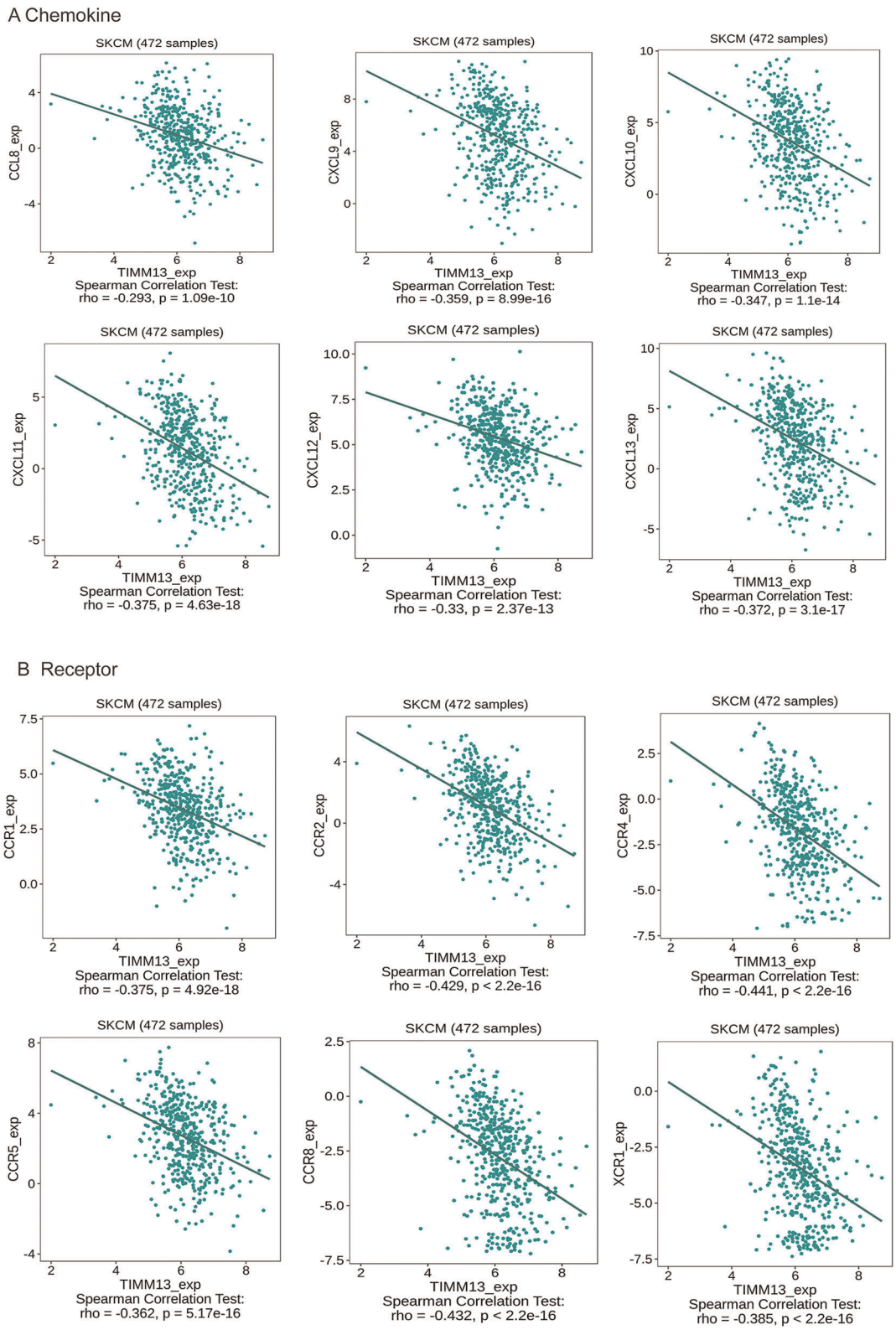


FIGURE 6
Correlation between the expression of TIMM13 and chemokines in SKCM. (**A**) Correlation between TIMM13 expression and chemokines in SKCM available at TISIDB database. (**B**) Correlation between TIMM13 expression and chemokine receptors in SKCM available at TISIDB database. Color images are available online.

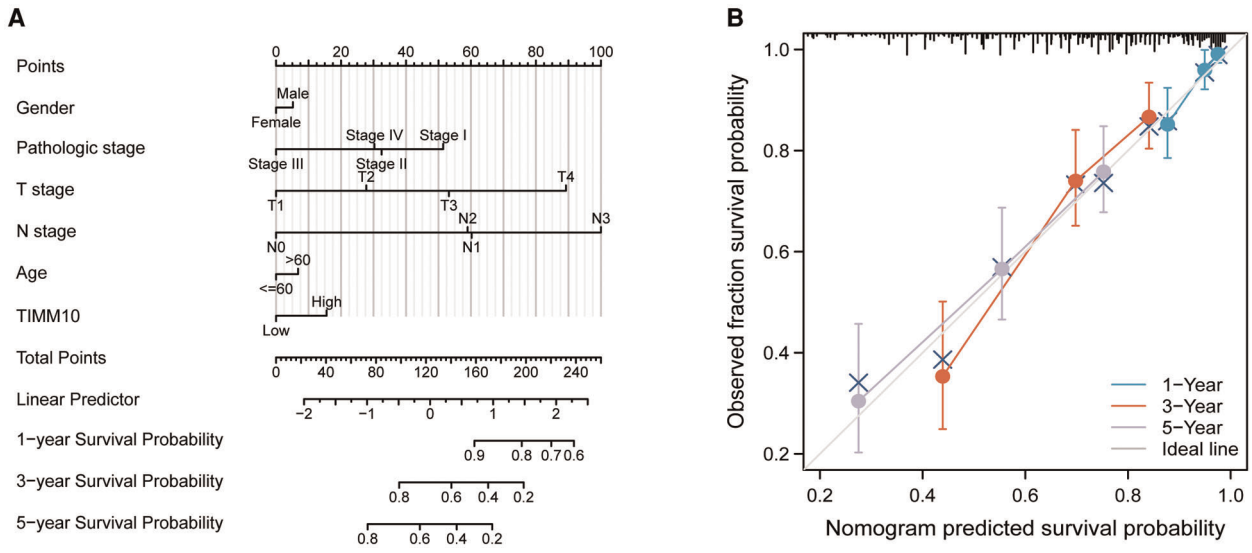


FIGURE 7
Nomogram model construction. (A) Nomogram. (B) Calibration plot.

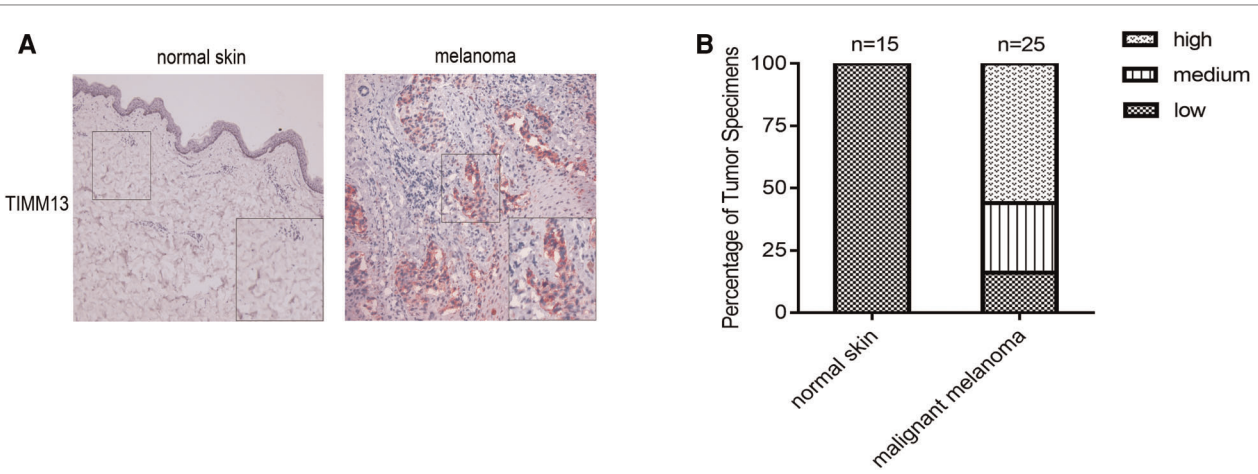


FIGURE 8
Gene expression of TIMM13 in melanoma tissue and normal skin specimens. Using IHC staining, TIMM13 was expressed at higher levels in the melanoma tissue ($n = 25$) when compared to normal skin ($n = 15$). (A) IHC staining. (B) Quantification of the TIMM13 levels. IHC: Immunohistochemistry. IHC stain, AEC, original magnification: 100× (inset, IHC stain, AEC, original magnification: 400×).

PPS of SKCM. In addition, upregulated TIMM13 expression had a significant correlation with a worse prognosis of SKCM in T4 stage, N1 stage, N2 stage, N3 stage. Taken together, these observations supported our hypothesis that TIMM13 was a prognostic biomarker in SKCM.

Additionally, this study found that TIMM13 was correlated with the degree of immune infiltration of SKCM. In the cancer microenvironment, immune cell infiltration had been proved to play a key role in the development and progression of cancer (23, 24). TIMM13 is a chaperone protein, which plays a key role in transporting cytoplasmic proteins into the mitochondrial inner membrane. At present, it is not clear whether the expression of TIMM13 is related to the immune infiltration of SKCM. Therefore, we systematically discussed the relationship between TIMM13 expression and immune infiltration degree of SKCM. Based on our results, it was found for the first time that TIMM13 modulates immune infiltration through SKCM.

The expression of TIMM13 was closely related to the expression of TILs in CD8 + T cells, CD4 + T cells, Treg cells, and TAM cells. Meanwhile, the increase of TIMM13 expression was related to immunoregulators, chemokines and

TABLE 5 Clinical characteristics of melanoma patients.

| ID | Sex | Age,y | Location | Primary/metastasis |
|---|---|---|---|---|
| Case1 | M | 54 | Right plantar | Primary |
| Case2 | F | 35 | Left plantar | Primary |
| Case3 | M | 82 | Left plantar | Primary |
| Case4 | F | 39 | Right ankle | Primary |
| Case5 | M | 62 | Left plantar | Metastasis |
| Case6 | M | 44 | Left plantar | Metastasis |
| Case7 | M | 55 | Right plantar | Metastasis |
| Case8 | F | 57 | Right plantar | Metastasis |
| Case9 | F | 48 | Face | Primary |
| Case10 | M | 73 | Left plantar | Primary |
| Case11 | M | 64 | Left plantar | Metastasis |
| Case12 | M | 65 | Right plantar | Primary |
| Case13 | M | 66 | Right plantar | Metastasis |
| Case14 | F | 58 | Right plantar | Primary |
| Case15 | F | 64 | Right plantar | Primary |
| Case16 | F | 74 | Right arm | Primary |
| Case17 | M | 66 | Right plantar | Metastasis |
| Case18 | M | 57 | Right plantar | Primary |
| Case19 | M | 52 | Back | Primary |
| Case20 | M | 63 | Left plantar | Metastasis |
| Case21 | F | 74 | Right plantar | Metastasis |
| Case22 | F | 71 | Left ankle | Primary |
| Case23 | M | 63 | Left plantar | Primary |
| Case24 | M | 41 | Left arm | Metastasis |
| Case25 | M | 52 | Head | Metastasis |

F, female; M, male.

receptors. Additionally, the study proposed the relationship between TIMM13 expression and TILs' marker genes of SKCM. The expression of TIMM13 was associated with M2 macrophage markers CD163, VSIG4, and MS4A4A, while M1 macrophage markers NOS2 and IRF5 were slightly associated with the expression of TIMM13. Macrophages played an important role in tumor proliferation (25), angiogenesis (26), invasion (27), metastasis (27) and tumor immunity (28). These results demonstrated that TIMM13 had the potential function of regulating TAMs polarization. The up-regulation of TIMM13 was closely related to Tregs markers (FOXP3, CCR8) and T lymphocyte depletion markers (PD1, CTLA4, LAG3). Blocking immune checkpoints is the main strategy of immunotherapy (29). The most important thing is to enhance the response of tumor cells to immune checkpoint inhibitors and cytokines (30, 31). According to TISIDB, TIMER and Xiantao tool, our results showed that the up-regulation of TIMM13 expression was not only related to PD1 and CTLA4, but also significantly related to cell response to chemokines. These results suggested that targeting TIMM13 may be a strategy to improve the efficacy of immunotherapy. It was also suggested that TIMM13 played an important role in the recruitment and regulation of TILs in SKCM, and its molecular mechanism and role in the regulation of tumor microenvironment deserve further study.

However, there are also some limitations in our research. One limitation is that most of the data is based on online platforms, which are constantly updated and extended; So, the research results may be influenced. Secondly, our study did not include any information about complications and therapy options. Thirdly, *in vivo* and *in vitro* experiments are not to verify the role of TIMM13 in SKCM. However, in future research, we are committed to paying more attention to the background information of patients and conducting experiments to further verify the expected results.

## Conclusions

The increased expression of TIMM13 was closely related to poor prognosis of SKCM and increased immune infiltration of CD8 + T lymphocytes, C4 + T lymphocytes, and myeloid dendritic cells. The expression of TIMM13 might be involved in the regulation of M2, Treg, and T -cell exhaustion. So, this study suggested that TIMM13 might have a new potential function in the regulation of immune cell infiltration in SKCM patients.

## Data availability statement

The original contributions presented in the study are included in the article/Suplementary Material, further inquiries can be directed to the corresponding author/s.

## Author contributions

RHY, XBP, and JHL designed the study. STZ and YYH conducted most of the experiments, data analysis, and wrote the manuscript. RHY, XBP, and JHL had full access to all of the data in the manuscript and takes responsibility for the integrity of the data and the accuracy of the data analysis. All authors contributed to the article and approved the submitted version.

## Funding

This study was supported by the National Natural Science Foundation of China (82002913), Guangdong Basic and Applied Basic Research Foundation (2021A1515011453, 2022A1515012160, 2021B1515120036, and 2022A1515012245), the Medical Scientific Research Foundation of Guangdong Province (A2022293), Foshan 14th - fifth high-level key

specialty construction project, Yunnan Fundamental Research Projects (grant NO. 202001AT070145, 202101AT070288).

## Conflict of interest

The authors declare that the research was conducted in the absence of any commercial or financial relationships that could be construed as a potential conflict of interest.

## Publisher's note

All claims expressed in this article are solely those of the authors and do not necessarily represent those of their affiliated organizations, or those of the publisher, the editors and the reviewers. Any product that may be evaluated in this article, or claim that may be made by its manufacturer, is not guaranteed or endorsed by the publisher.

## References

1. Elder DE, Bastian BC, Cree IA, Massi D, Scolyer RA. The 2018 world health organization classification of cutaneous, mucosal, and uveal melanoma: detailed analysis of 9 distinct subtypes defined by their evolutionary pathway. *Arch Pathol Lab Med*. (2020) 144(4):500–22. doi: 10.5858/arpa.2019-0561-RA

2. Timar J, Ladanyi A. Molecular pathology of skin melanoma: epidemiology, differential diagnostics, prognosis and therapy prediction. *Int J Mol Sci*. (2022) 23(10):5384. doi: 10.3390/ijms23105384

3. Villani A, Potestio L, Fabbrocini G, Troncone G, Malapelle U, Scalvenzi M. The treatment of advanced melanoma: therapeutic update. *Int J Mol Sci*. (2022) 23(12):6388. doi: 10.3390/ijms23126388

4. Rebecca VW, Somasundaram R, Herlyn M. Pre-clinical modeling of cutaneous melanoma. *Nat Commun*. (2020) 11(1):2858. doi: 10.1038/s41467-020-15546-9

5. Schadendorf D, van Akkooi ACJ, Berking C, Griewank KG, Gutzmer R, Hauschild A, et al. Melanoma. *Lancet*. (2018) 392(10151):971–84. doi: 10.1016/S0140-6736(18)31559-9

6. Kim G, McKee AE, Ning YM, Hazarika M, Theoret M, Johnson JR, et al. FDA Approval summary: vemurafenib for treatment of unresectable or metastatic melanoma with the BRAFV600E mutation. *Clin Cancer Res*. (2014) 20 (19):4994–5000. doi: 10.1158/1078-0432.CCR-14-0776

7. Rajkumar S, Berry D, Heney KA, Strong C, Ramsay L, Lajoie M, et al. Melanomas with concurrent BRAF non-p.V600 and NF1 loss-of-function mutations are targetable by BRAF/MEK inhibitor combination therapy. *Cell Rep*. (2022) 39(1):110634. doi: 10.1016/j.celrep.2022.110634

8. Kuryk L, Bertinato L, Staniszewska M, Pancer K, Wieczorek M, Salmaso S, et al. From conventional therapies to immunotherapy: melanoma treatment in review. *Cancers (Basel)*. (2020) 12(10):3057. doi: 10.3390/cancers12103057

9. Roesch K, Hynds PJ, Varga R, Tranebjaerg L, Koehler CM. The calcium-binding aspartate/glutamate carriers, citrin and aralar1, are new substrates for the DDP1/TIMM8a-TIMM13 complex. *Hum Mol Genet*. (2004) 13 (18):2101–11. doi: 10.1093/hmg/ddh217

10. Roesch K, Curran SP, Tranebjaerg L, Koehler CM. Human deafness dystonia syndrome is caused by a defect in assembly of the DDP1/TIMM8a-TIMM13 complex. *Hum Mol Genet*. (2002) 11(5):477–86. doi: 10.1093/hmg/11.5.477

11. Blesa JR, Solano A, Briones P, Prieto-Ruiz JA, Hernandez-Yago J, Coria F. Molecular genetics of a patient with Mohr-Tranebjaerg Syndrome due to a new mutation in the DDP1 gene. *Neuromolecular Med*. (2007) 9(4):285–91. doi: 10.1007/s12017-007-8000-3

12. Shi X, Huang Z, Zhou G, Li C. Dietary protein from different sources exerted a great impact on lipid metabolism and mitochondrial oxidative phosphorylation in rat liver. *Front Nutr*. (2021) 8:719144. doi: 10.3389/fnut.2021.719144

13. Hu Y, Wu G, Rusch M, Lukes L, Buetow KH, Zhang J, et al. Integrated cross-species transcriptional network analysis of metastatic susceptibility. *Proc Natl Acad Sci U S A*. (2012) 109(8):3184–9. doi: 10.1073/pnas.1117872109

14. Li Z, Song G, Guo D, Zhou Z, Qiu C, Xiao C, et al. Identification of GINS2 prognostic potential and involvement in immune cell infiltration in hepatocellular carcinoma. *J Cancer*. (2022) 13(2):610–22. doi: 10.7150/jca.53841

15. Sanchez-Alvarez R, De Francesco EM, Fiorillo M, Sotgia F, Lisanti MP. Mitochondrial fission factor (MFF) inhibits mitochondrial metabolism and reduces breast cancer stem cell (CSC) activity. *Front Oncol*. (2020) 10:1776. doi: 10.3389/fonc.2020.01776

16. Yan Y, Li J, Ye M, Li Z, Li S. Tropomyosin is potential markers for the diagnosis and prognosis of bladder cancer. *Dis Markers*. (2022) 2022:6936262. doi: 10.1155/2022/6936262

17. The Cancer Genome Atlas Network. Genomic classification of cutaneous melanoma. *Cell*. (2015) 161(7):1681–96. doi: 10.1016/j.cell.2015.05.044

18. Consortium GT. The genotype-tissue expression (GTEx) project. *Nat Genet*. (2013) 45(6):580–5. doi: 10.1038/ng.2653

19. Chandrashekar DS, Karthikeyan SK, Korla PK, Patel H, Shovon AR, Athar M, et al. UALCAN: an update to the integrated cancer data analysis platform. *Neoplasia*. (2022) 25:18–27. doi: 10.1016/j.neo.2022.01.001

20. Li T, Fu J, Zeng Z, Cohen D, Li J, Chen Q, et al. TIMER2.0 For analysis of tumor-infiltrating immune cells. *Nucleic Acids Res*. (2020) 48(W1):W509–14. doi: 10.1093/nar/gkaa407

21. Ru B, Wong CN, Tong Y, Zhong JY, Zhong SSW, Wu WC, et al. TISIDB: an integrated repository portal for tumor-immune system interactions. *Bioinformatics*. (2019) 35(20):4200–2. doi: 10.1093/bioinformatics/btz210

22. Kim SH, Choi KY, Park Y, McLean C, Park J, Lee JH, et al. Enhanced expression of microRNA-1273g-3p contributes to Alzheimer's disease pathogenesis by regulating the expression of mitochondrial genes. *Cells*. (2021) 10(10):2697. doi: 10.3390/cells10102697

23. Kim S, Kim A, Shin JY, Seo JS. The tumor immune microenvironmental analysis of 2,033 transcriptomes across 7 cancer types. *Sci Rep*. (2020) 10 (1):9536. doi: 10.1038/s41598-020-66449-0

24. Georgescu SR, Tampa M, Mitran CI, Mitran MI, Caruntu C, Caruntu A, et al. Tumour microenvironment in skin carcinogenesis. *Adv Exp Med Biol*. (2020) 1226:123–42. doi: 10.1007/978-3-030-36214-0_10

25. Yan K, Wang Y, Lu Y, Yan Z. Coexpressed genes that promote the infiltration of M2 macrophages in melanoma can evaluate the prognosis and immunotherapy outcome. *J Immunol Res*. (2021) 2021:6664791. doi: 10.1155/2021/6664791

26. Pratt HG, Steinberger KJ, Mihalik NE, Ott S, Whalley T, Szomolay B, et al. Macrophage and neutrophil interactions in the pancreatic tumor microenvironment drive the pathogenesis of pancreatic cancer. *Cancers (Basel)*. (2021) 14(1):194. doi: 10.3390/cancers14010194

27. Zhang H, Luo YB, Wu W, Zhang L, Wang Z, Dai Z, et al. The molecular feature of macrophages in tumor immune microenvironment of glioma patients. *Comput Struct Biotechnol J*. (2021) 19:4603–18. doi: 10.1016/j.csbj.2021.08.019

28. Yin W, Li Y, Song Y, Zhang J, Wu C, Chen Y, et al. CCRL2 Promotes antitumor T-cell immunity via amplifying TLR4-mediated immunostimulatory macrophage activation. *Proc Natl Acad Sci U S A*. (2021) 118(16):e2024171118. doi: 10.1073/pnas.2024171118

29. Pardoll DM. The blockade of immune checkpoints in cancer immunotherapy. *Nat Rev Cancer*. (2012) 12(4):252–64. doi: 10.1038/nrc3239

30. Jenkins L, Jungwirth U, Avgustinova A, Iravani M, Mills AP, Haider S, et al. Cancer-associated fibroblasts suppress CD8+ T cell infiltration and confer resistance to immune checkpoint blockade. *Cancer Res*. (2022). doi: 10.1158/0008-5472. [Epub ahead of print]

31. Asdourian MS, Shah N, Jacoby TV, Semenov YR, Otto T, Thompson LL, et al. Development of multiple cutaneous immune-related adverse events among cancer patients after immune checkpoint blockade. *J Am Acad Dermatol*. (2022). doi: 10.1016/j.jaad.2022.06.030. [Epub ahead of print]

frontiers | Frontiers in Surgery

TYPE Review
PUBLISHED 30 September 2022
DOI 10.3389/fsurg.2022.1030288

Check for updates

OPEN ACCESS

EDITED BY
Jiliang Zhou,
Georgia Health Sciences University,
United States

REVIEWED BY
Xiaojian Li,
Guangzhou Red Cross Hospital, China
Kunwu Fan,
Shenzhen Second People's Hospital, China

*CORRESPONDENCE
Xiaodong Chen
cxd234@163.com
Ronghua Yang
a_hwa991316 @163.com

SPECIALTY SECTION
This article was submitted to Reconstructive and Plastic Surgery, a section of the journal Frontiers in Surgery

RECEIVED 28 August 2022
ACCEPTED 12 September 2022
PUBLISHED 30 September 2022

CITATION
Long C, Wang J, Gan W, Qin X, Yang R and Chen X (2022) Therapeutic potential of exosomes from adipose-derived stem cells in chronic wound healing.
Front. Surg. 9:1030288.
doi: 10.3389/fsurg.2022.1030288

COPYRIGHT
© 2022 Long, Wang, Gan, Qin, Yang and Chen. This is an open-access article distributed under the terms of the Creative Commons Attribution License (CC BY). The use, distribution or reproduction in other forums is permitted, provided the original author(s) and the copyright owner(s) are credited and that the original publication in this journal is cited, in accordance with accepted academic practice. No use, distribution or reproduction is permitted which does not comply with these terms.

# Therapeutic potential of exosomes from adipose-derived stem cells in chronic wound healing

Chengmin Long[1,2], Jingru Wang[2,3], Wenjun Gan[1,2], Xinchi Qin[2,4], Ronghua Yang[1,5]* and Xiaodong Chen[1,2]*

[1]Guangdong Medical University, Zhanjiang, China, [2]Department of Burn Surgery and Skin Regeneration, the First People's Hospital of Foshan, Foshan, China, [3]Key Laboratory of Regenerative Medicine, Ministry of Education, Jinan University, Guangzhou, China, [4]Zunyi Medical University, Zhuhai, China, [5]Department of Burn and Plastic Surgery, Guangzhou First People's Hospital, South China University of Technology, Guangzhou, China

Chronic wound healing remains a challenging medical problem affecting society, which urgently requires anatomical and functional solutions. Adipose-derived stem cells (ADSCs), mesenchymal stem cells with self-renewal and multiple differentiation ability, play essential roles in wound healing and tissue regeneration. The exosomes from ADSCs (ADSC-EXOs) are extracellular vesicles that are essential for communication between cells. ADSC-EXOs release various bioactive molecules and subsequently restore tissue homeostasis and accelerate wound healing, by promoting various stages of wound repair, including regulating the inflammatory response, promoting wound angiogenesis, accelerating cell proliferation, and modulating wound remodeling. Compared with ADSCs, ADSC-EXOs have the advantages of avoiding ethical issues, being easily stored, and having high stability. In this review, a literature search of PubMed, Medline, and Google Scholar was performed for articles before August 1, 2022 focusing on exosomes from ADSCs, chronic wound repair, and therapeutic potential. This review aimed to provide new therapeutic strategies to help investigators explore how ADSC-EXOs regulate intercellular communication in chronic wounds.

KEYWORDS

adipose-Derived stem cells (ADSCs), exosome (EXO), chronic wounds, wound healing, therapeutic potential

Abbreviations

ADSCs, adipose-derived stem cells; ADSCs-EXOs, exosomes from adipose-derived stem cells; MSCs, mesenchymal stem cells; BMMSCs, bone marrow mesenchymal stem cells; EVs, extracellular vesicles; PM, plasma membrane; MVBs, multivesicular bodies; miRNAs, microRNAs; VEGF, vascular endothelial growth factor; TGF-β, transforming growth factor-β; MIF, macrophage migration inhibitory factor; TNF-α, tumor necrosis factor-alpha; MCSF, macrophage colony-stimulating factor; RBP-4, retinol-binding protein 4; NRF2, nuclear factor erythroid 2-related factor 2; FGF, fibroblast growth factor; TGF, transforming growth factor; VEGF-A, Vascular Endothelial Growth Factor A; PDGF-BB, platelet-derived growth factor BB; VECs, vascular endothelial cells; DLL4, Delta-like ligand 4; HIF-1, hypoxia-inducible factor-1; ECM, extracellular matrix; MMP3, matrix metalloproteinase-3; TIMP1, tissue inhibitor of metalloprotease 1; HDFs, human dermal fibroblasts.

## Background

The skin, the largest organ in humans, is a natural physical barrier against external stimulation (1). Loss of the balance between humans and the environment as a result of illness or trauma may result in substantial skin damage or even death (2, 3). Chronic wounds are long-lasting wounds that fail to achieve complete anatomical and functional repair through the normal healing process after 1 month of clinical treatment (4, 5). Chronic wounds, including vascular ulcers (venous and arterial ulcers), pressure ulcers, and diabetic foot ulcers, have complex pathogenesis and long disease courses, and are associated with high disability rates (6). Common features of chronic wounds include persistent bacterial biofilms, defective re-epithelization, decreased angiogenesis, and delayed extracellular matrix (ECM) remodeling (7, 8). Approximately 2.5% of the population in the United States is affected by chronic wounds (9, 10). According to conservative estimates, nearly $32 billion is spent on wound care, thus placing substantial pressure on the economy and healthcare system (11).

Many advanced therapies have been advocated as being effective for chronic wounds, such as negative pressure wound therapy; hyperbaric oxygen treatment; and biophysical, biological, and bioengineered therapies (4). Adipose-derived stem cells (ADSCs) are considered the most advantageous therapy for present-day regenerative medicine, given the abundant sources of adipose tissue, and the cells' outstanding proliferative ability and convenient isolation. ADSCs secrete paracrine factors and differentiate into multiple lineages (12, 13).

Exosomes from ADSCs (ADSC-EXOs) are small, single-membrane nanovesicles released by ADSCs through paracrine secretion, and are enriched in proteins, lipids, and nucleic acids (14–16) (**Figure 1**). As critical mediators of intercellular communication, they can alter the behaviors of recipient cells by transmitting signals and transporting molecules into target cells. Recent studies have shown that ADSC-EXOs had therapeutic effects in many aspects of disease, including wound healing (17, 18), organ diseases (19, 20), neurodegenerative diseases (21, 22), and cancer (23, 24). In regeneration and wound healing, ADSC-EXOs modulate persistent inflammation, angiogenesis, and ECM reconstruction. ADSC-EXO have functions resembling those of the parental stem cells, but are safer and more efficient in clinical applications, thus decreasing cell transplantation risks (25, 26).

## Adipose-derived stem cells

Mesenchymal stem cells (MSCs) have been a promising tool in tissue engineering and regenerative medicine (27, 28) since bone marrow mesenchymal stem cells (BMMSCs) were first discovered by Alexander Friedenstein in the late 1960s (29). MSCs have been successfully applied in corneal regeneration

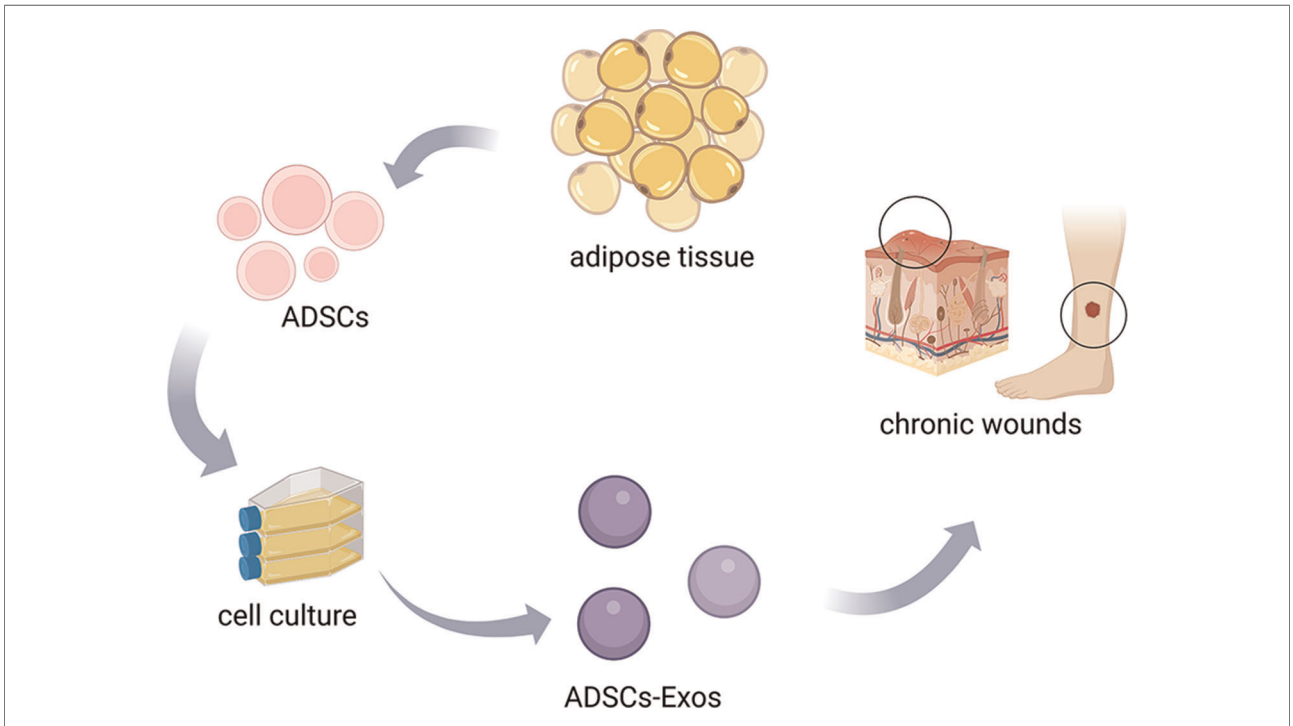


FIGURE 1
The production and applications of ADSCs-EXOs. Extracted from adipose tissue, ADSCs were collected and processed to obtain ADSCs-EXOs by cell culture. ADSCs-EXOs can apply to the treatment of chronic wound healing.

(30), wound healing, and skin rejuvenation (12, 28, 31). In their earlier studies, Friedenstein and colleagues demonstrated that MSCs, possibly derived from the mesoderm, can differentiate into various mesenchymal tissue lineages, such as osteoblasts, chondrocytes, adipocytes, myoblasts, and even neurons (32, 33) (**Figure 2**). In addition, these pluripotent cells can be isolated from a variety of tissues, such as adipose tissue, muscle, blood vessels, skin, and bone marrow (34, 35).

Among all these mesenchymal stem cells, ADSCs appear to be the most advantageous for clinical applications. Compared with other types of tissues, adipose tissue is available in relatively large quantities in humans. Furthermore, many ADSCs can be isolated from adipose tissue. Prior studies have indicated that 500 times more stem cells can be harvested from adipose tissue than from equal amounts of bone marrow (36, 37). In comparison with BMMSCs, ADSCs are relatively easily obtained, owing to their subcutaneous localization. Furthermore, patients tend to feel more comfortable with less donor site morbidity (12, 38). Moreover, ADSCs have higher proliferation ability than BMMSCs (39).

In recent studies, the roles of ADSCs in wound repair treatment have been confirmed. For example, ADSCs are crucial in wound repair in diabetic foot ulcers by enhancing VEGFR3-mediated lymphangiogenesis (40). In addition, ADSCs prevent scar formation and promote wound repair in skin-deficient mice by activating the PI3K/Akt pathway (41). However, barriers to the use of ADSCs must be addressed, such as their potential oncologic properties (42). Interestingly, ADSC-EXOs, the main factors through which ADSCs exert their biological effects (43), cannot actively contribute to tumorigenesis as adipose cell-free derivatives (44).

## Characteristic of exosomes

Extracellular vesicles (EVs) are membrane-contained vesicles secreted by cells from multiple organisms (45). On the basis of their contents, size, and membrane composition, three primary subgroups of EVs have been defined: apoptotic bodies, microvesicles, and exosomes (46) (**Figure 3**). EVs generally refer to vesicles ranging from 150 to 1,000 nm released by budding from the plasma membrane (PM) (47). The term "exosomes" was initially used to describe 40–1,000-nm vesicles released by all types of cultured cells and

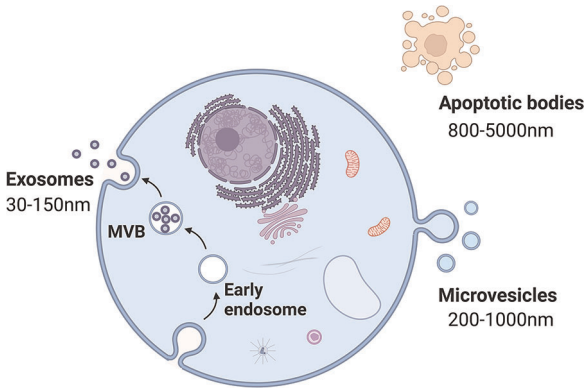


FIGURE 3
The biogenesis of each subtype of EVs. Apoptotic bodies (800–5,000 nm in size) are the result of the disintegration of apoptotic cells. Microvesicles (200–1,000 nm in size) arise from the plasma membrane. Exosomes (30–150 nm in size) originate from endosome.

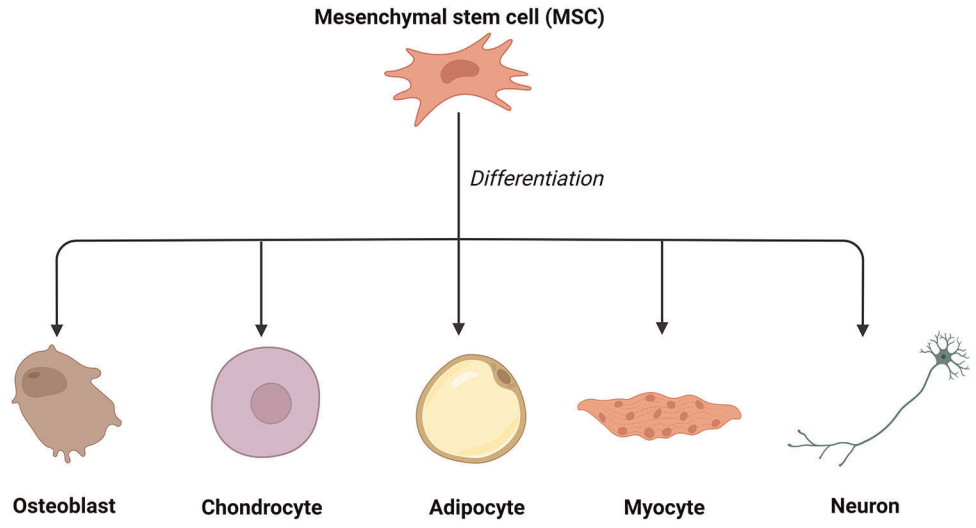


FIGURE 2
The differentiation of mesenchymal stem cells. Mesenchymal stem cells can differentiate into various mesenchymal tissue lineages, such as osteoblasts, chondrocytes, adipocytes, myoblasts, and even neurons.

exhibiting 5′-nucleotidase activity (48). Nevertheless, in the late 1980s, this term was used for small (30–100-nm) vesicles of endocytic origin, which are released outside cells as a result of the fusion of multivesicular bodies (MVBs) with the PM during reticulocyte differentiation (47, 49). Exosomes can be isolated from most biological fluids and cell types, such as saliva, urine, semen, nasal lavage fluid, plasma, and serum (50–53).

Exosomes contain many functional proteins, mRNAs, microRNAs (miRNAs), and complete organelles (**Figure 2**), which are released into the cytoplasm and mediate communication among target cells through surface membrane proteins (54, 55).

As the primary mediators of information transmission, miRNAs regulate the genes of recipient cells through self-degradation and re-expression; consequently, exosomes secreted by different cells vary in their biological functions (56). Current research on stem cell paracrine factors has indicated that exosomes secrete thousands of nutritional factors, such as stem cell factors, insulin-like growth factor I, vascular endothelial growth factor (VEGF), and transforming growth factor-β (TGF-β) (57). The uptake of exosomes by recipient cells occurs by fusion with the cell membrane, endocytosis, or receptor-ligand interaction. Adhesion-associated molecules on the surfaces of exosomes, such as glycoproteins, exosomal tetraspanin complexes, and integrins, determine the types of recipient cells (16, 58, 59).

## Inflammatory functions of ADSC-EXOs

ADSC-EXOs have immunomodulatory and anti-inflammatory effects, which remove necrotic tissue and pathogenic microorganisms from wounds, and consequently control local damage (60–62). ADSC-EXOs inhibit the differentiation and activation of T cells, thus inhibiting the release of the inflammatory factor IFN-γ and the proliferation of T cells (63, 64). ADSC-EXOs decrease adipose inflammation and obesity by regulating the phenotypic polarization of macrophages (65). Moreover, miRNAs, small, endogenous, non-coding nucleotides contained in ADSC-EXOs, play major roles in regulating metabolism and cell growth (66). One study has found that miRNA-451a enriched in ADSC-EXOs successfully promotes M1-to-M2 polarization of macrophages by downregulating macrophage migration inhibitory factor (MIF) (67). MIF is a pleiotropic pro-inflammatory mediator that participates in immune regulation *in vivo* (68). Some studies have indicated that inhibition of MIF suppresses the activation of macrophages and the expression of inflammatory factors, such as NO, tumor necrosis factor-alpha (TNF-α), and IL-6, thereby decreasing inflammatory responses and ameliorating arthritis and articular cartilage injury (68–70). Furthermore, ADSC-EXOs release many immunomodulatory proteins, such as TNF-α, macrophage colony-stimulating factor (MCSF), and retinol-binding protein 4 (RBP-4) (71). Macrophages and proteolytic enzymes are released after the destruction of cells, and subsequently digest cell debris and necrotic tissue, thus providing a suitable environment for wound repair (72–74). ADSC-EXOs have been found to contribute to wound healing in rats with diabetic foot ulcers, particularly in the presence of overexpression of nuclear factor erythroid 2-associated factor 2 (NRF2). The expression of oxidative stress-associated proteins and inflammatory cytokines is diminished (75). ADSC-EXOs have comparable properties to those of their parent cells. They can improve graft retention by upregulating early inflammation and angiogenesis (76). Similarly, ADSC-EXOs upregulate the expression of macrophage inflammatory protein-1α and monocyte chemoattractant protein-1, thus promoting early inflammation (76). Further research on immunomodulation and anti-inflammation of ADSC-EXOs in chronic wounds is needed.

## Angiogenesis regulation by ADSC-EXOs

Another function of ADSC-EXOs in wound repair is promoting angiogenesis, a dynamic process delivering sufficient nutrients and oxygen to the tissue. Emerging new capillaries, macrophages, and loose connective tissue contribute to granulation tissue formation. The elevated glucose levels in patients with diabetes can destroy the balance between vessel growth and maturation (77). In chronic wounds, perturbations in vascular integrity decrease vascularity and capillary density (78). VEGF, angiopoietin, fibroblast growth factor (FGF), and transforming growth factor (TGF) are key angiogenic cytokines in wound angiogenesis. Among these factors, VEGF-A is considered one of the most potent angiogenic factors in wounds (79). This protein, which is produced by many cells such as macrophages, binds its receptors on endothelial cells and subsequently induces migration, proliferation, and vessel growth. Mice deficient in VEGF-A 6, 7, or Flk1 8 succumb to a lack of angiogenesis early in development (80–82). ADSC-EXOs possess a higher ability to enhance angiogenesis in fat grafting by regulating VEGF/VEGF-R signaling and activating the protein kinase A (PKA) signaling pathway (83, 84). In addition to growth factors that mediate wound healing, such as VEGF-A and platelet-derived growth factor BB (PDGF-BB), ADSC-EXOs are enriched in miRNA-125a and miRNA-31 (85). ADSC-EXOs transfer miRNA-125a and miRNA-31 cargo into vascular endothelial cells (VECs), and consequently downregulate the expression of angiogenesis inhibitor Delta-like ligand 4 (DLL4), thereby promoting VEC proliferation

and angiogenesis (86). Lu et al. have found that ADSC-EXOs containing miRNA-486-5p promote angiogenesis and accelerate cutaneous wound healing (87). In addition, ADSC-EXOs inhibit the overexpression of the anti-angiogenic gene hypoxia-inducible factor-1 (HIF-1) after chronic wound injury (88). We propose that ADSC-EXOs significantly affect angiogenesis, a possibility requiring further investigation.

## Proliferation and ADSC-EXOs

ADSC-EXOs have a beneficial effect in accelerating cell proliferation, which is crucial for the treatment of chronic wounds. For example, exosomes from miRNA-199-3p-modified ADSCs contribute to the proliferation and migration of endothelial tip cells (89). Moreover, ADSC-EXOs facilitate osteosarcoma progression by increasing COLGALT2 expression in osteosarcoma cells (90). In the cell proliferation stage, fibroblasts stimulate wound healing by proliferating and synthesizing large amounts of ECM components, such as collagen and elastic fibers, under the stimulation of trauma (78). ADSC-EXOs are internalized by fibroblasts and affect cell migration, proliferation, and collagen synthesis by promoting gene expression of N-cadherin, cyclin 1, proliferating cell nuclear antigen, and collagen type I and III. In a dependent manner, higher doses of exosomes can achieve faster migration rates (91). Choi et al. have found that ADSC-EXOs promote the proliferation and differentiation of dermal fibroblasts through microRNAs inhibiting genes including NPM1, PDCD4, CCL5, and NUP62, thereby contributing to the regeneration of skin fibroblasts (92). Moreover, miRNA-21 is highly expressed in adipose-derived stem cell exosomes and has been found to enhance the migration and proliferation of HaCaT cells by increasing matrix metalloproteinase-9 expression through the PI3K/AKT pathway (93).

## ECM remodeling and ADSC-EXOs

ADSC-EXOs regulate remodeling of the ECM. During the wound remodeling stage, fibroblasts differentiate into myofibroblasts, and the granulation tissue gradually becomes fibrotic; collagen gradually increases; the wound begins to contract; and scar tissue is eventually formed. ADSC-EXOs promote collagen remodeling through the synthesis of collagen types I and III in early stages of wound healing. In late stages, they inhibit collagen formation and decrease scarring (94). ADSC-EXOs prevent fibroblast-to-myofibroblast differentiation by increasing the ratio of collagen III to collagen I, as well as the ratio of TGF-β3 to TGF-β1. Moreover, ADSC-EXOs increase the expression of matrix metalloproteinase-3 (MMP3) in skin dermal fibroblasts by activating the ERK/MAPK pathway, thus resulting in a high ratio of MMP3 to tissue inhibitor of metalloprotease 1 (TIMP1), and facilitating remodeling of the ECM and diminished scarring during wound healing (92). More research on wound remodeling is needed to achieve the goals of clinical application of ADSC-EXOs.

Wound healing is a complex and dynamic physiological process that can generally be divided into four highly integrated and overlapping stages: hemostasis, inflammation, proliferation, and remodeling. These phases and their biophysiological functions must occur in an appropriate sequence at a specific time. Otherwise, interruptions, abnormalities, or prolongations in the process may result in delayed or chronic wound non-healing. ADSC-EXOs are extensively involved in the above-mentioned wound repair process through their release of various bioactive molecules (95, 96).

All types of wounds may begin as small cuts and have the potential to evolve into chronic wounds. The repair process of chronic wounds usually begins with a normal acute wound. Similar features can be found in chronic wounds, although they are classified into different categories according to etiology. Persistent infections, excessive levels of proinflammatory cytokines, as well as senescent cells that do not respond to reparative stimuli lead to chronic wounds. Definitive evidence has indicated that wound dressing along with ADSC-EXOs alleviates diabetic and infectious wound healing (97) (**Figure 4**).

## Challenges and prospects

The exosome field has advanced remarkably rapidly. Extensive evidence has indicated that ADSC-EXOs have robust effects on multiple stages of chronic wound repair tissue regeneration as critical mediators of intercellular communication. For example, in a diabetic mouse model of delayed wound healing, ADSC-EXOs enhance skin collagen production, angiogenesis, and cell proliferation; inhibit apoptosis; promote skin barrier function repair; and decrease inflammation in skin lesions (98). Given these properties, ADSC-EXOs may have promise in applications in chronic wound repair, skin anti-aging therapy, and scarless cutaneous repair. ADSC-EXOs show positive effects in preventing skin aging through protecting human dermal fibroblasts (HDFs) against ultraviolet B-induced photoaging damage (99, 100). Wang and colleagues have demonstrated that ADSC-EXOs promote wound repair in diabetic mice during angiogenesis and remodeling (101). In genetic therapy, ADSC-EXOs have been found to be a new therapeutic target for curing PD in patients (102).

Despite the positive results obtained in pre-clinical studies, multiple issues must be considered before clinical application of

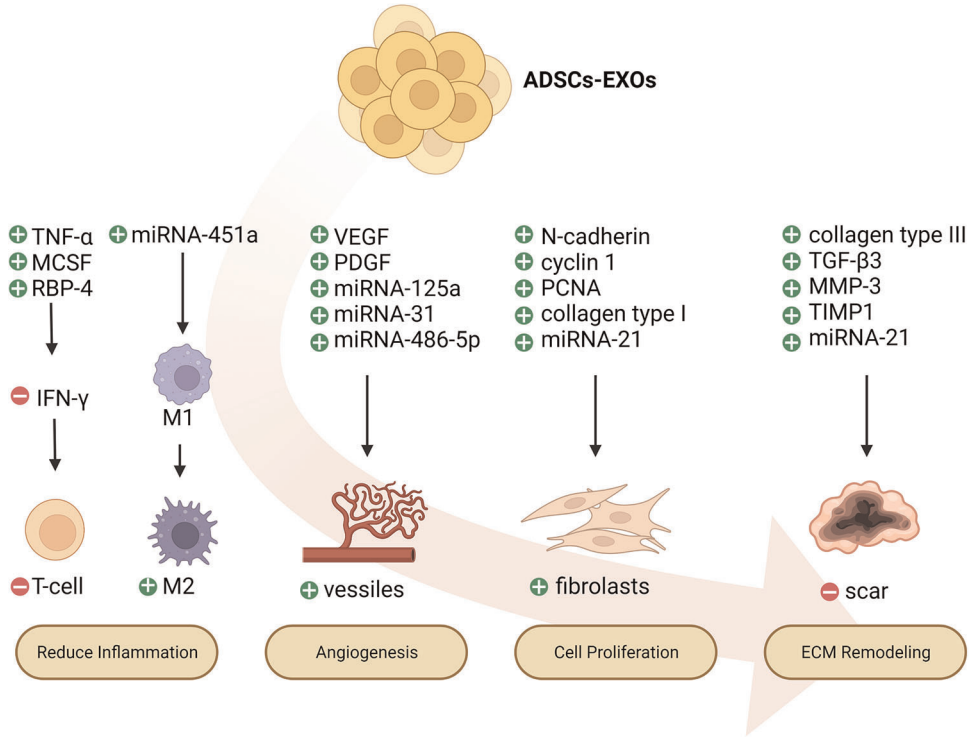


FIGURE 4
Potential mechanisms of ADSCs-EXOs regulating wound healing. ADSCs-EXOs might accelerate chronic wound repair by up-regulating early inflammation, promoting angiogenesis, enhancing proliferation, and regulating extracellular matrix (ECM) remodeling.

ADSC-EXOs. First, animal models for research are unable to fully reproduce the complexity of human chronic wounds, and clinical trials are scarce. Pigs or guinea pigs have skin structure somewhat similar to that in humans, thus providing a better animal model than mice in ADSC-EXO studies. Second, because they induce both effective pro-tumor and antitumor immune responses, ADSC-EXOs must be very carefully assessed in terms of safety and efficacy. Finally, technical issues such as extraction and purification of ADSC-EXOs must be simplified. The delivery and application methods are also worthy of consideration to achieve the development of large quantities of ADSC-EXOs capable of long-term storage of for clinical applications. Finally, although ADSC-EXOs appear to be a promising therapy for multiple diseases, further investigation and comprehensive information on isolating and identifying ADSC-EXOs is needed for widespread applications in clinical practice.

## Conclusion

In summary, chronic wound repair is a well-orchestrated process involving numerous factors participating in a sequence of steps. ADSC-EXOs appear to be a potential therapeutic agent for chronic wounds by promoting various stages of wound healing, including decreased oxidative stress, increased neo-vascularization, enhanced collagen deposition, and less scarring. With continuing discoveries in this field, ADSC-EXOs involved in various biological functions are expected to hold promise for treating a wide variety of disorders.

## Author contributions

All authors listed have made a substantial, direct, and intellectual contribution to the work, and approved it for publication. All authors contributed to the article and approved the submitted version.

## Funding

This work was funded by National Natural Science Foundation of China (No. 82172205), National Natural Science Foundation of China (No. 82272276), GuangDong

Basic and Applied Basic Research Foundation (Nos. 2021A1515011453, 2022A1515012160), Special Fund for Science and Technology Innovation Strategy of Guangdong Province (No. 2020A1515011402), Medical Research Fund of Guangdong Province (No. A2020322) and Research Grant of Key Laboratory of Regenerative Medicine, Ministry of Education, Jinan University (No. ZSYXM202209).

## Acknowledgments

The Figure was created in the web application BioRender.com (Available online: Biorender.com, accessed on 1 August 2022).

## Conflict of interest

The authors declare that the research was conducted in the absence of any commercial or financial relationships that could be construed as a potential conflict of interest.

## Publisher's note

All claims expressed in this article are solely those of the authors and do not necessarily represent those of their affiliated organizations, or those of the publisher, the editors and the reviewers. Any product that may be evaluated in this article, or claim that may be made by its manufacturer, is not guaranteed or endorsed by the publisher.

## References

1. Kanitakis J. Anatomy, histology and immunohistochemistry of normal human skin. *Eur J Dermatol*. (2002) 12(4):390–9.

2. Byrd AL, Belkaid Y, Segre JA. The human skin microbiome. *Nat Rev Microbiol*. (2018) 16(3):143–55. doi: 10.1038/nrmicro.2017.157

3. Grice EA, Segre JA. The skin microbiome. *Nat Rev Microbiol*. (2011) 9 (4):244–53. doi: 10.1038/nrmicro2537

4. Frykberg RG, Banks J. Challenges in the treatment of chronic wounds. *Adv Wound Care*. (2015) 4(9):560–82. doi: 10.1089/wound.2015.0635

5. Xue M, Zhao R, Lin H, Jackson C. Delivery systems of current biologicals for the treatment of chronic cutaneous wounds and severe burns. *Adv Drug Delivery Rev*. (2018) 129:219–41. doi: 10.1016/j.addr.2018.03.002

6. Nunan R, Harding KG, Martin P. Clinical challenges of chronic wounds: searching for an optimal animal model to recapitulate their complexity. *Dis Model Mech*. (2014) 7(11):1205–13. doi: 10.1242/dmm.016782

7. Huang Y-Z, Gou M, Da L-C, Zhang W-Q, Xie H-Q. Mesenchymal stem cells for chronic wound healing: current status of preclinical and clinical studies. *Tissue Eng Part B Rev*. (2020) 26(6):555–70. doi: 10.1089/ten.teb.2019.0351

8. Kim JH, Yang B, Tedesco A, Lebig EGD, Ruegger PM, Xu K, et al. High levels of oxidative stress and skin microbiome are critical for initiation and development of chronic wounds in diabetic mice. *Sci Rep*. (2019) 9(1):19318. doi: 10.1038/s41598-019-55644-3

9. Jones RE, Foster DS, Longaker MT. Management of chronic wounds-2018. *JAMA*. (2018) 320(14):1481–2. doi: 10.1001/jama.2018.12426

10. Sen CK. Human wound and its burden: updated 2020 compendium of estimates. *Adv Wound Care*. (2021) 10(5):281–92. doi: 10.1089/wound.2021.0026

11. Nussbaum SR, Carter MJ, Fife CE, DaVanzo J, Haught R, Nusgart M, et al. An economic evaluation of the impact, cost, and medicare policy implications of chronic nonhealing wounds. *Value Health*. (2018) 21(1):27–32. doi: 10.1016/j.jval.2017.07.007

12. Tobita M, Orbay H, Mizuno H. Adipose-derived stem cells: current findings and future perspectives. *Discov Med*. (2011) 11(57):160–70.

13. Bacakova L, Zarubova J, Travnickova M, Musilkova J, Pajorova J, Slepicka P, et al. Stem cells: their source, potency and use in regenerative therapies with focus on adipose-derived stem cells—a review. *Biotechnol Adv*. (2018) 36(4):1111–26. doi: 10.1016/j.biotechadv.2018.03.011

14. Liang Y, Duan L, Lu J, Xia J. Engineering exosomes for targeted drug delivery. *Theranostics*. (2021) 11(7):3183–95. doi: 10.7150/thno.52570

15. Pegtel DM, Gould SJ. Exosomes. *Annu Rev Biochem*. (2019) 88:487–514. doi: 10.1146/annurev-biochem-013118-111902

16. Zhang L, Yu D. Exosomes in cancer development, metastasis, and immunity. *Biochim Biophys Acta Rev Cancer*. (2019) 1871(2):455–68. doi: 10.1016/j.bbcan.2019.04.004

17. Shi R, Jin Y, Hu W, Lian W, Cao C, Han S, et al. Exosomes derived from mmu_circ_0000250-modified adipose-derived mesenchymal stem cells promote wound healing in diabetic mice by inducing miR-128-3p/SIRT1-mediated autophagy. *Am J Physiol Cell Physiol*. (2020) 318(5):C848–56. doi: 10.1152/ajpcell.00041.2020

18. Shao M, Jin M, Xu S, Zheng C, Zhu W, Ma X, et al. Exosomes from long noncoding RNA-Gm37494-ADSCs repair spinal cord injury via shifting microglial M1/M2 polarization. *Inflammation*. (2020) 43(4):1536–47. doi: 10.1007/s10753-020-01230-z

19. Shen W, Zhao X, Li S. Exosomes derived from ADSCs attenuate sepsis-induced lung injury by delivery of circ-fryl and regulation of the miR-490-3p/SIRT3 pathway. *Inflammation*. (2022) 45(1):331–42. doi: 10.1007/s10753-021-01548-2

20. Cao S, Huang Y, Dai Z, Liao Y, Zhang J, Wang L, et al. Circular RNA mmu_circ_0001295 from hypoxia pretreated adipose-derived mesenchymal stem cells (ADSCs) exosomes improves outcomes and inhibits sepsis-induced renal injury in a mouse model of sepsis. *Bioengineered*. (2022) 13(3):6323–31. doi: 10.1080/21655979.2022.2044720

21. Liu H, Jin M, Ji M, Zhang W, Liu A, Wang T. Hypoxic pretreatment of adipose-derived stem cell exosomes improved cognition by delivery of circ-Epc1 and shifting microglial M1/M2 polarization in an Alzheimer's Disease mice model. *Aging (Albany NY)*. (2022) 14(7):3070–83. doi: 10.18632/aging.203989

22. Hu X, Pan J, Li Y, Jiang Y, Zheng H, Shi R, et al. Extracellular vesicles from adipose-derived stem cells promote microglia M2 polarization and neurological recovery in a mouse model of transient middle cerebral artery occlusion. *Stem Cell Res Ther*. (2022) 13(1):21. doi: 10.1186/s13287-021-02668-0

23. Lou G, Chen L, Xia C, Wang W, Qi J, Li A, et al. MiR-199a-modified exosomes from adipose tissue-derived mesenchymal stem cells improve hepatocellular carcinoma chemosensitivity through mTOR pathway. *J Exp Clin Cancer Res*. (2020) 39(1):4. doi: 10.1186/s13046-019-1512-5

24. Liang Z, Liu H, Zhang Y, Xiong L, Zeng Z, He X, et al. Cyr61 from adipose-derived stem cells promotes colorectal cancer metastasis and vasculogenic mimicry formation via integrin $\alpha\,\beta$. *Mol Oncol*. (2021) 15(12):3447–67. doi: 10.1002/1878-0261.12998

25. He C, Zheng S, Luo Y, Wang B. Exosome theranostics: biology and translational medicine. *Theranostics*. (2018) 8(1):237–55. doi: 10.7150/thno.21945

26. Vu NB, Nguyen HT, Palumbo R, Pellicano R, Fagoonee S, Pham PV. Stem cell-derived exosomes for wound healing: current status and promising directions. *Minerva Med*. (2021) 112(3):384–400. doi: 10.23736/S0026-4806.20.07205-5

27. Kokai LE, Marra K, Rubin JP. Adipose stem cells: biology and clinical applications for tissue repair and regeneration. *Transl Res*. (2014) 163 (4):399–408. doi: 10.1016/j.trsl.2013.11.009

28. Nae S, Bordeianu I, Stăncioiu AT, Antohi N. Human adipose-derived stem cells: definition, isolation, tissue-engineering applications. *Rom J Morphol Embryol*. (2013) 54(4):919–24.

29. Bianco P, Robey PG, Simmons PJ. Mesenchymal stem cells: revisiting history, concepts, and assays. *Cell Stem Cell*. (2008) 2(4):313–9. doi: 10.1016/j.stem.2008.03.002

30. Saccu G, Menchise V, Giordano C, Delli Castelli D, Dastrù W, Pellicano R, et al. Regenerative approaches and future trends for the treatment of corneal burn injuries. *J Clin Med*. (2021) 10(2):317. doi: 10.3390/jcm10020317

31. Hanson SE, Gutowski KA, Hematti P. Clinical applications of mesenchymal stem cells in soft tissue augmentation. *Aesthet Surg J*. (2010) 30(6):838–42. doi: 10.1177/1090820X10386364

32. Prockop DJ. Marrow stromal cells as stem cells for nonhematopoietic tissues. *Science*. (1997) 276(5309):71–4. doi: 10.1126/science.276.5309.71

33. Caplan AI, Bruder SP. Mesenchymal stem cells: building blocks for molecular medicine in the 21st century. *Trends Mol Med*. (2001) 7(6):259–64. doi: 10.1016/S1471-4914(01)02016-0

34. Panchalingam KM, Jung S, Rosenberg L, Behie LA. Bioprocessing strategies for the large-scale production of human mesenchymal stem cells: a review. *Stem Cell Res Ther*. (2015) 6:225. doi: 10.1186/s13287-015-0228-5

35. Couto P S, Rotondi MC, Bersenev A, Hewitt CJ, Nienow AW, Verter F, et al. Expansion of human mesenchymal stem/stromal cells (hMSCs) in bioreactors using microcarriers: lessons learnt and what the future holds. *Biotechnol Adv*. (2020) 45:107636. doi: 10.1016/j.biotechadv.2020.107636

36. Zhang Y, Khan D, Delling J, Tobiasch E. Mechanisms underlying the osteo- and adipo-differentiation of human mesenchymal stem cells. *Sci World J*. (2012) 2012:793823. doi: 10.1100/2012/793823

37. Ong WK, Sugii S. Adipose-derived stem cells: fatty potentials for therapy. *Int J Biochem Cell Biol*. (2013) 45(6):1083–6. doi: 10.1016/j.biocel.2013.02.013

38. Ding D-C, Chou H-L, Hung W-T, Liu H-W, Chu T-Y. Human adipose-derived stem cells cultured in keratinocyte serum free medium: Donor's Age does not affect the proliferation and differentiation capacities. *J Biomed Sci*. (2013) 20:59. doi: 10.1186/1423-0127-20-59

39. Barba M, Cicione C, Bernardini C, Michetti F, Lattanzi W. Adipose-derived mesenchymal cells for bone regereneration: state of the art. *Biomed Res Int*. (2013) 2013:416391. doi: 10.1155/2013/416391

40. Zhou J, Wei T, He Z. ADSCs enhance VEGFR3-mediated lymphangiogenesis via METTL3-mediated VEGF-C mA modification to improve wound healing of diabetic foot ulcers. *Mol Med*. (2021) 27(1):146. doi: 10.1186/s10020-021-00406-z

41. Zhang W, Bai X, Zhao B, Li Y, Zhang Y, Li Z, et al. Cell-free therapy based on adipose tissue stem cell-derived exosomes promotes wound healing via the PI3K/Akt signaling pathway. *Exp Cell Res*. (2018) 370(2):333–42. doi: 10.1016/j.yexcr.2018.06.035

42. Behr B, Ko SH, Wong VW, Gurtner GC, Longaker MT. Stem cells. *Plast Reconstr Surg*. (2010) 126(4):1163–71. doi: 10.1097/PRS.0b013e3181ea42bb

43. Praveen Kumar L, Sangeetha K, Ranjita M, Vijayalakshmi S, Rajagopal K, Verma RS. The mesenchymal stem cell secretome: a new paradigm towards cell-free therapeutic mode in regenerative medicine. *Cytokine Growth Factor Rev*. (2019) 46:1–9. doi: 10.1016/j.cytogfr.2019.04.002

44. Cai Y, Li J, Jia C, He Y, Deng C. Therapeutic applications of adipose cell-free derivatives: a review. *Stem Cell Res Ther*. (2020) 11(1):312. doi: 10.1186/s13287-020-01831-3

45. Yáñez-Mó M, Siljander PRM, Andreu Z, Zavec AB, Borràs FE, Buzas EI, et al. Biological properties of extracellular vesicles and their physiological functions. *J Extracell Vesicles*. (2015) 4:27066. doi: 10.3402/jev.v4.27066

46. Gould SJ, Raposo G. As we wait: coping with an imperfect nomenclature for extracellular vesicles. *J Extracell Vesicles*. (2013) 2. doi: 10.3402/jev.v2i0.20389

47. Colombo M, Raposo G, Théry C. Biogenesis, secretion, and intercellular interactions of exosomes and other extracellular vesicles. *Annu Rev Cell Dev Biol*. (2014) 30:255–89. doi: 10.1146/annurev-cellbio-101512-122326

48. Trams EG, Lauter CJ, Salem N, Heine U. Exfoliation of membrane ecto-enzymes in the form of micro-vesicles. *Biochim Biophys Acta*. (1981) 645 (1):63–70. doi: 10.1016/0005-2736(81)90512-5

49. Johnstone RM, Adam M, Hammond JR, Orr L, Turbide C. Vesicle formation during reticulocyte maturation. Association of plasma membrane activities with released vesicles (exosomes). *J Biol Chem*. (1987) 262 (19):9412–20. doi: 10.1016/S0021-9258(18)48095-7

50. Lässer C, O'Neil SE, Ekerljung L, Ekström K, Sjöstrand M, Lötvall J. RNA-containing exosomes in human nasal secretions. *Am J Rhinol Allergy*. (2011) 25 (2):89–93. doi: 10.2500/ajra.2011.25.3573

51. Poliakov A, Spilman M, Dokland T, Amling CL, Mobley JA. Structural heterogeneity and protein composition of exosome-like vesicles (prostasomes) in human semen. *Prostate*. (2009) 69(2):159–67. doi: 10.1002/pros.20860

52. Pisitkun T, Shen R-F, Knepper MA. Identification and proteomic profiling of exosomes in human urine. *Proc Natl Acad Sci USA*. (2004) 101(36):13368–73. doi: 10.1073/pnas.0403453101

53. Caby M-P, Lankar D, Vincendeau-Scherrer C, Raposo G, Bonnerot C. Exosomal-like vesicles are present in human blood plasma. *Int Immunol*. (2005) 17(7):879–87. doi: 10.1093/intimm/dxh267

54. Valadi H, Ekström K, Bossios A, Sjöstrand M, Lee JJ, Lötvall JO. Exosome-mediated transfer of mRNAs and microRNAs is a novel mechanism of genetic exchange between cells. *Nat Cell Biol*. (2007) 9 (6):654–9. doi: 10.1038/ncb1596

55. Skog J, Würdinger T, van Rijn S, Meijer DH, Gainche L, Sena-Esteves M, et al. Glioblastoma microvesicles transport RNA and proteins that promote tumour growth and provide diagnostic biomarkers. *Nat Cell Biol*. (2008) 10 (12):1470–6. doi: 10.1038/ncb1800

56. Pegtel DM, Cosmopoulos K, Thorley-Lawson DA, van Eijndhoven MAJ, Hopmans ES, Lindenberg JL, et al. Functional delivery of viral miRNAs via exosomes. *Proc Natl Acad Sci USA*. (2010) 107(14):6328–33. doi: 10.1073/pnas.0914843107

57. Li X-Y, Zheng Z-H, Li X-Y, Guo J, Zhang Y, Li H, et al. Treatment of foot disease in patients with type 2 diabetes mellitus using human umbilical cord blood mesenchymal stem cells: response and correction of immunological anomalies. *Curr Pharm Des*. (2013) 19(27):4893–9. doi: 10.2174/1381612813199990326

58. Rana S, Yue S, Stadel D, Zöller M. Toward tailored exosomes: the exosomal tetraspanin web contributes to target cell selection. *Int J Biochem Cell Biol*. (2012) 44(9):1574–84. doi: 10.1016/j.biocel.2012.06.018

59. Nazarenko I, Rana S, Baumann A, McAlear J, Hellwig A, Trendelenburg M, et al. Cell surface tetraspanin Tspan8 contributes to molecular pathways of exosome-induced endothelial cell activation. *Cancer Res*. (2010) 70(4):1668–78. doi: 10.1158/0008-5472.CAN-09-2470

60. Chang C-L, Sung P-H, Chen K-H, Shao P-L, Yang C-C, Cheng B-C, et al. Adipose-derived mesenchymal stem cell-derived exosomes alleviate overwhelming systemic inflammatory reaction and organ damage and improve outcome in rat sepsis syndrome. *Am J Transl Res*. (2018) 10(4):1053–70.

61. Seo Y, Kim H-S, Hong I-S. Stem cell-derived extracellular vesicles as immunomodulatory therapeutics. *Stem Cells Int*. (2019) 2019:5126156. doi: 10.1155/2019/5126156

62. Cargnoni A, Papait A, Masserdotti A, Pasotti A, Stefani FR, Silini AR, et al. Extracellular vesicles from perinatal cells for anti-inflammatory therapy. *Front Bioeng Biotechnol*. (2021) 9:637737. doi: 10.3389/fbioe.2021.637737

63. Blazquez R, Sanchez-Margallo FM, de la Rosa O, Dalemans W, Alvarez V, Tarazona R, et al. Immunomodulatory potential of human adipose mesenchymal stem cells derived exosomes on in vitro stimulated T cells. *Front Immunol*. (2014) 5:556. doi: 10.3389/fimmu.2014.00556

64. Bolandi Z, Mokhberian N, Eftekhary M, Sharifi K, Soudi S, Ghanbarian H, et al. Adipose derived mesenchymal stem cell exosomes loaded with miR-10a promote the differentiation of Th17 and Treg from naive CD4 T cell. *Life Sci*. (2020) 259:118218. doi: 10.1016/j.lfs.2020.118218

65. Zhao H, Shang Q, Pan Z, Bai Y, Li Z, Zhang H, et al. Exosomes from adipose-derived stem cells attenuate adipose inflammation and obesity through polarizing M2 macrophages and beiging in white adipose tissue. *Diabetes*. (2018) 67(2):235–47. doi: 10.2337/db17-0356

66. Yu X, Odenthal M, Fries JWU. Exosomes as miRNA carriers: formation-function-future. *Int J Mol Sci*. (2016) 17(12):2028. doi: 10.3390/ijms17122028

67. Li R, Li D, Wang H, Chen K, Wang S, Xu J, et al. Exosomes from adipose-derived stem cells regulate M1/M2 macrophage phenotypic polarization to promote bone healing via miR-451a/MIF. *Stem Cell Res Ther*. (2022) 13(1):149. doi: 10.1186/s13287-022-02823-1

68. Zhang Y, Gu R, Jia J, Hou T, Zheng LT, Zhen X. Inhibition of macrophage migration inhibitory factor (MIF) tautomerase activity suppresses microglia-mediated inflammatory responses. *Clin Exp Pharmacol Physiol*. (2016) 43 (11):1134–44. doi: 10.1111/1440-1681.12647

69. Zhang Y, Xu L, Zhang Z, Zhang Z, Zheng L, Li D, et al. Structure-activity relationships and anti-inflammatory activities of N-carbamothioylformamide analogues as MIF tautomerase inhibitors. *J Chem Inf Model*. (2015) 55 (9):1994–2004. doi: 10.1021/acs.jcim.5b00445

70. Zhang Z, Zhang R, Li L, Zhu L, Gao S, Lu Q, et al. Macrophage migration inhibitory factor (MIF) inhibitor, Z-590 suppresses cartilage destruction in adjuvant-induced arthritis via inhibition of macrophage inflammatory activation. *Immunopharmacol Immunotoxicol*. (2018) 40(2):149–57. doi: 10.1080/08923973.2018.1424896

71. Kranendonk MEG, Visseren FLJ, van Balkom BWM, Nolte-'t Hoen ENM, van Herwaarden JA, de Jager W, et al. Human adipocyte extracellular vesicles

in reciprocal signaling between adipocytes and macrophages. *Obesity (Silver Spring)*. (2014) 22(5):1296–308. doi: 10.1002/oby.20679

72. Vannella KM, Wynn TA. Mechanisms of organ injury and repair by macrophages. *Annu Rev Physiol*. (2017) 79:593–617. doi: 10.1146/annurev-physiol-022516-034356

73. Wynn TA, Barron L. Macrophages: master regulators of inflammation and fibrosis. *Semin Liver Dis*. (2010) 30(3):245–57. doi: 10.1055/s-0030-1255354

74. Bevilacqua MP, Pober JS, Wheeler ME, Cotran RS, Gimbrone MA. Interleukin 1 acts on cultured human vascular endothelium to increase the adhesion of polymorphonuclear leukocytes, monocytes, and related leukocyte cell lines. *J Clin Invest*. (1985) 76(5):2003–11. doi: 10.1172/JCI112200

75. Li X, Xie X, Lian W, Shi R, Han S, Zhang H, et al. Exosomes from adipose-derived stem cells overexpressing Nrf2 accelerate cutaneous wound healing by promoting vascularization in a diabetic foot ulcer rat model. *Exp Mol Med*. (2018) 50(4):1–17. doi: 10.1038/s12276-018-0058-5

76. Chen B, Cai J, Wei Y, Jiang Z, Desjardins HE, Adams AE, et al. Exosomes are comparable to source adipose stem cells in fat graft retention with up-regulating early inflammation and angiogenesis. *Plast Reconstr Surg*. (2019) 144 (5):816e–27e. doi: 10.1097/PRS.0000000000006175

77. Burgess JL, Wyant WA, Abdo Abujamra B, Kirsner RS, Jozic I. Diabetic wound-healing science. *Medicina (Kaunas)*. (2021) 57(10):1072. doi: 10.3390/medicina57101072

78. Martin P. Wound healing–aiming for perfect skin regeneration. *Science*. (1997) 276(5309):75–81. doi: 10.1126/science.276.5309.75

79. Ferrara N, Gerber H-P, LeCouter J. The biology of VEGF and its receptors. *Nat Med*. (2003) 9(6):669–76. doi: 10.1038/nm0603-669

80. Carmeliet P, Ferreira V, Breier G, Pollefeyt S, Kieckens L, Gertsenstein M, et al. Abnormal blood vessel development and lethality in embryos lacking a single VEGF allele. *Nature*. (1996) 380(6573):435–9. doi: 10.1038/380435a0

81. Shalaby F, Rossant J, Yamaguchi TP, Gertsenstein M, Wu XF, Breitman ML, et al. Failure of blood-island formation and vasculogenesis in Flk-1-deficient mice. *Nature*. (1995) 376(6535):62–6. doi: 10.1038/376062a0

82. Ferrara N, Carver-Moore K, Chen H, Dowd M, Lu L, O'Shea KS, et al. Heterozygous embryonic lethality induced by targeted inactivation of the VEGF gene. *Nature*. (1996) 380(6573):439–42. doi: 10.1038/380439a0

83. Han Y, Ren J, Bai Y, Pei X, Han Y. Exosomes from hypoxia-treated human adipose-derived mesenchymal stem cells enhance angiogenesis through VEGF/VEGF-R. *Int J Biochem Cell Biol*. (2019) 109:59–68. doi: 10.1016/j.biocel.2019.01.017

84. Xue C, Shen Y, Li X, Li B, Zhao S, Gu J, et al. Exosomes derived from hypoxia-treated human adipose mesenchymal stem cells enhance angiogenesis through the PKA signaling pathway. *Stem Cells Dev*. (2018) 27(7):456–65. doi: 10.1089/scd.2017.0296

85. Hoang DH, Nguyen TD, Nguyen H-P, Nguyen X-H, Do PTX, Dang VD, et al. Differential wound healing capacity of mesenchymal stem cell-derived exosomes originated from bone marrow, adipose tissue and umbilical cord under serum- and xeno-free condition. *Front Mol Biosci*. (2020) 7:119. doi: 10.3389/fmolb.2020.00119

86. Liang X, Zhang L, Wang S, Han Q, Zhao RC. Exosomes secreted by mesenchymal stem cells promote endothelial cell angiogenesis by transferring miR-125a. *J Cell Sci*. (2016) 129(11):2182–9. doi: 10.1242/jcs.170373

87. Lu Y, Wen H, Huang J, Liao P, Liao H, Tu J, et al. Extracellular vesicle-enclosed miR-486-5p mediates wound healing with adipose-derived stem cells by promoting angiogenesis. *J Cell Mol Med*. (2020) 24(17):9590–604. doi: 10.1111/jcmm.15387

88. Kang T, Jones TM, Naddell C, Bacanamwo M, Calvert JW, Thompson WE, et al. Adipose-derived stem cells induce angiogenesis via microvesicle transport of miRNA-31. *Stem Cells Transl Med*. (2016) 5(4):440–50. doi: 10.5966/sctm.2015-0177

89. Du L, Li G, Yang Y, Yang G, Wan J, Ma Z, et al. Exosomes from microRNA-199-3p-modified adipose-derived stem cells promote proliferation and migration of endothelial tip cells by downregulation of semaphorin 3A. *Int J Clin Exp Pathol*. (2018) 11(10):4879–88.

90. Wang Y, Chu Y, Li K, Zhang G, Guo Z, Wu X, et al. Exosomes secreted by adipose-derived mesenchymal stem cells foster metastasis and osteosarcoma proliferation by increasing COLGALT2 expression. *Front Cell Dev Biol*. (2020) 8:353. doi: 10.3389/fcell.2020.00353

91. Hu L, Wang J, Zhou X, Xiong Z, Zhao J, Yu R, et al. Exosomes derived from human adipose mensenchymal stem cells accelerates cutaneous wound healing via optimizing the characteristics of fibroblasts. *Sci Rep*. (2016) 6:32993. doi: 10.1038/srep32993

92. Choi EW, Seo MK, Woo EY, Kim SH, Park EJ, Kim S. Exosomes from human adipose-derived stem cells promote proliferation and migration of skin fibroblasts. *Exp Dermatol*. (2018) 27(10):1170–2. doi: 10.1111/exd.13451

93. Yang C, Luo L, Bai X, Shen K, Liu K, Wang J, et al. Highly-expressed micoRNA-21 in adipose derived stem cell exosomes can enhance the migration and proliferation of the HaCaT cells by increasing the MMP-9 expression through the PI3K/AKT pathway. *Arch Biochem Biophys*. (2020) 681:108259. doi: 10.1016/j.abb.2020.108259

94. Wang L, Hu L, Zhou X, Xiong Z, Zhang C, Shehada HMA, et al. Exosomes secreted by human adipose mesenchymal stem cells promote scarless cutaneous repair by regulating extracellular matrix remodelling. *Sci Rep*. (2017) 7(1):13321. doi: 10.1038/s41598-017-12919-x

95. Guo S, Dipietro LA. Factors affecting wound healing. *J Dent Res*. (2010) 89 (3):219–29. doi: 10.1177/0022034509359125

96. Werner S, Grose R. Regulation of wound healing by growth factors and cytokines. *Physiol Rev*. (2003) 83(3):835–70. doi: 10.1152/physrev.2003.83.3.835

97. Shiekh PA, Singh A, Kumar A. Data supporting exosome laden oxygen releasing antioxidant and antibacterial cryogel wound dressing OxOBand alleviate diabetic and infectious wound healing. *Data Brief*. (2020) 31:105671. doi: 10.1016/j.dib.2020.105671

98. Zhao B, Zhang X, Zhang Y, Lu Y, Zhang W, Lu S, et al. Human exosomes accelerate cutaneous wound healing by promoting collagen synthesis in a diabetic mouse model. *Stem Cells Dev*. (2021) 30(18):922–33. doi: 10.1089/scd.2021.0100

99. Guo S, Wang T, Zhang S, Chen P, Cao Z, Lian W, et al. Adipose-derived stem cell-conditioned medium protects fibroblasts at different senescent degrees from UVB irradiation damages. *Mol Cell Biochem*. (2020) 463(1–2):67–78. doi: 10.1007/s11010-019-03630-8

100. Li L, Ngo HTT, Hwang E, Wei X, Liu Y, Liu J, et al. Conditioned medium from human adipose-derived mesenchymal stem cell culture prevents UVB-induced skin aging in human keratinocytes and dermal fibroblasts. *Int J Mol Sci*. (2019) 21(1):49. doi: 10.3390/ijms21010049

101. Wang J, Yi Y, Zhu Y, Wang Z, Wu S, Zhang J, et al. Effects of adipose-derived stem cell released exosomes on wound healing in diabetic mice. *Zhongguo Xiu Fu Chong Jian Wai Ke Za Zhi*. (2020) 34(1):124–31. doi: 10.7507/1002-1892.201903058

102. Li Q, Wang Z, Xing H, Wang Y, Guo Y. Exosomes derived from miR-188-3p-modified adipose-derived mesenchymal stem cells protect Parkinson's Disease. *Mol Ther Nucleic Acids*. (2021) 23:1334–44. doi: 10.1016/j.omtn.2021.01.022

frontiers | Frontiers in Surgery

TYPE Original Research
PUBLISHED 04 October 2022
DOI 10.3389/fsurg.2022.1029991

Check for updates

OPEN ACCESS

EDITED BY
Kun Xiong,
Central South University, China

REVIEWED BY
Xi Zhao,
Philips Healthcare, China
Fei Wenmin,
China-Japan Friendship Hospital, China

*CORRESPONDENCE
Jiehua Li
jiehuali_fs@163.com
Xiaobing Pi
pxbingice@163.com
Wei Luo
luowei_421@163.com

†These authors have contributed equally to this work

SPECIALTY SECTION
This article was submitted to Reconstructive and Plastic Surgery, a section of the journal Frontiers in Surgery

RECEIVED 28 August 2022
ACCEPTED 15 September 2022
PUBLISHED 04 October 2022

CITATION
Ou C, Zhou S, Yang R, Jiang W, He H, Gan W, Chen W, Qin X, Luo W, Pi X and Li J (2022) A deep learning based multimodal fusion model for skin lesion diagnosis using smartphone collected clinical images and metadata. Front. Surg. 9:1029991. doi: 10.3389/fsurg.2022.1029991

COPYRIGHT
© 2022 Ou, Zhou, Yang, Jiang, He, Gan, Chen, Qin, Luo, Pi and Li. This is an open-access article distributed under the terms of the Creative Commons Attribution License (CC BY). The use, distribution or reproduction in other forums is permitted, provided the original author(s) and the copyright owner(s) are credited and that the original publication in this journal is cited, in accordance with accepted academic practice. No use, distribution or reproduction is permitted which does not comply with these terms.

# A deep learning based multimodal fusion model for skin lesion diagnosis using smartphone collected clinical images and metadata

Chubin Ou[1,2†], Sitong Zhou[3†], Ronghua Yang[4†], Weili Jiang[2], Haoyang He[2], Wenjun Gan[5], Wentao Chen[5], Xinchi Qin[5], Wei Luo[1*], Xiaobing Pi[3*] and Jiehua Li[3*]

[1]Clinical Research Institute, The First People's Hospital of Foshan, Foshan, China, [2]R&D Center, Visionwise Medical Technology, Foshan, China, [3]Department of Dermatology, The First People's Hospital of Foshan, Foshan, China, [4]Department of Burn and Plastic Surgery, Guangzhou First People's Hospital, South China University of Technology, Guangzhou, China, [5]Guangdong Medical University, Zhanjiang, China

**Introduction:** Skin cancer is one of the most common types of cancer. An accessible tool to the public can help screening for malign lesion. We aimed to develop a deep learning model to classify skin lesion using clinical images and meta information collected from smartphones.

**Methods:** A deep neural network was developed with two encoders for extracting information from image data and metadata. A multimodal fusion module with intra-modality self-attention and inter-modality cross-attention was proposed to effectively combine image features and meta features. The model was trained on tested on a public dataset and compared with other state-of-the-art methods using five-fold cross-validation.

**Results:** Including metadata is shown to significantly improve a model's performance. Our model outperformed other metadata fusion methods in terms of accuracy, balanced accuracy and area under the receiver-operating characteristic curve, with an averaged value of $0.768 \pm 0.022$, $0.775 \pm 0.022$ and $0.947 \pm 0.007$.

**Conclusion:** A deep learning model using smartphone collected images and metadata for skin lesion diagnosis was successfully developed. The proposed model showed promising performance and could be a potential tool for skin cancer screening.

KEYWORDS

deep learning - artificial neural network, multimodal fusion, metadata, skin cancer, attention

## Introduction

Skin cancer is one of the most common types of cancer. The number of skin cancer diagnosed all over the world reached 1.2 million in 2020 (1). Skin cancer is caused by damaged skin cells or abnormal growth of skin cells, which is closely related to excessive exposure to ultraviolet radiation, chemical carcinogens, and radioactive

radiation (2). Early detection and treatment can improve the survival of patients. Dermoscope is a powerful tool used to observe pigmented skin disorders (2). By examining dermoscopic images, dermatologists can diagnose and grade a patient's lesion condition. However, reading dermoscopic images mainly relies on the experience and subjective judgments of dermatologists, which may introduce errors in the diagnosis process. Moreover, the cost of dermoscopy is relatively high, which imposes a considerable burden on patients in some underdeveloped country. Therefore, it is necessary to develop an automated tool to help to diagnose skin cancer and disease using affordable devices such as smartphone. Such a tool can reduce the cost, shorten the waiting time, and improve the accuracy of diagnosis.

Deep learning has emerged as a promising technology of artificial intelligence in recent years. With the continuous progress in the field of deep learning, artificial intelligence has made great breakthroughs in the field of medicine. Researchers have also shown positive outcomes in the smart diagnosis of skin cancer based on medical images. Various methods are proposed to diagnose skin cancers based on images (3). A mole classification system for early diagnosis of melanoma skin was proposed (4). The features were extracted according to the ABCD (5) rules of the lesions and classified them into common moles, rare moles and melanoma moles using a back-propagation feed-forward neural network. Aswin et al. (6) proposed a method for skin cancer detection based on Genetic Algorithm (GA) and Neural Network Algorithm, which divided lesion images into two categories: cancerous and non-cancerous. A skin cancer detection system based on convolutional neural network (CNN) was proposed by Mahbod et al. (7) who extracted deep features from pretrained deep CNNs for classification of skin diseases. Kalouche (8) proposed to finetune a pretrained deep CNN architecture VGG-16 and achieved an accuracy of 78%. A method combining a self-organizing neural network and a radial basis function (RBF) neural network was proposed to diagnose three different types of skin cancers with an accuracy of 93%, a significant improvement over traditional classifiers (9). Bisla et al. (10) proposed a deep learning method for data cleaning and a GAN method for data augmentation, which achieved 86.01% classification accuracy. Ali et al. also proposed a skin damage data enhancement method based on self-attention progressive GAN (11).

In real-world clinical setting, dermatologists make medical decision by considering a variety of information, including different types of imaging result, laboratory result, demographic information and patient feedback on their own feeling. To better utilize information from multiple sources, multi-modal fusion classification is introduced into the detection and classification of skin cancer. Cai et al. (12) proposed a multimodal transformer to fuse multimodal information. Chen et al. (13) proposed a skin cancer Multimodal Data Fusion Diagnosis Network (MDFNet) framework based on a data fusion strategy to effectively fuse clinical skin images with patient clinical data. Yap et al. (15) propose a method that combines multiple imaging modalities with patient metadata to improve the performance of automated skin lesion diagnosis. Li et al. proposed the MetaNet, which uses a sequence of 1D convolution on metadata to extract coefficients to assist visual features extracted from images in the classification task (16). Pacheco et al. developed a metadata processing block (MetaBlock) to fuse metadata with image data, which outperformed MetaNet and conventional feature concatenation method (17).

However, previous studies mainly focus the combination of metadata and image feature without exploring the underlying relationship between the two modalities. We argued that metadata provides extra information which can guide the interpretation of image. Similarly, image features also contain unique information which can guide the understanding of metadata. The two data modalities can facilitate each other to better unveil features that are most relevant to disease classification. We therefore proposed an attention-guided multimodal fusion network to better integrate imaging data and metadata for skin lesion diagnosis.

# Methods

## Model development

In medical diagnosis, clinicians are usually faced with multiple sources of information. Such information usually includes medical images and metadata (clinical or demographic supporting information that are not in the form of images). Medical decision is made after aggregating various aspects of information. In deep learning, the simplest method to combine information from different sources is channel concatenation. However, since imaging data is usually in higher dimensional than metadata, simply concatenating or adding them may not be the optimal solution for information fusion. We therefore proposed our method called multimodal fusion network (MMF-Net) to better solve the problem of image and metadata fusion.

## Experiment description

In this study, we used the images and meta information provided in PAD-UPES-20 as our experimental data (17). Data were obtained from the Dermatological and Surgical Assistance Program at the Federal University of Espírito Santo (UFES), and all samples were representative of skin lesions in patients and consisted of images and meta data. The dataset includes 2,298 images collected from smartphones including 6

different types of skin lesions. Each image also contains up to 21 clinical characteristics, including but not limited to age, lesion location, Fitzpatrick skin type, and lesion diameter. All data can be accessed on the following website https://data.mendeley.com/datasets/zr7vgbcyr2/1.1. In the dataset, among the 2,298 cases, 730 of them are actinic keratosis (ACK), 845 are Basal Cell Carcinoma (BCC), 52 are malignant melanoma (MEL), 244 are Melanocytic Nevus of Skin (NEV), 192 are Squamous Cell Carcinoma (SCC) and 235 are Seborrheic Keratosis (SEK).

## Model construction

To classify skin lesion types, each sample is given a smartphone photo and accompanying meta information, shown in Table 1. A convolutional neural network such as ResNet-50 was used to extract features from the smartphone image, denoted as $x_{img}$. Metadata is preprocessed as follow: numerical features were kept the same; Boolean features were converted to 0 and 1. Categorical features were one-hot encoded. For example, for the gender attribute, the one-hot encoding is [1,0] for male, [0,1] for female and [0,0] for missing information. A multi-layer perceptron was applied to extract features from meta information, denoted as $x_{meta}$. Our goal is to estimate the probability $y$ of a skin lesion belonging to a certain class $c$ in one of the six categories: Basal Cell Carcinoma (BCC), Squamous Cell Carcinoma (SCC), Actinic Keratosis (ACK), Seborrheic Keratosis (SEK), Melanoma (MEL), and Nevus (NEV), given the input image and meta information.

$$\hat{y} = p(y = c|x_{img}, x_{meta})$$

The overall design of the network is shown in Figure 1. The image encoder and meta encoder extract features from image and meta information, respectively. The extracted features are then fused together by the multimodal fusion module and passed into the classifier module composed of a fully connected layer. The final output is a six-channel vector representing the probability of six lesion types.

The simplest method of combining image and meta information, is by concatenating their corresponding features $x_{img}$ and $x_{meta}$ in the channel dimension or by summation. Yet these approaches essentially treat image and meta information as the same, ignoring the underlying differences between them. Moreover, there are inter-correlation between image and meta information, complementing of each other, which may be overlooked by simple combination. To exploit such intrinsic connection between two modalities, an attention-based multi-modality fusion module is proposed. Basically, what the attention mechanism does is to assign different weights to different features. Features with larger weights are considered to be more important in the diagnosis process and vice versa. One typical example for the use of attention mechanism is, if a specific body location is related to just one or few types of skin diseases, when such information is available as meta data, it could be used to directly suppress the prediction probability of other irrelevant diseases, thus guiding the network to focus on the rest possible types. The overall design of the fusion module, composed of intra-modality self-attention and inter-modality cross-attention, is shown in Figure 2.

TABLE 1 Description of attributes in meta information.

| Meta variable | Description | *P* value |
|---|---|---|
| Smoking | | <0.001 |
| Drinking | | 0.476 |
| Father country | Which country the patient's father is from | <0.001 |
| Mother country | Which country the patient's mother is from | 0.012 |
| Age | | <0.001 |
| Gender | | 0.032 |
| Cancer history | If the patient or someone in their family had history of any type of cancer in the past | 0.821 |
| Skin cancer history | If the patient or someone in their family had history of skin cancer in the past | 0.067 |
| Pesticide | If the patient use pesticide | <0.001 |
| Sewage system | If the patient has sewage system access in their home | 0.019 |
| Piped water | If the patient has piped water access in their home | 0.029 |
| Fitspatrick skin type | | <0.001 |
| Region | Living region | 0.598 |
| Diameter 1 | Horizontal diameter of lesion | <0.001 |
| Diameter 2 | Vertical diameter of lesion | <0.001 |
| Itch | If the lesion itches | <0.001 |
| Grew | If the lesion has grown recently | <0.001 |
| Hurt | If the lesion hurts | <0.001 |
| Changed | If the lesion has changed recently | <0.001 |
| Bleed | If the lesion has bled | <0.001 |
| Elevation | If the lesion has an elevation | <0.001 |

## Intra-modality self-attention

There may exist irrelevant information in each modality (e.g., image background in image). To avoid irrelevant information to confuse the neural network and to better guide the network to focus on key features, a multi-head self-attention module is applied to the two features, respectively. A typical attention module is consisting of two steps, linearly projecting the input feature $x$ into Query (Q), Key (K) and Value (V) vector, followed by multiplying $V$ by the attention

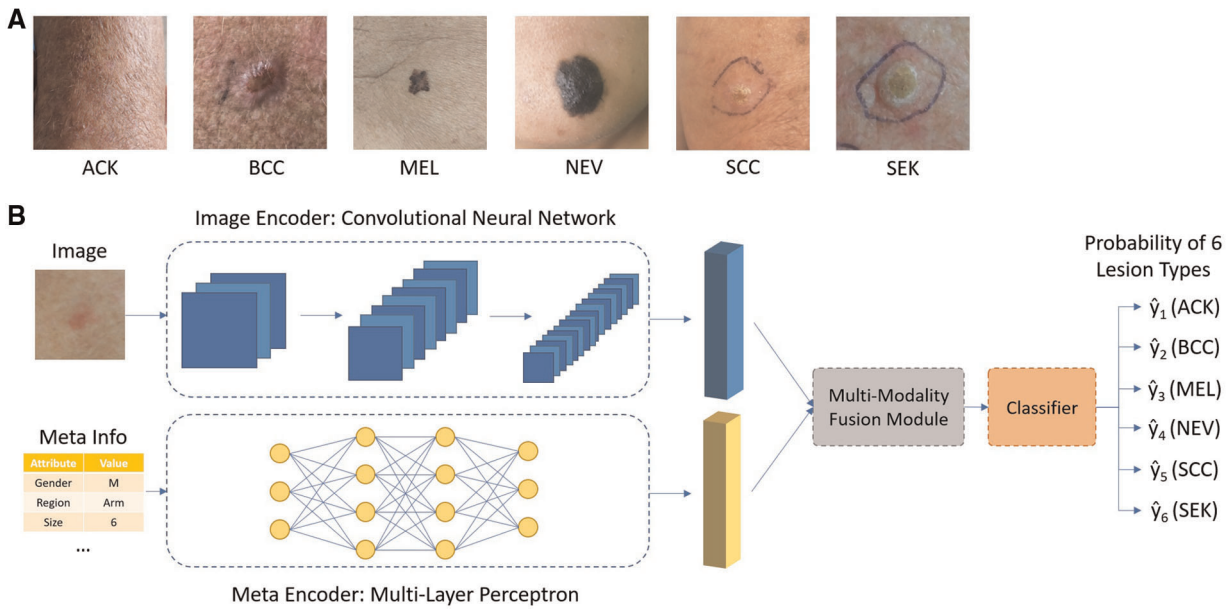


FIGURE 1
(A) Typical images of different types of skin lesions; (B) overall network architecture of the proposed network.

weight obtained from dot-product of $Q$ and $K$ to get the weighted feature $x'$, shown as below:

$$Q = W_q x, \quad K = W_k x, \quad V = W_v x$$

$$x' = Softmax\left(\frac{QK^T}{\sqrt{d}}\right)V$$

After passing through the self-attention module, we obtained the weighted $x_{img}$ and $x_{meta}$, which gives high weighting to cancer-relevant information and low weighting to irrelevant information.

## Inter-modality cross-attention

This module contains two paths. One path is designed to use meta information to guide the selection of most relevant information from image feature. The other path is designed the other way around, to use image feature to guide the selection of most relevant information from meta data. For the first path, a cross-attention module is designed with input vector Query and Value from $x_{img}$ projection and Key from $x_{meta}$, shown as below:

$$Q_1 = W_{q1}x'_{img}, \quad K_1 = W_{k1}x'_{imeta}, \quad V_1 = W_{v1}x'_{img}$$

$$x''_{img} = Softmax\left(\frac{Q_1{K_1}^T}{\sqrt{d}}\right)V_1$$

For the second part, a cross-attention module is designed with input vector Query and Value from $x_{meta}$ projection and Key from $x_{img}$, shown as below:

$$Q_2 = W_{q2}x'_{meta}, \quad K_2 = W_{k2}x'_{img}, \quad V_2 = W_{v2}x'_{meta}$$

$$x''_{meta} = Softmax\left(\frac{Q_2{K_2}^T}{\sqrt{d}}\right)V_2$$

We then concatenated $x_{meta}$" and $x_{img}$" to obtained the final feature vector $x_{final}$ that is passed into a fully connected layer and a softmax layer to output the probability of six lesion classes.

## Training and evaluation procedures

To ensure a fair comparison with other methods, we followed the experimental setup as that in Andre's work (14). We measured different methods' performance by calculating the following metrics including, accuracy (ACC), balanced accuracy (BACC) and aggregated area under the curve (AUC). The balanced accuracy is calculated by the arithmetic mean of sensitivity and specificity. As we can see that the portion of different diseases in the dataset is imbalanced, balanced accuracy is therefore more favored in such case as accuracy may be biased. The aggregated area under the curve is obtained by computing the average AUC of all possible pairwise combinations of the six classes, which will not be

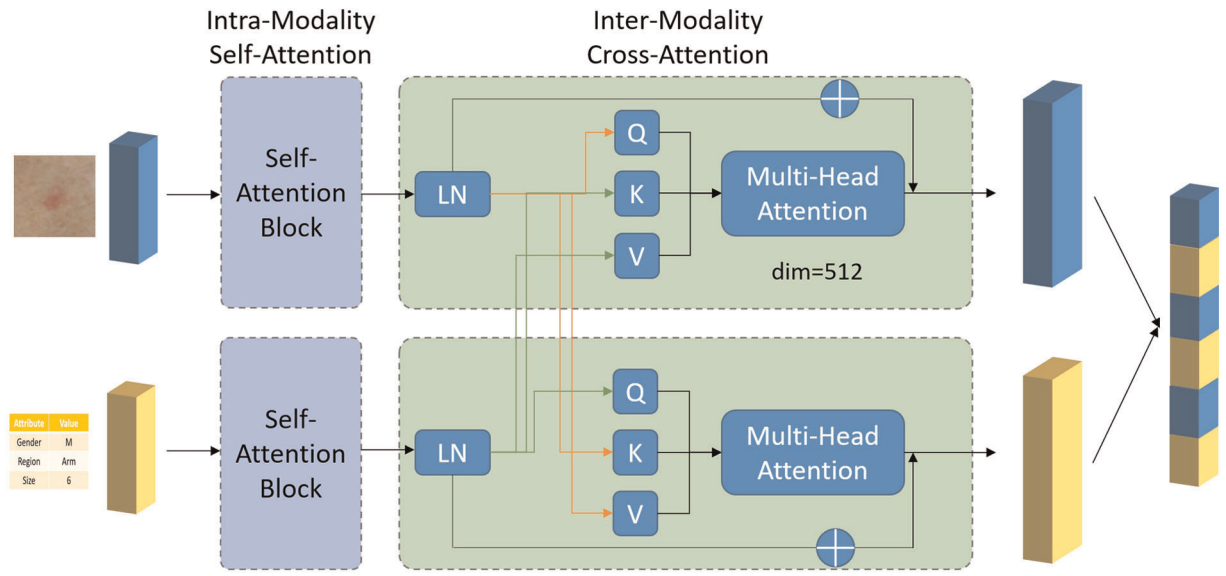


FIGURE 2
Network architecture of the proposed multimodal fusion module.

biased by imbalanced class distribution in our data. Five-fold cross-validation stratified by the label's frequency was applied for each competing method, namely baseline feature concatenation, MetaNet, MetaBlock and our proposed method. In each split, the whole dataset is split into five folds. Four folds were used as training set and the remaining fold was used as test set. The process was repeated five times until each fold has been used as test set at least once. The averaged performance of the five folds were reported.

During training, we used the SGD optimizer with an initial learning rate of 0.001. The learning rate is reduced to 0.1 of its current value if training loss stop to decrease within 10 epochs. A total of 100 epochs were trained for each method. Data augmentations such as horizontal and vertical flipping, color jittering, gaussian noise and random contrast were applied on-the-fly during training. All codes were written in Python 3.6.10. PyTorch framework (v1.7.0) was used by constructed the neural network.

## Statistical analysis

Metadata attributes were examined by univariate analysis. Continuous variables were first examined by Shapiro–Wilk test to determine if they were normally distributed. Student *t* test (for normally distributed parameters) or Mann–Whitney *U* test (for non-normally distributed parameters) were used to identify statistically significant variable between different skin lesion types. Categorical variables were compared by chi-square test. To compare different methods' performance, non-parametric Friedman test followed by the Wilcoxon test were used. $P < 0.05$ is consider to be statistically significant. The statistical analysis was performed with SPSS (IBM, version 26).

TABLE 2 Performance comparison of different methods.

| | ACC | BACC | AUC |
|---|---|---|---|
| No metadata | 0.616 ± 0.051 | 0.651 ± 0.050 | 0.901 ± 0.007 |
| Concatenation | 0.741 ± 0.014 | 0.728 ± 0.029 | 0.929 ± 0.006 |
| MetaBlock | 0.735 ± 0.013 | 0.765 ± 0.017 | 0.935 ± 0.004 |
| MetaNet | 0.732 ± 0.054 | 0.742 ± 0.019 | 0.936 ± 0.006 |
| Our Method | 0.768 ± 0.022 | 0.775 ± 0.022 | 0.947 ± 0.007 |

TABLE 3 Result of the Wilcoxon pair test for different methods.

| Pair | *P* value |
|---|---|
| No metadata—our method | <0.001 |
| MetaBlock—our method | 0.028 |
| MetaNet—our method | 0.035 |

# Results

The statistical significance of the difference of metadata attributes between different lesion types is shown in Table 1. Most metadata attributes are significantly correlated with different types of skin lesion. The averaged five-fold cross-validation performance of each method is presented in Table 2. Our proposed method achieved the best performance

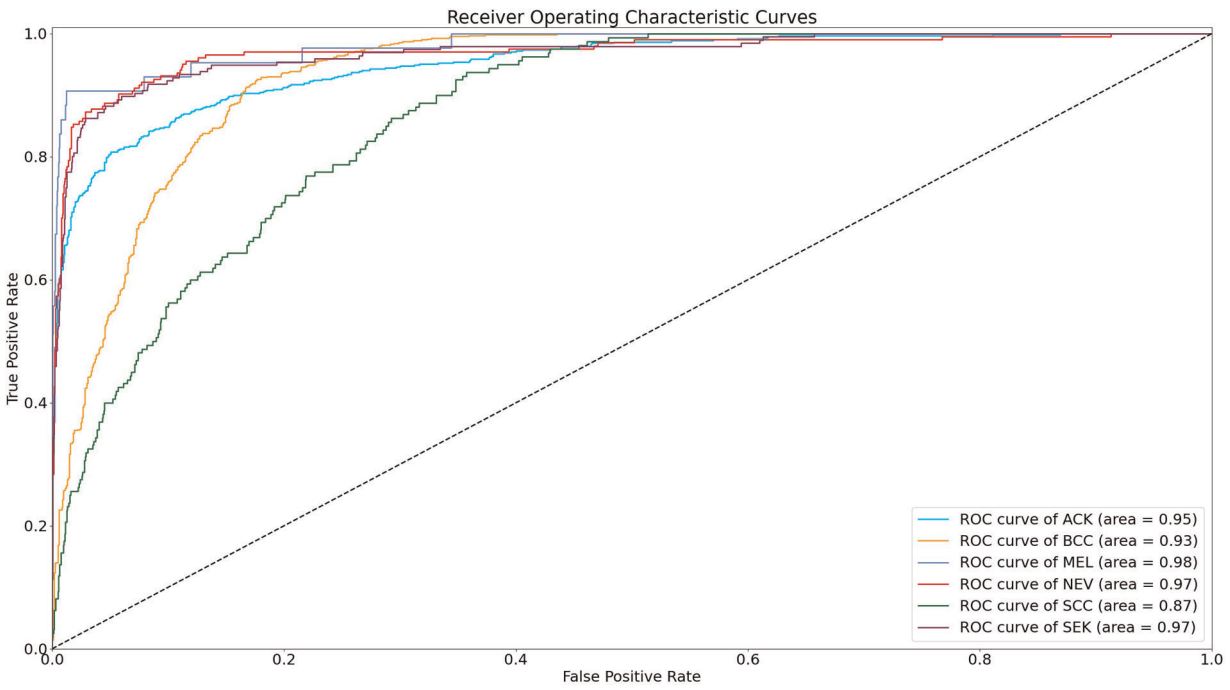


FIGURE 3
Receiver operating characteristic curves for different types of skin lesions.

in ACC ($0.768 \pm 0.022$), BACC ($0.775 \pm 0.022$) and AUC (s) metrics. We can observe that including meta information significantly improves the performance in terms of AUC ($0.947 \pm 0.007$ vs. $0.901 \pm 0.007$, $P < 0.001$), ACC ($0.768 \pm 0.022$ vs. $0.616 \pm 0.051$, $P < 0.001$) and BACC ($0.775 \pm 0.022$ vs. $0.651 \pm 0.050$, $P < 0.001$), as shown in **Table 3**. Our proposed method utilized meta information in a more effective way, which significantly outperformed the other two methods MetaNet ($P = 0.035$) and MetaBlock ($P = 0.028$). The ROC curves for six lesion types are plotted in **Figure 3**. The proposed method achieved the best performance for MEL (AUC = 0.98), followed by NEV (AUC = 0.97), SEK (AUC = 0.97), ACK (AUC = 0.95) and BCC (AUC = 0.93). SCC is the most difficult one to identify, with AUC = 0.87. The averaged AUC of six disease types is 0.947. We further examined the failed cases. **Figure 4** shows the averaged confusion matrix, from which we can see that SCC has the lowest accuracy because it is often mistaken as BCC. This is understandable as our images are collected from smartphone. Clinically, there is a tendency of SCC misdiagnosed as BCC. Using dermoscopy can improve the diagnostic accuracy (22). We further performed an ablation study to analyze different components' effect on the final result. **Table 4** shows the performance of the model without the inter-modality self-attention and model without the intra-modality cross-attention. This indicates that the two modules act synergistically to improve the fusion of image and metadata.

## Discussion

We have developed a deep learning model to diagnose skin lesion by using clinical images and meta information obtained from smartphones. We proposed a new module which uses the combination of intra-modality self-attention and inter-modality cross-attention to better fuse image and metadata. The proposed model achieved promising performance on the public dataset, outperforming other state-of-the-art methods.

Compared with previous work (MetaNet, MetaFuse) on metadata fusion, our method has made two improvements. First, we used a multi-head self-attention module which calculates the feature correlation matrix to assign attention weights to different features within the same modality, removing irrelevant information in each modality. Second, unlike previous works where the attention is one-way (metadata feature $\geq$ image feature), our attention mechanism works two-way. Metadata features are used to guide the attention on image features and vice versa, image features are also used to guide the attention on metadata features. This has enabled our model to better exploit the information in each modality and outperform the other methods, as demonstrated in our experiments.

Many previous studies applying artificial intelligence to skin disease diagnosis focused on dermoscopy images only. However, dermoscope is not always accessible to many people in rural area or in underdeveloped country. In contrast,

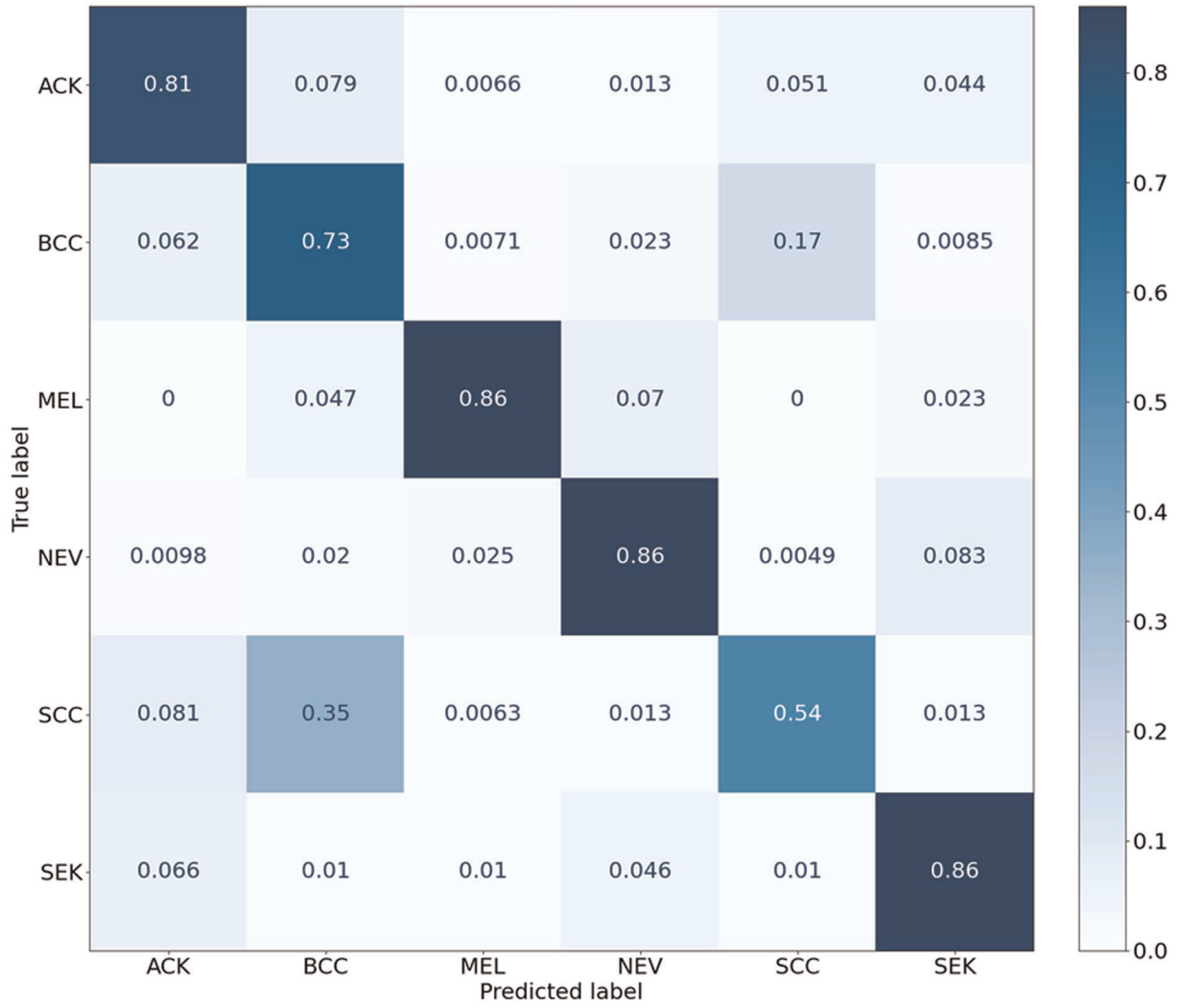


FIGURE 4
Confusion matrix of different types of skin lesions.

TABLE 4 Ablation study of the proposed method.

| | ACC | BACC | AUC |
|---|---|---|---|
| w/o Self-attention | 0.757 ± 0.026 | 0.765 ± 0.025 | 0.938 ± 0.008 |
| w/o Cross-attention | 0.743 ± 0.021 | 0.759 ± 0.021 | 0.936 ± 0.006 |
| Full module | 0.768 ± 0.022 | 0.775 ± 0.022 | 0.947 ± 0.007 |

smartphone is a more accessible tool to many patients. Moreover, many patients tend to seek advices online instead of scheduling a visit to the clinic at the early stage of skin disease, which can delay their treatment and result in poor prognosis. The model developed in the current study can be integrated into a smartphone-based automatic screening app, which can help to identify high risk lesion and urge the patient for immediate treatment.

In real world clinical settings, dermatologists seldom make decision solely based on images. They usually make their judgement based on patient demographics (age, gender) and lesion characteristics (anatomical region) (18) which cannot be simply obtained from images. They also consider other risk factors such as cancer history, exposure to chemical and types of skin (19). Including meta information and multiple sources of data has been proved to be helpful for deep learning model in some previous studies (20, 21). In this study, we incorporated meta information into neural network and have showed that it can significantly improve the skin lesion diagnostic performance. Such information can be easily obtained in the form of online questionnaire which costs only a few clicks on the app from the user.

Though we have developed a promising model for skin lesion diagnosis, there are several limitations in our study.

The number of included skin lesion types is relatively few compared to real world scenario. This can be improved by collecting data from more diseases in the future. External validation using data collected from different sites is needed before the model is put into clinical practice.

## Conclusion

We have developed a deep learning model to diagnose skin lesion using clinical images and meta information obtained from smartphones. A new module consisting of intra-modality self-attention and inter-modality cross-attention is proposed to better fuse image data and metadata and is shown to outperformed other state-of-the-art methods. Our proposed model could be integrated into smartphone as a potential and handy tool to screen for skin disease and skin cancer.

## Data availability statement

The original contributions presented in the study are included in the article/Supplementary Material, further inquiries can be directed to the corresponding author/s.

## Author contributions

CO, SZ, and RY contributed to conception and design of the study. CO, HH and WJ completed the code and analysis. SZ and RY performed the statistical analysis. CO and HH wrote the first draft of the manuscript. SZ, RY, WG, WC and XQ wrote sections of the manuscript. WL, XP and JL supervised the study. All authors contributed to the article and approved the submitted version.

## Funding

This study was supported by the National Natural Science Foundation of China (82002913), Guangdong Basic and Applied Basic Research Foundation (2021A1515011453, 2022A1515012160, 2021B1515120036, and 2022A1515012245) and the Medical Scientific Research Foundation of Guangdong Province (A2022293).

## Conflict of interest

The authors declare that the research was conducted in the absence of any commercial or financial relationships that could be construed as a potential conflict of interest.

## Publisher's note

All claims expressed in this article are solely those of the authors and do not necessarily represent those of their affiliated organizations, or those of the publisher, the editors and the reviewers. Any product that may be evaluated in this article, or claim that may be made by its manufacturer, is not guaranteed or endorsed by the publisher.

## References

1. Ferlay J, Colombet M, Soerjomataram I, Parkin DM, Piñeros M, Znaor A, et al. Cancer statistics for the year 2020: an overview. *Int J Cancer*. (2021) 149 (4):778–89. doi: 10.1002/ijc.33588

2. Khan IU, Aslam N, Anwar T, Aljameel SS, Ullah M, Khan R, et al. Remote diagnosis and triaging model for skin cancer using efcientnet and extreme gradient boosting. *Complexity*. (2021) 2021:5591614. doi: 10.1155/2021/5591614

3. Dildar M, Akram S, Irfan M, Khan HU, Ramzan M, Mahmood AR, et al. Skin cancer detection: a review using deep learning techniques. *Int J Environ Res Public Health*. (2021) 18(10):5479. doi: 10.3390/ijerph18105479

4. Cueva WF, Munoz F, Vasquez G, Delgado G. *Detection of skin cancer "melanoma" through computer vision*. In: *Proceedings of the 2017 IEEE XXIV international conference on electronics, electrical engineering and computing (INTERCON), Cusco, Peru*; 15–18 August 2017. p. 1–4.

5. Nachbar F, Stolz W, Merkle T, Cognetta AB, Vogt T, Landthaler M, et al. The ABCD rule of dermatoscopy: high prospective value in the diagnosis of doubtful melanocytic skin lesions. *J Am Acad Dermatol*. (1994) 30(4):551–9. doi: 10.1016/S0190-9622(94)70061-3

6. Aswin RB, Jaleel JA, Salim S. *Hybrid genetic algorithm: artificial neural network classifier for skin cancer detection*. In: *Proceedings of the 2014 international conference on control, instrumentation, communication and computational technologies (ICCICCT), kanyakumari, India*; 10–11 July 2014. p. 1304–9.

7. Mahbod A, Schaefer G, Wang C, Ecker R, Ellinge I. *Skin lesion classification using hybrid deep neural networks*. In: *Proceedings of the ICASSP 2019–2019 IEEE international conference on acoustics, speech and signal processing (ICASSP), brighton, UK*; 12–17 May 2019. p. 1229–33.

8. Kalouche S. Vision-based classification of skin cancer using deep learning (2016). Available at: https://www.semanticscholar.org/paper/Vision-Based-Classification-of-Skin-Cancer-using-Kalouche/b57ba909756462d812dc20fca157b397 2bc1f533 (Accessed January 10, 2021).

9. Mengistu AD, Alemayehu DM. Computer vision for skin cancer diagnosis and recognition using RBF and SOM. *Int J Image Process*. (2015) 9:311–9. doi: 10.1007/s00432-022-04180-1

10. Bisla D, Choromanska A, Stein JA, Polsky D, Berman R. Towards automated melanoma detection with deep learning: data purification and augmentation. *arXiv*. (2019) 2720–28. doi: 10.48550/arXiv.1902.06061

11. Abdelhalim ISA, Mohamed MF, Mahdy YB. Data augmentation for skin lesion using self-attention based progressive generative adversarial network. *Expert Systems with Applications*. (2021) 165:113922. doi: 10.48550/arXiv.1910.11960

12. Cai G, Zhu Y, Wu Y, Jiang X, Ye J, Yang D. A multimodal transformer to fuse images and metadata for skin disease classification. *Vis Comput*. (2022):1–13. doi: 10.1007/s00371-022-02492-4

13. Chen Q, Li M, Chen C, Zhou P, Lv X, Chen C. MDFNet: application of multimodal fusion method based on skin image and clinical data to skin cancer

classification. *J Cancer Res Clin Oncol*. (2022) 1–13. doi: 10.1007/s00432-022-04180-1

14. Pacheco AG, Krohling RA. An attention-based mechanism to combine images and metadata in deep learning models applied to skin cancer classification. *IEEE J Biomed Health Inform*. (2021) 25(9):3554–63. doi: 10.1109/JBHI.2021.3062002

15. Yap J, Yolland W, Tschandl P. Multimodal skin lesion classification using deep learning. *Exp Dermatol*. (2018) 27(11):1261–7. doi: 10.1111/exd.13777

16. Li W, Zhuang J, Wang R, Zhang J, Zheng W-S. Fusing metadata and dermoscopy images for skin disease diagnosis. In: *2020 IEEE 17th international symposium on biomedical imaging (ISBI)*. IEEE (2020). pp. 1996–2000.

17. Pacheco AG, Lima GR, Salomão AS, Krohling B, Biral IP, de Angelo GG, et al. PAD-UFES-20: a skin lesion dataset composed of patient data and clinical images collected from smartphones. *Data Brief*. (2020) 32:106221. doi: 10.1016/j.dib.2020.106221

18. Wolff K, Johnson RA, Saavedra AP, Roh EK. *Fitzpatrick's color atlas and synopsis of clinical dermatology*. 8th edn. New York, USA: McGraw-Hill Education (2017).

19. Duarte AF, Sousa-Pinto B, Haneke E, Correia O. Risk factors for development of new skin neoplasms in patients with past history of skin cancer: a survival analysis. *Sci Rep*. (2018) 8(1):1–6. doi: 10.1038/s41598-018-33763-7

20. Kharazmi P, Kalia S, Lui H, Wang Z, Lee T. A feature fusion system for basal cell carcinoma detection through data-driven feature learning and patient profile. *Skin Res Technol*. (2018) 24(2):256–64. doi: 10.1111/srt.12422

21. Ou C, Li C, Qian Y, Duan CZ, Si W, Zhang X, et al. Morphology-aware multi-source fusion–based intracranial aneurysms rupture prediction. *Eur Radiol*. (2022) 32:5633–41. doi: 10.1007/s00330-022-08608-7

22. Ryu TH, Kye H, Choi JE, Ahn HH, Kye YC, Seo SH. Features causing confusion between basal cell carcinoma and squamous cell carcinoma in clinical diagnosis. *Ann Dermatol*. (2018) 30(1):64–70. doi: 10.5021/ad.2018.30.1.64

frontiers | Frontiers in Surgery

TYPE Review
PUBLISHED 14 October 2022
DOI 10.3389/fsurg.2022.988843

Check for updates

OPEN ACCESS

EDITED BY
Kun Xiong,
Independent researcher, China

REVIEWED BY
Khondoker Mehedi Akram,
The University of Sheffield, United Kingdom
Bob Liu,
Tsinghua University, China

*CORRESPONDENCE
Yuansen Luo
drjasonlaw@outlook.com
Yongjun Du
fsdyjun@163.com

†These authors have contributed equally to this work

SPECIALTY SECTION
This article was submitted to Reconstructive and Plastic Surgery, a section of the journal Frontiers in Surgery

RECEIVED 07 July 2022
ACCEPTED 20 September 2022
PUBLISHED 14 October 2022

CITATION
Luo Y, Xu X, Ye Z, Xu Q, Li J, Liu N and Du Y (2022) 3D bioprinted mesenchymal stromal cells in skin wound repair.
Front. Surg. 9:988843.
doi: 10.3389/fsurg.2022.988843

COPYRIGHT
© 2022 Luo, Xu, Ye, Xu, Li, Liu and Du. This is an open-access article distributed under the terms of the Creative Commons Attribution License (CC BY). The use, distribution or reproduction in other forums is permitted, provided the original author(s) and the copyright owner(s) are credited and that the original publication in this journal is cited, in accordance with accepted academic practice. No use, distribution or reproduction is permitted which does not comply with these terms.

# 3D bioprinted mesenchymal stromal cells in skin wound repair

Yuansen Luo*†, Xuefeng Xu†, Zhiming Ye, Qikun Xu, Jin Li, Ning Liu and Yongjun Du*

Department of the Second Plastic and Aesthetic Surgery, the First People's Hospital of Foshan, Foshan, China

Skin tissue regeneration and repair is a complex process involving multiple cell types, and current therapies are limited to promoting skin wound healing. Mesenchymal stromal cells (MSCs) have been proven to enhance skin tissue repair through their multidifferentiation and paracrine effects. However, there are still difficulties, such as the limited proliferative potential and the biological processes that need to be strengthened for MSCs in wound healing. Recently, three-dimensional (3D) bioprinting has been applied as a promising technology for tissue regeneration. 3D-bioprinted MSCs could maintain a better cell ability for proliferation and expression of biological factors to promote skin wound healing. It has been reported that 3D-bioprinted MSCs could enhance skin tissue repair through anti-inflammatory, cell proliferation and migration, angiogenesis, and extracellular matrix remodeling. In this review, we will discuss the progress on the effect of MSCs and 3D bioprinting on the treatment of skin tissue regeneration, as well as the perspective and limitations of current research.

KEYWORDS
skin tissue regeneration, biological engineering, 3D bioprinting, mesenchymal stromal cells, paracrine

## Introduction

Skin is the first barrier to protect us from invading pathogens and environmental challenges. However, skin tissue injury is common due to trauma and pathological situations such as diabetes mellitus and vascular disorder (1). Wound healing is a complex process which approximately may divide into three phases: inflammation, proliferation, and extracellular matrix (ECM) remodeling (2–4). Multiple cell types, such as platelets, neutrophils, macrophages, fibroblasts (FBs), and myofibroblasts, take part in the skin

Abbreviations
MSCs, mesenchymal stromal cells; 3D, three-dimensional; ECM, extracellular matrix; ESCs, embryonic stromal cells; iPSCs, induced pluripotent stromal cells; dECM, decellularized extracellular matrix; FBs, fibroblasts; ECs, endothelial cells; HDFs, human dermal fibroblasts; BMSCs, bone marrow stromal cells; ADSCs, adipose-derived stromal cells; HUC-MSCs, human umbilical cord-derived mesenchymal stromal cells; DFU, diabetic foot ulcers; HUVECs, human umbilical vein endothelial cells; LIFT, laser-induced forward transfer; NSCs, neural stromal cells; PCL, polycaprolactone; PLA, polylactic acid; PLGA, poly lactic-co-glycolic acid; Alg-Gel, alginate-gelatin; DLP, digital light processing; SLA, stereolithography; EVs, extracellular vehicles; GelMA, gelatin methacryloyl; ECFCs, endothelial colony-forming cells; KCs, keratinocytes; EPCs, endothelial progenitor cells; SG, sweat gland.

wound healing process, regulated by biological factors (5). As a result of various reasons, including physiological inflammatory, infection, or systemic diseases, it turns into a chronic wound, which brings an enormous economic burden and influences the population's health (6, 7). Over the decades, the field of skin tissue regeneration has made progress in acute and chronic wound healing. However, there is not enough solid evidence to support general therapeutic modalities that noticeably improve wound healing, including negative pressure or hyperbaric oxygen therapy. Further studies are needed to figure out a superior therapeutic method of skin wound healing (8).

Mesenchymal stromal cells (MSCs) make a novel and effective contribution to wound healing. They can be obtained from bone marrow, adipose, umbilical cord tissue (9–11), etc. Unlike embryonic stromal cells (ESCs) or induced pluripotent stromal cells (iPSCs), MSCs are easy to isolate from original tissues with less severe ethical issues and a lower risk of teratoma formation (12, 13). Both clinical and preclinical studies suggested that MSCs can accelerate re-epithelization, neovascularization, and collagen deposition to promote wound healing (14, 15). Recently, MSCs have been introduced as a new treatment for wound healing because of their biological characteristics and paracrine function, which could secrete various bioactive factors, such as vascular endothelial growth factor (VEGF), hepatocyte growth factor (HGF), transforming growth factor β1 (TGF-β1), KGF, IL-8, and IL-6 (16, 17). Moreover, as a cell-free therapy, extracellular vesicles (EVs) derived from MSCs have become a promising wound healing treatment. Extracellular vesicles contain abundant messenger RNA (mRNA), microRNAs (miRNAs), and long noncoding RNA (LncRNA) to regulate the activity of host cells and promote wound healing, avoiding risks related to cell transplant (18). Exosomes derived from MSCs have been confirmed that remarkably promote angiogenesis (19, 20), increase collagen synthesis (21), and expression of growth factors (22) in wound healing. Despite all the advantages of MSCs therapy, there are still difficulties, such as the limited proliferative potential and the biological processes that need to be strengthened.

Recently, three-dimensional (3D) bioprinting as additive manufacturing technology has been applied to fabricate tissues/organs to achieve the controllable spatial distribution of living cells and biological materials (23–25). With biocompatibility biomaterials, such as decellularized extracellular matrix (dECM), alginate and hyaluronic acid, 3D-bioprinted cells have been used for tissue repair (26). In the field of skin tissue regeneration, 3D-bioprinted bioengineered skin grafts containing FBs, endothelial cells (ECs), or human dermal fibroblasts (HDFs), have been proved could enhance skin wound repair (27, 28). In recent years, a variety of research explored the potential of MSCs as effective

TABLE 1 Research about 3D-bioprinted MSCs in skin tissue regeneration.

| Bioprinting strategies | Bioinks and seeded cell | Biological features | References |
|---|---|---|---|
| LIFT | Blood plasma/alginate and FBs/KCs/BMSCs/ADSCs | Bioprinted cells maintain the ability to proliferate and did not show an increase in apoptosis or DNA fragmentation. | (29) |
| | HA–fibrinogen and ADSCs/ECFCs | Bioprinted cells trigger the development of stable vascular-like networks by direct cell–cell contacts in vascular endothelial growth factor-free medium. | (129) |
| | Fibrin-collagen gel and AFSs/BMSCs | Bioprinted cells increased wound healing and angiogenesis in full-thickness skin mice wounds due to secreted trophic factors. | (30) |
| Extrusion and inkjet printing | S-dECM and EPCs/ADSCs | Bioprinted cells accelerated re-epithelization, neovascularization, and wound healing *in vivo*. | (130) |
| Extrusion-based | Collagen/alginate and ADSCs | Bioprinted cells accelerated wound contraction and healing with faster epithelization and formation of a multilayered epidermis *in vivo*. | (124) |
| | Gelatine/alginate/PMNT and UC-MSCs | Bioprinted cells accelerated the healing of full-thickness excisional wounds with preferable cell proliferation in the nutritionally deficient environment. | (11) |
| | Gelatine/alginate/SNAP and ADSCs | Bioprinted cells enhanced the migration and angiogenesis of HUVECs, as well as promoted severe burn wound healing through increased neovascularization *via* the VEGF signaling pathway. | (125) |
| | Alginate and BMSCs | Bioprinted cells maintained stemness and proangiogenic properties, with more extracellular vesicles. | (123) |
| | GelMA/curcumin and ADSCs | Bioprinted cells mitigated AGE/AGER/p65 axis-induced ROS and apoptosis, as well as promoted cell survival and diabetic wound healing *in vivo*. | (10) |
| Core–shell (c/s) extrusion-based | GelMA/succinylated chitosan/dextran aldehyde (D) and BMSCs/HUVECs | Bioprinted cells show cord-like, natural microvascularization and promote skin wound healing *in vivo*. | (126) |
| | Gelatin/chitosan and MSC (T0523)/HUVECs | Bioprinted cells increased the secretion of wound healing factors EGF, MMP-9, TGF-α, PDGF, decrease pro-inflammatory factor IL-6, and promote neovascularization *in vivo*. | (127) |

MSCs, mesenchymal stromal cells; FBs, fibroblasts; KCs, keratinocytes; BMSCs, bone marrow stromal cells; ADSCs, adipose-derived stromal cells; LIFT, laser-induced forward transfer; ECFCs, endothelial colony-forming cells; dECM, decellularized extracellular matrix; EPCs, endothelial progenitor cells; UC-MSC, umbilical cord-derived mesenchymal stromal cells; GelMA, gelatin methacryloyl; HUVEC, human umbilical vein endothelial cells; EGF, endothelial growth factor; TGF-α, transforming growth factor-α; PDGF, platelet-derived growth factor.

seed cells for the treatment of skin wound healing. 3D-bioprinted MSCs maintained a better ability to proliferate increased biological factors to promote skin wound healing (29, 30). With their ability to differentiate and paracrine effect, MSCs show infinite potentialities based on 3D bioprinting technology (31).

Accordingly, in this review, we will discuss current knowledge about the role of MSCs and 3D bioprinting in the treatment of skin wound healing, as well as the perspective and limitations of recent research.

## The process of skin wound repair

Following injury, mammalian wound healing is traditionally divided into three phases: inflammation, proliferation, and ECM remodeling (32). The first stage of wound healing, inflammation, will happen from the moment of tissue damage. Platelets, neutrophils, macrophages, and fibrin matrices work together to prevent ongoing blood and fluid losses as well as infection. In contrast, macrophages are considered vital for coordinating other issues in the wound healing process (33). The second stage, proliferation, is attributed to the proliferation and migration of fibroblasts, myofibroblasts, and keratinocytes. These different cell types are associated with angiogenesis and re-epithelialization to restore the barrier function of the epidermis (2, 34). In the third stage, ECM remodeling, all the activities after injury cease. Macrophages and myofibroblasts will undergo apoptosis, leaving collagen and other extracellular matrix proteins (35). Matrix metalloproteinases secreted by macrophages, fibroblasts, and endothelial cells strengthen the repaired tissue (36). However, the incongruity of any stage will occur in chronic wounds or keloid scar formation (37).

Chronic wounds or impaired wound healing are defects in the skin for more than 6 weeks (38). Typically, chronic wounds may be divided into three types: vascular dysfunction, diabetes, and pressure ulcers (39). Inappropriate physiological inflammatory reactions, underlying systemic diseases, such as diabetes mellitus and vascular disorders, and infections will lead to impairments of cell proliferation and migration and extracellular matrix damage (6, 8). The formation of myofibroblasts is compromised, partly due to hypoxic conditions or vascular insufficiency, which will contribute to the lack of granulation tissue and delayed wound healing (40).

Unfortunately, damaged tissue could not regain the properties of unwounded tissue (41). Importantly, nonhealing and dysfunctional healing cause lifelong disability and a significant economic burden (42). Therefore, the emphasis of research should be on enhancing wound healing and regeneration of original tissues in the future.

## MSCs and skin wound healing

Recently, MSCs have become a promising therapy in the field of regenerative medicine because of their pluripotency, self-renewal, and paracrine of biological factors (43). MSCs, possibly derived from the mesoderm, could differentiate into various mesenchymal tissue lineages, such as chondrocytes, adipocytes, osteoblasts, and even myoblasts (44). The most MSCs used in skin regeneration are adult stromal cells because of less ethical controversy and substantial legal restrictions (45). MSCs would accelerate skin wound healing by regulating multiple phases of wound reconstruction, including inflammatory response, cell proliferation, wound angiogenesis, and wound remodeling (46). Fifty years ago, Friedenstein et al. have been isolated bone marrow stromal cells (BMSCs) from bone marrow (47). In the last few decades, adipose-derived stromal cells (ADSCs) have been a new source of MSCs introduced to wound healing because they are obtained from adipose tissues with less invasive methods and less ethical concerns (16). Including human umbilical cord-derived mesenchymal stromal cells (HUC-MSCs), MSCs play an important role in wound healing (**Figure 1**).

### MSCs and anti-inflammatory/immunoregulatory

There is an amount of literature about skin wound healing, pointing out that skin wound healing is a complex process that depends on many cell types. Molecular and cellular mechanisms are critical for the process of cutaneous wound healing. At the early stage of wound healing, keratinocytes and inflammatory cells seem necessary. First, leukocytes, especially neutrophil granulocytes, transmigrate to the injury site to initiate and perpetuate inflammation (48, 49). Inflammation is a self-defense mechanism against noxious stimuli in the early stages of wound healing, with a significant objective of removing necrotic debris and pathogenic microorganisms from the wound bed and controlling local area damage (50). MSCs can cooperate with various immune cells to modulate inflammatory responses such as B cells, T cells, natural killer (NK) cells, neutrophils, and macrophages (51, 52). Moreover, MSCs promote the polarization of macrophages to an M2-like phenotype, which reduces inflammation and immunosuppressive function through a prostaglandin E2-dependent mechanism (53). Recent studies have demonstrated that MSCs encourage the polarization of macrophages toward an anti-inflammatory, reparative M2 phenotype by a paracrine mechanism. It has been reported that MSCs could secrete transforming growth factor beta (TGF-β) (54), C-X-C motif chemokine ligand 12 (CXCL12) (55), tumor necrosis factor-α-induced gene/protein-6 (TSG-6) (56), and prostaglandin E2 (53) to induce macrophage M2 polarization

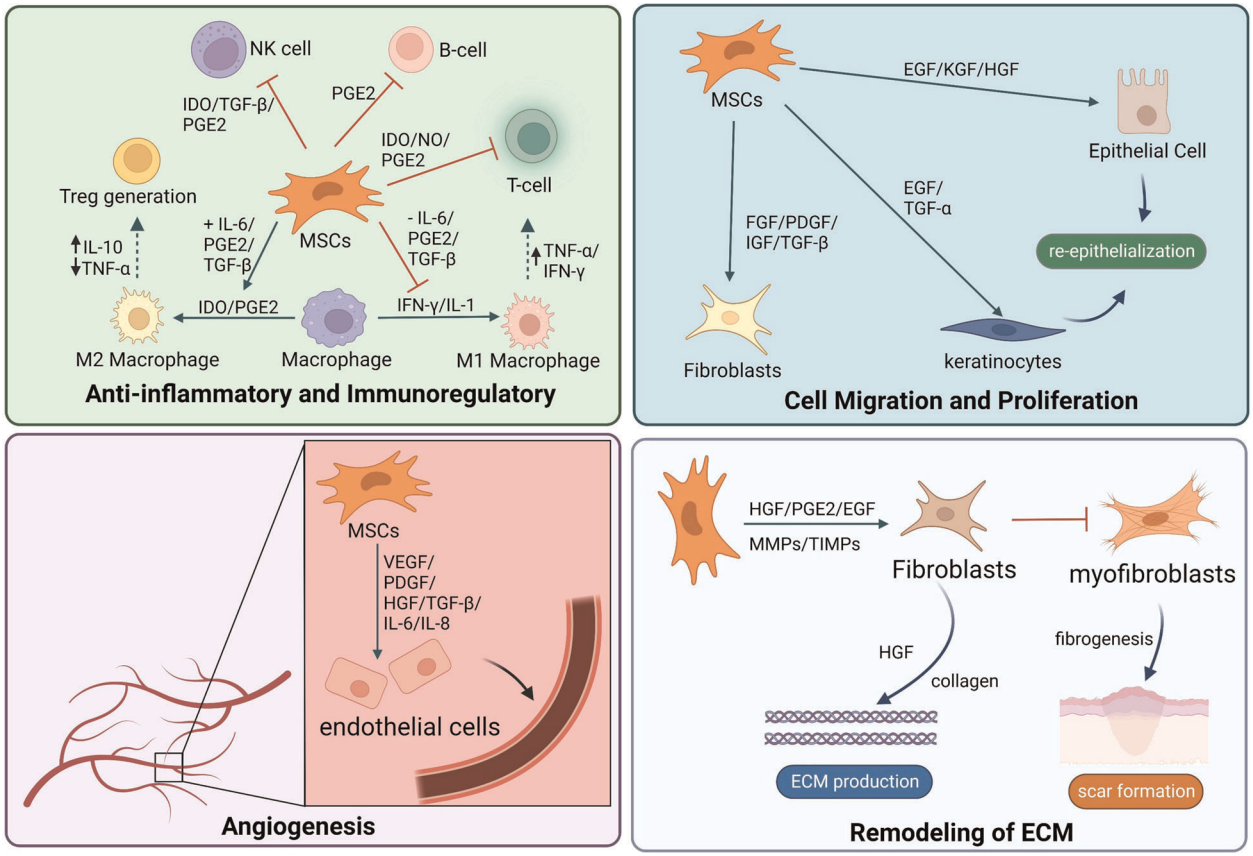


FIGURE 1
MSCs promote skin tissue regeneration through anti-inflammatory and immunoregulatory, cell migration and proliferation, angiogenesis, and ECM remodeling. MSCs, mesenchymal stromal cells; ECM, extracellular matrix.

(53, 57). The cell–cell interaction between MSCs and macrophages in the progress of skin wound healing can accelerate skin tissue regeneration (58).

Meanwhile, MSCs also inhibit the proliferation of activated helper T (Th) cells (59). Mo et al. found that MSCs suppressed Th2 inflammation by regulating macrophage activation *via* soluble mediators rather than direct cell-to-cell contact (60). Besides, the extracts of MSCs could suppress Th2 cells and reduce the expression of IL-17 and IFN-γ, which further demonstrate that MSCs inhibit Th2 cells through paracrine factors (61, 62). In clinical, the immunomodulatory ability of MSCs could reverse the ratio of Th1 cells to Th2 cells, with an increase in Th1 and a decrease in Th2 achieving a new balance (63). This interaction could decrease the production of interferon γ (IFN-γ) and interleukin (IL)-17 and increase the production of IL-4 secreted by Th cells, thus leading to T cells polarizing from a pro-inflammatory to an anti-inflammatory phenotype (64).

MSC sheet technology enables cultured MSC harvest without enzymatic treatment or cell or protein disruption using temperature-responsive cell culture dishes (65). With this application, changes in culture temperature cause oscillation between hydrophilic and hydrophobic states. Cells adhere to and proliferate on the surface of the culture dish at 37 °C, and a monolayer cell sheet with ECM detach spontaneously at temperatures below 32 °C without enzymatic digestion (66). Application of MSCs sheet also brings preferable wound healing and less scar formation, believed that it can suppress macrophage infiltration and chemotactic response of macrophages (67, 68). In clinical research, MSCs could reduce the expression of inflammation and oxidative stress-related proteins to improve diabetic foot ulcers (DFU) healing by Nrf2 (69). It has been reported that MSCs therapy may reduce inflammation and has been applied in acute and chronic liver injury, which suggests MSCs improve tissue regeneration using their anti-inflammatory properties (70).

## MSCs and proliferation/migration

The intermediate stage of wound healing contains proliferation and migration of keratinocytes, the proliferation

of fibroblasts, matrix deposition, and angiogenesis. Stationary keratinocytes are converted to flat migratory keratinocytes to start re-epithelialization (27). In this stage, fibroblasts stimulate wound healing by proliferating and synthesizing a large amount of ECM components such as collagen and elastic fibers under the stimulation of trauma (71). MSCs stimulate the migration and proliferation of keratinocytes by the expression of epidermal growth factor (EGF) and transforming growth factor-α (TGF-α) (72). The treatment of MSCs improves the survival rate of fibroblasts and enhances the healing effects (73). Evidence shows that BMSCs improve the proliferation and migration of dermal fibroblasts (74). *In vivo*, MSCs increased the expression of CK19 and proliferating cell nuclear antigen (PCNA) and promoted the regeneration of dermal tissue (75, 76). Specifically, PCNA participates in cell proliferation by mediating DNA polymerase while blocking the PCNA production in cells severely affects cell division, which takes a significant part in the synthesis of DNA and its repair, cell proliferation, and progression of the cell cycle (77, 78). Studies show treatment of MSCs could elevate the expression of PCNA, promote wound healing, and enhance re-epithelialization (79–81).

Animals treated with MSCs show improving wound healing with no detectable side effects related to increasing viability, proliferation, and migration of epithelial cells (82). *In vivo*, the application of MSCs could promote re-epithelialization by enhancing the proliferation of epidermal keratinocytes (83). Moreover, MSCs strengthened the dermal and epidermal cell proliferation ability in a dose-dependent manner and positively impacted oxidative stress injury, which could improve cutaneous wound healing (84). All the evidence indicates that MSCs have a positive effect on wound healing.

## MSCs and angiogenesis

Angiogenesis plays an essential role in the process of wound healing. Creating new capillaries will bring oxygen and nutrients to growing tissues and remove catabolic wastes. Therefore, angiogenesis contributes to the repair of wound tissue (85). Angiogenesis is strictly regulated by a variety of factors, mainly through the secretion of proangiogenic factors, such as VEGF and platelet-derived growth factor (PDGF), leading to stimulating endothelial cell proliferation and migration and angiogenesis (86). Rehman et al. found that MSCs secreted synergistic proangiogenic growth factors, such as VEGF and HGF, which enhance angiogenesis (87). The previous review reported that MSCs could promote re-epithelialization, angiogenesis, collagen synthesis, and neovascularization by secretion of multiple growth factors including VEGF, HGF, TGF-β1, KGF, IL-8, and IL-6 during the progress of wound healing (88). MSCs improved cell viability, migration, and angiogenesis of the high glucose-damaged human umbilical vein endothelial cells (HUVECs) through paracrine, increasing the expression of IL-6, TNF-α, ICAM-1, VCAM-1, BAX, P16, P53, and ET-1(89). Different experimental models mimic the effect of MSCs in wound healing, performed preferentially in rodents. Subcutaneously injecting MSCs into the full-thickness wounds of mice will result in more angiogenesis and promote wound healing (90). With treatment of MSCs, the density of neovascularization in wound bed was increased, also with the expression of VEGF, while the expression of IL-10, IL-6, IL-1β, and TNF-α were significantly decreased (91). Meanwhile, MSCs could enhance angiogenesis and improve the survival rate of graft skin *in vivo* (92). MSCs also positively impacted vascular regeneration and endothelial leukocyte adhesion modulation in critical ischemic skin (93).

## MSCs and ECM remodeling

Late-stage healing involves remodeling of ECM, resulting in scar formation and barrier restoration (28). During the wound remodeling stage, fibroblasts differentiate into myofibroblasts, and the granulation tissue gradually becomes fibrotic; collagen gradually increases; the wound begins to contract, and eventually, scar tissue is formed (94). MSCs would release plenty of cytokines and growth factors with anti-fibrotic properties (95, 96). In the early progress, MSCs improve collagen remodeling through synthesizing collagen types I and III of wound healing while reducing scarring in the late stage by inhibiting collagen formation (97). Treated with MSCs, fibroblasts secret more HGF and increase collagen production. With the inhibition of excessive fibrogenesis, fibroblast proliferation, and α-smooth muscle actin expression, MSCs can reduce scar formation during wound healing (98). MSCs also inhibited fibrosis by decreasing the expression of profibrotic genes and protein, promoting extracellular matrix regeneration, inhibiting fibroblast contraction, and reversing myofibroblast activation (99). It has been reported that MSCs were capable of myofibroblast suppression and anti-scar formation *in vivo* and *in vitro* (100). MSCs have been considered significant in skin wound repair. However, further research is still needed to increase the biological regulation of wound healing.

## MSC-EVs and skin wound healing

Although mesenchymal stem cells could regulate inflammation, promote cell proliferation and migration, and improve angiogenesis during skin wound healing, a few disadvantages limit its wide application. Mesenchymal stem cell therapy may have a problem with storage and transportation, as well as the risk of cancer and deformities. As a result, it is not a definitive treatment without a long-term study on safety (101). EVs, including exosomes, have taken part in various

pathological physiology processes and significantly contributed to MSCs (102). It has been reported that EVs derived from MSC carried a large number of regulatory factors, such as active protein, miRNA, and lncRNA (103). EVs play a key role in several biological processes that activate downstream target cells through a paracrine effect (104). Like MSCs, researchers have discovered that EVs derived from MSCs could modulate the inflammatory response, accelerate cell proliferation, promote angiogenesis, and regulate ECM remodeling during wound healing (105).

In the early stage, exosome derived from MSCs (MSCs-exo) helps monocytes translate into M1 macrophages through many immunomodulatory proteins released, such as tumor necrosis factor-alpha (TNF-α), macrophage colony-stimulating factor (MCSF) and retinol-binding protein 4(RBP-4) (106). The expression level of oxidative stress-related proteins and inflammatory cytokines is reduced (69). MSC-EVs upregulate the expression of monocyte chemoattractant protein-1and macrophage inflammatory protein-1α reduces early inflammation and oxidative stress (69, 107). In the proliferation stage, MSC-EVs are internalized by fibroblasts as well as epidermal keratinocytes and promote cell migration and proliferation by expression of N-cadherin, cyclin 1, proliferating cell nuclear antigen, collagen type I and III (22). Besides, MSC-EVs are enriched in vascular endothelial growth factor A (VEGF-A), platelet-derived growth factor BB (PDGF-BB), and noncoding RNAs, which promote proliferation and angiogenesis of vascular endothelial cells (19, 108). In the late stage, MSC-EVs prevented fibroblast-to-myofibroblast differentiation by increasing the ratio of collagen III to collagen I and the ratio of TGF-β3 to TGF-β1 to reduce scar formation (109). Therefore, MSC-EVs have become a hot topic in the field of skin wound regeneration as a cell-free therapy.

## Three-dimensional (3D) bioprinting

Inspired by traditional inkjet printer technology, Thomas Boland directly printed viable mammalian cells onto hydrogel-bases papers with a cell printer, successfully exploring the field of 3D bioprinting technology used in tissue engineering (110). Bioink is a biomaterial composed of living cells, biological factors, and biological glue (111). With sufficient mechanical properties and biocompatibility, bioink can provide a stable and harmless environment of proliferation and differentiation for cells (112). Depending on the type of cell deposition, 3D bioprinting technology can be classified into three main strategies: drop-based, filament-based, and plane-based (113) (**Figure 2**).

### Drop-based bioprinting

Inkjet or laser bioprinting are two commonly used strategies of drop-based 3D bioprinting. In inkjet-based bioprinting, inkjet bioprinters utilize heat or mechanical compression to create and

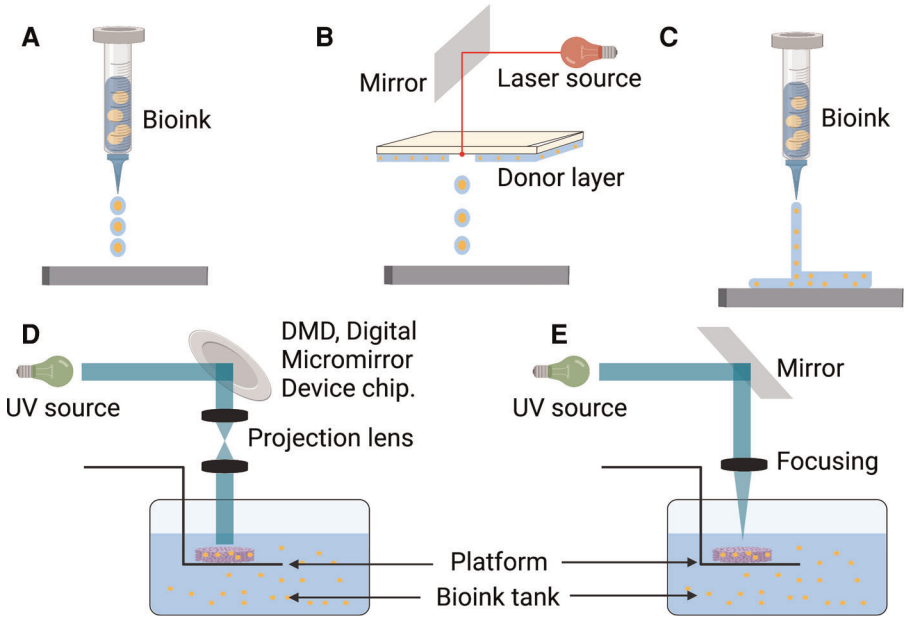


FIGURE 2
There are multiple strategies of 3D bioprinting, including inkjet bioprinting (**A**), laser bioprinting (**B**), extrusion-based bioprinting (**C**), SLA-based bioprinting (**D**), and DLP-based bioprinting (**E**). DLP, digital light processing; SLA, stereolithography.

eject drops. In this bioprinting process, various volumes of ink drops are created based on computer control, in which each drop of bioink contains $10^4$–$30^4$ cells (114). Laser-based bioprinting utilizes the laser-induced forward transfer (LIFT) effect to print different biomaterials and living cells (115). During the process, the incident laser light causes the ejection of bioink droplets, which are subsequently received on a receiving substrate (116, 117). It has been reported that inkjet printing can be combined with gene delivery to effectively control stromal cell differentiation while bioprinting neural stromal cells (NSCs) (118). Sorkio et al. used laser-based bioprinting to demonstrate tissues mimicking the structure of the corneal tissue with stromal cells (119). A separate study indicated that MSCs could keep the predefined structure and maintain cell competency for tissue repair (120). Inkjet and laser bioprinting allow the printing of cells, materials, and protein molecules rapidly and inexpensively. However, the smooth printing process would frequently disrupt by the clogging of nozzles because of bioink gelation and the unequal-sized drops in inkjet bioprinting (121). Meanwhile, long-fabrication times and gravitational settling of cells in solution are other challenges in drop-based bioprinting (122).

## Filament-based bioprinting

Extrusion-based bioprinting is the most popular approach in the research of filament-based bioprinting strategy. Based on mechanical driven force (displacement driven) or pneumatic driven force (pressure driven), extrusion bioprinting mechanisms can directly dispense the higher viscosity bioinks out of the biomaterial cartridge (123). During the development of extrusion-based bioprinting, the scaffold of acellular polymers, such as polycaprolactone (PCL), polylactic acid (PLA), and poly lactic-co-glycolic acid (PLGA), was used for 3D cell culture by extrusion printing (124–126). With the different applications of bioinert hydrogel materials such as sodium alginate, extrusion bioprinting can print bioinks of living cells to a particular flow out as seamless circular cylindrical filaments with computer manufacturing (127, 128). Extrusion-based bioprinting device creates a scaffold of adipose-derived mesenchymal stromal cells (ADSCs) in alginate-gelatin (Alg-Gel) hydrogel for tissue repair and regeneration (129). Moreover, this technology can provide a kidney organoid with highly reproducible cell numbers and viability (130). Extrusion-based bioprinting brings a promising future of producing rapid and high-throughput organoids for drug screening, disease modeling, and tissue repair. However, rapid speed and high pressure can enhance shear stress, which decreases cell viability (131). The current research focuses on extrusion bioprinting study intensively on cell-instructive hydrogels as bioinks to provide a cell-friendly microenvironment (132).

## Plane-based bioprinting

Compared with other 3D bioprinting strategies, plane-based bioprinting technology, such as digital light processing (DLP) and stereolithography (SLA) bioprinting, has significant advantages in efficiency, printing resolution, and working conditions (133). DLP-based bioprinting employs projection light to biomaterials to obtain the predesigned structures. In contrast, SLA-based bioprinting achieves photo polymerization by a light pencil scanning the surface of liquid bioink (133, 134). With light-based techniques, DLP/SLA-based bioprinting can print the entire layer with higher accuracy and speed (135). Through a DLP-based 3D printer, Ma et al. printed a 3D triculture hepatic model encapsulated kind of cells, including induced iPSCs and ADSCs. The microstructure can promote maturation and maintain the functions of cells (136). With SLA-based bioprinting technology, the 3D cell-laden hydrogel scaffolds represent high cell viability and cell adhesion (137). Although this technique has shown the characteristics of high precision, fast speed, and mild condition, its running cost, and the lack of compatible bioinks limit its broader applicability (138).

# 3D-bioprinted MSCs in skin tissue regeneration

Traditional 2D cell cultures cannot recreate the native three-dimensional (3D) cell microenvironment, which provides cell–matrix and cell–cell interactions that readjust cell morphology and gene expression (139–141). 3D bioprinting is a promising biofabrication strategy, using living cells and biomaterials as bioink to create artificial multicellular tissues (142). In the field of skin tissue repair, 3D bioprinting is currently being explored in developing more complex synthetic skin models (143, 144). Nowadays, various biomaterials have been widely investigated as scaffolds for bioprinting in tissue engineering and skin wound healing (145, 146). Usually, hydrogel containing FBs, keratinocytes (KCs), and HUVECs are bioprinted as scaffolds directly applied on the wound bed (147). Jin et al. *had* taken advantage of the acellular dermal matrix (ADM) and HUVECs as bioink to 3D-bioprinted functional skin model, which maintained the ECM components to promote cell viability and form the vascular network and framework (148). Recently, 3D bioprinting has been successfully performed using multiple mesenchymal stromal cell types for tissue repair, including cardiovascular, hepatic, and skin (149). 3D-bioprinted MSCs preserved proangiogenic properties and secreted more EVs containing a greater variety of proteins (150). However, not much research focuses on adult stromal cells as seeded cells in skin wound regeneration (**Table 1**).

In 2010, Koch and colleagues utilized skin cell lines (fibroblasts/keratinocytes) and MSCs as bioink for skin

regeneration based on laser printing. MSCs maintained the ability to proliferate and did not show an increase in apoptosis after 3D bioprinting (29). 3D-bioprinted MSCs increased angiogenesis and wound closure rates due to secretion of biological factors rather than direct cell–cell interactions, such as basic fibroblast growth factor (bFGF), and fibroblast growth factor (FGF) and growth differentiation factor (GDF) (30). Moreover, Roshangar et al. evaluated a 3D bioprinting scaffold loaded with MSCs on rat skin burn defects. Data showed that the scaffold promoted wound healing by creating a continuous epidermal layer without scar formation (151).

3D-bioprinted MSCs could improve wound healing *in vivo* by generating collagen and enhancing cell proliferation. Besides, 3D-bioprinted MSCs would maintain a preferable cell proliferation in the nutritionally deficient environment (11). In addition to utilizing hydrogel and MSCs for 3D bioprinting, various bioactive substances have been applied to enhance the abilities of MSCs, such as angiogenesis. A 3D-bioprinted scaffold loaded with MSCs and SNAP, which could release NO, can improve the migration and angiogenesis of HUVECs. On the other hand, the hydrogel scaffolds accelerated the serve burn wound healing by promoting epithelialization and collagen deposition (152). It has been reported that 3D-bioprinted MSCs could accelerate diabetic wound healing by combining bioink with curcumin and gelatin methacryloyl (GelMA). 3D-bioprinted MSCs with curcumin could better exert antioxidant and anti-apoptotic activity to promote wound healing (10). As widely used biological material with biocompatibility and multichannel printing technology, Turner et al. established a regenerative, dual cell delivery 3D core/shell (c/s) "living dressing" system using MSCs. It indicated that the construct provided an appropriate microenvironment to improve the proliferation and differentiation of MSCs (153). In addition, Turner et al. discovered the 3D core/shell MSCs dressing would accelerate angiogenesis and anti-inflammatory to promote wound healing in thermal injury by increasing the expression of wound healing factors and neovascularization EGF, PDGF, MMP-9, TGF-α and decreasing pro-inflammatory factor IL-6 (154).

In the last few decades, new materials and technologies have been developed to fabricate skin substitutes (31). Compared to conventional tissue engineering technologies, 3D bioprinting can deposit different cell types and specific biomaterials with a high spatial resolution (155). In 2011, Gruene et al. utilized endothelial colony-forming cells (ECFCs) and ADSCs to build a layer-by-layer scaffold using laser-assisted bioprinting and discovered direct cell–cell contacts, which may promote angiogenesis (156). Skin tissue contains a variety of cell types. Baltazar et al. have created artificial dermis using bioink containing human foreskin dermal FBs, human ECs derived from cord blood human endothelial colony-forming cells (HECFCs), and human placental pericytes (PCs) suspended in rat tail type I collagen and printed epidermis with human foreskin KCs. The result showed the 3D bioprinting of artificial dermis enhanced the formation of microvessels and the epidermal rete *in vivo* (28). Another research used endothelial progenitor cells (EPCs) and MSCs to 3D bioprint a full-thickness skin model. This model accelerated re-epithelization, wound closure, and neovascularization (157). For skin appendages, 3D-bioprinted MSCs have been confirmed could enhance stemness maintenance by sweat gland (SG) lineage *in vitro* (158). With 3D bioprinting, alginate-gelatin and epidermal progenitors could enhance sweat gland regeneration (159). Through bioprinting an SG-like matrix, MSCs could differentiate into functional SGs and facilitate SGs recovery in mice (160). Despite MSCs and 3D bioprinting technology showing great potential for preparing artificial skin, future research should concentrate on skin tissue bioprinting and make it more adaptable to clinical needs.

## Discussion

The objective of skin tissue regeneration is to realize structural and functional reconstruction, at the same time promoting wound healing and reducing scar formation (161). MSCs have been considered to have a promising potential in skin tissue regeneration with their differentiation abilities and paracrine effect (15). Many studies have shown that MSCs could regulate inflammation, promote cell proliferation and migration, and improve angiogenesis during skin wound healing (15). However, MSCs therapy still has obstacles, such as its low frequency in tissues and the limited proliferative potential (162). Recently, studies have focused on the therapeutic potential of EVs derived from MSCs in skin wound regeneration. MSC-EVs and exosomes are considered to affect skin wound healing significantly. Unlike MSC-based therapy, MSC-EVs therapy has advantages in delivery and storage, as well as a lack of endogenous tumor-formation potential (163). One of the most significant advantages of MSC-EVs therapy is the possibility to inject EVs locally, thus minimizing the side effects of cell administration (102). Nevertheless, clinical applications of MSC-EVs require a long-term study on safety to prevent the development of uncontrolled immunosuppression in MSC-EVs recipients (164). Although evidence suggests the therapeutic potential of MSCs and MSC-EVs, there are still further studies to be done before MSCs and MSC-EVs could be offered as a common clinical therapy for skin wound healing.

On the other hand, with the application of 3D bioprinting, MSCs have more ability to proliferate and secrete biological factors to enhance cell–cell interaction. As 3D bioprinting technology developed, *in situ* bioprinting or "*in vivo*" bioprinting has been applied to tissue regeneration, including skin, cartilage, and bone (165). It's reported that autologous

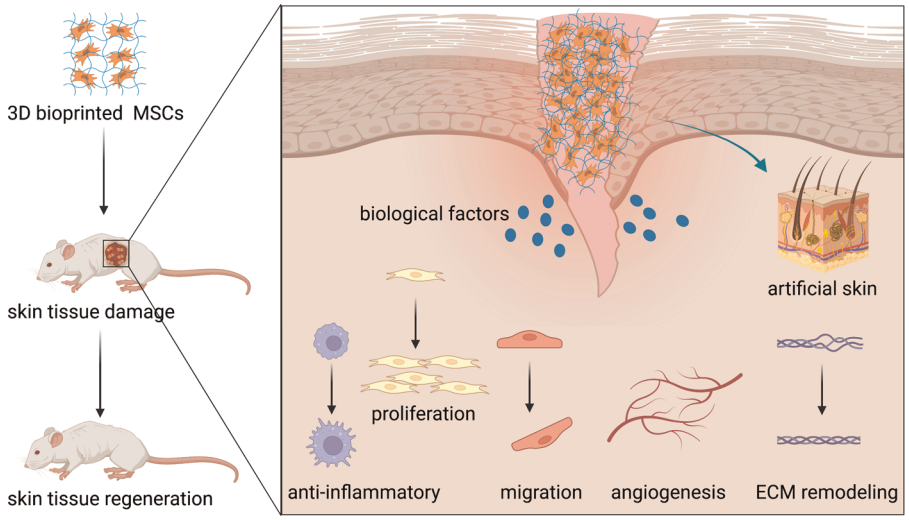


FIGURE 3
3D-bioprinted MSCs promote skin tissue regeneration. MSCs, mesenchymal stromal cells

dermal fibroblasts and epidermal keratinocytes, along with the fibrinogen-collagen hydrogel, were directly printed into the wound of a porcine model, with better re-epithelialization and reducing the healing time (147). Besides, through cellular self-assembly bioprinting, upregulated expression of tissue-specific functional genes indicated increased tissue functionality to realize multitissue organs-on-a-chip with different cell types (166). There is substantial evidence supporting various methods of MSCs culture influence the release of EVs, while little research concerned EVs derived from 3D-bioprinted MSCs (167). According to a recent study, Chen et al. combined 3D core–shell bioprinting and MSCs to increase MSC-derived EVs' production (150). In his platform, the 3D-bioprinted MSCs enriched particles by ~1,009-fold compared to traditional 2D culture, expressing higher stemness markers and preserving proangiogenic properties. Moreover, 3D-EVs contained hundreds of unique protein profiles compared to 2D-EVs. Supported by 3D bioprinting technology, the bioprinted 3D structures loaded with EVs recapitulated the blood-perfused microvessels with a new functional vasculature *in situ* (168). Besides, Bari had found that 3D-bioprinted MSC-EVs could release the secretome from the scaffold with a fast speed for tissue regeneration (169). Moreover, the release was governed by the scaffold shape and the application of different biomaterials, for example, increasing alginate concentration or cross-linking with protamine. Technological developments may present new opportunities and challenges for MSCs in skin tissue regeneration.

Although MSCs and 3D bioprinting technology bring a new therapeutic strategy for skin wound healing, some obstacles still need to be overcome. The skin is one of the most vital organs as a protective barrier against various external agents (170). At present, the mechanical strength of 3D bioprinting hydrogels is insufficient, which could not be satisfied with the unique physical and mechanical characteristics of human skin. In addition, the skin contains various appendages, such as sweat glands, adipose glands, hair follicles, and blood vessels, along with nerve endings (171). Despite the sweat gland regeneration function of 3D bioprinting MSCs, 3D bioprinting skin tissue could not simulate every structure or functional reconstruction, especially nerve regeneration.

After all, 3D-bioprinted MSCs have played a positive role in skin wound healing. With the progress of related technologies and the application of new biomaterials, 3D bioprinting will hopefully overcome the difficulties mentioned above and make a big difference in skin tissue regeneration (**Figure 3**).

## Conclusion

Wound healing and skin tissue regeneration have been critical clinical issues for decades. Various methods have been used to promote skin wound healing by better regulating every phase of wound healing. As depicted in the published studies, 3D-bioprinted MSCs are a promising therapeutic strategy for skin tissue regeneration because of their preferable differentiation and paracrine effect of biological factors. However, interdisciplinary collaboration is still needed to overcome the difficulties, such as the mechanical strength and skin appendages of bioprinted MSCs. In conclusion, 3D-bioprinted MSCs have been proven to have a positive role in skin tissue regeneration. Further studies are needed to assess the long-term outcomes and well-designed clinical studies to apply this strategy in clinical medicine.

## Author contributions

YL and XX wrote the original draft. ZY and QX reviewed and edited the manuscript. JL and NL supervised the data. YD and YL critically reviewed and revised the manuscript. All authors contributed to the article and approved the submitted version.

## Funding

This review was funded by the Basic and Applied Basic Research Foundation of Guangdong Province, China (No. 2021A1515220120).

## Acknowledgments

The Figure was created in the web application BioRender.com (Available online: Biorender.com, accessed on 26 June 2022).

## Conflict of interest

The authors declare that the research was conducted in the absence of any commercial or financial relationships that could be construed as a potential conflict of interest.

## Publisher's note

All claims expressed in this article are solely those of the authors and do not necessarily represent those of their affiliated organizations, or those of the publisher, the editors and the reviewers. Any product that may be evaluated in this article, or claim that may be made by its manufacturer, is not guaranteed or endorsed by the publisher.

## References

1. Karimkhani C, Dellavalle RP, Coffeng LE, Flohr C, Hay RJ, Langan SM, et al. Global skin disease morbidity and mortality: an update from the global burden of disease study 2013. *JAMA Dermatol.* (2017) 153(5):406–12. doi: 10.1001/jamadermatol.2016.5538

2. Werner S, Krieg T, Smola H. Keratinocyte-fibroblast interactions in wound healing. *J Invest Dermatol.* (2007) 127(5):998–1008. doi: 10.1038/sj.jid.5700786

3. Richardson R, Slanchev K, Kraus C, Knyphausen P, Eming S, Hammerschmidt M. Adult zebrafish as a model system for cutaneous wound-healing research. *J Invest Dermatol.* (2013) 133(6):1655–65. doi: 10.1038/jid.2013.16

4. Velnar T, Bailey T, Smrkolj V. The wound healing process: an overview of the cellular and molecular mechanisms. *J Int Med Res.* (2009) 37(5):1528–42. doi: 10.1177/147323000903700531

5. Lawrence WT. Physiology of the acute wound. *Clin Plast Surg.* (1998) 25 (3):321–40. doi: 10.1016/S0094-1298(20)32467-6

6. Eming SA, Krieg T, Davidson JM. Inflammation in wound repair: molecular and cellular mechanisms. *J Invest Dermatol.* (2007) 127(3):514–25. doi: 10.1038/sj.jid.5700701

7. Demidova-Rice TN, Hamblin MR, Herman IM. Acute and impaired wound healing: pathophysiology and current methods for drug delivery, part 2: role of growth factors in normal and pathological wound healing: therapeutic potential and methods of delivery. *Adv Skin Wound Care.* (2012) 25(8):349–70. doi: 10.1097/01.ASW.0000418541.31366.a3

8. Otero-Viñas M, Falanga V. Mesenchymal stem cells in chronic wounds: the spectrum from basic to advanced therapy. *Adv Wound Care (New Rochelle).* (2016) 5(4):149–63. doi: 10.1089/wound.2015.0627

9. Kim WS, Park BS, Sung JH, Yang JM, Park SB, Kwak SJ, et al. Wound healing effect of adipose-derived stem cells: a critical role of secretory factors on human dermal fibroblasts. *J Dermatol Sci.* (2007) 48(1):15–24. doi: 10.1016/j.jdermsci.2007.05.018

10. Xia S, Weng T, Jin R, Yang M, Yu M, Zhang W, et al. Curcumin-incorporated 3D bioprinting gelatin methacryloyl hydrogel reduces reactive oxygen species-induced adipose-derived stem cell apoptosis and improves implanting survival in diabetic wounds. *Burns Trauma.* (2022) 10:tkac001. doi: 10.1093/burnst/tkac001

11. Zhao H, Xu J, Zhang E, Qi R, Huang Y, Lv F, et al. 3D Bioprinting of polythiophene materials for promoting stem cell proliferation in a nutritionally deficient environment. *ACS Appl Mater Interfaces.* (2021) 13(22):25759–70. doi: 10.1021/acsami.1c04967

12. Steens J, Klein D. Current strategies to generate human mesenchymal stem cells in vitro. *Stem Cells Int.* (2018) 2018:6726185. doi: 10.1155/2018/6726185

13. Beeravolu N, McKee C, Alamri A, Mikhael S, Brown C, Perez-Cruet M, et al. Isolation and characterization of mesenchymal stromal cells from human umbilical cord and fetal placenta. *J. Visualized Exp.* (2017) 122:1–13. doi: 10.3791/55224

14. Isakson M, de Blacam C, Whelan D, McArdle A, Clover AJP. Mesenchymal stem cells and cutaneous wound healing: current evidence and future potential. *Stem Cells Int.* (2015) 2015:1–12. doi: 10.1155/2015/831095

15. Jo H, Brito S, Kwak BM, Park S, Lee MG, Bin BH. Applications of mesenchymal stem cells in skin regeneration and rejuvenation. *Int J Mol Sci.* (2021) 22(5):1–19. doi: 10.3390/ijms22052410

16. Kern S, Eichler H, Stoeve J, Kluter H, Bieback K. Comparative analysis of mesenchymal stem cells from bone marrow, umbilical cord blood, or adipose tissue. *Stem Cells.* (2006) 24(5):1294–301. doi: 10.1634/stemcells.2005-0342

17. Teng M, Huang Y, Zhang H. Application of stems cells in wound healing–an update. *Wound Repair Regen.* (2014) 22(2):151–60. doi: 10.1111/wrr.12152

18. Wu P, Zhang B, Shi H, Qian H, Xu W. MSC-exosome: a novel cell-free therapy for cutaneous regeneration. *Cytotherapy.* (2018) 20(3):291–301. doi: 10.1016/j.jcyt.2017.11.002

19. Liang X, Zhang L, Wang S, Han Q, Zhao RC. Exosomes secreted by mesenchymal stem cells promote endothelial cell angiogenesis by transferring miR-125a. *J Cell Sci.* (2016) 129(11):2182–9. doi: 10.1242/jcs.170373

20. Kang T, Jones TM, Naddell C, Bacanamwo M, Calvert JW, Thompson WE, et al. Adipose-derived stem cells induce angiogenesis via microvesicle transport of miRNA-31. *Stem Cells Transl Med.* (2016) 5(4):440–50. doi: 10.5966/sctm.2015-0177

21. Choi EW, Seo MK, Woo EY, Kim SH, Park EJ, Kim S. Exosomes from human adipose-derived stem cells promote proliferation and migration of skin fibroblasts. *Exp Dermatol.* (2017) 27(10):1170–2. doi: 10.5966/sctm.2015-0177

22. Hu L, Wang J, Zhou X, Xiong Z, Zhao J, Yu R, et al. Exosomes derived from human adipose mensenchymal stem cells accelerates cutaneous wound healing via optimizing the characteristics of fibroblasts. *Sci Rep.* (2016) 6(1):1–11. doi: 10.1038/srep32993

23. Liu J, Sun L, Xu W, Wang Q, Yu S, Sun J. Current advances and future perspectives of 3D printing natural-derived biopolymers. *Carbohydr Polym.* (2019) 207:297–316. doi: 10.1016/j.carbpol.2018.11.077

24. Liu N, Ye X, Yao B, Zhao M, Wu P, Liu G, et al. Advances in 3D bioprinting technology for cardiac tissue engineering and regeneration. *Bioact Mater*. (2021) 6 (5):1388–401. doi: 10.1016/j.bioactmat.2020.10.021

25. Koçak E, Yıldız A, Acartürk F. Three dimensional bioprinting technology: applications in pharmaceutical and biomedical area. *Colloids Surf B Biointerfaces*. (2021) 197:111396. doi: 10.1016/j.colsurfb.2020.111396

26. Osidak EO, Karalkin PA, Osidak MS, Parfenov VA, Sivogrivov DE, Pereira F, et al. Viscoll collagen solution as a novel bioink for direct 3D bioprinting. *J Mater Sci Mater Med*. (2019) 30(3):31. doi: 10.1007/s10856-019-6233-y

27. Won JY, Lee MH, Kim MJ, Min KH, Ahn G, Han JS, et al. A potential dermal substitute using decellularized dermis extracellular matrix derived bio-ink. *Artif Cells Nanomed Biotechnol*. (2019) 47(1):644–9. doi: 10.1080/21691401.2019.1575842

28. Baltazar T, Merola J, Catarino C, Xie CB, Kirkiles-Smith NC, Lee V, et al. Three dimensional bioprinting of a vascularized and perfusable skin graft using human keratinocytes, fibroblasts, pericytes, and endothelial cells. *Tissue Eng Part A*. (2020) 26(5-6):227–38. doi: 10.1089/ten.tea.2019.0201

29. Koch L, Kuhn S, Sorg H, Gruene M, Schlie S, Gaebel R, et al. Laser printing of skin cells and human stem cells. *Tissue Eng Part C*. (2010) 16(5):847–54. doi: 10.1089/ten.tec.2009.0397

30. Skardal A, Mack D, Kapetanovic E, Atala A, Jackson JD, Yoo J, et al. Bioprinted amniotic fluid-derived stem cells accelerate healing of large skin wounds. *Stem Cells Transl Med*. (2012) 1(11):792–802. doi: 10.5966/sctm.2012-0088

31. Tottoli EM, Dorati R, Genta I, Chiesa E, Pisani S, Conti B. Skin wound healing process and new emerging technologies for skin wound care and regeneration. *Pharmaceutics*. (2020) 12(8):1–30. doi: 10.3390/pharmaceutics12080735

32. Gurtner GC, Werner S, Barrandon Y, Longaker MT. Wound repair and regeneration. *Nature*. (2008) 453(7193):314–21. doi: 10.1038/nature07039

33. Grose R, Werner S. Wound-healing studies in transgenic and knockout mice. *Mol Biotechnol*. (2004) 28(2):147–66. doi: 10.1385/MB:28:2:147

34. Opalenik SR, Davidson JM. Fibroblast differentiation of bone marrow-derived cells during wound repair. *FASEB J*. (2005) 19(11):1561–3. doi: 10.1096/fj.04-2978fje

35. Szabowski A, Maas-Szabowski N, Andrecht S, Kolbus A, Schorpp-Kistner M, Fusenig NE, et al. c-Jun and JunB antagonistically control cytokine-regulated mesenchymal-epidermal interaction in skin. *Cell*. (2000) 103 (5):745–55. doi: 10.1016/S0092-8674(00)00178-1

36. Baum CL, Arpey CJ. Normal cutaneous wound healing: clinical correlation with cellular and molecular events. *Dermatol Surg*. (2005) 31(6):674–86, discussion 686. doi: 10.1097/00042728-200506000-00011

37. Martin P, Leibovich SJ. Inflammatory cells during wound repair: the good, the bad and the ugly. *Trends Cell Biol*. (2005) 15(11):599–607. doi: 10.1016/j.tcb.2005.09.002

38. Markova A, Mostow EN. US skin disease assessment: ulcer and wound care. *Dermatol Clin*. (2012) 30(1):107–11, ix. doi: 10.1016/j.det.2011.08.005

39. Medina A, Scott PG, Ghahary A, Tredget EE. Pathophysiology of chronic nonhealing wounds. *J Burn Care Rehabil*. (2005) 26(4):306–19. doi: 10.1097/01.BCR.0000169887.04973.3A

40. Van De Water L, Varney S, Tomasek JJ. Mechanoregulation of the myofibroblast in wound contraction, scarring, and fibrosis: opportunities for new therapeutic intervention. *Adv Wound Care (New Rochelle)*. (2013) 2 (4):122–41. doi: 10.1089/wound.2012.0393

41. Levenson SM, Geever EF, Crowley LV, Oates JF, Berard CW, Rosen H. The healing of rat skin wounds. *Ann Surg*. (1965) 161(2):293–308. doi: 10.1097/00000658-196502000-00019

42. Aarabi S, Longaker MT, Gurtner GC. Hypertrophic scar formation following burns and trauma: new approaches to treatment. *PLoS Med*. (2007) 4(9):e234. doi: 10.1371/journal.pmed.0040234

43. Behr B, Ko SH, Wong VW, Gurtner GC, Longaker MT. Stem cells. *Plast Reconstr Surg*. (2010) 126(4):1163–71. doi: 10.1097/PRS.0b013e3181ea42bb

44. Biancone L, Bruno S, Deregibus MC, Tetta C, Camussi G. Therapeutic potential of mesenchymal stem cell-derived microvesicles. *Nephrol Dial Transplant*. (2012) 27(8):3037–42. doi: 10.1093/ndt/gfs168

45. Chen M, Przyborowski M, Berthiaume F. Stem cells for skin tissue engineering and wound healing. *Crit Rev Biomed Eng*. (2009) 37(4-5):399–421. doi: 10.1615/CritRevBiomedEng.v37.i4-5.50

46. An Y, Lin S, Tan X, Zhu S, Nie F, Zhen Y, et al. Exosomes from adipose-derived stem cells and application to skin wound healing. *Cell Prolif*. (2021) 54 (3):e12993. doi: 10.1111/cpr.12993

47. Friedenstein AJ, Petrakova KV, Kurolesova AI, Frolova GP. Heterotopic of bone marrow. Analysis of precursor cells for osteogenic and hematopoietic tissues. *Transplantation*. (1968) 6(2):230–47. doi: 10.1097/00007890-196803000-00009

48. Sinno H, Prakash S. Complements and the wound healing cascade: an updated review. *Plast Surg Int*. (2013) 2013:146764. doi: 10.1155/2013/146764

49. Vestweber D. How leukocytes cross the vascular endothelium. *Nat Rev Immunol*. (2015) 15(11):692–704. doi: 10.1038/nri3908

50. Takeo M, Lee W, Ito M. Wound healing and skin regeneration. *Cold Spring Harbor Perspect Med*. (2015) 5(1):a023267. doi: 10.1101/cshperspect.a023267

51. Wang Y, Chen X, Cao W, Shi Y. Plasticity of mesenchymal stem cells in immunomodulation: pathological and therapeutic implications. *Nat Immunol*. (2014) 15(11):1009–16. doi: 10.1038/ni.3002

52. Aboalola D, Han VKM. Different effects of insulin-like growth factor-1 and insulin-like growth factor-2 on myogenic differentiation of human mesenchymal stem cells. *Stem Cells Int*. (2017) 2017:8286248. doi: 10.1155/2017/8286248

53. Chiossone L, Conte R, Spaggiari GM, Serra M, Romei C, Bellora F, et al. Mesenchymal stromal cells induce peculiar alternatively activated macrophages capable of dampening both innate and adaptive immune responses. *Stem Cells*. (2016) 34(7):1909–21. doi: 10.1002/stem.2369

54. Liu F, Qiu H, Xue M, Zhang S, Zhang X, Xu J, et al. MSC-secreted TGF-β regulates lipopolysaccharide-stimulated macrophage M2-like polarization via the Akt/FoxO1 pathway. *Stem Cell Res Ther*. (2019) 10(1):345. doi: 10.1186/s13287-019-1447-y

55. Babazadeh S, Nassiri SM, Siavashi V, Sahlabadi M, Hajinasrollah M, Zamani-Ahmadmahmudi M. Macrophage polarization by MSC-derived CXCL12 determines tumor growth. *Cell Mol Biol Lett*. (2021) 26(1):30. doi: 10.1186/s11658-021-00273-w

56. Zhao Y, Zhu XY, Song T, Zhang L, Eirin A, Conley S, et al. Mesenchymal stem cells protect renal tubular cells via TSG-6 regulating macrophage function and phenotype switching. *Am J Physiol Renal Physiol*. (2021) 320(3):F454–63. doi: 10.1152/ajprenal.00426.2020

57. Song JY, Kang HJ, Hong JS, Kim CJ, Shim JY, Lee CW, et al. Umbilical cord-derived mesenchymal stem cell extracts reduce colitis in mice by re-polarizing intestinal macrophages. *Sci Rep*. (2017) 7(1):9412. doi: 10.1038/s41598-017-09827-5

58. He X, Dong Z, Cao Y, Wang H, Liu S, Liao L, et al. MSC-derived exosome promotes M2 polarization and enhances cutaneous wound healing. *Stem Cells Int*. (2019) 2019:7132708. doi: 10.1155/2019

59. Regmi S, Pathak S, Kim JO, Yong CS, Jeong JH. Mesenchymal stem cell therapy for the treatment of inflammatory diseases: challenges, opportunities, and future perspectives. *Eur J Cell Biol*. (2019) 98(5-8):151041. doi: 10.1016/j.ejcb.2019.04.002

60. Mo Y, Kang H, Bang JY, Shin JW, Kim HY, Cho SH, et al. Intratracheal administration of mesenchymal stem cells modulates lung macrophage polarization and exerts anti-asthmatic effects. *Sci Rep*. (2022) 12(1):11728. doi: 10.1038/s41598-022-14846-y

61. Goodwin M, Sueblinvong V, Eisenhauer P, Ziats NP, LeClair L, Poynter ME, et al. Bone marrow-derived mesenchymal stromal cells inhibit Th2-mediated allergic airways inflammation in mice. *Stem Cells*. (2011) 29(7):1137–48. doi: 10.1002/stem.656

62. Song JY, Kang HJ, Ju HM, Park A, Park H, Hong JS, et al. Umbilical cord-derived mesenchymal stem cell extracts ameliorate atopic dermatitis in mice by reducing the T cell responses. *Sci Rep*. (2019) 9(1):6623. doi: 10.1038/s41598-019-42964-7

63. Zhou H, Guo M, Bian C, Sun Z, Yang Z, Zeng Y, et al. Efficacy of bone marrow-derived mesenchymal stem cells in the treatment of sclerodermatous chronic graft-versus-host disease: clinical report. *Biol Blood Marrow Transplant*. (2010) 16(3):403–12. doi: 10.1016/j.bbmt.2009.11.006

64. Aggarwal S, Pittenger MF. Human mesenchymal stem cells modulate allogeneic immune cell responses. *Blood*. (2005) 105(4):1815–22. doi: 10.1182/blood-2004-04-1559

65. Okano T, Yamada N, Okuhara M, Sakai H, Sakurai Y. Mechanism of cell detachment from temperature-modulated, hydrophilic-hydrophobic polymer surfaces. *Biomaterials*. (1995) 16(4):297–303. doi: 10.1016/0142-9612(95)93257-E

66. Kobayashi J, Kikuchi A, Aoyagi T, Okano T. Cell sheet tissue engineering: cell sheet preparation, harvesting/manipulation, and transplantation. *J Biomed Mater Res A*. (2019) 107(5):955–67. doi: 10.1002/jbm.a.36627

67. Yu J, Wang MY, Tai HC, Cheng NC. Cell sheet composed of adipose-derived stem cells demonstrates enhanced skin wound healing with reduced scar formation. *Acta Biomater*. (2018) 77:191–200. doi: 10.1016/j.actbio.2018.07.022

68. Sun L, Huang Y, Bian Z, Petrosino J, Fan Z, Wang Y, et al. Sundew-Inspired adhesive hydrogels combined with adipose-derived stem cells for wound healing. *ACS Appl Mater Interfaces*. (2016) 8(3):2423–34. doi: 10.1021/acsami.5b11811

69. Li X, Xie X, Lian W, Shi R, Han S, Zhang H, et al. Exosomes from adipose-derived stem cells overexpressing Nrf2 accelerate cutaneous wound healing by promoting vascularization in a diabetic foot ulcer rat model. *Exp Mol Med*. (2018) 50(4):1–14. doi: 10.1038/s12276-018-0058-5

70. Wang W, Du Z, Yan J, Ma D, Shi M, Zhang M, et al. Mesenchymal stem cells promote liver regeneration and prolong survival in small-for-size liver grafts: involvement of C-jun N-terminal kinase, cyclin D1, and NF-κB. *PloS One*. (2014) 9(12):e112532. doi: 10.1371/journal.pone.0112532

71. Martin P. Wound healing—aiming for perfect skin regeneration. *Science*. (1997) 276(5309):75–81. doi: 10.1126/science.276.5309.75

72. Smith AN, Willis E, Chan VT, Muffley LA, Isik FF, Gibran NS, et al. Mesenchymal stem cells induce dermal fibroblast responses to injury. *Exp Cell Res*. (2010) 316(1):48–54. doi: 10.1016/j.yexcr.2009.08.001

73. Yates CC, Rodrigues M, Nuschke A, Johnson ZI, Whaley D, Stolz D, et al. Multipotent stromal cells/mesenchymal stem cells and fibroblasts combine to minimize skin hypertrophic scarring. *Stem Cell Res Ther*. (2017) 8(1):193. doi: 10.1186/s13287-017-0644-9

74. McBride JD, Rodriguez-Menocal L, Guzman W, Candanedo A, Garcia-Contreras M, Badiavas EV. Bone marrow mesenchymal stem cell-derived CD63 (+) exosomes transport Wnt3a exteriorly and enhance dermal fibroblast proliferation, migration, and angiogenesis in vitro. *Stem Cells Dev*. (2017) 26 (19):1384–98. doi: 10.1089/scd.2017.0087

75. Zhang B, Wang M, Gong A, Zhang X, Wu X, Zhu Y, et al. HucMSC-exosome mediated-Wnt4 signaling is required for cutaneous wound healing. *Stem Cells*. (2015) 33(7):2158–68. doi: 10.1002/stem.1771

76. Kaita Y, Tarui T, Yoshino H, Matsuda T, Yamaguchi Y, Nakagawa T, et al. Sufficient therapeutic effect of cryopreserved frozen adipose-derived regenerative cells on burn wounds. *Regener Ther*. (2019) 10:92–103. doi: 10.1016/j.reth.2019.01.001

77. Strzalka W, Ziemienowicz A. Proliferating cell nuclear antigen (PCNA): a key factor in DNA replication and cell cycle regulation. *Ann Bot*. (2011) 107 (7):1127–40. doi: 10.1093/aob/mcq243

78. Tsai WC, Cheng JW, Chen JL, Chen CY, Chang HN, Liao YH, et al. Low-level laser irradiation stimulates tenocyte proliferation in association with increased NO synthesis and upregulation of PCNA and cyclins. *Lasers Med Sci*. (2014) 29(4):1377–84. doi: 10.1007/s10103-014-1528-1

79. Zhou Y, Zhao B, Zhang XL, Lu YJ, Lu ST, Cheng J, et al. Combined topical and systemic administration with human adipose-derived mesenchymal stem cells (hADSC) and hADSC-derived exosomes markedly promoted cutaneous wound healing and regeneration. *Stem Cell Res Ther*. (2021) 12(1):257. doi: 10.1186/s13287-021-02287-9

80. Pan H, Lam PK, Tong SW, Leung KK, Teoh AY, Ng EK. Mesenchymal stem cells combined with tissue fusion technology promoted wound healing in porcine bowel anastomosis. *Stem Cells Int*. (2020) 2020:5142797. doi: 10.1155/2020/5142797

81. Pelizzo G, Avanzini MA, Icaro Cornaglia A, Osti M, Romano P, Avolio L, et al. Mesenchymal stromal cells for cutaneous wound healing in a rabbit model: pre-clinical study applicable in the pediatric surgical setting. *J Transl Med*. (2015) 13:219. doi: 10.1186/s12967-015-0580-3

82. Cases-Perera O, Blanco-Elices C, Chato-Astrain J, Miranda-Fernández C, Campos F, Crespo PV, et al. Development of secretome-based strategies to improve cell culture protocols in tissue engineering. *Sci Rep*. (2022) 12(1):10003. doi: 10.1038/s41598-022-14115-y

83. Hassanzadeh H, Matin MM, Naderi-Meshkin H, Bidkhori HR, Mirahmadi M, Raeesolmohaddeseen M, et al. Using paracrine effects of Ad-MSCs on keratinocyte cultivation and fabrication of epidermal sheets for improving clinical applications. *Cell Tissue Bank*. (2018) 19(4):531–47. doi: 10.1007/s10561-018-9702-5

84. Bellei B, Migliano E, Tedesco M, Caputo S, Papaccio F, Lopez G, et al. Adipose tissue-derived extracellular fraction characterization: biological and clinical considerations in regenerative medicine. *Stem Cell Res Ther*. (2018) 9 (1):207. doi: 10.1186/s13287-018-0956-4

85. Guerra A, Belinha J, Jorge RN. Modelling skin wound healing angiogenesis: a review. *J Theor Biol*. (2018) 459:1–17. doi: 10.1016/j.jtbi.2018.09.020

86. Huang M, Huang X, Jiang B, Zhang P, Guo L, Cui X, et al. linc00174-EZH2-ZNF24/Runx1-VEGFA regulatory mechanism modulates post-burn wound healing. *Mol Ther Nucleic Acids*. (2020) 21:824–36. doi: 10.1016/j.omtn.2020.07.010

87. Rehman J, Traktuev D, Li J, Merfeld-Clauss S, Temm-Grove CJ, Bovenkerk JE, et al. Secretion of angiogenic and antiapoptotic factors by human adipose stromal cells. *Circulation*. (2004) 109(10):1292–8. doi: 10.1161/01.CIR.0000121425.42966.F1

88. Goodarzi P, Alavi-Moghadam S, Sarvari M, Tayanloo Beik A, Falahzadeh K, Aghayan H, et al. Adipose tissue-derived stromal cells for wound healing. *Adv Exp Med Biol*. (2018) 1119:133–49. doi: 10.1007/5584

89. Liu Y, Chen J, Liang H, Cai Y, Li X, Yan L, et al. Human umbilical cord-derived mesenchymal stem cells not only ameliorate blood glucose but also protect vascular endothelium from diabetic damage through a paracrine mechanism mediated by MAPK/ERK signaling. *Stem Cell Res Ther*. (2022) 13 (1):258. doi: 10.1186/s13287-022-02927-8

90. Cheng NC, Lin WJ, Ling TY, Young TH. Sustained release of adipose-derived stem cells by thermosensitive chitosan/gelatin hydrogel for therapeutic angiogenesis. *Acta Biomater*. (2017) 51:258–67. doi: 10.1016/j.actbio.2017.01.060

91. Xue J, Sun N, Liu Y. Self-Assembled nano-peptide hydrogels with human umbilical cord mesenchymal stem cell spheroids accelerate diabetic skin wound healing by inhibiting inflammation and promoting angiogenesis. *Int J Nanomed*. (2022) 17:2459–74. doi: 10.2147/IJN.S363777

92. Luo Y, Yi X, Liang T, Jiang S, He R, Hu Y, et al. Autograft microskin combined with adipose-derived stem cell enhances wound healing in a full-thickness skin defect mouse model. *Stem Cell Res Ther*. (2019) 10(1):279. doi: 10.1186/s13287-019-1389-4

93. Schweizer R, Kamat P, Schweizer D, Dennler C, Zhang S, Schnider JT, et al. Bone marrow-derived mesenchymal stromal cells improve vascular regeneration and reduce leukocyte-endothelium activation in critical ischemic murine skin in a dose-dependent manner. *Cytotherapy*. (2014) 16(10):1345–60. doi: 10.1016/j.jcyt.2014.05.008

94. Pugliese E, Coentro JQ, Raghunath M, Zeugolis DI. Wound healing and scar wars. *Adv Drug Delivery Rev*. (2018) 129:1–3. doi: 10.1016/j.addr.2018.05.010

95. Li L, Zhang S, Zhang Y, Yu B, Xu Y, Guan Z. Paracrine action mediate the antifibrotic effect of transplanted mesenchymal stem cells in a rat model of global heart failure. *Mol Biol Rep*. (2009) 36(4):725–31. doi: 10.1007/s11033-008-9235-2

96. Li L, Zhang Y, Li Y, Yu B, Xu Y, Zhao S, et al. Mesenchymal stem cell transplantation attenuates cardiac fibrosis associated with isoproterenol-induced global heart failure. *Transplant Int*. (2008) 21(12):1181–9. doi: 10.1111/j.1432-2277.2008.00742.x

97. Wang L, Hu L, Zhou X, Xiong Z, Zhang C, Shehada HMA, et al. Exosomes secreted by human adipose mesenchymal stem cells promote scarless cutaneous repair by regulating extracellular matrix remodelling. *Sci Rep*. (2017) 7(1):13321. doi: 10.1038/s41598-017-12919-x

98. Yuan B, Broadbent JA, Huan J, Yang H. The effects of adipose stem cell-conditioned media on fibrogenesis of dermal fibroblasts stimulated by transforming growth factor-beta1. *J Burn Care Res*. (2018) 39(1):129–40. doi: 10.1097/BCR.0000000000000558

99. Hu CH, Tseng YW, Chiou CY, Lan KC, Chou CH, Tai CS, et al. Bone marrow concentrate-induced mesenchymal stem cell conditioned medium facilitates wound healing and prevents hypertrophic scar formation in a rabbit ear model. *Stem Cell Res Ther*. (2019) 10(1):275. doi: 10.1186/s13287-019-1383-x

100. Fang S, Xu C, Zhang Y, Xue C, Yang C, Bi H, et al. Umbilical cord-derived mesenchymal stem cell-derived exosomal microRNAs suppress myofibroblast differentiation by inhibiting the transforming growth factor-β/SMAD2 pathway during wound healing. *Stem Cells Transl Med*. (2016) 5(10):1425–39. doi: 10.5966/sctm.2015-0367

101. Trounson A, McDonald C. Stem cell therapies in clinical trials: progress and challenges. *Cell Stem Cell*. (2015) 17(1):11–22. doi: 10.1016/j.stem.2015.06.007

102. Taverna S, Pucci M, Alessandro R. Extracellular vesicles: small bricks for tissue repair/regeneration. *Ann Transl Med*. (2017) 5(4):83. doi: 10.21037/atm.2017.01.53

103. Harrell CR, Jovicic N, Djonov V, Arsenijevic N, Volarevic V. Mesenchymal stem cell-derived exosomes and other extracellular vesicles as new remedies in the therapy of inflammatory diseases. *Cells*. (2019) 8(12):1–22. doi: 10.3390/cells8121605

104. Mathivanan S, Ji H, Simpson RJ. Exosomes: extracellular organelles important in intercellular communication. *J Proteomics*. (2010) 73(10):1907–20. doi: 10.1016/j.jprot.2010.06.006

105. Casado-Díaz A, Quesada-Gómez JM, Dorado G. Extracellular vesicles derived from mesenchymal stem cells (MSC) in regenerative medicine: applications in skin wound healing. *Front Bioeng Biotechnol*. (2020) 8:146. doi: 10.3389/fbioe.2020.00146

106. Kranendonk MEG, Visseren FLJ, van Balkom BWM, Nolte't Hoen ENM, van Herwaarden JA, de Jager W, et al. Human adipocyte extracellular vesicles in reciprocal signaling between adipocytes and macrophages. *Obesity*. (2014) 22 (5):1296–308. doi: 10.1002/oby.20679

107. Chen B, Cai J, Wei Y, Jiang Z, Desjardins HE, Adams AE, et al. Exosomes are comparable to source adipose stem cells in fat graft retention with up-regulating early inflammation and angiogenesis. *Plast Reconstr Surg*. (2019) 144 (5):816e–27e. doi: 10.1097/PRS.0000000000006175

108. Hoang DH, Nguyen TD, Nguyen HP, Nguyen XH, Do PTX, Dang VD, et al. Differential wound healing capacity of mesenchymal stem cell-derived exosomes originated from bone marrow, adipose tissue and umbilical cord under serum- and xeno-free condition. *Front Mol Biosci*. (2020) 7:119. doi: 10.3389/fmolb.2020.00119

109. Choi EW, Seo MK, Woo EY, Kim SH, Park EJ, Kim S. Exosomes from human adipose-derived stem cells promote proliferation and migration of skin fibroblasts. *Exp Dermatol*. (2018) 27(10):1170–2. doi: 10.1111/exd.13451

110. Xu T, Jin J, Gregory C, Hickman JJ, Boland T. Inkjet printing of viable mammalian cells. *Biomaterials*. (2005) 26(1):93–9. doi: 10.1016/j.biomaterials.2004.04.011

111. Gao C, Lu C, Jian Z, Zhang T, Chen Z, Zhu Q, et al. 3D bioprinting for fabricating artificial skin tissue. *Colloids Surf B Biointerfaces*. (2021) 208:112041. doi: 10.1016/j.colsurfb.2021.112041

112. Faulkner-Jones A, Fyfe C, Cornelissen DJ, Gardner J, King J, Courtney A, et al.. Bioprinting of human pluripotent stem cells and their directed differentiation into hepatocyte-like cells for the generation of mini-livers in 3D. *Biofabrication*. (2015) 7(4):044102. doi: 10.1088/1758-5090/7/4/044102

113. Germain N, Dhayer M, Dekiouk S, Marchetti P. Current advances in 3D bioprinting for cancer modeling and personalized medicine. *Int J Mol Sci*. (2022) 23(7):1–31. doi: 10.3390/ijms23073432

114. Zhu W, Ma X, Gou M, Mei D, Zhang K, Chen S. 3D Printing of functional biomaterials for tissue engineering. *Curr Opin Biotechnol*. (2016) 40:103–12. doi: 10.1016/j.copbio.2016.03.014

115. Schiele NR, Corr DT, Huang Y, Raof NA, Xie Y, Chrisey DB. Laser-based direct-write techniques for cell printing. *Biofabrication*. (2010) 2(3):032001. doi: 10.1088/1758-5082/2/3/032001

116. Guillemot F, Souquet A, Catros S, Guillotin B. Laser-assisted cell printing: principle, physical parameters versus cell fate and perspectives in tissue engineering. *Nanomedicine*. (2010) 5(3):507–15. doi: 10.2217/nnm.10.14

117. Ringeisen BR, Othon CM, Barron JA, Young D, Spargo BJ. Jet-based methods to print living cells. *Biotechnol J*. (2006) 1(9):930–48. doi: 10.1002/biot.200600058

118. Ilkhanizadeh S, Teixeira AI, Hermanson O. Inkjet printing of macromolecules on hydrogels to steer neural stem cell differentiation. *Biomaterials*. (2007) 28(27):3936–43. doi: 10.1016/j.biomaterials.2007.05.018

119. Sorkio A, Koch L, Koivusalo L, Deiwick A, Miettinen S, Chichkov B, et al. Human stem cell based corneal tissue mimicking structures using laser-assisted 3D bioprinting and functional bioinks. *Biomaterials*. (2018) 171:57–71. doi: 10.1016/j.biomaterials.2018.04.034

120. Gruene M, Deiwick A, Koch L, Schlie S, Unger C, Hofmann N, et al. Laser printing of stem cells for biofabrication of scaffold-free autologous grafts. *Tissue Eng Part C Methods*. (2011) 17(1):79–87. doi: 10.1089/ten.tec.2010.0359

121. Gao Q, He Y, Fu JZ, Liu A, Ma L. Coaxial nozzle-assisted 3D bioprinting with built-in microchannels for nutrients delivery. *Biomaterials*. (2015) 61:203–15. doi: 10.1016/j.biomaterials.2015.05.031

122. Dinca V, Kasotakis E, Catherine J, Mourka A, Ranella A, Ovsianikov A, et al. Directed three-dimensional patterning of self-assembled peptide fibrils. *Nano Lett*. (2008) 8(2):538–43. doi: 10.1021/nl072798r

123. Gao G, Kim BS, Jang J, Cho DW Recent strategies in extrusion-based three-dimensional cell printing toward organ biofabrication. *ACS Biomater Sci Eng*. (2019) 5(3):1150–69. doi: 10.1021/acsbiomaterials.8b00691

124. Buyuksungur S, Endogan Tanir T, Buyuksungur A, Bektas EI, Torun Kose G, Yucel D, et al. 3D Printed poly(ϵ-caprolactone) scaffolds modified with hydroxyapatite and poly(propylene fumarate) and their effects on the healing of rabbit femur defects. *Biomater Sci*. (2017) 5(10):2144–58. doi: 10.1039/C7BM00514H

125. Sherwood JK, Riley SL, Palazzolo R, Brown SC, Monkhouse DC, Coates M, et al. A three-dimensional osteochondral composite scaffold for articular cartilage repair. *Biomaterials*. (2002) 23(24):4739–51. doi: 10.1016/S0142-9612(02)00223-5

126. Das P, DiVito MD, Wertheim JA, Tan LP. Collagen-I and fibronectin modified three-dimensional electrospun PLGA scaffolds for long-term in vitro maintenance of functional hepatocytes. *Mater Sci Eng C Mater Biol Appl*. (2020) 111:110723. doi: 10.1016/j.msec.2020.110723

127. Knowlton S, Anand S, Shah T, Tasoglu S. Bioprinting for neural tissue engineering. *Trends Neurosci*. (2018) 41(1):31–46. doi: 10.1016/j.tins.2017.11.001

128. Lee H, Ahn S, Bonassar LJ, Kim G. Cell(MC3T3-E1)-printed poly(ε-caprolactone)/alginate hybrid scaffolds for tissue regeneration. *Macromol Rapid Commun*. (2013) 34(2):142–9. doi: 10.1002/marc.201200524

129. Kolan KCR, Semon JA, Bromet B, Day DE, Leu MC. Bioprinting with human stem cell-laden alginate-gelatin bioink and bioactive glass for tissue engineering. *Int J Bioprint*. (2019) 5(2.2):204. doi: 10.18063/ijb.v5i2.2.204

130. Lawlor KT, Vanslambrouck JM, Higgins JW, Chambon A, Bishard K, Arndt D, et al. Cellular extrusion bioprinting improves kidney organoid reproducibility and conformation. *Nat Mater*. (2021) 20(2):260–71. doi: 10.1038/s41563-020-00853-9

131. Chang R, Nam J, Sun W. Effects of dispensing pressure and nozzle diameter on cell survival from solid freeform fabrication-based direct cell writing. *Tissue Eng Part A*. (2008) 14(1):41–8. doi: 10.1089/ten.a.2007.0004

132. Ji S, Guvendiren M. Recent advances in bioink design for 3D bioprinting of tissues and organs. *Front Bioeng Biotechnol*. (2017) 5:23. doi: 10.3389/fbioe.2017.00023

133. Lu Y, Mapili G, Suhali G, Chen S, Roy K. A digital micro-mirror device-based system for the microfabrication of complex, spatially patterned tissue engineering scaffolds. *J Biomed Mater Res A*. (2006) 77(2):396–405. doi: 10.1002/jbm.a.30601

134. Xu C, Chai W, Huang Y, Markwald RR. Scaffold-free inkjet printing of three-dimensional zigzag cellular tubes. *Biotechnol Bioeng*. (2012) 109 (12):3152–60. doi: 10.1002/bit.24591

135. Leberfinger AN, Ravnic DJ, Dhawan A, Ozbolat IT. Concise review: bioprinting of stem cells for transplantable tissue fabrication. *Stem Cells Transl Med*. (2017) 6(10):1940–8. doi: 10.1002/sctm.17-0148

136. Ma X, Qu X, Zhu W, Li YS, Yuan S, Zhang H, et al. Deterministically patterned biomimetic human iPSC-derived hepatic model via rapid 3D bioprinting. *Proc Natl Acad Sci U S A*. (2016) 113(8):2206–11. doi: 10.1073/pnas.1524510113

137. Hossain Rakin R, Kumar H, Rajeev A, Natale G, Menard F, Li ITS, et al. Tunable metacrylated hyaluronic acid-based hybrid bioinks for stereolithography 3D bioprinting. *Biofabrication*. (2021) 13(4). doi: 10.1088/1758-5090/ac25cb

138. Ngo TD, Kashani A, Imbalzano G, Nguyen KTQ, Hui D. Additive manufacturing (3D printing): a review of materials, methods, applications and challenges. *Composites Part B*. (2018) 143:172–96. doi: 10.1016/j.compositesb.2018.02.012

139. Wang X, Dai X, Zhang X, Li X, Xu T, Lan Q. Enrichment of glioma stem cell-like cells on 3D porous scaffolds composed of different extracellular matrix. *Biochem Biophys Res Commun*. (2018) 498(4):1052–7. doi: 10.1016/j.bbrc.2018.03.114

140. Wang X, Li X, Dai X, Zhang X, Zhang J, Xu T, et al. Coaxial extrusion bioprinted shell-core hydrogel microfibers mimic glioma microenvironment and enhance the drug resistance of cancer cells. *Colloids Surf B Biointerfaces*. (2018) 171:291–9. doi: 10.1016/j.colsurfb.2018.07.042

141. Li X, Wang X, Chen H, Jin Z, Dai X, Zhang X, et al. A comparative study of the behavior of neural progenitor cells in extrusion-based in vitro hydrogel models. *Biomed Mater*. (2019) 14(6):065001. doi: 10.1088/1748-605X/ab3b4b

142. Matai I, Kaur G, Seyedsalehi A, McClinton A, Laurencin CT. Progress in 3D bioprinting technology for tissue/organ regenerative engineering. *Biomaterials*. (2020) 226:119536. doi: 10.1016/j.biomaterials.2019.119536

143. Derr K, Zou J, Luo K, Song MJ, Sittampalam GS, Zhou C, et al. Fully three-dimensional bioprinted skin equivalent constructs with validated morphology and barrier function. *Tissue Eng Part C Methods*. (2019) 25(6):334–43. doi: 10.1089/ten.tec.2018.0318

144. Cubo N, Garcia M, Del Cañizo JF, Velasco D, Jorcano JL. 3D bioprinting of functional human skin: production and in vivo analysis. *Biofabrication*. (2016) 9 (1):015006. doi: 10.1088/1758-5090/9/1/015006

145. Do AV, Khorsand B, Geary SM, Salem AK. 3D printing of scaffolds for tissue regeneration applications. *Adv Healthcare Mater*. (2015) 4(12):1742–62. doi: 10.1002/adhm.201500168

146. Guvendiren M, Molde J, Soares RM, Kohn J. Designing biomaterials for 3D printing. *ACS Biomater Sci Eng*. (2016) 2(10):1679–93. doi: 10.1021/acsbiomaterials.6b00121

147. Albanna M, Binder KW, Murphy SV, Kim J, Qasem SA, Zhao W, et al. In situ bioprinting of autologous skin cells accelerates wound healing of extensive excisional full-thickness wounds. *Sci Rep*. (2019) 9(1):1856. doi: 10.1038/s41598-018-38366-w

148. Jin R, Cui Y, Chen H, Zhang Z, Weng T, Xia S, et al. Three-dimensional bioprinting of a full-thickness functional skin model using acellular dermal

matrix and gelatin methacrylamide bioink. *Acta Biomater*. (2021) 131:248–61. doi: 10.1016/j.actbio.2021.07.012

149. Ong CS, Yesantharao P, Huang CY, Mattson G, Boktor J, Fukunishi T, et al. 3D Bioprinting using stem cells. *Pediatr Res*. (2018) 83(1-2):223–31. doi: 10.1038/pr.2017.252

150. Chen J, Zhou D, Nie Z, Lu L, Lin Z, Zhou D, et al. A scalable coaxial bioprinting technology for mesenchymal stem cell microfiber fabrication and high extracellular vesicle yield. *Biofabrication*. (2021) 14(1):1–17. doi: 10.1088/1758-5090/ac3b90

151. Roshangar L, Rad JS, Kheirjou R, Khosroshahi AF. Using 3D-bioprinting scaffold loaded with adipose-derived stem cells to burns wound healing. *J Tissue Eng Regen Med*. (2021) 15(6):546–55. doi: 10.1002/term.3194

152. Wu Y, Liang T, Hu Y, Jiang S, Luo Y, Liu C, et al. 3D Bioprinting of integral ADSCs-NO hydrogel scaffolds to promote severe burn wound healing. *Regen Biomater*. (2021) 8(3):rbab014.

153. Turner PR, Murray E, McAdam CJ, McConnell MA, Cabral JD. Peptide chitosan/dextran core/shell vascularized 3D constructs for wound healing. *ACS Appl Mater Interfaces*. (2020) 12(29):32328–39. doi: 10.1021/acsami.0c07212

154. Turner PR, McConnell M, Young SL, Cabral JD. 3D living dressing improves healing and modulates immune response in a thermal injury model. *Tissue Eng Part C Methods*. (2022) 28(8):431–9. doi: 10.1093/rb/rbab014

155. Shapira A, Dvir T. 3D tissue and organ printing-hope and reality. *Adv Sci*. (2021) 8(10):2003751. doi: 10.1002/advs.202003751

156. Gruene M, Pflaum M, Hess C, Diamantouros S, Schlie S, Deiwick A, et al. Laser printing of three-dimensional multicellular arrays for studies of cell-cell and cell-environment interactions. *Tissue Eng Part C Methods*. (2011) 17(10):973–82. doi: 10.1089/ten.tec.2011.0185

157. Kim BS, Kwon YW, Kong JS, Park GT, Gao G, Han W, et al. 3D Cell printing of in vitro stabilized skin model and in vivo pre-vascularized skin patch using tissue-specific extracellular matrix bioink: a step towards advanced skin tissue engineering. *Biomaterials*. (2018) 168:38–53. doi: 10.1016/j.biomaterials.2018.03.040

158. Li J, Zhang Y, Enhe J, Yao B, Wang Y, Zhu D, et al. Bioactive nanoparticle reinforced alginate/gelatin bioink for the maintenance of stem cell stemness. *Mater Sci Eng C Mater Biol Appl*. (2021) 126:112193. doi: 10.1016/j.msec.2021.112193

159. Cheng L, Yao B, Hu T, Cui X, Shu X, Tang S, et al. Properties of an alginate-gelatin-based bioink and its potential impact on cell migration, proliferation, and differentiation. *Int J Biol Macromol*. (2019) 135:1107–13. doi: 10.1016/j.ijbiomac.2019.06.017

160. Yao B, Wang R, Wang Y, Zhang Y, Hu T, Song W, et al. Biochemical and structural cues of 3D-printed matrix synergistically direct MSC differentiation for functional sweat gland regeneration. *Sci Adv*. (2020) 6(10):eaaz1094. doi: 10.1126/sciadv.aaz1094

161. Nourian Dehkordi A, Mirahmadi Babaheydari F, Chehelgerdi M, Raeisi Dehkordi S. Skin tissue engineering: wound healing based on stem-cell-based therapeutic strategies. *Stem Cell Res Ther*. (2019) 10(1):111. doi: 10.1186/s13287-019-1212-2

162. Bojanic C, To K, Hatoum A, Shea J, Seah KTM, Khan W, et al. Mesenchymal stem cell therapy in hypertrophic and keloid scars. *Cell Tissue Res*. (2021) 383(3):915–30. doi: 10.1007/s00441-020-03361-z

163. Giebel B, Kordelas L, Börger V. Clinical potential of mesenchymal stem/stromal cell-derived extracellular vesicles. *Stem Cell Invest*. (2017) 4:84. doi: 10.21037/sci.2017.09.06

164. Kusuma GD, Barabadi M, Tan JL, Morton DAV, Frith JE, Lim R. To protect and to preserve: novel preservation strategies for extracellular vesicles. *Front Pharmacol*. (2018) 9:1199. doi: 10.3389/fphar.2018.01199

165. Singh S, Choudhury D, Yu F, Mironov V, Naing MW. In situ bioprinting—bioprinting from benchside to bedside? *Acta Biomater*. (2020) 101:14–25. doi: 10.1016/j.actbio.2019.08.045

166. Rothbauer M, Eilenberger C, Spitz S, Bachmann BEM, Kratz SRA, Reihs EI, et al. Recent advances in additive manufacturing and 3D bioprinting for organs-on-A-chip and microphysiological systems. *Front Bioeng Biotechnol*. (2022) 10:837087. doi: 10.3389/fbioe.2022.837087

167. Tsiapalis D, O'Driscoll L. Mesenchymal stem cell derived extracellular vesicles for tissue engineering and regenerative medicine applications. *Cells*. (2020) 9(4):1–27. doi: 10.3390/cells9040991

168. Maiullari F, Chirivì M, Costantini M, Ferretti AM, Recchia S, Maiullari S, et al. In vivo organized neovascularization induced by 3D bioprinted endothelial-derived extracellular vesicles. *Biofabrication*. (2021) 13(3). doi: 10.1088/1758-5090/abdacf

169. Bari E, Scocozza F, Perteghella S, Sorlini M, Auricchio F, Torre ML, et al. 3D bioprinted scaffolds containing mesenchymal stem/stromal lyosecretome: next generation controlled release device for bone regenerative medicine. *Pharmaceutics*. (2021) 13(4):1–23. doi: 10.3390/pharmaceutics13040515

170. Kanitakis J. Anatomy, histology and immunohistochemistry of normal human skin. *Eur J Dermatol*. (2002) 12(4):390–9, quiz 400–1. PMID: 12095893

171. Vig K, Chaudhari A, Tripathi S, Dixit S, Sahu R, Pillai S, et al. Advances in skin regeneration using tissue engineering. *Int J Mol Sci*. (2017) 18(4):1–19. doi: 10.3390/ijms18040789

frontiers | Frontiers in Surgery

TYPE Original Research
PUBLISHED 21 October 2022
DOI 10.3389/fsurg.2022.1025557

Check for updates

OPEN ACCESS

EDITED BY
Jiliang Zhou,
Georgia Health Sciences University,
United States

REVIEWED BY
Zhang Jianglin,
Jinan University, China
Fang Wang,
Sun Yat-sen University, China

*CORRESPONDENCE
Rong-hua Yang
21720091@qq.com
Kun Xiong
xiongkun2001@163.com

†These authors have contributed equally to this work

SPECIALTY SECTION
This article was submitted to Reconstructive and Plastic Surgery, a section of the journal Frontiers in Surgery

RECEIVED 23 August 2022
ACCEPTED 28 September 2022
PUBLISHED 21 October 2022

CITATION
Zheng S-y, Hu X-m, Huang K, Li Z-h, Chen Q-n, Yang R-h and Xiong K (2022) Proteomics as a tool to improve novel insights into skin diseases: what we know and where we should be going.
Front. Surg. 9:1025557.
doi: 10.3389/fsurg.2022.1025557

COPYRIGHT
© 2022 Zheng, Hu, Huang, Li, Chen, Yang and Xiong. This is an open-access article distributed under the terms of the Creative Commons Attribution License (CC BY). The use, distribution or reproduction in other forums is permitted, provided the original author(s) and the copyright owner(s) are credited and that the original publication in this journal is cited, in accordance with accepted academic practice. No use, distribution or reproduction is permitted which does not comply with these terms.

# Proteomics as a tool to improve novel insights into skin diseases: what we know and where we should be going

Sheng-yuan Zheng[1,2†], Xi-min Hu[1,2†], Kun Huang[3], Zi-han Li[3], Qing-ning Chen[3], Rong-hua Yang[4*] and Kun Xiong[2,5,6*]

[1]Department of Dermatology, Xiangya Hospital, Central South University, Changsha, China, [2]Department of Anatomy and Neurobiology, School of Basic Medical Science, Central South University, Changsha, China, [3]Clinical Medicine Eight-Year Program, Xiangya School of Medicine, Central South University, Changsha, China, [4]Department of Burn and Plastic Surgery, Guangzhou First People's Hospital, School of 173 Medicine, South China University of Technology, Guangzhou, China, [5]Key Laboratory of Emergency and Trauma, Ministry of Education, College of Emergency and Trauma, Hainan Medical University, Haikou, China, [6]Hunan Key Laboratory of Ophthalmology, Central South University, Changsha, China

**Background:** Biochemical processes involved in complex skin diseases (skin cancers, psoriasis, and wound) can be identified by combining proteomics analysis and bioinformatics tools, which gain a next-level insight into their pathogenesis, diagnosis, and therapeutic targets.
**Methods:** Articles were identified through a search of PubMed, Embase, and MEDLINE references dated to May 2022, to perform system data mining, and a search of the Web of Science (WoS) Core Collection was utilized to conduct a visual bibliometric analysis.
**Results:** An increased trend line revealed that the number of publications related to proteomics utilized in skin diseases has sharply increased recent years, reaching a peak in 2021. The hottest fields focused on are skin cancer (melanoma), inflammation skin disorder (psoriasis), and skin wounds. After deduplication and title, abstract, and full-text screening, a total of 486 of the 7,822 outcomes met the inclusion/exclusion criteria for detailed data mining in the field of skin disease tooling with proteomics, with regard to skin cancer. According to the data, cell death, metabolism, skeleton, immune, and inflammation enrichment pathways are likely the major part and hotspots of proteomic analysis found in skin diseases. Also, the focuses of proteomics in skin disease are from superficial presumption to depth mechanism exploration within more comprehensive validation, from basic study to a combination or guideline for clinical applications. Furthermore, we chose skin cancer as a typical example, compared with other skin disorders. In addition to finding key pathogenic proteins and differences between diseases, proteomic analysis is also used for therapeutic evaluation or can further obtain in-depth mechanisms in the field of skin diseases.
**Conclusion:** Proteomics has been regarded as an irreplaceable technology in the study of pathophysiological mechanism and/or therapeutic targets of skin diseases, which could provide candidate key proteins for the insight into the biological information after gene transcription. However, depth pathogenesis and potential clinical applications need further studies with stronger evidence within a wider range of skin diseases.

KEYWORDS

proteomics, skin disease, bibliometric analysis, data mining study, pathogenesis, treatment, molecular biomarker

## Introduction

Skin, as the human body's largest and one of the most important organs, exerts an essential function, such as protecting from external insults and maintaining microenvironment homeostasis, based on the exquisite balance of intestinal microbiota, metabolites, and so on. Once this balance is damaged or out of the compensatory range, various skin disorders occur concomitantly, resulting in physical impairment and adversely impacting the quality of life worldwide. As for this, a majority of studies have focused on the pathophysiological mechanisms of different skin diseases, benefited for accurate diagnosis and identifying the subtype of skin diseases, finding an efficient therapeutic target, and/or evaluating the treatment or nursing care effect. However, there are still multiple challenges during the basic investigation, clinical diagnosis, and treatment (e.g., a low specific mechanism or biomarker in skin diseases, preliminary inquiry of the critical molecules, ignoring the co-network in different skin diseases or other systemic changes, and arduous process in mining problem). For these aspects, the emergence of proteomics provides a systematic and reliable prediction tool or verification method (1, 2).

Mass spectrometry (MS)-based high-throughput proteomics has been regarded as a core technique for large-scale protein characterization in cells, tissues, or organisms. It mainly provides a qualitative and quantitative analysis of proteins in samples as complementary bio-information to genomics and transcriptomics, which is essential for better understanding the complex biochemical processes (3–5). From the production of proteins to function execution, it refers to various conditions for multiple post-translational mechanisms. So, proteomics has not been limited to be performed in a quantitative fashion of a conventional protein. It has also been improved to be used in the analysis of specific modifications (e.g., acetylations, methylations, and phosphorylations), leading to an insightful analysis of protein function (6–8). As we can see, the proteomic analysis aims to increase the depth of protein coverage of cells or tissues. Notably, with the development of technologies, proteomics has integrated computer elements to improve the accuracy and comprehensiveness (7–9). Meanwhile, public databases and analysis platforms began to appear and continued to innovate (10, 11), promoting proteomics data sharing and analysis applications in various fields.

In the past decade, proteomics has been used in skin diseases, which significantly contributed to skin disease's pathogenesis and clinical applications. For instance, in research on the pathophysiological mechanism, proteomics can provide candidate hub proteins (12). It can also identify similarities and differences in the proteome of different skin diseases with similar symptoms (13). Furthermore, proteomics can reveal biomarkers of different degrees of skin diseases, drug treatment targets, and treatment effects (14–16). However, the application of proteomics in skin disease research has not shown a corresponding high growth rate with the innovation of key technologies (17, 18). Moreover, only conventional proteomics methods have been used widely in most studies, and a few attempted to combine proteomics with other techniques or used multi-omics analysis (19, 20). These may make some of the limitations of proteomics irreparable, and the single application solution may also hinder the advantages of proteomics. So, the necessity to fully understand the advantages and limitations of proteomics in skin disease research is one of the keys to promoting this research. As far as we are concerned, there are no comprehensive and systemic information and suggestions for proteomics applied in skin diseases based on accurate data. Data mining and analysis is a suitable statistical and analysis method that can analyze the value and future trend of proteomics in skin diseases based on the published literature and provide more practical information in the direction of research and methods of proteomics application.

Generally, bibliometrics has been used as a visual analysis for trend and hot spot prediction through publications, citations, and keywords (21–23). However, since the datasets "Proteomics for Skin Disease Research" were accessed through searching online databases, the qualifier "skin disease" in the search cannot comprehensively and accurately represent all skin disease research using proteomics. Thus, we chose to use more accurate and heavier workload data mining to screen and analyze the datasets retrieved from three databases—PubMed, MEDLINE, and Embase. By manually analyzing the data, we summarized the proportion of research directions and the characteristics of time migration according to the application of proteomics in skin diseases, supplemented by quantitative analysis (**Figure 1**). For specific proteomics research designs, we analyzed the advantages and limitations of proteomics in dermatology based on the overall situation and specific dataset records and proposed more complete research methods. We also made a detailed record and analysis of the current research hotspots, prospects, and trends by collecting skin disease research using proteomics. The results showed that the application of proteomics in skin

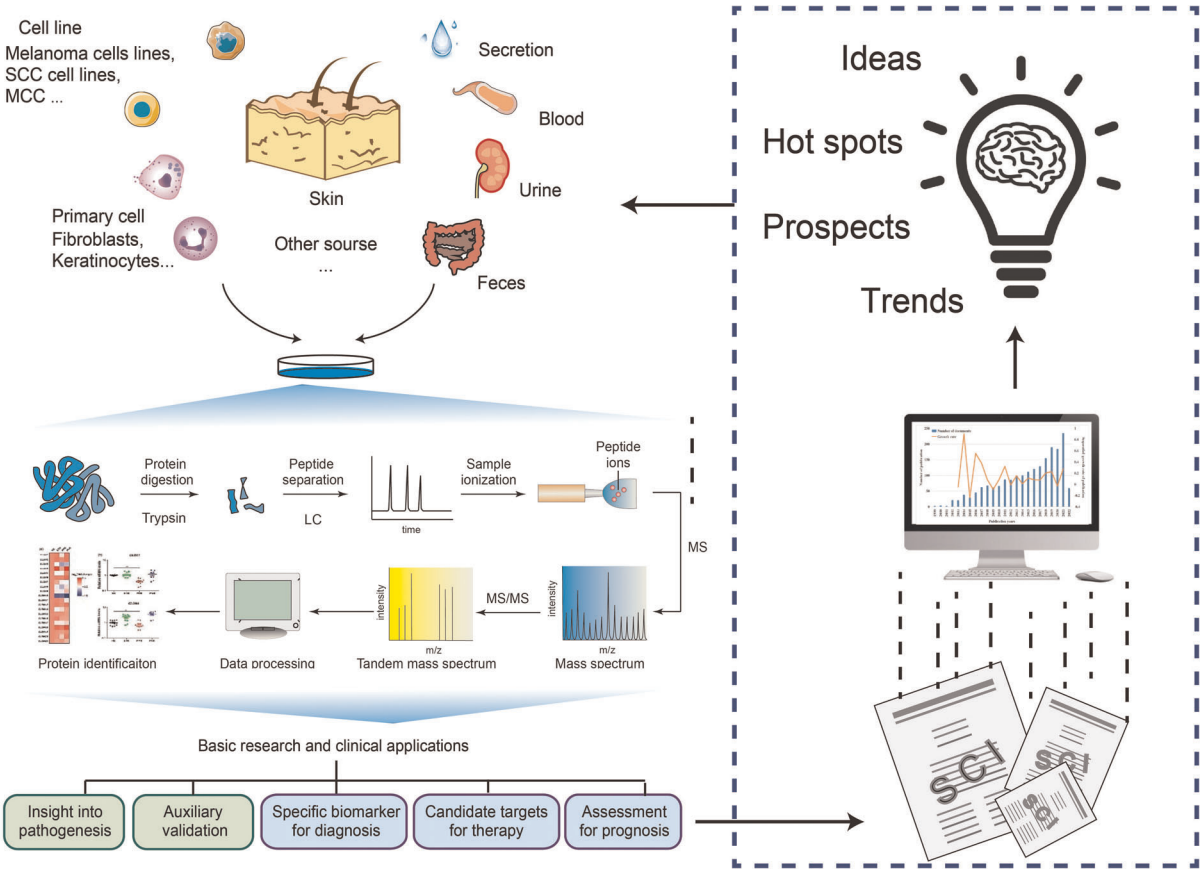


FIGURE 1
Bibliometric and data mining provide insights and trend analysis of proteomics in skin disorder. SCC, squamous cell carcinoma; MCC, Merkel cell carcinoma; LC, liquid chromatogram; MS, mass spectrum.

disease research had differences worth summarizing in terms of sample sources, techniques, and result analysis methods. In terms of pathogenesis research, we took skin cancer as a typical example and conducted a comprehensive analysis from exploring molecular functions to finding out biomarkers or take insight into the depth mechanism, which illustrated the irreplaceable importance of proteomics in skin diseases. Ultimately, we hope to summarize the contributions of proteomics and make rational research recommendations with accurate data analysis and comprehensive discussions.

# Data and methods

## Data retrieval and analysis for data mining

### Search strategy

We selected a systematic approach to make a document collection: PubMed, MEDLINE and Embase. The retrieval strategy of each database is customized according to the usage standard of the database and the scale of the retrieved documents. After screening within the inclusion/exclusion criteria, part of the literature has been used for a full-text screening and data collection. The process of literature screening is shown in Figure 2, and more details are as follows.

To perform a systematic analysis of skin and proteomics, we chose articles for inclusion using a data mining analysis. The terms "skin" and "proteomic" were used in the MeSH (https://www.ncbi.nlm.nih.gov/mesh) search, whereas "proteomics," and "proteome," "skin," "cutaneous," "dermal," "dermatis" and "tegumental" were represented by other expressions.

### Preliminary screening according to exclusion/inclusion criteria by screened titles, abstracts, and keywords

Exclusion criteria conducted were as follows:

(1) Not research article: review, letter, book, comment, etc.;
(2) Not skin diseases or not main;
(3) Full-text not available; and
(4) Duplicate articles.

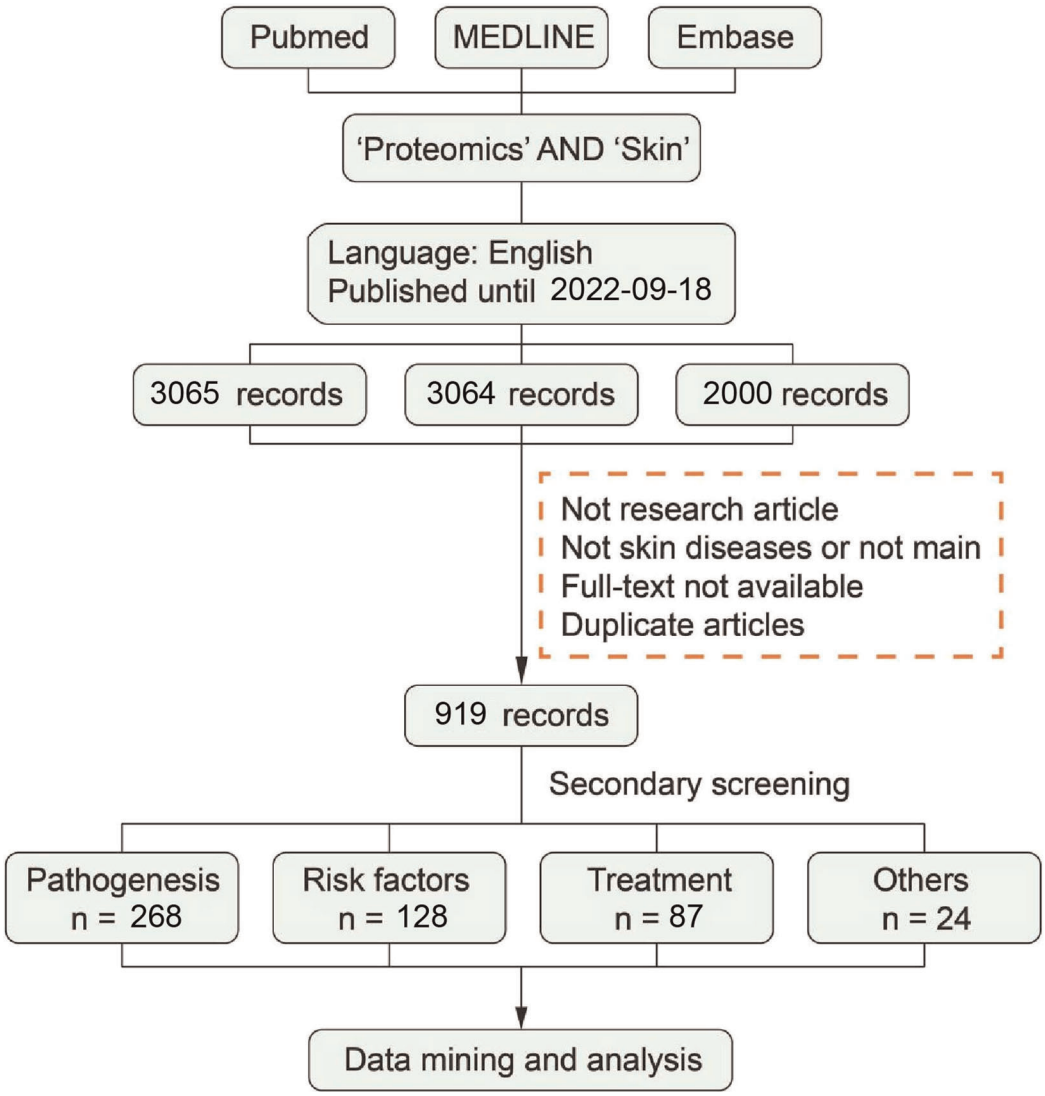


FIGURE 2
Systematic literature search and outcome identification.

After the preliminary screening was completed, 919 literature studies were included for secondary screening.

## Secondary screening according to inclusion criteria by screened full-texts

Inclusion criteria conducted were as follows:

(1) Type of documents: original proteomic data;
(2) Topic of documents: studied on skin diseases using proteomics; and
(3) Contents of documents: Reporting of at least one statistically significant protein were included;

After the secondary screening was completed, 486 literature studies were included for secondary screening.

## Grouping the literature in tables

Literature studies included finally were divided into several groups according to research topics and the four groups are as follows: (1) Pathogenesis; (2) Risk factor; (3) Treatment; (4) Others.

## Data extraction and analysis

Then, we made whole summaries of the literature in publication, situation of development, and analyzed the details in each table. In the process of selecting article data, we mainly extracted disease types, proteomic sample sources, key enrichment pathways, and in-depth research based on differential proteins. In addition, we extracted risk factors for disease in the Risk factor group, and considering that some

studies have also given novel solutions for the corresponding factors, we also extracted Options for risk factors in particular. For the Treatment group, we have additionally extracted treatments for better understanding. Comprehensively analyzing these contents, we have drawn some research characteristics of proteomics in various aspects.

## Data retrieval and analysis for bibliometrics study

To make our summary more credible, we also used bibliometrics to analyze the characteristics of published articles from the perspective of big data. Due to "skin" or "skin diseases" being inaccurate in searching the literature from the databases, we chose skin diseases using data mining. The search was conducted in the Web of Science (WoS) Core Collection database with citation indexes, including Science Citation Index Expanded (SCIE), Social Science Citation Index (SSCI), and Emerging Sources Citation Index (ESCI). A total of 2,060 documents were retrieved to make visual bibliometric analysis with the duration from 1 Jan 2002 to 18 Sep 2022.

# Results

## The overview of the application and distribution of proteomics in skin diseases

All included articles were counted according to respectively related diseases. According to the type of skin diseases, we classified the diseases in different color and performed the publication search by year through manual statistics (**Figure 3**). From 2002 to 2021, the total number of publications was on an upward trend with volatility. Especially from 2015 to 2021, a successive growth trend in proteomics was shown using the field of skin, and our bibliometric data also indicated this increasing trend (**Supplementary Figure S1**). Among these skin diseases, skin cancer seems to be a major part of studies using proteomics that reached the highest growth rate in 2018 and peaked in 2020 and 2021. Also, the publications on psoriasis and atopic dermatitis (AD) showed an increased trend and reached a peak in 2021. As for skin wounds, the growth trend of publications leveled off owing to a massive growth in 2018. The overall trend of cutaneous leishmaniasis has been relatively stable from 2013 and increased slightly in the past

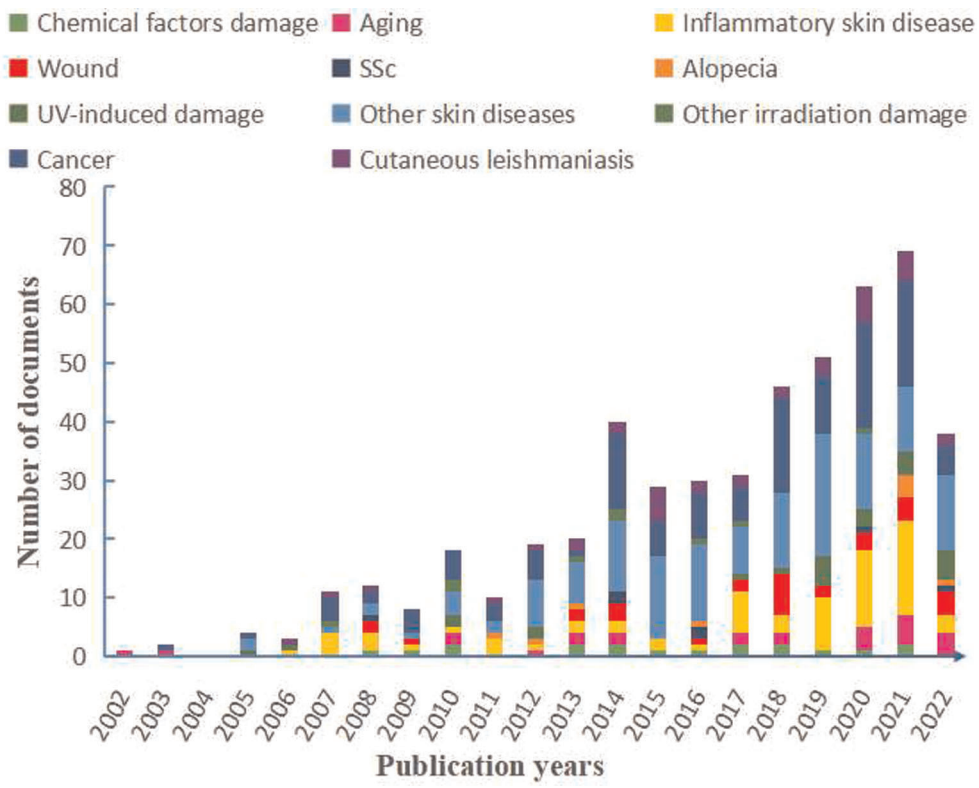


FIGURE 3
Distribution of publications on the studies of skin diseases according to year and each part contributions have also shown. SSc, systemic sclerosis; UV, ultraviolet; AD, atopic dermatitis.

two years (Figure 3). In addition, our bibliometric data have showed that some keywords of skin disease that have co-occurred in recent years are consistent with the above results (Supplementary Figure S2).

In addition, to further analyze the research on skin diseases using proteomics, we noted the diseases with the above conditions. The proportion of different skin diseases varied widely across all studies. Here, we mainly highlighted cancer, inflammatory skin diseases, wound, aging, alopecia, and systemic sclerosis (SSc) (Figure 4). Cancer accounted for the largest proportion of all disease categories (25.514%). Among these, melanoma (18.107%) had the highest proportion, followed by squamous cell carcinoma (SCC) (3.086%). In addition, there were studies involving lymphoma, Merkel cell carcinoma (MCC), and cholesteatoma. Inflammatory skin disease is the second largest category accounting for 14.609%. Psoriasis and AD are the primarily researched diseases, accounting for 7.819% and 6.173%, respectively. Wound, aging, alopecia, and SSc account for a smaller proportion, whose subordinate diseases are more diverse. Cutaneous leishmaniasis, UV-induced damage, and chemical factors damage were classified as other skin diseases here because they are not further subdivided.

Overall, the increased trend line and broad application showed good progress in the study of skin diseases using proteomics. The range of skin diseases is large and diverse within complex pathogenesis, and proteomic analysis provides a systematic analysis of the proteins during the disease development. Notably, proteomic analysis has begun to be incorporated in many other diseases in recent years (Figures 3, 4). However, the sample source, research significance, and their depth and breadth are different, so we conducted full-text mining to obtain more detailed information.

## Pathophysiological research analysis

### Proteomics in pathogenesis, taking skin cancers as the example

A total of 268 articles studied on pathophysiology were obtained and divided into seven parts of different types of skin diseases, including skin cancer, inflammation skin disease, wound, skin aging, hair disorder, systemic sclerosis, and others. According to the data, we suppose that there is something that is common to these skin diseases. For a better understanding of the proteomic application in skin disease,

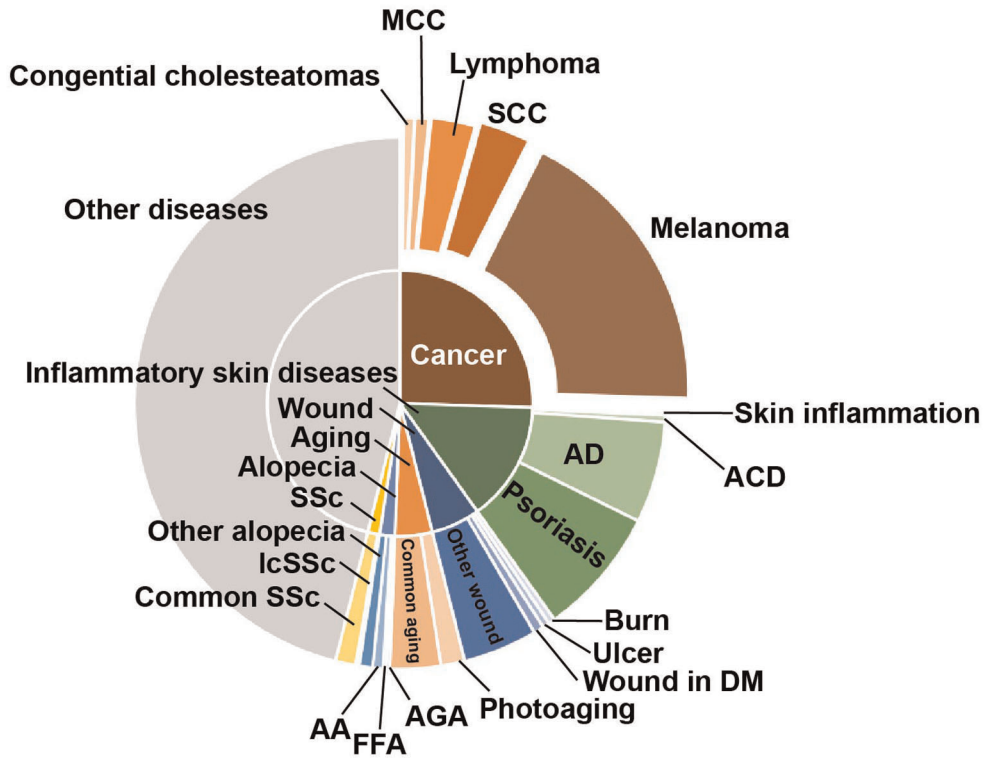


FIGURE 4
The proportion of research on the different skin diseases. The main application directions of proteomics are skin cancer and inflammatory skin diseases, among which melanoma, AD, and psoriasis are the main ones. SCC, squamous cell carcinoma; MCC, Merkel cell carcinoma; AD, atopic dermatitis; ACD, atopic contact dermatitis; DM, diabetes mellitus; FFA, frontal fibrosing alopecia; AA, alopecia areata; AGA, androgenetic alopecia; SSc, systemic sclerosis; lcSSc, limited cutaneous SSc.

we used skin cancer, the most significant proportion in the above profiling, as a typical example in pathogenesis compared with other skin diseases. To elucidate some of the crucial mechanisms of skin cancer and the role of proteomics, we screened the differential proteins in each article, shown as the top upregulated and downregulated ones in **Table 1** and **Supplementary Table S1**.

In data, skin cancers mainly included melanoma, SCC, lymphoma, etc. Some differential proteins with similar functions in cancer appeared in different studies. Moreover, these proteins can be mainly clustered into inflammation, immunity, survival/death, metabolism, metastasis, cyclin-dependent kinase (CDK), and heat shock protein (HSP). (Many of the following proteins have multiple functions, and the clustering here is only based on the main function, rather than an absolute distinction.)

Inflammation-related proteins are detected to upregulate in nearly all skin cancers, such as the interleukin family in melanoma, the S100 calcium-binding proteins in SCC, and tumor necrosis factor(TNF) in cutaneous T-cell lymphomas (CTCL). Some immunity-related proteins were detected in melanoma, like CD14 as a particular protein in stage II melanoma and upregulated Endoglin/CD105. The proteins related to the survival of melanoma cells mainly include Galectin-3, Survivin, Dickkopf (DKK), Bcl-2, and so on.

Proteins related to the metabolism of melanoma cancer cells mainly include heme oxygenase-1 (HO-1/HMOX1), Cathepsin S, Progranulin, FBXO32, etc. For SCC, they mainly include CDC-like kinase 2 (CLK2), serine/threonine kinase 10 (STK10), aldo-keto reductase family 1 member C3 (AKR1C3), etc. There are also some proteins related to cancer migration, such as intercellular adhesion molecule 1 (ICAM-1), tubulin and vascular cellular adhesion molecule-1 (VCAM-1) in melanoma, transforming growth factor-$\beta$ (TGF$\beta$), and calmodulin-like 5 (CALML5) in SCC. In addition, some proteins are involved in many life activities such as tumor cell proliferation and migration, such as serine/threonine kinase 2 (AKT2).

In addition to functional distinction, some proteins can also be considered promising markers for skin cancer diagnosis. HSPs are associated with many characteristics of cancer, such as cell proliferation and metastasis. In addition, there are Survivin, CDK12, Vimentin, and Galectin-3. These proteins may be potential biomarkers for some skin cancers. In addition, some studies focus on markers in the pathogenesis process, but it has not been confirmed experimentally (**Table 1**, **Supplementary Table S1**).

Based on differential proteins, many studies have further enriched their functions to explain critical pathways and biological processes in the development or progression of skin cancer. In melanoma-related proteomic studies, PI3K/AKT pathway, mTOR pathway, and mitogen-activated protein kinase (MAPK)/ERK pathway are the most frequently mentioned signaling pathways (**Supplementary Table S1**). Upstream of the mTOR pathway, PI3K/AKT signaling initiates several selective signaling cascades that lead to increased cell growth and proliferation (24). Whether it is tripartite motif-containing 14 (TRIM14)-promoted melanoma progression or Hey1-promoted melanoma invasion and migration, the PI3K/AKT pathway is an important part (25, 26). Activation of the mTOR signaling pathway plays a role in melanocytic tumorigenesis by regulating extracellular signals that control cell growth, proliferation, and apoptosis (27, 28). MAPK/ERK pathway also plays a vital role in the tumorigenic effects of transcription co-activators 1–3 (29). In addition, most enrichment results focused on biological processes, especially functions related to tumor progressions such as cell adhesion, proliferation, and migration. SCC is similar to melanoma, except that JNK/SAPK signaling, cell division cycle 42 (CDC42) signaling, and Hippo signaling also appears in the pathway enrichment of the former (**Table 1**, **Supplementary Table S1**).

From the data and analysis of skin cancer, proteomics can provide changes in fundamental proteins for disease research and can also explore important functional changes in the pathogenesis through enrichment or in-depth research. This situation is also prominent in other skin diseases. Whether searching for psoriasis biomarkers or the research on the pathogenesis of AD, the application and analysis of proteomics is similar to skin cancer.

## Sample of proteomics

The sources of samples for proteomic analysis were diverse, and the mainstream sample used for each disease was different. The choices of samples are related to the characteristics of the disease and the purpose of the proteome.

The most important source of samples for cancer was tumor cell lines cultured *in vitro*, accounting for 59.302% (**Table 1**, **Supplementary Table S1**). The second was cancer tissue samples, most of which were cancer samples of the skin, and a small number of studies used fibroblasts (30), serum (31), and metastatic cancer tissue (32) to study the progression and metastasis of cancer. Compared with skin cancer, blood samples from diseased individuals are essential and frequently used in research on inflammatory skin diseases (41.818% in **Table 2** and **Supplementary Table S2**). Blood samples include serum, plasma, and biologically active substances and cells in the blood environment. These samples provide an accurate and detailed reflection of inflammatory changes in skin diseases. Based on these changes, biomarkers can obtain biomarkers (33), diseases can be distinguished (13, 34), and also the pathogenesis can be studied with hub proteins (35, 36). In addition, the use of skin tissue samples and primary cell samples was also common. In recent years, studies have begun to use blood samples and skin tissue samples from the

TABLE 1 Mechanism of squamous cell carcinoma pathogenesis within proteomic analysis.

| Type of disease | Sample | TOP differential proteins | Biological process of cancer | Highlighting mechanism | Depth mechanism | Ref. |
|---|---|---|---|---|---|---|
| SCC | SCC cell lines | ANO1, CE350, NRBF2, NSUN4, K1C14, KT33B, HORN in 10% $O_2$; TRI18, TRY3, ZN714, VAT1, AL1B1 in 5% $O_2$; TRFL, HBA, PI3R4, CTL1, K2C8, TTLL1, FGFR2, DKK2, CCD73, STON2, SHRM3 in 1% $O_2$ | Levels of hypoxia | Energy, metabolism, nucleic acid regulation | — | Głuszko et al. (2021) |
| SCC | SCC cell lines | Up: CK19, tropomyosin 1α chain, HSP27, CK8, AHCY, NNMT, GSTO1 | Proliferation, invasion (NNMT) | — | NNMT knockdown inhibits cell migration and invasion | Hah et al. (2019) |
| SCC | SCC cell lines | A431: FUCA2, LRG1, MAGEA4, CSF1, PROS1, PLAT, LCP1, AXL, EGFR, DNAJB11;<br>HaCaT: SERPINB7, MMP13, GSN, DSG4, MXRA5, SEMA3A, FN1, SPARC, MMP2, DSC3 | — | Metabolism, mTOR, PI3K-AKT, RAP1 signaling | Secretome of A431 cancer cells accelerates migration and proliferation | Hoesl et al. (2020) |
| SCC | SCC cell lines | Down: AKT2, MAP4K4, PRKCD, ERBB2, CLK2, STK10, MAP2K1, EGFR, PTK2B, MAP2K2;<br>Up: YES1, CDK11, PRPF4B, BMP2K, CDK12, PNKP, MNAT, MINK | Invasion | MAPK, mTOR pathways; adhesions, skeleton | YAP1 and SOX2 are related to mesenchymal and epithelial transcriptional programs | Pastushenko et al. (2021) |
| SCC | SCC cell lines | Up: FABP5, S100A9, S100A8, SPRR1A, AKR1C3, AKR1C2, SPRR1B | Proliferation | — | — | Shintani et al. (2021) |
| SCC | SCC cell lines | $CDK1^{T14,Y15}$, $EIF4EBP1^{T46,T50}$, $EIF4B^{S422}$, $AKT1S1^{T246,S247}$, $CTTN1^{T401,S405,Y421}$, $CAP1^{S307/309}$ in K8-S73A/D mutant; $CTTN1^{T401,S405,Y421}$, $BUB1B^{S1043}$, $CARHSP1^{S30,S32}$ in K8-S431A/D mutant | Metastasis, Proliferation, Invasion | Junction, JNK/SAPK, CDC42 signaling, Hippo signaling | — | Tiwari et al. (2017) |
| SCC | SCC cell lines | — | — | Cholesterol and steroid metabolic process | HMGCS1 partly was related to A431 cell proliferation | Xu et al. (2022) |
| SCC | SCC cell lines | KRT8, KRT14, KRT18 | — | — | — | Yamashiro et al. (2010) |
| SCC | SCC cell lines | — | — | — | — | Yanagi et al. (2018) |
| SCC | Human [SCC ($n = 5$)] | Up: G3BP, Filamin-A, NDRG1, Myosin-9, Plectin, 40S Ribosomal protein S4, Actin-related protein 2/3 complex subunit 1B, Fascin, Transgelin, Superoxide dismutase [Mn];<br>Down: FLG2, Suprabasin, FLG, Dermokine, Apolipoprotein EArginase-1, Galectin-7, Desmoglein-1, Desmoplakin, Collagen alpha-1(III) chain, Corneodesmosin | — | Cell survival, proliferation | — | Azimi et al. (2016) |
| SCC | Human [SCC ($n = 20$)] | — | — | Gene, metabolism | — | Chen et al. (2021) |

(*continued*)

TABLE 1 Continued

| Type of disease | Sample | TOP differential proteins | Biological process of cancer | Highlighting mechanism | Depth mechanism | Ref. |
|---|---|---|---|---|---|---|
| SCC | Human [samples of primary ($n$ = 19 patients, $n$ = 20 lesions) and metastatic SCC lesions ($n$ = 20 patients, 25 lesions)] | Up: ISG15 ubiquitin like modifier, APOA1, MARCKS, EFHD2, STMN1, ACBD3; Down: CMA1, CST6, KRT79, CPA3, APCS, DMKN | Metastasis | Invasion, migration, immune response | — | Azimi et al. (2020) |
| SCC | Human [primary ($n$ = 52), metastasize ($n$ = 53)] | Up: TNC, POSTN, TGFB1, PRDX5, SFPQ, FGB, LCP1, PHB2, HNRNPA2B1, P4HB; Down: CALML5, KRT2, KRT6B | Metastasis | PI3K-Akt signaling | — | Shapanis et al. (2021) |
| SCC | Human [AK ($n$ = 19), SCC ($n$ = 21), HCs ($n$ = 40)] | — | — | MEK-ERK, EGFR, mTOR pathways | — | Einspahr et al. (2021) |
| SCC | Human | — | — | Cell motility, cell death, survival, growth, proliferation, morphology | KRT17 protein is related to caspase-mediated degradation, supporting by altered TMS1-NF-κB signaling | Tiwari et al. (2018) |

SCC: squamous cell carcinoma; HCs, human controls; AK, actinic keratosis; MAPK, mitogen-activated protein kinase; PI3K, phosphatidylinositol-4,5-bisphosphate 3-kinase; mTOR, mechanistic target of rapamycin; JNK/SAPK, c-Jun N-terminal kinase/stress-activated protein kinase; CDC42, cell division cycle 42; RAP1, role of ras-associated protein 1; EGFR, epidermal growth factor receptor; Panx1, pannexin 1; AKT, protein kinase B; NNMT, N-nicotinamide methyltransferase; YAP1, yes-associated protein 1; SOX2, SRY-box transcription factor 2; HMGCS1, 3-hydroxy-3-methylglutaryly-CoA synthase 1; NF-κB, nuclear factor-kappaB; KRT17, keratin 17; AKT2, AKT serine/threonine kinase 2; CLK2, cdc2-like kinase 2; MAP2K1, mitogen-activated protein kinase kinase 1; MAP4K4, mitogen-activated protein kinase kinase kinase kinase 4; PRKCD, protein kinase C, delta; ERBB2, epidermal growth factor receptor 2; STK10, serine threonine kinase 10; PTK2B, protein tyrosine kinase 2 beta; MAP2K2, mitogen-activated protein Kinase Kinase 2; YES1, YES proto-oncogene 1 tyrosine kinase; CDK11, cyclin-dependent kinase 11; PRPF4B, PRP4 pre-mRNA processing factor 4 homolog B; BMP2K, BMP-2-inducible protein kinase isoform b; PNKP, polynucleotide kinase 3′-phosphatase; FABP5, fatty acid-binding protein 5; S100A9, S100 calcium-binding protein A9; AKR1C3, aldo-keto reductase family 1 member C3; SPRR1B, small proline-rich protein 1B; TNC, tenascin C; TGFB1, transforming growth factor, beta 1; PRDX5, peroxiredoxin 5; LCP1, lymphocyte cytosolic protein 1; PHB2, prohibitin 2; P4HB, prolyl 4-hydroxylase beta-subunit; CALML5, calmodulin-like 5; KRT, keratin; NRBF2, nuclear receptor binding factor 2; CTL1, choline transporter-like 1; K2C8, keratin, type II cytoskeletal 8; TTL1, Tubulin tyrosine ligase-like family, member 1; FGFR2, fibroblast growth factor receptor 2; DDK2, Dickkopf-2; STON2, Stonin 2; LRG1, leucine-rich alpha-2-glycoprotein 1; CSF1, colony-stimulating factor 1; PROS1, protein S; PLAT, plasminogen activator; MMP13, matrix metallopeptidase-13; GSN, gelsolin; DSG4, desmoglein 4; MXRA5, matrix-remodeling associated 5; SEMA3A, semaphorin 3A; FN1, fibronectin 1; SPARC, secreted protein acidic and rich in cysteine; DSC3, desmocollin 3; CK19, cytokeratin 19; AHCY, adenosylhomosysteinase; GSTO1, glutathione S-transferase omega 1; EIF4EBP1, eukaryotic translation initiation factor 4E binding protein 1; EIF4B, eukaryotic translation initiation factor 4B; AKT1S1, AKT1 substrate 1; CAP1, cyclase-associated protein 1; CARHSP1, calcium-regulated heat stable protein 1; G3BP, galectin-3-binding protein; FLNA, Filamin-A; NDRG1, N-myc downstream regulated gene 1; FLG2, Filaggrin-2.

same individual to obtain more comprehensive information on pathological changes (37, 38).

In the study of other diseases, there were also applications of specific samples corresponding to particular diseases (**Supplementary Tables S5–S8**). As for skin wounds, we often focused on the surrounding skin tissue but ignored the exudates of the wound. Studies by Krisp et al., van der Plas et al., and Bekeschus et al. reported that the exudates of skin wounds might have important implications for the progression of wounds (39–41). In the study of bullous pemphigoid, blister fluid was used as a sample for proteomic analysis (42). Moreover, with the continuous improvement of online databases in recent years, some studies have begun to download online data for analysis (43, 44). However, the skin proteomic database still needs to enrich and improved. The use of online analysis may be one of the future development trends of skin disease research.

## Application of proteomics in skin pathophysiological research

Turning back to the total articles of skin disease benefited for proteomics, most of them were based on proteomic analysis to raise a presumption and explore the pathology of skin diseases. The typical analysis process consists of five steps: sample acquisition, protein purification, qualitative and quantitative, acquisition of differential protein information, and validation (Western blot, ELISA, etc.). However, this routine process can only provide insights into the study of the pathological mechanism but cannot concretize the results of protein profiling (45).

With the improvement and promotion of bioinformatic platforms, such as the Kyoto Encyclopedia of Genes and Genomes (KEGG), Gene Ontology (GO), and Ingenuity Pathway Analysis (IPA), the results of proteomics can be analyzed online to correlate with information on cellular

TABLE 2 Mechanism of atopic dermatitis pathogenesis within proteomic analysis.

| Type of disease | Sample | Highlighting mechanism | Depth mechanism | Ref. |
|---|---|---|---|---|
| AD | Human [AD ($n = 12$), HCs ($n = 13$)] | Localization, regulation of biological quality, platelet activation, etc. | — | Chang et al. (2021) |
| AD | Human [AA ($n = 35$), HCs ($n = 36$), psoriasis ($n = 19$), AD ($n = 49$)] | Atherosclerosis signaling, immune pathways, cardiovascular pathway | — | Glickman et al. (2021) |
| AD | Human [AD ($n = 4$), HCs ($n = 7$), spontaneously healed AD ($n = 4$)] | — | — | Rindler et al. (2021) |
| AD | Human [AD ($n = 34$), HCs ($n = 20$)] | — | Insufficiency of IL-37 leads to dysregulation of serum protein and skin disruption in AD | Hou et al. (2021) |
| AD | Human [AD ($n = 8$), HCs ($n = 8$)] | Biological regulation, cellular component organization, etc. | — | Morelli et al. (2021) |
| AD | Human [AD ($n = 20$), HCs ($n = 28$)] | — | — | Pavel et al. (2020) |
| AD | Skin suction blisters and skin | — | — | Rojahn et al. (2020) |
| AD | Human [18–40 years old ($n = 26$), 41–60 years ($n = 24$),>60 years ($n = 21$), HCs ($n = 37$)] | Th1/Th2 differentiation, IL-4-mediated signaling, IL-5-mediated signaling, etc. | — | He et al. (2020) |
| AD | Human [AD + FA ($n = 21$), AD ($n = 19$), HCs ($n = 22$)] | Inflammatory response, glycolysis, oxidative stress response | — | Goleva et al. (2020) |
| AD | Human [AD ($n = 20$), HCs ($n = 7$)] | — | — | Umayahara et al. (2020) |
| ACD | Mice TGs | Response to stimulus, metabolic process, immune system process, etc. | — | Su et al. (2020) |
| AD | Human [AD ($n = 76$), HCs ($n = 39$)] | — | — | Leonard et al. (2020) |
| AD | Human | — | — | Yin et al. (2019) |
| AD | Human [AD pediatric ($n = 30$), healthy pediatric ($n = 19$), AD adult ($n = 58$), healthy adult ($n = 18$)] | — | — | Brunner et al. (2019) |
| AD | Human [HCs ($n = 84$),severe AD ($n = 50$), moderate AD ($n = 123$)] | — | — | Mikus et al. (2019) |
| AD | Human [HC ($n = 10$), AD ($n = 20$), CD ($n = 10$), AD and CD ($n = 10$), psoriasis ($n = 12$)] | — | — | Wang et al. (2017) |
| AD | Human [psoriasis ($n = 22$), AD ($n = 59$), HCs ($n = 18$)] | — | — | Brunner et al. (2017) |
| ACD | Dendritic-like cell line | Cell signaling, transcriptional regulation, protein transport, ubiquitination, etc. | MLK is one of FITC targets leading the specific protein haptenation and the subsequent pathway of dermal dendritic cells activation | Guedes et al. (2017) |
| AD | Spleen and thymus Treg cells | — | — | Lee et al. (2016) |
| AD | AD-NC/Nga mice | — | — | Kawasaki et al. (2014) |
| AD | Human [EH− ($n = 18$), EH+ ($n = 17$), non-atopic controls ($n = 6$)] | Skin barrier, generation of natural moisturizing factor | — | Broccardo et al. (2011) |
| AD | Human [AD ($n = 8$), HCs] | — | — | Kim et al. (2008) |
| AD | Human [ADe ($n = 14$), ADi ($n = 10$), HCs ($n = 14$)] | — | — | Park et al. (2007) |
| AD | Human [ADe ($n = 14$), ADi ($n = 10$), HCs ($n = 14$)] | — | — | Park et al. (2007) |
| AD | Human [ADe, ADi, HCs] | — | — | Park et al. (2006) |
| AD | Human [ADe, ADi, HCs] | — | — | Park et al. (2004) |

AD, atopic dermatitis; ACD, atopic contact dermatitis; HCs, human controls; AA, alopecia areata; TGs, trigeminal ganglions; CD, contact dermatitis; EH, eczema herpeticum; ADe, extrinsic AD; ADi, intrinsic AD; PsA, psoriatic arthritis; FITC, fluorescein isothiocyanate; MLK, mixed-lineage protein kinase.

pathways and biological processes. The proteomic protein function analysis could provide comprehensive and specific information for the progress of pathogenesis. According to the statistical results of the pathophysiological group, 50.988% of the studies conducted functional analyses of the online database on the proteome results (**Tables 1**, **2**, **Supplementary Tables S1, S2, S5–S8**). Taking the melanoma study by *Konstantakou* et al. as an example, after obtaining the proteome, a series of online database analyses were used to provide insights into the core proteins and pathways from tumorigenesis to therapeutic targets (2).

In addition, some studies use proteomics as a reliable method for validating research findings (46) or replenishing proof of results (47). These may be new approaches to applying proteomics to skin disease research. Online database analysis of proteomes is not a necessary research process. Follow-up studies based on proteomic analysis results can be comprehensive (such as GO analysis) or precise (only targeting one core protein or core pathway). For example, PSMB9 in systemic lupus erythematosus (SLE) and TRIM29 in SCC were obtained through proteomic screening, and further functional studies were conducted precisely (12, 48). Moreover, a study identified the critical mechanism associated with melanoma metastasis through specific changes obtained by proteomics (49). At present, such precise functional research has a more specific role in promoting the research on the pathophysiological mechanism of skin diseases. However, as the basis of precise studies, extensive functional studies like GO analysis and KEGG analysis are essential and non-negligible.

## Risk factors research analysis

A total of 128 articles were included in the risk factor group, and these articles were divided into two tables according to biological risk factors and abiotic risk factors. Non-biological risk factors include UV exposure, chemical exposure, and other irradiation, while biological risk factors are all about microbial skin infections (**Supplementary Tables S3, S9**). Among the 44 articles related to non-biological risk factors, the research on radiation (including UV and laser) accounts for the most significant proportion (50.000%). As for biological risk factors, *Leishmania* and its subspecies infection studies account for the vast majority (46.913%).

The focus of research on risk factors is to lead a guideline for preventing or treating diseases, which is further beneficial for discovering the critical pathogenic proteins and mechanisms of risk factors.

## Treatment research analysis

A total of 87 articles were included in the skin disease therapy. Skin cancer has the highest number of studies, while the wound is as the second but less than half the number of cancers. The number of remaining studies on psoriasis, aging, UV-induced damage, and AD is not much different (**Supplementary Table S4**).

Among 28 studies related to skin cancer therapy, 19 studies used *in vitro* cells, and 89.473% were tumor cell lines. For samples, de Groot et al. have reported that combined treatment of IACS-010759 (IACS) and atorvastatin (STN) could induce tumor regression, and they further explored the mechanism MAPK pathway using functional proteomic analysis (50). In researching glucocorticoid treatment for vitiligo, Qian et al. pioneered urine as a sample source for proteomics to identify the differentially expressed proteins and ingenuity pathway analysis (such as retinol binding protein-1 and torsin 1A interacting protein 1) (51). In these studies, proteomics exerts as a screener, accurately reflecting changes in proteins before and after interventions. Similar to the study of pathophysiological mechanisms, only a few studies carried out precise therapeutic mechanism studies based on core proteins after obtaining the proteomic results. However, unlike the study of pathophysiological mechanisms, the application of proteomics in therapeutic research was more inclined to investigate the effectiveness of the intervention substance or the main therapeutic effect of the intervention substance. For example, BRAF inhibitors were used in melanoma therapy, and MS-based chemical proteomics were used to identify never-in-mitosis-gene-A related kinase 9 (NEK9) and CDK16 as unique targets of dabrafenib (52). The situation may be related to the different purposes of the two types of research. The study of pathophysiological mechanisms explores the possibility of disease grading and treatment, and the study of therapy is to judge the degree of cure and effectiveness.

# Discussion

Over the hundreds of years of studies in skin diseases, the curve of its annual publications showed a sharply increasing trend in recent 20 years. During the preceding 12 years covered by the proteomic analysis utilized in the studies of skin diseases, a number of annual publications have contributed to the development of skin diseases, which reached a peak in 2021. Among these, skin cancer as a major part exerted a sharply increasing trend in recent five years for the cancer hotspot or most research groups, a wide range of samples and multiple cell lines, and high prevalence, a limited therapeutic effect, and sorely needed treatment targets (53). Skin inflammation disease, as a major category of skin disease that ranked second, may be related to its prevalence with a well therapeutic response (54). We have summarized the timeline of some key discoveries in different skin diseases according to our data (**Figure 5**). In all, this curve suggests that an increasing number of researchers pay attention to

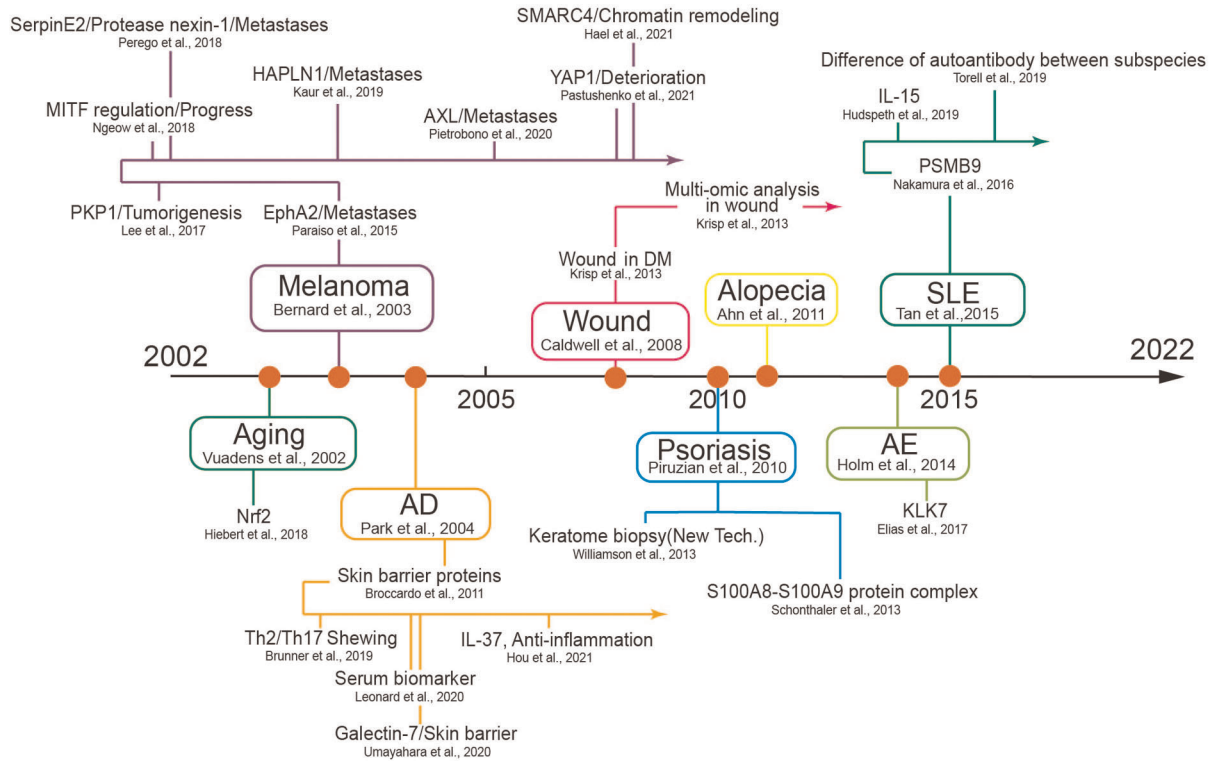


FIGURE 5
The timeline of some key discoveries in the field of the skin disease using proteomics. The first records of proteomics used in several diseases and their subsequent development are listed here. We selected primary skin diseases that began in different periods to list and used high-impact factor articles as developing nodes to display in the follow-up development process AD, atopic dermatitis; SLE, systemic lupus erythematosus; AE, atopic eczema; PKP1, plakophilin-1; HAPLN1, hyaluronan and proteoglycan link protein 1; AXL, AXL receptor tyrosine kinase; YAP1, yes-associated protein 1; MITF, microphthalmia-associated transcription factor: DM, diabetes mellitus; KLK7, kallikrein-7.

improved technologies, which indicates a continuously increasing hotspot of proteomic analysis in skin disorders over the next few years.

Proteomic assays have been extensively used in the field of skin, providing significance to nucleotide sequences by giving a direct link to biological activity, such as functional proteomics and phosphoproteomics (55, 56), so that the knowledge of structural–functional cellular complexities and their changes under skin physiological and pathological conditions could advance at a faster pace (57). Numerous studies have identified skin lesion-related changes (including systemic changes) in protein expression or modification to enrich the specific pathogenesis well or find a special biomarker for diagnosis and a therapeutic target for a particular disease (58). Recently, a more improved and delicate proteomic analysis has been developed, such as spatial proteomics (protein subcellular localization tightly combined with its functions) (59), multi-omics analysis (genetics-proteomics) (60), and single-cell proteomics (61).

As for the pathogenesis of skin diseases, we analyzed the application and characteristics of proteomics in skin disease and selected skin cancer as a typical example for further explanations. We enumerated differential proteins with similar functions. Whether related to inflammation or cancer cell survival, these proteins are undoubtedly of great significance for the study of skin cancer. S100A9 is a protein involved in the recruitment of immune cells and has been shown to be a molecule in the epidermal layer of the skin that controls skin tumor formation (62). As survival-related molecules, DKK proteins can also affect the phenotype of melanoma in various ways (63, 64), and studies have also shown that the invasive activity of melanoma cells can be inhibited by DKK1 (65). Knockdown of FBXO32, which is related to the metabolism of melanoma cancer cells, was able to induce global changes in melanoma gene expression profiles and was shown to correlate with melanoma cell migration, proliferation, and tumor development (66). ICAM-1, a cell surface glycoprotein and adhesion receptor, was shown to be expressed together with LFA-1 under melanoma-endothelial cell co-culture conditions to facilitate melanoma metastasis *in vitro* (67, 68). However, there are still many high-fold change proteins whose real functions are still unclear (**Table 1**,

Supplementary Table S1). In addition, we also tried to find some common biomarkers, such as HSPs, Survivin, Galectin-3, and other markers that have been experimentally verified. The detection of HSPs in the serum of sick individuals can play an essential role in cancer diagnosis (69). Survivin, one of the inhibitors of the apoptosis protein family, is overexpressed in cancer and has been proved to be a biomarker for cancer diagnosis (70). CDK12, a member of the CDK family, has also been shown to play an important role in various human cancers, suggesting that it is a potential biomarker of cancer (71). Vimentin is proved to be not only the diagnostic marker but also the hematogenous metastasis predictor for melanomas clinically (72). Galectin-3 shows high serum levels in advanced melanoma patients and is also regarded as an important biomarker for prognosis in stage III and IV melanoma patients (73). There are also many potential biomarkers that have not been further confirmed. For instance, the study by Welinder et al. identified several proteins correlated with tumor tissue content by combining proteomics with histopathology and clinical outcomes, of which HEXB, PKM, and GPNMB were relatively prominent and may serve as biomarkers in progression from stage III to IV melanoma (74).

Proteomics is mainly involved in screening differential proteins and enriched functions, as well as in the search for biomarkers in the pathogenesis of skin cancer. Most of the research relies on proteomics to obtain the general protein set related to cancer, obtain the enriched protein function through platform analysis or other approaches, and then highlight or research the part related to cancer. For example, Eumorphia et al. used nano-liquid chromatography-tandem mass spectrometry (nLC-MS/MS) proteomic technology to dissect the deep proteome of WM-266-4 human metastatic melanoma cells and found 6,681 unique proteins. Ultimately, they focused on 1433G and ADT3 proteins, which are related to epithelial-to-mesenchymal (EMT) and mesenchymal-to-epithelial (MET) programs (2). Some studies focused on specific proteins and explored the relationship between proteins and cancer. For example, to explore the role of heparin-binding protein 17 (HBp17) and FAT1 in the progression of cutaneous squamous cell carcinoma, both adopted the knockout-first pattern and finally proved their mechanisms in promoting keratinization and deterioration, respectively (75, 76). Identifying FAM83H as a TRIM29 interactor through comprehensive proteomic and immunoprecipitation analysis is similar (48).

In exploring biomarkers, researchers obtain candidate proteins by comparing differential proteins from the tissue or cells from different stages of diseases. However, the screened candidate proteins often cannot become efficient markers. Whether for tumors and tumors, or tumors and other diseases, due to the existence of similar biological processes, the specificity of differential molecules expressed in clusters is not enough to distinguish similar diseases. At present, the solution is to adopt the combined detection of immunolabeling to meet the specific identification, but this is not a universal and cost-effective method. In some respects, proteomics has similar functions to genomics, transcriptomics, etc. However, in particular, the proteome is dynamic, regulated by post-translational modifications (PTMs), and the prediction of impaired PTMs cannot be achieved by genomic and transcriptomic analysis but only by proteomic approaches (77). Therefore, developing proteomic technologies and applications is very important for skin cancer. Likewise, these conditions are suitable for other skin disorders.

Among the research on skin disorders, proteomics seems to be a key part and a research hotspot in skin research. According to our data, we have found that proteomics contributed to a more profound discovery of the physiology and pathology of the skin. Both in circulation and skin of systemic sclerosis, CXC-l4 was found as a special biomarker *via* proteome-wide analysis, which provided a meaningful guideline for clinical diagnosis both for the presence and progression of complications (78). As for shrimp allergen analysis (most of the allergens were protein), Pen m2 was identified as a novel cross-reactive crustacea allergen through matrix-assisted laser desorption ionization time-of-flight mass spectrometry analysis (79). For depth mechanism, Yoon et al. found a specific defect in an internal ribosome entry site-dependent translation in X-linked dyskeratosis congenita using an unbiased proteomic strategy (80). Also, secretory proteome has been used for skin-related microbiomes, such as to reveal the pathogenicity of extracellular hydrolases from dandruff-associated *Malassezia* (81). Proteomics has been used to identify protein-interacting proteins, such as ERK-interacting protein analysis during cell fate decisions (82). Besides research articles, various high-cited reviews have also pointed out that proteomic strategies improved our ability to understand skin disorders, such as the structure and function of the microbiome in both diseased skin and its healthy states (83). In general, the proteomic technology contributed to the development of diagnosing skin disease and improved more sophisticatedly with high universality, practicality, and accuracy.

Initially, proteomics emerged as one of the technologies that gave a better explanation of the pathogenesis of disease within a simple verification. For example, the process of injured skin healing refers to a complex and highly regulated mechanism, such as growth factor (GF)-related clotting cascade, proteases-related necrotic tissue removal, and inflammation response-related repair and cell growth (84, 85). These findings have only described part of the pathogenesis of wound healing, whereas a broader perspective of proteins in the wound area is detected by proteomic technology. Proteomic analysis revealed the altered abundance of proteins in wound skin, suggesting the pathogenesis progress of myofibroblast contractility, extracellular matrix production, response to

oxidative stress, and energy metabolism (86). Through mass spectrometric investigation, the progress of an antiangiogenic environment, excessive inflammation, and accelerated cell death have been found in exudates from chronic wounds (41). It has also found that neutrophil extracellular trap components were enriched in wound tissue, which may delay wound healing (87). Besides skin wounds, proteomic analysis has also been used in other skin diseases. As for chronic hand eczema (CHE), skin barrier dysfunction plays an essential role in the pathogenesis of CHE (88). An integrated quantitative proteomics approach was used to detect proteomic changes in the SARS-CoV-2-infected skin to provide a functional analysis of the response to microorganisms, apoptosis, and immune response, which leads to an insight into the virus-damaged skin response (89).

At present, in the research process of skin diseases, multi-omics combined analysis methods are more and more popular. Proteomics is often combined with genome, epigenome, transcriptome, metabolome, lipidome, exposure group, and microbiome for the exploration of various aspects of skin diseases. Take AD as an example. Genomics can help identify some of the underlying root causes of AD lesions, such as mutations in genes such as *BAT1*, *LCE3E*, *PCDH9*, and *PRR5l* (90–93). Proteomics can provide AD information in the form of phenomena during pathogenesis, namely, the protein profile of diseased tissue at specific time points (94, 95). Adipomics, microbiome, and exposome can also provide detailed information on various aspects (20). When these omics serve the same experiment or the same goal, they can reflect the pathogenesis of AD at multiple levels and broadly (96). Multi-omics are used more frequently and in depth in melanoma research. Such analysis can not only identify the multi-omics features that drive the molecular classification of melanoma but also provide precise guidance for subsequent treatment (97, 98). In fact, the advantage of multi-omics is that each project can help make up for the shortcomings of other projects, especially when one kind of omics is not enough to get a full picture of the disease process.

Recently, it has raised great attention on the mechanism of skin factors for skin diseases, such as UV damage, microorganism, and chemical agents. According to our data, proteomics plays an essential role in bridging the basic mechanism and risk factors. The research process generally uses risk factors to intervene on skin or cells. Second, proteomics has been used to analyze the proteome changes after the intervention. In addition, some studies further explored the effectiveness of specific agents against risk factors based on proteomic results. For instance, the research on diesel particulate extract conducted by Rajagopalan et al. investigated the treatment of vitamin E according to oxidant changes from proteomics (99). Most studies on microbial risk factors focus on screening virulence proteins from microorganisms *via* proteomics. For example, comparing the performance of RT4 and RT6 subtypes of *Cutibacterium acnes* in different living environments, triacylglycerol lipase and Christie–Atkins–Munch–Petersen (CAMP) factor were the critical virulence factors in pathogenesis (100). In addition, some studies examined infected skin or cells and have focused on pathogenic proteins derived from tissue cells (101). Using proteomics to study risk factors can provide detailed molecular changes and even mechanism predictions for the pathogenesis of particular diseases.

Interestingly, we have found the sample source differed from in various skin diseases. The most important source of samples for cancer was tumor cell lines cultured *in vitro* (59.302%). The advantage of using cell lines *in vitro* as research samples is that the results can reflect the characteristics of tumor cells in more detail and specially, which could exclude the interference of various other cells compared to skin tissue or tumor tissue sample. However, tissue samples, cell samples, and blood samples derived from patients or diseased mice are more realistic and comprehensive than *in vitro* cell lines in reflecting disease conditions and more conducive to studying the impact of tumor invasion, metastasis, and other deterioration processes. Moreover, cancer skin samples, primary fibroblasts (30), serum (31), and metastatic cancer tissue (32) have also been used in the study of progression and metastasis in cancer. Blood samples include serum, plasma, and biologically active substances and cells in the blood environment. These samples provide an accurate and detailed reflection of inflammatory changes in skin diseases. Based on these changes, biomarkers can obtain biomarkers (33), diseases can be distinguished (13, 34), and also pathogenesis can be studied with hub proteins (35, 36). In addition, the use of skin tissue samples and primary cell samples was also common. The advantage of skin tissue samples is that the proteomic results are closer to the actual pathological situation. In contrast, the primary cells can be used for detailed studies of single cells in the diseased site. In recent years, studies have begun to use blood samples and skin tissue samples from the same individual to obtain more comprehensive information on pathological changes (37, 38).

With the development of the enriched complex mechanism, proteomics helps gain a next-level insight or offer a breakthrough to guide further study. For example, CDK7 was identified by proteomics, and then its related function was proved by further experience to reveal that the downstream mechanism CDK7 could promote $CD^{4+}$ T-cell activation and Th17/Th1 cell differentiation by regulating glycolysis, contributing to the pathogenesis of psoriasis (36). The phosphoproteomic analysis identified the signaling cascades downstream of FAT1 deletion. Then, combined with mechanistic studies, it jointly revealed that loss of function of

FAT1 could activate a CAMK2-CD44-SRC axis to promote tumor initiation, progression, invasiveness, stemness, and metastasis (75). However, many more concerns remain for continued and improved research: (1) although the proteomic analysis could provide strong indications of expression level protein differences or the highlighted pathways, the hypothesized implications in several pathways or their co-network have to be confirmed not only in presentation but also their functions during the disease; (2) a specific or causative candidate has failed to identify for the certain skin disease, as well as the analysis mostly provided with the same inflammation factors or immune pathways in disease; (3) the different source of tissue (skin, guy, blood, urine, etc.) for proteomics may suggest systematic pathological changes during skin disorder, but it is still unclear to understanding their interface; (4) it is important to recognize the control populations included in the study, which should be appropriately matched in terms of other factors, and the subtype, the progression, and the interruption should be also provided in evidence; (5) strong evidence needs a large scale of samples limited to sample source and cost. However, there is no denying that proteomics leads to a well-founded hypothesis and a more systematic understanding of the pathogenesis of skin disorders.

Furthermore, a more accurate and systematic proteomic analysis has been contributed to clinical applications. According to our data, a majority of studies in proteomics utilized in skin disease focused on the specific proteins and their corresponding functions presented with a sensitive option for biomarker monitoring of diagnosis and disease progression evaluation. As for acute alopecia, Krt5 has been found as a novel biological marker for acute radiation symptoms *via* liquid chromatography/electrospray-ionization mass spectrometry (102) and a series of specific inflammation candidates have been reported for disease monitoring (38). Also other biomarkers were discovered through proteomics, such as acetaldehyde dehydrogenase 1 (ALDH1) for atopic dermatitis (103) and GPX5 for melanoma (104). Recently, the proteins in the circulatory system mirror an individual's physiology, which could be utilized as a specific marker within a convenient sampling method (105). As plasma biomarkers' specific analysis, a large-scale quantitative proteomic discovery helped identify the specific biomarker elafin for skin graft-versus-host disease and proved the specificity with enzyme-linked immunosorbent assay in samples from 492 patients (106). Interestingly, a series of specific proteins have been detected in the CD81-positive small extracellular vesicles through proteomics in melanoma, strengthening the circulating sEV as a systematic biomarker for early diagnosis for melanoma patients (107). Although multiple biomarkers have been termed, they tend to develop with high accuracy, specificity, and cost-effective combination of these candidates rather than a single indicator.

Also, proteomics has been utilized in the evaluation of the therapeutic strategy, and it is also benefited from a better understanding of the elusive mechanism of drug targets. As for the drugs for wound healing, it significant changes of abundance proteins have been found from the topical peri-wounding tissue after extracorporeal shock wave therapy (ESWT). After that, the related MAPK signaling might involve ESWT-enhanced diabetic wound healing (108). Also, through proteomic microarrays of the wound exudate, significantly higher levels of matrix metalloproteinases (MMPs) and lower levels of inflammation factors (e.g., CX3CL1, FLT-3 L, IL-1ra, IL-1a, IL-9, IL-2, IL-3) have been found to evaluate the therapeutic effect (109). The therapeutic effect also provided an optimal dose guiding drug therapy. For example, using collagen to treat aging could reduce the MMP-1, IL-1b, and IL-6 protein expression, especially in high concentration-treated in 160 mg/kg (110). Proteomics may lead to a systematic analysis, but Western blot and ELISA are still irreplaceable and classic methods, while part of certain proteins needs to be detected in skin disorders.

## Conclusion

Proteomics is a technique that provides the ability to identify changes in proteins at specific time points. It can provide key molecules, candidate biomarkers, and other information in the research of skin diseases. Based on this information, skin diseases can be more comprehensively explored through multichannel analysis methods, precise in-depth research, and the combination of multiple technologies. Various proteomic analyses have significantly contributed to a better understanding of the pathophysiology progress of skin, which is closely related to clinical applications. Although initial studies emerged to enrich skin proteomes and/or their related systemic disorder to establish comprehensive inventories, subsequent quantitative analysis paved the way to more in-depth studies addressing the detailed pathways underlying skin disease, guiding diagnosis, and therapy. Furthermore, spatial proteomics, multi-omics analysis, single-cell proteomics, and others may lead to a richer brainstorming for a deeper mechanism.

## Data availability statement

The original contributions presented in the study are included in the article/**Supplementary Material**, further inquiries can be directed to the corresponding authors.

## Author contributions

S-yZ and X-mH were the major contributors who reviewed the literature, wrote the manuscript writing, and created descriptive figures. S-yZ, KH, Z-hL, and Q-nC were the major contributors who screened the literature. X-mH and KX were the major contributors who designed the study. S-yZ assisted in the literature review and editing the tables. KX and R-hY were major contributors who revised the manuscript. All authors contributed to the article and approved the submitted version.

## Funding

This work was supported by the National Natural Science Foundation of China (81971891, 82172196, and 82272276), Guangdong Basic and Applied Basic Research Foundation (2021A1515011453 and 2022A1515012160), Key Laboratory of Emergency and Trauma (Hainan Medical University) of Ministry of Education (KLET-202108), and the College Students' Innovation and Entrepreneurship Project (S20210026020013).

## Conflict of interest

The authors declare that the research was conducted in the absence of any commercial or financial relationships that could be construed as a potential conflict of interest.

## Publisher's note

All claims expressed in this article are solely those of the authors and do not necessarily represent those of their affiliated organizations, or those of the publisher, the editors and the reviewers. Any product that may be evaluated in this article, or claim that may be made by its manufacturer, is not guaranteed or endorsed by the publisher.

## Supplementary material

The Supplementary Material for this article can be found online at: https://www.frontiersin.org/articles/10.3389/fsurg.2022.1025557/full#supplementary-material.

## References

1. Kaufman KL, Belov L, Huang P, Mactier S, Scolyer RA, Mann GJ, et al. An extended antibody microarray for surface profiling metastatic melanoma. *J Immunol Methods*. (2010) 358(1–2):23–34. doi: 10.1016/j.jim.2010.03.017

2. Konstantakou EG, Velentzas AD, Anagnostopoulos AK, Litou ZI, Konstandi OA, Giannopoulou AF, et al. Deep-proteome mapping of WM-266-4 human metastatic melanoma cells: from oncogenic addiction to druggable targets. *PLoS One*. (2017) 12(2):e0171512. doi: 10.1371/journal.pone.0171512

3. Chen C, Hou J, Tanner JJ, Cheng J. Bioinformatics methods for mass spectrometry-based proteomics data analysis. *Int J Mol Sci*. (2020) 21(8):2873. doi: 10.3390/ijms21082873

4. Noor Z, Ahn SB, Baker MS, Ranganathan S, Mohamedali A. Mass spectrometry-based protein identification in proteomics—a review. *Brief Bioinform*. (2021) 22(2):1620–38. doi: 10.1093/bib/bbz163

5. Zhang Y, Fonslow BR, Shan B, Baek MC, Yates 3rd JR. Protein analysis by shotgun/bottom-up proteomics. *Chem Rev*. (2013) 113(4):2343–94. doi: 10.1021/cr3003533

6. Brinkerhoff H, Kang ASW, Liu J, Aksimentiev A, Dekker C. Multiple rereads of single proteins at single-amino acid resolution using nanopores. *Science*. (2021) 374(6574):1509–13. doi: 10.1126/science.abl4381

7. Keskin O, Tuncbag N, Gursoy A. Predicting protein-protein interactions from the molecular to the proteome level. *Chem Rev*. (2016) 116(8):4884–909. doi: 10.1021/acs.chemrev.5b00683

8. Mumby M, Brekken D. Phosphoproteomics: new insights into cellular signaling. *Genome Biol*. (2005) 6(9):230. doi: 10.1186/gb-2005-6-9-230

9. Lennicke C, Rahn J, Heimer N, Lichtenfels R, Wessjohann LA, Seliger B. Redox proteomics: methods for the identification and enrichment of redox-modified proteins and their applications. *Proteomics*. (2016) 16(2):197–213. doi: 10.1002/pmic.201500268

10. Schmidt T, Samaras P, Frejno M, Gessulat S, Barnert M, Kienegger H, et al. ProteomicsDB. *Nucleic Acids Res*. (2018) 46(D1):D1271–81. doi: 10.1093/nar/gkx1029

11. Xiao Q, Zhang F, Xu L, Yue L, Kon OL, Zhu Y, et al. High-throughput proteomics and AI for cancer biomarker discovery. *Adv Drug Deliv Rev*. (2021) 176:113844. doi: 10.1016/j.addr.2021.113844

12. Nakamura K, Jinnin M, Kudo H, Inoue K, Nakayama W, Honda N, et al. The role of PSMB9 upregulated by interferon signature in the pathophysiology of cutaneous lesions of dermatomyositis and systemic lupus erythematosus. *Br J Dermatol*. (2016) 174(5):1030–41. doi: 10.1111/bjd.14385

13. Glickman JW, Dubin C, Renert-Yuval Y, Dahabreh D, Kimmel GW, Auyeung K, et al. Cross-sectional study of blood biomarkers of patients with moderate to severe alopecia areata reveals systemic immune and cardiovascular biomarker dysregulation. *J Am Acad Dermatol*. (2021) 84(2):370–80. doi: 10.1016/j.jaad.2020.04.138

14. Harel M, Ortenberg R, Varanasi SK, Mangalhara KC, Mardamshina M, Markovits E, et al. Proteomics of melanoma response to immunotherapy reveals mitochondrial dependence. *Cell*. (2019) 179(1):236–50.e18. doi: 10.1016/j.cell.2019.08.012

15. Matharoo-Ball B, Ratcliffe L, Lancashire L, Ugurel S, Miles AK, Weston DJ, et al. Diagnostic biomarkers differentiating metastatic melanoma patients from healthy controls identified by an integrated MALDI-TOF mass spectrometry/bioinformatic approach. *Proteomics Clin Appl*. (2007) 1(6):605–20. doi: 10.1002/prca.200700022

16. Xu M, Deng J, Xu K, Zhu T, Han L, Yan Y, et al. In-depth serum proteomics reveals biomarkers of psoriasis severity and response to traditional Chinese medicine. *Theranostics*. (2019) 9(9):2475–88. doi: 10.7150/thno.31144

17. Kaleja P, Emmert H, Gerstel U, Weidinger S, Tholey A. Evaluation and improvement of protein extraction methods for analysis of skin proteome by noninvasive tape stripping. *J Proteomics*. (2020) 217:103678. doi: 10.1016/j.jprot.2020.103678

18. Perez-Riverol Y, Csordas A, Bai J, Bernal-Llinares M, Hewapathirana S, Kundu DJ, et al. The PRIDE database and related tools and resources in 2019: improving support for quantification data. *Nucleic Acids Res*. (2019) 47(D1):D442–50. doi: 10.1093/nar/gky1106

19. Echevarria-Vargas IM, Reyes-Uribe PI, Guterres AN, Yin X, Kossenkov AV, Liu Q, et al. Co-targeting BET and MEK as salvage therapy for MAPK and checkpoint inhibitor-resistant melanoma. *EMBO Mol Med*. (2018) 10(5):e8446. doi: 10.15252/emmm.201708446

20. Ghosh D, Bernstein JA, Khurana Hershey GK, Rothenberg ME, Mersha TB. Leveraging multilayered "omics" data for atopic dermatitis: a road map to

precision medicine. *Front Immunol*. (2018) 9:2727. doi: 10.3389/fimmu.2018.02727

21. Chen Y, Li Y, Guo L, Hong J, Zhao W, Hu X, et al. Bibliometric analysis of the inflammasome and pyroptosis in brain. *Front Pharmacol*. (2020) 11:626502. doi: 10.3389/fphar.2020.626502

22. Yan WT, Lu S, Yang YD, Ning WY, Cai Y, Hu XM, et al. Research trends, hot spots and prospects for necroptosis in the field of neuroscience. *Neural Regen Res*. (2021) 16(8):1628–37. doi: 10.4103/1673-5374.303032

23. Yan WT, Yang YD, Hu XM, Ning WY, Liao LS, Lu S, et al. Do pyroptosis, apoptosis, and necroptosis (PANoptosis) exist in cerebral ischemia? Evidence from cell and rodent studies. *Neural Regen Res*. (2022) 17(8):1761–8. doi: 10.4103/1673-5374.331539

24. Engelman JA, Luo J, Cantley LC. The evolution of phosphatidylinositol 3-kinases as regulators of growth and metabolism. *Nat Rev Genet*. (2006) 7(8):606–19. doi: 10.1038/nrg1879

25. Chen J, Huang L, Quan J, Xiang D. TRIM14 regulates melanoma malignancy via PTEN/PI3K/AKT and STAT3 pathways. *Aging (Albany NY)*. (2021) 13(9):13225–38. doi: 10.18632/aging.203003

26. Pu Y, Lei M, Chen Y, Huang Y, Zhang L, Chen J, et al. Hey1 promotes migration and invasion of melanoma cells via GRB2/PI3K/AKT signaling cascade. *J Cancer*. (2021) 12(23):6979–88. doi: 10.7150/jca.60974

27. Dahl C, Guldberg P. The genome and epigenome of malignant melanoma. *APMIS*. (2007) 115(10):1161–76. doi: 10.1111/j.1600-0463.2007.apm_855.xml.x

28. Populo H, Soares P, Faustino A, Rocha AS, Silva P, Azevedo F, et al. mTOR pathway activation in cutaneous melanoma is associated with poorer prognosis characteristics. *Pigment Cell Melanoma Res*. (2011) 24(1):254–7. doi: 10.1111/j.1755-148X.2010.00796.x

29. Ostojic J, Yoon YS, Sonntag T, Nguyen B, Vaughan JM, Shokhirev M, et al. Transcriptional co-activator regulates melanocyte differentiation and oncogenesis by integrating cAMP and MAPK/ERK pathways. *Cell Rep*. (2021) 35(7):109136. doi: 10.1016/j.celrep.2021.109136

30. Kaur A, Ecker BL, Douglass SM, Kugel 3rd CH, Webster MR, Almeida FV, et al. Remodeling of the collagen matrix in aging skin promotes melanoma metastasis and affects immune cell motility. *Cancer Discov*. (2019) 9(1):64–81. doi: 10.1158/2159-8290.CD-18-0193

31. Longo C, Gambara G, Espina V, Luchini A, Bishop B, Patanarut AS, et al. A novel biomarker harvesting nanotechnology identifies Bak as a candidate melanoma biomarker in serum. *Exp Dermatol*. (2011) 20(1):29–34. doi: 10.1111/j.1600-0625.2010.01187.x

32. Murillo JR, Kuras M, Rezeli M, Miliotis T, Betancourt L, Marko-Varga G. Automated phosphopeptide enrichment from minute quantities of frozen malignant melanoma tissue. *PLoS One*. (2018) 13(12):e0208562. doi: 10.1371/journal.pone.0208562

33. Yin SJ, Cho IH, Yang HS, Park YD, Yang JM. Analysis of the peptides detected in atopic dermatitis and various inflammatory diseases patients-derived sera. *Int J Biol Macromol*. (2018) 106:1052–61. doi: 10.1016/j.ijbiomac.2017.08.109

34. Kim WK, Hwang HR, Kim DH, Lee PY, In YJ, Ryu HY, et al. Glycoproteomic analysis of plasma from patients with atopic dermatitis: CD5L and ApoE as potential biomarkers. *Exp Mol Med*. (2008) 40(6):677–85. doi: 10.3858/emm.2008.40.6.677

35. Leonard A, Wang J, Yu L, Liu H, Estrada Y, Greenlees L, et al. Atopic dermatitis endotypes based on allergen sensitization, reactivity to *Staphylococcus aureus* antigens, and underlying systemic inflammation. *J Allergy Clin Immunol Pract*. (2020) 8(1):236–47.e3. doi: 10.1016/j.jaip.2019.08.013

36. Lin Y, Xue K, Li Q, Liu Z, Zhu Z, Chen J, et al. Cyclin-dependent kinase 7 promotes Th17/Th1 cell differentiation in psoriasis by modulating glycolytic metabolism. *J Invest Dermatol*. (2021) 141(11):2656–67.e11. doi: 10.1016/j.jid.2021.04.018

37. Gegotek A, Domingues P, Wronski A, Ambrozewicz E, Skrzydlewska E. The proteomic profile of keratinocytes and lymphocytes in psoriatic patients. *Proteomics Clin Appl*. (2019) 13(4):e1800119. doi: 10.1002/prca.201800119

38. Pavel AB, Zhou L, Diaz A, Ungar B, Dan J, He H, et al. The proteomic skin profile of moderate-to-severe atopic dermatitis patients shows an inflammatory signature. *J Am Acad Dermatol*. (2020) 82(3):690–9. doi: 10.1016/j.jaad.2019.10.039

39. van der Plas MJ, Cai J, Petrlova J, Saleh K, Kjellstrom S, Schmidtchen A. Method development and characterisation of the low-molecular-weight peptidome of human wound fluids. *Elife*. (2021) 10:e66876. doi: 10.7554/eLife.66876

40. Bekeschus S, Lackmann JW, Gumbel D, Napp M, Schmidt A, Wende K. A neutrophil proteomic signature in surgical trauma wounds. *Int J Mol Sci*. (2018) 19(3):761. doi: 10.3390/ijms19030761

41. Krisp C, Jacobsen F, McKay MJ, Molloy MP, Steinstraesser L, Wolters DA. Proteome analysis reveals antiangiogenic environments in chronic wounds of diabetes mellitus type 2 patients. *Proteomics*. (2013) 13(17):2670–81. doi: 10.1002/pmic.201200502

42. Solimani F, Didona D, Li J, Bao L, Patel PM, Gasparini G, et al. Characterizing the proteome of bullous pemphigoid blister fluid utilizing tandem mass tag labeling coupled with LC-MS/MS. *Arch Dermatol Res*. (2021) 314(9):921–8. doi: 10.1007/s00403-021-02253-8

43. Hoffman LK, Tomalin LE, Schultz G, Howell MD, Anandasabapathy N, Alavi A, et al. Integrating the skin and blood transcriptomes and serum proteome in hidradenitis suppurativa reveals complement dysregulation and a plasma cell signature. *PLoS One*. (2018) 13(9):e0203672. doi: 10.1371/journal.pone.0203672

44. Frew JW, Navrazhina K. In silico analysis of gamma-secretase-complex mutations in hidradenitis suppurativa demonstrates disease-specific substrate recognition and cleavage alterations. *Front Med (Lausanne)*. (2019) 6:206. doi: 10.3389/fmed.2019.00206

45. Javad F, Day PJ. Protein profiling of keloidal scar tissue. *Arch Dermatol Res*. (2012) 304(7):533–40. doi: 10.1007/s00403-012-1224-6

46. Jiang M, Fang H, Shao S, Dang E, Zhang J, Qiao P, et al. Keratinocyte exosomes activate neutrophils and enhance skin inflammation in psoriasis. *FASEB J*. (2019) 33(12):13241–53. doi: 10.1096/fj.201900642R

47. Gao L, van Nieuwpoort FA, Out-Luiting JJ, Hensbergen PJ, de Snoo FA, Bergman W, et al. Genome-wide analysis of gene and protein expression of dysplastic naevus cells. *J Skin Cancer*. (2012) 2012:981308. doi: 10.1155/2012/981308

48. Yanagi T, Watanabe M, Hata H, Kitamura S, Imafuku K, Yanagi H, et al. Loss of TRIM29 alters keratin distribution to promote cell invasion in squamous cell carcinoma. *Cancer Res*. (2018) 78(24):6795–806. doi: 10.1158/0008-5472.CAN-18-1495

49. Pietrobono S, Anichini G, Sala C, Manetti F, Almada LL, Pepe S, et al. ST3GAL1 is a target of the SOX2-GLI1 transcriptional complex and promotes melanoma metastasis through AXL. *Nat Commun*. (2020) 11(1):5865. doi: 10.1038/s41467-020-19575-2

50. de Groot E, Varghese S, Tan L, Knighton B, Sobieski M, Nguyen N, et al. Combined inhibition of HMGCoA reductase and mitochondrial complex I induces tumor regression of BRAF inhibitor-resistant melanomas. *Cancer Metab*. (2022) 10(1):6. doi: 10.1186/s40170-022-00281-0

51. Qian YT, Liu XY, Sun HD, Xu JY, Sun JM, Liu W, et al. Urinary proteomics analysis of active vitiligo patients: biomarkers for steroid treatment efficacy prediction and monitoring. *Front Mol Biosci*. (2022) 9:761562. doi: 10.3389/fmolb.2022.761562

52. Phadke M, Remsing Rix LL, Smalley I, Bryant AT, Luo Y, Lawrence HR, et al. Dabrafenib inhibits the growth of BRAF-WT cancers through CDK16 and NEK9 inhibition. *Mol Oncol*. (2018) 12(1):74–88. doi: 10.1002/1878-0261.12152

53. Guo W, Wang H, Li C. Signal pathways of melanoma and targeted therapy. *Signal Transduct Target Ther*. (2021) 6(1):424. doi: 10.1038/s41392-021-00827-6

54. Turner CT, Lim D, Granville DJ. Granzyme B in skin inflammation and disease. *Matrix Biol*. (2019) 75–76:126–40. doi: 10.1016/j.matbio.2017.12.005

55. Wladis EJ, Swamy S, Herrmann A, Yang J, Carlson JA, Adam AP. Activation of p38 and Erk mitogen-activated protein kinases signaling in ocular Rosacea. *Invest Ophthalmol Vis Sci*. (2017) 58(2):843–8. doi: 10.1167/iovs.16-20275

56. Fedorenko IV, Abel EV, Koomen JM, Fang B, Wood ER, Chen YA, et al. Fibronectin induction abrogates the BRAF inhibitor response of BRAF V600E/PTEN-null melanoma cells. *Oncogene*. (2016) 35(10):1225–35. doi: 10.1038/onc.2015.188

57. Kanduc D. The role of proteomics in defining autoimmunity. *Expert Rev Proteomics*. (2021) 18(3):177–84. doi: 10.1080/14789450.2021.1914595

58. Hanash S. Disease proteomics. *Nature*. (2003) 422(6928):226–32. doi: 10.1038/nature01514

59. Lundberg E, Borner GHH. Spatial proteomics: a powerful discovery tool for cell biology. *Nat Rev Mol Cell Biol*. (2019) 20(5):285–302. doi: 10.1038/s41580-018-0094-y

60. Suhre K, McCarthy MI, Schwenk JM. Genetics meets proteomics: perspectives for large population-based studies. *Nat Rev Genet*. (2021) 22(1):19–37. doi: 10.1038/s41576-020-0268-2

61. Vistain LF, Tay S. Single-cell proteomics. *Trends Biochem Sci*. (2021) 46(8):661–72. doi: 10.1016/j.tibs.2021.01.013

62. McNeill E, Hogg N. S100a9 has a protective role in inflammation-induced skin carcinogenesis. *Int J Cancer*. (2014) 135(4):798–808. doi: 10.1002/ijc.28725

63. Hartman ML, Talar B, Noman MZ, Gajos-Michniewicz A, Chouaib S, Czyz M. Gene expression profiling identifies microphthalmia-associated transcription

factor (MITF) and Dickkopf-1 (DKK1) as regulators of microenvironment-driven alterations in melanoma phenotype. *PLoS One*. (2014) 9(4):e95157. doi: 10.1371/journal.pone.0095157

64. Huo J, Zhang Y, Li R, Wang Y, Wu J, Zhang D. Upregulated microRNA-25 mediates the migration of melanoma cells by targeting DKK3 through the WNT/beta-catenin pathway. *Int J Mol Sci*. (2016) 17(11):1124. doi: 10.3390/ijms17111124

65. Chen J, Li H, Chen H, Hu D, Xing Q, Ren G, et al. Dickkopf-1 inhibits the invasive activity of melanoma cells. *Clin Exp Dermatol*. (2012) 37(4):404–10. doi: 10.1111/j.1365-2230.2011.04276.x

66. Habel N, El-Hachem N, Soysouvanh F, Hadhiri-Bzioueche H, Giuliano S, Nguyen S, et al. FBXO32 links ubiquitination to epigenetic reprograming of melanoma cells. *Cell Death Differ*. (2021) 28(6):1837–48. doi: 10.1038/s41418-020-00710-x

67. Bui TM, Wiesolek HL, Sumagin R. ICAM-1: a master regulator of cellular responses in inflammation, injury resolution, and tumorigenesis. *J Leukoc Biol*. (2020) 108(3):787–99. doi: 10.1002/JLB.2MR0220-549R

68. Ghislin S, Obino D, Middendorp S, Boggetto N, Alcaide-Loridan C, Deshayes F. LFA-1 and ICAM-1 expression induced during melanoma-endothelial cell co-culture favors the transendothelial migration of melanoma cell lines in vitro. *BMC Cancer*. (2012) 12:455. doi: 10.1186/1471-2407-12-455

69. Saini J, Clinical SP. Prognostic and therapeutic significance of heat shock proteins in cancer. *Curr Drug Targets*. (2018) 19(13):1478–90. doi: 10.2174/1389450118666170823121248

70. Piras F, Murtas D, Minerba L, Ugalde J, Floris C, Maxia C, et al. Nuclear survivin is associated with disease recurrence and poor survival in patients with cutaneous malignant melanoma. *Histopathology*. (2007) 50(7):835–42. doi: 10.1111/j.1365-2559.2007.02695.x

71. Liang S, Hu L, Wu Z, Chen Z, Liu S, Xu X, et al. CDK12: a potent target and biomarker for human cancer therapy. *Cells*. (2020) 9(6):1483. doi: 10.3390/cells9061483

72. Li M, Zhang B, Sun B, Wang X, Ban X, Sun T, et al. A novel function for vimentin: the potential biomarker for predicting melanoma hematogenous metastasis. *J Exp Clin Cancer Res*. (2010) 29:109. doi: 10.1186/1756-9966-29-109

73. Vereecken P, Awada A, Suciu S, Castro G, Morandini R, Litynska A, et al. Evaluation of the prognostic significance of serum galectin-3 in American Joint Committee on Cancer stage III and stage IV melanoma patients. *Melanoma Res*. (2009) 19(5):316–20. doi: 10.1097/CMR.0b013e32832ec001

74. Welinder C, Pawlowski K, Szasz AM, Yakovleva M, Sugihara Y, Malm J, et al. Correlation of histopathologic characteristics to protein expression and function in malignant melanoma. *PLoS One*. (2017) 12(4):e0176167. doi: 10.1371/journal.pone.0176167

75. Pastushenko I, Mauri F, Song Y, de Cock F, Meeusen B, Swedlund B, et al. Fat1 deletion promotes hybrid EMT state, tumour stemness and metastasis. *Nature*. (2021) 589(7842):448–55. doi: 10.1038/s41586-020-03046-1

76. Shintani T, Higaki M, Okamoto T. Heparin-binding protein 17/fibroblast growth factor-binding protein-1 knockout inhibits proliferation and induces differentiation of squamous cell carcinoma cells. *Cancers (Basel)*. (2021) 13(11):2684. doi: 10.3390/cancers13112684

77. Mann M, Jensen ON. Proteomic analysis of post-translational modifications. *Nat Biotechnol*. (2003) 21(3):255–61. doi: 10.1038/nbt0303-255

78. van Bon L, Affandi AJ, Broen J, Christmann RB, Marijnissen RJ, Stawski L, et al. Proteome-wide analysis and CXCL4 as a biomarker in systemic sclerosis. *N Engl J Med*. (2014) 370(5):433–43. doi: 10.1056/NEJMoa1114576

79. Yu CJ, Lin YF, Chiang BL, Chow LP. Proteomics and immunological analysis of a novel shrimp allergen, Pen m 2. *J Immunol*. (2003) 170(1):445–53. doi: 10.4049/jimmunol.170.1.445

80. Yoon A, Peng G, Brandenburger Y, Zollo O, Xu W, Rego E, et al. Impaired control of IRES-mediated translation in X-linked dyskeratosis congenita. *Science*. (2006) 312(5775):902–6. doi: 10.1126/science.1123835

81. Xu J, Saunders CW, Hu P, Grant RA, Boekhout T, Kuramae EE, et al. Dandruff-associated *Malassezia* genomes reveal convergent and divergent virulence traits shared with plant and human fungal pathogens. *Proc Natl Acad Sci U S A*. (2007) 104(47):18730–5. doi: 10.1073/pnas.0706756104

82. von Kriegsheim A, Baiocchi D, Birtwistle M, Sumpton D, Bienvenut W, Morrice N, et al. Cell fate decisions are specified by the dynamic ERK interactome. *Nat Cell Biol*. (2009) 11(12):1458–64. doi: 10.1038/ncb1994

83. Fan Y, Pedersen O. Gut microbiota in human metabolic health and disease. *Nat Rev Microbiol*. (2021) 19(1):55–71. doi: 10.1038/s41579-020-0433-9

84. Smola H, Thiekotter G, Fusenig NE. Mutual induction of growth factor gene expression by epidermal-dermal cell interaction. *J Cell Biol*. (1993) 122(2):417–29. doi: 10.1083/jcb.122.2.417

85. Hackam DJ, Ford HR. Cellular, biochemical, and clinical aspects of wound healing. *Surg Infect (Larchmt)*. (2002) 3(Suppl 1):S23–35. doi: 10.1089/10962960260496316

86. Aden N, Shiwen X, Aden D, Black C, Nuttall A, Denton CP, et al. Proteomic analysis of scleroderma lesional skin reveals activated wound healing phenotype of epidermal cell layer. *Rheumatology (Oxford)*. (2008) 47(12):1754–60. doi: 10.1093/rheumatology/ken370

87. Fadini GP, Menegazzo L, Rigato M, Scattolini V, Poncina N, Bruttocao A, et al. NETosis delays diabetic wound healing in mice and humans. *Diabetes*. (2016) 65(4):1061–71. doi: 10.2337/db15-0863

88. Molin S, Merl J, Dietrich KA, Regauer M, Flaig M, Letule V, et al. The hand eczema proteome: imbalance of epidermal barrier proteins. *Br J Dermatol*. (2015) 172(4):994–1001. doi: 10.1111/bjd.13418

89. Ma J, Liu J, Gao D, Li X, Zhang Q, Lv L, et al. Establishment of human pluripotent stem cell-derived skin organoids enabled pathophysiological model of SARS-CoV-2 infection. *Adv Sci (Weinh)*. (2022) 9(7):e2104192. doi: 10.1002/advs.202104192

90. Kim KW, Myers RA, Lee JH, Igartua C, Lee KE, Kim YH, et al. Genome-wide association study of recalcitrant atopic dermatitis in Korean children. *J Allergy Clin Immunol*. (2015) 136(3):678–84.e4. doi: 10.1016/j.jaci.2015.03.030

91. Paternoster L, Standl M, Waage J, Baurecht H, Hotze M, Strachan DP, et al. Multi-ancestry genome-wide association study of 21,000 cases and 95,000 controls identifies new risk loci for atopic dermatitis. *Nat Genet*. (2015) 47(12):1449–56. doi: 10.1038/ng.3424

92. Schaarschmidt H, Ellinghaus D, Rodriguez E, Kretschmer A, Baurecht H, Lipinski S, et al. A genome-wide association study reveals 2 new susceptibility loci for atopic dermatitis. *J Allergy Clin Immunol*. (2015) 136(3):802–6. doi: 10.1016/j.jaci.2015.01.047

93. Weidinger S, Willis-Owen SA, Kamatani Y, Baurecht H, Morar N, Liang L, et al. A genome-wide association study of atopic dermatitis identifies loci with overlapping effects on asthma and psoriasis. *Hum Mol Genet*. (2013) 22(23):4841–56. doi: 10.1093/hmg/ddt317

94. Broccardo CJ, Mahaffey SB, Strand M, Reisdorph NA, Leung DY. Peeling off the layers: skin taping and a novel proteomics approach to study atopic dermatitis. *J Allergy Clin Immunol*. (2009) 124(5):1113–5.e11. doi: 10.1016/j.jaci.2009.07.057

95. Sakabe J, Kamiya K, Yamaguchi H, Ikeya S, Suzuki T, Aoshima M, et al. Proteome analysis of stratum corneum from atopic dermatitis patients by hybrid quadrupole-orbitrap mass spectrometer. *J Allergy Clin Immunol*. (2014) 134(4):957–60.e8. doi: 10.1016/j.jaci.2014.07.054

96. Bangert C, Rindler K, Krausgruber T, Alkon N, Thaler FM, Kurz H, et al. Persistence of mature dendritic cells, TH2A, and Tc2 cells characterize clinically resolved atopic dermatitis under IL-4Ralpha blockade. *Sci Immunol*. (2021) 6(55):eabe2749. doi: 10.1126/sciimmunol.abe2749

97. Mo Q, Wan L, Schell MJ, Jim H, Tworoger SS, Peng G. Integrative analysis identifies multi-omics signatures that drive molecular classification of uveal melanoma. *Cancers (Basel)*. (2021) 13(24):6168. doi: 10.3390/cancers13246168

98. Valenti F, Falcone I, Ungania S, Desiderio F, Giacomini P, Bazzichetto C, et al. Precision medicine and melanoma: multi-omics approaches to monitoring the immunotherapy response. *Int J Mol Sci*. (2021) 22(8):3837. doi: 10.3390/ijms22083837

99. Rajagopalan P, Jain AP, Nanjappa V, Patel K, Mangalaparthi KK, Babu N, et al. Proteome-wide changes in primary skin keratinocytes exposed to diesel particulate extract—a role for antioxidants in skin health. *J Dermatol Sci*. (2018) 91(3):239–49. doi: 10.1016/j.jdermsci.2018.05.003

100. Borrel V, Gannesen AV, Barreau M, Gaviard C, Duclairoir-Poc C, Hardouin J, et al. Adaptation of acneic and non acneic strains of *Cutibacterium acnes* to sebum-like environment. *Microbiologyopen*. (2019) 8(9):e00841. doi: 10.1002/mbo3.841

101. Wichit S, Hamel R, Zanzoni A, Diop F, Cribier A, Talignani L, et al. SAMHD1 enhances Chikungunya and Zika virus replication in human skin fibroblasts. *Int J Mol Sci*. (2019) 20(7):1695. doi: 10.3390/ijms20071695

102. Nanashima N, Ito K, Ishikawa T, Nakano M, Nakamura T. Damage of hair follicle stem cells and alteration of keratin expression in external radiation-induced acute alopecia. *Int J Mol Med*. (2012) 30(3):579–84. doi: 10.3892/ijmm.2012.1018

103. Park YD, Lyou YJ, Yang JM. Detection of down-regulated acetaldehyde dehydrogenase 1 in atopic dermatitis patients by two-dimensional electrophoresis. *Exp Dermatol*. (2007) 16(2):130–4. doi: 10.1111/j.1600-0625.2006.00524.x

104. Paulitschke V, Kunstfeld R, Mohr T, Slany A, Micksche M, Drach J, et al. Entering a new era of rational biomarker discovery for early detection of melanoma metastases: secretome analysis of associated stroma cells. *J Proteome Res*. (2009) 8(5):2501–10. doi: 10.1021/pr8010827

105. Geyer PE, Kulak NA, Pichler G, Holdt LM, Teupser D, Mann M. Plasma proteome profiling to assess human health and disease. *Cell Syst*. (2016) 2 (3):185–95. doi: 10.1016/j.cels.2016.02.015

106. Paczesny S, Braun TM, Levine JE, Hogan J, Crawford J, Coffing B, et al. Elafin is a biomarker of graft-versus-host disease of the skin. *Sci Transl Med*. (2010) 2(13):13ra2. doi: 10.1126/scitranslmed.3000406

107. Paolino G, Huber V, Camerini S, Casella M, Macone A, Bertuccini L, et al. The fatty acid and protein profiles of circulating CD81-positive small extracellular vesicles are associated with disease stage in melanoma patients. *Cancers (Basel)*. (2021) 13(16):4157. doi: 10.3390/cancers13164157

108. Chen RF, Yang MY, Wang CJ, Wang CT, Kuo YR. Proteomic analysis of peri-wounding tissue expressions in extracorporeal shock wave enhanced diabetic wound healing in a streptozotocin-induced diabetes model. *Int J Mol Sci*. (2020) 21(15):5445. doi: 10.3390/ijms21155445.

109. McQuilling JP, Carter MJ, Fulton JA, Patel K, Doner B, Serena TE, et al. A prospective clinical trial evaluating changes in the wound microenvironment in patients with chronic venous leg ulcers treated with a hypothermically stored amniotic membrane. *Int Wound J*. (2022) 19(1):144–55. doi: 10.1111/iwj.13606

110. Yun MK, Lee SJ, Song HJ, Yu HJ, Rha CS, Kim DO, et al. Protein expression level of skin wrinkle-related factors in hairless mice fed hyaluronic acid. *J Med Food*. (2017) 20(4):420–4. doi: 10.1089/jmf.2016.3873

# Frontiers in Surgery

**Explores and improves surgical practice and clinical patient management**

A multidisciplinary journal which explores surgical practices - from fundamental principles to advances in microsurgery and minimally invasive techniques. It fosters innovation and improves the clinical management of patients.

---

## Discover the latest Research Topics

See more →


**Frontiers**

Avenue du Tribunal-Fédéral 34
1005 Lausanne, Switzerland
frontiersin.org

**Contact us**

+41 (0)21 510 17 00
frontiersin.org/about/contact